

On the adaptation of reference sets using niching and pair-potential energy functions for multi-objective optimization

Supplementary material

Luis A. Márquez-Vega, Jesús Guillermo Falcón-Cardona, and Edgar Covantes Osuna

Tecnológico de Monterrey, School of Engineering and Sciences, Ave. Eugenio Garza Sada
2501, Monterrey, Nuevo León, 64849, Mexico

Abstract

This supplementary material provides additional results to discuss further the performance of multi-objective evolutionary algorithms (MOEAs) using our adaptation method Ada \mathcal{K} on multi-objective optimization problems (MOPs) with regular and irregular Pareto front (PF) shapes. First, a sensitivity analysis of the parameters required by our adaptation method is shown. Then, the performance comparison of MOEAs using our adaptation method against state-of-the-art MOEAs is performed. After that, additional tables containing the complete numerical results of the performance assessment of MOEAs using the main framework of NSGA-III, RVEA, and MOEA/D are provided. Finally, all final populations and additional convergence and diversity graphs obtained by MOEAs based on the main framework of NSGA-III, RVEA, and MOEA/D on MOPs with regular and irregular PF shapes are given.

1 Sensitivity analysis

This section shows a sensitivity analysis of our adaptation method regarding the parameters f_{step} and f_{last} on multi-objective optimization problems (MOPs) with regular and irregular Pareto front (PF) shapes. Since multi-objective evolutionary algorithms (MOEAs) can employ different features of our adaptation method Ada \mathcal{K} , performing the sensitivity analysis on MOEAs using different frameworks is important. For instance, NSGA-III provides the nadir vector approximation at each generation to our adaptation method, while it is not given by RVEA and MOEA/D. Also, MOEA/D requires including the information of differently scaled objective functions on the adaptation of the weight vector-based reference set (WVRS), while NSGA-III and RVEA do not since they have mechanisms to handle these MOPs. Finally, MOEA/D requires updating the population and neighborhoods each time its WVRS is adapted. Thus, in representation of MOEAs with our adaptation method, we employ the NSGA-III-AdaRSE, RVEA-AdaRSE, and MOEA/D-AdaRSE to perform this sensitivity analysis using all combinations between $f_{\text{step}} \in \{0.01, 0.025, 0.05, 0.1\}$ and $f_{\text{last}} \in \{0.5, 0.7, 0.9, 0.95\}$. On the one hand, the parameter f_{step} indicates that the WVRS should be adapted at each $f_{\text{step}} \cdot g_{\max}$ generations, where g_{\max} is the maximum number of generations. Thus, the selected values for f_{step} are useful to study the performance of our adaptation method having different frequencies of adaptation, where the values $f_{\text{step}} = 0.01$ and $f_{\text{step}} = 0.1$ are sufficiently small and large, respectively, to observe the effect of adapting the WVRS at a fast and slow rate. On the other hand, the parameter f_{last} is used to indicate that the WVRS should not be adapted after the generation $f_{\text{last}} \cdot g_{\max}$. Consequently, the selected values f_{last} allow us to study our adaptation method with a last adaptation of the WVRS too far or too close to the end of the evolutionary process, where $f_{\text{last}} = 0.5$ is useful to observe the effect of adapting the WVRS during a small portion of the evolutionary process and $f_{\text{last}} = 0.95$ represents an adaptation of the WVRS too near to the end of the evolutionary process. Finally, it is worth noting that larger values for f_{step} and smaller values for f_{last} will produce that our adaptation method be scarcely utilized.

1.1 Regular PF shapes

Figures 1 to 4 show the sensitivity analysis in terms of hypervolume (HV) and Solow Polasky diversity (SPD) of NSGA-III-AdaRSE, RVEA-AdaRSE, and MOEA/D-AdaRSE on DTLZ1, DTLZ2, WFG1, and WFG4,

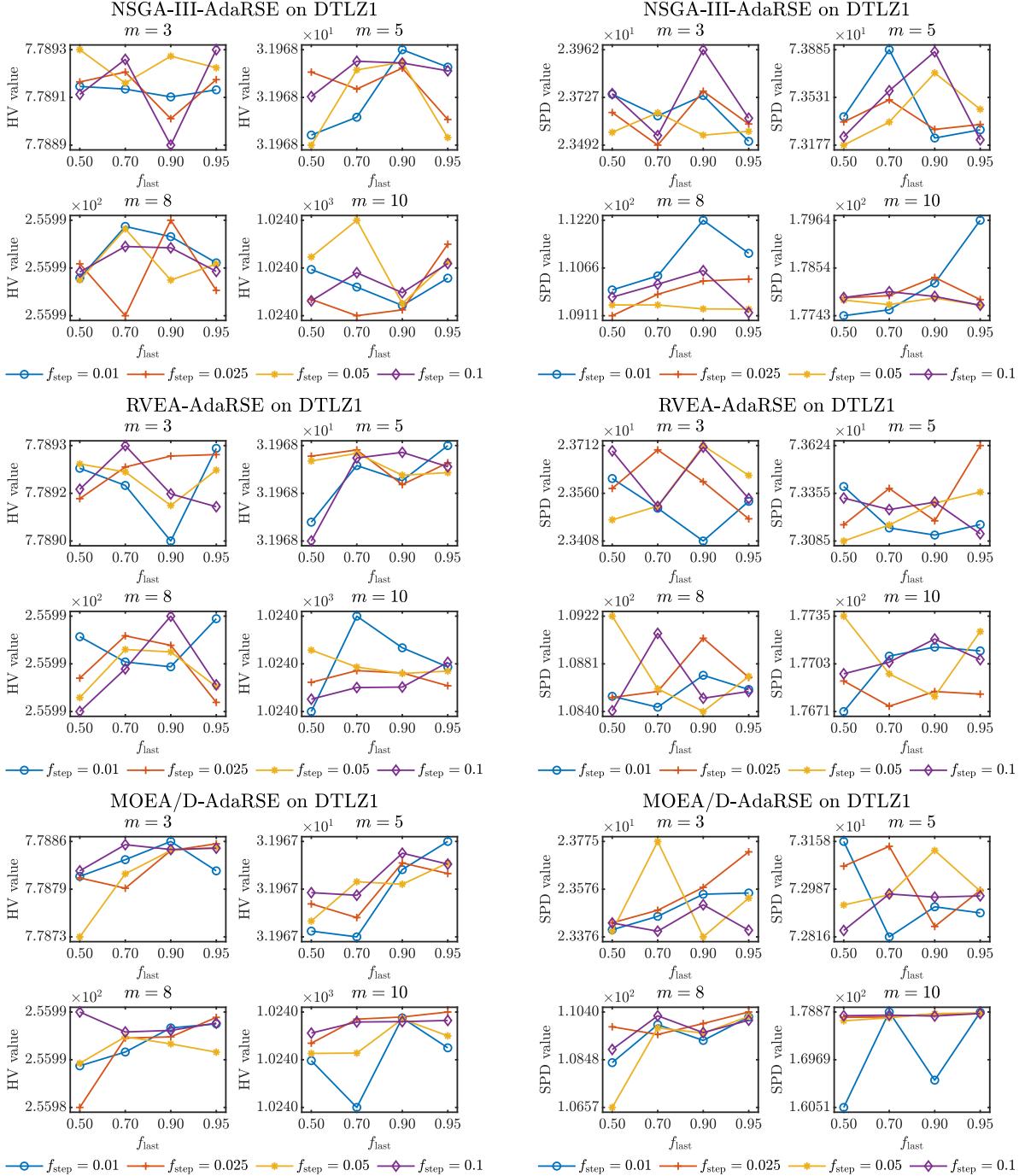


Figure 1: Performance comparison using the mean values of HV and SPD among 30 independent runs of NSGA-III-AdaRSE, RVEA-AdaRSE, and MOEA/D-AdaRSE with different configurations for f_{step} and f_{last} on DTLZ1 with 3, 5, 8, and 10 objective functions, where m represents the number of objective functions.

respectively, with 3, 5, 8, and 10 objective functions. Figure 1 shows that all configurations of MOEAs get similar performance on most instances of DTLZ1 since they achieve similar HV values. However, a small value of f_{last} may reduce their performance in this MOP. This observation is more evident on MOEA/D-AdaRSE, where its performance is improved in most cases as the value of f_{last} increases. Nevertheless, performing the adaptation too close to the end of the evolutionary process may degrade its performance. Similar results are shown in Figure 2, where similar HV and SPD values are obtained by all configurations on most instances of DTLZ2. However, small values for f_{last} systematically get the best performance in terms of HV on DTLZ2

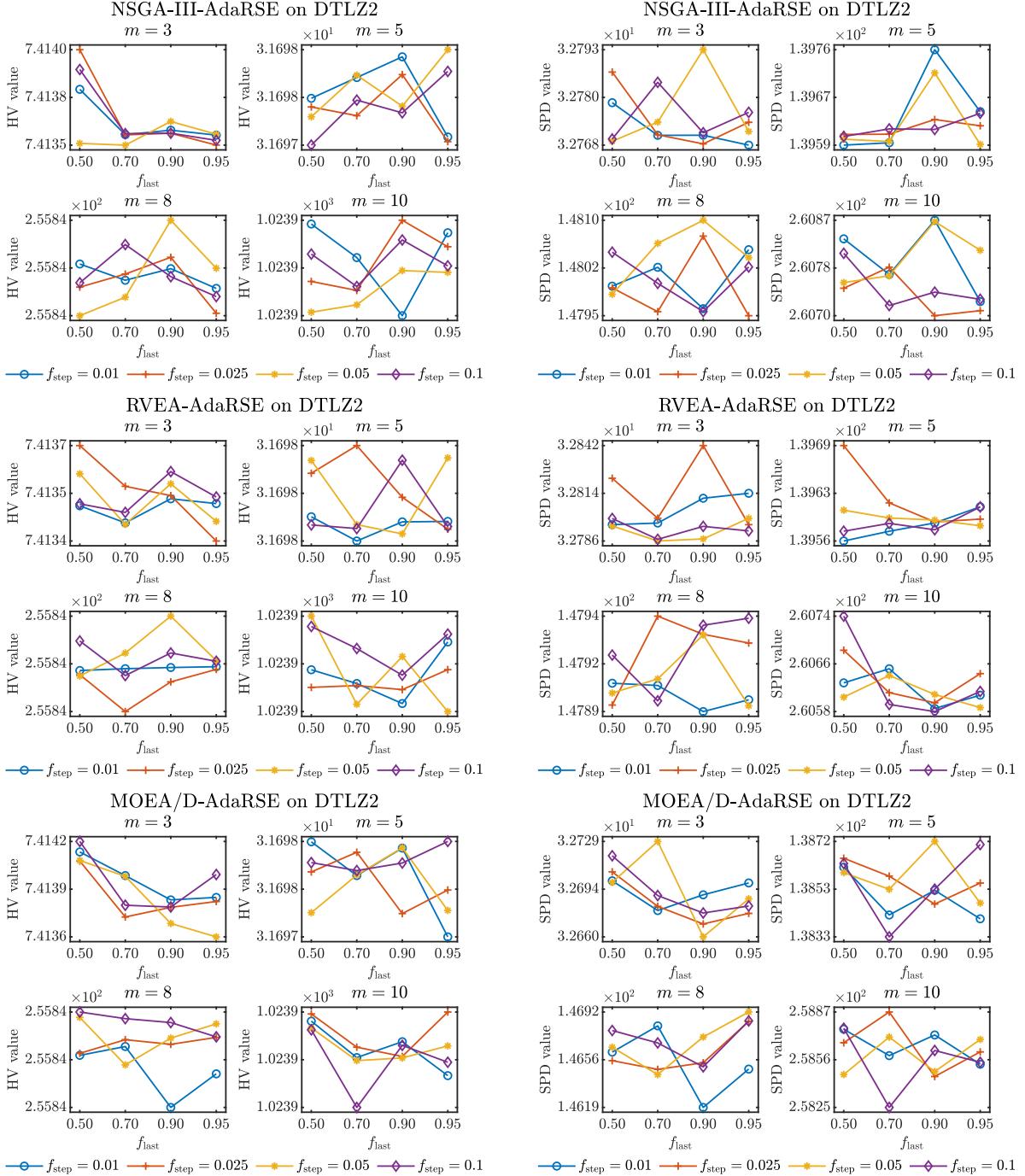


Figure 2: Performance comparison using the mean values of HV and SPD among 30 independent runs of NSGA-III-AdaRSE, RVEA-AdaRSE, and MOEA/D-AdaRSE with different configurations for f_{step} and f_{last} on DTLZ2 with 3, 5, 8, and 10 objective functions, where m represents the number of objective functions.

with 3 objective functions. Figure 3 shows that large values for f_{step} are preferred on NSGA-III-AdaRSE and RVEA-AdaRSE, while small values promote better results on MOEA/D-AdaRSE on most instances of WFG1. In addition, it can be seen that similar results are obtained by different values of f_{last} on NSGA-III-AdaRSE and RVEA-AdaRSE. However, large values of f_{last} are preferred for MOEA/D-AdaRSE, especially on WFG1 with 3 and 10 objective functions. Similarly to the results obtained on DTLZ2, Figure 4 indicates that different configurations of f_{last} get similar HV and SPD values on WFG4. However, adapting the WVRS too close to the end of the evolutionary process degrades the performance of the MOEA in most cases.

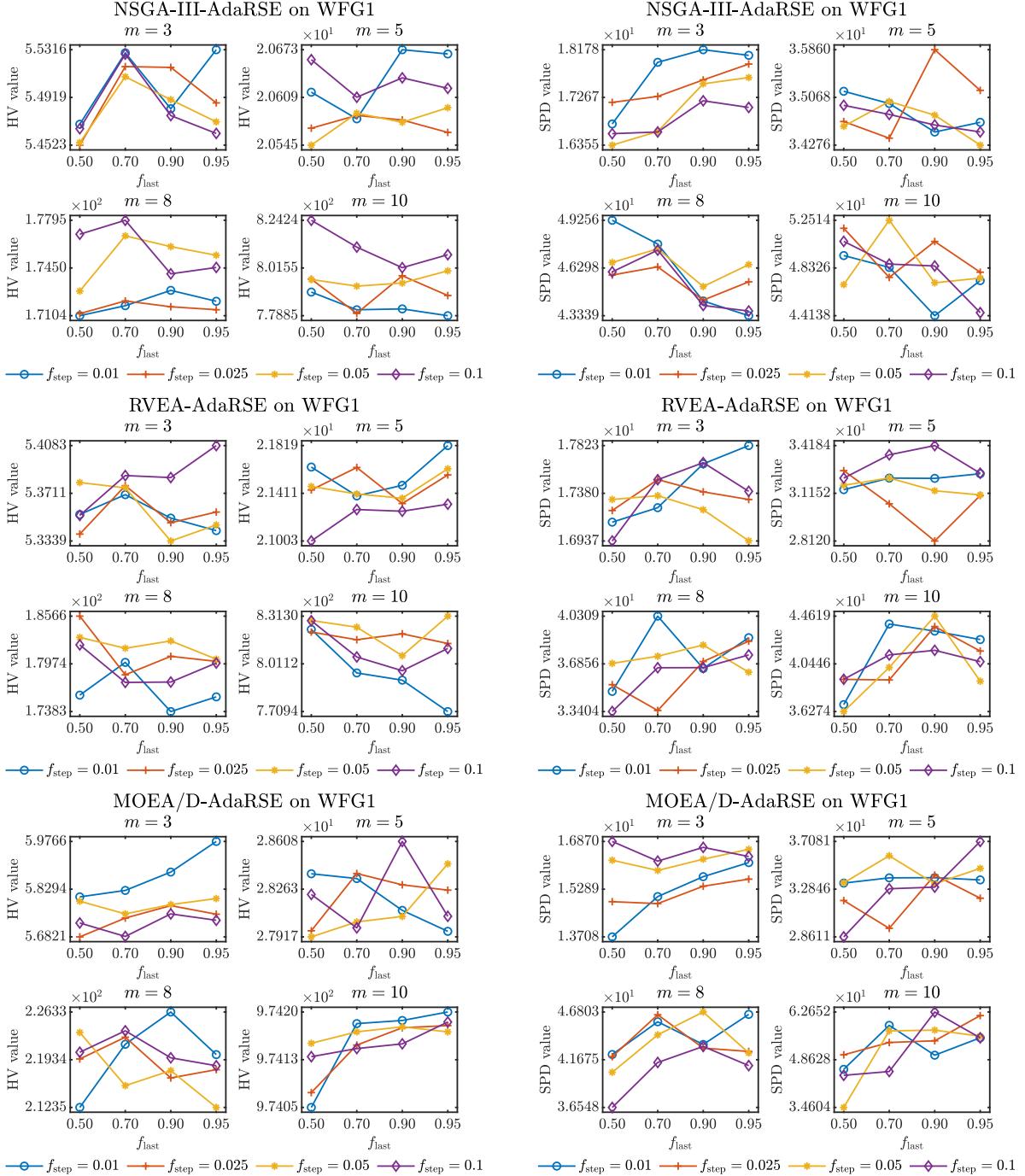


Figure 3: Performance comparison using the mean values of HV and SPD among 30 independent runs of NSGA-III-AdaRSE, RVEA-AdaRSE, and MOEA/D-AdaRSE with different configurations for f_{step} and f_{last} on WFG1 with 3, 5, 8, and 10 objective functions, where m represents the number of objective functions.

Among the obtained results, it can be seen that our adaptation method is capable of getting similar results on some MOPs with regular PF shapes regardless of the configuration of the parameters f_{step} and f_{last} . The explanation of this observation is that the task of our adaption method when tackling MOPs with regular PF shape is to determine that all weight vectors of the original WVRs are useful. Thus, our adaptation method can achieve such a task on some MOPs with regular PF shapes, even with different configurations of parameters. For instance, MOEAs with our adaptation method using different parameters obtain similar performance on DTLZ2 and WFG4 since these MOPs do not include complex search difficulties. However, it

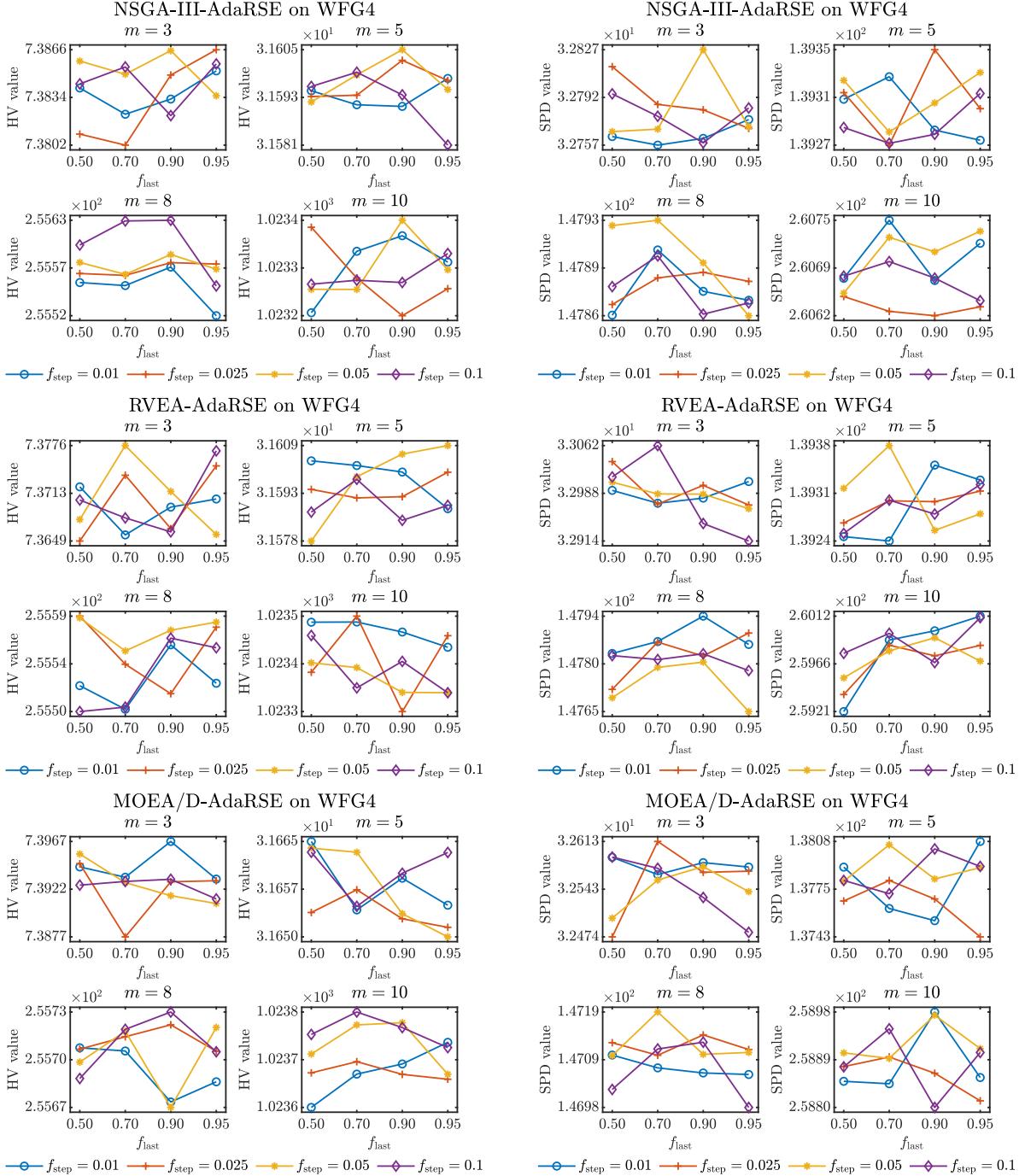


Figure 4: Performance comparison using the mean values of HV and SPD among 30 independent runs of NSGA-III-AdaRSE, RVEA-AdaRSE, and MOEA/D-AdaRSE with different configurations for f_{step} and f_{last} on WFG4 with 3, 5, 8, and 10 objective functions, where m represents the number of objective functions.

can be observed that stopping the adaptation too early may harm the performance on DTLZ1 and WFG1, which have multi-modality and bias difficulty, respectively. Furthermore, results on WFG1 show that a slow adaptation frequency may benefit NSGA-III-AdaRSE and RVEA-AdaRSE, while a fast adaptation frequency is better on MOEA/D-AdaRSE. This result can be because MOEA/D employs our adaptation method to include the ranges of objective functions. Consequently, regularly updating such information can be beneficial when dealing with a MOP having bias difficulty and differently scaled objective functions. Finally, it is worth noting that in most cases is not recommended to adapt the WVRS very close to the end of the evolutionary

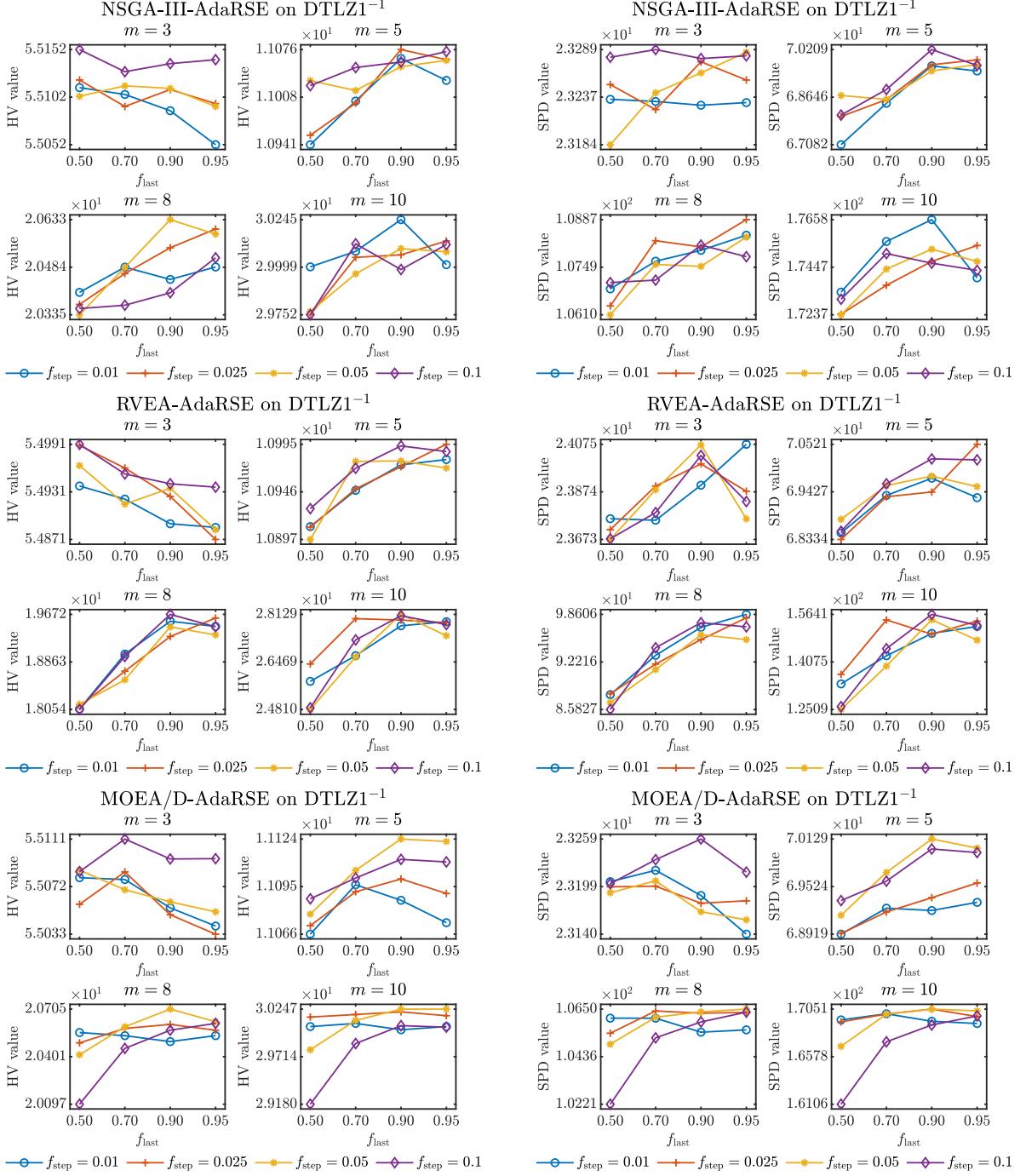


Figure 5: Performance comparison using the mean values of HV and SPD among 30 independent runs of NSGA-III-AdaRSE, RVEA-AdaRSE, and MOEA/D-AdaRSE with different configurations for f_{step} and f_{last} on DTLZ1⁻¹ with 3, 5, 8, and 10 objective functions, where m represents the number of objective functions.

process since some weight vectors can be replaced, leading to new search directions that cannot be reached due to the limited number of remaining generations.

1.2 Irregular PF shapes

Figures 5 to 8 show the sensitivity analysis in terms of HV and SPD of NSGA-III-AdaRSE, RVEA-AdaRSE, and MOEA/D-AdaRSE on DTLZ1⁻¹, DTLZ2⁻¹, WFG1⁻¹, and WFG4⁻¹, respectively, under 3, 5, 8, and 10 objective functions. Also, Figure 9 presents the sensitivity analysis results on IMOP4, IMOP5, IMOP7,

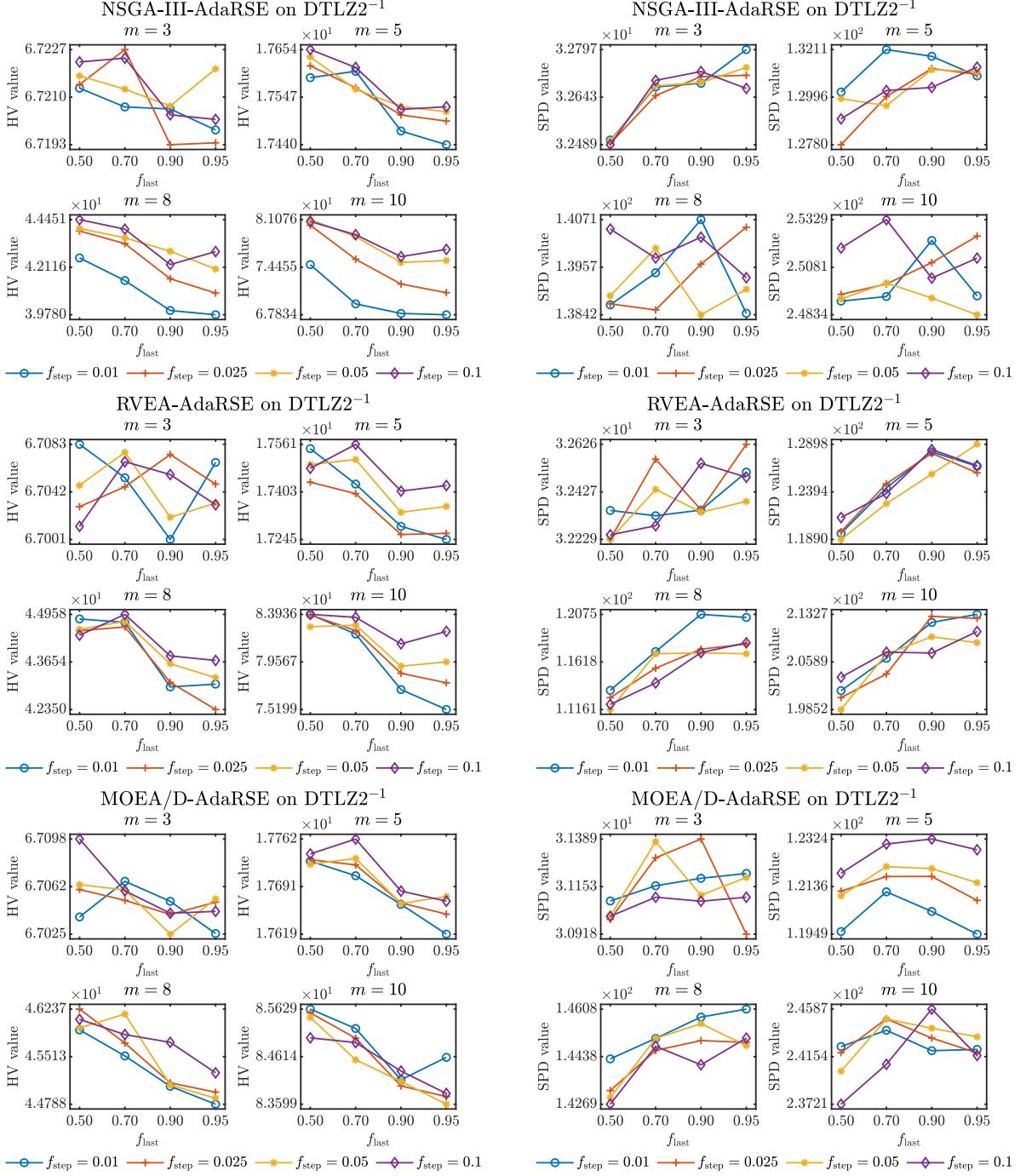


Figure 6: Performance comparison using the mean values of HV and SPD among 30 independent runs of NSGA-III-AdaRSE, RVEA-AdaRSE, and MOEA/D-AdaRSE with different configurations for f_{step} and f_{last} on DTLZ2^{-1} with 3, 5, 8, and 10 objective functions, where m represents the number of objective functions.

and VNT1. Figure 5 shows that the performance can be improved by increasing the parameter f_{last} on DTLZ1^{-1} with 5, 8, and 10 objective functions. However, such a parameter does not strongly affect the performance on DTLZ1^{-1} with 3 objectives. Also, performing the adaptation during the last generations may degrade the performance of MOEAs in most cases of DTLZ1^{-1} . Regarding the parameter f_{step} , large values get good performance on DTLZ1^{-1} with low dimensional objective space. However, a small value can be useful in high-dimensional objective space. Thus, an intermediate value promotes consistent performance. Figure 6 shows that small values of f_{last} promote better HV values on most instances of DTLZ2^{-1} , while

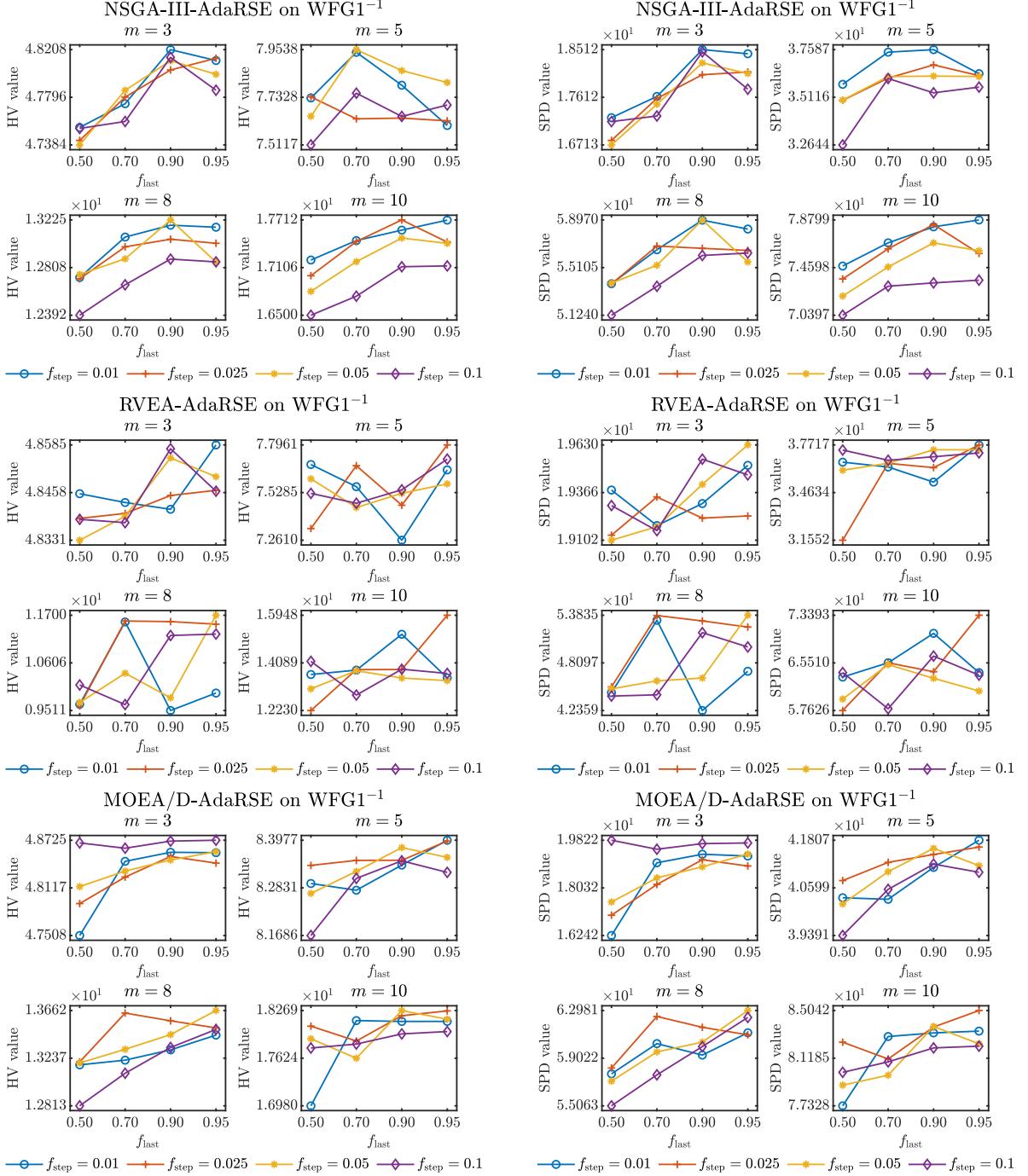


Figure 7: Performance comparison using the mean values of HV and SPD among 30 independent runs of NSGA-III-AdaRSE, RVEA-AdaRSE, and MOEA/D-AdaRSE with different configurations for f_{step} and f_{last} on WFG1 $^{-1}$ with 3, 5, 8, and 10 objective functions, where m represents the number of objective functions.

these values produce worse SPD values. These results may be because stopping the adaptation process too early prevents the entire PF from being covered. Thus, most solutions may be located around the center of the PF. Such solutions have large HV contributions on inverted convex PF shapes, producing large HV values. In contrast, the SPD value is small since the entire PF is not covered. However, similar observations to the obtained on DTLZ1 $^{-1}$ can be seen on DTLZ2 $^{-1}$ when analyzing the performance in terms of SPD. Regarding WFG1 $^{-1}$, Figure 7 shows that larger values for f_{last} are preferred. However, letting to perform the adaptation process during the last generations may degrade the performance. Also, small values for f_{step}

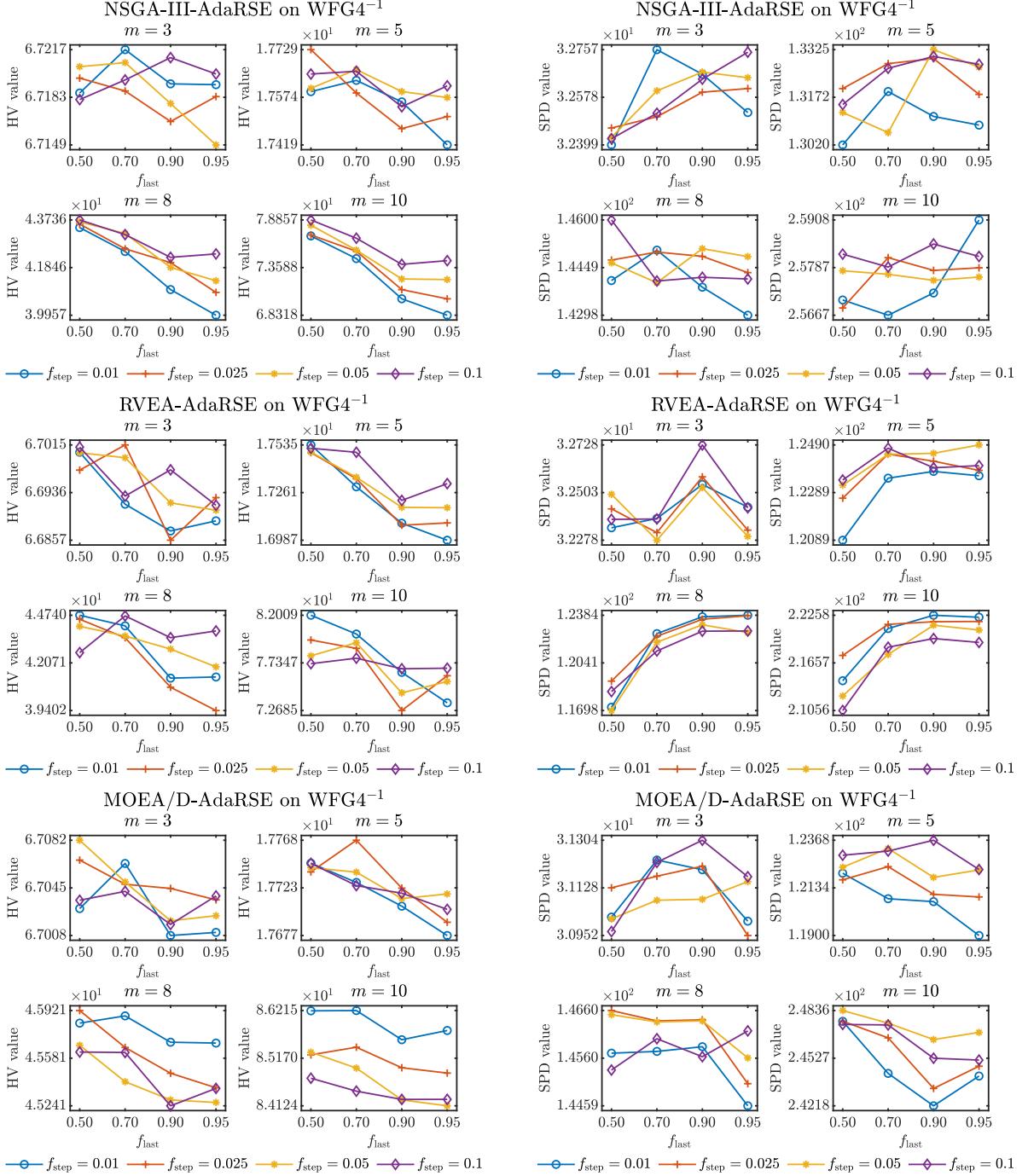


Figure 8: Performance comparison using the mean values of HV and SPD among 30 independent runs of NSGA-III-AdaRSE, RVEA-AdaRSE, and MOEA/D-AdaRSE with different configurations for f_{step} and f_{last} on WFG4^{-1} with 3, 5, 8, and 10 objective functions, where m represents the number of objective functions.

systematically perform better on most cases of WFG1^{-1} since a fast frequency of adaptation is beneficial to discover the entire PF on a MOP with bias difficulty. Similar observations to the obtained on DTLZ2^{-1} can be seen in Figure 8 since WFG4^{-1} also has an inverted convex PF shape but differently scaled objective functions. Thus, some differences in the performance of MOEA/D-AdaRSE can be seen between DTLZ2^{-1} and WFG4^{-1} . Specifically, the performance is not generally improved by using large values of f_{last} on WFG4^{-1} with 5, 8, and 10 objective functions. Finally, Figure 9 shows that large values for f_{last} are better than small values on IMOP4, IMOP5, and IMOP7. Also, using small values of f_{step} consistently performs well

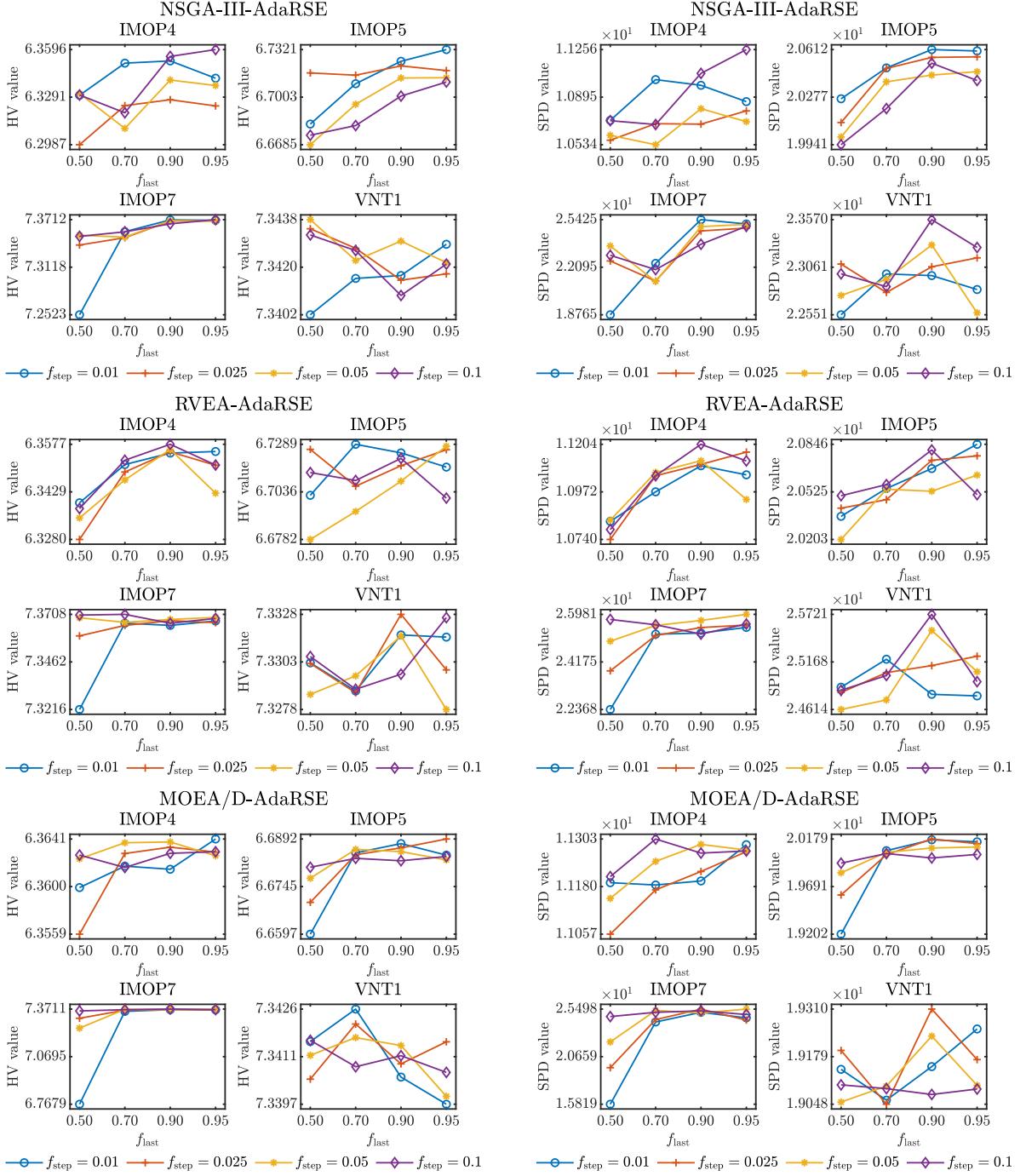


Figure 9: Performance comparison using the mean values of HV and SPD among 30 independent runs of NSGA-III-AdaRSE, RVEA-AdaRSE, and MOEA/D-AdaRSE with different configurations for f_{step} and f_{last} on IMOP4, IMOP5, IMOP7, and VNT1.

on these MOPs. However, such observations are not maintained on VNT1, where the employed parameters do not strongly affect the performance of MOEAs since different parameter configurations obtain similar HV values. Such results suggest that a careful setting of parameters is required to improve the performance of our adaptation method on IMOP4, IMOP5, and IMOP7, where it is difficult to cover the entire PF rapidly.

The obtained results highlight that the performance of our adaptation method can be improved by selecting the parameters depending on the characteristics of the MOP to be tackled. However, a consistent behavior can be observed when dealing with MOPs having irregular PF shapes. In general, stopping the

adaptation process too early during the evolutionary process is not recommended since the PF may only be covered partially. In the same way, allowing an adaptation after the 90% of the evolutionary process may lead to a degradation in the performance of the MOEA since new search directions can be provided near the end of the evolutionary process. Consequently, a large value for f_{last} that does not exceed 0.9 is consistently a good option for our adaptation method. Additionally, tuning the frequency of adaptation controlled by f_{step} is useful to improve the performance of our adaptation method when tackling MOPs with irregular PF shapes having a different number of objective functions or complex search difficulties. For instance, it can be observed that large values for f_{step} can be helpful on some MOPs with 3 and 5 objective functions, while small values are better on such MOPs with 8 and 10 objective functions. Similarly, small values for f_{step} can be helpful to cover the PF of MOPs having bias difficulty rapidly. Therefore, an intermediate value between 0.01 and 0.1 can appropriately handle MOPs with different characteristics. Based on the obtained results, we found that our adaptation method using the values $f_{\text{step}} = 0.05$ and $f_{\text{last}} = 0.9$ promotes a balanced performance among MOPs with different characteristics. Such values promote utilizing the adaptation method sufficiently to represent the PF shape better and letting sufficient time to the current adapted WVRs guide the population toward the PF while adapting the WVRs too close to the end of the evolutionary process is avoided. Additionally, these values for f_{step} and f_{last} have been employed for other MOEAs with adaptation methods such as AdaW [1].

2 Comparison against state-of-the-art MOEAs

Section 5 of the main paper presents the performance assessment of our adaptation method plugged into well-known MOEAs that use a predefined WVRs, namely NSGA-III, RVEA, and MOEA/D. The MOEAs employing our adaptation method are termed as NSGA-III-Ada \mathcal{K} , RVEA-Ada \mathcal{K} , and MOEA/D-Ada \mathcal{K} , where different pair-potential kernels \mathcal{K} can be used. Our experimental results show that our adaptation method enhances the performance of these MOEAs on MOPs with irregular PF shapes. At the same time, our adaptation method maintains their good performance on MOPs with regular PF shapes. Therefore, these results highlight the capability of our adaptation method to promote a Pareto front invariant performance on MOEAs that use a predefined WVRs. In contrast, this supplementary material presents an additional study to compare the performance of NSGA-III-Ada \mathcal{K} , RVEA-Ada \mathcal{K} , and MOEA/D-Ada \mathcal{K} against state-of-the-art MOEAs that have shown good results on MOPs with regular and irregular PF shapes, namely, Two_Arch2 [2], VaEA [3], AR-MOEA [4], hpaEA [5], PREA [6], and RVEA-iGNG [7].

First, we compare the performance of state-of-the-art MOEAs against NSGA-III-AdaRSE and NSGA-III-AdaCOU. Then, the performance of these MOEAs is compared against RVEA-AdaRSE and RVEA-AdaCOU. Finally, we assess the performance of the selected MOEAs against MOEA/D-AdaRSE and MOEA/D-AdaCOU. Hence, this study is also useful to compare the performance of our adaptation method when plugged into different algorithmic frameworks. The state-of-the-art MOEAs selected for this study are briefly described as follows:

- Two_Arch2 employs two archives to focus on convergence and diversity independently. The convergence archive is maintained using an indicator-based selection mechanism based on the binary ϵ^+ indicator [8]. In contrast, the diversity archive uses the $L_{1/m}$ -norm to enhance the diversity among non-dominated solutions, where m is the number of objective functions. Two_Arch2 has demonstrated good performance on MaOPs, while their performance does not depend on the PF shape.
- VaEA follows a similar framework to NSGA-III. However, it does not rely on a predefined WVRs to generate niches. In contrast, it associates candidate solutions to currently selected solutions based on an angular distance, where solutions with the largest distance are chosen to enhance diversity. In addition, the worst solutions in terms of convergence are removed. Therefore, VaEA shows a good balance between convergence and diversity on MOPs with different PF shapes.
- AR-MOEA uses an environmental selection based on an enhanced IGD indicator. The reference set required to calculate the enhanced IGD indicator is adjusted at each generation using a predefined WVRs and selected solutions from an external archive. Consequently, AR-MOEA has demonstrated good versatility when tackling MOPs with various PF geometries.
- hpaEA proposes an environmental selection to balance convergence and diversity. First, prominent solutions are detected using a hyperplane generated from neighboring solutions to strengthen the selection pressure. The prominent solutions are first selected when the number of nondominated solutions

is larger than the population size. Then, the remaining nondominated solutions are chosen based on the angular distance to enhance the diversity. Otherwise, all nondominated solutions are first selected, while a predefined WVRS divides dominated solutions into sub-spaces, where the best solutions in terms of convergence are chosen. Thus, hpaEA exhibits good performance on a wide variety of MOPs.

- PREA uses a ratio-based indicator with infinite norm to identify a promising region in the objective space. Then, the solutions outside this promising region are discarded. Finally, a diversity maintenance mechanism based on the parallel distance is used to select solutions within the promising region. By using these mechanisms, PREA obtains good results in convergence and diversity and exhibits robustness against various PF shapes.
- RVEA-iGNG is a reference vector-guided MOEA using an improved growing neural gas (iGNG) network to adapt the distribution of reference vectors. The iGNG is used to learn the topology of the PF, where the nodes of the iGNG are used as reference vectors, and the solutions from the current and past generations are used as training data. Consequently, RVEA-iGNG can effectively guide the population toward regular and irregular PF shapes.

In this study, we employ MOPs with different PF shapes from the DTLZ and WFG test suites, namely DTLZ1, DTLZ2, DTLZ5, DTLZ7, and WFG1-WFG4 with 3, 5, 8, and 10 objective functions. Furthermore, the corresponding minus versions of such MOPs from the DTLZ⁻¹ and WFG⁻¹ test suites are also employed. Additionally, the benchmark problems IMOP1-IMOP8 and VNT1-VNT3 from the IMOP and VNT test suites are included in the study. The population size, the number of decision variables, and the maximum number of generations for each MOP are set in the same manner described in the main paper.

The simulated binary crossover (SBX) and polynomial mutation are used as genetic operators. For all MOEAs, the crossover probability is set to 1, and the mutation probability is set to $1/n$, where n is the number of decision variables. In the main paper, the crossover index is set to 30, and the mutation index is set to 20 for MOEAs using the NSGA-III and RVEA frameworks. In contrast, for MOEAs using the MOEA/D framework, both crossover and mutation indexes are set to 20. Consequently, we execute the state-of-the-art MOEAs using the crossover and mutation indexes of 30 and 20, respectively, to be compared against NSGA-III-AdaRSE, NSGA-III-AdaCOU, RVEA-AdaRSE, and RVEA-AdaCOU. Also, the state-of-the-art MOEAs using the crossover and mutation indexes of 20 are executed to be compared against MOEA/D-AdaRSE and MOEA/D-AdaCOU. All state-of-the-art MOEAs were performed using their implementations available in PlatEMO with the recommended parameters by their authors.

To assess the performance of MOEAs, we employ the HV and SPD indicators in the same way as the performance assessment provided in the main paper. We performed 30 independent runs of each MOEA on each test problem. The one-tailed Wilcoxon test with a significance level of $\alpha = 0.05$ is used to determine significance difference between state-of-the-art MOEAs and MOEAs with our adaptation method. The symbols “+”, “-”, and “=” indicate when the performance of state-of-the-art MOEAs was significantly better, significantly worse, or statistically equivalent to NSGA-III-AdaRSE, RVEA-AdaRSE, and MOEA/D-AdaRSE. Similarly, the symbols “⊕”, “⊖”, and “≈” indicate when the performance of state-of-the-art MOEAs was significantly better, significantly worse, or statistically equivalent to NSGA-III-AdaCOU, RVEA-AdaCOU, and MOEA/D-AdaCOU. All experiments were run on a computer with a processor Intel Core i7-8700 CPU @ 3.20GHz and 32.0 GB of RAM, running 64-bit Windows 10.

2.1 Regular PF shapes

Tables 1 and 2 present the performance comparison of state-of-the-art MOEAs against NSGA-III-AdaRSE and NSGA-III-AdaCOU on MOPs with regular PF shapes in terms of HV and SPD, respectively. The numerical results from these tables show that both versions of NSGA-III-Ada \mathcal{K} perform significantly better than Two_Arch2, VaEA, hpaEA, and RVEA-iGNG on most test instances regarding HV and SPD. In contrast, AR-MOEA performs better than NSGA-III-AdaRSE and NSGA-III-AdaCOU on most test instances in terms of HV. However, both versions of NSGA-III-Ada \mathcal{K} outperform AR-MOEA on most MOPs in terms of SPD. Especially, results show that NSGA-III-AdaRSE and NSGA-III-AdaCOU are competitive against AR-MOEA in terms of HV and SPD on DTLZ1, DTLZ2, and WFG4 with 3 and 5 objective functions. Also, they show good performance on IMOP2. Finally, results regarding HV and SPD show that PREA performs significantly better than NSGA-III-AdaRSE and NSGA-III-AdaCOU on most test instances. However, both versions of NSGA-III-Ada \mathcal{K} significantly outperform PREA on all the cases of DTLZ1 and DTLZ2 in terms of HV.

Table 1: Mean and standard deviations (in parenthesis) of the HV indicator obtained by state-of-the-art MOEAs, NSGA-III-AdaRSE, and NSGA-III-AdaCOU on MOPs with regular PF shapes. The two best mean values per MOP are highlighted in grayscale, where the darker tone corresponds to the best one. The symbols in the tuples (+, -, =) and (\oplus , \ominus , \approx) are placed when the MOEA performs significantly better, significantly worse, or statistically equivalent to NSGA-III-AdaRSE and NSGA-III-AdaCOU, respectively, based on a one-tailed Wilcoxon test using a significance level of $\alpha = 0.05$. The superscripts are the obtained rank in the comparison.

MOP	Obj.	Gen.	Two_Arch2	VaEA	AR-MOEA	hpaEA	PREA	RVEA-iGNG	NSGA-III-AdaRSE	NSGA-III-AdaCOU
DTLZ1	3	400	7.7720e+0 ⁰ (9.04e-3) \ominus	7.6728e+0 ⁰ (1.17e-1) \ominus	7.7878e+0 ⁰ (9.01e-4) \approx	7.7890e+0 ⁰ (2.12e-3) \approx	7.7832e+0 ⁰ (1.73e-3) \oplus	7.7838e+0 ⁰ (1.76e-3) \ominus	7.7872e+0 ⁰ (1.44e-3) \oplus	7.7871e+0 ⁰ (2.19e-3)
	5	600	3.1962e+0 ¹ (8.30e-4) \ominus	3.1758e+0 ¹ (1.89e-1) \ominus	3.1967e+0 ¹ (1.10e-4) \approx	3.1970e+0 ¹ (2.71e-4) \approx	3.1967e+0 ¹ (2.41e-4) \oplus	3.1964e+0 ¹ (3.24e-3) \ominus	3.1967e+0 ¹ (1.97e-4) \oplus	3.1967e+0 ¹ (1.85e-4)
	8	750	2.5598e+0 ² (1.54e-3) \ominus	2.5535e+0 ² (8.65e-1) \ominus	2.5600e+0 ² (5.47e-5) \oplus	2.5595e+0 ² (2.19e-1) \approx	2.5599e+0 ² (2.41e-4) \oplus	2.5595e+0 ² (2.86e-2) \oplus	2.5599e+0 ² (2.93e-5) \oplus	2.5599e+0 ² (1.63e-4)
	10	1000	1.0240e+0 ³ (8.76e-4) \ominus	1.0237e+0 ³ (2.22e-1) \ominus	1.0240e+0 ³ (1.11e-5) \oplus	1.0240e+0 ³ (1.51e-4) \oplus	1.0240e+0 ³ (2.94e-4) \oplus	1.0240e+0 ³ (2.73e-2) \oplus	1.0240e+0 ³ (1.29e-5) \oplus	1.0240e+0 ³ (1.45e-5)
DTLZ2	3	250	7.4105e+0 ⁰ (1.72e-3) \ominus	7.4079e+0 ⁰ (1.92e-3) \ominus	7.4134e+0 ⁰ (1.90e-4) \approx	7.4143e+0 ⁰ (5.07e-4) \oplus	7.4106e+0 ⁰ (1.16e-3) \ominus	7.4081e+0 ⁰ (5.33e-3) \ominus	7.4134e+0 ⁰ (1.34e-4) \oplus	7.4134e+0 ⁰ (1.52e-4)
	5	350	3.1617e+0 ¹ (1.37e-2) \ominus	3.1666e+0 ¹ (3.57e-3) \ominus	3.1697e+0 ¹ (2.80e-4) \ominus	3.1702e+0 ¹ (1.17e-3) \oplus	3.1692e+0 ¹ (1.96e-3) \oplus	3.1686e+0 ¹ (3.98e-3) \ominus	3.1697e+0 ¹ (1.53e-4) \oplus	3.1697e+0 ¹ (1.44e-4)
	8	500	2.5462e+0 ² (5.50e-1) \ominus	2.5579e+0 ² (7.59e-3) \ominus	2.5584e+0 ² (8.61e-4) \oplus	2.5564e+0 ² (2.03e-1) \approx	2.5583e+0 ² (3.68e-3) \oplus	2.5582e+0 ² (8.79e-3) \oplus	2.5584e+0 ² (4.38e-4) \oplus	2.5584e+0 ² (3.13e-4)
	10	750	1.0198e+0 ³ (1.62e-0) \ominus	1.0239e+0 ³ (3.47e-3) \ominus	1.0234e+0 ³ (4.38e-1) \ominus	1.0234e+0 ³ (7.36e-3) \oplus	1.0234e+0 ³ (7.53e-3) \oplus	1.0234e+0 ³ (1.71e-1) \oplus	1.0234e+0 ³ (1.42e-4) \oplus	1.0234e+0 ³ (1.42e-4)
WFG1	3	400	5.4144e+0 ⁰ (3.36e-2) \approx	5.2681e+0 ⁰ (2.41e-2) \ominus	5.5136e+0 ⁰ (4.85e-2) \oplus	4.2230e+0 ⁰ (5.51e-1) \ominus	5.6594e+0 ⁰ (1.01e-1) \oplus	5.3980e+0 ⁰ (3.75e-2) \ominus	5.4305e+0 ⁰ (2.67e-2) \oplus	5.4225e+0 ⁰ (2.48e-2)
	5	750	2.2220e+0 ¹ (3.61e-1) \ominus	1.9266e+0 ¹ (6.52e-2) \ominus	2.1869e+0 ¹ (3.15e-1) \oplus	2.0107e+0 ¹ (9.64e-1) \oplus	2.4627e+0 ¹ (3.92e-1) \oplus	2.1216e+0 ¹ (2.54e-1) \oplus	2.0455e+0 ¹ (6.17e-2) \oplus	2.0479e+0 ¹ (5.99e-2)
	8	1500	1.9415e+0 ² (7.51e-0) \ominus	1.4596e+0 ² (1.10e-0) \ominus	1.9068e+0 ² (4.70e-0) \oplus	1.6148e+0 ² (8.02e-0) \oplus	2.2588e+0 ² (6.25e-0) \oplus	1.8761e+0 ² (6.06e-0) \oplus	1.6668e+0 ² (3.85e-0) \oplus	1.6597e+0 ² (3.24e-0)
	10	2000	9.3666e+0 ² (1.88e-1) \ominus	5.6877e+0 ² (3.92e-0) \ominus	8.5588e+0 ² (2.10e-1) \oplus	7.8047e+0 ² (3.66e-1) \oplus	9.7337e+0 ² (4.81e-0) \oplus	8.7986e+0 ² (8.42e-0) \oplus	7.5135e+0 ² (1.81e-1) \oplus	7.7138e+0 ² (2.00e-1)
WFG4	3	400	7.3668e+0 ⁰ (8.20e-3) \ominus	7.3450e+0 ⁰ (1.06e-2) \ominus	7.3695e+0 ⁰ (7.34e-3) \ominus	7.3265e+0 ⁰ (5.43e-2) \approx	7.3971e+0 ⁰ (5.22e-3) \oplus	7.3734e+0 ⁰ (6.43e-3) \oplus	7.3717e+0 ⁰ (6.14e-3) \oplus	7.3731e+0 ⁰ (6.96e-3)
	5	750	3.1432e+0 ¹ (2.50e-0) \ominus	3.1287e+0 ¹ (5.54e-1) \ominus	3.1551e+0 ¹ (4.24e-2) \oplus	3.1161e+0 ¹ (1.34e-1) \oplus	3.1690e+0 ¹ (3.07e-3) \oplus	3.1456e+0 ¹ (3.21e-2) \oplus	3.1557e+0 ¹ (2.46e-2) \oplus	3.1561e+0 ¹ (1.67e-2)
	8	1500	2.5453e+0 ² (2.25e-1) \ominus	2.5478e+0 ² (2.76e-1) \ominus	2.5545e+0 ² (9.71e-2) \oplus	2.4626e+0 ² (2.58e-0) \oplus	2.5583e+0 ² (4.30e-3) \oplus	2.5409e+0 ² (3.43e-1) \oplus	2.5541e+0 ² (9.31e-2) \oplus	2.5538e+0 ² (1.20e-1)
	10	2000	1.0207e+0 ³ (5.49e-1) \ominus	1.0204e+0 ³ (8.12e-1) \ominus	1.0231e+0 ³ (5.21e-1) \oplus	9.9956e+0 ² (5.24e-0) \oplus	1.0239e+0 ³ (2.95e-3) \oplus	1.0176e+0 ³ (3.16e-1) \oplus	1.0230e+0 ³ (2.70e-1) \oplus	1.0229e+0 ³ (2.76e-1)
IMOP1	2	500	3.9851e+0 ⁰ (3.79e-5) \oplus	3.9811e+0 ⁰ (6.39e-4) \ominus	3.9818e+0 ⁰ (5.84e-5) \oplus	3.2096e+0 ⁰ (1.07e-1) \ominus	3.9847e+0 ⁰ (6.83e-5) \oplus	3.9848e+0 ⁰ (2.02e-4) \oplus	3.9817e+0 ⁰ (7.41e-5) \oplus	3.9817e+0 ⁰ (2.94e-4)
IMOP2	2	500	2.4710e+0 ⁰ (5.33e-1) \ominus	3.0694e+0 ⁰ (1.99e-3) \oplus	2.4928e+0 ⁰ (5.13e-1) \ominus	1.9036e+0 ⁰ (1.24e-2) \ominus	3.0706e+0 ⁰ (1.17e-4) \oplus	3.0053e+0 ⁰ (2.41e-1) \ominus	3.0649e+0 ⁰ (6.12e-3) \oplus	3.0341e+0 ⁰ (1.80e-1)
+/-/-		4/14/0	1/17/0	11/2/5	4/11/3	10/8/0	4/12/2			
@/⊖/≈		4/13/1	1/17/0	11/3/4	4/12/2	10/8/0	4/12/2			

Table 2: Mean and standard deviations (in parenthesis) of the SPD indicator obtained by state-of-the-art MOEAs, NSGA-III-AdaRSE, and NSGA-III-AdaCOU on MOPs with regular PF shapes. The two best mean values per MOP are highlighted in grayscale, where the darker tone corresponds to the best one. The symbols in the tuples (+, -, =) and (\oplus , \ominus , \approx) are placed when the MOEA performs significantly better, significantly worse, or statistically equivalent to NSGA-III-AdaRSE and NSGA-III-AdaCOU, respectively, based on a one-tailed Wilcoxon test using a significance level of $\alpha = 0.05$. The superscripts are the obtained rank in the comparison.

MOP	Obj.	Gen.	Two_Arch2	VaEA	AR-MOEA	hpaEA	PREA	RVEA-iGNG	NSGA-III-AdaRSE	NSGA-III-AdaCOU
DTLZ1	3	400	2.1470e+0 ¹ (8.16e-1) \ominus	1.9635e+0 ¹ (2.42e+0) \ominus	2.3336e+0 ¹ (4.41e-2) \approx	2.3501e+0 ¹ (1.03e-1) \oplus	2.2806e+0 ¹ (1.42e-1) \ominus	2.2716e+0 ¹ (1.52e-1) \ominus	2.3370e+0 ¹ (6.90e-2) \oplus	2.3381e+0 ¹ (1.04e-1)
	5	600	5.5433e+0 ¹ (9.24e-1) \ominus	3.7463e+0 ¹ (9.32e+0) \ominus	7.2991e+0 ¹ (8.19e-2) \oplus	7.5333e+0 ¹ (2.89e-1) \oplus	6.8147e+0 ¹ (7.31e-1) \oplus	6.4870e+0 ¹ (9.43e-1) \oplus	7.3070e+0 ¹ (1.63e-1) \oplus	7.3098e+0 ¹ (1.49e-1)
	8	750	6.2834e+0 ² (2.42e+0) \ominus	4.0932e+0 ² (9.36e-0) \ominus	1.0357e+0 ² (6.62e-1) \oplus	1.2496e+0 ² (7.20e+0) \oplus	1.0674e+0 ² (2.00e+0) \oplus	9.7151e+0 ¹ (3.73e+0) \oplus	1.0866e+0 ² (2.65e-1) \oplus	1.0868e+0 ² (3.16e-1)
	10	1000	7.5486e+0 ² (3.07e-0) \ominus	7.6857e+0 ² (1.36e+1) \ominus	1.7886e+0 ² (7.89e-1) \oplus	2.1003e+0 ² (1.86e+1) \oplus	2.1189e+0 ² (7.80e+0) \oplus	1.6603e+0 ² (1.12e+1) \oplus	1.7698e+0 ² (3.16e-1) \oplus	1.7701e+0 ² (4.53e-2)
DTLZ2	3	250	3.2255e+0 ¹ (3.07e-1) \ominus	3.2255e+0 ¹ (2.04e-1) \ominus	3.2742e+0 ¹ (2.07e-2) \oplus	3.2957e+0 ¹ (6.96e-2) \oplus	3.2178e+0 ¹ (1.49e-1) \oplus	3.2178e+0 ¹ (1.85e-1) \oplus	3.2188e+0 ¹ (1.86e-3) \oplus	3.2765e+0 ¹ (6.86e-3) \oplus
	5	350	1.0835e+0 ² (1.57e-0) \ominus	1.3318e+0 ² (9.57e-1) \ominus	1.3955e+0 ² (1.24e-1) \oplus	1.5017e+0 ² (8.47e-1) \oplus	1.3148e+0 ² (8.29e-1) \oplus	1.3126e+0 ² (9.05e-1) \oplus	1.3955e+0 ² (4.25e-2) \oplus	1.3952e+0 ² (3.04e-2)
	8	500	1.3307e+0 ² (1.54e-0) \ominus	1.4435e+0 ² (9.13e-1) \ominus	1.4791e+0 ² (2.34e-1) \oplus	1.5999e+0 ² (2.62e-0) \oplus	1.4912e+0 ² (2.48e-1) \oplus	1.4926e+0 ² (4.19e-1) \oplus	1.4790e+0 ² (6.38e-2) \oplus	1.4789e+0 ² (5.34e-2)
	10	750	2.3286e+0 ² (2.61e-0) \ominus	2.3286e+0 ² (1.08e-1) \oplus	2.6059e+0 ² (3.72e-1) \oplus	2.6688e+0 ² (1.63e-1) \oplus	2.6320e+0 ² (4.10e-1) \oplus	2.6428e+0 ² (5.03e-2) \oplus	2.6058e+0 ² (3.09e-2) \oplus	2.6060e+0 ² (4.83e-2)
WFG1	3	400	1.7665e+0 ¹ (2.66e-1) \ominus	1.6128e+0 ¹ (2.67e-1) \ominus	1.7838e+0 ¹ (4.70e-1) \oplus	3.9753e+0 ¹ (2.32e+0) \oplus	3.9248e+0 ¹ (3.90e-1) \oplus	1.6597e+0 ¹ (3.90e-1) \oplus	1.6597e+0 ¹ (4.49e-1) \oplus	1.6370e+0 ¹ (3.58e-1)
	5	750	3.0194e+0 ¹ (6.82e-0) \ominus	2.5148e+0 ¹ (9.50e-1) \ominus	3.5145e+0 ¹ (6.29e-1) \oplus	1.1474e+0 ¹ (5.46e-0) \oplus	3.9571e+0 ¹ (5.52e-1) \oplus	3.0162e+0 ¹ (6.06e-0) \oplus	3.3411e+0 ¹ (6.81e-1) \oplus	3.3039e+0 ¹ (7.74e-1)
	8	1500	3.1749e+0 ² (1.11e-0) \ominus	9.2933e+0 ¹ (1.32e-0) \ominus	4.6378e+0 ¹ (1.74e-0) \oplus	1.0119e+0 ¹ (3.14e-0) \oplus	6.0675e+0 ¹ (1.09e+0) \oplus	3.4304e+0 ¹ (1.30e+0) \oplus	3.5954e+0 ¹ (2.19e+0) \oplus	4.0091e+0 ¹ (2.03e+0)
	10	2000	3.4280e+0 ² (1.15e-1) \ominus	3.7074e+0 ² (3.11e-0) \ominus	5.5142e+0 ² (1.31e-1) \oplus	1.6728e+0 ² (5.84e-0) \oplus	8.4538e+0 ² (1.39e-0) \oplus	3.8606e+0 ² (2.09e+0) \oplus	4.0868e+0 ² (2.90e+0) \oplus	4.0900e+0 ² (3.46e+0)
WFG4	3	400	3.0573e+0 ¹ (2.95e-1) \ominus	3.2301e+0 ¹ (1.73e-1) \ominus	3.2306e+0 ¹ (4.38e-2) \oplus	3.2387e+0 ¹ (1.09e-1) \oplus	3.2387e+0 ¹ (1.58e-1) \oplus	3.1709e+0 ¹ (1.61e-1) \oplus	3.2370e+0 ¹ (3.22e-2) \oplus	3.2735e+0 ¹ (2.17e-2)
	5	750	1.0929e+0 ^{2</}							

Table 3: Mean and standard deviations (in parenthesis) of the HV indicator obtained by state-of-the-art MOEAs, RVEA-AdaRSE, and RVEA-AdaCOU on MOPs with regular PF shapes. The two best mean values per MOP are highlighted in grayscale, where the darker tone corresponds to the best one. The symbols in the tuples (+, -, =) and (\oplus , \ominus , \approx) are placed when the MOEA performs significantly better, significantly worse, or statistically equivalent to RVEA-AdaRSE and RVEA-AdaCOU, respectively, based on a one-tailed Wilcoxon test using a significance level of $\alpha = 0.05$. The superscripts are the obtained rank in the comparison.

MOP	Obj.	Gen.	Two_Arch2	VaEA	AR-MOEA	hpaEA	PREA	RVEA-iGNG	RVEA-AdaRSE	RVEA-AdaCOU
DTLZ1	3	400	7.7720e+0 ⁷ (9.04e-3) \ominus	7.6728e+0 ⁷ (1.17e-1) \ominus	7.7878e+0 ⁷ (9.01e-4) \ominus	7.7890e+0 ⁷ (2.12e-3) \ominus	7.7838e+0 ⁷ (1.76e-3) \ominus	7.7880e+0 ⁷ (1.72e-3) \ominus	7.7875e+0 ⁷ (1.42e-3)	
	5	600	3.1962e+1 ⁷ (5.30e-4) \ominus	3.1758e+1 ⁷ (1.89e-1) \ominus	3.1967e+1 ⁷ (1.10e-4) \ominus	3.1970e+1 ⁷ (2.71e-1) \oplus	3.1967e+1 ⁷ (2.41e-1) \ominus	3.1964e+1 ⁷ (3.24e-3) \ominus	3.1967e+1 ⁷ (1.13e-4) \ominus	3.1967e+1 ⁷ (8.64e-5)
	8	750	2.5598e+2 ⁸ (1.54e-3) \ominus	2.5535e+2 ⁸ (6.65e-1) \ominus	2.5600e+2 ⁸ (5.47e-1) \ominus	2.5599e+2 ⁸ (2.41e-1) \ominus	2.5599e+2 ⁸ (2.86e-1) \oplus	2.5599e+2 ⁸ (4.43e-4) \ominus	2.5599e+2 ⁸ (7.34e-5) \ominus	
	10	1000	1.0240e+3 ⁸ (5.76e-4) \ominus	1.0237e+3 ⁸ (2.22e-1) \ominus	1.0240e+3 ⁸ (1.11e-5) \ominus	1.0240e+3 ⁸ (1.51e-2) \ominus	1.0240e+3 ⁸ (2.94e-4) \ominus	1.0240e+3 ⁸ (2.73e-2) \ominus	1.0240e+3 ⁸ (3.15e-5) \ominus	1.0240e+3 ⁸ (7.65e-6) \ominus
DTLZ2	3	250	7.4079e+0 ⁷ (1.72e-3) \ominus	7.4079e+0 ⁷ (1.92e-3) \ominus	7.4134e+0 ⁷ (1.90e-4) \oplus	7.4106e+0 ⁷ (1.66e-4) \ominus	7.4081e+0 ⁷ (5.53e-3) \ominus	7.4131e+0 ⁷ (2.11e-4) \ominus	7.4131e+0 ⁷ (2.03e-4) \ominus	
	5	350	3.1617e+1 ⁷ (1.37e-2) \ominus	3.1666e+1 ⁷ (3.57e-3) \ominus	3.1697e+1 ⁷ (2.80e-1) \ominus	3.1702e+1 ⁷ (1.17e-0) \ominus	3.1692e+1 ⁷ (1.96e-3) \ominus	3.1686e+1 ⁷ (3.08e-3) \ominus	3.1698e+1 ⁷ (1.04e-4) \ominus	3.1698e+1 ⁷ (1.09e-4) \ominus
	8	500	2.5579e+2 ⁸ (5.50e-1) \ominus	2.5579e+2 ⁸ (7.59e-3) \ominus	2.5584e+2 ⁸ (8.61e-4) \ominus	2.5584e+2 ⁸ (2.03e-1) \ominus	2.5583e+2 ⁸ (3.68e-3) \ominus	2.5582e+2 ⁸ (8.70e-3) \ominus	2.5584e+2 ⁸ (1.62e-4) \ominus	2.5584e+2 ⁸ (1.75e-4) \ominus
	10	750	1.0199e+3 ⁸ (7.79e+0) \ominus	1.0239e+3 ⁸ (5.58e-3) \ominus	1.0239e+3 ⁸ (4.38e-1) \ominus	1.0239e+3 ⁸ (2.17e-3) \ominus	1.0239e+3 ⁸ (5.75e-5) \ominus	1.0239e+3 ⁸ (5.75e-5) \ominus	1.0239e+3 ⁸ (5.99e-5) \ominus	
WFG1	3	400	5.4144e+0 ⁷ (3.36e-2) \oplus	5.2681e+0 ⁷ (2.41e-2) \oplus	5.5136e+0 ⁷ (4.85e-2) \oplus	4.2230e+0 ⁷ (5.51e-1) \ominus	5.1659e+0 ⁷ (1.01e-1) \ominus	5.3989e+0 ⁷ (3.75e-2) \oplus	5.2736e+0 ⁷ (3.66e-2) \oplus	5.2747e+0 ⁷ (3.66e-2) \oplus
	5	750	2.2220e+1 ⁷ (3.61e-1) \ominus	1.9266e+1 ⁷ (6.52e-2) \ominus	2.1869e+1 ⁷ (3.15e-1) \ominus	2.0127e+1 ⁷ (9.64e-1) \ominus	2.4627e+1 ⁷ (3.92e-1) \oplus	2.0866e+1 ⁷ (2.03e-1) \ominus	2.0920e+1 ⁷ (2.47e-1) \ominus	
	8	1500	1.9415e+2 ⁸ (5.71e-0) \ominus	1.4596e+2 ⁸ (1.10e+0) \ominus	1.9068e+2 ⁸ (4.70e+0) \oplus	1.6148e+2 ⁸ (8.02e+0) \oplus	2.2588e+2 ⁸ (6.25e+0) \oplus	1.8761e+2 ⁸ (6.06e+0) \oplus	1.7263e+2 ⁸ (3.73e+0) \oplus	1.7366e+2 ⁸ (4.47e+0) \oplus
	10	2000	9.3606e+2 ⁸ (1.88e+0) \ominus	3.1555e+2 ⁸ (2.10e+0) \ominus	8.5585e+2 ⁸ (2.10e+0) \oplus	7.9847e+2 ⁸ (3.66e+1) \oplus	9.7337e+2 ⁸ (4.81e+0) \oplus	7.7076e+2 ⁸ (1.99e+1) \oplus	7.8851e+2 ⁸ (1.85e+1) \oplus	
WFG4	3	400	7.3665e+0 ⁷ (8.20e-3) \oplus	7.3450e+0 ⁷ (1.06e-2) \ominus	7.3696e+0 ⁷ (7.34e-3) \oplus	7.3236e+0 ⁷ (5.43e-3) \oplus	7.3971e+0 ⁷ (5.22e-3) \oplus	7.3734e+0 ⁷ (6.43e-3) \oplus	7.3543e+0 ⁷ (1.10e-2) \oplus	7.3539e+0 ⁷ (8.42e-3) \oplus
	5	750	3.1432e+1 ⁷ (2.50e-2) \ominus	3.1287e+1 ⁷ (5.54e-2) \ominus	3.1155e+1 ⁷ (1.42e-1) \oplus	3.1116e+1 ⁷ (1.34e-1) \oplus	3.1690e+1 ⁷ (3.07e-3) \oplus	3.1456e+1 ⁷ (3.21e-2) \oplus	3.1561e+1 ⁷ (2.14e-2) \oplus	3.1557e+1 ⁷ (2.41e-2) \oplus
	8	1500	2.5453e+2 ⁸ (2.25e-1) \ominus	2.5478e+2 ⁸ (2.76e-1) \ominus	2.5545e+2 ⁸ (9.71e-2) \oplus	2.4626e+2 ⁸ (2.88e-0) \oplus	2.5583e+2 ⁸ (4.30e-3) \oplus	2.5409e+2 ⁸ (3.43e-1) \oplus	2.5534e+2 ⁸ (1.35e-1) \oplus	2.5535e+2 ⁸ (1.44e-1) \oplus
	10	2000	1.0207e+3 ⁸ (5.49e-1) \ominus	1.0231e+3 ⁸ (2.15e-1) \ominus	9.9956e+2 ⁸ (5.24e-1) \oplus	1.0239e+3 ⁸ (2.76e-3) \oplus	1.0239e+3 ⁸ (1.16e+0) \oplus	1.0176e+3 ⁸ (1.31e+0) \oplus	1.0229e+3 ⁸ (2.77e-1) \oplus	1.0230e+3 ⁸ (2.55e-1) \oplus
IMOP1	2	500	3.9851e+0 ⁷ (3.79e-5) \oplus	3.9811e+0 ⁷ (6.39e-4) \ominus	3.9818e+0 ⁷ (5.84e-5) \ominus	3.2096e+0 ⁷ (1.07e-1) \ominus	3.9847e+0 ⁷ (6.83e-3) \oplus	3.9848e+0 ⁷ (2.02e-0) \oplus	3.9823e+0 ⁷ (8.78e-4) \oplus	3.9825e+0 ⁷ (8.44e-4) \oplus
IMOP2	2	500	2.4710e+0 ⁷ (5.53e-1) \approx	3.0694e+0 ⁷ (1.99e-3) \oplus	2.4928e+0 ⁷ (5.13e-1) \approx	1.9936e+0 ⁷ (1.24e-2) \oplus	3.0705e+0 ⁷ (1.17e-1) \oplus	3.0053e+0 ⁷ (2.14e-1) \oplus	2.6820e+0 ⁷ (5.01e-1) \oplus	2.6565e+0 ⁷ (5.02e-1) \oplus
+/-/-		6/11/1	1/16/1	12/4/2	4/13/1	10/8/0	7/11/0			
$\oplus/\ominus/\approx$		6/11/1	1/16/1	11/3/4	4/13/1	10/8/0	7/11/0			

Table 4: Mean and standard deviations (in parenthesis) of the SPD indicator obtained by state-of-the-art MOEAs, RVEA-AdaRSE, and RVEA-AdaCOU on MOPs with regular PF shapes. The two best mean values per MOP are highlighted in grayscale, where the darker tone corresponds to the best one. The symbols in the tuples (+, -, =) and (\oplus , \ominus , \approx) are placed when the MOEA performs significantly better, significantly worse, or statistically equivalent to RVEA-AdaRSE and RVEA-AdaCOU, respectively, based on a one-tailed Wilcoxon test using a significance level of $\alpha = 0.05$. The superscripts are the obtained rank in the comparison.

MOP	Obj.	Gen.	Two_Arch2	VaEA	AR-MOEA	hpaEA	PREA	RVEA-iGNG	RVEA-AdaRSE	RVEA-AdaCOU	
DTLZ1	3	400	2.1479e+1 ⁷ (8.16e-1) \ominus	1.9635e+1 ⁸ (2.42e+0) \ominus	2.3336e+1 ⁴ (4.41e-2) \ominus	2.3501e+1 ¹ (1.03e-1) \oplus	2.2806e+1 ⁵ (1.42e-1) \ominus	2.2716e+1 ⁶ (1.52e-1) \ominus	2.3339e+1 ³ (7.91e-2) \ominus	2.3364e+1 ² (7.11e-2) \ominus	
	5	600	5.7433e+1 ⁷ (0.24e-1) \ominus	3.7465e+1 ⁸ (0.32e+0) \ominus	3.1551e+1 ⁸ (1.81e-2) \ominus	7.5333e+1 ⁸ (2.89e-1) \oplus	6.8147e+1 ⁵ (7.31e-1) \oplus	6.4870e+1 ⁶ (9.43e-1) \ominus	7.3008e+1 ³ (1.07e-1) \ominus	7.3008e+1 ² (7.08e-2) \ominus	
	8	750	6.2834e+1 ⁷ (2.42e+0) \ominus	4.0932e+1 ⁸ (0.36e+0) \ominus	1.0957e+2 ² (6.62e-1) \oplus	1.2495e+2 ² (7.20e+0) \oplus	1.0674e+2 ⁵ (2.00e+0) \oplus	9.7915e+1 ⁶ (3.73e+0) \oplus	1.0803e+2 ⁴ (4.70e-1) \oplus	1.0824e+2 ² (2.05e-1) \oplus	
	10	1000	7.5486e+1 ⁷ (3.07e+0) \ominus	7.6857e+1 ⁷ (1.36e+0) \ominus	1.7886e+2 ² (7.89e-1) \oplus	2.1003e+2 ² (1.86e+1) \oplus	2.1189e+2 ² (7.80e+0) \oplus	1.6603e+2 ⁶ (1.12e+1) \oplus	1.7636e+2 ⁵ (4.77e-1) \oplus	1.7656e+2 ⁴ (2.27e-1) \oplus	
DTLZ2	3	250	3.0573e+0 ⁷ (3.07e-1) \ominus	3.2255e+0 ⁷ (2.04e-1) \oplus	3.2742e+0 ⁷ (2.07e-2) \ominus	3.2187e+0 ⁷ (6.96e-2) \oplus	3.2187e+0 ⁷ (1.49e-1) \ominus	3.2187e+0 ⁷ (1.85e-2) \oplus	3.2769e+0 ⁷ (1.85e-2) \oplus	3.2775e+0 ⁷ (7.22e-3) \oplus	
	5	350	1.8356e+2 ⁸ (1.57e-0) \ominus	1.3318e+2 ⁸ (0.57e-1) \ominus	1.3955e+2 ⁸ (1.24e-1) \oplus	1.5017e+2 ⁸ (4.87e-1) \oplus	1.3814e+2 ⁸ (8.29e-1) \oplus	1.3949e+2 ⁸ (9.05e-1) \oplus	1.3954e+2 ⁸ (2.81e-1) \oplus	1.3954e+2 ⁸ (2.51e-2) \oplus	
	8	500	1.3307e+2 ⁸ (1.54e-0) \ominus	1.4435e+2 ⁸ (9.13e-1) \ominus	1.4791e+2 ⁸ (2.34e-1) \oplus	1.5999e+2 ⁸ (6.22e+0) \oplus	1.4912e+2 ⁸ (2.48e-1) \oplus	1.4926e+2 ⁸ (4.19e-1) \oplus	1.4786e+2 ⁸ (2.81e-2) \oplus	1.4786e+2 ⁸ (2.78e-2) \oplus	
	10	750	2.3286e+2 ⁸ (2.61e-0) \ominus	3.0740e+1 ⁰ (1.31e-0) \oplus	2.6059e+2 ⁸ (3.72e-1) \oplus	2.6686e+2 ⁸ (1.63e+1) \oplus	2.6329e+2 ⁸ (4.10e-1) \oplus	2.6428e+2 ⁸ (5.03e-1) \oplus	2.6044e+2 ⁸ (2.29e-1) \oplus	2.6051e+2 ⁸ (1.22e-1) \oplus	
WFG1	3	400	1.7665e+1 ⁷ (2.66e-1) \oplus	1.6128e+1 ⁸ (2.67e-1) \ominus	1.7835e+1 ² (4.79e-2) \oplus	3.9751e+0 ⁸ (2.32e+0) \oplus	1.9248e+1 ⁷ (1.92e-1) \oplus	1.6997e+1 ⁴ (3.99e-1) \oplus	1.5657e+1 ⁶ (1.03e+0) \oplus	1.5112e+1 ⁷ (1.21e+0) \oplus	
	5	750	1.0929e+2 ⁸ (1.34e-1) \oplus	1.3892e+2 ⁸ (2.74e-1) \ominus	1.2892e+2 ⁸ (7.92e-0) \oplus	1.3314e+2 ⁸ (7.88e-1) \oplus	1.3216e+2 ⁸ (7.51e-1) \oplus	1.3910e+2 ⁸ (8.59e-2) \oplus	1.3912e+2 ⁸ (8.60e-2) \oplus		
	8	1500	1.3121e+2 ⁸ (1.42e-0) \oplus	1.4490e+2 ⁸ (1.34e-0) \oplus	1.4775e+2 ⁸ (9.59e-2) \oplus	1.1103e+2 ⁸ (7.35e-0) \oplus	1.4481e+2 ⁸ (2.86e-1) \oplus	1.4447e+2 ⁸ (6.61e-1) \oplus	1.4737e+2 ⁸ (2.75e-1) \oplus	1.4743e+2 ⁸ (1.99e-1) \oplus	
	10	2000	2.2728e+2 ⁸ (2.38e+0) \oplus	2.5553e+2 ⁸ (1.94e+0) \oplus	2.6038e+2 ⁸ (1.81e-1) \oplus	1.7550e+2 ⁸ (1.61e+0) \oplus	2.6269e+2 ⁸ (3.80e-1) \oplus	2.5502e+2 ⁸ (8.83e-1) \oplus	2.5586e+2 ⁸ (6.76e-1) \oplus	2.5831e+2 ⁸ (8.10e-1) \oplus	
IMOP1	2	500	9.6251e+0 ² (1.12e-1) \oplus	5.4188e+0 ⁷ (1.45e-1) \approx	8.8110e+0 ⁸ (6.62e-1) \oplus	5.6638e+0 ⁸ (2.35e+0) \approx	2.0068e+0 ⁸ (3.12e-1) \oplus	9.0896e+0 ⁸ (6.13e-1) \oplus	6.9588e+0 ⁸ (4.95e-1) \oplus	5.7022e+0 ⁸ (6.77e-1) \oplus	5.6497e+0 ⁸ (6.60e-1) \oplus
IMOP2	2	500	4.9156e+0								

Table 5: Mean and standard deviations (in parenthesis) of the HV indicator obtained by state-of-the-art MOEAs, MOEA/D-AdaRSE, and MOEA/D-AdaCOU on MOPs with regular PF shapes. The two best mean values per MOP are highlighted in grayscale, where the darker tone corresponds to the best one. The symbols in the tuples (+, −, =) and (\oplus , \ominus , \approx) are placed when the MOEA performs significantly better, significantly worse, or statistically equivalent to MOEA/D-AdaRSE and MOEA/D-AdaCOU, respectively, based on a one-tailed Wilcoxon test using a significance level of $\alpha = 0.05$. The superscripts are the obtained rank in the comparison.

MOP	Obj.	Gen.	Two_Arch2	VaEA	AR-MOEA	hpEA	PREA	RVEA-IGNG	MOEA/D-AdaRSE	MOEA/D-AdaCOU
DTLZ1	3	400	7.7786e+0 ² (6.18e-3) \ominus	7.6850e+0 ² (9.38e-2) \ominus	7.7866e+0 ² (2.75e-3) \approx	7.7892e+0 ² (2.21e-3) \approx	7.7832e+0 ² (1.78e-3) \oplus	7.7841e+0 ² (1.50e-3) \ominus	7.7870e+0 ² (1.27e-3) \approx	7.7873e+0 ² (9.42e-4) \approx
	5	600	3.1962e+1 ² (6.13e-4) \ominus	3.1751e+1 ² (1.45e-1) \ominus	3.1967e+1 ² (1.59e-4) \ominus	3.1970e+1 ² (2.80e-4) \ominus	3.1967e+1 ² (2.66e-4) \oplus	3.1965e+1 ² (1.15e-3) \approx	3.1964e+1 ² (9.88e-3) \ominus	3.1963e+1 ² (9.57e-3) \approx
	8	750	2.5598e+2 ² (1.35e-3) \ominus	2.5202e+2 ² (1.37e-1) \ominus	2.5600e+2 ² (8.38e-3) \oplus	2.5576e+2 ² (1.21e+0) \oplus	2.5596e+2 ² (2.79e-4) \oplus	2.5596e+2 ² (2.37e-2) \oplus	2.5596e+2 ² (5.14e-2) \oplus	2.5596e+2 ² (8.21e-2) \oplus
	10	1000	1.0240e+3 ² (7.68e-4) \oplus	1.0236e+3 ² (2.90e-1) \oplus	1.0240e+3 ² (1.38e-5) \oplus	1.0240e+3 ² (4.12e-1) \oplus	1.0240e+3 ² (2.47e-4) \oplus	1.0240e+3 ² (7.61e-3) \oplus	1.0239e+3 ² (5.86e-2) \oplus	1.0238e+3 ² (1.99e-1) \oplus
DTLZ2	3	250	7.4098e+0 ² (1.74e-3) \ominus	7.4074e+0 ² (1.50e-3) \ominus	7.4133e+0 ² (1.97e-4) \approx	7.4142e+0 ² (4.96e-4) \oplus	7.4095e+0 ² (1.18e-3) \ominus	7.4068e+0 ² (5.62e-3) \ominus	7.4134e+0 ² (1.94e-3) \oplus	7.4133e+0 ² (1.80e-4) \oplus
	5	350	3.1610e+1 ² (2.47e-2) \ominus	3.1663e+1 ² (3.64e-3) \ominus	3.1697e+1 ² (3.11e-4) \ominus	3.1701e+1 ² (1.21e-3) \ominus	3.1691e+1 ² (1.52e-3) \oplus	3.1682e+1 ² (4.93e-3) \ominus	3.1697e+1 ² (1.08e-3) \ominus	3.1694e+1 ² (1.69e-2) \approx
	8	500	2.5439e+2 ² (7.43e-1) \ominus	2.5579e+2 ² (6.81e-3) \ominus	2.5584e+2 ² (8.70e-4) \oplus	2.5572e+2 ² (1.49e-1) \oplus	2.5583e+2 ² (3.49e-3) \oplus	2.5582e+2 ² (8.46e-2) \oplus	2.5579e+2 ² (8.46e-2) \oplus	2.5581e+2 ² (1.10e-1) \oplus
	10	750	1.0199e+3 ² (2.73e-1) \ominus	1.0238e+3 ² (2.90e-1) \ominus	1.0234e+3 ² (5.24e-1) \ominus	1.0234e+3 ² (7.03e-1) \ominus	1.0239e+3 ² (2.56e-1) \oplus	1.0239e+3 ² (8.05e-2) \oplus	1.0239e+3 ² (3.17e-1) \oplus	1.0239e+3 ² (7.86e-2) \oplus
WFG1	3	400	5.4103e+0 ² (3.23e-2) \oplus	5.2478e+0 ² (2.13e-2) \ominus	5.4952e+0 ² (2.59e-2) \ominus	4.3533e+0 ² (5.90e-1) \ominus	5.6339e+0 ² (5.27e-2) \oplus	5.3799e+0 ² (2.89e-2) \ominus	5.0138e+0 ² (6.20e-2) \ominus	5.5946e+0 ² (5.70e-2) \oplus
	5	750	2.1816e+1 ² (2.71e-1) \ominus	1.9104e+1 ² (0.08e-2) \ominus	2.1607e+1 ² (2.84e-1) \ominus	1.9861e+1 ² (8.68e-1) \ominus	2.4503e+1 ² (4.11e-1) \oplus	2.0292e+1 ² (1.45e-1) \oplus	2.7081e+1 ² (6.80e-1) \oplus	2.6684e+1 ² (7.63e-1) \oplus
	8	1500	1.9331e+2 ² (3.94e+0) \oplus	1.4477e+2 ² (1.07e+0) \oplus	1.9022e+2 ² (4.65e+0) \oplus	1.6227e+2 ² (7.71e+0) \oplus	2.3143e+2 ² (4.14e+0) \oplus	1.8277e+2 ² (3.87e+0) \oplus	2.0373e+2 ² (6.18e+0) \oplus	2.0549e+2 ² (6.12e+0) \oplus
	10	2000	9.3207e+2 ² (1.73e+1) \oplus	5.6695e+2 ² (4.18e+0) \oplus	8.4289e+2 ² (2.11e+1) \oplus	6.9151e+2 ² (3.23e+1) \oplus	9.7425e+2 ² (8.96e-7) \oplus	8.4710e+2 ² (1.09e+1) \oplus	9.6527e+2 ² (1.37e+1) \oplus	9.5269e+2 ² (2.25e+1) \oplus
WFG4	3	400	7.3609e+0 ² (1.04e-2) \ominus	7.3295e+0 ² (1.06e-2) \ominus	7.3573e+0 ² (1.02e-2) \ominus	7.2768e+0 ² (8.52e-2) \ominus	7.3921e+0 ² (5.25e-2) \oplus	7.3624e+0 ² (6.57e-3) \ominus	7.3813e+0 ² (6.13e-3) \oplus	7.3821e+0 ² (6.02e-3) \oplus
	5	750	3.1360e+1 ² (2.99e-2) \ominus	3.1182e+1 ² (5.61e-2) \ominus	3.1472e+1 ² (2.47e-2) \oplus	3.1107e+1 ² (1.07e-1) \oplus	3.1687e+1 ² (2.54e-3) \oplus	3.1397e+1 ² (3.22e-2) \oplus	3.1627e+1 ² (1.74e-2) \oplus	3.1631e+1 ² (1.33e-2) \oplus
	8	1500	2.5410e+2 ² (2.92e-1) \ominus	2.5431e+2 ² (3.63e-1) \ominus	2.5515e+2 ² (1.48e-1) \oplus	2.4576e+2 ² (4.20e+0) \oplus	2.5583e+2 ² (5.75e-2) \oplus	2.5553e+2 ² (2.79e-1) \oplus	2.5554e+2 ² (8.23e-2) \oplus	2.5554e+2 ² (8.23e-2) \oplus
	10	2000	1.0196e+3 ² (5.91e-1) \ominus	1.0189e+3 ² (9.42e-1) \ominus	1.0221e+3 ² (4.19e-1) \oplus	9.9582e+2 ² (7.03e-0) \oplus	1.0239e+3 ² (3.89e-3) \oplus	1.0161e+3 ² (1.26e-1) \oplus	1.0234e+3 ² (2.06e-1) \oplus	1.0233e+3 ² (1.89e-1) \oplus
IMOP1	2	500	3.9851e+0 ¹ (3.64e-5) \oplus	3.9807e+0 ¹ (6.42e-4) \ominus	3.9818e+0 ¹ (6.72e-5) \approx	3.2669e+0 ¹ (1.20e-1) \ominus	3.9847e+0 ¹ (8.51e-5) \oplus	3.9849e+0 ¹ (1.33e-4) \oplus	3.9817e+0 ¹ (1.97e-3) \oplus	3.9815e+0 ¹ (3.24e-3) \oplus
IMOP2	2	500	2.5012e+0 ² (5.41e-1) \oplus	3.0699e+0 ² (1.14e-3) \oplus	2.7909e+0 ² (4.60e-1) \oplus	1.9962e+0 ² (9.23e-3) \oplus	3.0705e+0 ² (1.18e-4) \oplus	3.0311e+0 ² (1.92e-1) \oplus	2.0154e+0 ² (7.24e-2) \oplus	2.0502e+0 ² (2.08e-1) \oplus
+/-/-		4/14/0	1/16/1	6/8/4	5/11/2	12/4/2	3/11/4			
@/⊖/≈		3/14/1	1/17/0	6/8/4	5/11/2	12/4/2	3/11/4			

Table 6: Mean and standard deviations (in parenthesis) of the SPD indicator obtained by state-of-the-art MOEAs, MOEA/D-AdaRSE, and MOEA/D-AdaCOU on MOPs with regular PF shapes. The two best mean values per MOP are highlighted in grayscale, where the darker tone corresponds to the best one. The symbols in the tuples (+, −, =) and (\oplus , \ominus , \approx) are placed when the MOEA performs significantly better, significantly worse, or statistically equivalent to MOEA/D-AdaRSE and MOEA/D-AdaCOU, respectively, based on a one-tailed Wilcoxon test using a significance level of $\alpha = 0.05$. The superscripts are the obtained rank in the comparison.

MOP	Obj.	Gen.	Two_Arch2	VaEA	AR-MOEA	hpEA	PREA	RVEA-IGNG	MOEA/D-AdaRSE	MOEA/D-AdaCOU
DTLZ1	3	400	2.1932e+1 ² (6.56e-1) \ominus	1.9867e+1 ² (1.90e+0) \ominus	2.3390e+1 ² (1.35e-1) \oplus	2.3506e+1 ² (1.06e-1) \oplus	2.2750e+1 ² (1.08e-1) \ominus	2.2724e+1 ² (2.68e-1) \ominus	2.3294e+1 ² (5.13e-2) \ominus	2.3279e+1 ² (6.11e-2) \oplus
	5	600	5.5742e+1 ² (7.56e-1) \ominus	3.5077e+1 ² (9.48e+0) \ominus	7.2986e+1 ² (1.59e-1) \ominus	7.5289e+1 ² (2.75e-1) \ominus	6.8051e+1 ² (4.85e-1) \oplus	6.4296e+1 ² (7.24e-1) \oplus	7.2329e+1 ² (2.07e+0) \oplus	7.2023e+1 ² (2.11e+0) \oplus
	8	750	6.4167e+1 ² (1.18e-1) \ominus	4.5846e+1 ² (1.89e-1) \ominus	1.0963e+2 ² (4.63e-1) \oplus	1.3016e+2 ² (1.52e+1) \oplus	1.0713e+2 ² (2.48e-0) \oplus	9.7370e+1 ² (1.07e+0) \oplus	9.7578e+1 ² (1.16e+1) \oplus	1.0020e+2 ² (1.37e+1) \oplus
	10	1000	7.6721e+1 ² (2.69e+0) \oplus	7.8061e+1 ² (1.60e+1) \oplus	2.1735e+2 ² (3.56e+1) \oplus	2.1693e+2 ² (6.04e+0) \oplus	1.6297e+2 ² (1.19e+1) \oplus	1.6000e+2 ² (1.57e+1) \oplus	1.3944e+2 ² (3.43e+1) \oplus	
DTLZ2	3	250	3.0488e+1 ² (1.53e-1) \ominus	3.2753e+1 ² (1.03e-2) \oplus	3.2961e+1 ² (6.49e-2) \oplus	3.2326e+1 ² (2.05e-1) \oplus	3.2157e+1 ² (1.58e-1) \oplus	3.2621e+1 ² (2.84e-2) \oplus	3.2632e+1 ² (3.50e-2) \oplus	
	5	350	1.0897e+2 ² (1.27e+0) \oplus	1.3285e+2 ² (9.25e-2) \oplus	1.5022e+2 ² (1.03e-0) \oplus	1.3149e+2 ² (8.08e-1) \oplus	1.3207e+2 ² (1.09e+0) \oplus	1.3698e+2 ² (2.85e+0) \oplus	1.3642e+2 ² (5.21e+0) \oplus	
	8	500	1.3358e+2 ² (1.52e+0) \ominus	1.4452e+2 ² (1.25e+0) \oplus	1.4785e+2 ² (2.39e-1) \oplus	1.6431e+2 ² (5.32e+0) \oplus	1.4895e+2 ² (2.59e-1) \oplus	1.4925e+2 ² (5.80e-1) \oplus	1.3777e+2 ² (8.07e+0) \oplus	1.4090e+2 ² (8.17e+0) \oplus
	10	750	2.3320e+2 ² (2.55e+0) \oplus	2.5815e+2 ² (8.97e-1) \oplus	2.6047e+2 ² (3.14e-1) \oplus	2.7041e+2 ² (1.44e+1) \oplus	2.6323e+2 ² (3.14e-1) \oplus	2.6148e+2 ² (4.34e-1) \oplus	2.5266e+2 ² (1.09e+1) \oplus	2.4989e+2 ² (1.57e+1) \oplus
WFG1	3	400	1.7644e+1 ² (1.80e-1) \oplus	1.6117e+1 ² (5.00e-1) \oplus	1.7783e+1 ² (5.36e-1) \oplus	1.5924e+1 ² (3.46e-0) \oplus	1.6998e+1 ² (5.10e-1) \oplus	1.4545e+1 ² (1.09e+0) \oplus	1.4654e+1 ² (6.99e-1) \oplus	
	5	750	3.0379e+1 ² (5.66e-1) \ominus	2.5527e+1 ² (8.54e-1) \ominus	3.4768e+1 ² (8.17e-1) \ominus	1.3267e+1 ² (6.80e-0) \ominus	3.9515e+1 ² (5.80e-1) \oplus	3.0004e+1 ² (4.83e-1) \oplus	2.5187e+1 ² (3.73e+0) \oplus	2.6043e+1 ² (3.67e+0) \oplus
	8	1500	3.1804e+1 ² (1.11e+0) \oplus	2.9583e+1 ² (1.04e+0) \oplus	4.5580e+1 ² (2.04e+0) \oplus	1.2093e+1 ² (4.31e+0) \oplus	6.0261e+1 ² (1.40e+0) \oplus	3.4153e+1 ² (1.39e+0) \oplus	3.6753e+1 ² (3.16e+0) \oplus	3.1608e+1 ² (3.17e+0) \oplus
	10	2000	3.4049e+1 ² (1.20e+0) \oplus	3.6924e+1 ² (1.25e+0) \oplus	3.5760e+1 ² (2.88e+0) \oplus	2.1157e+1 ² (5.06e-0) \oplus	8.4791e+1 ² (1.24e+0) \oplus	3.8408e+1 ² (1.60e+0) \oplus	3.3673e+1 ² (8.17e+0) \oplus	3.5697e+1 ² (8.66e+0) \oplus
WFG4	3	400	3.0567e+1 ² (2.77e-1) \ominus	3.2330e+1 ² (2.30e-1) \oplus	3.2612e+1 ² (4.65e-2) \oplus	3.1884e+1 ² (1.32e-1) \oplus	3.2304e+1 ² (1.50e-1) \oplus	3.1680e+1 ² (1.71e-1) \oplus	3.2228e+1 ² (2.98e-1)	

Table 7: Mean and standard deviations (in parenthesis) of the HV indicator obtained by state-of-the-art MOEAs, NSGA-III-AdaRSE, and NSGA-III-AdaCOU on MOPs with irregular PF shapes. The two best mean values per MOP are highlighted in grayscale, where the darker tone corresponds to the best one. The symbols in the tuples (+, -, =) and (\oplus , \ominus , \approx) are placed when the MOEA performs significantly better, significantly worse, or statistically equivalent to NSGA-III-AdaRSE and NSGA-III-AdaCOU, respectively, based on a one-tailed Wilcoxon test using a significance level of $\alpha = 0.05$. The superscripts are the obtained rank in the comparison.

MOP	Obj.	Gen.	Two_Arch2	VaEA	AR-MOEA	hpaEA	PREA	RVEA-iGNG	NSGA-III-AdaRSE	NSGA-III-AdaCOU
DTLZ5	3	400	5.5131e+0 ³ (3.90e-4) \oplus	5.5095e+0 ³ (5.54e-4) \oplus	5.5101e+0 ⁴ (5.23e-4) \ominus	5.5101e+0 ⁴ (6.15e-4) \oplus	5.5120e+0 ³ (3.75e-4) \oplus	5.5074e+0 ⁷ (8.57e-3) \oplus	5.5060e+0 ⁸ (1.66e-2)	
	5	600	3.1306e+1 ³ (5.76e-3) \oplus	3.1255e+1 ³ (1.69e-2) \oplus	3.1294e+1 ² (6.25e-3) \oplus	3.1140e+1 ⁶ (2.54e-2) \oplus	3.1282e+1 ³ (8.89e-3) \oplus	3.1080e+1 ⁷ (1.68e-1) \oplus	3.0881e+1 ⁸ (1.76e-1) \oplus	3.1143e+1 ⁵ (8.07e-2)
	8	750	2.5017e+2 ³ (7.73e-2) \oplus	2.4901e+2 ³ (2.89e-1) \oplus	2.4953e+2 ³ (1.29e-1) \oplus	2.4789e+2 ³ (7.24e-1) \oplus	2.4985e+2 ³ (2.23e-1) \oplus	2.4610e+2 ⁷ (2.04e+0) \oplus	2.4499e+2 ⁸ (2.03e+0) \oplus	2.4789e+2 ⁶ (8.97e-1)
	10	1000	1.0011e+3 ³ (3.42e-1) \oplus	9.9144e+2 ³ (1.44e+0) \oplus	9.9858e+2 ³ (4.34e-1) \oplus	9.9131e+2 ⁹ (3.35e+0) \oplus	9.9892e+2 ² (4.87e-1) \oplus	9.8645e+2 ⁹ (9.04e+0) \oplus	9.8255e+2 ⁹ (7.33e+0) \oplus	9.9683e+2 ⁴ (2.82e+0)
DTLZ7	3	1000	6.4304e+0 ³ (3.31e-1) \ominus	6.5191e+0 ³ (3.01e-1) \ominus	6.3754e+0 ⁶ (4.30e-1) \oplus	6.1821e+0 ⁸ (3.48e-1) \oplus	6.2538e+0 ⁷ (4.63e-1) \oplus	6.3787e+0 ⁷ (4.33e-1) \oplus	6.4453e+0 ¹ (2.11e-1) \oplus	6.5438e+0 ² (2.11e-1) \oplus
	5	1000	2.4098e+1 ⁷ (1.92e-1) \ominus	2.4973e+1 ⁶ (8.94e-1) \ominus	2.5471e+1 ⁶ (3.91e-1) \oplus	2.4093e+1 ⁸ (5.91e-1) \oplus	2.5251e+1 ³ (3.95e-1) \oplus	2.5479e+1 ¹ (2.41e-1) \oplus	2.5224e+1 ⁴ (7.79e-2) \oplus	2.5210e+1 ⁵ (1.11e-1) \oplus
	8	1000	1.7443e+2 ⁸ (1.48e-1) \ominus	1.8215e+2 ⁹ (7.96e-1) \ominus	1.7755e+2 ⁷ (7.96e-1) \oplus	1.8305e+2 ⁸ (8.27e-1) \oplus	1.8707e+2 ² (7.00e-1) \oplus	1.8891e+2 ¹ (1.85e+0) \oplus	1.8639e+2 ⁹ (4.94e-1) \oplus	1.8578e+2 ⁴ (2.70e-1) \oplus
	10	1500	6.6098e+2 ⁸ (3.14e+0) \ominus	7.0568e+2 ⁹ (5.01e+0) \ominus	6.5553e+2 ⁹ (5.01e+0) \oplus	7.0247e+2 ⁹ (2.53e+0) \oplus	7.3945e+2 ⁹ (6.75e-1) \oplus	7.3781e+2 ² (3.93e+0) \oplus	7.1469e+2 ⁹ (3.45e+0) \oplus	7.1991e+2 ³ (1.29e+0) \oplus
	20	2000	7.8377e+0 ⁷ (2.19e-2) \oplus	8.7423e+0 ⁷ (1.47e-2) \oplus	7.9648e+0 ⁷ (2.24e-2) \oplus	7.8153e+0 ⁸ (2.66e-2) \oplus	7.9825e+0 ⁷ (7.44e-3) \oplus	7.8412e+0 ⁷ (3.67e-2) \oplus	7.8653e+0 ² (8.79e-3) \oplus	7.8596e+0 ⁴ (1.48e-2) \oplus
WFG2	5	750	3.1918e+1 ³ (1.99e-2) \ominus	3.1811e+1 ⁷ (2.82e-2) \ominus	3.1930e+1 ² (1.93e-1) \oplus	3.1806e+1 ⁸ (3.09e-2) \oplus	3.1982e+1 ⁶ (6.24e-3) \oplus	3.1882e+1 ⁶ (4.21e-2) \oplus	3.1901e+1 ⁹ (1.74e-2) \oplus	3.1906e+1 ⁴ (1.41e-2) \oplus
	8	1500	2.5567e+2 ⁸ (1.14e-1) \ominus	2.5517e+2 ⁷ (2.19e-1) \ominus	2.5570e+2 ⁹ (1.21e-1) \oplus	2.5400e+2 ⁸ (2.37e-1) \oplus	2.5592e+2 ² (3.82e-2) \oplus	2.5571e+2 ⁰ (1.15e-1) \oplus	2.5561e+2 ⁹ (9.63e-2) \oplus	2.5561e+2 ⁴ (9.63e-2) \oplus
	10	2000	1.0219e+3 ³ (5.52e-1) \ominus	1.0235e+3 ³ (5.72e-1) \ominus	1.0213e+3 ³ (5.83e-1) \oplus	1.0240e+3 ³ (3.15e-1) \oplus	1.0240e+3 ³ (3.15e-1) \oplus	1.0224e+3 ³ (4.57e-1) \oplus	1.0232e+3 ³ (2.93e-1) \oplus	1.0233e+3 ³ (2.54e-1) \oplus
	20	3000	7.0549e+0 ² (1.86e-2) \oplus	6.9987e+0 ⁷ (1.81e-2) \oplus	7.0065e+0 ⁶ (1.95e-2) \oplus	6.8544e+0 ⁸ (1.04e-1) \oplus	7.0458e+0 ⁶ (9.51e-3) \oplus	7.0174e+0 ⁷ (1.56e-2) \oplus	7.0054e+0 ⁶ (2.31e-2) \oplus	7.0154e+0 ⁴ (1.98e-2) \oplus
WFG3	5	750	2.9039e+1 ² (7.54e-2) \ominus	2.8433e+1 ⁷ (1.45e-1) \ominus	2.8595e+1 ⁴ (1.40e-1) \oplus	2.7863e+1 ⁸ (4.12e-1) \oplus	2.9184e+1 ¹¹ (8.29e-1) \oplus	2.9490e+1 ¹⁰ (0.95e-2) \oplus	2.8867e+1 ¹³ (0.95e-2) \oplus	2.8900e+1 ¹⁰ (1.01e-1) \oplus
	8	1500	2.3280e+2 ⁸ (7.57e-2) \ominus	2.3203e+2 ⁹ (1.16e+0) \ominus	2.1984e+2 ⁷ (2.95e-0) \oplus	2.1943e+2 ⁸ (6.15e+0) \oplus	2.3307e+2 ¹ (1.15e+0) \oplus	2.3162e+2 ⁵ (1.22e+0) \oplus	2.2526e+2 ⁶ (1.66e+0) \oplus	2.3236e+2 ³ (1.04e+0) \oplus
	10	2000	9.3930e+2 ⁸ (2.06e+0) \ominus	9.3693e+2 ⁹ (2.37e+0) \ominus	8.5941e+2 ⁹ (2.17e+1) \oplus	8.6001e+2 ⁹ (2.98e+1) \oplus	9.3604e+2 ⁹ (3.54e+0) \oplus	9.3625e+2 ⁹ (2.41e+0) \oplus	9.1245e+2 ⁹ (6.46e+0) \oplus	9.4403e+2 ² (2.74e+0) \oplus
	20	3000	5.4526e+0 ² (7.73e-3) \oplus	5.4328e+0 ⁷ (1.65e-2) \oplus	5.4482e+0 ⁶ (5.91e-3) \oplus	5.2238e+0 ⁸ (8.20e-2) \oplus	5.4821e+0 ⁷ (4.57e-3) \oplus	5.5049e+0 ³ (3.21e-3) \oplus	5.5049e+0 ² (2.46e-3) \oplus	
DTLZ1-1	5	600	1.0125e+1 ⁵ (5.68e-2) \ominus	1.0668e+1 ⁵ (5.11e-2) \ominus	1.0549e+1 ⁶ (9.29e-2) \oplus	1.0278e+1 ⁷ (1.32e-1) \oplus	1.0937e+1 ² (3.57e-2) \oplus	1.0699e+1 ⁴ (5.26e-2) \oplus	1.0960e+1 ³ (4.90e-2) \oplus	1.1274e+1 ¹ (1.87e-2) \oplus
	8	750	1.5439e+1 ² (2.81e-1) \ominus	1.9527e+1 ⁴ (1.42e-1) \ominus	1.8538e+1 ⁵ (2.35e-1) \oplus	1.6905e+1 ⁵ (5.47e-1) \oplus	2.0092e+1 ² (1.67e-1) \oplus	1.2263e+1 ³ (1.21e+0) \oplus	2.0239e+1 ² (2.19e-1) \oplus	2.0364e+1 ⁴ (4.94e-2) \oplus
	10	1000	1.5901e+1 ⁷ (3.19e-1) \ominus	2.7743e+1 ⁶ (3.85e-1) \ominus	2.4852e+1 ⁶ (6.59e-1) \oplus	2.8493e+1 ⁶ (9.51e-1) \oplus	9.3634e+2 ⁹ (2.41e+0) \oplus	9.3625e+2 ⁹ (6.46e-1) \oplus	9.1245e+2 ⁹ (6.46e-1) \oplus	9.4403e+2 ² (2.74e+0) \oplus
	20	2000	6.6037e+0 ² (6.89e-3) \oplus	6.6108e+0 ⁷ (3.72e-2) \oplus	6.6558e+0 ⁶ (2.94e-3) \oplus	6.5637e+0 ⁸ (3.73e-2) \oplus	6.6899e+0 ⁴ (6.51e-3) \oplus	6.6575e+0 ⁷ (6.89e-3) \oplus	6.7162e+0 ¹ (2.09e-3) \oplus	6.7128e+0 ² (3.33e-3) \oplus
DTLZ2-1	5	350	1.7363e+1 ⁴ (6.03e-2) \ominus	1.6899e+1 ⁸ (9.69e-2) \ominus	1.6959e+5 ⁵ (8.52e-2) \oplus	1.6940e+1 ⁵ (5.47e-1) \oplus	2.0092e+1 ² (1.67e-1) \oplus	1.6981e+1 ⁶ (8.65e-2) \oplus	1.9060e+1 ³ (4.90e-2) \oplus	1.1274e+1 ¹ (1.87e-2) \oplus
	8	500	4.0478e+1 ² (4.40e-1) \ominus	4.2256e+1 ⁴ (4.42e-1) \ominus	3.8907e+1 ⁵ (5.32e-1) \oplus	4.2700e+1 ³ (4.89e-1) \oplus	5.4526e+1 ⁶ (3.63e-1) \oplus	4.2025e+1 ⁵ (8.74e-1) \oplus	4.1104e+1 ⁶ (7.17e-1) \oplus	3.9000e+1 ⁷ (4.18e-1) \oplus
	10	750	7.9799e+1 ⁴ (1.13e+0) \ominus	7.8092e+1 ⁴ (6.58e-1) \ominus	7.1161e+1 ⁷ (1.65e+0) \oplus	7.8493e+1 ³ (9.51e-1) \oplus	8.3897e+1 ² (6.86e-1) \oplus	7.5936e+1 ⁵ (2.17e+0) \oplus	7.2094e+1 ⁶ (1.13e+0) \oplus	6.4514e+1 ⁸ (5.20e-1) \oplus
	20	2000	7.2417e+0 ² (6.21e-3) \oplus	7.2240e+0 ⁷ (1.61e-2) \oplus	7.1928e+0 ⁶ (2.04e-1) \oplus	6.7645e+0 ⁸ (2.49e-1) \oplus	7.1331e+0 ⁷ (4.07e-1) \oplus	7.2384e+0 ⁷ (1.75e-1) \oplus	7.2941e+0 ⁹ (4.51e-3) \oplus	7.6770e+0 ² (7.66e-3) \oplus
DTLZ5-1	5	600	1.8475e+1 ⁵ (4.62e-2) \ominus	1.8210e+1 ⁵ (7.63e-2) \ominus	1.7863e+1 ⁵ (1.72e-2) \oplus	1.8035e+1 ⁶ (1.10e-1) \oplus	1.8633e+1 ² (4.21e-2) \oplus	1.8024e+1 ⁷ (1.65e-1) \oplus	1.8526e+1 ⁶ (7.86e-2) \oplus	1.8807e+1 ³ (3.56e-2) \oplus
	8	750	5.3665e+1 ⁴ (4.78e-1) \ominus	5.4749e+1 ⁴ (4.38e-1) \ominus	5.0917e+1 ⁶ (8.40e-1) \oplus	5.1001e+1 ⁷ (1.65e-1) \oplus	5.6641e+1 ¹ (4.44e-1) \oplus	5.1300e+1 ⁹ (8.77e-1) \oplus	5.3639e+1 ⁹ (5.85e-1) \oplus	5.4995e+1 ² (2.95e-1) \oplus
	10	1000	1.0693e+2 ² (1.22e+0) \ominus	1.1317e+2 ³ (8.95e-1) \ominus	1.0100e+2 ⁷ (1.22e+0) \oplus	1.0404e+2 ⁸ (1.20e+0) \oplus	1.0320e+2 ⁹ (1.72e+0) \oplus	1.0745e+2 ¹ (1.37e+0) \oplus	1.1048e+2 ² (4.83e-1) \oplus	
	20	2000	3.7212e+1 ² (1.76e+1) \oplus	7.1846e+2 ⁹ (4.33e+0) \oplus	8.4376e+2 ⁹ (3.37e+0) \oplus	8.6755e+2 ⁹ (2.92e+0) \oplus	8.6755e+2 ⁹ (2.92e+0) \oplus			
WFG1 ⁻¹	5	750	4.4736e+0 ² (3.62e-2) \ominus	4.8314e+0 ⁷ (3.56e-2) \ominus	4.8356e+0 ⁶ (6.60e-3) \oplus	4.8356e+0 ⁸ (1.18e-0) \oplus	4.8043e+0 ⁷ (1.96e-2) \oplus	4.8308e+0 ⁷ (4.75e-1) \oplus	4.8203e+0 ⁷ (7.32e-2) \oplus	4.8281e+0 ¹ (1.18e-1) \oplus
	8	1500	7.1606e+0 ² (5.51e-2) \ominus	7.0318e+0 ⁷ (2.19e-2) \ominus	7.0214e+0 ⁸ (2.22e-2) \oplus	7.0214e+0 ⁸ (2.22e-2) \oplus	1.3561e+1 ² (1.80e-1) \oplus	7.6102e+0 ⁹ (7.53e-1) \oplus	1.2260e+1 ⁹ (7.75e-1) \oplus	1.2934e+1 ³ (8.30e-1) \oplus
	10	2000	1.1196e+1 ² (1.23e-1) \ominus	1.2492e+1 ⁴ (1.46e-1) \ominus	1.1261e+2 ⁴ (2.42e-1) \oplus	1.1708e+2 ⁴ (1.72e-1) \oplus	1.8275e+1 ² (1.85e-1) \oplus	1.8427e+0 ⁹ (1.88e-1) \oplus	1.6031e+1 ⁹ (1.05e+0) \oplus	1.8109e+1 ³ (1.11e+0) \oplus
	20	3000	6.1310e+0 ² (0.97e-1) \oplus	6.1435e+0 ⁷ (3.15e-1) \oplus	6.1494e+0 ⁸ (3.57e-1) \oplus	5.3913e+0 ⁸ (4.48e-2) \oplus	4.5741e+0 ⁷ (6.80e-3) \oplus	4.8783e+0 ⁷ (9.55e-2) \oplus	4.8296e+0 ⁴ (2.23e-2) \oplus	4.7559e+0 ² (1.23e-2) \oplus
WFG2 ⁻¹	5	750	9.0605e+0 ² (0.92e-2) \oplus	8.3143e+0 ⁷ (2.19e-2) \oplus	8.0129e+0 ⁸ (7.90e-2) \oplus	7.0214e+0 ⁹ (2.22e-2) \oplus	1.1256e+1 ² (3.65e-1)			

Table 8: Mean and standard deviations (in parenthesis) of the SPD indicator obtained by state-of-the-art MOEAs, NSGA-III-AdaRSE, and NSGA-III-AdaCOU on MOPs with irregular PF shapes. The two best mean values per MOP are highlighted in grayscale, where the darker tone corresponds to the best one. The symbols in the tuples (+, -, =) and (\oplus , \ominus , \approx) are placed when the MOEA performs significantly better, significantly worse, or statistically equivalent to NSGA-III-AdaRSE and NSGA-III-AdaCOU, respectively, based on a one-tailed Wilcoxon test using a significance level of $\alpha = 0.05$. The superscripts are the obtained rank in the comparison.

MOP	Obj.	Gen.	Two_Arch2	VaEA	AR-MOEA	hpaEA	PREA	RVEA-iGNG	NSGA-III-AdaRSE	NSGA-III-AdaCOU
DTLZ5	3	400	1.0469e+1 ² (7.52e-3) \ddagger	1.0500e+1 ² (8.87e-3) \ddagger	1.0483e+1 ² (5.97e-3) \ddagger	1.0502e+1 ² (1.29e-3) \ddagger	1.0484e+1 ² (8.52e-3) \ddagger	1.0486e+1 ² (3.98e-3) \ddagger	1.0427e+1 ² (1.33e-1) \ddagger	1.0439e+1 ² (1.12e-1)
	5	600	2.5923e+1 ² (4.70e-1) \ddagger	2.3898e+1 ² (9.27e-1) \ddagger	2.5085e+1 ² (4.45e-1) \ddagger	9.3836e+0 ² (5.21e-1) \ddagger	1.7775e+1 ² (2.93e+0) \ddagger	2.1266e+1 ² (3.60e+0) \ddagger	2.2743e+1 ² (2.00e+0) \ddagger	2.2315e+1 ² (1.32e+0)
	8	750	4.5964e+1 ² (1.92e+0) \ddagger	6.7311e+1 ² (5.86e+0) \ddagger	4.7971e+1 ² (1.79e+0) \ddagger	1.7073e+1 ² (1.78e+0) \ddagger	5.8668e+1 ² (2.94e+0) \ddagger	3.9608e+1 ² (1.98e+0) \ddagger	4.5677e+1 ² (7.99e+0) \ddagger	3.7864e+1 ² (3.79e+0)
	10	1000	7.1879e+1 ² (2.81e+0) \ddagger	1.6640e+2 ² (1.10e+1) \ddagger	7.5343e+1 ² (3.86e+0) \ddagger	2.3543e+1 ² (2.44e+0) \ddagger	1.1377e+2 ² (6.42e+0) \ddagger	6.3197e+1 ² (2.85e+0) \ddagger	7.3127e+1 ² (1.29e+1) \ddagger	6.5351e+1 ² (6.10e+0)
DTLZ7	3	1000	2.1776e+1 ² (5.00e+0) \ddagger	2.4431e+1 ² (3.54e+0) \ddagger	2.1456e+1 ² (5.05e+0) \ddagger	1.9212e+1 ² (4.14e+0) \ddagger	1.7918e+1 ² (5.70e+0) \ddagger	2.0782e+1 ² (5.78e+0) \ddagger	2.4403e+1 ² (3.39e+0) \ddagger	2.4352e+1 ² (3.37e+0)
	5	1000	1.2899e+2 ² (8.77e+0) \ddagger	1.5532e+2 ² (1.82e+0) \ddagger	1.2456e+2 ² (1.81e+0) \ddagger	1.2508e+2 ² (1.75e+0) \ddagger	1.2794e+2 ² (1.51e+1) \ddagger	1.3287e+2 ² (8.21e+0) \ddagger	1.5273e+2 ² (1.77e+0) \ddagger	1.4101e+2 ² (3.12e+0)
	8	1000	1.5173e+2 ² (2.72e+0) \ddagger	1.4443e+2 ² (8.13e-1) \ddagger	1.0533e+2 ² (2.08e+0) \ddagger	1.4818e+2 ² (1.77e+0) \ddagger	1.5543e+2 ² (8.29e-1) \ddagger	1.5248e+2 ² (1.93e+0) \ddagger	1.5445e+2 ² (6.42e-1) \ddagger	1.5286e+2 ² (8.16e-1)
	10	1500	2.7024e+2 ² (7.72e-1) \ddagger	1.6124e+2 ² (3.55e+0) \ddagger	2.6427e+2 ² (1.91e+0) \ddagger	2.7490e+2 ² (3.61e+0) \ddagger	2.7354e+2 ² (1.23e+0) \ddagger	2.7354e+2 ² (5.75e-1) \ddagger	2.7085e+2 ² (8.41e+0) \ddagger	
	20	2000	3.1812e+2 ² (1.11e+0) \ddagger	3.2507e+2 ² (2.19e+0) \ddagger	7.0492e+2 ² (1.57e+0) \ddagger	2.3345e+2 ² (4.47e+0) \ddagger	1.2350e+2 ² (4.47e+0) \ddagger	1.2350e+2 ² (4.47e+0) \ddagger	1.2350e+2 ² (4.47e+0) \ddagger	
WFG2	3	400	2.0145e+1 ² (4.19e-1) \ddagger	1.8201e+1 ² (4.99e-1) \ddagger	2.0535e+1 ² (2.60e-1) \ddagger	1.6683e+1 ² (1.31e+0) \ddagger	2.1863e+1 ² (6.15e-1) \ddagger	1.8045e+1 ² (5.24e-1) \ddagger	2.0548e+1 ² (1.78e-1) \ddagger	2.0565e+1 ² (2.72e-1)
	5	750	3.4397e+1 ² (1.58e+0) \ddagger	3.0365e+1 ² (1.50e+0) \ddagger	4.0622e+1 ² (6.60e-1) \ddagger	2.9433e+1 ² (1.76e+0) \ddagger	5.0477e+1 ² (2.14e+0) \ddagger	2.7140e+1 ² (1.24e+0) \ddagger	3.9776e+1 ² (7.57e-1) \ddagger	3.9979e+1 ² (6.03e-1)
	8	1500	3.5302e+1 ² (1.68e+0) \ddagger	3.0418e+1 ² (1.81e+0) \ddagger	5.2631e+1 ² (1.05e+0) \ddagger	2.0109e+1 ² (1.54e+0) \ddagger	7.7828e+1 ² (3.62e+0) \ddagger	2.3518e+1 ² (1.22e+0) \ddagger	5.1740e+1 ² (6.43e-1) \ddagger	5.1387e+1 ² (1.35e+0)
	10	2000	6.8129e+1 ² (1.11e+0) \ddagger	3.7812e+1 ² (2.97e+0) \ddagger	1.27162e+1 ² (3.83e+0) \ddagger	1.5521e+1 ² (2.10e+0) \ddagger	1.1993e+2 ² (4.23e+0) \ddagger	1.0163e+2 ² (2.27e+0) \ddagger	1.2416e+2 ² (1.98e+0) \ddagger	6.8740e+1 ² (2.33e+0)
	20	2500	1.2933e+2 ² (3.97e-1) \ddagger	1.2571e+2 ² (4.35e-1) \ddagger	1.3077e+2 ² (3.97e-1) \ddagger	1.0203e+2 ² (4.68e-1) \ddagger	1.0253e+2 ² (4.01e-1) \ddagger	1.2610e+2 ² (3.70e-1) \ddagger	1.2733e+2 ² (3.90e-1) \ddagger	1.2341e+2 ² (3.64e-1)
WFG3	3	400	1.2933e+1 ² (3.97e-1) \ddagger	1.2571e+1 ² (4.35e-1) \ddagger	1.3077e+1 ² (3.97e-1) \ddagger	1.0203e+1 ² (4.68e-1) \ddagger	1.0253e+1 ² (4.01e-1) \ddagger	1.2610e+1 ² (3.70e-1) \ddagger	1.2733e+1 ² (3.90e-1) \ddagger	1.2341e+1 ² (3.64e-1)
	5	750	3.9505e+1 ² (5.59e-1) \ddagger	3.9886e+1 ² (9.26e-1) \ddagger	4.4953e+1 ² (5.62e-1) \ddagger	1.9467e+1 ² (1.60e+0) \ddagger	4.1666e+1 ² (9.85e-1) \ddagger	3.9101e+1 ² (0.01e+1) \ddagger	4.3611e+1 ² (7.41e-1) \ddagger	4.4278e+1 ² (7.56e-1)
	8	1500	5.2506e+1 ² (1.02e+0) \ddagger	7.5829e+1 ² (2.13e+0) \ddagger	7.9885e+1 ² (2.27e+0) \ddagger	1.6231e+1 ² (1.73e-1) \ddagger	7.7977e+1 ² (1.89e+0) \ddagger	6.7345e+1 ² (2.33e+0) \ddagger	8.2002e+1 ² (1.27e+0) \ddagger	7.7952e+1 ² (8.50e+0)
	10	2000	6.8129e+1 ² (1.11e+0) \ddagger	7.8129e+1 ² (2.79e+0) \ddagger	1.27162e+1 ² (3.83e+0) \ddagger	1.5521e+1 ² (2.10e+0) \ddagger	1.1993e+2 ² (4.23e+0) \ddagger	1.0163e+2 ² (2.27e+0) \ddagger	1.2416e+2 ² (1.98e+0) \ddagger	1.2248e+2 ² (3.77e+0)
DTLZ1-1	3	400	2.2248e+1 ² (1.25e-1) \ddagger	2.2241e+1 ² (1.21e-1) \ddagger	2.2221e+1 ² (1.29e-1) \ddagger	1.9805e+1 ² (8.96e-1) \ddagger	2.2279e+1 ² (1.30e-1) \ddagger	2.2279e+1 ² (1.30e-1) \ddagger	2.3035e+1 ² (9.88e-2) \ddagger	2.3169e+1 ² (3.86e-2)
	5	600	5.1963e+1 ² (8.02e-1) \ddagger	6.4556e+1 ² (6.75e-1) \ddagger	6.2537e+1 ² (1.14e+0) \ddagger	5.8298e+1 ² (1.57e+0) \ddagger	6.3316e+1 ² (5.57e-1) \ddagger	6.3351e+1 ² (6.42e-1) \ddagger	6.8367e+1 ² (5.89e-1) \ddagger	7.2030e+1 ² (2.88e-1)
	8	750	1.0487e+2 ² (1.72e+0) \ddagger	1.0185e+2 ² (1.26e+0) \ddagger	8.7852e+2 ² (1.06e+0) \ddagger	7.6206e+2 ² (3.68e+0) \ddagger	1.0403e+2 ² (1.34e+0) \ddagger	7.6237e+2 ² (1.34e+0) \ddagger	1.0593e+2 ² (1.02e+0) \ddagger	9.7898e+1 ² (1.01e+0)
	10	1000	1.0591e+2 ² (1.49e-1) \ddagger	1.5595e+2 ² (1.70e+0) \ddagger	1.4521e+2 ² (3.67e+0) \ddagger	1.6185e+2 ² (5.36e+0) \ddagger	1.6480e+2 ² (1.96e+0) \ddagger	1.7271e+2 ² (1.49e+0) \ddagger	1.5596e+2 ² (2.15e+0) \ddagger	
DTLZ2-1	3	250	2.9729e+1 ² (4.35e-1) \ddagger	2.8336e+1 ² (4.00e-1) \ddagger	2.8841e+1 ² (1.61e-1) \ddagger	2.2215e+1 ² (1.47e+0) \ddagger	2.2215e+1 ² (1.47e+0) \ddagger	2.2279e+1 ² (1.30e-1) \ddagger	2.3035e+1 ² (9.88e-2) \ddagger	2.3169e+1 ² (3.86e-2)
	5	350	1.0345e+2 ² (1.37e-1) \ddagger	1.1698e+2 ² (1.73e-1) \ddagger	1.1959e+2 ² (1.57e+0) \ddagger	1.0621e+2 ² (4.03e+0) \ddagger	1.1304e+2 ² (1.74e+0) \ddagger	1.0624e+2 ² (2.14e+0) \ddagger	1.0624e+2 ² (1.62e-1) \ddagger	1.0624e+2 ² (1.62e-1) \ddagger
	8	500	1.2380e+2 ² (1.72e+0) \ddagger	1.3912e+2 ² (5.11e-1) \ddagger	1.4294e+2 ² (3.48e+0) \ddagger	1.3105e+2 ² (2.36e+0) \ddagger	1.3632e+2 ² (1.59e+0) \ddagger	1.2022e+2 ² (1.86e+0) \ddagger	1.2671e+2 ² (1.32e+0) \ddagger	1.2671e+2 ² (1.32e+0) \ddagger
	10	750	2.0464e+2 ² (2.71e+0) \ddagger	2.4818e+2 ² (8.93e-1) \ddagger	1.9599e+2 ² (5.38e+0) \ddagger	2.2603e+2 ² (3.30e+0) \ddagger	2.3829e+2 ² (2.19e+0) \ddagger	2.3685e+2 ² (3.26e+0) \ddagger	2.4543e+2 ² (2.42e+0) \ddagger	2.3973e+2 ² (2.46e+0) \ddagger
	20	2500	2.9729e+1 ² (4.34e-1) \ddagger	2.8336e+1 ² (4.34e-1) \ddagger	2.4411e+1 ² (4.34e-1) \ddagger	2.4529e+1 ² (1.02e-1) \ddagger	1.9724e+1 ² (1.37e-1) \ddagger	2.4794e+1 ² (4.27e-1) \ddagger	2.6980e+1 ² (1.06e-1) \ddagger	2.6581e+1 ² (1.14e-1)
DTLZ5-1	3	400	2.5389e+1 ² (2.34e-1) \ddagger	2.4411e+1 ² (4.83e-1) \ddagger	2.4529e+1 ² (1.02e-1) \ddagger	1.9724e+1 ² (1.37e-1) \ddagger	2.2211e+1 ² (1.37e-1) \ddagger	2.2211e+1 ² (1.37e-1) \ddagger	2.2211e+1 ² (1.37e-1) \ddagger	
	5	600	8.4557e+1 ² (1.16e+0) \ddagger	8.0958e+1 ² (1.28e+0) \ddagger	8.5028e+1 ² (1.57e+0) \ddagger	8.0556e+1 ² (2.19e+0) \ddagger	8.7639e+1 ² (1.34e+0) \ddagger	8.5878e+1 ² (1.41e+0) \ddagger	9.7868e+1 ² (6.92e-1) \ddagger	1.0155e+2 ² (4.70e-1)
	8	750	1.0887e+2 ² (1.56e+0) \ddagger	1.2418e+2 ² (1.33e+0) \ddagger	1.0590e+2 ² (3.71e+0) \ddagger	1.0277e+2 ² (2.27e+0) \ddagger	1.1302e+2 ² (1.26e+0) \ddagger	1.1628e+2 ² (1.85e+0) \ddagger	1.2671e+2 ² (1.32e+0) \ddagger	1.2528e+2 ² (1.69e+0)
	10	1000	1.7297e+2 ² (2.36e+0) \ddagger	1.2585e+2 ² (2.05e+0) \ddagger	1.5906e+2 ² (3.52e+0) \ddagger	1.5906e+2 ² (3.55e+0) \ddagger	1.5906e+2 ² (3.55e+0) \ddagger	1.5906e+2 ² (2.92e+0) \ddagger	2.2174e+2 ² (2.26e+0) \ddagger	2.2174e+2 ² (2.26e+0) \ddagger
	20	2000	3.8678e+1 ² (1.40e-1) \ddagger	8.6589e+1 ² (1.08e+0) \ddagger	7.7207e+1 ² (1.58e+0) \ddagger	7.9220e+1 ² (1.41e+0) \ddagger	8.4836e+1 ² (1.03e+0) \ddagger	8.4836e+1 ² (1.03e+0) \ddagger	8.6393e+1 ² (4.08e+0) \ddagger	8.9087e+1 ² (5.06e+0) \ddagger
WFG1 ⁻¹	3	400	9.0358e+1 ² (1.37e-1) \ddagger	3.0805e+1 ² (2.37e-1) \ddagger	2.8768e+1 ² (1.56e-1) \ddagger	2.8060e+1 ² (3.07e-1) \ddagger	3.1118e+1 ² (2.23e-1) \ddagger	2.4910e+1 ² (4.19e-1) \ddagger	2.2727e+1 ² (1.90e-1) \ddagger	2.1722e+1 ² (4.91e-1) \ddagger
	5	750	2.3013e+2 ² (8.81e-1) \ddagger	7.6132e+2 ² (5.36e-1) \ddagger	6.7056e+2 ² (6.81e-1) \ddagger	7.5503e+2 ² (1.08e-1) \ddagger	7.0574e+2 ² (1.76e-1) \ddagger	6.4237e+2 ² (1.37e-1) \ddagger	6.2848e+2 ² (1.37e-1) \ddagger	6.1051e+2 ² (3.28e+0) <math

Table 9: Mean and standard deviations (in parenthesis) of the HV indicator obtained by state-of-the-art MOEAs, RVEA-AdaRSE, and RVEA-AdaCOU on MOPs with irregular PF shapes. The two best mean values per MOP are highlighted in grayscale, where the darker tone corresponds to the best one. The symbols in the tuples (+, -, =) and (\oplus , \ominus , \approx) are placed when the MOEA performs significantly better, significantly worse, or statistically equivalent to RVEA-AdaRSE and RVEA-AdaCOU, respectively, based on a one-tailed Wilcoxon test using a significance level of $\alpha = 0.05$. The superscripts are the obtained rank in the comparison.

MOP	Obj.	Gen.	Two_Arch2	VaEA	AR-MOEA	hpaEA	PREA	RVEA-iGNG	RVEA-AdaRSE	RVEA-AdaCOU	
DTLZ5	3	400	5.5131e+0 ³ (1.90e-4) \oplus	5.5095e+0 ³ (5.54e-4) \oplus	5.5100e+0 ³ (5.23e-4) \oplus	5.5101e+0 ³ (6.15e-4) \oplus	5.5120e+0 ³ (3.75e-4) \oplus	5.5121e+0 ³ (1.04e-3) \oplus	5.4937e+0 ³ (7.79e-3)	5.4947e+0 ³ (8.73e-3)	
	5	600	3.1306e+1 ³ (5.76e-3) \oplus	3.1255e+1 ³ (1.69e-2) \oplus	3.1294e+1 ³ (6.25e-3) \oplus	3.1140e+1 ³ (2.54e-2) \oplus	3.1282e+1 ³ (8.80e-3) \oplus	3.1080e+1 ³ (1.68e-1) \oplus	3.1215e+1 ³ (1.58e-2)	3.1272e+1 ³ (9.10e-3)	
	8	750	2.5017e+2 ³ (7.73e-2) \oplus	2.4901e+2 ³ (2.89e-1) \oplus	2.4953e+2 ³ (1.29e-1) \oplus	2.4789e+2 ³ (7.24e-1) \oplus	2.4985e+2 ³ (1.23e-1) \oplus	2.4610e+2 ³ (2.04e+0) \oplus	2.4877e+2 ³ (2.86e-1)	2.4980e+2 ³ (1.36e-1)	
	10	1000	1.0011e+3 ³ (3.42e-1) \oplus	9.9144e+2 ³ (1.44e+0) \oplus	9.9858e+2 ³ (4.34e+0) \oplus	9.9131e+2 ³ (3.35e+0) \oplus	9.9892e+2 ³ (4.87e-1) \oplus	9.8645e+2 ³ (9.04e+0) \oplus	9.9525e+2 ³ (1.13e+0) \oplus	1.0000e+3 ³ (4.27e-1) \oplus	
DTLZ7	3	1000	6.4304e+0 ³ (3.31e-1) \approx	6.5191e+0 ³ (3.01e-1) \approx	6.3754e+0 ³ (4.30e-1) \approx	6.1821e+0 ³ (3.48e-1) \approx	6.2528e+0 ³ (4.63e-1) \approx	6.3787e+0 ³ (4.33e-1) \approx	6.5617e+0 ³ (8.95e-3) \approx	6.5575e+0 ³ (1.13e-2) \approx	
	5	1000	2.4908e+1 ³ (1.92e-1) \oplus	2.4973e+1 ³ (8.94e-2) \oplus	2.5471e+1 ³ (3.91e-2) \oplus	2.4693e+1 ³ (5.91e-1) \oplus	2.5251e+1 ³ (3.95e-1) \oplus	2.5470e+1 ³ (4.21e-1) \oplus	2.4424e+1 ³ (9.76e-2) \oplus	2.4831e+1 ³ (7.01e-2)	2.4980e+1 ³ (1.76e-1)
	8	1000	1.7443e+2 ³ (1.48e-1) \oplus	1.8215e+2 ³ (7.96e-1) \oplus	1.7785e+2 ³ (7.96e-1) \oplus	1.8305e+2 ³ (8.27e-1) \oplus	1.8707e+2 ³ (7.00e-1) \oplus	1.8991e+2 ³ (1.85e+0) \oplus	1.7011e+2 ³ (4.33e+0) \oplus	1.7555e+2 ³ (2.90e+0)	1.7555e+2 ³ (2.90e+0)
	10	1500	6.6098e+2 ³ (5.52e-1) \oplus	7.0568e+2 ³ (5.01e+0) \oplus	7.0247e+2 ³ (2.53e+0) \oplus	7.3945e+2 ³ (6.75e-1) \oplus	7.3781e+2 ³ (3.91e+0) \oplus	6.5590e+2 ³ (1.12e+1) \oplus	6.8857e+2 ³ (6.93e+0) \oplus	6.8857e+2 ³ (6.93e+0) \oplus	6.8857e+2 ³ (6.93e+0) \oplus
WFG2	3	400	7.8377e+0 ³ (2.19e-2) \oplus	7.8423e+0 ³ (1.47e-2) \oplus	7.8648e+0 ³ (2.24e-2) \oplus	7.8150e+0 ³ (2.06e-2) \oplus	7.8925e+0 ³ (7.44e-3) \oplus	7.8412e+0 ³ (3.67e-2) \oplus	7.8126e+0 ³ (3.60e-2)	7.8126e+0 ³ (3.60e-2)	7.8126e+0 ³ (3.60e-2)
	5	750	3.1918e+1 ³ (1.92e-2) \oplus	3.1811e+1 ³ (1.93e-2) \oplus	3.1806e+1 ³ (3.09e-2) \oplus	3.1930e+1 ³ (2.82e-2) \oplus	3.1982e+1 ³ (8.00e-2) \oplus	3.1828e+1 ³ (2.01e-2) \oplus	3.1849e+1 ³ (3.17e-2)	3.1865e+1 ³ (3.09e-2)	3.1865e+1 ³ (3.09e-2)
	8	1500	2.5567e+2 ³ (1.14e-1) \oplus	2.5517e+2 ³ (2.19e-1) \oplus	2.5570e+2 ³ (2.12e-1) \oplus	2.5490e+2 ³ (2.37e-1) \oplus	2.5592e+2 ³ (3.82e-2) \oplus	2.5517e+2 ³ (1.15e-1) \oplus	2.5411e+2 ³ (4.13e-1) \oplus	2.5412e+2 ³ (1.32e+0)	2.5412e+2 ³ (1.32e+0)
	10	2000	1.0235e+3 ³ (1.40e-1) \oplus	1.0219e+3 ³ (5.72e-1) \oplus	1.0235e+3 ³ (1.83e-1) \oplus	1.0213e+3 ³ (6.52e-1) \oplus	1.0240e+3 ³ (3.15e-1) \oplus	1.0224e+3 ³ (4.11e-1) \oplus	1.0200e+3 ³ (1.23e+0) \oplus	1.0203e+3 ³ (1.31e+0) \oplus	1.0203e+3 ³ (1.31e+0) \oplus
WFG3	3	400	7.0549e+0 ³ (1.86e-2) \oplus	6.9987e+0 ³ (1.81e-2) \oplus	7.0065e+0 ³ (1.95e-2) \oplus	6.8544e+0 ³ (1.04e-1) \oplus	7.0586e+0 ³ (9.51e-2) \oplus	7.0174e+0 ³ (1.56e-2) \oplus	6.9331e+0 ³ (2.30e-2) \oplus	6.9328e+0 ³ (2.58e-2)	6.9328e+0 ³ (2.58e-2)
	5	750	2.9030e+1 ³ (7.54e-2) \oplus	2.8433e+1 ³ (1.45e-1) \oplus	2.8593e+1 ³ (1.40e-1) \oplus	2.7863e+1 ³ (4.12e-1) \oplus	2.7863e+1 ³ (2.77e-1) \oplus	2.8687e+1 ³ (9.95e-2) \oplus	2.8260e+1 ³ (1.85e-1) \oplus	2.8473e+1 ³ (1.30e-1)	2.8473e+1 ³ (1.30e-1)
	8	1500	2.3280e+2 ³ (7.57e-1) \oplus	2.3203e+2 ³ (1.16e+0) \oplus	2.1984e+2 ³ (2.95e-0) \oplus	2.1943e+2 ³ (6.15e+0) \oplus	2.3307e+2 ³ (1.15e+0) \oplus	2.3162e+2 ³ (2.12e+0) \oplus	1.9811e+2 ³ (1.38e+1) \oplus	2.2784e+2 ³ (2.79e+0)	2.2784e+2 ³ (2.79e+0)
	10	2000	9.3930e+2 ³ (2.06e+0) \oplus	9.3693e+2 ³ (2.37e+0) \oplus	8.5941e+2 ³ (2.17e+1) \oplus	8.6081e+2 ³ (2.98e+0) \oplus	9.3666e+2 ³ (3.54e+0) \oplus	9.3625e+2 ³ (2.41e+0) \oplus	7.5023e+2 ³ (5.26e+1) \oplus	9.3406e+2 ³ (1.47e+1) \oplus	9.3406e+2 ³ (1.47e+1) \oplus
DTLZ1 ⁻¹	3	400	5.4526e+0 ³ (1.73e-2) \oplus	5.4528e+0 ³ (1.65e-2) \oplus	5.4482e+0 ³ (5.91e-3) \oplus	5.2238e+0 ³ (5.05e-2) \oplus	5.4821e+0 ³ (7.89e-3) \oplus	5.4821e+0 ³ (5.37e-3) \oplus	5.4763e+0 ³ (1.71e-2) \oplus	5.4811e+0 ³ (9.71e-3) \oplus	5.4811e+0 ³ (9.71e-3) \oplus
	5	600	1.0125e+1 ³ (5.68e-2) \oplus	1.00688e+1 ³ (1.11e-2) \oplus	1.0549e+1 ³ (9.29e-2) \oplus	1.0278e+1 ³ (3.82e-2) \oplus	1.0973e+1 ³ (3.57e-2) \oplus	1.0699e+1 ³ (5.26e-2) \oplus	1.0916e+1 ³ (5.27e-2) \oplus	1.1229e+1 ³ (4.80e-2)	1.1229e+1 ³ (4.80e-2)
	8	750	7.1430e+2 ³ (2.81e-2) \oplus	7.1527e+2 ³ (1.42e-1) \oplus	1.8583e+2 ³ (2.35e-1) \oplus	1.6905e+2 ³ (5.47e-1) \oplus	2.0092e+2 ³ (1.167e-1) \oplus	1.2263e+2 ³ (1.21e+0) \oplus	1.7224e+2 ³ (1.44e+0) \oplus	1.9373e+2 ³ (1.12e+0)	1.9373e+2 ³ (1.12e+0)
	10	1000	1.5901e+3 ³ (1.39e-1) \oplus	2.8493e+2 ³ (2.39e-0) \oplus	2.7743e+2 ³ (1.65m-1) \oplus	2.4825e+2 ³ (6.59e-1) \oplus	2.9613e+2 ³ (2.11e-1) \oplus	1.3435e+2 ³ (1.42e+0) \oplus	2.4340e+2 ³ (2.76e+0) \oplus	2.8243e+2 ³ (2.51e+0) \oplus	2.8243e+2 ³ (2.51e+0) \oplus
DTLZ2 ⁻¹	3	250	6.6937e+0 ³ (6.88e-3) \oplus	6.6108e+0 ³ (1.72e-2) \oplus	6.6558e+0 ³ (2.94e-3) \oplus	6.5633e+0 ³ (3.73e-2) \oplus	6.6898e+0 ³ (6.51m-3) \oplus	6.6575e+0 ³ (2.16e-2) \oplus	6.6881e+0 ³ (8.03e-3) \oplus	6.6753e+0 ³ (9.51e-2) \oplus	6.6753e+0 ³ (9.51e-2) \oplus
	5	350	1.7363e+1 ³ (6.03e-2) \oplus	1.6890e+1 ³ (9.69e-2) \oplus	1.6985e+1 ³ (8.52e-2) \oplus	1.6954e+1 ³ (9.64e-2) \oplus	1.7514e+1 ³ (4.66e-2) \oplus	1.6981e+1 ³ (8.65e-2) \oplus	1.7213e+1 ³ (7.62e-2) \oplus	1.7347e+1 ³ (6.60e-2)	1.7347e+1 ³ (6.60e-2)
	8	500	4.4078e+2 ³ (4.40e-1) \oplus	4.2256e+2 ³ (4.42e-1) \oplus	3.8697e+2 ³ (5.32e-1) \oplus	4.2700e+2 ³ (4.89e-1) \oplus	4.5266e+2 ³ (3.63e-1) \oplus	4.2025e+2 ³ (8.74e-1) \oplus	4.2700e+2 ³ (5.55e-1) \oplus	4.1448e+2 ³ (6.72e-1)	4.1448e+2 ³ (6.72e-1)
	10	750	7.7979e+2 ³ (1.13e-0) \oplus	7.8092e+2 ³ (6.58e-1) \oplus	7.1161e+2 ³ (1.65e-1) \oplus	7.8489e+2 ³ (9.51e-1) \oplus	8.3897e+2 ³ (6.68e-1) \oplus	7.5936e+2 ³ (1.27e+0) \oplus	7.6947e+2 ³ (1.25e+0) \oplus	6.8701e+2 ³ (9.90e-1)	6.8701e+2 ³ (9.90e-1)
DTLZ5 ⁻¹	3	400	6.7666e+0 ³ (6.60e-3) \oplus	6.7031e+0 ³ (0.07e-2) \oplus	6.7015e+0 ³ (2.67e-3) \oplus	6.6171e+0 ³ (5.16e-2) \oplus	6.7653e+0 ³ (6.89e-3) \oplus	6.7653e+0 ³ (1.07e-2) \oplus	6.7747e+0 ³ (8.66e-2) \oplus	6.7544e+0 ³ (1.01e-2)	6.7544e+0 ³ (1.01e-2)
	5	600	1.8478e+1 ³ (4.62e-2) \oplus	1.7847e+1 ³ (4.88e-2) \oplus	1.7824e+1 ³ (1.72e-2) \oplus	1.8243e+1 ³ (1.72e-2) \oplus	1.8036e+1 ³ (1.10e-1) \oplus	1.8683e+1 ³ (4.21e-2) \oplus	1.8024e+1 ³ (1.65e-1) \oplus	1.8401e+1 ³ (4.89e-2) \oplus	1.8724e+1 ³ (3.48e-2) \oplus
	8	1000	5.3665e+2 ³ (4.78e-1) \oplus	5.1479e+2 ³ (4.78e-1) \oplus	5.0917e+2 ³ (8.40e-1) \oplus	5.1001e+2 ³ (6.35e-1) \oplus	5.6641e+2 ³ (4.44e-1) \oplus	5.1032e+2 ³ (1.26e-1) \oplus	5.1023e+2 ³ (1.26e-1) \oplus	1.0325e+2 ³ (2.95e-1) \oplus	1.0325e+2 ³ (2.95e-1) \oplus
	10	1500	1.1317e+3 ³ (1.22e-0) \oplus	1.1317e+3 ³ (1.22e-0) \oplus	1.0100e+3 ³ (2.10e-0) \oplus	1.0404e+3 ³ (2.10e-0) \oplus	1.1534e+3 ³ (1.26e-1) \oplus	1.0320e+3 ³ (1.26e-1) \oplus			
WFG1 ⁻¹	3	400	4.7368e+0 ³ (0.36e-2) \oplus	4.8384e+0 ³ (1.56e-2) \oplus	4.8536e+0 ³ (6.60e-3) \oplus	3.1600e+0 ³ (1.18e-0) \oplus	4.8783e+0 ³ (9.55e-3) \oplus	4.8296e+0 ³ (4.07e-2) \oplus	4.2236e+0 ³ (7.44e-1) \oplus	4.1215e+0 ³ (7.55e-1) \oplus	4.1215e+0 ³ (7.55e-1) \oplus
	5	750	7.1606e+1 ³ (5.51e-2) \oplus	8.3143e+1 ³ (2.19e-2) \oplus	8.0129e+1 ³ (7.90e-2) \oplus	8.2048e+1 ³ (2.22e-2) \oplus	8.4038e+1 ³ (1.96e-2) \oplus	6.3027e+0 ³ (4.75e-1) \oplus	7.2845e+1 ³ (5.78e-2) \oplus	7.2845e+1 ³ (5.78e-2) \oplus	7.2845e+1 ³ (5.78e-2) \oplus
	8	1500	9.8030e+2 ³ (8.58e-2) \oplus	1.3772e+2 ³ (8.49e-1) \oplus	1.2334e+2 ³ (1.89e-1) \oplus	1.1256e+2 ³ (3.65e-0) \oplus	1.2136e+2 ³ (1.80e-1) \oplus	1.2530e+2 ³ (2.14e+0) \oplus	2.0598e+2 ³ (4.21e+0) \oplus	2.0489e+2 ³ (3.16e+0)	2.0489e+2 ³ (3.16e+0)

Table 10: Mean and standard deviations (in parenthesis) of the SPD indicator obtained by state-of-the-art MOEAs, RVEA-AdaRSE, and RVEA-AdaCOU on MOPs with irregular PF shapes. The two best mean values per MOP are highlighted in grayscale, where the darker tone corresponds to the best one. The symbols in the tuples (+, -, =) and (\oplus , \ominus , \approx) are placed when the MOEA performs significantly better, significantly worse, or statistically equivalent to RVEA-AdaRSE and RVEA-AdaCOU, respectively, based on a one-tailed Wilcoxon test using a significance level of $\alpha = 0.05$. The superscripts are the obtained rank in the comparison.

MOP	Obj.	Gen.	Two_Arch2	VaEA	AR-MOEA	hpEA	PREA	RVEA-iGNG	RVEA-AdaRSE	RVEA-AdaCOU
DTLZ5	3	400	1.0469e+1 ³ (5.52e-0) \ominus	1.0500e+1 ³ (5.97e-0) \ominus	1.0483e+1 ³ (5.97e-0) \ominus	1.0502e+1 ³ (1.29e-2) \ominus	1.0484e+1 ³ (8.52e-3) \ominus	1.0486e+1 ³ (3.98e-3) \ominus	1.0579e+1 ² (1.67e-1) \ominus	1.0619e+1 ² (2.47e-1) \ominus
	5	600	2.5923e+1 ³ (4.70e-0) \ominus	2.3898e+1 ³ (9.27e-0) \ominus	2.5058e+1 ³ (4.45e-1) \oplus	9.3836e+1 ² (5.21e-1) \ominus	1.7775e+1 ² (2.93e+0) \ominus	1.2626e+1 ² (3.60e+0) \oplus	3.3509e+1 ² (2.72e+0) \ominus	2.2010e+1 ² (1.47e+0) \ominus
	8	750	4.5964e+1 ³ (1.92e+0) \oplus	6.7311e+1 ³ (5.86e+0) \oplus	4.7971e+1 ³ (2.79e+0) \oplus	1.7073e+1 ² (1.78e+0) \oplus	5.8668e+1 ² (2.94e+0) \oplus	3.9608e+1 ² (1.98e+0) \oplus	4.4195e+1 ² (9.61e+0) \oplus	3.6301e+1 ² (4.02e+0) \oplus
	10	1000	7.1879e+1 ³ (2.81e+0) \oplus	1.6640e+2 ³ (1.10e+1) \oplus	7.5343e+1 ³ (3.86e+0) \oplus	2.3543e+1 ³ (2.44e+0) \oplus	1.1377e+2 ² (6.42e+0) \oplus	6.3197e+1 ² (2.85e+0) \oplus	7.6640e+1 ² (1.75e+1) \oplus	6.6458e+1 ² (6.69e+0) \oplus
DTLZ7	3	1000	2.1776e+1 ³ (5.00e+0) \ominus	2.4431e+1 ³ (3.54e+0) \ominus	2.1456e+1 ³ (5.95e+0) \ominus	1.9212e+1 ³ (4.14e+0) \ominus	1.7918e+1 ³ (5.70e+0) \ominus	2.0782e+1 ³ (5.78e+0) \ominus	2.5905e+1 ³ (3.28e-1) \oplus	2.5586e+1 ² (4.66e-1) \oplus
	5	1000	1.2890e+2 ³ (8.77e+0) \oplus	1.5532e+2 ³ (1.82e+0) \oplus	1.2456e+2 ³ (1.81e+0) \oplus	1.2598e+2 ³ (1.75e+1) \oplus	1.2794e+2 ³ (1.51e+1) \oplus	1.3287e+2 ³ (8.21e+0) \oplus	1.3802e+2 ² (2.59e+0) \oplus	1.3042e+2 ² (2.50e+0) \oplus
	8	1000	1.5173e+2 ³ (2.72e+0) \oplus	1.4443e+2 ³ (8.13e-1) \oplus	1.0533e+2 ³ (2.08e+0) \oplus	1.4818e+2 ³ (1.77e+0) \oplus	1.5543e+2 ³ (8.29e-1) \oplus	1.5248e+2 ³ (1.93e+0) \oplus	8.7357e+1 ³ (7.13e+0) \oplus	9.1355e+1 ³ (2.48e+0) \oplus
	10	1500	2.7024e+2 ³ (5.62e+0) \oplus	2.6012e+2 ³ (7.72e+0) \oplus	1.6124e+2 ³ (3.55e+0) \oplus	2.6422e+2 ³ (1.91e+0) \oplus	2.7490e+2 ³ (3.61e+0) \oplus	2.7354e+2 ³ (1.23e+0) \oplus	1.4442e+2 ³ (6.64e+0) \oplus	1.4086e+2 ³ (6.66e+0) \oplus
WFG2	3	400	2.0145e+1 ³ (4.19e-1) \ominus	1.8201e+1 ³ (4.99e-1) \ominus	2.0535e+1 ³ (2.60e-0) \oplus	1.6683e+1 ³ (1.31e+0) \oplus	2.1863e+1 ³ (6.15e-1) \oplus	1.8405e+1 ³ (5.24e-1) \oplus	1.9792e+1 ³ (3.71e-1) \oplus	1.9931e+1 ³ (5.78e-1) \oplus
	5	750	3.4397e+1 ³ (1.58e+0) \oplus	3.0365e+1 ³ (4.06e+1) \oplus	4.0622e+1 ³ (6.60e-1) \oplus	9.29433e+1 ² (1.76e+0) \oplus	5.0471e+1 ² (1.24e+0) \oplus	2.7140e+1 ² (1.24e+0) \oplus	2.9343e+1 ² (1.26e+0) \oplus	2.9602e+1 ² (1.15e+0) \oplus
	8	1500	3.5302e+1 ³ (1.68e+0) \oplus	3.0418e+1 ³ (1.81e+0) \oplus	5.2631e+1 ³ (1.05e+0) \oplus	2.0190e+1 ³ (1.54e+0) \oplus	7.7828e+1 ² (3.62e+0) \oplus	3.2518e+1 ² (1.22e+0) \oplus	2.0073e+1 ² (1.42e+0) \oplus	2.0408e+1 ² (1.20e+0) \oplus
	10	2000	3.7814e+1 ³ (1.39e+0) \oplus	3.2507e+1 ³ (1.22e+0) \oplus	7.0492e+1 ³ (2.07e+0) \oplus	3.2545e+1 ³ (1.23e+0) \oplus	1.1260e+2 ² (4.47e+0) \oplus	2.7339e+1 ² (1.71e+0) \oplus	2.2293e+1 ² (1.49e+0) \oplus	2.3628e+1 ² (1.98e+0) \oplus
WFG3	3	400	1.2933e+1 ² (3.97e-1) \oplus	1.2571e+1 ² (4.35e-1) \oplus	1.30377e+1 ² (3.97e-1) \oplus	1.0293e+1 ² (4.68e-1) \oplus	1.0252e+1 ² (4.01e-1) \oplus	1.2610e+1 ² (3.70e-1) \oplus	1.1900e+1 ² (4.02e-1) \oplus	1.1632e+1 ² (5.29e-1) \oplus
	5	750	3.9595e+1 ² (5.59e-1) \oplus	4.4953e+1 ² (5.62e-1) \oplus	1.9467e+1 ² (1.60e+0) \oplus	4.1666e+1 ² (9.85e-1) \oplus	3.9101e+1 ² (9.01e-1) \oplus	4.1319e+1 ² (1.10e+0) \oplus	4.1777e+1 ² (8.84e-1) \oplus	
	8	1500	5.2506e+1 ² (1.02e+0) \oplus	7.5829e+1 ² (1.23e+0) \oplus	7.9885e+1 ² (2.27e+0) \oplus	1.6321e+1 ² (1.73e+0) \oplus	7.7977e+1 ² (1.89e+0) \oplus	6.7345e+1 ² (2.33e+0) \oplus	7.2323e+1 ² (2.77e+0) \oplus	
	10	2000	6.8129e+1 ² (1.11e+0) \oplus	1.1406e+2 ² (2.79e+0) \oplus	1.2716e+2 ² (3.83e+0) \oplus	1.5521e+2 ² (2.10e+0) \oplus	1.1993e+2 ² (2.43e+0) \oplus	1.0163e+2 ² (2.27e+0) \oplus	1.1649e+2 ² (5.95e+0) \oplus	1.1721e+2 ² (2.10e+0) \oplus
DTLZ1 ⁻¹	3	400	2.2248e+1 ² (1.25e-1) \ominus	2.2427e+1 ² (2.11e-0) \ominus	2.2221e+1 ² (1.29e-1) \ominus	1.9805e+1 ² (8.96e-1) \ominus	2.2797e+1 ² (1.30e-1) \ominus	2.3035e+1 ² (9.88e-1) \ominus	2.3554e+1 ² (2.45e-1) \ominus	2.3400e+1 ² (1.91e-1) \ominus
	5	600	5.1963e+1 ² (8.02e-1) \oplus	6.4556e+1 ² (6.75e-1) \oplus	6.2537e+1 ² (1.14e+0) \oplus	5.8292e+1 ² (1.45e+0) \oplus	6.7316e+1 ² (5.57e-1) \oplus	6.5351e+1 ² (4.62e-1) \oplus	6.8803e+1 ² (6.72e-1) \oplus	7.0509e+1 ² (4.00e-1) \oplus
	8	750	9.0478e+1 ² (1.72e+0) \oplus	1.0185e+2 ² (1.26e+0) \oplus	7.6296e+1 ² (3.68e+0) \oplus	1.0403e+2 ² (1.34e+0) \oplus	4.7274e+1 ² (6.75e+0) \oplus	8.0385e+1 ² (1.18e+1) \oplus	8.7010e+1 ² (8.08e+0) \oplus	
	10	1000	4.0591e+2 ² (1.49e+0) \oplus	1.15959e+2 ² (2.70e+0) \oplus	1.4521e+2 ² (3.67e+0) \oplus	1.1658e+2 ² (5.36e+0) \oplus	1.6480e+2 ² (1.96e+0) \oplus	4.7096e+2 ² (9.32e+0) \oplus	1.2000e+2 ² (2.61e+1) \oplus	1.3837e+2 ² (2.05e+0) \oplus
DTLZ2 ⁻¹	3	250	2.9729e+1 ² (4.35e-1) \ominus	2.8336e+1 ² (4.06e-1) \ominus	2.8841e+1 ² (1.61e-0) \ominus	2.9073e+1 ² (1.47e-0) \ominus	2.9973e+1 ² (6.70e-1) \ominus	2.8581e+1 ² (7.02e-1) \ominus	3.2031e+1 ² (1.82e-1) \oplus	3.1569e+1 ² (3.66e-1) \oplus
	5	350	1.0345e+2 ² (1.37e+0) \oplus	1.1696e+2 ² (1.73e+0) \oplus	1.1959e+2 ² (1.57e+0) \oplus	1.0621e+2 ² (4.03e+0) \oplus	1.1304e+2 ² (1.74e+0) \oplus	1.0674e+2 ² (2.12e+0) \oplus	1.2302e+2 ² (2.30e+0) \oplus	1.2688e+2 ² (1.94e+0) \oplus
	8	500	1.2380e+2 ² (1.72e+0) \oplus	1.3912e+2 ² (5.11e+0) \oplus	1.2492e+2 ² (3.48e+0) \oplus	1.3105e+2 ² (2.36e+0) \oplus	1.3652e+2 ² (1.58e+0) \oplus	1.3488e+2 ² (1.57e+0) \oplus	1.1431e+2 ² (1.60e+0) \oplus	1.1805e+2 ² (1.06e+0) \oplus
	10	750	2.0464e+2 ² (2.71e+0) \oplus	2.4818e+2 ² (8.93e+0) \oplus	1.9599e+2 ² (5.38e+0) \oplus	2.2639e+2 ² (3.30e+0) \oplus	2.3829e+2 ² (2.19e+0) \oplus	2.3686e+2 ² (2.83e+0) \oplus	2.0356e+2 ² (3.57e+0) \oplus	2.1551e+2 ² (1.34e+0) \oplus
DTLZ5 ⁻¹	3	400	2.5389e+1 ² (2.34e-1) \ominus	2.4411e+1 ² (4.83e-1) \ominus	2.4529e+1 ² (1.02e-0) \ominus	1.9724e+1 ² (1.37e-0) \ominus	2.5147e+1 ² (3.56e-1) \ominus	2.4794e+1 ² (4.27e-1) \ominus	2.6784e+1 ² (1.38e-1) \ominus	2.6333e+1 ² (1.72e-1) \ominus
	5	600	8.4557e+1 ² (1.16e+0) \oplus	9.0958e+1 ² (1.28e+0) \oplus	8.5205e+1 ² (1.57e+0) \oplus	8.0556e+1 ² (2.19e+0) \oplus	8.0272e+1 ² (2.37e+0) \oplus	2.0222e+2 ² (1.86e+0) \oplus	8.5878e+1 ² (1.34e+1) \oplus	1.0236e+2 ² (1.56e+0) \oplus
	8	750	1.0887e+2 ² (1.56e+0) \oplus	1.2418e+2 ² (1.33e+0) \oplus	1.05090e+2 ² (3.71e+0) \oplus	1.0272e+2 ² (2.27e+0) \oplus	2.0222e+2 ² (1.86e+0) \oplus	2.0222e+2 ² (1.85e+0) \oplus	1.0658e+2 ² (2.26e+0) \oplus	1.1298e+2 ² (1.36e+0) \oplus
	10	1000	1.7297e+2 ² (2.36e+0) \oplus	1.2586e+2 ² (2.36e+0) \oplus	1.55006e+2 ² (3.35e+0) \oplus	2.0236e+2 ² (3.42e+0) \oplus	1.9290e+2 ² (3.82e+0) \oplus	2.0236e+2 ² (3.42e+0) \oplus	1.8093e+2 ² (4.64e+0) \oplus	1.9903e+2 ² (2.09e+0) \oplus
DTLZ7 ⁻¹	3	1000	1.4466e+1 ² (1.62e-1) \ominus	1.4953e+1 ² (1.73e-1) \ominus	1.4775e+1 ² (2.19e-0) \ominus	1.1914e+1 ² (6.98e-1) \ominus	1.4946e+1 ² (2.44e+0) \ominus	1.4496e+1 ² (1.73e-1) \ominus	1.6278e+1 ² (1.90e+0) \oplus	1.5910e+1 ² (1.71e+0) \oplus
	5	1000	5.6188e+1 ² (5.83e+0) \oplus	4.4144e+1 ² (2.45e+0) \oplus	9.9821e+1 ² (1.45e+0) \oplus	2.7551e+1 ² (8.14e+0) \oplus	5.8491e+1 ² (1.26e+1) \oplus	6.7253e+1 ² (7.54e+0) \oplus	1.1612e+2 ² (1.04e+1) \oplus	1.1615e+2 ² (1.47e+1) \oplus
	8	1000	1.4013e+2 ² (3.05e+0) \oplus	1.4779e+2 ² (3.83e+0) \oplus	1.0003e+2 ² (2.12e+0) \oplus	1.4742e+2 ² (3.64e+0) \oplus	1.4904e+2 ² (3.31e+0) \oplus	1.3743e+2 ² (4.18e+0) \oplus	8.9402e+2 ² (4.51e+0) \oplus	1.0086e+2 ² (5.88e+0) \oplus
	10	1500	2.6654e+2 ² (2.17e+0) \oplus	2.6411e+2 ² (2.92e+0) \oplus	1.2455e+2 ² (1.26e+0) \oplus	2.5747e+2 ² (3.77e+0) \oplus	2.7307e+2 ² (9.43e+0) \oplus	2.5399e+2 ² (4.17e+0) \oplus	1.4205e+2 ² (7.42e+0) \oplus	1.5778e+2 ² (2.33e+1) \oplus
WFG1 ⁻¹	3	400	2.16740e+1 ² (6.81e-1) \ominus	1.8960e+1 ² (5.28e-1) \ominus	2.17520e+1 ² (1.44e-1) \ominus	2.0758e+1 ² (7.56e-2) \ominus	2.0600e+1 ² (7.48e-0) \ominus	1.9770e+1 ² (1.90e-1) \ominus	1.4542e+1 ² (5.50e+0) \oplus	1.3733e+1 ² (5.60e+0) \oplus
	5	750	2.3013e+1 ² (8.81e-1) \oplus	4.1033e+1 ² (3.01e-1) $\$						

Table 11: Mean and standard deviations (in parenthesis) of the HV indicator obtained by state-of-the-art MOEAs, MOEA/D-AdaRSE, and MOEA/D-AdaCOU on MOPs with irregular PF shapes. The two best mean values per MOP are highlighted in grayscale, where the darker tone corresponds to the best one. The symbols in the tuples $(+, -, =)$ and $(\oplus, \ominus, \approx)$ are placed when the MOEA performs significantly better, significantly worse, or statistically equivalent to MOEA/D-AdaRSE and MOEA/D-AdaCOU, respectively, based on a one-tailed Wilcoxon test using a significance level of $\alpha = 0.05$. The superscripts are the obtained rank in the comparison.

MOP	Obj.	Gen.	Two-Arch2	VaEA	AR-MOEAs	hpEA	PREA	RVEA-IGNG	MOEA/D-AdaRSE	MOEA/D-AdaCOU
DTLZ5	3	400	5.5130e+0 ² (2.03e-1) \ddagger	5.5089e+0 ² (2.82e-3) \ddagger	5.5100e+0 ² (5.03e-0) \ddagger	5.5099e+0 ² (5.36e-4) \ddagger	5.5118e+0 ² (4.32e-4) \ddagger	5.5122e+0 ² (8.96e-4) \ddagger	5.5045e+0 ² (1.74e-3)	5.5046e+0 ² (1.82e-3)
	5	600	3.1303e+0 ² (6.64e-3) \ddagger	3.1253e+0 ² (1.17e-2) \ddagger	3.1249e+0 ² (7.05e-3) \ddagger	3.1140e+0 ² (1.23e-2) \ddagger	3.1280e+0 ² (1.00e-2) \ddagger	3.1071e+0 ² (1.72e-1) \ddagger	3.1296e+0 ² (1.39e-2) \ddagger	3.1310e+0 ² (1.87e-1)
	8	750	2.5013e+0 ² (1.05e-1) \ddagger	2.4888e+0 ² (2.63e-1) \ddagger	2.4951e+0 ² (1.18e-1) \ddagger	2.4771e+0 ² (8.74e-1) \ddagger	2.4985e+0 ² (1.09e-0) \ddagger	2.4580e+0 ² (2.33e-0) \ddagger	2.5016e+0 ² (2.16e-1) \ddagger	2.5038e+0 ² (6.94e-2)
	10	1000	1.0000e+0 ³ (4.60e-1) \ddagger	9.9234e+0 ² (1.65e+0) \ddagger	9.9848e+0 ² (5.50e-1) \ddagger	9.9189e+0 ² (3.43e+0) \ddagger	9.9879e+0 ² (3.70e-1) \ddagger	9.8901e+0 ² (6.86e+0) \ddagger	1.0014e+0 ³ (4.11e-1) \ddagger	1.0024e+0 ³ (2.06e-1)
	3	1000	6.4317e+0 ⁴ (3.31e-1) \ddagger	6.5162e+0 ⁴ (2.05e-1) \ddagger	6.3404e+0 ⁴ (4.91e-1) \ddagger	6.2432e+0 ⁴ (2.97e-1) \ddagger	6.3086e+0 ⁴ (4.98e-1) \ddagger	6.4315e+0 ⁴ (3.34e-1) \ddagger	6.6044e+0 ⁴ (3.44e-3) \ddagger	6.5979e+0 ⁴ (3.12e-2) \ddagger
DTLZ7	3	400	4.2846e+0 ² (4.69e-1) \ddagger	4.2916e+0 ² (8.59e-2) \ddagger	4.2542e+0 ² (2.90e-0) \ddagger	4.2630e+0 ² (1.58e-1) \ddagger	4.2568e+0 ² (3.21e-1) \ddagger	4.2554e+0 ² (3.36e-2) \ddagger	4.2523e+0 ² (3.72e-1) \ddagger	4.2526e+0 ² (1.37e-1) \ddagger
	5	1000	1.4826e+0 ² (1.46e-1) \ddagger	1.4916e+0 ² (8.59e-2) \ddagger	1.4802e+0 ² (2.90e-0) \ddagger	1.7744e+0 ² (8.42e-1) \ddagger	1.8703e+0 ² (5.89e-1) \ddagger	1.8923e+0 ² (2.66e-0) \ddagger	1.8242e+0 ² (9.57e-1) \ddagger	1.8173e+0 ² (2.75e-0) \ddagger
	8	1000	1.7371e+0 ² (9.92e-0) \ddagger	1.8155e+0 ² (9.33e-1) \ddagger	1.7744e+0 ² (8.42e-1) \ddagger	1.8299e+0 ² (4.79e-1) \ddagger	1.8703e+0 ² (5.89e-1) \ddagger	1.8923e+0 ² (2.66e-0) \ddagger	1.8242e+0 ² (9.57e-1) \ddagger	1.8173e+0 ² (2.75e-0) \ddagger
	10	1500	6.4568e+0 ² (8.23e-1) \ddagger	7.0648e+0 ² (2.32e+0) \ddagger	6.5639e+0 ² (5.11e+0) \ddagger	7.3050e+0 ² (2.16e+0) \ddagger	7.3862e+0 ² (8.27e-1) \ddagger	7.3695e+0 ² (2.43e+0) \ddagger	6.9628e+0 ² (9.52e-1) \ddagger	7.1055e+0 ² (1.36e+0) \ddagger
	3	1000	6.4317e+0 ⁴ (3.31e-1) \ddagger	6.5162e+0 ⁴ (2.05e-1) \ddagger	6.3404e+0 ⁴ (4.91e-1) \ddagger	6.2432e+0 ⁴ (2.97e-1) \ddagger	6.3086e+0 ⁴ (4.98e-1) \ddagger	6.4315e+0 ⁴ (3.34e-1) \ddagger	6.6044e+0 ⁴ (3.44e-3) \ddagger	6.5979e+0 ⁴ (3.12e-2) \ddagger
WFG2	3	400	7.8178e+0 ⁸ (1.40e-1) \ddagger	7.8415e+0 ⁸ (1.72e-2) \ddagger	7.8726e+0 ⁸ (1.28e-2) \ddagger	7.8215e+0 ⁸ (1.86e-2) \ddagger	7.8802e+0 ⁸ (7.67e-2) \ddagger	7.8470e+0 ⁸ (2.25e-2) \ddagger	7.8810e+0 ⁸ (1.87e-2) \ddagger	7.8796e+0 ⁸ (1.80e-2) \ddagger
	5	750	3.1928e+0 ⁸ (1.28e-2) \ddagger	3.1803e+0 ⁸ (2.65e-2) \ddagger	3.1936e+0 ⁸ (1.14e-1) \ddagger	3.1805e+0 ⁸ (3.44e-2) \ddagger	3.1985e+0 ⁸ (4.75e-3) \ddagger	3.1898e+0 ⁸ (2.08e-2) \ddagger	3.1944e+0 ⁸ (1.68e-2) \ddagger	3.1934e+0 ⁸ (1.17e-1) \ddagger
	8	1500	2.5572e+0 ⁸ (8.70e-2) \ddagger	2.5524e+0 ⁸ (2.02e-1) \ddagger	2.5575e+0 ⁸ (9.20e-2) \ddagger	2.5482e+0 ⁸ (2.39e-1) \ddagger	2.5594e+0 ⁸ (3.71e-2) \ddagger	2.5524e+0 ⁸ (1.65e-1) \ddagger	2.5562e+0 ⁸ (1.01e-1) \ddagger	2.5526e+0 ⁸ (2.19e-1) \ddagger
	10	2000	1.0236e+0 ⁹ (3.14e-1) \ddagger	1.0219e+0 ⁹ (5.36e-2) \ddagger	1.0236e+0 ⁹ (3.14e-1) \ddagger	1.0214e+0 ⁹ (4.75e-1) \ddagger	1.0240e+0 ⁹ (3.70e-2) \ddagger	1.0226e+0 ⁹ (3.18e-1) \ddagger	1.0232e+0 ⁹ (3.09e-1) \ddagger	1.0232e+0 ⁹ (3.01e-1) \ddagger
	3	400	7.0509e+0 ² (1.5e-2) \ddagger	6.9908e+0 ² (2.08e-2) \ddagger	7.0067e+0 ² (1.65e-2) \ddagger	6.9717e+0 ² (1.34e-2) \ddagger	7.0226e+0 ² (7.35e-2) \ddagger	7.0251e+0 ² (1.92e-2) \ddagger	7.0631e+0 ² (2.37e-2) \ddagger	7.0616e+0 ² (1.95e-2) \ddagger
WFG3	5	750	2.9021e+0 ⁴ (8.42e-2) \ddagger	2.8441e+0 ⁴ (1.73e-1) \ddagger	2.8717e+0 ⁴ (1.33e-1) \ddagger	2.7959e+0 ⁴ (3.38e-2) \ddagger	2.9171e+0 ⁴ (7.81e-2) \ddagger	2.8659e+0 ⁴ (9.93e-2) \ddagger	2.9028e+0 ⁴ (1.17e-1) \ddagger	2.9268e+0 ⁴ (1.10e-1) \ddagger
	8	1500	2.3268e+0 ⁴ (6.94e-2) \ddagger	2.3172e+0 ⁴ (1.50e+0) \ddagger	2.2020e+0 ⁴ (4.11e-1) \ddagger	2.1761e+0 ⁴ (5.68e+0) \ddagger	2.3317e+0 ⁴ (1.02e+0) \ddagger	2.3124e+0 ⁴ (1.29e+0) \ddagger	2.2290e+0 ⁴ (2.42e+0) \ddagger	2.3469e+0 ⁴ (1.12e+0) \ddagger
	10	2000	9.3930e+0 ³ (1.83e-1) \ddagger	9.3691e+0 ³ (2.49e-1) \ddagger	8.5819e+0 ³ (2.30e+0) \ddagger	8.5613e+0 ³ (3.54e-1) \ddagger	9.3561e+0 ³ (4.35e-1) \ddagger	8.9352e+0 ³ (2.35e+0) \ddagger	8.9662e+0 ³ (1.32e+0) \ddagger	9.4971e+0 ³ (4.99e-1) \ddagger
	3	400	4.5450e+0 ² (7.36e-3) \ddagger	5.0357e+0 ² (1.19e-2) \ddagger	5.4487e+0 ² (6.92e-3) \ddagger	5.2458e+0 ² (8.69e-2) \ddagger	5.4781e+0 ² (8.26e-3) \ddagger	5.0143e+0 ² (5.70e-3) \ddagger	5.4813e+0 ² (5.70e-3) \ddagger	5.4986e+0 ² (8.40e-3) \ddagger
	5	600	1.0144e+0 ² (4.59e-2) \ddagger	1.0646e+0 ² (6.39e-2) \ddagger	1.0573e+0 ² (7.78e-2) \ddagger	1.0314e+0 ² (1.17e-1) \ddagger	1.0506e+0 ² (3.88e-2) \ddagger	1.0688e+0 ² (5.82e-2) \ddagger	1.1068e+0 ² (2.70e-2) \ddagger	1.1285e+0 ² (1.76e-1) \ddagger
DTLZ1 ⁻¹	3	400	4.5450e+0 ² (7.36e-3) \ddagger	5.0357e+0 ² (1.19e-2) \ddagger	5.4487e+0 ² (6.92e-3) \ddagger	5.2458e+0 ² (8.69e-2) \ddagger	5.4781e+0 ² (8.26e-3) \ddagger	5.0143e+0 ² (5.70e-3) \ddagger	5.4813e+0 ² (5.70e-3) \ddagger	5.4986e+0 ² (8.40e-3) \ddagger
	5	600	1.0144e+0 ² (4.59e-2) \ddagger	1.0646e+0 ² (6.39e-2) \ddagger	1.0573e+0 ² (7.78e-2) \ddagger	1.0314e+0 ² (1.17e-1) \ddagger	1.0506e+0 ² (3.88e-2) \ddagger	1.0688e+0 ² (5.82e-2) \ddagger	1.1068e+0 ² (2.70e-2) \ddagger	1.1285e+0 ² (1.76e-1) \ddagger
	8	750	1.3368e+0 ² (3.45e-1) \ddagger	1.9372e+0 ² (1.28e-1) \ddagger	1.8684e+0 ² (2.00e-1) \ddagger	1.7016e+0 ² (4.05e-1) \ddagger	2.0045e+0 ² (1.50e-1) \ddagger	1.2194e+0 ² (9.80e-1) \ddagger	2.0438e+0 ² (1.43e-1) \ddagger	2.0731e+0 ² (1.52e-1) \ddagger
	10	1000	1.5706e+0 ² (3.75e-1) \ddagger	2.8502e+0 ² (2.52e-1) \ddagger	2.7694e+0 ² (3.04e-1) \ddagger	2.3545e+0 ² (4.04e-1) \ddagger	2.9597e+0 ² (2.18e-1) \ddagger	1.3324e+0 ² (1.38e+0) \ddagger	2.9997e+0 ² (1.45e-1) \ddagger	2.9963e+0 ² (7.34e-2) \ddagger
	3	250	6.6915e+0 ² (6.31e-2) \ddagger	6.6084e+0 ² (2.06e-2) \ddagger	6.6550e+0 ² (2.37e-3) \ddagger	6.5580e+0 ² (5.06e-2) \ddagger	6.6913e+0 ² (4.93e-3) \ddagger	6.6548e+0 ² (1.71e-2) \ddagger	6.6984e+0 ² (3.37e-3) \ddagger	6.6887e+0 ² (5.33e-3) \ddagger
DTLZ2 ⁻¹	3	400	6.6915e+0 ² (6.31e-2) \ddagger	6.6084e+0 ² (2.06e-2) \ddagger	6.6550e+0 ² (2.37e-3) \ddagger	6.5580e+0 ² (5.06e-2) \ddagger	6.6913e+0 ² (4.93e-3) \ddagger	6.6548e+0 ² (1.71e-2) \ddagger	6.6984e+0 ² (3.37e-3) \ddagger	6.6887e+0 ² (5.33e-3) \ddagger
	5	350	1.7350e+0 ² (7.17e-2) \ddagger	1.6832e+0 ² (9.30e-2) \ddagger	1.6950e+0 ² (6.17e-1) \ddagger	1.6938e+0 ² (7.37e-2) \ddagger	1.7522e+0 ² (4.65e-2) \ddagger	1.7054e+0 ² (1.04e-1) \ddagger	1.7614e+0 ² (3.04e-2) \ddagger	1.7552e+0 ² (2.60e-2) \ddagger
	8	500	4.3990e+0 ¹ (4.87e-1) \ddagger	4.2426e+0 ¹ (3.75e-1) \ddagger	3.8518e+0 ¹ (6.78e-1) \ddagger	4.2396e+0 ¹ (5.65e-1) \ddagger	4.5101e+0 ¹ (3.84e-1) \ddagger	4.2129e+0 ¹ (6.66e-1) \ddagger	4.4648e+0 ¹ (2.96e-1) \ddagger	4.2317e+0 ¹ (2.98e-1) \ddagger
	10	750	7.8889e+0 ¹ (1.37e+0) \ddagger	7.8261e+0 ¹ (7.14e-1) \ddagger	7.9388e+0 ¹ (6.67e+0) \ddagger	7.7239e+0 ¹ (2.07e+0) \ddagger	7.1760e+0 ¹ (5.00e+0) \ddagger	8.4057e+0 ¹ (4.47e+0) \ddagger	8.6857e+0 ¹ (2.33e+0) \ddagger	8.4437e+0 ¹ (2.14e+0) \ddagger
	3	400	4.7297e+0 ² (7.80e-2) \ddagger	4.8344e+0 ² (2.11e-2) \ddagger	4.8347e+0 ² (6.18e-3) \ddagger	3.5702e+0 ² (1.24e+0) \ddagger	4.8721e+0 ² (1.16e-2) \ddagger	4.8326e+0 ² (3.60e-2) \ddagger	4.7976e+0 ² (3.47e-2) \ddagger	4.8112e+0 ² (3.35e-2) \ddagger
WFG1 ⁻¹	3	500	7.1737e+0 ⁷ (5.41e-1) \ddagger	8.2922e+0 ⁷ (4.84e-2) \ddagger	8.0706e+0 ⁷ (7.23e-2) \ddagger	7.7205e+0 ⁷ (1.39e+0) \ddagger	8.4054e+0 ⁷ (2.05e-2) \ddagger	6.4316e+0 ⁷ (2.78e-1) \ddagger	8.2817e+0 ⁷ (7.09e-1) \ddagger	8.2871e+0 ⁷ (1.04e-2) \ddagger
	5	1000	2.8094e+0 ⁷ (3.14e-1) \ddagger	2.8205e+0 ⁷ (6.18e-2) \ddagger	2.8597e+0 ⁷ (3.19e-2) \ddagger	2.8136e+0 ⁷ (2.40e-1) \ddagger	2.8841e+0 ⁷ (5.88e-2) \ddagger	2.8469e+0 ⁷ (9.17e-2) \ddagger	2.8217e+0 ⁷ (7.09e-1) \ddagger	2.8497e+0 ⁷ (6.42e-2) \ddagger
	8	1500	2.0994e+0 ⁷ (2.08e-1) \ddagger	2.0469e+0 ⁷ (2.17e+0) \ddagger	2.9233e+0 ⁷ (3.48e-0) \ddagger	2.1454e+0 ⁷ (2.08e+0) \ddagger	2.1455e+0 ⁷ (2.54e+0) \ddagger	2.1400e+0 ⁷ (2.54e+0) \ddagger	2.1702e+0 ⁷ (2.16e+0) \ddagger	2.1720e+0 ⁷ (2.14e+0) \ddagger
	10	2000	1.7154e+0 ⁷ (1.76e-1) \ddagger	1.8623e+0 ⁷ (1.27e-1) \ddagger	1.5983e+0 ⁷ (2.80e-1) \ddagger	1.7039e+0 ⁷ (1.79e-1) \ddagger	1.8383e+0 ⁷ (2.02e-1) \ddagger	9.8401e+0 ⁷ (1.58e+0) \ddagger	1.5730e+0 ⁷ (1.61e+0) \ddagger	1.6521e+0 ⁷ (1.96e+0) \ddagger
	3	400	5.4401e+0 ⁹ (9.25e-3) \ddagger	5.4233e+0 ⁹ (7.23e-2) \ddagger	5.4510e+0 ⁹ (5.89e-3) \ddagger	5.3996e+0 ⁹ (4.84e-2) \ddagger	5.4745e+0 ⁹ (7.08e-3) \ddagger	5.4705e+0 ⁹ (5.75e-3) \ddagger	5.4956e+0 ⁹ (5.90e-3) \ddagger	5.4893e+0 ⁹ (4.86e-3) \ddagger
WFG3 ⁻¹	5	500	1.0251e+0 ⁹ (7.30e-2) \ddagger	1.0654e+0 ⁹ (6.85e-2) \ddagger	1.0161e+0 ⁹ (6.25e-2) \ddagger	1.0195e+0 ⁹ (4.10e-2) \ddagger	1.0598e+0 ⁹ (4.51e-2) \ddagger	1.1076e+0 ⁹ (1.76e-2) \ddagger	1.1269e+0 ⁹ (1.14e-2) \ddagger	1.1269e+0 ⁹ (1.14e-2) \ddagger
	8	1500	1.3883e+0 ⁹ (3.68e-2) \ddagger	1.9482e+0 ⁹ (1.77e-1) \ddagger	1.4748e+0 ⁹ (1.19e-1) \ddagger	1.6738e+0 ⁹ (1.62e-1) \ddagger	1.2500e+0 ⁹ (1.76e-1) \ddagger	1.3604e+0 ⁹ (1.36		

Consequently, it is less likely to reduce the cardinality of the population. Furthermore, when the number of selected solutions is larger than the population size, crowding solutions are deleted until the population size is reached. Regarding the performance of NSGA-III and MOEA/D with our adaptation method, results in terms of HV and SPD indicate that they are competitive against state-of-the-art MOEAs on MOPs with disconnected, inverted linear, inverted convex, and inverted concave PF shapes. Also, MOEA/D-AdaRSE and MOEA/D-AdaCOU show a competitive performance in terms of HV on MOPs with mostly degenerated PF shapes such as DTLZ5 with 5, 8, and 10 objective functions and WFG3. Furthermore, MOEAs with our adaptation method show good results on IMOP6, IMOP7, IMOP8, and all MOPs from the VNT test suite due to the capability of our adaptation method to promote an invariant performance regardless of the PF shape. Finally, it is worth noting that our adaptation method does not modify the main framework of MOEAs since it only provides an adapted WVRS employed by MOEAs during their environmental selection. Consequently, the performance of MOEAs with our adaptation method can be improved by modifying their main frameworks. Especially the performance of RVEA with our adaptation method can be further enhanced by modifying its environmental selection to avoid providing approximation sets with fewer solutions than the population size. These results show that our adaptation method can make MOEAs that originally do not perform well on MOPs with irregular PF shapes competitive against state-of-the-art MOEAs.

Table 12: Mean and standard deviations (in parenthesis) of the SPD indicator obtained by state-of-the-art MOEAs, MOEA/D-AdaRSE, and MOEA/D-AdaCOU on MOPs with irregular PF shapes. The two best mean values per MOP are highlighted in grayscale, where the darker tone corresponds to the best one. The symbols in the tuples (+, -, =) and (\oplus , \ominus , \approx) are placed when the MOEA performs significantly better, significantly worse, or statistically equivalent to MOEA/D-AdaRSE and MOEA/D-AdaCOU, respectively, based on a one-tailed Wilcoxon test using a significance level of $\alpha = 0.05$. The superscripts are the obtained rank in the comparison.

MOP	Obj.	Gen.	Two_Arch2	VaEA	AR-MOEA	hpEA	PREA	RVEA-IGNG	MOEA/D-AdaRSE	MOEA/D-AdaCOU
DTLZ5	3	400	1.0469e+1 ⁶ (7.49e-3) $\frac{+}{\ominus}$	1.0501e+1 ⁶ (1.49e-2) $\frac{+}{\ominus}$	1.0484e+1 ⁶ (6.88e-3) $\frac{+}{\ominus}$	1.0500e+1 ² (9.61e-3) $\frac{+}{\ominus}$	1.0486e+1 ⁴ (6.64e-3) $\frac{+}{\ominus}$	1.0488e+1 ³ (5.65e-3) $\frac{+}{\ominus}$	1.0441e+1 ⁸ (8.88e-3) $\frac{+}{\ominus}$	1.0443e+1 ⁷ (8.95e-3)
	5	600	2.5827e+1 ⁴ (4.03e-0) $\frac{+}{\ominus}$	2.3549e+1 ³ (9.51e-1) $\frac{+}{\ominus}$	2.4956e+1 ² (3.84e-1) $\frac{+}{\ominus}$	9.2231e+0 ³ (5.61e-1) $\frac{+}{\ominus}$	1.7405e+1 ⁶ (2.64e+0) $\frac{+}{\ominus}$	2.1969e+1 ⁴ (3.66e+0) $\frac{+}{\ominus}$	1.7421e+1 ⁵ (2.46e+0) $\frac{+}{\ominus}$	1.6918e+1 ⁷ (2.53e+0)
	8	750	4.5974e+1 ⁴ (1.60e+0) $\frac{+}{\ominus}$	6.8175e+1 ³ (5.69e+0) $\frac{+}{\ominus}$	4.6964e+1 ³ (2.59e+0) $\frac{+}{\ominus}$	1.7884e+1 ⁸ (2.10e+0) $\frac{+}{\ominus}$	5.8321e+1 ² (2.73e+0) $\frac{+}{\ominus}$	4.0304e+1 ⁵ (2.10e+0) $\frac{+}{\ominus}$	1.9340e+17 (3.18e+0) $\frac{+}{\ominus}$	2.3886e+1 ⁶ (3.11e+0)
	10	1000	7.2133e+1 ² (2.86e+0) $\frac{+}{\ominus}$	1.5726e+2 ¹ (3.13e+1) $\frac{+}{\ominus}$	7.4173e+1 ⁰ (5.92e+0) $\frac{+}{\ominus}$	2.3438e+1 ⁸ (3.01e+0) $\frac{+}{\ominus}$	1.1106e+2 ¹ (4.73e+0) $\frac{+}{\ominus}$	6.3952e+1 ⁵ (3.34e+0) $\frac{+}{\ominus}$	2.4657e+17 (3.57e+0) $\frac{+}{\ominus}$	3.2873e+1 ⁶ (1.96e+0)
DTLZ7	3	1000	2.1881e+1 ⁴ (5.03e-0) $\frac{+}{\ominus}$	2.4040e+1 ² (3.22e+0) $\frac{+}{\ominus}$	2.1259e+1 ⁶ (6.33e+0) $\frac{+}{\ominus}$	1.9958e+1 ⁷ (3.47e+0) $\frac{+}{\ominus}$	1.8751e+1 ⁸ (5.73e+0) $\frac{+}{\ominus}$	2.1364e+1 ⁵ (4.94e+0) $\frac{+}{\ominus}$	2.3538e+1 ² (4.12e+0) $\frac{+}{\ominus}$	2.3421e+1 ³ (5.02e-1)
	5	1000	1.2584e+2 ⁴ (1.71e+0) $\frac{+}{\ominus}$	1.5458e+2 ² (1.63e+0) $\frac{+}{\ominus}$	1.2435e+2 ⁵ (2.03e+0) $\frac{+}{\ominus}$	1.2192e+2 ⁶ (2.11e+1) $\frac{+}{\ominus}$	1.2196e+2 ³ (1.27e+1) $\frac{+}{\ominus}$	1.3462e+2 ² (1.56e+0) $\frac{+}{\ominus}$	1.2045e+2 ⁵ (1.19e+1) $\frac{+}{\ominus}$	1.1139e+2 ⁸ (9.80e+0)
	8	1000	1.5184e+2 ⁴ (2.57e+0) $\frac{+}{\ominus}$	1.4425e+2 ² (7.74e-1) $\frac{+}{\ominus}$	1.0478e+2 ⁸ (2.48e+0) $\frac{+}{\ominus}$	1.4769e+2 ² (1.72e+0) $\frac{+}{\ominus}$	1.5538e+2 ¹ (1.65e-1) $\frac{+}{\ominus}$	1.5169e+2 ³ (3.13e+0) $\frac{+}{\ominus}$	1.2014e+2 ⁶ (1.17e+0) $\frac{+}{\ominus}$	1.1522e+2 ⁷ (5.07e+0)
	10	1500	2.7102e+2 ⁴ (8.50e+0) $\frac{+}{\ominus}$	1.6070e+2 ² (3.88e+0) $\frac{+}{\ominus}$	2.6474e+2 ⁴ (2.17e+0) $\frac{+}{\ominus}$	2.7340e+2 ⁵ (3.56e-3) $\frac{+}{\ominus}$	2.7340e+2 ⁴ (1.90e+0) $\frac{+}{\ominus}$	1.9025e+2 ⁶ (9.33e-1) $\frac{+}{\ominus}$	1.8818e+2 ⁷ (1.39e+0) $\frac{+}{\ominus}$	
WFG2	3	400	2.0265e+1 ³ (1.35e+0) $\frac{+}{\ominus}$	1.8251e+1 ⁷ (6.91e-1) $\frac{+}{\ominus}$	2.0675e+1 ² (2.95e-1) $\frac{+}{\ominus}$	1.6713e+1 ⁸ (7.22e-1) $\frac{+}{\ominus}$	2.1077e+1 ¹ (3.11e+0) $\frac{+}{\ominus}$	1.8725e+1 ⁰ (5.05e-1) $\frac{+}{\ominus}$	1.8938e+1 ¹ (3.79e-1) $\frac{+}{\ominus}$	1.8909e+1 ⁵ (4.08e-1)
	5	750	3.5584e+1 ⁵ (1.46e+0) $\frac{+}{\ominus}$	3.1165e+1 ² (1.51e+0) $\frac{+}{\ominus}$	4.0502e+1 ⁶ (5.24e-1) $\frac{+}{\ominus}$	2.8934e+1 ⁷ (5.69e+0) $\frac{+}{\ominus}$	4.9827e+1 ¹ (1.90e+0) $\frac{+}{\ominus}$	2.7773e+1 ² (1.23e+0) $\frac{+}{\ominus}$	3.6620e+1 ³ (3.92e-1) $\frac{+}{\ominus}$	3.6461e+1 ⁴ (4.54e+0)
	8	1500	3.5150e+1 ⁵ (1.40e+0) $\frac{+}{\ominus}$	3.0272e+1 ² (2.11e+0) $\frac{+}{\ominus}$	5.3186e+1 ² (7.11e-1) $\frac{+}{\ominus}$	2.1155e+1 ⁸ (2.05e+0) $\frac{+}{\ominus}$	7.8084e+1 ¹ (3.24e+0) $\frac{+}{\ominus}$	2.4136e+1 ⁷ (1.40e+0) $\frac{+}{\ominus}$	4.4678e+1 ³ (9.55e-1) $\frac{+}{\ominus}$	
	10	2000	3.8319e+1 ⁵ (1.55e+0) $\frac{+}{\ominus}$	3.1163e+1 ² (2.12e+0) $\frac{+}{\ominus}$	7.1444e+1 ⁶ (1.44e+0) $\frac{+}{\ominus}$	2.3946e+1 ⁸ (4.15e+0) $\frac{+}{\ominus}$	1.1293e+2 ¹ (4.15e+0) $\frac{+}{\ominus}$	6.2559e+1 ⁴ (1.67e+0) $\frac{+}{\ominus}$	5.2704e+1 ³ (1.35e+0) $\frac{+}{\ominus}$	
WFG3	3	400	1.2937e+1 ² (3.27e-1) $\frac{+}{\ominus}$	1.2639e+1 ³ (5.28e-1) $\frac{+}{\ominus}$	1.3169e+1 ⁹ (3.29e-1) $\frac{+}{\ominus}$	1.0114e+1 ⁸ (5.24e-1) $\frac{+}{\ominus}$	1.0317e+1 ⁷ (3.74e-1) $\frac{+}{\ominus}$	1.2584e+1 ⁴ (4.51e-1) $\frac{+}{\ominus}$	1.2515e+1 ⁵ (3.56e-1) $\frac{+}{\ominus}$	1.2232e+1 ⁶ (3.28e-1)
	5	750	3.9618e+1 ⁴ (6.04e-0) $\frac{+}{\ominus}$	3.9633e+1 ³ (7.87e-1) $\frac{+}{\ominus}$	4.4344e+1 ¹ (6.88e-1) $\frac{+}{\ominus}$	1.9548e+1 ⁸ (1.43e-0) $\frac{+}{\ominus}$	4.1368e+1 ² (9.35e-1) $\frac{+}{\ominus}$	3.9096e+1 ⁵ (0.10e-1) $\frac{+}{\ominus}$	3.8083e+1 ⁷ (1.66e+0) $\frac{+}{\ominus}$	3.8644e+1 ⁶ (1.52e+0)
	8	1500	5.2592e+1 ⁴ (1.24e+0) $\frac{+}{\ominus}$	7.3783e+1 ³ (7.20e+0) $\frac{+}{\ominus}$	7.9183e+1 ² (1.80e+0) $\frac{+}{\ominus}$	5.9908e+1 ⁸ (1.85e+0) $\frac{+}{\ominus}$	7.6853e+1 ² (1.80e+0) $\frac{+}{\ominus}$	6.6919e+1 ⁴ (2.24e+0) $\frac{+}{\ominus}$	6.9430e+1 ⁴ (2.97e+0) $\frac{+}{\ominus}$	6.6311e+1 ⁶ (2.75e+0)
	10	2000	6.7671e+1 ⁴ (1.55e+0) $\frac{+}{\ominus}$	1.1181e+2 ² (2.88e+0) $\frac{+}{\ominus}$	1.2677e+2 ² (4.50e+0) $\frac{+}{\ominus}$	1.6093e+1 ⁹ (2.12e+0) $\frac{+}{\ominus}$	1.8236e+2 ¹ (2.71e+0) $\frac{+}{\ominus}$	1.0146e+2 ⁶ (2.21e+0) $\frac{+}{\ominus}$	1.1130e+2 ⁴ (4.28e+0) $\frac{+}{\ominus}$	1.0948e+2 ⁵ (3.86e-1) $\frac{+}{\ominus}$
DTLZ1-1	3	400	2.2126e+1 ⁷ (1.21e-1) $\frac{+}{\ominus}$	2.2434e+1 ⁵ (1.68e-1) $\frac{+}{\ominus}$	2.2248e+1 ⁶ (1.31e-1) $\frac{+}{\ominus}$	2.0065e+1 ⁸ (9.60e-1) $\frac{+}{\ominus}$	2.2782e+1 ² (1.75e-1) $\frac{+}{\ominus}$	2.3004e+1 ³ (8.82e-2) $\frac{+}{\ominus}$	2.3103e+1 ² (6.64e-2) $\frac{+}{\ominus}$	2.3134e+1 ³ (3.40e-2)
	5	600	5.2140e+1 ⁵ (6.58e-0) $\frac{+}{\ominus}$	6.4171e+1 ² (8.60e-1) $\frac{+}{\ominus}$	6.2515e+1 ⁶ (1.07e+0) $\frac{+}{\ominus}$	5.8811e+1 ⁷ (1.17e+0) $\frac{+}{\ominus}$	6.5811e+1 ¹ (1.56e-1) $\frac{+}{\ominus}$	6.6915e+1 ⁵ (5.50e-1) $\frac{+}{\ominus}$	6.5176e+1 ² (7.93e-1) $\frac{+}{\ominus}$	6.6198e+1 ⁰ (4.18e-1) $\frac{+}{\ominus}$
	8	750	1.0178e+1 ⁸ (2.13e+0) $\frac{+}{\ominus}$	1.0502e+2 ² (1.05e+0) $\frac{+}{\ominus}$	8.8817e+1 ² (1.98e+0) $\frac{+}{\ominus}$	7.7221e+1 ⁸ (3.16e+0) $\frac{+}{\ominus}$	1.0336e+2 ² (1.36e+1) $\frac{+}{\ominus}$	4.6324e+1 ⁷ (6.13e+0) $\frac{+}{\ominus}$	1.0518e+2 ² (7.55e-1) $\frac{+}{\ominus}$	9.9943e+1 ⁴ (7.24e-1)
	10	1000	4.0223e+1 ⁸ (1.63e+0) $\frac{+}{\ominus}$	1.5560e+2 ² (2.38e+0) $\frac{+}{\ominus}$	1.4469e+2 ² (3.58e+0) $\frac{+}{\ominus}$	1.1894e+2 ² (3.45e+0) $\frac{+}{\ominus}$	1.6397e+2 ² (1.89e+0) $\frac{+}{\ominus}$	4.6606e+1 ⁷ (8.48e-1) $\frac{+}{\ominus}$	1.6896e+2 ⁰ (1.10e+0) $\frac{+}{\ominus}$	1.5303e+2 ⁴ (8.87e-1) $\frac{+}{\ominus}$
DTLZ2-1	3	250	2.9763e+1 ³ (4.40e-1) $\frac{+}{\ominus}$	2.8506e+1 ² (5.41e-1) $\frac{+}{\ominus}$	2.8829e+1 ⁵ (1.19e-1) $\frac{+}{\ominus}$	2.1838e+1 ³ (1.69e-1) $\frac{+}{\ominus}$	3.0178e+1 ² (3.67e-1) $\frac{+}{\ominus}$	2.8534e+1 ⁴ (6.36e-1) $\frac{+}{\ominus}$	3.0463e+1 ¹ (8.87e-1) $\frac{+}{\ominus}$	2.9625e+1 ⁴ (4.19e-1)
	5	350	1.0373e+2 ⁴ (1.58e+0) $\frac{+}{\ominus}$	1.1638e+1 ² (1.31e+0) $\frac{+}{\ominus}$	1.1943e+2 ⁴ (1.71e+0) $\frac{+}{\ominus}$	1.0729e+2 ⁶ (2.94e+0) $\frac{+}{\ominus}$	1.1255e+2 ² (1.47e+0) $\frac{+}{\ominus}$	1.0602e+2 ² (1.78e+0) $\frac{+}{\ominus}$	1.1975e+2 ² (1.30e+0) $\frac{+}{\ominus}$	1.2234e+2 ² (7.86e-1)
	8	500	1.2362e+2 ⁴ (1.46e+0) $\frac{+}{\ominus}$	1.3905e+2 ² (5.91e-1) $\frac{+}{\ominus}$	1.2334e+2 ⁸ (3.75e+0) $\frac{+}{\ominus}$	1.3038e+2 ⁶ (2.52e+0) $\frac{+}{\ominus}$	1.3692e+2 ⁴ (1.12e+0) $\frac{+}{\ominus}$	1.4350e+2 ⁵ (2.11e+0) $\frac{+}{\ominus}$	1.4158e+2 ² (2.18e+0) $\frac{+}{\ominus}$	1.4517e+2 ⁴ (1.54e+0) $\frac{+}{\ominus}$
	10	750	2.0292e+2 ⁴ (2.99e+0) $\frac{+}{\ominus}$	2.3474e+2 ² (1.78e+0) $\frac{+}{\ominus}$	1.9490e+2 ⁸ (6.85e+0) $\frac{+}{\ominus}$	2.2748e+2 ² (4.15e+0) $\frac{+}{\ominus}$	2.3712e+2 ² (2.33e+0) $\frac{+}{\ominus}$	2.3591e+2 ² (2.74e+0) $\frac{+}{\ominus}$	2.3742e+2 ³ (3.40e+0) $\frac{+}{\ominus}$	2.4443e+2 ² (3.99e+0) $\frac{+}{\ominus}$
DTLZ5-1	3	400	2.5425e+1 ² (8.18e-1) $\frac{+}{\ominus}$	2.4373e+1 ⁷ (4.64e-1) $\frac{+}{\ominus}$	2.4572e+1 ⁶ (9.11e-1) $\frac{+}{\ominus}$	1.9850e+1 ⁸ (1.27e+0) $\frac{+}{\ominus}$	2.5367e+1 ¹ (3.01e-1) $\frac{+}{\ominus}$	2.4616e+1 ⁵ (5.66e-1) $\frac{+}{\ominus}$	2.6463e+1 ³ (1.36e-1) $\frac{+}{\ominus}$	2.5919e+1 ² (2.05e-1) $\frac{+}{\ominus}$
	5	600	8.4538e+1 ⁵ (1.09e+0) $\frac{+}{\ominus}$	9.0191e+1 ² (1.19e+0) $\frac{+}{\ominus}$	8.5042e+1 ⁶ (1.28e+0) $\frac{+}{\ominus}$	8.0587e+1 ⁸ (1.97e+0) $\frac{+}{\ominus}$	8.1550e+1 ² (1.24e+0) $\frac{+}{\ominus}$	8.6332e+1 ⁵ (1.48e+0) $\frac{+}{\ominus}$	1.0021e+2 ² (4.84e-1) $\frac{+}{\ominus}$	1.0185e+2 ⁴ (4.88e-1) $\frac{+}{\ominus}$
	8	750	1.0883e+2 ⁴ (1.57e+0) $\frac{+}{\ominus}$	1.2396e+2 ² (1.57e+0) $\frac{+}{\ominus}$	1.0647e+2 ⁷ (3.86e+0) $\frac{+}{\ominus}$	1.0291e+2 ⁹ (3.13e+0) $\frac{+}{\ominus}$	1.1964e+2 ² (2.09e+0) $\frac{+}{\ominus}$	1.1696e+2 ² (3.36e+0) $\frac{+}{\ominus}$	1.2906e+2 ² (2.03e+0) $\frac{+}{\ominus}$	1.3174e+2 ⁴ (1.68e+0) $\frac{+}{\ominus}$
	10	1000	1.7387e+2 ⁴ (2.13e+0) $\frac{+}{\ominus}$	2.1472e+2 ² (2.27e+0) $\frac{+}{\ominus}$	1.6626e+2 ² (5.05e+0) $\frac{+}{\ominus}$	1.5918e+2 ⁹ (1.54e+0) $\frac{+}{\ominus}$	1.7053e+2 ² (8.01e-1) $\frac{+}{\ominus}$	1.5246e+0 ² (1.17e+0) $\frac{+}{\ominus}$	1.5977e+2 ⁶ (2.09e+0) $\frac{+}{\ominus}$	1.5886e+2 ⁷ (2.42e+0) $\frac{+}{\ominus}$
WFG1 ⁻¹	3	400	1.4517e+1 ³ (1.50e-1) $\frac{+}{\ominus}$	1.4995e+1 ² (1.99e-1) $\frac{+}{\ominus}$	1.4750e+1 ² (1.66e-1) $\frac{+}{\ominus}$	1.2029e+1 ⁸ (2.00e+0) $\frac{+}{\ominus}$	1.3294e+1 ⁷ (1.74e-1) $\frac{+}{\ominus}$	1.4454e+1 ⁴ (1.35e-1) $\frac{+}{\ominus}$	1.3925e+1 ⁵ (2.00e-1) $\frac{+}{\ominus}$	1.3870e+1 ⁶ (2.14e-1) $\frac{+}{\ominus}$
	5	1000	5.5619e+1 ⁶ (1.47e+0) $\frac{+}{\ominus}$	1.4232e+2 ² (1.52e+0) $\frac{+}{\ominus}$	1.0484e+2 ⁶ (1.93e+0) $\frac{+}{\ominus}$	5.9902e+1 ⁴ (3.92e+0) $\frac{+}{\ominus}$	5.9614e+1 ⁵ (1.07e+0) $\frac{+}{\ominus}$	6.2509e+1 ³ (6.23e+0) $\frac{+}{\ominus}$	4.6627e+1 ⁸ (6.23e+0) $\frac{+}{\ominus}$	4.9331e+1 ⁷ (6.11e-1) $\frac{+}{\ominus}$
	8	1000	1.4016e+2 ⁴ (2.78e+0) $\frac{+}{\ominus}$	1.4809e+2 ² (9.24e-1) $\frac{+}{\ominus}$	9					

Table 13: Mean and standard deviations (in parenthesis) of the HV indicator obtained by MOEAs using the NSGA-III framework on MOPs with regular PF shapes. The two best mean values per MOP are highlighted in grayscale, where the darker tone corresponds to the best one. The symbols “+”, “-”, and “=” are placed when the MOEA performs significantly better, significantly worse, or statistically equivalent to NSGA-III based on a one-tailed Wilcoxon test using a significance level of $\alpha = 0.05$. The % of satisfaction refers to the percentage of MOPs where the MOEA performs significantly better or statistically equivalent to NSGA-III. The superscripts are the obtained rank in the comparison.

MOP	Obj.	Gen.	NSGA-III	A-NSGA-III	NSGA-III-AdaRSE	NSGA-III-AdaGAE	NSGA-III-AdaMPT	NSGA-III-AdaCOU	NSGA-III-AdaPT	NSGA-III-AdaKRA
DTLZ1	3	400	7.7868e+0 ⁷ (2.36e-3)	7.7845e+0 ⁸ (3.65e-3)	-	7.7872e+0 ⁸ (1.44e-3)	-	7.7873e+0 ⁸ (1.96e-3)	-	7.7871e+0 ⁸ (2.19e-3)
	5	600	3.1967e+1 ¹ (1.19e-4)	3.1967e+1 ⁸ (3.10e-4)	-	3.1967e+1 ⁵ (1.97e-4)	-	3.1967e+1 ⁸ (1.38e-4)	-	3.1967e+1 ² (1.10e-4)
	8	750	2.5599e+2 ² (1.20e-4)	2.5599e+2 ² (3.11e-4)	-	2.5599e+2 ² (9.23e-5)	-	2.5599e+2 ² (1.42e-4)	-	2.5599e+2 ² (1.13e-4)
	10	1000	1.0240e+3 ² (9.45e-5)	1.0240e+3 ² (3.35e-5)	-	1.0240e+3 ² (1.29e-5)	-	1.0240e+3 ² (8.42e-6)	-	1.0240e+3 ² (1.56e-5)
DTLZ2	3	250	7.4134e+0 ⁸ (1.01e-4)	7.4116e+0 ⁸ (0.75e-4)	-	7.4134e+0 ⁸ (1.34e-4)	-	7.4134e+0 ⁸ (1.44e-4)	-	7.4134e+0 ⁸ (1.52e-4)
	5	350	3.1697e+1 ¹ (1.97e-4)	3.1696e+1 ⁸ (0.50e-4)	-	3.1697e+1 ⁵ (1.53e-4)	-	3.1697e+1 ⁸ (1.96e-4)	-	3.1697e+1 ² (1.35e-4)
	8	500	2.5584e+2 ² (3.97e-4)	2.5584e+2 ² (1.35e-4)	-	2.5584e+2 ² (4.38e-4)	-	2.5584e+2 ² (3.03e-4)	-	2.5584e+2 ² (4.60e-4)
	10	750	1.0239e+3 ² (1.55e-4)	1.0239e+3 ² (3.88e-4)	-	1.0239e+3 ² (1.71e-4)	-	1.0239e+3 ² (1.40e-4)	-	1.0239e+3 ² (1.32e-4)
DTLZ3	3	1000	7.4072e+0 ⁸ (5.50e-3)	7.4037e+0 ⁸ (6.27e-3)	-	7.4072e+0 ⁸ (3.41e-3)	-	7.4066e+0 ⁸ (7.00e-3)	-	7.4066e+0 ⁸ (5.91e-3)
	5	1000	3.1696e+1 ¹ (2.28e-3)	3.1696e+1 ⁸ (2.80e-3)	-	3.1696e+1 ⁷ (0.22e-3)	-	3.1695e+1 ⁸ (2.58e-3)	-	3.1695e+1 ² (2.03e-3)
	8	1000	2.5582e+2 ² (9.60e-3)	2.5582e+2 ² (9.16e-3)	-	2.5582e+2 ² (9.31e-3)	-	2.5582e+2 ² (9.03e-3)	-	2.5582e+2 ² (1.34e-2)
	10	1500	1.0239e+3 ² (1.94e-3)	1.0239e+3 ² (1.31e-3)	-	1.0239e+3 ² (1.53e-4)	-	1.0239e+3 ² (1.05e-3)	-	1.0239e+3 ² (1.77e-3)
DTLZ4	3	600	7.1862e+0 ⁸ (8.66e-1)	7.2980e+0 ⁸ (6.23e-1)	-	7.0044e+0 ⁸ (1.05e-0)	-	7.2661e+0 ⁸ (6.44e-4)	-	7.3000e+0 ⁸ (6.23e-1)
	5	1000	3.1698e+1 ² (2.57e-4)	3.1698e+1 ⁸ (3.32e-4)	-	3.1698e+1 ⁵ (1.27e-4)	-	3.1698e+1 ⁸ (1.12e-4)	-	3.1698e+1 ² (2.33e-4)
	8	1250	2.5584e+2 ² (1.82e-4)	2.5584e+2 ² (6.05e-4)	-	2.5584e+2 ² (2.33e-4)	-	2.5584e+2 ² (2.10e-4)	-	2.5584e+2 ² (1.99e-4)
	10	2000	1.0239e+3 ² (2.84e-4)	1.0239e+3 ² (1.24e-4)	-	1.0239e+3 ² (1.26e-4)	-	1.0239e+3 ² (1.24e-4)	-	1.0239e+3 ² (9.71e-5)
WFG1	3	400	7.3974e+0 ⁸ (1.92e-2)	5.4059e+0 ⁸ (2.11e-2)	-	5.4403e+0 ⁸ (2.67e-2)	-	5.4182e+0 ⁸ (1.94e-2)	-	5.4182e+0 ⁸ (2.47e-2)
	5	750	2.0487e+1 ¹ (7.68e-2)	2.0339e+1 ⁸ (7.50e-2)	-	2.0455e+1 ⁶ (1.76e-2)	-	2.0441e+1 ⁸ (6.84e-2)	-	2.0465e+1 ⁵ (7.36e-2)
	8	1500	1.6764e+2 ² (3.65e-0)	1.6363e+2 ² (3.86e-0)	-	1.6668e+2 ² (3.85e-0)	-	1.6660e+2 ² (3.18e-0)	-	1.6597e+2 ² (3.24e-0)
	10	2000	7.8149e+2 ² (1.47e+0)	7.8061e+2 ² (2.36e-1)	-	7.5135e+2 ² (1.81e+1)	-	7.5482e+2 ² (2.41e+1)	-	7.5692e+2 ² (1.91e+1)
WFG4	3	400	7.3736e+0 ⁸ (5.60e-3)	7.3657e+0 ⁸ (7.61e-3)	-	7.3717e+0 ⁸ (6.14e-3)	-	7.3716e+0 ⁸ (5.73e-3)	-	7.3714e+0 ⁸ (6.13e-3)
	5	750	3.1558e+1 ³ (1.81e-2)	3.1535e+1 ⁸ (2.18e-2)	-	3.1557e+1 ⁴ (2.46e-2)	-	3.1554e+1 ² (2.32e-2)	-	3.1554e+1 ² (2.09e-2)
	8	1500	2.5539e+2 ² (1.18e-1)	2.5534e+2 ² (1.21e-1)	-	2.5541e+2 ² (9.31e-0)	-	2.5542e+2 ² (1.08e-1)	-	2.5538e+2 ² (1.12e-1)
	10	2000	1.0229e+3 ² (2.20e-1)	1.0229e+3 ² (2.70e-1)	-	1.0230e+3 ² (2.70e-1)	-	1.0230e+3 ² (2.57e-1)	-	1.0229e+3 ² (2.62e-1)
WFG5	3	400	7.2281e+0 ⁸ (1.45e-3)	7.2258e+0 ⁸ (3.53e-3)	-	7.2281e+0 ⁸ (1.05e-3)	-	7.2279e+0 ⁸ (1.63e-3)	-	7.2281e+0 ⁸ (1.27e-3)
	5	750	3.0787e+1 ² (1.62e-3)	3.0785e+1 ⁸ (2.92e-3)	-	3.0787e+1 ⁵ (1.49e-3)	-	3.0787e+1 ⁸ (2.51e-3)	-	3.0787e+1 ² (1.30e-3)
	8	1500	2.4724e+2 ² (6.38e-3)	2.4724e+2 ² (6.13e-3)	-	2.4724e+2 ² (4.39e-3)	-	2.4724e+2 ² (4.85e-3)	-	2.4724e+2 ² (5.06e-3)
	10	2000	9.8697e+2 ² (7.25e-3)	9.8697e+2 ² (4.12e-2)	-	9.8697e+2 ² (7.07e-2)	-	9.8697e+2 ² (6.35e-3)	-	9.8697e+2 ² (6.51e-3)
WFG6	3	400	7.2288e+0 ⁸ (2.23e-2)	7.2333e+0 ⁸ (2.30e-2)	-	7.2263e+0 ⁸ (2.06e-2)	-	7.2344e+0 ⁸ (1.99e-2)	-	7.2261e+0 ⁸ (1.97e-2)
	5	750	3.0608e+1 ² (8.98e-2)	3.0806e+1 ⁸ (7.85e-2)	-	3.0828e+1 ⁵ (6.73e-2)	-	3.0801e+1 ² (7.81e-2)	-	3.0828e+1 ² (7.33e-2)
	8	1500	2.4742e+2 ² (3.68e-2)	2.4742e+2 ² (4.13e-2)	-	2.4742e+2 ² (3.99e-2)	-	2.4742e+2 ² (4.56e-2)	-	2.4742e+2 ² (3.59e-2)
	10	2000	9.8544e+2 ² (3.97e+0)	9.8390e+2 ² (4.75e+0)	-	9.8439e+2 ² (6.63e+0)	-	9.8359e+2 ² (5.07e+0)	-	9.8361e+2 ² (6.37e+0)
WFG7	3	400	7.3857e+0 ⁸ (3.56e-3)	7.3801e+0 ⁸ (5.28e-3)	-	7.3852e+0 ⁸ (4.14e-3)	-	7.3841e+0 ⁸ (4.89e-3)	-	7.3845e+0 ⁸ (5.01e-3)
	5	750	3.1640e+1 ² (7.89e-3)	3.1631e+1 ⁸ (1.23e-2)	-	3.1643e+1 ⁵ (8.14e-3)	-	3.1639e+1 ² (9.58e-3)	-	3.1643e+1 ² (9.81e-3)
	8	1500	2.5574e+2 ² (2.95e-2)	2.5570e+2 ² (4.75e-2)	-	2.5573e+2 ² (3.63e-2)	-	2.5573e+2 ² (3.15e-2)	-	2.5572e+2 ² (3.62e-2)
	10	2000	1.0237e+3 ² (7.68e-2)	1.0236e+3 ² (8.28e-2)	-	1.0237e+3 ² (5.64e-2)	-	1.0237e+3 ² (4.58e-2)	-	1.0237e+3 ² (5.37e-2)
WFG8	3	400	7.2338e+0 ⁸ (1.53e-2)	7.2030e+0 ⁸ (3.27e-2)	-	7.2277e+0 ⁸ (1.60e-2)	-	7.2304e+0 ⁸ (1.52e-2)	-	7.2334e+0 ⁸ (1.42e-2)
	5	750	3.1142e+1 ² (5.03e-2)	3.1072e+1 ⁸ (5.65e-2)	-	3.1136e+1 ⁵ (5.37e-2)	-	3.1121e+1 ² (5.10e-2)	-	3.1124e+1 ² (4.62e-2)
	8	1500	2.5126e+2 ² (4.76e-1)	2.5126e+2 ² (6.33e-2)	-	2.5233e+2 ² (5.01e-1)	-	2.5247e+2 ² (3.76e-2)	-	2.5244e+2 ² (4.02e-1)
	10	2000	1.0157e+3 ² (1.34e-0)	1.0097e+3 ² (2.29e-0)	-	1.0154e+3 ² (1.18e-0)	-	1.0153e+3 ² (1.30e-0)	-	1.0156e+3 ² (1.46e-0)
WFG9	3	400	7.1726e+0 ⁸ (8.56e-2)	7.1696e+0 ⁸ (8.14e-2)	-	7.1698e+0 ⁸ (7.87e-2)	-	7.1676e+0 ⁸ (6.86e-2)	-	7.1682e+0 ⁸ (5.93e-2)
	5	750	3.0826e+1 ² (2.75e-1)	3.0845e+1 ⁸ (2.16e-1)	-	3.0823e+1 ⁵ (2.42e-1)	-	3.0904e+1 ² (1.04e-1)	-	3.0871e+1 ² (2.23e-1)
	8	1500	2.4832e+2 ² (2.35e-0)	2.4806e+2 ² (4.04e-0)	-	2.4826e+2 ² (4.48e-0)	-	2.4796e+2 ² (3.23e-0)	-	2.4812e+2 ² (2.70e-0)
	10	2000	9.9774e+2 ² (1.26e+0)	9.9770e+2 ² (1.72e+0)	-	9.9502e+2 ² (1.72e+0)	-	1.0000e+3 ² (2.69e+0)	-	9.9952e+2 ² (2.35e+0)
IMOP1	2	500	3.9817e+0 ⁸ (6.15e-0)	3.9812e+0 ⁸ (1.80e-3)	-	3.9817e+0 ⁸ (7.41e-0)	-	3.9816e+0 ⁸ (4.91e-5)	-	3.9817e+0 ⁸ (2.94e-4)
	5	500	3.0695e+0 ⁸ (9.37e-4)	3.0647e+0 ⁸ (6.45e-3)	-	3.0649e+0 ⁸ (6.12e-3)	-	3.0662e+0 ⁸ (3.84e-3)	-	3.0339e+0 ⁸ (1.69e-1)
IMOP2	2	500	0/24/22	2/3/41	-	1/5/40	-	3/3/40	-	5/3/38
	5	500	47.83%	93.48%	-	89.13%	-	93.48%	-	89.13%
% of satisfaction										
47.83% 93.48% 89.13% 93.48%										

versions of MOEA/D-Ada \mathcal{K} on MOPs with regular PF shapes in terms of HV and SPD, respectively. The obtained results show that all versions of NSGA-III-Ada \mathcal{K} , RVEA-Ada \mathcal{K} , and MOEA/D-Ada \mathcal{K} can maintain or improve the performance of NSGA-III, RVEA, and MOEA/D, respectively, on most MOPs in terms of HV and SPD. In contrast, A-NSGA-III and RVEA* degrade the performance of their original versions on most MOPs in terms of HV and SPD. Also, AdaW degrades the performance of MOEA/D on most MOPs in terms of HV, while it maintains or improves the performance of MOEA/D on slightly more than half of the MOPs in terms of SPD. However, all versions of MOEA/D-Ada \mathcal{K} maintain or improve the performance of MOEA/D on more MOPs than AdaW based on HV and SPD. Thus, results show that our proposed adaptation method avoids degrading the performance of MOEAs that use a predefined WVRs on most MOPs with regular PF shapes regardless of their algorithmic framework.

3.2 Irregular PF shapes

The performance comparison of NSGA-III, A-NSGA-III, and all versions of NSGA-III-Ada \mathcal{K} on MOPs with irregular PF shapes based on HV and SPD can be observed in Tables 19 and 20, respectively. Then, Tables 21 and 22 show the results of RVEA, RVEA*, and all versions of RVEA-Ada \mathcal{K} on MOPs with irregular PF shapes in terms of HV and SPD, respectively. Finally, the results of MOEA/D, AdaW, and all versions of MOEA/D-Ada \mathcal{K} on MOPs with irregular PF shapes in terms of HV and SPD are shown in Tables 23 and 24, respectively. The obtained results in terms of HV and SPD indicate that all MOEAs with our adaptation method improve the performance of their original versions on most MOPs. Also, RVEA* and AdaW can enhance the performance of RVEA and MOEA/D on most MOPs. However, A-NSGA-III cannot improve the performance of NSGA-III on most MOPs based on HV and SPD. Additionally, it can be seen that

Table 14: Mean and standard deviations (in parenthesis) of the SPD indicator obtained by MOEAs using the NSGA-III framework on MOPs with regular PF shapes. The two best mean values per MOP are highlighted in grayscale, where the darker tone corresponds to the best one. The symbols “+”, “-”, and “=” are placed when the MOEA performs significantly better, significantly worse, or statistically equivalent to NSGA-III based on a one-tailed Wilcoxon test using a significance level of $\alpha = 0.05$. The % of satisfaction refers to the percentage of MOPs where the MOEA performs significantly better or statistically equivalent to NSGA-III. The superscripts are the obtained rank in the comparison.

MOP	Obj.	Gen.	NSGA-III	A-NSGA-III	NSGA-III-AdaRSE	NSGA-III-AdaGAE	NSGA-III-AdaMPT	NSGA-III-AdaCOU	NSGA-III-AdaPT	NSGA-III-AdaKRA
DTLZ1	3	400	$2.3395e+1^3$ (1.09e-1)	$2.3325e+1^3$ (2.30e-1)	$-2.3379e+1^3$ (6.90e-2)	$-2.3371e+1^3$ (9.43e-2)	$-2.3371e+1^3$ (7.74e-2)	$-2.3381e+1^3$ (1.04e-1)	$-2.3357e+1^3$ (5.52e-2)	$-2.3388e+1^2$ (8.27e-2)
	5	600	$7.3039e+1^2$ (1.02e-1)	$7.2767e+1^2$ (3.60e-1)	$-7.3070e+1^2$ (1.63e-1)	$-7.3049e+1^2$ (1.07e-1)	$-7.3055e+1^2$ (1.13e-1)	$-7.3098e+1^2$ (1.49e-1)	$-7.3056e+1^2$ (1.01e-1)	$-7.3104e+1^2$ (1.64e-1)
	8	750	$1.0869e+2^2$ (3.79e-1)	$1.0800e+2^2$ (9.47e-1)	$-1.0866e+2^2$ (2.65e-1)	$-1.0882e+2^2$ (3.98e-1)	$-1.0876e+2^2$ (3.50e-1)	$-1.0868e+2^2$ (3.48e-1)	$-1.0846e+2^2$ (1.17e+0)	$-1.0811e+2^2$ (2.42e+0)
	10	1000	$1.7699e+2^2$ (3.30e-1)	$1.7662e+2^2$ (5.99e-1)	$-1.7698e+2^2$ (1.36e-1)	$-1.7683e+2^2$ (1.75e-1)	$-1.7697e+2^2$ (2.79e-1)	$-1.7701e+2^2$ (4.53e-1)	$-1.7607e+2^2$ (4.66e+0)	$-1.7702e+2^2$ (4.04e-1)
DTLZ2	3	250	$3.2763e+1^3$ (4.15e-3)	$3.2614e+1^3$ (1.15e-1)	$-3.2765e+1^3$ (6.86e-3)	$-3.2760e+1^3$ (8.46e-3)	$-3.2763e+1^3$ (5.42e-3)	$-3.2763e+1^3$ (3.97e-3)	$-3.2762e+1^3$ (4.86e-3)	$-3.2762e+1^3$ (6.09e-3)
	5	350	$1.3054e+2^2$ (4.02e-2)	$1.3898e+2^2$ (3.44e-1)	$-1.3055e+2^2$ (4.25e-2)	$-1.3054e+2^2$ (3.06e-2)	$-1.3054e+2^2$ (2.93e-2)	$-1.3052e+2^2$ (3.04e-2)	$-1.3054e+2^2$ (2.63e-2)	$-1.3054e+2^2$ (2.51e-2)
	8	500	$1.4787e+2^2$ (5.15e-2)	$1.4753e+2^2$ (3.01e-1)	$-1.4790e+2^2$ (6.38e-2)	$-1.4790e+2^2$ (6.71e-2)	$-1.4788e+2^2$ (5.98e-2)	$-1.4789e+2^2$ (5.34e-2)	$-1.4788e+2^2$ (6.40e-2)	$-1.4788e+2^2$ (4.62e-2)
	10	750	$2.6059e+2^2$ (8.06e-2)	$2.6026e+2^2$ (2.55e-1)	$-2.6058e+2^2$ (9.03e-2)	$-2.6058e+2^2$ (6.85e-2)	$-2.6058e+2^2$ (5.88e-2)	$-2.6058e+2^2$ (8.27e-2)	$-2.6057e+2^2$ (8.73e-2)	$-2.6057e+2^2$ (8.42e-2)
DTLZ3	3	1000	$3.2921e+1^4$ (1.36e-1)	$3.2819e+1^4$ (1.90e-1)	$-3.2926e+1^4$ (3.87e-2)	$-3.2936e+1^4$ (1.78e-1)	$-3.2938e+1^4$ (1.50e-1)	$-3.2893e+1^4$ (1.06e-1)	$-3.2915e+1^4$ (1.29e-1)	$-3.2915e+1^4$ (1.29e-1)
	5	1000	$1.3978e+2^4$ (2.65e-1)	$1.3918e+2^4$ (6.46e-1)	$-1.3981e+2^4$ (2.61e-1)	$-1.3975e+2^4$ (2.21e-1)	$-1.3982e+2^4$ (3.15e-1)	$-1.3982e+2^4$ (3.43e-1)	$-1.3977e+2^4$ (2.23e-1)	$-1.3977e+2^4$ (2.33e-1)
	8	1000	$4.4809e+2^4$ (2.81e-1)	$4.4712e+2^4$ (6.91e-1)	$-4.4785e+2^4$ (2.75e-1)	$-4.4798e+2^4$ (7.00e-1)	$-4.4786e+2^4$ (9.00e-1)	$-4.4775e+2^4$ (7.90e-1)	$-4.4769e+2^4$ (1.50e+0)	$-4.4791e+2^4$ (9.78e-1)
	10	1500	$6.6059e+2^4$ (1.37e-1)	$6.2014e+2^4$ (2.75e-1)	$-6.6060e+2^4$ (1.75e-1)	$-6.6063e+2^4$ (1.49e-1)	$-6.6059e+2^4$ (1.26e-1)	$-6.6056e+2^4$ (2.37e-1)	$-6.6054e+2^4$ (2.37e-1)	$-6.6054e+2^4$ (2.11e-1)
DTLZ4	3	600	$3.0633e+1^7$ (8.06e-0)	$3.1497e+1^7$ (5.81e-0)	$-2.7958e+1^7$ (1.10e-1)	$-3.0891e+1^7$ (7.16e-0)	$-3.1369e+1^7$ (6.50e-0)	$-3.2323e+1^7$ (2.36e-0)	$-3.0640e+1^7$ (8.06e-0)	$-3.0633e+1^7$ (8.06e-0)
	5	1000	$1.3946e+2^2$ (2.66e-2)	$1.3938e+2^2$ (1.41e-1)	$-1.3946e+2^2$ (2.95e-2)	$-1.3945e+2^2$ (6.75e-2)	$-1.3945e+2^2$ (3.05e-2)	$-1.3945e+2^2$ (2.01e-2)	$-1.3946e+2^2$ (3.02e-2)	$-1.3945e+2^2$ (2.79e-2)
	8	1250	$1.4785e+2^2$ (5.18e-2)	$1.4782e+2^2$ (1.39e-1)	$-1.4785e+2^2$ (4.46e-2)	$-1.4785e+2^2$ (4.14e-2)	$-1.4785e+2^2$ (4.60e-2)	$-1.4785e+2^2$ (5.33e-2)	$-1.4787e+2^2$ (3.84e-2)	$-1.4785e+2^2$ (4.82e-2)
	10	2000	$2.6056e+2^2$ (6.71e-2)	$2.6049e+2^2$ (2.25e-1)	$-2.6059e+2^2$ (6.46e-2)	$-2.6058e+2^2$ (5.79e-2)	$-2.6060e+2^2$ (6.29e-2)	$-2.6058e+2^2$ (7.18e-2)	$-2.6058e+2^2$ (7.63e-2)	$-2.6057e+2^2$ (7.63e-2)
WFG1	3	400	$1.7603e+1^3$ (5.07e-1)	$1.7188e+1^3$ (5.33e-1)	$-1.6597e+1^3$ (4.49e-1)	$-1.6329e+1^3$ (4.00e-1)	$-1.6446e+1^3$ (3.39e-1)	$-1.6370e+1^3$ (3.75e-1)	$-1.6465e+1^3$ (3.02e-1)	$-1.6531e+1^3$ (3.76e-1)
	5	750	$3.3548e+1^2$ (6.48e-1)	$3.2039e+1^2$ (6.24e-1)	$-3.3411e+1^2$ (6.81e-1)	$-3.2868e+1^2$ (6.89e-1)	$-3.3077e+1^2$ (7.20e-1)	$-3.3039e+1^2$ (7.74e-1)	$-3.3137e+1^2$ (7.84e-1)	$-3.3137e+1^2$ (7.84e-1)
	8	1500	$3.9677e+1^2$ (2.41e-0)	$3.7928e+1^2$ (2.74e-0)	$-3.9594e+1^2$ (2.19e-0)	$-4.0223e+1^2$ (2.41e+0)	$-4.0246e+1^2$ (2.89e-0)	$-4.0091e+1^2$ (2.03e+0)	$-4.0008e+1^2$ (2.20e+0)	$-4.0335e+1^2$ (2.42e+0)
	10	2000	$3.7512e+1^2$ (2.04e+0)	$3.3866e+1^2$ (1.96e+0)	$-4.0868e+1^2$ (1.90e+0)	$-4.0487e+1^2$ (3.13e+0)	$-4.0900e+1^2$ (3.48e+0)	$-4.1395e+1^2$ (3.76e+0)	$-4.1833e+1^2$ (3.61e+0)	$-4.1833e+1^2$ (3.61e+0)
WFG4	3	400	$3.2757e+1^3$ (1.39e-2)	$3.2575e+1^3$ (1.11e-1)	$-3.2730e+1^3$ (3.22e-2)	$-3.2740e+1^3$ (1.66e-2)	$-3.2737e+1^3$ (1.52e-2)	$-3.2735e+1^3$ (2.17e-2)	$-3.2736e+1^3$ (2.42e-2)	$-3.2735e+1^3$ (1.90e-2)
	5	750	$1.3919e+2^2$ (5.32e-2)	$1.3875e+2^2$ (3.70e-1)	$-1.3920e+2^2$ (6.26e-2)	$-1.3920e+2^2$ (5.62e-2)	$-1.3919e+2^2$ (5.55e-2)	$-1.3920e+2^2$ (4.82e-2)	$-1.3919e+2^2$ (5.16e-2)	$-1.3919e+2^2$ (4.57e-2)
	8	1500	$1.4780e+2^2$ (3.97e-2)	$1.4778e+2^2$ (4.11e-1)	$-1.4781e+2^2$ (4.61e-2)	$-1.4778e+2^2$ (4.46e-2)	$-1.4778e+2^2$ (4.47e-2)	$-1.4780e+2^2$ (4.60e-2)	$-1.4778e+2^2$ (4.75e-2)	$-1.4779e+2^2$ (3.36e-2)
	10	2000	$2.6054e+2^2$ (6.12e-2)	$2.6047e+2^2$ (1.64e-1)	$-2.6054e+2^2$ (6.82e-2)	$-2.6053e+2^2$ (6.55e-2)	$-2.6053e+2^2$ (6.26e-2)	$-2.6053e+2^2$ (6.64e-2)	$-2.6053e+2^2$ (5.86e-2)	$-2.6054e+2^2$ (6.45e-2)
WFG5	3	400	$3.2725e+1^4$ (1.46e-2)	$3.2595e+1^4$ (1.25e-1)	$-3.2723e+1^4$ (1.22e-2)	$-3.2717e+1^4$ (3.13e-2)	$-3.2727e+1^4$ (1.27e-2)	$-3.2727e+1^4$ (1.29e-2)	$-3.2726e+1^4$ (1.29e-2)	$-3.2718e+1^4$ (2.44e-2)
	5	750	$1.3931e+2^4$ (2.00e-2)	$1.3900e+2^4$ (3.50e-1)	$-1.3931e+2^4$ (2.15e-2)	$-1.3931e+2^4$ (2.01e-2)	$-1.3931e+2^4$ (1.96e-2)	$-1.3930e+2^4$ (2.01e-2)	$-1.3930e+2^4$ (1.93e-2)	$-1.3930e+2^4$ (1.93e-2)
	8	1500	$1.4779e+2^4$ (1.36e-2)	$1.4777e+2^4$ (2.14e-1)	$-1.4779e+2^4$ (1.19e-2)	$-1.4779e+2^4$ (1.08e-2)	$-1.4779e+2^4$ (9.12e-2)	$-1.4779e+2^4$ (1.84e-2)	$-1.4779e+2^4$ (2.15e-2)	$-1.4779e+2^4$ (2.15e-2)
	10	2000	$2.6049e+2^4$ (2.59e-2)	$2.6036e+2^4$ (1.76e-1)	$-2.6044e+2^4$ (2.75e-2)	$-2.6044e+2^4$ (2.60e-2)	$-2.6044e+2^4$ (2.96e-2)	$-2.6044e+2^4$ (2.72e-2)	$-2.6045e+2^4$ (3.08e-2)	$-2.6045e+2^4$ (3.08e-2)
WFG6	3	400	$3.2763e+1^4$ (1.15e-2)	$3.2554e+1^4$ (1.36e-1)	$-3.2767e+1^4$ (1.16e-2)	$-3.2765e+1^4$ (1.27e-2)	$-3.2761e+1^4$ (1.15e-2)	$-3.2760e+1^4$ (1.04e-2)	$-3.2761e+1^4$ (1.45e-2)	$-3.2760e+1^4$ (1.57e-2)
	5	750	$1.3935e+2^4$ (2.60e-2)	$1.3905e+2^4$ (2.77e-1)	$-1.3937e+2^4$ (2.15e-2)	$-1.3935e+2^4$ (2.85e-2)	$-1.3936e+2^4$ (2.85e-2)	$-1.3936e+2^4$ (2.20e-2)	$-1.3936e+2^4$ (2.52e-2)	$-1.3936e+2^4$ (2.52e-2)
	8	1500	$1.4783e+2^4$ (2.86e-2)	$1.4780e+2^4$ (1.02e-1)	$-1.4783e+2^4$ (2.32e-2)	$-1.4784e+2^4$ (2.92e-2)	$-1.4783e+2^4$ (3.50e-2)	$-1.4783e+2^4$ (4.24e-2)	$-1.4782e+2^4$ (3.36e-2)	$-1.4782e+2^4$ (3.36e-2)
	10	2000	$2.6054e+2^4$ (5.48e-2)	$2.6030e+2^4$ (2.94e-1)	$-2.6053e+2^4$ (6.05e-2)	$-2.6052e+2^4$ (6.20e-2)	$-2.6054e+2^4$ (6.43e-2)	$-2.6054e+2^4$ (5.68e-2)	$-2.6054e+2^4$ (6.49e-2)	$-2.6054e+2^4$ (6.20e-2)
WFG8	3	400	$3.2484e+1^6$ (2.37e-2)	$3.2462e+1^6$ (1.47e-1)	$-3.2485e+1^6$ (2.19e-2)	$-3.2485e+1^6$ (2.10e-2)	$-3.2484e+1^6$ (2.10e-2)	$-3.2484e+1^6$ (2.41e-2)	$-3.2485e+1^6$ (2.10e-2)	$-3.2484e+1^6$ (2.03e-2)
	5	750	$1.3970e+2^6$ (7.95e-2)	$1.3933e+2^6$ (3.35e-1)	$-1.3969e+2^6$ (5.94e-2)	$-1.3972e+2^6$ (6.64e-2)	$-1.3970e+2^6$ (7.71e-2)	$-1.3970e+2^6$ (6.95e-2)	$-1.3970e+2^6$ (8.08e-2)	$-1.3973e+2^6$ (7.47e-2)
	8	1500	$1.4791e+2^6$ (4.16e-2)	$1.4789e+2^6$ (1.16e-1)	$-1.4791e+2^6$ (4.27e-2)	$-1.4791e+2^6$ (4.57e-2)	$-1.4791e+2^6$ (4.16e-2)	$-1.4793e+2^6$ (5.36e-2)	$-1.4792e+2^6$ (4.09e-2)	$-1.4792e+2^6$ (4.09e-2)
	10	2000	$2.6079e+2^6$ (1.04e-1)	$2.6061e+2^6$ (2.96e-1)	$-2.6077e+2^6$ (1.81e-1)	$-2.6076e+2^6$ (1.06e-1)	$-2.6076e+2^6$ (1.39e-1)	$-2.6081e+2^6$ (9.97e-2)	$-2.6077e+2^6$ (9.98e-2)	$-2.6077e+2^6$ (9.98e-2)
WFG9	3	400	$3.2273e+1^8$ (9.43e-2)	$3.2273e+1^8$ (2.34e-1)	$-3.2258e+1^8$ (8.96e-2)	$-3.2255e+1^8$ (8.26e-2)	$-3.2255e+1^8$ (8.12e-2)	$-3.2255e+1^8$ (8.12e-2)	$-3.2257e+1^8$ (9.36e-2)	$-3.2254e+1^8$ (9.16e-2)
	5	750	$1.3910e+2^8$ (7.35e-2)	$1.3858e+2^8$ (4.20e-1)	$-1.3910e+2^8$ (1.00e-1)	$-1.3908e+2^8$ (4.85e-2)	$-1.3908e+2^8$ (1.06e-1)	$-1.3908e+2^8$ (6.63e-2)	$-1.3911e+2^8$ (1.01e-1)	$-1.3911e+2^8$ (8.16e-2)
	8	1500	$1.4774e+2^8$ (2.51e-1)	$1.4649e+2^8$ (6.02e-1)	$-1.4774e+2^8$ (1.21e-1)	$-1.4774e+2^8$ (1.63e-1)	$-1.4775e+2^8$ (1.47e-1)	$-1.4776e+2^8$ (1.79e-1)	$-1.4776e+2^8$ (1.56e-1)	$-1.4773e+2^8$ (2.15e-1)
	10	2000	$2.6019e+2^8$ (6.70e-1)	$2.5850e+2^8</$						

Table 15: Mean and standard deviations (in parenthesis) of the HV indicator obtained by MOEAs using the RVEA framework on MOPs with regular PF shapes. The two best mean values per MOP are highlighted in grayscale, where the darker tone corresponds to the best one. The symbols “+”, “-”, and “=” are placed when the MOEA performs significantly better, significantly worse, or statistically equivalent to RVEA based on a one-tailed Wilcoxon test using a significance level of $\alpha = 0.05$. The % of satisfaction refers to the percentage of MOPs where the MOEA performs significantly better or statistically equivalent to RVEA. The superscripts are the obtained rank in the comparison.

MOP	Obj.	Gen.	RVEA	RVEA*	RVEA-AdaRSE	RVEA-AdaGAE	RVEA-AdaMPT	RVEA-AdaCOU	RVEA-AdaPT	RVEA-AdaKRA
DTLZ1	3	400	7.7876e+0 ³ (2.09e-3)	7.7705e+0 ³ (6.04e-3)	7.7880e+0 ³ (1.72e-3)	7.7873e+0 ³ (1.55e-3)	7.7875e+0 ³ (1.42e-3)	7.7874e+0 ³ (2.52e-3)	7.7874e+0 ³ (2.37e-3)	
	5	600	3.1967e+1 ⁹ (1.30e-4)	3.1958e+1 ⁹ (2.04e-3)	3.1967e+1 ⁹ (1.13e-4)	3.1967e+1 ⁹ (1.03e-4)	3.1967e+1 ⁹ (8.08e-5)	3.1967e+1 ⁹ (8.64e-5)	3.1967e+1 ⁹ (1.29e-4)	3.1967e+1 ⁹ (1.35e-4)
	8	750	2.5599e+2 ⁹ (6.09e-4)	2.5599e+2 ⁹ (5.51e-3)	2.5599e+2 ⁹ (4.43e-4)	2.5599e+2 ⁹ (7.34e-5)	2.5599e+2 ⁹ (2.63e-4)	2.5599e+2 ⁹ (2.13e-4)	2.5599e+2 ⁹ (1.15e-4)	
	10	1000	1.0240e+3 ⁹ (2.67e-6)	1.0240e+3 ⁹ (5.02e-3)	1.0240e+3 ⁹ (3.15e-5)	1.0240e+3 ⁹ (6.98e-6)	1.0240e+3 ⁹ (3.86e-6)	1.0240e+3 ⁹ (4.90e-6)	1.0240e+3 ⁹ (8.14e-6)	
DTLZ2	3	250	7.4131e+0 ³ (1.41e-4)	7.3880e+0 ³ (6.03e-3)	7.4131e+0 ³ (2.11e-4)	7.4132e+0 ³ (2.11e-4)	7.4131e+0 ³ (2.54e-4)	7.4131e+0 ³ (2.03e-4)	7.4131e+0 ³ (2.17e-4)	7.4131e+0 ³ (1.81e-4)
	5	350	3.1698e+1 ⁹ (1.21e-4)	3.1666e+1 ⁹ (8.65e-3)	3.1698e+1 ⁹ (1.40e-4)	3.1698e+1 ⁹ (1.23e-4)	3.1698e+1 ⁹ (1.05e-4)	3.1698e+1 ⁹ (1.09e-4)	3.1698e+1 ⁹ (1.16e-4)	3.1698e+1 ⁹ (1.03e-4)
	8	500	2.5584e+2 ⁹ (1.27e-4)	2.5583e+2 ⁹ (4.93e-4)	2.5584e+2 ⁹ (1.62e-4)	2.5584e+2 ⁹ (1.35e-4)	2.5584e+2 ⁹ (1.74e-4)	2.5584e+2 ⁹ (1.75e-4)	2.5584e+2 ⁹ (1.36e-4)	2.5584e+2 ⁹ (1.65e-4)
	10	750	1.0239e+3 ⁹ (4.97e-5)	1.0239e+3 ⁹ (6.60e-3)	1.0239e+3 ⁹ (5.09e-5)	1.0239e+3 ⁹ (6.75e-5)	1.0239e+3 ⁹ (5.58e-5)	1.0239e+3 ⁹ (5.99e-5)	1.0239e+3 ⁹ (6.64e-5)	1.0239e+3 ⁹ (5.14e-5)
DTLZ3	3	1000	7.4085e+0 ³ (2.98e-3)	7.3844e+0 ³ (1.00e-2)	7.4066e+0 ³ (5.91e-3)	7.4089e+0 ³ (4.33e-3)	7.4088e+0 ³ (3.54e-3)	7.4077e+0 ³ (5.19e-3)	7.4069e+0 ³ (5.03e-3)	7.4079e+0 ³ (4.21e-3)
	5	1000	3.1696e+1 ⁹ (3.17e-3)	3.1670e+1 ⁹ (7.40e-3)	3.1696e+1 ⁹ (1.49e-3)	3.1696e+1 ⁹ (1.04e-3)	3.1696e+1 ⁹ (1.82e-3)	3.1696e+1 ⁹ (1.60e-3)	3.1697e+1 ⁹ (1.41e-3)	3.1697e+1 ⁹ (9.22e-4)
	8	1000	2.5583e+2 ⁹ (4.22e-3)	2.5581e+2 ⁹ (1.04e-2)	2.5583e+2 ⁹ (4.10e-3)	2.5583e+2 ⁹ (4.37e-3)	2.5583e+2 ⁹ (3.26e-3)	2.5583e+2 ⁹ (3.61e-3)	2.5583e+2 ⁹ (4.23e-3)	2.5583e+2 ⁹ (3.40e-3)
	10	1500	1.0239e+3 ⁹ (5.24e-4)	1.0239e+3 ⁹ (4.89e-5)	1.0239e+3 ⁹ (3.02e-5)	1.0239e+3 ⁹ (3.45e-5)	1.0239e+3 ⁹ (3.88e-5)	1.0239e+3 ⁹ (6.51e-4)	1.0239e+3 ⁹ (4.54e-4)	1.0239e+3 ⁹ (4.87e-4)
DTLZ4	3	600	7.4131e+0 ³ (8.27e-5)	7.4020e+0 ³ (7.17e-6)	7.4138e+0 ³ (3.20e-5)	7.4138e+0 ³ (3.34e-5)	7.3802e+0 ³ (3.57e-5)	7.4138e+0 ³ (1.84e-1)	7.4138e+0 ³ (5.38e-5)	7.4138e+0 ³ (3.05e-5)
	5	1000	3.1698e+1 ⁹ (2.36e-5)	3.1681e+1 ⁹ (7.08e-3)	3.1698e+1 ⁹ (2.55e-5)	3.1698e+1 ⁹ (2.77e-5)	3.1698e+1 ⁹ (2.59e-5)	3.1698e+1 ⁹ (3.03e-5)	3.1698e+1 ⁹ (2.25e-5)	3.1698e+1 ⁹ (2.14e-5)
	8	1250	2.5583e+2 ⁹ (1.06e-4)	2.5583e+2 ⁹ (1.54e-4)	2.5583e+2 ⁹ (1.68e-4)	2.5583e+2 ⁹ (6.06e-5)	2.5583e+2 ⁹ (6.52e-5)	2.5583e+2 ⁹ (4.06e-2)	2.5583e+2 ⁹ (7.79e-2)	2.5583e+2 ⁹ (4.04e-2)
	10	2000	1.0239e+3 ⁹ (4.64e-5)	1.0239e+3 ⁹ (2.00e-5)	1.0239e+3 ⁹ (4.29e-5)	1.0239e+3 ⁹ (3.83e-5)	1.0239e+3 ⁹ (4.53e-5)	1.0239e+3 ⁹ (3.40e-5)	1.0239e+3 ⁹ (3.34e-5)	
WFG1	3	400	7.4085e+0 ³ (4.70e-4)	5.2803e+0 ³ (3.41e-2)	5.2736e+0 ³ (3.66e-2)	5.2812e+0 ³ (4.19e-2)	5.2786e+0 ³ (3.57e-2)	5.2747e+0 ³ (3.66e-2)	5.2786e+0 ³ (3.79e-2)	5.2824e+0 ³ (4.08e-2)
	5	750	2.1186e+1 ⁹ (3.40e-4)	1.9492e+1 ⁹ (1.21e-1)	2.0666e+1 ⁹ (2.03e-1)	2.0789e+1 ⁹ (2.35e-1)	2.0902e+1 ⁹ (2.77e-1)	2.0920e+1 ⁹ (2.47e-1)	2.0759e+1 ⁹ (1.95e-1)	2.0727e+1 ⁹ (1.81e-1)
	8	1500	1.8773e+2 ⁹ (4.95e-0)	1.5131e+2 ⁹ (1.46e-0)	1.7263e+2 ⁹ (3.73e-0)	1.7266e+2 ⁹ (4.73e-0)	1.7169e+2 ⁹ (3.93e+0)	1.7366e+2 ⁹ (4.47e+0)	1.7341e+2 ⁹ (4.77e+0)	1.7371e+2 ⁹ (4.34e+0)
	10	2000	9.1929e+2 ⁹ (2.15e+0)	7.1806e+2 ⁹ (2.38e+1)	7.7076e+2 ⁹ (1.99e+1)	7.7482e+2 ⁹ (1.99e+1)	7.8111e+2 ⁹ (2.07e+1)	7.8851e+2 ⁹ (1.85e+1)	7.8249e+2 ⁹ (1.73e+1)	7.7888e+2 ⁹ (1.95e+1)
WFG4	3	400	3.3563e+0 ³ (6.18e-3)	3.73042e+0 ³ (2.38e-2)	3.73453e+0 ³ (1.10e-2)	3.73453e+0 ³ (6.88e-3)	3.73526e+0 ³ (7.97e-3)	3.73526e+0 ³ (8.42e-3)	3.73526e+0 ³ (9.83e-3)	3.73549e+0 ³ (8.45e-3)
	5	750	3.1564e+1 ⁹ (1.84e-2)	3.1209e+1 ⁹ (4.83e-2)	3.1561e+1 ⁹ (1.24e-2)	3.1558e+1 ⁹ (1.99e-2)	3.15162e+1 ⁹ (2.05e-2)	3.1557e+1 ⁹ (2.41e-2)	3.1554e+1 ⁹ (1.89e-2)	3.1554e+1 ⁹ (2.34e-2)
	8	1500	2.5539e+2 ⁹ (9.39e-1)	2.5263e+2 ⁹ (4.51e-1)	2.5534e+2 ⁹ (1.35e-1)	2.5529e+2 ⁹ (1.37e-1)	2.5534e+2 ⁹ (1.31e-1)	2.5533e+2 ⁹ (1.44e-1)	2.5533e+2 ⁹ (1.37e-1)	2.5533e+2 ⁹ (1.13e-1)
	10	2000	1.0231e+3 ⁹ (1.81e-1)	1.0165e+3 ⁹ (2.16e-1)	1.0229e+3 ⁹ (2.77e-1)	1.0229e+3 ⁹ (3.41e-1)	1.0229e+3 ⁹ (2.33e-1)	1.0230e+3 ⁹ (2.55e-1)	1.0231e+3 ⁹ (2.22e-1)	1.0230e+3 ⁹ (2.40e-1)
WFG5	3	400	7.2228e+0 ³ (2.91e-3)	7.1859e+0 ³ (1.98e-2)	7.2199e+0 ³ (1.47e-2)	7.2234e+0 ³ (1.46e-3)	7.2235e+0 ³ (1.79e-3)	7.2235e+0 ³ (2.18e-3)	7.2222e+0 ³ (3.12e-3)	7.2220e+0 ³ (3.90e-3)
	5	750	3.0788e+1 ⁹ (1.83e-4)	3.0663e+1 ⁹ (4.22e-2)	3.0788e+1 ⁹ (2.23e-2)	3.0788e+1 ⁹ (1.91e-2)	3.0788e+1 ⁹ (1.49e-2)	3.0788e+1 ⁹ (1.56e-2)	3.0788e+1 ⁹ (2.13e-2)	
	8	1500	2.4725e+2 ⁹ (2.75e-3)	2.4678e+2 ⁹ (8.57e-2)	2.4726e+2 ⁹ (2.76e-3)	2.4726e+2 ⁹ (2.91e-2)	2.4726e+2 ⁹ (1.88e-3)	2.4726e+2 ⁹ (3.29e-3)	2.4726e+2 ⁹ (2.97e-3)	2.4726e+2 ⁹ (2.49e-3)
	10	2000	9.8697e+2 ⁹ (5.02e-3)	9.8613e+2 ⁹ (1.93e-2)	9.8697e+2 ⁹ (5.26e-3)	9.8696e+2 ⁹ (4.18e-3)	9.8696e+2 ⁹ (3.01e-3)	9.8697e+2 ⁹ (4.35e-3)	9.8697e+2 ⁹ (4.06e-3)	
WFG6	3	400	7.2119e+0 ³ (1.68e-2)	7.1699e+0 ³ (2.64e-2)	7.2084e+0 ³ (2.27e-2)	7.2137e+0 ³ (2.12e-2)	7.2196e+0 ³ (2.55e-2)	7.2196e+0 ³ (2.31e-2)	7.2192e+0 ³ (2.43e-2)	7.2211e+0 ³ (1.82e-2)
	5	750	3.0840e+1 ⁹ (9.96e-2)	3.0539e+1 ⁹ (8.48e-2)	3.0874e+1 ⁹ (1.00e-1)	3.0837e+1 ⁹ (8.47e-2)	3.0837e+1 ⁹ (9.29e-2)	3.0832e+1 ⁹ (8.71e-2)	3.0842e+1 ⁹ (1.18e-1)	3.0855e+1 ⁹ (9.60e-2)
	8	1500	2.4735e+2 ⁹ (1.44e+0)	2.4534e+2 ⁹ (1.37e+0)	2.4732e+2 ⁹ (1.59e+0)	2.4685e+2 ⁹ (1.40e+0)	2.4682e+2 ⁹ (1.65e+0)	2.4750e+2 ⁹ (1.20e+0)	2.4730e+2 ⁹ (1.72e+0)	2.4705e+2 ⁹ (1.53e+0)
	10	2000	9.8498e+2 ⁹ (6.57e+0)	9.7843e+2 ⁹ (6.16e+0)	9.8390e+2 ⁹ (7.55e+0)	9.8351e+2 ⁹ (7.64e+0)	9.8376e+2 ⁹ (6.95e+0)	9.8341e+2 ⁹ (7.85e+0)	9.8322e+2 ⁹ (7.36e+0)	9.8524e+2 ⁹ (5.07e+0)
WFG7	3	400	7.3701e+0 ³ (7.26e-3)	7.3362e+0 ³ (1.93e-2)	7.3666e+0 ³ (8.29e-3)	7.3662e+0 ³ (5.52e-3)	7.3714e+0 ³ (5.58e-3)	7.3694e+0 ³ (6.02e-3)	7.3677e+0 ³ (4.32e-3)	7.3685e+0 ³ (6.17e-3)
	5	750	3.1646e+1 ⁹ (8.17e-3)	3.1461e+1 ⁹ (3.68e-2)	3.1642e+1 ⁹ (9.38e-3)	3.1642e+1 ⁹ (7.51e-3)	3.1640e+1 ⁹ (7.68e-3)	3.1642e+1 ⁹ (8.98e-3)	3.1642e+1 ⁹ (7.05e-3)	3.1641e+1 ⁹ (8.03e-3)
	8	1500	2.5568e+2 ⁹ (3.70e-2)	2.5407e+2 ⁹ (3.92e-1)	2.5549e+2 ⁹ (1.03e-1)	2.5547e+2 ⁹ (1.72e-1)	2.5556e+2 ⁹ (1.25e-1)	2.5559e+2 ⁹ (7.14e-2)	2.5558e+2 ⁹ (6.87e-2)	
	10	2000	1.0236e+3 ⁹ (9.66e-2)	1.0196e+3 ⁹ (1.01e-0)	1.0233e+3 ⁹ (2.23e-1)	1.0233e+3 ⁹ (2.52e-1)	1.0233e+3 ⁹ (2.31e-1)	1.0235e+3 ⁹ (1.09e-1)	1.0235e+3 ⁹ (1.56e-1)	1.0235e+3 ⁹ (1.19e-1)
WFG8	3	400	7.1906e+0 ³ (1.37e-2)	7.1066e+0 ³ (1.41e-2)	7.1956e+0 ³ (4.16e-2)	7.1831e+0 ³ (4.16e-2)	7.1916e+0 ³ (3.00e-2)	7.2002e+0 ³ (2.43e-2)	7.1897e+0 ³ (3.54e-2)	
	5	750	3.0969e+1 ⁹ (7.33e-2)	3.0622e+1 ⁹ (1.12e-1)	3.0948e+1 ⁹ (6.96e-2)	3.0943e+1 ⁹ (7.26e-2)	3.0939e+1 ⁹ (7.60e-2)	3.0956e+1 ⁹ (7.05e-2)	3.0972e+1 ⁹ (8.14e-2)	3.0944e+1 ⁹ (7.48e-2)
	8	1500	2.4135e+2 ⁹ (8.54e-0)	2.3847e+2 ⁹ (1.21e+0)	2.4167e+2 ⁹ (6.07e+0)	2.4148e+2 ⁹ (6.18e+0)	2.4173e+2 ⁹ (4.04e+0)	2.4171e+2 ⁹ (4.04e+0)	2.4171e+2 ⁹ (8.98e+0)	2.4162e+2 ⁹ (6.66e+0)
	10	2000	9.0506e+2 ⁹ (5.70e+1)	9.1865e+2 ⁹ (5.46e+1)	9.3569e+2 ⁹ (5.72e+1)	9.4663e+2 ⁹ (5.89e+1)	9.2628e+2 ⁹ (6.26e+1)	9.4933e+2 ⁹ (6.41e+1)	9.3337e+2 ⁹ (6.71e+1)	
WFG9	3	400	7.1480e+0 ³ (8.01e-2)	7.1227e+0 ³ (7.33e-2)	7.1431e+0 ³ (6.67e-2)	7.1419e+0 ³ (7.48e-2)	7.1612e+0 ³ (6.88e-2)	7.1608e+0 ³ (5.63e-2)	7.1550e+0 ³ (5.55e-2)	7.1432e+0 ³ (7.04e-2)
	5	750	3.0849e+1 ⁹ (8.82e-2)	3.0566e+1 ⁹ (1.92e-1)	3.0812e+1 ⁹ (1.50e-1)	3.0838e+1 ⁹ (9.76e-2)	3.0847e+1 ⁹ (1.22e-1)	3.0835e+1 ⁹ (1.31e-1)	3.0837e+1 ⁹ (1.56e-1)	3.0863e+1 ⁹ (1.14e-1)

Table 16: Mean and standard deviations (in parenthesis) of the SPD indicator obtained by MOEAs using the RVEA framework on MOPs with regular PF shapes. The two best mean values per MOP are highlighted in grayscale, where the darker tone corresponds to the best one. The symbols “+”, “-”, and “=” are placed when the MOEA performs significantly better, significantly worse, or statistically equivalent to RVEA based on a one-tailed Wilcoxon test using a significance level of $\alpha = 0.05$. The % of satisfaction refers to the percentage of MOPs where the MOEA performs significantly better or statistically equivalent to RVEA. The superscripts are the obtained rank in the comparison.

MOP	Obj.	Gen.	RVEA	RVEA*	RVEA-AdaRSE	RVEA-AdaGAE	RVEA-AdaMPT	RVEA-AdaCOU	RVEA-AdaPT	RVEA-AdaKRA
DTLZ1	3	400	$2.3357e+1^8$ (9.76e-2)	$2.2423e+1^8$ (1.95e-1)	$2.3339e+1^8$ (7.91e-2)	$2.3349e+1^8$ (6.97e-2)	$2.3337e+1^8$ (9.00e-2)	$2.3364e+1^8$ (7.11e-2)	$2.3368e+1^8$ (1.27e-1)	$2.3365e+1^8$ (1.11e-1)
	5	600	$7.3023e+1^2$ (1.12e-1)	$6.6500e+1^2$ (7.02e-1)	$7.3008e+1^2$ (1.07e-1)	$7.3016e+1^2$ (8.68e-2)	$7.2995e+1^2$ (6.72e-2)	$7.3008e+1^2$ (7.08e-2)	$7.3036e+1^2$ (1.08e-1)	$7.3006e+1^2$ (1.06e-1)
	8	750	$1.0782e+2^2$ (5.92e-1)	$9.6977e+2^2$ (1.21e+0)	$1.0803e+2^2$ (4.70e-1)	$1.0805e+2^2$ (2.80e-1)	$1.0816e+2^2$ (4.61e-1)	$1.0824e+2^2$ (2.05e-1)	$1.0804e+2^2$ (3.82e-1)	$1.0819e+2^2$ (2.12e-1)
	10	1000	$1.7619e+2^2$ (5.13e-1)	$1.5156e+2^2$ (3.16e+0)	$1.7636e+2^2$ (4.77e-1)	$1.7647e+2^2$ (2.48e-1)	$1.7656e+2^2$ (2.27e-1)	$1.7652e+2^2$ (1.91e-1)	$1.7657e+2^2$ (2.36e-1)	
DTLZ2	3	250	$3.2775e+1^2$ (4.45e-3)	$3.2171e+1^2$ (1.49e-1)	$3.2769e+1^2$ (1.85e-2)	$3.2767e+1^2$ (1.65e-2)	$3.2772e+1^2$ (1.53e-2)	$3.2775e+1^2$ (7.22e-3)	$3.2775e+1^2$ (1.32e-2)	$3.2768e+1^2$ (1.84e-2)
	5	350	$1.3055e+2^2$ (2.76e-2)	$1.3817e+2^2$ (4.70e-1)	$1.3054e+2^2$ (2.81e-1)	$1.3056e+2^2$ (2.11e-2)	$1.3054e+2^2$ (2.36e-2)	$1.3054e+2^2$ (2.51e-2)	$1.3054e+2^2$ (2.31e-2)	$1.3054e+2^2$ (2.69e-2)
	8	500	$1.4781e+2^2$ (1.83e-1)	$1.4964e+2^2$ (1.18e-1)	$1.4786e+2^2$ (2.81e-2)	$1.4780e+2^2$ (1.82e-1)	$1.4785e+2^2$ (3.03e-2)	$1.4786e+2^2$ (2.78e-2)	$1.4785e+2^2$ (2.35e-2)	$1.4778e+2^2$ (2.20e-1)
	10	750	$2.6051e+2^2$ (1.38e-1)	$2.6406e+2^2$ (3.76e-1)	$2.6047e+2^2$ (1.29e-1)	$2.6047e+2^2$ (1.29e-1)	$2.6050e+2^2$ (1.29e-1)	$2.6051e+2^2$ (1.28e-1)	$2.6049e+2^2$ (1.28e-1)	$2.6043e+2^2$ (3.00e-1)
DTLZ3	3	1000	$3.2889e+1^2$ (7.20e-2)	$3.2461e+1^2$ (2.43e-1)	$3.2936e+1^2$ (1.44e-1)	$3.2877e+1^2$ (1.10e-1)	$3.2884e+1^2$ (9.04e-2)	$3.2911e+1^2$ (1.27e-1)	$3.2948e+1^2$ (1.23e-1)	$3.2907e+1^2$ (1.07e-1)
	5	1000	$1.3056e+2^2$ (1.86e-1)	$1.3833e+2^2$ (7.48e-1)	$1.3971e+2^2$ (2.19e-1)	$1.3967e+2^2$ (4.70e-1)	$1.3965e+2^2$ (1.67e-1)	$1.3965e+2^2$ (1.67e-1)	$1.3961e+2^2$ (1.14e-1)	
	8	1000	$1.4796e+2^2$ (2.18e-1)	$1.4951e+2^2$ (2.98e-1)	$1.4799e+2^2$ (3.00e-1)	$1.4798e+2^2$ (1.46e-1)	$1.4795e+2^2$ (1.15e-1)	$1.4796e+2^2$ (1.18e-1)	$1.4791e+2^2$ (2.45e-1)	$1.4781e+2^2$ (5.43e-1)
	10	1500	$2.6048e+2^2$ (3.72e-1)	$2.6408e+2^2$ (3.20e-1)	$2.6047e+2^2$ (2.86e-1)	$2.6047e+2^2$ (5.65e-2)	$2.6046e+2^2$ (1.88e-1)	$2.6046e+2^2$ (1.32e-1)	$2.6047e+2^2$ (1.43e-1)	$2.6051e+2^2$ (6.39e-2)
DTLZ4	3	600	$3.2758e+1^2$ (2.71e-3)	$2.4895e+1^2$ (1.14e-1)	$3.2757e+1^2$ (9.88e-4)	$3.2757e+1^2$ (9.31e-4)	$3.1954e+1^2$ (4.40e-0)	$3.2757e+1^2$ (1.07e-3)	$3.2757e+1^2$ (1.44e-3)	$3.2757e+1^2$ (1.18e-3)
	5	1000	$1.3043e+2^2$ (5.82e-3)	$1.3771e+2^2$ (4.46e-1)	$1.3943e+2^2$ (5.73e-3)	$1.3943e+2^2$ (6.54e-3)	$1.3943e+2^2$ (5.37e-3)	$1.3943e+2^2$ (7.01e-3)	$1.3943e+2^2$ (4.81e-3)	$1.3943e+2^2$ (4.88e-3)
	8	1250	$1.4785e+2^2$ (2.93e-2)	$1.4951e+2^2$ (1.99e-1)	$1.4581e+2^2$ (1.10e-1)	$1.4784e+2^2$ (2.44e-2)	$1.4785e+2^2$ (2.46e-2)	$1.4645e+2^2$ (5.30e-0)	$1.4526e+2^2$ (6.67e+0)	$1.4714e+2^2$ (3.86e+0)
	10	2000	$2.6055e+2^2$ (4.31e-2)	$2.6501e+2^2$ (1.85e-1)	$2.6050e+2^2$ (1.17e-1)	$2.6049e+2^2$ (1.77e-1)	$2.6051e+2^2$ (1.19e-1)	$2.6050e+2^2$ (1.81e-1)	$2.6053e+2^2$ (1.09e-1)	
WFG1	3	400	$1.7499e+1^2$ (2.33e-1)	$1.5934e+1^2$ (4.43e-1)	$1.5657e+1^2$ (1.03e-0)	$1.5829e+1^2$ (9.89e-1)	$1.5493e+1^2$ (1.42e-0)	$1.5112e+1^2$ (1.21e+0)	$1.5298e+1^2$ (1.19e+0)	$1.5384e+1^2$ (1.19e+0)
	5	750	$3.0556e+1^2$ (7.75e-1)	$2.8783e+1^2$ (8.15e-1)	$2.7317e+1^2$ (1.62e-0)	$2.7567e+1^2$ (2.43e-0)	$2.6686e+1^2$ (1.71e-0)	$2.7305e+1^2$ (2.16e+0)	$2.8131e+1^2$ (2.24e+0)	$2.8477e+1^2$ (1.99e-0)
	8	1500	$3.2394e+1^2$ (2.56e-0)	$2.3680e+1^2$ (2.31e-0)	$3.2689e+1^2$ (2.14e-0)	$3.1619e+1^2$ (1.60e-0)	$3.2455e+1^2$ (1.87e-0)	$3.2497e+1^2$ (1.58e-0)	$3.4046e+1^2$ (1.83e-0)	$3.4732e+1^2$ (2.36e-0)
	10	2000	$2.4462e+1^2$ (2.04e-0)	$2.8583e+1^2$ (1.46e-0)	$3.9023e+1^2$ (1.63e-0)	$3.8408e+1^2$ (2.37e-0)	$3.8720e+1^2$ (2.17e-0)	$0.40177e+1^2$ (2.45e-0)	$4.2794e+1^2$ (2.38e-0)	$4.2965e+1^2$ (2.17e-0)
WFG4	3	400	$3.2795e+1^2$ (8.90e-2)	$3.1056e+1^2$ (1.32e-1)	$3.2806e+1^2$ (1.08e-0)	$3.2811e+1^2$ (8.80e-2)	$3.2806e+1^2$ (1.02e-1)	$3.2806e+1^2$ (1.25e-0)	$3.2828e+1^2$ (8.63e-2)	$3.2795e+1^2$ (9.00e-2)
	5	750	$1.3914e+2^2$ (9.61e-2)	$1.2184e+2^2$ (1.64e-0)	$1.3910e+2^2$ (8.59e-2)	$1.3912e+2^2$ (8.34e-2)	$1.3910e+2^2$ (8.89e-2)	$1.3912e+2^2$ (8.60e-2)	$1.3913e+2^2$ (1.07e-1)	$1.3913e+2^2$ (7.10e-2)
	8	1500	$1.4740e+2^2$ (2.54e-1)	$1.3071e+2^2$ (1.78e-0)	$1.4737e+2^2$ (2.75e-1)	$1.4730e+2^2$ (2.11e-1)	$1.4732e+2^2$ (3.42e-1)	$1.4743e+2^2$ (2.82e-1)	$1.4744e+2^2$ (1.99e-1)	$1.4731e+2^2$ (3.37e-1)
	10	2000	$2.5547e+2^2$ (8.43e-1)	$1.9407e+2^2$ (2.94e-0)	$2.5588e+2^2$ (6.76e-1)	$2.5587e+2^2$ (6.22e-1)	$2.5584e+2^2$ (4.10e-1)	$2.5583e+2^2$ (8.10e-1)	$2.5587e+2^2$ (8.12e-1)	$2.5519e+2^2$ (9.95e-1)
WFG6	3	400	$3.2800e+1^2$ (4.60e-2)	$3.0862e+1^2$ (2.68e-1)	$3.2759e+1^2$ (2.38e-1)	$3.2810e+1^2$ (3.35e-2)	$3.2807e+1^2$ (3.84e-2)	$3.2781e+1^2$ (6.41e-2)	$3.2782e+1^2$ (9.03e-2)	$3.2765e+1^2$ (1.34e-1)
	5	750	$3.0393e+2^2$ (4.21e-2)	$1.1881e+2^2$ (9.47e-1)	$3.0933e+2^2$ (4.95e-2)	$3.0933e+2^2$ (4.90e-2)	$3.0932e+2^2$ (3.14e-2)	$3.0933e+2^2$ (2.58e-2)	$3.1033e+2^2$ (3.64e-2)	$3.1033e+2^2$ (4.52e-2)
	8	1500	$3.4737e+2^2$ (2.06e-1)	$1.9296e+2^2$ (1.76e-0)	$1.4732e+2^2$ (2.28e-1)	$1.4734e+2^2$ (2.09e-0)	$1.4729e+2^2$ (1.93e-1)	$1.4735e+2^2$ (1.77e-1)	$1.4733e+2^2$ (2.42e-1)	$1.4731e+2^2$ (2.37e-1)
	10	2000	$2.5547e+2^2$ (8.43e-1)	$1.8586e+2^2$ (2.67e-0)	$2.5581e+2^2$ (7.09e-1)	$2.5585e+2^2$ (5.46e-1)	$2.5586e+2^2$ (7.99e-1)	$2.5584e+2^2$ (7.56e-1)	$2.5585e+2^2$ (8.32e-1)	$2.5538e+2^2$ (7.85e-1)
WFG7	3	400	$3.2964e+1^2$ (1.00e-1)	$3.1178e+1^2$ (9.43e-1)	$3.2955e+1^2$ (8.82e-2)	$3.2965e+1^2$ (8.82e-2)	$3.2957e+1^2$ (8.00e-2)	$3.2996e+1^2$ (8.35e-2)	$3.2882e+1^2$ (1.32e-1)	$3.2828e+1^2$ (1.17e-1)
	5	750	$1.3090e+2^2$ (3.27e-2)	$1.2076e+2^2$ (1.36e-0)	$1.3939e+2^2$ (5.44e-2)	$1.3939e+2^2$ (4.07e-2)	$1.3939e+2^2$ (4.65e-2)	$1.3939e+2^2$ (6.08e-2)	$1.3939e+2^2$ (3.70e-2)	$1.3939e+2^2$ (3.67e-2)
	8	1500	$1.4654e+2^2$ (8.15e-1)	$1.2761e+2^2$ (2.54e-0)	$1.4599e+2^2$ (6.88e-1)	$1.4605e+2^2$ (1.02e-0)	$1.4567e+2^2$ (8.04e-1)	$1.4613e+2^2$ (8.94e-1)	$1.4626e+2^2$ (9.03e-1)	$1.4625e+2^2$ (1.03e-0)
	10	2000	$2.5726e+2^2$ (1.13e+0)	$1.9057e+2^2$ (3.16e+0)	$2.5711e+2^2$ (1.10e+0)	$2.5753e+2^2$ (1.17e+0)	$2.5703e+2^2$ (9.21e-1)	$2.5719e+2^2$ (1.33e+0)	$2.5729e+2^2$ (1.08e+0)	$2.5755e+2^2$ (9.10e-1)
WFG8	3	400	$3.2964e+1^2$ (2.02e-1)	$3.1010e+1^2$ (2.59e-1)	$3.2449e+1^2$ (2.49e-1)	$3.2955e+1^2$ (2.31e-1)	$3.2820e+1^2$ (1.02e-1)	$3.2823e+1^2$ (1.32e-1)	$3.2813e+1^2$ (1.32e-1)	$3.2827e+1^2$ (1.15e-1)
	5	750	$1.3894e+2^2$ (1.62e-1)	$1.2212e+2^2$ (1.12e-0)	$1.3895e+2^2$ (1.90e-1)	$1.3897e+2^2$ (1.76e-1)	$1.3899e+2^2$ (2.52e-1)	$1.3901e+2^2$ (2.86e-2)	$1.3912e+2^2$ (1.86e-2)	$1.3913e+2^2$ (1.07e-1)
	8	1500	$1.4595e+2^2$ (1.30e-1)	$1.3521e+2^2$ (1.50e-0)	$1.4501e+2^2$ (1.18e-0)	$1.4480e+2^2$ (9.73e-1)	$1.4517e+2^2$ (9.32e-1)	$1.4480e+2^2$ (9.69e-1)	$1.4506e+2^2$ (9.03e-1)	$1.4484e+2^2$ (7.88e-1)
	10	2000	$2.5586e+2^2$ (1.05e+0)	$1.9558e+2^2$ (7.25e-1)	$2.5526e+2^2$ (1.83e-0)	$2.5554e+2^2$ (1.93e-0)	$2.5560e+2^2$ (8.59m-1)	$2.5546e+2^2$ (9.68e-1)	$2.5572e+2^2$ (1.01e+0)	$2.5548e+2^2$ (1.30e+0)
WFG9	3	400	$3.2853e+1^2$ (8.69m-2)	$3.1243e+1^2$ (2.68e-1)	$3.2828e+1^2$ (1.23e-1)	$3.2820e+1^2$ (1.02e-1)	$3.2823e+1^2$ (8.82e-2)	$3.2813e+1^2$ (1.32e-1)	$3.2828e+1^2$ (1.17e-1)	$3.2827e+1^2$ (1.15e-1)
	5	750	$1.3094e+2^2$ (2.37e-2)	$1.2076e+2^2$ (1.36e-0)	$1.3939e+2^2$ (5.44e-2)	$1.3939e+2^2$ (4.07e-2)	$1.3939e+2^2$ (4.65e-2)	$1.3939e+2^2$ (6.08e-2)	$1.3939e+2^2$ (3.70e-2)	$1.3939e+2^2$ (3.67e-2)
	8	1500	$1.4564e+2^2$ (8.15e-1)	$1.2761e+2^2$ (2.54e-0)	$1.4599e+2^2$ (6.88e-1)	$1.4605e+2^2$ (1.02e-0)	$1.4567e+2^2$ (8.04e-1)	$1.4613e+2^2$ (8.94e-1)	$1.4626e+2^2$ (9.03e-1)	$1.4625e+2^2$ (1.03e-0)
	10	2000	$2.5726e+2^2$ (9.65m-1)	$1.8759e+2^2$ (3.42e-0)	$2.5653e+2^2$ (9.95m-1)	$2.5606e+2^2$ (7.89m-1)	$2.5653e+2^2$ (9.64m-1)	$2.5636e+2^2$ (7.88m-1)	$2.5653e+2^2$ (9.12m-1)	$2.5656e+2^2$ (8.03m-1)
IMOP1	2	500	$5.1290e+0^2$ (1.01e-1)	$1.1510e+0^2$ (8.27e-1)	$5.7022e+0^2$ (6.77e-1)	$5.6764e+0^2$ (8.51e-1)	$5.7576e+0^2$ (8.00e-1)	$5.6497e+0^2$ (6.60e-1)	$5.7919e+0^2$ (6.43e-1)	$5.6512e+0^2$ (5.83e-1)
	2	500	$6.7915e+0^2$ (2.47e+0)	$3.8686e+0^2$ (3.38e+0)	$5.5312e+0^2$ (2.70e+0)	$6.2634e$				

Table 17: Mean and standard deviations (in parenthesis) of the HV indicator obtained by MOEAs using the MOEA/D framework on MOPs with regular PF shapes. The two best mean values per MOP are highlighted in grayscale, where the darker tone corresponds to the best one. The symbols “+”, “-”, and “=” are placed when the MOEA performs significantly better, significantly worse, or statistically equivalent to MOEA/D based on a one-tailed Wilcoxon test using a significance level of $\alpha = 0.05$. The % of satisfaction refers to the percentage of MOPs where the MOEA performs significantly better or statistically equivalent to MOEA/D. The superscripts are the obtained rank in the comparison.

MOP	Obj.	Gen.	MOEA/D	AdaW	MOEA/D-AdaRSE	MOEA/D-AdaGAE	MOEA/D-AdaMPT	MOEA/D-AdaCOU	MOEA/D-AdaPT	MOEA/D-AdaKRA
DTLZ1	3	400	$7.7870e+0^0$ (1.25e-3)	$7.7843e+0^0$ (1.82e-3)	$7.7869e+0^0$ (1.93e-3)	$7.7869e+0^0$ (1.72e-3)	$7.7873e+0^0$ (9.42e-4)	$7.7871e+0^0$ (1.03e-3)	$7.7871e+0^0$ (1.18e-3)	
	5	600	$3.1960e+1^7$ (1.94e-2)	$3.1965e+1^7$ (2.67e-3)	$3.1964e+1^7$ (9.88e-3)	$3.1964e+1^7$ (8.10e-3)	$3.1955e+1^7$ (2.43e-2)	$3.1963e+1^7$ (9.57e-3)	$3.1962e+1^7$ (1.17e-2)	$3.1963e+1^7$ (1.16e-2)
	8	750	$2.5594e+2^9$ (5.02e-2)	$2.5594e+2^9$ (1.02e-1)	$2.5596e+2^9$ (5.14e-2)	$2.5596e+2^9$ (6.26e-2)	$2.5594e+2^9$ (7.43e-2)	$2.5596e+2^9$ (8.21e-2)	$2.5596e+2^9$ (4.63e-2)	$2.5597e+2^9$ (2.17e-2)
	10	1000	$1.0239e+3^7$ (1.62e-1)	$1.0240e+3^7$ (4.60e-2)	$1.0239e+3^7$ (3.56e-2)	$1.0239e+3^7$ (1.18e-1)	$1.0239e+3^7$ (7.44e-2)	$1.0238e+3^7$ (1.99e-1)	$1.0239e+3^7$ (9.56e-2)	$1.0239e+3^7$ (1.10e-1)
DTLZ2	3	250	$3.4134e+0^0$ (1.53e-4)	$7.4022e+0^0$ (9.28e-3)	$7.4134e+0^0$ (1.94e-4)	$7.4134e+0^0$ (1.57e-4)	$7.4133e+0^0$ (2.26e-4)	$7.4133e+0^0$ (1.80e-4)	$7.4133e+0^0$ (1.88e-4)	$7.4133e+0^0$ (1.85e-4)
	5	350	$3.1695e+1^7$ (1.10e-2)	$3.1696e+1^7$ (1.68e-2)	$3.1697e+1^7$ (1.08e-3)	$3.1696e+1^7$ (4.62e-3)	$3.1692e+1^7$ (1.80e-2)	$3.1694e+1^7$ (1.69e-2)	$3.1697e+1^7$ (1.79e-1)	$3.1697e+1^7$ (2.70e-1)
	8	500	$2.5580e+2^9$ (6.70e-2)	$2.5586e+2^9$ (6.35e-2)	$2.5570e+2^9$ (8.46e-2)	$2.5580e+2^9$ (1.53e-1)	$2.5578e+2^9$ (1.69e-1)	$2.5581e+2^9$ (1.10e-1)	$2.5584e+2^9$ (6.84e-3)	$2.5583e+2^9$ (2.50e-2)
	10	750	$1.0238e+3^7$ (3.38e-1)	$1.0238e+3^7$ (3.93e-2)	$1.0239e+3^7$ (8.05e-2)	$1.0238e+3^7$ (1.09e-1)	$1.0239e+3^7$ (7.86e-2)	$1.0239e+3^7$ (7.54e-3)	$1.0239e+3^7$ (1.07e-3)	$+1.0239e+3^7$ (1.76e-3)
DTLZ3	3	1000	$7.4111e+0^0$ (1.64e-3)	$7.3988e+0^0$ (1.29e-2)	$7.4100e+0^0$ (3.07e-3)	$7.4096e+0^0$ (2.41e-3)	$7.4105e+0^0$ (1.82e-3)	$7.4107e+0^0$ (2.40e-3)	$7.4104e+0^0$ (2.09e-3)	$7.4098e+0^0$ (3.45e-3)
	5	1000	$3.1695e+1^7$ (1.60e-3)	$3.1650e+1^7$ (2.04e-2)	$3.1662e+1^7$ (8.58e-2)	$3.1634e+1^7$ (1.56e-1)	$3.1648e+1^7$ (1.85e-1)	$3.1643e+1^7$ (1.30e-1)	$3.1690e+1^7$ (3.22e-2)	$3.1687e+1^7$ (2.86e-2)
	8	1000	$2.5530e+2^9$ (1.12e+0)	$2.5529e+2^9$ (5.98e-1)	$2.5561e+2^9$ (4.40e-1)	$2.5541e+2^9$ (6.75e-1)	$2.5520e+2^9$ (1.40e+0)	$2.5535e+2^9$ (7.31e-1)	$2.5557e+2^9$ (5.92e-1)	$2.5559e+2^9$ (5.12e-1)
	10	1500	$1.0237e+3^7$ (2.52e-1)	$1.0234e+3^7$ (1.76e+0)	$1.0233e+3^7$ (3.04e-1)	$1.0233e+3^7$ (1.04e-1)	$1.0233e+3^7$ (1.92e+0)	$1.0235e+3^7$ (1.92e+0)	$1.0235e+3^7$ (3.19e+0)	$1.0239e+3^7$ (7.07e-2)
DTLZ4	3	600	$7.2784e+0^0$ (3.50e-1)	$7.4090e+0^0$ (6.65e-3)	$7.1650e+0^0$ (6.92e-1)	$7.2114e+0^0$ (4.11e-1)	$7.1056e+0^0$ (4.67e-1)	$7.3459e+0^0$ (2.57e-1)	$7.1452e+0^0$ (4.52e-1)	$7.1787e+0^0$ (4.32e-1)
	5	1000	$3.1517e+1^7$ (4.32e-1)	$3.1675e+1^7$ (9.27e-2)	$3.1509e+1^7$ (2.18e-1)	$3.1536e+1^7$ (4.27e-1)	$3.1538e+1^7$ (2.44e-1)	$3.1290e+1^7$ (5.40e-1)	$3.1471e+1^7$ (4.12e-1)	$3.1329e+1^7$ (6.16e-1)
	8	1250	$2.5553e+2^9$ (3.63e-1)	$2.5578e+2^9$ (6.66e-2)	$2.5562e+2^9$ (2.58e-1)	$2.5559e+2^9$ (3.53e-1)	$2.5571e+2^9$ (1.93e-1)	$2.5551e+2^9$ (3.69e-1)	$2.5560e+2^9$ (3.06e-1)	$2.5567e+2^9$ (1.94e-1)
	10	2000	$1.0236e+3^7$ (2.84e-1)	$1.0239e+3^7$ (9.42e-3)	$1.0237e+3^7$ (1.21e-1)	$1.0237e+3^7$ (3.23e-1)	$1.0236e+3^7$ (2.64e-1)	$1.0237e+3^7$ (1.55e-1)	$1.0236e+3^7$ (2.73e-1)	
WFG1	3	400	$5.5941e+0^0$ (4.88e-2)	$5.4299e+0^0$ (2.57e-2)	$5.6138e+0^0$ (6.20e-2)	$5.6151e+0^0$ (5.13e-2)	$5.6156e+0^0$ (6.98e-2)	$5.5946e+0^0$ (5.70e-2)	$5.6082e+0^0$ (5.72e-2)	$5.5965e+0^0$ (6.93e-2)
	5	750	$2.5795e+1^7$ (1.07e+0)	$2.1581e+1^7$ (3.47e-1)	$2.7081e+1^7$ (8.18e-1)	$2.6763e+1^7$ (7.57e-1)	$2.7059e+1^7$ (9.73e-1)	$2.6684e+1^7$ (7.63e-1)	$2.7083e+1^7$ (8.23e-1)	$2.7098e+1^7$ (8.88e-1)
	8	1500	$2.2088e+2^9$ (1.00e+1)	$1.7255e+2^9$ (4.58e-0)	$2.0373e+2^9$ (6.18e+0)	$2.0423e+2^9$ (6.28e+0)	$2.0372e+2^9$ (6.38e+0)	$2.0495e+2^9$ (6.12e+0)	$2.1696e+2^9$ (6.24e+0)	$2.1622e+2^9$ (5.59e+0)
	10	2000	$9.3962e+2^9$ (3.34e+1)	$7.3907e+2^9$ (2.71e+1)	$9.6527e+2^9$ (1.37e+1)	$9.6149e+2^9$ (1.98e+1)	$9.6286e+2^9$ (1.20e+1)	$9.5269e+2^9$ (2.25e+1)	$9.6406e+2^9$ (1.48e+1)	$9.7036e+2^9$ (1.34e+1)
WFG4	3	400	$7.3813e+0^0$ (5.38e-2)	$7.3397e+0^0$ (1.37e-2)	$7.3813e+0^0$ (6.13e-3)	$7.3814e+0^0$ (6.64e-3)	$7.3779e+0^0$ (1.46e-2)	$7.3822e+0^0$ (6.02e-3)	$7.3768e+0^0$ (1.77e-2)	$7.3801e+0^0$ (5.14e-3)
	5	750	$3.1625e+1^7$ (1.54e-2)	$3.1488e+1^7$ (3.31e-2)	$3.1627e+1^7$ (1.74e-2)	$3.1632e+1^7$ (1.43e-2)	$3.1626e+1^7$ (1.76e-2)	$3.1631e+1^7$ (1.33e-2)	$3.1633e+1^7$ (1.79e-2)	$3.1636e+1^7$ (1.12e-2)
	8	1500	$2.5557e+2^9$ (9.23e-2)	$2.5372e+2^9$ (4.94e-1)	$2.5553e+2^9$ (9.14e-2)	$2.5554e+2^9$ (7.85e-2)	$2.5555e+2^9$ (7.57e-2)	$2.5554e+2^9$ (8.23e-2)	$2.5555e+2^9$ (7.78e-2)	$2.5555e+2^9$ (8.02e-2)
	10	2000	$1.0234e+3^7$ (1.53e-1)	$1.0185e+3^7$ (3.17e-0)	$1.0234e+3^7$ (2.06e-1)	$1.0234e+3^7$ (3.20e-1)	$1.0233e+3^7$ (2.03e-1)	$1.0233e+3^7$ (1.89e-1)	$1.0234e+3^7$ (1.50e-1)	$1.0233e+3^7$ (1.91e-1)
WFG5	3	400	$7.1945e+0^0$ (3.97e-2)	$7.1717e+0^0$ (3.31e-2)	$7.1691e+0^0$ (4.77e-2)	$7.1874e+0^0$ (4.26e-2)	$7.1966e+0^0$ (4.47e-2)	$7.1673e+0^0$ (5.02e-2)	$7.1938e+0^0$ (4.51e-2)	$7.1898e+0^0$ (4.34e-2)
	5	750	$2.5795e+1^7$ (1.70e-1)	$3.0700e+1^7$ (4.96e-2)	$3.0785e+1^7$ (1.66e-2)	$3.0787e+1^7$ (2.12e-2)	$3.0788e+1^7$ (1.76e-3)	$3.0785e+1^7$ (1.69e-2)	$3.0785e+1^7$ (1.60e-2)	$3.0784e+1^7$ (1.65e-2)
	8	1500	$2.4717e+2^9$ (5.23e-2)	$2.4633e+2^9$ (2.19e-1)	$2.4718e+2^9$ (2.07e-2)	$2.4717e+2^9$ (3.41e-2)	$2.4718e+2^9$ (2.70e-2)	$2.4717e+2^9$ (2.28e-2)	$2.4717e+2^9$ (2.70e-2)	$2.4717e+2^9$ (2.70e-2)
	10	2000	$9.6861e+2^9$ (4.22e-2)	$9.8537e+2^9$ (4.63e-2)	$9.8681e+2^9$ (3.73e-2)	$9.8681e+2^9$ (2.42e-2)	$9.8682e+2^9$ (4.24e-2)	$9.8682e+2^9$ (4.85e-2)	$9.8686e+2^9$ (4.74e-2)	$9.8686e+2^9$ (4.74e-2)
WFG6	3	400	$7.2387e+0^0$ (2.75e-2)	$7.2269e+0^0$ (3.24e-2)	$7.2401e+0^0$ (3.41e-2)	$7.2493e+0^0$ (2.56e-2)	$7.2476e+0^0$ (2.97e-2)	$7.2527e+0^0$ (4.29e-2)	$7.2509e+0^0$ (1.90e-2)	$7.2517e+0^0$ (2.37e-2)
	5	750	$3.0922e+1^7$ (1.39e-1)	$3.0784e+1^7$ (1.64e-1)	$3.0914e+1^7$ (1.53e-1)	$3.0887e+1^7$ (1.64e-1)	$3.0916e+1^7$ (1.47e-1)	$3.0897e+1^7$ (1.63e-1)	$3.0912e+1^7$ (1.67e-1)	$3.0903e+1^7$ (1.54e-1)
	8	1500	$2.4775e+2^9$ (1.72e+0)	$2.4646e+2^9$ (1.78e+0)	$2.4753e+2^9$ (1.67e+0)	$2.4776e+2^9$ (2.02e+0)	$2.4736e+2^9$ (1.91e+0)	$2.4733e+2^9$ (1.66e+0)	$2.4756e+2^9$ (1.84e+0)	$2.4778e+2^9$ (1.76e+1)
	10	2000	$9.8631e+2^9$ (9.53e+0)	$9.8271e+2^9$ (9.98e+0)	$9.8349e+2^9$ (8.25e+0)	$9.8755e+2^9$ (1.02e+1)	$9.8240e+2^9$ (9.57e+0)	$9.8294e+2^9$ (1.01e+1)	$9.8744e+2^9$ (1.29e+1)	$9.8599e+2^9$ (9.61e+0)
WFG7	3	400	$7.0343e+0^0$ (1.52e-3)	$7.3787e+0^0$ (1.04e-2)	$7.4025e+0^0$ (1.92e-3)	$7.4026e+0^0$ (1.84e-3)	$7.4024e+0^0$ (1.43e-3)	$7.4033e+0^0$ (1.60e-3)	$7.4034e+0^0$ (1.99e-3)	$7.4028e+0^0$ (1.88e-3)
	5	750	$3.1676e+1^7$ (3.85e-3)	$3.1559e+1^7$ (2.26e-2)	$3.1673e+1^7$ (2.57e-2)	$3.1668e+1^7$ (2.88e-2)	$3.1676e+1^7$ (3.56e-3)	$3.1676e+1^7$ (4.23e-3)	$3.1676e+1^7$ (3.88e-3)	
	8	1500	$2.5573e+2^9$ (2.96e-2)	$2.5391e+2^9$ (4.31e-1)	$2.5573e+2^9$ (3.18e-2)	$2.5572e+2^9$ (2.82e-2)	$2.5572e+2^9$ (3.30e-2)	$2.5573e+2^9$ (2.37e-2)	$2.5573e+2^9$ (2.48e-2)	
	10	2000	$1.0236e+3^7$ (1.16e-1)	$1.0191e+3^7$ (2.12e-0)	$1.0236e+3^7$ (3.92e-2)	$1.0236e+3^7$ (8.16e-2)	$1.0236e+3^7$ (9.57e-2)	$1.0236e+3^7$ (9.44e-2)	$1.0236e+3^7$ (3.08e-1)	
WFG8	3	400	$7.2062e+0^0$ (1.07e-2)	$7.2258e+0^0$ (1.51e-2)	$7.2115e+0^0$ (2.52e-2)	$7.2100e+0^0$ (1.61e-2)	$7.2150e+0^0$ (3.25e-2)	$7.2205e+0^0$ (1.56e-2)	$7.2205e+0^0$ (1.87e-2)	
	5	750	$3.0998e+1^7$ (3.83e-2)	$3.1026e+1^7$ (6.51e-2)	$3.0991e+1^7$ (9.22e-2)	$3.0966e+1^7$ (9.47e-2)	$3.0937e+1^7$ (8.38e-2)	$3.1116e+1^7$ (7.48e-2)	$3.1080e+1^7$ (8.23e-2)	$3.1094e+1^7$ (7.50e-2)
	8	1500	$2.5456e+2^9$ (2.51e-1)	$2.4902e+2^9$ (9.00e-1)	$2.5447e+2^9$ (2.10e-1)	$2.5446e+2^9$ (8.18e-1)	$2.5446e+2^9$ (8.47e-2)	$2.5463e+2^9$ (8.47e-2)	$2.5458e+2^9$ (1.16e-1)	
	10	2000	$1.0219e+3^7$ (3.39e-1)	$1.0092e+3^7$ (2.60e-1)	$1.0217e+3^7$ (4.92e-1)	$1.0216e+3^7$ (4.19e-1)	$1.0216e+3^7$ (3.21e-1)	$1.0222e+3^7$ (1.78e-1)	$1.0221e+3^7$ (1.63e-1)	$1.0220e+3^7$ (2.12e-1)
WFG9	3	400	$7.1780e+0^0$ (8.59e-2)	$7.0898e+0^0$ (7.97e-2)	$7.1590e+0^0$ (1.00e-1)	$7.1597e+0^0$ (8.68e-2)	$7.1886e+0^0$ (9.80e-2)	$7.1976e+0^0$ (7.61e-2)	$7.1510e+0^0$ (9.84e-2)	$7.1826e+0^0$ (8.26e-2)
	5	750	$2.9915e+1^7$ (4.36e-1)	$2.9704e+1^7$ (3.18e-1)	$3.0204e+1^7$ (6.51e-1)	$3.0153e+1^7$ (5.91e-1)	$3.0032e+1^7$ (4.93e-1)	$3.0222e+1^7$ (6.30e-1)	$3.0018e$	

Table 18: Mean and standard deviations (in parenthesis) of the SPD indicator obtained by MOEAs using the MOEA/D framework on MOPs with regular PF shapes. The two best mean values per MOP are highlighted in grayscale, where the darker tone corresponds to the best one. The symbols “+”, “-”, and “=” are placed when the MOEA performs significantly better, significantly worse, or statistically equivalent to MOEA/D based on a one-tailed Wilcoxon test using a significance level of $\alpha = 0.05$. The % of satisfaction refers to the percentage of MOPs where the MOEA performs significantly better or statistically equivalent to MOEA/D. The superscripts are the obtained rank in the comparison.

MOP	Obj.	Gen.	MOEA/D	AdaW	MOEA/D-AdaRSE	MOEA/D-AdaGAE	MOEA/D-AdaMPT	MOEA/D-AdaCOU	MOEA/D-AdaPT	MOEA/D-AdaKRA
DTLZ1	3	400	2.3292e+1 ² (7.42e-2)	2.2924e+1 ² (1.35e-1)	-	2.3294e+1 ² (1.12e-2)	-	2.3315e+1 ² (9.78e-2)	-	2.3279e+1 ² (6.11e-2)
	5	600	7.1189e+1 ² (4.45e+0)	6.6112e+1 ² (1.96e+0)	-	7.2320e+1 ² (2.07e+0)	-	7.1993e+1 ² (2.68e+0)	-	7.0120e+1 ² (5.65e+0)
	8	750	9.4488e+1 ² (1.38e+1)	7.6885e+1 ² (6.30e+0)	-	9.7578e+1 ² (1.16e+1)	-	9.6831e+1 ² (1.34e+0)	-	9.4327e+1 ² (1.35e+1)
	10	1000	1.4262e+2 ² (2.26e+1)	9.6369e+1 ² (7.73e+0)	-	1.6000e+2 ² (1.57e+1)	-	1.3724e+2 ² (2.54e+1)	-	1.5726e+2 ² (1.74e+1)
DTLZ2	3	250	3.2626e+1 ² (4.73e-2)	3.2140e+1 ² (2.22e-1)	-	3.2626e+1 ² (3.97e-2)	-	3.3060e+1 ² (3.37e-2)	-	3.2632e+1 ² (3.50e-2)
	5	350	1.3644e+2 ² (5.64e+0)	1.3451e+2 ² (1.17e+0)	-	1.3698e+2 ² (2.85e+0)	-	1.3657e+2 ² (3.78e+0)	-	1.3551e+2 ² (7.34e+0)
	8	500	1.3904e+2 ² (8.57e+0)	1.4825e+2 ² (7.09e-1)	-	1.3777e+2 ² (8.07e+0)	-	1.4042e+2 ² (7.82e+0)	-	1.3828e+2 ² (1.03e+1)
	10	750	2.3936e+2 ² (3.23e+1)	2.5898e+2 ² (1.09e+1)	-	2.5269e+2 ² (2.52e+1)	-	2.4878e+2 ² (1.74e+1)	-	2.4412e+2 ² (1.71e+1)
DTLZ3	3	1000	3.2770e+1 ² (4.55e-2)	3.1751e+1 ² (4.94e-1)	-	3.2775e+1 ² (3.37e-1)	-	3.2801e+1 ² (7.78e-2)	-	3.2770e+1 ² (5.72e-2)
	5	1000	3.3923e+1 ² (2.30e-1)	1.2371e+2 ² (8.42e+0)	-	3.1468e+2 ² (8.93e+0)	-	1.3206e+2 ² (1.50e+1)	-	1.3024e+2 ² (1.00e+1)
	8	1000	1.2078e+2 ² (3.00e+1)	9.6715e+1 ² (2.16e+1)	-	1.2999e+2 ² (1.12e+1)	-	1.2409e+2 ² (1.34e+1)	-	1.2313e+2 ² (1.86e+1)
	10	1500	2.2376e+2 ² (3.53e+1)	1.6965e+2 ² (3.77e+1)	-	2.1330e+2 ² (3.93e+1)	-	2.1504e+2 ² (3.70e+0)	-	2.2622e+2 ² (3.70e+0)
DTLZ4	3	600	2.9445e+1 ² (8.30e+0)	3.2338e+1 ² (2.17e-1)	-	2.8436e+1 ² (9.77e+0)	-	2.7892e+1 ² (9.78e+0)	-	2.8415e+1 ² (1.13e+1)
	5	1000	1.2324e+2 ² (3.06e+1)	1.3481e+2 ² (9.57e+0)	-	1.2702e+2 ² (2.39e+0)	-	1.2460e+2 ² (2.86e+1)	-	1.2460e+2 ² (2.68e+1)
	8	1250	1.2793e+2 ² (2.08e+1)	1.4877e+2 ² (1.55e+1)	+	1.3386e+2 ² (1.59e+1)	-	1.3591e+2 ² (1.69e+1)	-	1.4111e+2 ² (8.55e+0)
	10	2000	2.4519e+2 ² (1.98e+1)	2.6263e+2 ² (1.01e+0)	-	2.5239e+2 ² (9.67e+0)	-	2.5239e+2 ² (1.69e+0)	-	2.4608e+2 ² (2.20e+0)
WFG1	3	400	1.5666e+1 ² (5.74e-1)	1.7062e+1 ² (7.89e-1)	-	1.4545e+1 ² (1.09e+0)	-	1.4744e+1 ² (9.79e-1)	-	1.4670e+1 ² (1.03e+0)
	5	750	2.8848e+1 ² (5.16e+0)	3.2463e+1 ² (1.12e+0)	-	2.5187e+1 ² (3.73e+0)	-	2.4044e+1 ² (3.83e+0)	-	2.5132e+1 ² (3.76e+0)
	8	1500	3.6051e+1 ² (5.55e+0)	4.4348e+1 ² (1.23e+0)	-	3.6753e+1 ² (5.16e+0)	-	3.1467e+1 ² (4.85e+0)	-	3.5686e+1 ² (5.47e+0)
	10	2000	5.7761e+1 ² (4.90e+0)	5.2920e+1 ² (4.76e+0)	-	3.9673e+1 ² (6.78e+0)	-	3.6273e+1 ² (6.29e+0)	-	3.5697e+1 ² (8.66e+0)
WFG4	3	400	3.2192e+1 ² (2.48e-1)	3.1920e+1 ² (2.58e-1)	-	3.2228e+1 ² (2.98e-1)	-	3.2249e+1 ² (2.23e-1)	-	3.2211e+1 ² (4.17e-1)
	5	750	1.3589e+2 ² (2.95e+0)	1.3401e+2 ² (6.26e+0)	-	1.3587e+2 ² (4.33e+0)	-	1.3673e+2 ² (7.37e-0)	-	1.3575e+2 ² (4.39e+0)
	8	1500	1.4615e+2 ² (1.97e+0)	1.4940e+2 ² (2.78e-1)	-	1.4616e+2 ² (2.10e+0)	-	1.4595e+2 ² (2.92e+0)	-	1.4606e+2 ² (2.20e+0)
	10	2000	2.5382e+2 ² (9.58e-1)	2.6402e+2 ² (6.88e-1)	-	2.5773e+2 ² (3.71e+0)	-	2.5784e+2 ² (3.92e+0)	-	2.5743e+2 ² (4.17e-1)
WFG5	3	400	3.1709e+1 ² (9.26e-1)	3.1279e+1 ² (4.17e-1)	-	3.1292e+1 ² (1.03e+0)	-	3.1548e+1 ² (9.49e-1)	-	3.1794e+1 ² (9.60e-1)
	5	750	1.3189e+2 ² (4.05e+0)	1.3189e+2 ² (9.77e-1)	-	1.3773e+2 ² (4.13e+0)	-	1.3806e+2 ² (1.21e+0)	-	1.3638e+2 ² (3.67e+0)
	8	1500	1.4237e+2 ² (7.57e+0)	1.4883e+2 ² (2.23e+1)	-	1.4399e+2 ² (1.44e+0)	-	1.4432e+2 ² (4.18e+0)	-	1.4243e+2 ² (6.21e+0)
	10	2000	2.5378e+2 ² (5.82e+0)	2.6308e+2 ² (3.93e+1)	-	2.5450e+2 ² (4.87e+0)	-	2.5351e+2 ² (7.19e+0)	-	2.5359e+2 ² (5.38e+0)
WFG6	3	400	3.2200e+1 ² (4.19e-1)	3.1981e+1 ² (2.06e-1)	-	3.2240e+1 ² (3.28e-1)	-	3.2328e+1 ² (3.31e-1)	-	3.2199e+1 ² (3.68e-1)
	5	750	1.3850e+2 ² (4.05e+0)	1.3369e+2 ² (6.92e-1)	-	1.3845e+2 ² (5.11e+0)	-	1.3845e+2 ² (5.82e-1)	-	1.3824e+2 ² (1.50e+0)
	8	1500	1.4719e+2 ² (8.80e-2)	1.4947e+2 ² (1.74e-1)	-	1.4561e+2 ² (8.53e+0)	-	1.4678e+2 ² (2.01e+0)	-	1.4715e+2 ² (1.86e+0)
	10	2000	2.5827e+2 ² (4.57e+0)	2.6421e+2 ² (3.66e-1)	-	2.5693e+2 ² (6.93e+0)	-	2.5662e+2 ² (9.12e+0)	-	2.5585e+2 ² (2.88e+0)
WFG7	3	400	3.2200e+1 ² (4.19e-1)	3.1981e+1 ² (2.06e-1)	-	3.2240e+1 ² (3.28e-1)	-	3.2328e+1 ² (3.31e-1)	-	3.2199e+1 ² (3.68e-1)
	5	750	1.3850e+2 ² (2.82e-1)	1.3369e+2 ² (6.92e-1)	-	1.3845e+2 ² (5.11e+0)	-	1.3824e+2 ² (5.82e-1)	-	1.3824e+2 ² (1.50e+0)
	8	1500	1.4719e+2 ² (8.80e-2)	1.4947e+2 ² (1.74e-1)	-	1.4713e+2 ² (8.53e+0)	-	1.4678e+2 ² (2.01e+0)	-	1.4703e+2 ² (6.73e-1)
	10	2000	2.5859e+2 ² (1.74e-1)	2.6491e+2 ² (5.46e-1)	-	2.5830e+2 ² (1.79e-0)	-	2.5804e+2 ² (2.40e+0)	-	2.5802e+2 ² (3.13e-0)
WFG8	3	400	2.6718e+1 ² (2.82e-1)	2.6168e+1 ² (2.38e-1)	-	2.6977e+1 ² (3.65e-1)	-	2.6801e+1 ² (3.16e-1)	-	2.6711e+1 ² (3.41e-1)
	5	750	3.7058e+1 ² (4.58e+0)	3.1339e+1 ² (4.55e+0)	-	3.5602e+1 ² (6.84e+0)	-	3.5458e+1 ² (5.48e+0)	-	3.4947e+1 ² (5.24e+0)
	8	1500	4.1982e+1 ² (5.37e+0)	3.7842e+1 ² (9.19e+0)	-	4.1704e+1 ² (9.89e+0)	-	7.6460e+1 ² (9.71e+0)	-	7.1594e+1 ² (4.82e+0)
	10	2000	9.8031e+1 ² (1.07e+1)	2.6508e+2 ² (4.61e-1)	-	1.4166e+2 ² (1.91e+1)	-	1.5388e+2 ² (1.89e+1)	-	1.4140e+2 ² (2.07e+0)
WFG9	3	400	2.8712e+1 ² (5.29e-1)	3.0056e+1 ² (5.62e-1)	-	2.8006e+1 ² (5.36e-1)	-	2.8706e+1 ² (5.73e-1)	-	2.8955e+1 ² (4.84e-2)
	5	750	7.5531e+1 ² (1.84e+1)	1.2744e+2 ² (1.33e+0)	-	8.0588e+1 ² (1.27e+1)	-	8.3063e+1 ² (1.31e+1)	-	8.1044e+1 ² (1.30e+1)
	8	1500	6.0203e+2 ² (6.42e+0)	1.4680e+2 ² (6.61e+1)	-	5.8478e+2 ² (6.31e+0)	-	5.9708e+2 ² (6.51e+0)	-	6.0287e+2 ² (6.73e+0)
	10	2000	2.5943e+2 ² (1.72e+1)	1.7031e+2 ² (1.60e+1)	-	9.6907e+2 ² (1.04e+1)	-	1.0238e+2 ² (2.39e+1)	-	9.3121e+2 ² (8.32e+0)
IMOP1	2	500	4.9527e+0 ² (2.30e-1)	5.4948e+0 ² (1.69e-1)	-	4.9344e+0 ² (2.57e-1)	-	5.0429e+0 ² (2.76e-1)	-	5.0039e+0 ² (2.19e-1)
	2	500	1.4286e+0 ² (1.58e+0)	1.3643e+0 ² (1.47e+0)	-	1.3652e+0 ² (1.12e+0)	-	1.7680e+0 ² (2.17e+0)	-	1.1995e+0 ² (8.63e-1)
+/−/-			24/19/3	5/6/35		7/5/34		5/5/36		9/7/30
% of satisfaction			58.70%	86.96%		89.13%		89.13%		84.78%
										93.48%
										91.30%

adaptation method does not strongly modify the behavior of MOEAs that use predefined WVRSs on MOPs with regular PF shapes.

5.2 Irregular PF shapes

The convergence and diversity graphs generated with the mean HV and the mean SPD value of 30 independent runs of MOEAs using the NSGA-III, RVEA, and MOEA/D frameworks on DTLZ1⁻¹ and WFG4⁻¹ with 3, 5, 8 and 10 objective functions are shown in Figures 157 to 164. They show that RVEA*, AdaW, and all versions of NSGA-III-Ada \mathcal{K} , RVEA-Ada \mathcal{K} , and MOEA/D-Ada \mathcal{K} improve the convergence and diversity of their original versions on all instances of DTLZ1⁻¹ and WFG4⁻¹. However, A-NSGA-III cannot improve the performance of NSGA-III on DTLZ1⁻¹ and WFG4⁻¹ with 8 and 10 objective functions. Also, it can be seen that RVEA* maintains a better performance than all versions of RVEA-Ada \mathcal{K} at the beginning of the evolution because RVEA* adapts the WVRS at each generation. However, most versions of RVEA-Ada \mathcal{K} obtain better HV and SPD values than RVEA* at the end of the evolution. Additionally, the convergence and diversity of AdaW and MOEAs with our adaptation method are improved at each 0.05 · g_{\max} generations due to the adaptation frequency. However, the performance of all versions of RVEA-Ada \mathcal{K} begins to be improved until the generation 0.1 · g_{\max} on DTLZ1⁻¹ with 8 and 10 objective functions and all instances of WFG4⁻¹. This behavior occurs because, following the RVEA framework, the information of the ranges of objective functions is included in the WVRS at each 0.1 · g_{\max} generations. Finally, it is worth noting that the performance of MOEAs with our adaptation method is slightly degraded at each adaptation step due to the inclusion of new weight vectors, which have no associated solutions. However, the performance increases rapidly as good solutions are found for new weight vectors. Since AdaW includes additional solutions

from the archive into the main population at each adaptation step, its diversity is improved. However, it decreases during the next generations. In addition, it can be seen that all versions of NSGA-III-Ada \mathcal{K} have smoother convergence and diversity graphs than all versions of RVEA-Ada \mathcal{K} and MOEA/D-Ada \mathcal{K} . The selection mechanism and the normalization procedure of the NSGA-III framework may produce this result. When empty sub-populations are generated, a second solution is selected randomly from sub-populations with multiple solutions preventing the diversity loss at each adaptation step. In addition, the normalization procedure includes information of the ranges of objective functions at each generation instead of including it with a specific frequency promoting a smoother evolution. The presented convergence and diversity graphs indicate that our adaptation method enhances the performance of MOEAs using predefined WVRSSs on MOPs with irregular PF shapes.

References

- [1] M. Li, X. Yao, What Weights Work for You? Adapting Weights for Any Pareto Front Shape in Decomposition-Based Evolutionary Multiobjective Optimisation, *Evolutionary Computation* 28 (2) (2020) 227–253. [doi:10.1162/evco_a_00269](https://doi.org/10.1162/evco_a_00269).
- [2] H. Wang, L. Jiao, X. Yao, Two_Arch2: An Improved Two-Archive Algorithm for Many-Objective Optimization, *IEEE Transactions on Evolutionary Computation* 19 (4) (2015) 524–541. [doi:10.1109/TEVC.2014.2350987](https://doi.org/10.1109/TEVC.2014.2350987).
- [3] Y. Xiang, Y. Zhou, M. Li, Z. Chen, A Vector Angle-Based Evolutionary Algorithm for Unconstrained Many-Objective Optimization, *IEEE Transactions on Evolutionary Computation* 21 (1) (2017) 131–152. [doi:10.1109/TEVC.2016.2587808](https://doi.org/10.1109/TEVC.2016.2587808).
- [4] Y. Tian, R. Cheng, X. Zhang, F. Cheng, Y. Jin, An Indicator-Based Multiobjective Evolutionary Algorithm With Reference Point Adaptation for Better Versatility, *IEEE Transactions on Evolutionary Computation* 22 (4) (2018) 609–622. [doi:10.1109/TEVC.2017.2749619](https://doi.org/10.1109/TEVC.2017.2749619).
- [5] H. Chen, Y. Tian, W. Pedrycz, G. Wu, R. Wang, L. Wang, Hyperplane Assisted Evolutionary Algorithm for Many-Objective Optimization Problems, *IEEE Transactions on Cybernetics* 50 (7) (2020) 3367–3380. [doi:10.1109/TCYB.2019.2899225](https://doi.org/10.1109/TCYB.2019.2899225).
- [6] J. Yuan, H.-L. Liu, F. Gu, Q. Zhang, Z. He, Investigating the Properties of Indicators and an Evolutionary Many-Objective Algorithm Using Promising Regions, *IEEE Transactions on Evolutionary Computation* 25 (1) (2021) 75–86. [doi:10.1109/TEVC.2020.2999100](https://doi.org/10.1109/TEVC.2020.2999100).
- [7] Q. Liu, Y. Jin, M. Heiderich, T. Rodemann, G. Yu, An Adaptive Reference Vector-Guided Evolutionary Algorithm Using Growing Neural Gas for Many-Objective Optimization of Irregular Problems, *IEEE Transactions on Cybernetics* 52 (5) (2022) 2698–2711. [doi:10.1109/TCYB.2020.3020630](https://doi.org/10.1109/TCYB.2020.3020630).
- [8] E. Zitzler, S. Künzli, Indicator-Based Selection in Multiobjective Search, in: X. Yao, E. K. Burke, J. A. Lozano, J. Smith, J. J. Merelo-Guervós, J. A. Bullinaria, J. E. Rowe, P. Tiño, A. Kabán, H.-P. Schwefel (Eds.), *Parallel Problem Solving from Nature, PPSN VIII*, Vol. 3242 of *Lecture Notes in Computer Science*, Springer, 2004, pp. 832–842. [doi:10.1007/978-3-540-30217-9_84](https://doi.org/10.1007/978-3-540-30217-9_84).

Table 19: Mean and standard deviations (in parenthesis) of the HV indicator obtained by MOEAs using the NSGA-III framework on MOPs with irregular PF shapes. The two best mean values per MOP are highlighted in grayscale, where the darker tone corresponds to the best one. The symbols “+”, “-”, and “=” are placed when the MOEA performs significantly better, significantly worse, or statistically equivalent to NSGA-III based on a one-tailed Wilcoxon test using a significance level of $\alpha = 0.05$. The % of satisfaction refers to the percentage of MOPs where the MOEA performs significantly better than NSGA-III. The superscripts are the obtained rank in the comparison.

MOP	Obj.	Gen.	NSGA-III	A-NSGA-III	NSGA-III-AdaRSE	NSGA-III-AdaGAE	NSGA-III-AdaMPT	NSGA-III-AdaCOU	NSGA-III-AdaPT	NSGA-III-AdaKRA
DTLZ5	3	400	5.4810e+0 ³ (5.67e-3)	5.4900e+0 ³ (3.43e-3)	5.5074e+0 ³ (8.57e-3)	5.5040e+0 ³ (1.12e-2)	+ 5.5076e+0 ² (1.21e-3) +	5.5000e+0 ² (1.66e-2) +	5.5077e+0 ¹ (6.22e-3) +	5.5000e+0 ⁰ (4.21e-2) +
	5	600	3.1188e+0 ¹ (4.91e-1)	3.1082e+0 ¹ (9.72e-1)	3.0818e+0 ¹ (1.76e-1)	3.0312e+0 ¹ (2.42e-1)	+ 3.0957e+0 ¹ (1.32e-1)	+ 3.1143e+0 ² (8.07e-1) +	+ 3.1096e+0 ¹ (1.21e-1) +	- 3.0988e+0 ¹ (1.25e-1) -
	8	750	2.4790e+0 ² (3.76e-1)	2.4781e+0 ² (4.24e-1)	2.4499e+0 ² (2.03e+0)	2.4617e+0 ² (1.63e+0)	+ 2.4789e+0 ² (8.97e-1) +	+ 2.4789e+0 ² (1.63e+0) +	+ 2.4276e+0 ² (1.63e+0) +	- 2.4252e+0 ² (3.14e+0) -
	10	1000	9.9280e+0 ² (1.22e+0)	9.9255e+0 ² (7.33e+0)	9.8255e+0 ² (1.84e+0)	9.8236e+0 ² (6.99e+0)	+ 9.9484e+0 ² (5.69e+0) +	+ 9.9683e+0 ² (2.82e+0) +	+ 9.7152e+0 ² (7.06e+0) +	- 9.6961e+0 ² (5.16e+0) -
DTLZ6	3	400	5.4793e+0 ³ (6.74e-3)	5.4893e+0 ³ (3.20e-3)	+ 5.5116e+0 ³ (3.62e-3)	+ 5.5056e+0 ³ (9.96e-4)	+ 5.5058e+0 ³ (8.24e-4)	+ 5.5110e+0 ³ (4.65e-3) +	+ 5.5117e+0 ² (3.46e-3) +	+ 5.5119e+0 ¹ (2.69e-3) +
	5	600	3.1882e+0 ¹ (1.73e-1)	3.1870e+0 ¹ (1.92e-1)	3.1820e+0 ¹ (4.03e-2)	+ 3.1828e+0 ¹ (3.43e-2) +	+ 3.1829e+0 ¹ (4.08e-2) +	+ 3.1873e+0 ¹ (3.50e-2) +	+ 3.1829e+0 ¹ (4.23e-2) +	- 3.1848e+0 ¹ (3.66e-2) -
	8	750	2.5507e+0 ² (2.42e-1)	2.5503e+0 ² (1.48e-1)	+ 2.5455e+0 ² (2.89e-1) +	+ 2.5444e+0 ² (4.04e-1) +	+ 2.5457e+0 ² (2.58e-1) +	+ 2.5485e+0 ² (1.58e-1) +	+ 2.5460e+0 ² (3.71e-1) +	- 2.5459e+0 ² (3.06e-1) -
	10	1000	1.0207e+0 ² (3.24e-1)	1.0177e+0 ² (7.27e+0)	+ 1.0179e+0 ³ (1.73e+0) +	+ 1.0182e+0 ³ (1.47e+0) +	+ 1.0183e+0 ³ (1.83e+0) +	+ 1.0197e+0 ³ (3.87e+0) +	+ 1.0182e+0 ³ (1.25e+0) +	- 1.0182e+0 ³ (1.47e+0) -
DTLZ7	3	1000	6.5509e+0 ² (2.06e-1)	6.5140e+0 ² (2.54e-1)	+ 6.5455e+0 ² (2.11e-1) +	+ 6.5708e+0 ² (3.62e-1) +	+ 6.5716e+0 ² (1.50e-1) +	+ 6.5438e+0 ² (2.11e-1) +	+ 6.5730e+0 ¹ (1.51e-1) +	+ 6.5181e+0 ⁰ (2.54e-1) +
	5	1000	2.5042e+0 ² (7.65e-2)	2.4889e+0 ² (6.34e-2)	+ 2.5224e+0 ² (1.79e-2) +	+ 2.5126e+0 ² (1.95e-2) +	+ 2.5097e+0 ² (1.21e-1) +	+ 2.5210e+0 ¹ (1.11e-1) +	+ 2.5230e+0 ¹ (6.88e-2) +	+ 2.5231e+0 ¹ (6.92e-2) +
	8	1000	1.8183e+0 ² (6.41e-1)	1.7840e+0 ² (5.15e-1)	+ 1.8639e+0 ² (4.94e-1) +	+ 1.8574e+0 ² (4.84e-1) +	+ 1.8686e+0 ² (5.01e-1) +	+ 1.8578e+0 ² (2.70e-1) +	+ 1.8656e+0 ² (4.41e-1) +	+ 1.8644e+0 ² (5.55e-1) +
	10	1500	7.0037e+0 ² (2.64e+0)	6.8765e+0 ² (3.25e+0)	+ 7.1469e+0 ² (3.45e+0) +	+ 7.1431e+0 ² (2.44e+0) +	+ 7.1544e+0 ² (1.80e+0) +	+ 7.1991e+0 ² (1.29e+0) +	+ 7.0767e+0 ² (3.77e+0) +	+ 7.0839e+0 ² (4.28e+0) +
WFG2	3	400	7.8650e+0 ⁰ (1.08e-2)	7.8515e+0 ⁰ (1.34e-2)	+ 7.8653e+0 ⁰ (8.79e-3) +	+ 7.8574e+0 ⁰ (1.70e-2) +	+ 7.8601e+0 ⁰ (1.34e-2) +	+ 7.8556e+0 ⁰ (1.48e-2) +	+ 7.8595e+0 ⁰ (1.67e-2) +	+ 7.8644e+0 ⁰ (1.24e-2) +
	5	750	3.1900e+0 ¹ (1.96e-2)	3.1893e+0 ¹ (1.76e-2)	+ 3.1901e+0 ¹ (1.74e-2) +	+ 3.1900e+0 ¹ (1.59e-2) +	+ 3.1905e+0 ¹ (1.92e-2) +	+ 3.1906e+0 ¹ (1.41e-1) +	+ 3.1903e+0 ¹ (1.74e-2) +	+ 3.1901e+0 ¹ (1.89e-2) +
	8	1500	2.5560e+0 ² (1.14e-1)	2.5553e+0 ² (1.56e-1)	+ 2.5561e+0 ² (9.20e-2) +	+ 2.5564e+0 ² (9.19e-2) +	+ 2.5550e+0 ² (1.29e-1) +	+ 2.5561e+0 ² (1.02e-1) +	+ 2.5556e+0 ² (1.59e-2) +	+ 2.5556e+0 ² (9.58e-2) +
	10	2000	1.0232e+0 ² (2.58e-1)	1.0229e+0 ² (4.06e-1)	+ 1.0232e+0 ² (2.93e-1) +	+ 1.0233e+0 ² (2.64e-1) +	+ 1.0233e+0 ² (3.21e-1) +	+ 1.0233e+0 ² (3.28e-1) +	+ 1.0233e+0 ² (3.27e-1) +	+ 1.0233e+0 ² (3.27e-1) +
WFG3	3	400	7.0237e+0 ¹ (2.22e-2)	7.0148e+0 ¹ (2.10e-2)	+ 7.0054e+0 ¹ (2.31e-1) +	+ 6.9911e+0 ¹ (2.47e-2) +	+ 7.0054e+0 ¹ (1.72e-2) +	+ 7.0154e+0 ¹ (1.98e-2) +	+ 7.0066e+0 ⁰ (2.56e-2) +	+ 7.0087e+0 ⁰ (1.80e-2) +
	5	750	2.8861e+0 ¹ (1.76e-2)	2.8504e+0 ¹ (1.06e-1)	+ 2.8490e+0 ¹ (1.01e-1) +	+ 2.8370e+0 ¹ (1.21e-1) +	+ 2.8435e+0 ¹ (1.01e-1) +	+ 2.8500e+0 ¹ (1.46e-1) +	+ 2.8558e+0 ¹ (1.29e-1) +	+ 2.8603e+0 ¹ (1.23e-1) +
	8	1500	2.2820e+0 ² (9.69e-2)	2.2558e+0 ² (1.55e-0)	+ 2.2526e+0 ² (1.66e-0) +	+ 2.2556e+0 ² (1.72e-0) +	+ 2.2556e+0 ² (1.80e-0) +	+ 2.3232e+0 ² (1.04e-0) +	+ 2.3011e+0 ² (1.39e-0) +	+ 2.3005e+0 ² (1.59e-0) +
	10	2000	9.1788e+0 ¹ (2.87e-0)	9.0989e+0 ¹ (5.45e-0)	+ 9.1245e+0 ¹ (6.46e-0) +	+ 9.0867e+0 ¹ (6.38e-0) +	+ 9.0928e+0 ¹ (4.91e-0) +	+ 9.4403e+0 ¹ (2.74e-0) +	+ 9.3276e+0 ¹ (5.04e-0) +	+ 9.3371e+0 ¹ (4.11e-0) +
DTLZ1-1	3	400	5.4225e+0 ⁰ (1.07e-2)	5.4037e+0 ⁰ (6.38e-3)	+ 5.5049e+0 ⁰ (3.21e-3) +	+ 5.4966e+0 ⁰ (2.87e-3) +	+ 5.5004e+0 ⁰ (2.46e-3) +	+ 5.5004e+0 ⁰ (2.46e-3) +	+ 5.5039e+0 ⁰ (3.59e-3) +	+ 5.5042e+0 ⁰ (3.81e-3) +
	5	600	9.3299e+0 ⁰ (1.41e-1)	9.1697e+0 ⁰ (4.23e-1)	+ 1.0900e+0 ¹ (4.90e-2) +	+ 1.0498e+0 ¹ (7.05e-2) +	+ 1.0636e+0 ¹ (7.95e-2) +	+ 1.1274e+0 ¹ (1.38e-2) +	+ 1.1259e+0 ¹ (2.22e-2) +	+ 1.1289e+0 ¹ (2.04e-2) +
	8	750	7.4554e+0 ⁰ (4.15e-1)	7.5658e+0 ⁰ (3.43e-1)	+ 2.0239e+0 ¹ (2.19e-1) +	+ 1.8903e+0 ¹ (3.15e-1) +	+ 1.9724e+0 ¹ (2.43e-1) +	+ 2.0364e+0 ¹ (4.94e-1) +	+ 2.0396e+0 ¹ (4.93e-2) +	+ 2.0398e+0 ¹ (4.80e-1) +
	10	1000	8.4726e+0 ⁰ (5.56e-1)	8.5496e+0 ⁰ (5.54e-1)	+ 2.9734e+0 ¹ (2.05e-1) +	+ 2.7414e+0 ¹ (4.31e-1) +	+ 2.9734e+0 ¹ (5.93e-1) +	+ 2.9754e+0 ¹ (6.14e-1) +	+ 2.9763e+0 ¹ (8.28e-2) +	+ 2.9749e+0 ¹ (7.36e-2) +
DTLZ2-1	3	250	6.6630e+0 ⁰ (4.99e-3)	6.6810e+0 ⁰ (6.12e-3)	+ 6.7162e+0 ⁰ (2.09e-3) +	+ 6.7128e+0 ⁰ (2.76e-3) +	+ 6.7114e+0 ⁰ (3.23e-3) +	+ 6.7128e+0 ⁰ (3.33e-3) +	+ 6.7150e+0 ⁰ (2.57e-3) +	+ 6.7159e+0 ⁰ (2.47e-3) +
	5	350	1.6429e+0 ¹ (19.9e-2)	1.6080e+0 ¹ (9.86e-2)	+ 1.7409e+0 ¹ (5.46e-2) +	+ 1.7142e+0 ¹ (7.50e-2) +	+ 1.7214e+0 ¹ (8.36e-2) +	+ 1.7476e+0 ¹ (3.92e-2) +	+ 1.7424e+0 ¹ (5.63e-2) +	+ 1.7421e+0 ¹ (5.63e-2) +
	8	500	2.7872e+0 ¹ (1.05e+0)	2.1528e+0 ¹ (9.66e-1)	+ 4.1104e+0 ¹ (7.17e-1) +	+ 4.1928e+0 ¹ (5.90e-1) +	+ 4.1920e+0 ¹ (6.39e-1) +	+ 3.9006e+0 ¹ (4.18e-1) +	+ 3.7589e+0 ¹ (3.36e-1) +	+ 3.7904e+0 ¹ (5.03e-1) +
	10	750	4.5254e+0 ¹ (1.30e+0)	4.5131e+0 ¹ (1.13e+0)	+ 7.2049e+0 ¹ (1.96e-1) +	+ 7.4089e+0 ¹ (1.65e-0) +	+ 7.4959e+0 ¹ (1.56e-0) +	+ 6.4514e+0 ¹ (5.20e-1) +	+ 6.1845e+0 ¹ (5.67e-1) +	+ 1.1582e+0 ¹ (5.13e-1) +
DTLZ3-1	3	1000	6.6636e+0 ⁰ (5.25e-3)	6.6814e+0 ⁰ (4.70e-3)	+ 6.7138e+0 ⁰ (1.76e-3) +	+ 6.7185e+0 ⁰ (1.77e-3) +	+ 6.7189e+0 ⁰ (1.55e-3) +	+ 6.7195e+0 ⁰ (1.51e-3) +	+ 6.7188e+0 ⁰ (1.85e-3) +	+ 6.7185e+0 ⁰ (1.95e-3) +
	5	1000	1.6308e+0 ¹ (1.56e-1)	1.5908e+0 ¹ (1.27e-1)	+ 1.7518e+0 ¹ (5.99e-2) +	+ 1.7226e+0 ¹ (8.86e-2) +	+ 1.7300e+0 ¹ (1.21e-1) +			
	8	1000	2.6243e+0 ¹ (6.58e-1)	2.0862e+0 ¹ (1.08e-0)	+ 3.9950e+0 ¹ (8.04e-1) +	+ 3.8758e+0 ¹ (1.19e-0) +	+ 4.1272e+0 ¹ (1.44e-0) +	+ 4.1272e+0 ¹ (1.44e-0) +	+ 3.8510e+0 ¹ (1.56e-0) +	+ 3.7270e+0 ¹ (5.38e-1) +
	10	1500	4.2963e+0 ¹ (1.89e-0)	4.2629e+0 ¹ (1.63e-0)	+ 7.1398e+0 ¹ (1.96e-0) +	+ 7.1997e+0 ¹ (2.56e-0) +	+ 7.1928e+0 ¹ (1.68e-0) +	+ 6.4103e+0 ¹ (3.94e-1) +	+ 6.1393e+0 ¹ (6.07e-1) +	+ 6.1393e+0 ¹ (7.06e-1) +
DTLZ5-1	3	600	6.6669e+0 ⁰ (4.87e-3)	6.6744e+0 ⁰ (4.78e-3)	+ 6.7015e+0 ⁰ (4.51e-3) +	+ 6.7018e+0 ⁰ (4.52e-3) +	+ 6.7180e+0 ⁰ (4.52e-3) +	+ 6.7180e+0 ⁰ (1.89e-3) +	+ 6.7184e+0 ⁰ (2.54e-3) +	+ 6.7186e+0 ⁰ (1.95e-3) +
	5	600	1.6730e+0 ¹ (1.03e-1)	1.6460e+0 ¹ (1.24e-1)	+ 1.7096e+0 ¹ (3.45e-2) +	+ 1.7449e+0 ¹ (4.10e-2) +	+ 1.7416e+0 ¹ (4.22e-2) +	+ 1.7586e+0 ¹ (2.30e-2) +	+ 1.7506e+0 ¹ (3.25e-2) +	+ 1.7575e+0 ¹ (3.00e-2) +
	8	1250	3.7093e+0 ¹ (1.76e-1)	3.7076e+0 ¹ (2.67e-1)	+ 3.9412e+0 ¹ (7.16e-1) +	+ 3.9728e+0 ¹ (5.01e-1) +	+ 3.9944e+0 ¹ (5.01e-1) +	+ 3.8194e+0 ¹ (1.77e-1) +	+ 3.7048e+0 ¹ (2.17e-1) +	+ 3.7095e+0 ¹ (2.77e-1) +
	10	2000	6.6342e+0 ¹ (1.46e-1)	6.5165e+0 ¹ (1.26e-1)	+ 6.7474e+0 ¹ (2.52e-1) +	+ 6.7194e+0 ¹ (1.96e-1) +	+ 6.7325e+0 ¹ (2.27e-1) +	+ 6.7316e+0 ¹ (1.99e-3) +	+ 6.7318e+0 ¹ (1.85e-3) +	+ 6.7318e+0 ¹ (1.95e-3) +
DTLZ7-1	3	1000	9.2317e+0 ¹ (2.31e-1)	7.2438e+0 ¹ (1.82e-1)	+ 7.2454e+0 ¹ (1.42e-1) +	+ 7.2485e+0 ¹ (3.16e-2) +	+ 7.2435e+			

Table 20: Mean and standard deviations (in parenthesis) of the SPD indicator obtained by MOEAs using the NSGA-III framework on MOPs with irregular PF shapes. The two best mean values per MOP are highlighted in grayscale, where the darker tone corresponds to the best one. The symbols “+”, “-”, and “=” are placed when the MOEA performs significantly better, significantly worse, or statistically equivalent to NSGA-III based on a one-tailed Wilcoxon test using a significance level of $\alpha = 0.05$. The % of satisfaction refers to the percentage of MOPs where the MOEA performs significantly better than NSGA-III. The superscripts are the obtained rank in the comparison.

MOP	Obj.	Gen.	NSGA-III	A-NSGA-III	NSGA-III-AdaRSE	NSGA-III-AdaGAE	NSGA-III-AdaMPT	NSGA-III-AdaCOU	NSGA-III-AdaPT	NSGA-III-AdaKRA
DTLZ5	3	400	1.0047e+1 ⁸ (1.18e-1)	1.0248e+1 ⁷ (6.63e-2)	+ 1.0427e+1 ⁴ (1.33e-1)	+ 1.044e+1 ⁵ (7.81e-2)	+ 1.0437e+1 ³ (1.59e-2)	+ 1.0439e+1 ² (1.12e-1)	+ 1.0449e+1 ¹ (3.75e-2)	+ 1.0375e+1 ⁰ (3.51e-1)
	5	600	2.2132e+1 ⁵ (1.42e+0)	2.0791e+1 ⁴ (1.72e+0)	+ 2.2743e+1 ³ (2.00e+0)	+ 2.1600e+1 ² (2.25e+0)	+ 2.1288e+1 ¹ (2.36e+0)	+ 2.2315e+1 ⁰ (1.32e-0)	+ 2.5661e+1 ⁻¹ (2.07e+0)	+ 2.5146e+1 ⁻² (2.43e+0)
	8	750	3.3044e+1 ⁸ (4.14e+0)	3.8213e+1 ⁴ (4.59e+0)	+ 4.5677e+1 ³ (7.99e+0)	+ 3.3671e+1 ² (4.09e+0)	+ 3.6354e+1 ¹ (5.71e+0)	+ 3.7864e+1 ⁰ (3.79e+0)	+ 9.1547e+1 ⁻¹ (7.02e+0)	+ 9.446e+1 ⁻² (5.90e+0)
	10	1000	6.1875e+1 ⁵ (5.47e+0)	9.4568e+1 ² (2.24e+1)	+ 7.3127e+1 ¹ (1.29e+1)	+ 5.2289e+1 ⁰ (6.84e+0)	+ 6.3535e+1 ⁻¹ (9.07e+0)	+ 6.3535e+1 ⁻² (5.42e+0)	+ 1.7743e+2 ⁻³ (5.98e+0)	+ 1.7743e+2 ⁻⁴ (9.33e+0)
DTLZ6	3	400	9.9043e+1 ⁷ (1.52e-1)	1.0194e+1 ⁷ (1.84e-1)	1.0480e+1 ³ (1.83e-2)	+ 1.0425e+1 ⁶ (1.12e-2)	+ 1.0443e+1 ⁵ (7.54e-3)	+ 1.0478e+1 ⁴ (2.30e-2)	+ 1.0513e+1 ³ (1.65e-1)	+ 1.0481e+1 ² (1.36e-2)
	5	600	1.3755e+1 ⁷ (1.20e+0)	1.2791e+1 ⁸ (1.04e+0)	+ 1.7708e+1 ² (2.19e+0)	+ 1.7001e+1 ⁴ (1.78e+0)	+ 1.6929e+1 ⁵ (2.11e+0)	+ 1.5402e+1 ⁶ (1.80e+0)	+ 1.9259e+1 ⁷ (1.83e+0)	+ 1.8738e+1 ⁸ (1.55e+0)
	8	750	2.5631e+1 ⁷ (3.40e+0)	3.4547e+1 ⁴ (4.53e+0)	+ 2.9918e+1 ³ (3.16e+0)	+ 2.8114e+1 ² (3.37e+0)	+ 2.8967e+1 ¹ (3.99e+0)	+ 2.4846e+1 ⁰ (3.60e+0)	+ 4.1893e+1 ⁻¹ (6.04e+0)	+ 4.3082e+1 ⁻² (4.69e+0)
	10	1000	4.0761e+1 ⁵ (5.03e+0)	9.9001e+1 ² (1.31e+1)	+ 4.2746e+1 ⁴ (5.00e+0)	+ 3.9190e+1 ³ (1.40e+0)	+ 4.2121e+1 ² (6.84e+0)	+ 3.7647e+1 ¹ (4.32e+0)	+ 7.8144e+1 ⁻¹ (7.69e+0)	+ 7.3480e+1 ⁻² (9.33e+0)
DTLZ7	3	400	2.3038e+1 ⁷ (2.07e+0)	2.2156e+1 ³ (3.52e+0)	+ 2.4040e+1 ⁴ (3.93e+0)	+ 2.4615e+1 ² (2.45e+0)	+ 2.4705e+1 ² (2.44e+0)	+ 2.4325e+1 ³ (3.37e+0)	+ 2.4863e+1 ⁴ (3.469e+0)	+ 2.4010e+1 ⁵ (4.104e+0)
	5	1000	1.1640e+2 ⁸ (1.86e+0)	1.2835e+2 ⁷ (2.55e+0)	+ 1.5273e+2 ⁴ (1.77e+0)	+ 1.5080e+2 ² (2.27e+0)	+ 1.5043e+2 ⁰ (2.10e+0)	+ 1.4101e+2 ⁻² (3.12e+0)	+ 1.4545e+2 ⁻⁴ (2.06e+0)	+ 1.4502e+2 ⁻⁵ (2.53e+0)
	8	1000	1.3578e+2 ⁸ (2.17e+0)	1.3999e+2 ⁷ (1.77e+0)	+ 1.5454e+2 ² (5.42e+1)	+ 1.5421e+2 ⁰ (5.82e+1)	+ 1.5437e+2 ⁻¹ (4.75e+1)	+ 1.5286e+2 ⁻² (8.12e+1)	+ 1.5434e+2 ⁻³ (4.46e+1)	+ 1.5447e+2 ⁻⁴ (4.42e+1)
	10	1500	2.4481e+2 ⁸ (2.30e+0)	2.5074e+2 ⁷ (2.74e+0)	+ 2.7315e+2 ² (5.75e+1)	+ 2.7330e+2 ¹ (7.63e+1)	+ 2.7278e+2 ⁰ (4.21e+0)	+ 2.7085e+2 ⁻¹ (8.41e+1)	+ 2.7309e+2 ⁻² (6.29e+1)	+ 2.7263e+2 ⁻³ (2.44e+0)
WFG2	3	400	2.0618e+1 ⁷ (2.51e+0)	2.0190e+1 ⁸ (3.62e-1)	+ 2.0548e+1 ⁷ (1.78e-1)	+ 2.0648e+1 ² (2.64e-1)	+ 2.0622e+1 ⁰ (3.88e-1)	+ 2.0565e+1 ⁻¹ (2.72e-1)	+ 2.0548e+1 ⁻² (9.95e-1)	+ 2.0637e+1 ⁻³ (2.13e-1)
	5	750	4.0023e+1 ⁶ (6.65e-1)	3.9234e+1 ⁸ (8.08e-1)	+ 3.9767e+1 ⁷ (7.57e-1)	+ 3.9755e+1 ³ (6.60e-1)	+ 3.9774e+1 ² (6.96e-1)	+ 3.9979e+1 ¹ (6.03e-1)	+ 3.9973e+1 ⁰ (7.39e-1)	+ 3.9853e+1 ⁻¹ (5.50e-1)
	8	1500	5.1547e+1 ⁷ (1.24e+0)	4.9080e+1 ⁸ (2.48e+0)	+ 5.1740e+1 ⁶ (4.63e-1)	+ 5.1412e+1 ⁴ (1.26e-0)	+ 5.1204e+1 ² (1.82e-0)	+ 5.1387e+1 ¹ (1.35e-0)	+ 5.1402e+1 ⁰ (1.12e+0)	+ 5.1423e+1 ⁻¹ (1.24e-0)
	10	2000	6.9279e+1 ⁵ (1.25e+0)	5.9667e+1 ⁸ (8.72e+0)	+ 6.9726e+1 ⁴ (1.30e+0)	+ 6.7954e+1 ² (3.18e+0)	+ 6.9314e+1 ¹ (4.14e+0)	+ 6.8740e+1 ⁰ (2.33e+0)	+ 6.8896e+1 ⁻¹ (1.78e+0)	+ 6.9190e+1 ⁻² (1.61e+0)
WFG3	3	400	1.2655e+1 ⁵ (5.81e+0)	1.2431e+1 ⁷ (5.03e-1)	+ 1.2733e+1 ² (3.90e-1)	+ 1.2639e+1 ⁶ (4.48e-1)	+ 1.2684e+1 ⁴ (4.20e-1)	+ 1.2341e+1 ³ (3.64e-1)	+ 1.2700e+1 ² (3.73e-1)	+ 1.2799e+1 ¹ (4.00e-1)
	5	750	4.4270e+1 ⁶ (6.26e-1)	4.4337e+1 ⁸ (6.01e+1)	+ 4.3614e+1 ⁷ (7.41e-1)	+ 4.3734e+1 ² (7.34e-1)	+ 4.3655e+1 ¹ (1.06e-0)	+ 4.4278e+1 ⁰ (7.56e-1)	+ 4.8558e+1 ⁻¹ (6.04e-1)	+ 4.8529e+1 ⁻² (5.34e-1)
	8	1500	6.3767e+1 ⁷ (1.40e+0)	7.3978e+1 ⁷ (8.11e-1)	+ 8.2602e+1 ² (1.27e+0)	+ 7.4583e+1 ⁶ (2.07e+0)	+ 7.7576e+1 ⁵ (1.80e+0)	+ 7.7952e+1 ⁴ (8.50e+0)	+ 8.5092e+1 ³ (1.12e+0)	+ 8.5172e+1 ² (1.27e+0)
	10	2000	1.0317e+2 ⁸ (1.50e+0)	1.1389e+2 ⁸ (8.40e-1)	+ 1.2416e+2 ⁸ (1.98e+0)	+ 1.0911e+2 ⁷ (1.20e+0)	+ 1.1799e+2 ⁶ (3.26e+0)	+ 1.2248e+2 ⁵ (3.77e+0)	+ 1.2991e+2 ⁴ (1.47e+0)	+ 1.2982e+2 ³ (1.51e+0)
DTLZ1 ⁻¹	3	400	2.1750e+1 ⁸ (2.43e+0)	2.3014e+1 ⁷ (1.00e-1)	+ 2.3181e+1 ⁴ (4.77e-2)	+ 2.3148e+1 ⁶ (5.76e-2)	+ 2.3162e+1 ⁵ (4.54e-2)	+ 2.3169e+1 ³ (3.80e-2)	+ 2.3162e+1 ² (3.18e-2)	+ 2.3174e+1 ¹ (4.59e-2)
	5	600	4.2123e+1 ⁸ (1.18e+0)	5.0507e+1 ⁷ (2.44e+0)	+ 6.8336e+1 ² (5.59e-1)	+ 6.8336e+1 ⁴ (9.38e-1)	+ 6.3581e+1 ⁵ (8.66e-1)	+ 7.2038e+1 ⁶ (2.288e+0)	+ 7.1699e+1 ⁷ (2.74e-1)	+ 7.1640e+1 ⁸ (1.38e-1)
	8	750	2.4003e+1 ⁸ (1.19e+0)	2.5673e+1 ⁷ (1.59e+0)	+ 1.0593e+2 ⁹ (1.02e+0)	+ 9.7300e+1 ⁶ (1.25e+0)	+ 1.0279e+2 ² (1.20e+0)	+ 9.7888e+1 ¹ (1.01e+0)	+ 9.7627e+1 ⁰ (9.76e-1)	+ 9.7617e+1 ⁻¹ (9.60e-1)
	10	1000	2.3717e+1 ⁸ (2.36e+0)	2.4039e+1 ⁷ (2.37e+0)	+ 1.7271e+2 ² (1.49e+0)	+ 1.5559e+2 ² (2.69e+0)	+ 1.6892e+2 ² (1.86e+0)	+ 1.5356e+2 ² (2.15e+0)	+ 1.5545e+2 ² (1.36e+0)	+ 1.5555e+2 ² (1.24e+0)
DTLZ2 ⁻¹	3	250	2.9548e+1 ⁸ (3.11e+0)	2.9796e+1 ⁷ (3.99e-1)	+ 3.2463e+1 ² (3.14e-1)	+ 3.2053e+1 ⁶ (3.94e-2)	+ 3.2052e+1 ⁴ (2.10e-1)	+ 3.2180e+1 ² (2.32e-1)	+ 3.2175e+1 ⁰ (1.60e-1)	+ 3.2367e+1 ⁻¹ (1.72e-1)
	5	350	1.0153e+2 ⁸ (1.75e-1)	1.0080e+2 ⁸ (1.53e+0)	+ 1.2848e+2 ⁶ (1.57e+0)	+ 1.1705e+2 ⁶ (3.09e+0)	+ 1.2130e+2 ⁵ (3.34e+0)	+ 1.3120e+2 ⁴ (1.20e+0)	+ 1.3120e+2 ² (1.19e+0)	+ 1.2491e+2 ¹ (1.49e+0)
	8	500	8.6972e+1 ⁷ (4.38e+0)	8.6035e+1 ⁸ (1.53e+0)	+ 1.3627e+2 ⁷ (1.39e+0)	+ 1.2741e+2 ⁶ (2.20e+0)	+ 1.3215e+2 ⁵ (2.05e+0)	+ 1.3438e+2 ⁴ (1.51e+0)	+ 1.3206e+2 ² (1.51e+0)	+ 1.3279e+2 ¹ (1.85e+0)
	10	750	1.2427e+2 ⁸ (6.09e+0)	1.2386e+2 ⁸ (5.69e+0)	+ 2.4543e+2 ² (2.42e+0)	+ 2.3235e+2 ² (5.48e+0)	+ 2.3533e+2 ² (3.33e+0)	+ 2.3973e+2 ² (2.37e+0)	+ 2.3539e+2 ² (2.08e+0)	+ 2.3395e+2 ² (2.08e+0)
DTLZ3 ⁻¹	3	1000	2.9623e+1 ⁸ (3.09e-1)	2.9700e+1 ⁷ (3.13e-1)	+ 3.2700e+1 ² (9.64e-2)	+ 3.2464e+1 ⁶ (1.96e-2)	+ 3.2510e+1 ⁵ (1.10e-1)	+ 3.2510e+1 ⁴ (5.99e-2)	+ 3.2772e+1 ³ (5.57e-2)	+ 3.2704e+1 ² (8.27e-2)
	5	1000	1.0425e+2 ⁸ (1.99e+0)	1.0011e+2 ⁸ (1.10e+0)	+ 1.3139e+2 ⁶ (1.34e+0)	+ 1.1917e+2 ⁶ (2.29e+0)	+ 1.2205e+2 ⁵ (3.59e+0)	+ 1.3120e+2 ⁴ (1.19e+0)	+ 1.3120e+2 ² (1.19e+0)	+ 1.2852e+2 ¹ (1.44e+0)
	8	1000	9.0102e+1 ⁷ (3.42e+0)	8.6076e+1 ⁸ (2.06e+0)	+ 1.3636e+2 ⁴ (2.41e+0)	+ 1.1481e+2 ⁴ (2.06e+0)	+ 1.2706e+2 ³ (2.63e+0)	+ 1.3519e+2 ² (1.82e+0)	+ 1.3275e+2 ¹ (1.75e+0)	+ 1.3242e+2 ⁰ (1.50e+0)
	10	1500	1.2796e+2 ⁸ (8.32e+0)	1.2796e+2 ⁸ (6.60e+0)	+ 2.4638e+2 ² (2.05e+0)	+ 2.1153e+2 ² (4.09e+0)	+ 2.2376e+2 ² (3.42e+0)	+ 2.4227e+2 ² (1.98e+0)	+ 2.3737e+2 ² (2.83e+0)	+ 2.3737e+2 ² (2.83e+0)
DTLZ4 ⁻¹	3	600	2.4637e+1 ⁸ (1.86e-1)	2.4801e+1 ⁷ (2.01e-1)	+ 2.6908e+1 ² (1.06e-1)	+ 2.6110e+1 ⁶ (1.50e-1)	+ 2.6311e+1 ⁵ (1.60e-1)	+ 2.6518e+1 ⁴ (1.14e-1)	+ 2.7024e+1 ³ (1.17e-1)	+ 2.7030e+1 ² (1.06e-1)
	5	600	7.7505e+1 ⁷ (1.32e-0)	7.5470e+1 ⁸ (1.51e-1)	+ 9.7868e+1 ⁴ (2.69e-2)	+ 8.0503e+1 ⁶ (1.46e-1)	+ 8.9001e+1 ² (1.64e-0)	+ 1.0155e+2 ¹ (4.70e-1)	+ 9.9716e+1 ³ (6.75e-1)	+ 9.9749e+1 ⁴ (7.45e-1)
	8	750	9.3157e+1 ⁷ (1.36e-0)	9.4250e+1 ⁸ (1.47e-0)	+ 1.3499e+2 ² (1.77e-0)	+ 1.3500e+2 ² (1.74e-0)	+ 1.3500e+2 ¹ (1.43e-0)	+ 1.3703e+2 ⁰ (1.41e-0)	+ 1.3038e+2 ⁻¹ (1.22e-0)	+ 1.3038e+2 ⁻² (1.22e-0)
	10	1000	1.3700e+2 ⁸ (5.30e+0)	1.3184e+2 ⁸ (4.52e+0)	+ 1.5348e+2 ² (3.09e+0)	+ 1.5091e+2 ⁶ (4.51e+0)	+ 1.5390e+2 ⁹ (3.70e+0)	+ 1.5167e+2 ⁸ (2.99e+0)	+ 1.5421e+2 ⁷ (2.92e+0)	+ 1.5444e+2 ⁶ (1.11e+0)
WFG1 ⁻¹	3	400	1.6628e+1 ⁵ (5.51e-1)	1.8172e+1 ⁷ (5.81e-1)	+ 1.7272e+1 ² (4.91e-1)	+ 1.6764e+1 ⁶ (1.56e-1)	+ 1.7060e+1 ⁴ (3.50e-1)	+ 1.7055e+1 ³ (2.32e-1)	+ 1.7224e+1 ² (4.36e-1)	+ 1.7025e+1 ¹ (4.55e-1)
	5	750	2.1282e+1 ⁷ (6.79e-1)	1.6162e+1 ⁸ (8.04e-1)	+ 3.4721e+1 ² (8.76e-1)	+ 3.1724e+1 ⁶ (1.11e+0)	+ 3.3396e+1 ⁴ (8.85e-1)	+ 3.8404e+1 ³ (6.57e-1)	+ 3.8167e+1 ² (7.61e-1)	+ 3.8232e+1 ¹ (6.47e-1)
	8	1500	2.6738e+1 ⁷ (1.97e-0)	2.6730e+1 ⁸ (2.06e+0)	+ 5.1378e+1 ⁵ (3.68e+0)	+ 4.8024e+1 ⁶ (3.19e+0)	+ 5.1807e+1 ⁴ (3.74e-0)	+ 6.0071e+1 ² (4.00e+0)	+ 6.0071e+1 ⁻¹ (4.00e+0)	+ 5.9850e+1 ⁻² (3.87e+0)
	10	2000	2.7707e+1 ⁸ (1.82e-0)	2.8689e+1 ⁷ (2.12e+0)	+ 6.8639e+1 ⁵ (4.08e+0)	+ 6.5101e+1 ⁶ (3.93e+0)	+ 6.7086e+1 ⁴ (5.49e+0)	+ 6.8362e+1 ² (6.57e+0)	+ 6.8362e+1 ^{-1</}	

Table 21: Mean and standard deviations (in parenthesis) of the HV indicator obtained by MOEAs using the RVEA framework on MOPs with irregular PF shapes. The two best mean values per MOP are highlighted in grayscale, where the darker tone corresponds to the best one. The symbols “+”, “-”, and “=” are placed when the MOEA performs significantly better, significantly worse, or statistically equivalent to RVEA based on a one-tailed Wilcoxon test using a significance level of $\alpha = 0.05$. The % of satisfaction refers to the percentage of MOPs where the MOEA performs significantly better than RVEA. The superscripts are the obtained rank in the comparison.

MOP	Obj.	Gen.	RVEA	RVEA*	RVEA-AdaRSE	RVEA-AdaGAE	RVEA-AdaMPT	RVEA-AdaCOU	RVEA-AdaPT	RVEA-AdaKRA
DTLZ5	3	400	5.2469e+0 ³ (5.26e-2)	5.5074e+0³ (1.27e-3)	5.4937e+0 ³ (7.79e-3)	5.4858e+0 ³ (5.68e-3)	5.4867e+0 ³ (5.82e-3)	5.4947e+0 ³ (6.73e-3)	5.4878e+0 ³ (2.89e-2)	5.4047e+0 ³ (7.30e-3)
	5	600	3.1213e+1 ⁵ (1.17e-1)	3.1162e+1 ⁵ (2.69e-2)	3.1215e+1 ⁵ (1.58e-2)	3.1203e+1 ⁵ (1.86e-2)	3.1202e+1 ⁵ (1.75e-2)	3.1272e+1 ⁵ (9.10e-3)	3.1222e+1 ³ (1.73e-2)	3.1224e+1 ² (1.74e-2)
	8	750	2.4797e+0 ³ (3.68e-1)	2.4824e+0 ³ (4.55e-1)	2.4877e+0 ³ (2.86e-1)	2.4861e+0 ³ (2.99e-1)	2.4864e+0 ³ (2.59e-1)	2.4908e+0 ² (1.36e-1)	2.4886e+0 ² (2.28e-1)	2.4886e+0 ² (2.33e-1)
	10	1000	9.9364e+0 ² (7.06e-1)	9.9467e+0 ² (1.13e+0)	9.9525e+0 ² (1.13e+0)	9.9529e+0 ² (1.35e-1)	9.9551e+0 ² (9.06e-1)	1.0000e+0 ³ (4.27e-1)	9.9566e+0 ² (9.59e-1)	9.9588e+0 ² (6.97e-1)
DTLZ6	3	400	5.2647e+0 ² (7.03e-2)	5.5070e+0 ² (1.23e-3)	5.5075e+0 ² (6.86e-3)	5.5032e+0 ² (9.30e-3)	5.5009e+0 ² (1.89e-2)	5.5072e+0 ² (6.90e-2)	5.5076e+0 ² (7.51e-3)	5.5065e+0 ² (1.29e-2)
	5	600	3.1913e+1 ⁵ (1.21e-1)	3.1922e+1 ⁵ (2.77e-2)	3.1917e+1 ⁵ (3.36e-3)	3.1919e+1 ⁵ (3.36e-3)	3.1918e+1 ⁵ (3.13e-2)	3.1925e+1 ⁵ (6.25e-3)	3.1919e+1 ⁵ (2.78e-3)	3.1920e+1 ⁵ (2.71e-3)
	8	750	2.5498e+0 ² (7.08e-2)	2.5528e+0 ² (3.40e-2)	2.5527e+0 ² (3.83e-2)	2.5526e+0 ² (3.38e-2)	2.5525e+0 ² (4.19e-2)	2.5534e+0 ² (2.52e-2)	2.5528e+0 ² (2.75e-2)	2.5528e+0 ² (2.27e-2)
	10	1000	1.0198e+0 ³ (8.28e-2)	1.0210e+0³ (1.24e-1)	1.0209e+0 ³ (1.35e-1)	1.0209e+0 ³ (1.43e-1)	1.0209e+0 ³ (1.20e-1)	1.0210e+0 ³ (8.29e-2)	1.0210e+0 ³ (9.63e-2)	1.0210e+0 ³ (8.40e-2)
DTLZ7	3	1000	6.5137e+0 ² (6.20e-2)	6.4793e+0 ² (2.80e-1)	6.5617e+0² (8.95e-3)	6.5551e+0 ² (1.19e-2)	6.5586e+0 ² (1.14e-2)	6.5575e+0 ² (1.13e-2)	6.5556e+0 ² (1.15e-2)	6.5626e+0 ² (1.21e-2)
	5	1000	2.3430e+0 ³ (6.40e-2)	2.5043e+0³ (3.69e-2)	2.4424e+0 ³ (9.76e-2)	2.4256e+0 ³ (7.36e-2)	2.4282e+0 ³ (8.36e-2)	2.4381e+0 ³ (7.01e-2)	2.4722e+0 ³ (8.27e-2)	2.4724e+0 ³ (5.89e-2)
	8	1000	1.5744e+0 ² (2.95e-0)	1.7863e+0 ² (1.88e+0)	1.7011e+0 ² (4.33e+0)	1.6536e+0 ² (2.66e+0)	1.6893e+0 ² (3.30e+0)	1.7555e+0 ² (2.90e+0)	1.7226e+0 ² (3.13e+0)	1.7258e+0 ² (3.02e+0)
	10	1500	5.8589e+0 ² (1.35e+1)	6.8911e+0 ² (2.31e+0)	6.5590e+0 ² (1.12e+1)	6.5436e+0 ² (9.87e+0)	6.5453e+0 ² (9.78e+0)	6.8857e+0 ² (6.93e+0)	6.4067e+0 ² (1.87e+1)	6.3766e+0 ² (1.61e+1)
WFG2	3	400	7.8154e+0 ² (3.74e-2)	7.7950e+0 ² (3.19e-2)	7.7813e+0 ² (2.07e-2)	7.7810e+0 ² (2.85e-2)	7.8126e+0 ² (3.60e-2)	7.8120e+0 ² (3.78e-2)	7.8180e+0 ² (3.09e-2)	7.8163e+0 ² (2.85e-2)
	5	750	3.1851e+1 ⁵ (2.80e-2)	3.1651e+1 ⁵ (4.76e-2)	3.1849e+1 ⁵ (3.17e-2)	3.1861e+1 ⁵ (3.11e-2)	3.1857e+1 ⁵ (3.42e-2)	3.1865e+1 ⁵ (3.09e-2)	3.1849e+1 ⁵ (2.47e-2)	3.1855e+1 ⁵ (3.61e-2)
	8	1500	2.5434e+0 ² (4.69e-1)	2.5212e+0 ² (8.36e-1)	2.5411e+0 ² (4.13e-1)	2.5433e+0 ² (4.48e-1)	2.5422e+0 ² (4.12e-1)	2.5412e+0 ² (1.32e-0)	2.5344e+0 ² (5.69e-1)	2.5447e+0 ² (5.90e-1)
	10	2000	1.0193e+0 ³ (1.12e+0)	1.0137e+0 ³ (2.58e+0)	1.0200e+0 ³ (1.23e+0)	1.0199e+0 ³ (9.19e+0)	1.0200e+0 ³ (1.19e+0)	1.0203e+0 ³ (3.13e+0)	1.0208e+0 ³ (1.21e+0)	1.0208e+0 ³ (1.25e+0)
WFG3	3	400	6.9429e+0 ² (2.14e-0)	6.9547e+0² (6.07e-2)	6.9331e+0 ² (2.39e-3)	6.9089e+0 ² (2.98e-2)	6.9307e+0 ² (3.27e-2)	6.9323e+0 ² (3.20e-2)	6.9323e+0 ² (3.20e-2)	6.9217e+0 ² (3.93e-2)
	5	750	2.8631e+0 ³ (1.82e-1)	2.7634e+0³ (6.27e-1)	2.8260e+0 ³ (1.85e-1)	2.8086e+0 ³ (1.43e-1)	2.8100e+0 ³ (1.28e-1)	2.8473e+0 ³ (1.30e-1)	2.8385e+0 ³ (1.24e-1)	2.8417e+0 ³ (1.63e-1)
	8	1500	2.0104e+0 ² (1.43e-0)	2.0269e+0 ² (1.01e+1)	1.9811e+0 ² (1.38e-1)	1.9933e+0 ² (1.26e-1)	1.9665e+0 ² (1.09e-1)	1.9574e+0 ² (1.32e-0)	2.1762e+0 ² (5.12e+0)	2.1623e+0 ² (4.92e+0)
	10	2000	7.8494e+0 ² (5.57e+1)	8.1663e+0 ² (5.11e+1)	7.5023e+0 ² (5.26e+1)	7.4238e+0 ² (4.79e+1)	7.4238e+0 ² (4.79e+1)	8.6563e+0 ² (5.07e+1)	8.7151e+0 ² (2.81e+1)	8.7151e+0 ² (2.81e+1)
DTLZ1	3	400	5.3421e+0 ² (7.47e-4)	5.4331e+0 ² (2.18e-2)	5.4763e+0 ² (4.71e-2)	5.4745e+0 ² (2.16e-2)	5.4750e+0 ² (1.97e-2)	5.4811e+0 ² (9.71e-3)	5.4838e+0 ² (5.30e-3)	5.4821e+0 ² (1.03e-2)
	5	600	7.1834e+0 ² (2.24e-1)	8.9725e+0² (4.42e-1)	1.0916e+0 ² (5.27e-1)	1.0307e+0 ² (7.33e-2)	1.0507e+0 ² (7.33e-2)	1.1229e+0 ¹ (4.88e-2)	1.1213e+0 ¹ (1.66e-2)	1.1213e+0 ¹ (9.84e-2)
	8	750	3.6154e+0 ² (1.33e+0)	3.5241e+0² (6.05e-1)	1.7242e+0 ² (1.44e+0)	1.5747e+0 ² (1.45e+0)	1.6110e+0 ² (1.83e+0)	1.0373e+0 ² (1.12e+0)	1.0414e+0 ² (1.35e+0)	1.0414e+0 ² (1.35e+0)
	10	1000	2.7397e+0 ² (6.89e-1)	2.1858e+0 ² (8.22e-1)	2.4340e+0 ² (2.76e+0)	2.1509e+0 ² (2.69e+0)	2.3206e+0 ² (2.97e+0)	2.8243e+0 ¹ (2.51e+0)	2.7662e+0 ¹ (2.92e+0)	2.7837e+0 ¹ (2.45e+0)
DTLZ2	3	250	6.6223e+0 ² (8.64e-4)	6.6613e+0 ² (2.13e-2)	6.6881e+0² (8.03e-3)	6.6691e+0 ² (1.49e-2)	6.6778e+0 ² (1.29e-2)	6.6775e+0 ² (1.40e-2)	6.6910e+0 ² (9.51e-3)	6.6868e+0 ² (9.42e-3)
	5	350	1.4318e+0 ³ (1.89e-1)	1.5702e+0³ (2.77e-1)	1.7136e+0 ³ (1.76e-2)	1.6717e+0 ³ (1.31e-1)	1.6861e+0 ³ (1.19e-1)	1.7347e+0 ³ (1.60e-2)	1.7267e+0 ³ (1.72e-2)	1.7276e+0 ³ (1.53e-2)
	8	500	8.1825e+0 ² (8.08e-1)	8.5217e+0² (1.40e-0)	4.2700e+0 ² (5.55e-1)	4.0378e+0 ² (8.80e-1)	4.1265e+0 ² (9.17e-1)	4.1448e+0 ² (6.72e-1)	3.8990e+0 ¹ (6.02e-1)	3.9018e+0 ¹ (6.26e-1)
	10	750	2.4020e+0 ² (1.04e-0)	6.6312e+0² (1.25e-0)	7.1967e+0 ² (1.25e-0)	7.4241e+0 ² (1.45e-0)	7.5594e+0 ² (1.42e-0)	8.6701e+0 ² (9.09e-1)	6.4292e+0 ¹ (1.12e-0)	6.4068e+0 ¹ (1.35e+0)
DTLZ3	3	600	6.6345e+0 ² (3.64e-4)	6.6870e+0 ² (4.66e-3)	6.7050e+0² (4.86e-3)	6.6973e+0 ² (1.11e-2)	6.6986e+0 ² (8.42e-3)	6.7030e+0 ² (4.24e-3)	6.7022e+0 ² (8.97e-3)	6.7015e+0 ² (1.16e-2)
	5	1000	1.4311e+0 ³ (2.14e-2)	1.5926e+0³ (1.99e-1)	1.7294e+0 ³ (4.75e-2)	1.6966e+0 ³ (1.61e-1)	1.6884e+0 ³ (1.55e-2)	1.7406e+0 ³ (5.55e-2)	1.7424e+0 ³ (4.66e-2)	1.7424e+0 ³ (4.66e-2)
	8	1000	1.8201e+0 ³ (8.91e-1)	3.3952e+0² (1.31e+0)	4.0409e+0 ² (7.73e-1)	3.7239e+0 ² (8.84e-1)	3.8602e+0 ² (1.02e+0)	3.9170e+0 ² (7.32e+1)	3.7118e+0 ² (7.50e-1)	3.7323e+0 ² (5.23e-1)
	10	1500	3.2849e+0 ² (7.36e-1)	6.4799e+0² (2.70e+0)	7.4078e+0 ¹ (9.33e-1)	6.9160e+0 ¹ (1.68e+0)	7.1987e+0 ¹ (1.50e+0)	6.6952e+0 ¹ (1.09e+0)	6.6952e+0 ¹ (1.07e+0)	6.1140e+0 ¹ (1.11e+0)
DTLZ4	3	600	6.6540e+0 ² (5.26e-2)	6.6940e+0 ² (4.56e-3)	6.7160e+0² (3.26e-3)	6.7201e+0 ² (3.07e-3)	6.7275e+0 ² (1.29e-2)	6.7376e+0 ² (1.28e-2)	6.6905e+0 ² (5.36e-1)	6.6905e+0 ² (3.51e-1)
	5	1000	1.4174e+0 ³ (6.67e-1)	1.6425e+0³ (1.67e-1)	1.7243e+0 ³ (1.67e-1)	1.6477e+0 ³ (1.86e-1)	1.6995e+0 ³ (1.12e-1)	1.7508e+0 ¹ (2.60e-2)	1.7463e+0 ¹ (3.85e-2)	1.7528e+0 ¹ (1.14e-0)
	8	1250	4.1477e+0 ² (1.34e-0)	4.2177e+0² (2.33e+0)	3.1349e+0 ² (5.76e-1)	3.0344e+0 ² (5.01e+0)	3.0931e+0 ² (6.84e-1)	3.0275e+0 ² (5.64e-1)	2.8354e+0 ² (6.48e-1)	2.9636e+0 ² (6.02e+0)
	10	2000	2.0180e+0 ² (1.39e-0)	8.4602e+0² (4.22e+0)	1.0325e+0 ² (3.66e-0)	5.1626e+0 ² (5.95e-1)	8.8339e+0 ² (3.38e-0)	5.1963e+0 ² (1.06e+1)	4.9830e+0 ² (8.44e-0)	5.1617e+0 ² (7.26e+0)
DTLZ5	3	400	6.6532e+0 ² (2.85e-5)	6.6870e+0 ² (1.17e-2)	6.7250e+0² (3.33e-3)	6.7154e+0 ² (4.30e-3)	6.7188e+0 ² (3.40e-3)	6.7193e+0 ² (3.09e-3)	6.7262e+0 ² (2.07e-3)	6.7255e+0 ² (3.29e-3)
	5	600	1.4468e+0 ³ (3.89e-0)	1.5933e+0³ (2.12e-1)	1.7701e+0 ³ (3.42e-1)	1.7506e+0 ³ (5.93e-2)	1.7591e+0 ³ (2.12e-1)	1.7715e+0 ¹ (5.90e-2)	1.7715e+0 ¹ (3.19e-2)	1.7726e+0 ¹ (3.33e-1)
	8	750	3.1797e+0 ² (4.80e-1)	3.6376e+0² (1.29e+0)	4.4539e+0 ² (5.50e-1)	4.5352e+0 ² (4.74e-1)	4.3002e+0 ² (3.55e-1)	4.1866e+0 ² (3.34e-1)	4.1186e+0 ² (2.67e-1)	4.1388e+0 ² (2.67e-1)
	10	1000	7.0174e+0 ² (1.86e-1)	7.0711e+0² (2.03e+0)	8.0178e+0 ² (1.79e+0)	7.9506e+0 ² (1.86e+0)	8.2213e+0 ² (2.03e+0)	7.6464e+0 ² (1.87e+0)	7.6464e+0 ² (1.87e+0)	7.2273e+0 ² (1.87e-1)
DTLZ7	3	1000	7.2190e+0 ² (1.63e-2)	7.2395e+0² (3.71e-3)	7.2088e+0 ² (8.13e-3)	7.2120e+0² (0.94e-3)</b				

Table 22: Mean and standard deviations (in parenthesis) of the SPD indicator obtained by MOEAs using the RVEA framework on MOPs with irregular PF shapes. The two best mean values per MOP are highlighted in grayscale, where the darker tone corresponds to the best one. The symbols “+”, “-”, and “=” are placed when the MOEA performs significantly better, significantly worse, or statistically equivalent to RVEA based on a one-tailed Wilcoxon test using a significance level of $\alpha = 0.05$. The % of satisfaction refers to the percentage of MOPs where the MOEA performs significantly better than RVEA. The superscripts are the obtained rank in the comparison.

MOP	Obj.	Gen.	RVEA	RVEA*	RVEA-AdaRSE	RVEA-AdaGAE	RVEA-AdaMPT	RVEA-AdaCOU	RVEA-AdaPT	RVEA-AdaKRA
DTLZ5	3	400	9.9863e+0 ⁸ (1.68e+0)	1.0430e+1 ⁷ (2.08e-2)	+ 1.0570e+1 ² (1.67e-1)	+ 1.0545e+1 ⁵ (9.04e-2)	+ 1.0560e+1 ³ (7.83e-2)	+ 1.0619e+1 ⁹ (2.47e-1)	+ 1.0453e+1 ⁶ (5.83e-1)	+ 1.0549e+1 ⁴ (1.09e-1)
	5	600	2.5690e+1 ² (2.29e+0)	9.4552e+0 ⁸ (1.57e+0)	+ 2.3590e+1 ² (1.72e+0)	+ 2.1817e+1 ⁷ (1.72e+0)	+ 2.1868e+1 ⁶ (2.46e+0)	+ 2.2010e+1 ³ (1.47e+0)	+ 2.0211e+1 ⁷ (2.48e+0)	+ 2.6380e+1 ¹ (2.61e+0)
	8	750	4.3742e+1 ² (9.61e+0)	1.0077e+1 ⁸ (3.37e+0)	+ 4.4195e+1 ³ (9.61e+0)	+ 3.5497e+1 ⁷ (6.96e+0)	+ 3.9339e+1 ⁵ (8.09e+0)	+ 3.6301e+1 ⁸ (4.02e+0)	+ 6.2517e+1 ² (1.11e+1)	+ 6.4966e+1 ¹ (1.27e+1)
	10	1000	6.4458e+1 ² (1.56e+0)	1.4688e+1 ⁸ (1.56e+0)	+ 6.7640e+1 ² (1.75e+0)	+ 6.2726e+1 ⁷ (1.36e+1)	+ 7.1055e+1 ⁴ (6.69e+1)	+ 6.6458e+1 ⁸ (1.23e+1)	+ 1.3283e+2 ² (1.84e+1)	+ 1.2952e+2 ² (1.90e+1)
DTLZ6	3	400	1.0028e+1 ⁸ (1.59e+0)	1.0417e+1 ⁷ (1.85e-2)	- 1.0594e+1 ² (2.20e-1)	- 1.0434e+1 ⁶ (8.90e-2)	- 1.0461e+1 ⁷ (7.80e-2)	- 1.0657e+1 ¹ (2.36e-1)	- 1.0554e+1 ⁴ (1.54e-1)	- 1.0606e+1 ² (2.47e-1)
	5	600	1.4365e+1 ² (1.46e+0)	1.0368e+1 ⁸ (1.31e+0)	- 1.4636e+1 ² (1.57e+0)	- 1.5379e+1 ⁵ (2.07e+0)	- 1.6180e+1 ⁸ (1.93e+0)	+ 1.3031e+1 ⁷ (1.62e-1)	+ 1.7206e+1 ² (1.79e+0)	+ 1.7344e+1 ¹ (1.91e+0)
	8	750	2.2878e+1 ² (4.29e+0)	1.3931e+1 ⁸ (2.02e+0)	- 3.5321e+1 ² (4.01e+0)	- 3.1030e+1 ⁵ (3.86e+0)	- 3.2405e+1 ⁸ (2.11e+0)	+ 2.6510e+1 ² (2.11e+0)	+ 4.2783e+1 ² (5.45e+0)	+ 4.0760e+1 ² (4.64e+0)
	10	1000	3.6744e+1 ² (6.55e+0)	2.4455e+1 ⁸ (8.12e+0)	- 5.0852e+1 ² (8.12e+0)	+ 5.0638e+1 ⁵ (8.25e+0)	+ 5.5432e+1 ⁸ (3.12e+0)	+ 4.5753e+1 ² (3.12e+0)	+ 7.8586e+1 ¹ (1.14e+1)	+ 7.3618e+1 ² (1.05e+1)
DTLZ7	3	400	2.3108e+1 ⁷ (3.53e-1)	2.2052e+1 ⁸ (4.15e+0)	- 2.5905e+1 ² (3.28e-1)	- 2.5293e+1 ⁵ (3.25e-1)	- 2.5552e+1 ⁵ (3.25e-1)	- 2.5586e+1 ¹ (4.66e-1)	- 2.5003e+1 ³ (3.50e-1)	- 2.5016e+1 ² (3.80e-1)
	5	1000	6.8259e+1 ⁸ (2.64e+0)	1.2519e+1 ² (1.32e+0)	+ 1.3802e+2 ² (2.59e+0)	+ 1.3652e+2 ⁵ (2.63e+0)	+ 1.3672e+2 ² (2.79e+0)	+ 1.3024e+2 ² (2.50e+0)	+ 1.3807e+2 ² (2.77e+0)	+ 1.3710e+2 ² (2.71e+0)
	8	1000	4.7925e+1 ⁸ (5.92e+0)	1.5053e+2 ² (5.75e+0)	+ 8.7357e+1 ⁷ (7.13e+0)	+ 8.7705e+1 ⁶ (5.93e+0)	+ 8.9278e+1 ⁵ (6.06e+0)	+ 9.1355e+1 ² (2.48e+0)	+ 8.8362e+1 ³ (3.53e+0)	+ 9.0977e+1 ² (3.24e+0)
	10	1500	7.0384e+1 ⁸ (1.12e+1)	2.7214e+2 ² (1.88e+0)	+ 1.4442e+2 ² (6.64e+0)	+ 1.4281e+2 ⁶ (9.55e+0)	+ 1.4614e+2 ² (8.84e+0)	+ 1.4086e+2 ² (6.66e+0)	+ 1.4382e+2 ² (1.00e+1)	+ 1.4392e+2 ² (7.80e+0)
WFG2	3	400	1.9965e+1 ⁷ (4.94e-1)	1.7700e+1 ⁸ (4.76e-1)	- 1.9792e+1 ² (3.71e-1)	- 1.9902e+1 ³ (4.59e-1)	- 1.9931e+1 ¹ (5.78e-1)	- 1.9931e+1 ¹ (5.78e-1)	- 1.9777e+1 ⁹ (5.52e-1)	- 1.9824e+1 ⁴ (4.16e-1)
	5	750	3.0137e+1 ⁷ (9.19e-1)	2.1123e+1 ⁸ (1.26e+0)	- 2.9343e+1 ² (1.21e+0)	- 2.9858e+1 ⁵ (1.21e+0)	- 2.9702e+1 ² (1.33e+0)	- 2.9602e+1 ⁹ (1.15e+0)	- 2.9913e+1 ³ (1.12e+0)	- 3.0159e+1 ² (9.84e-1)
	8	1500	2.0408e+1 ⁷ (1.38e+0)	1.1152e+1 ⁸ (1.31e+0)	- 2.0073e+1 ² (1.42e+0)	- 2.0407e+1 ⁵ (1.46e+0)	- 1.9947e+1 ² (1.62e+0)	- 2.0408e+1 ⁹ (1.20e+0)	- 2.1276e+1 ² (1.73e+0)	- 2.1593e+1 ² (1.85e+0)
	10	2000	2.0636e+1 ⁷ (1.50e+0)	9.8858e+1 ⁸ (1.06e+0)	- 2.2293e+1 ² (1.19e+0)	- 2.2836e+1 ⁵ (1.65e+0)	- 2.2995e+1 ² (1.81e+0)	- 2.3628e+1 ⁹ (1.98e+0)	- 2.4639e+1 ² (2.38e+0)	- 2.4636e+1 ² (1.89e+0)
WFG3	3	400	1.1568e+1 ⁷ (4.68e-1)	1.0258e+1 ⁸ (3.67e-1)	- 1.1900e+1 ² (4.02e-1)	- 1.1980e+1 ⁴ (5.06e-1)	- 1.2029e+1 ² (5.74e-1)	- 1.1632e+1 ⁹ (5.29e-1)	- 1.2004e+1 ³ (5.08e-1)	- 1.2117e+1 ¹ (5.77e-1)
	5	750	2.6363e+1 ⁷ (1.05e+0)	2.0371e+1 ⁸ (2.23e+0)	- 4.1319e+1 ² (1.10e+0)	- 6.3069e+1 ⁵ (1.06e+0)	- 3.8153e+1 ⁹ (1.04e+0)	- 4.1777e+1 ² (8.84e-1)	- 4.6941e+1 ³ (1.04e+0)	- 4.6929e+1 ² (7.99e-1)
	8	1500	7.3213e+1 ⁷ (5.02e+0)	4.9923e+1 ⁸ (4.23e+0)	- 7.2323e+1 ² (2.77e+0)	- 6.4093e+1 ⁷ (3.95e-0)	- 6.7373e+1 ² (3.89e-0)	- 7.3207e+1 ⁹ (1.49e+0)	- 7.6326e+1 ² (1.21e+0)	- 7.6065e+1 ² (1.11e+0)
	10	2000	1.2129e+2 ² (7.77e+0)	9.1133e+1 ⁸ (8.38e+0)	- 1.1649e+2 ⁵ (9.59e+0)	- 1.0597e+2 ² (9.59e+0)	- 1.0989e+2 ² (8.48e-0)	- 1.1721e+2 ² (2.10e+0)	- 1.2001e+2 ² (1.74e+0)	- 1.1985e+2 ² (1.81e+0)
DTLZ1 ⁻¹	3	400	1.8410e+1 ⁸ (1.50e-2)	2.1969e+1 ⁷ (1.91e-1)	- 2.3554e+1 ² (4.25e-1)	- 2.3484e+1 ⁶ (1.62e-1)	- 2.3400e+1 ² (2.27e-1)	- 2.3490e+1 ³ (1.91e-1)	- 2.3507e+1 ² (2.02e-1)	- 2.3481e+1 ² (2.09e-1)
	5	600	2.4558e+1 ⁸ (1.45e-0)	4.4724e+1 ⁷ (3.56e+0)	- 6.8803e+1 ² (6.72e-1)	- 6.0527e+1 ⁶ (1.49e+0)	- 6.1253e+1 ² (7.58e-1)	- 7.0505e+1 ³ (1.06e+0)	- 7.1494e+1 ² (3.98e-1)	- 7.1332e+1 ² (3.20e+0)
	8	750	3.3299e+1 ⁸ (3.16e+0)	6.7949e+1 ⁷ (4.72e+0)	- 8.0385e+1 ² (1.18e+1)	- 7.0310e+1 ⁶ (1.21e+1)	- 7.1885e+1 ² (6.45e-1)	- 8.7010e+1 ³ (8.08e+0)	- 8.7209e+1 ² (3.38e+0)	- 8.2099e+1 ² (1.22e+1)
	10	1000	3.1396e+1 ⁸ (1.09e+0)	9.8027e+1 ⁷ (6.63e+0)	- 1.2000e+2 ² (1.68e+1)	- 9.6939e+1 ² (1.73e+1)	- 1.1120e+2 ² (2.62e+1)	- 1.3332e+2 ² (2.34e+1)	- 1.3459e+2 ² (2.03e+1)	- 1.3459e+2 ² (2.03e+1)
DTLZ2 ⁻¹	3	250	2.7581e+1 ⁷ (1.47e-1)	2.8527e+1 ⁷ (9.61e-1)	- 3.2018e+1 ² (1.82e-1)	- 3.1340e+1 ⁶ (4.80e-1)	- 3.1764e+1 ² (4.34e-1)	- 3.1596e+1 ⁹ (3.66e-1)	- 3.2046e+1 ² (2.75e-1)	- 3.2003e+1 ³ (3.11e-1)
	5	350	4.3039e+1 ⁷ (2.83e-1)	7.3369e+1 ⁸ (5.03e+0)	- 1.2302e+2 ² (2.30e+0)	- 1.0628e+2 ⁶ (4.64e+0)	- 1.1222e+2 ² (3.71e+0)	- 1.2688e+2 ² (1.94e+0)	- 1.1891e+2 ² (1.44e+0)	- 1.1921e+2 ² (1.37e+0)
	8	500	1.3618e+1 ⁸ (2.40e+0)	6.1817e+1 ⁷ (6.36e+0)	- 1.1431e+2 ² (1.60e+0)	- 1.0140e+2 ⁶ (3.05e+0)	- 1.0603e+2 ² (2.88e+0)	- 1.1805e+2 ² (1.06e+0)	- 1.1517e+2 ² (1.54e+0)	- 1.1513e+2 ² (1.34e+0)
	10	750	4.0778e+1 ⁷ (1.09e+0)	1.0955e+2 ² (9.15e+0)	- 2.0356e+2 ² (3.57e+0)	- 1.7935e+2 ⁶ (4.23e+0)	- 1.8934e+2 ² (3.32e+0)	- 2.1557e+2 ² (2.05e+1)	- 2.0877e+2 ² (2.31e+0)	- 2.0912e+2 ² (2.12e+0)
DTLZ3 ⁻¹	3	1000	2.7663e+1 ⁷ (9.36e-2)	3.0080e+1 ⁷ (4.12e-1)	- 3.2404e+1 ² (1.98e-1)	- 3.2128e+1 ⁶ (1.63e-1)	- 3.2160e+1 ² (1.52e-1)	- 3.2148e+1 ⁹ (1.65e-1)	- 3.2390e+1 ² (2.13e-1)	- 3.2363e+1 ² (2.01e-1)
	5	1000	4.3127e+1 ⁷ (1.66e-1)	7.8838e+1 ⁷ (5.36e+0)	- 1.2948e+2 ² (1.12e+0)	- 1.1726e+2 ⁶ (4.76e-1)	- 1.2128e+2 ² (3.70e+0)	- 1.3250e+2 ² (0.37e+1)	- 1.3275e+2 ² (1.38e+0)	- 1.2400e+2 ² (1.74e+0)
	8	1000	3.1523e+1 ⁸ (2.58e+0)	5.6711e+1 ⁷ (6.07e+0)	- 1.1813e+2 ² (1.16e+0)	- 1.0320e+2 ⁶ (3.57e+0)	- 1.1912e+2 ² (3.03e+0)	- 1.2185e+2 ² (3.64e+0)	- 1.1943e+2 ² (3.14e-1)	- 1.1937e+2 ² (9.33e-1)
	10	1500	4.0493e+1 ⁷ (7.58e-1)	1.0552e+2 ² (1.21e+1)	- 2.1267e+2 ² (1.19e+0)	- 1.8517e+2 ⁶ (2.95e+0)	- 1.9857e+2 ² (2.78e+0)	- 2.1987e+2 ² (0.54e+0)	- 2.1529e+2 ² (1.07e+0)	- 2.1539e+2 ² (1.09e+0)
DTLZ4 ⁻¹	3	600	2.7026e+1 ⁷ (3.62e+0)	3.0202e+1 ⁷ (2.75e+0)	- 3.1737e+1 ² (1.73e-1)	- 2.9733e+1 ⁶ (1.73e-1)	- 2.9733e+1 ² (1.73e-1)	- 2.6633e+1 ⁹ (1.72e-1)	- 2.6783e+1 ² (1.34e-1)	- 2.6755e+1 ² (1.47e-1)
	5	1000	4.3371e+1 ⁷ (1.14e+0)	8.7714e+1 ⁷ (2.67e+0)	- 1.3123e+2 ² (9.81e+0)	- 1.2030e+2 ⁶ (2.05e+0)	- 1.2500e+2 ² (9.12e+0)	- 1.3392e+2 ² (8.07e+0)	- 1.2610e+2 ² (1.50e+0)	- 1.2497e+2 ² (8.46e+0)
	8	1250	2.7482e+1 ⁷ (5.32e+0)	1.0811e+2 ² (1.12e+1)	- 1.2408e+2 ² (6.94e+0)	- 1.2150e+2 ⁶ (2.75e+0)	- 1.2146e+2 ² (7.30e+0)	- 1.2146e+2 ² (1.20e+1)	- 1.1920e+2 ² (1.20e+1)	- 1.1984e+2 ² (7.46e+0)
	10	2000	3.8324e+1 ⁷ (1.70e+0)	1.8774e+2 ² (9.19e+0)	- 2.2101e+2 ² (6.40e+0)	- 2.1571e+2 ⁶ (2.95e+0)	- 2.2001e+2 ² (7.71e+0)	- 2.1920e+2 ² (8.93e+0)	- 2.1477e+2 ² (9.74e+0)	- 2.1572e+2 ² (7.57e+0)
DTLZ5 ⁻¹	3	400	2.2753e+1 ⁷ (2.03e-1)	2.4278e+1 ⁷ (3.03e+0)	- 2.6874e+1 ² (1.87e-1)	- 2.5857e+1 ⁶ (2.50e-1)	- 2.5857e+1 ² (2.50e-1)	- 2.3131e+1 ⁹ (1.70e-1)	- 2.3133e+1 ² (1.70e-1)	- 2.6753e+1 ² (2.25e-1)
	5	600	4.0393e+1 ⁷ (3.67e-1)	5.6717e+1 ⁷ (3.76e-1)	- 6.0362e+1 ² (1.63e+0)	- 8.5015e+1 ⁶ (1.36e+0)	- 8.4156e+1 ² (5.85e-1)	- 9.8104e+1 ¹ (5.85e-1)	- 9.6342e+1 ² (4.41e-1)	- 9.6398e+1 ² (4.48e-1)
	8	750	2.5221e+1 ⁸ (7.40e-1)	5.1946e+1 ⁷ (6.42e+0)	- 1.0658e+2 ² (2.26e+0)	- 8.7748e+1 ⁶ (3.03e+0)	- 1.0254e+2 ² (2.36e+0)	- 1.1928e+2 ² (1.36e+0)	- 1.0816e+2 ² (1.36e+0)	- 1.0791e+2 ² (1.36e+0)
	10	1000	2.7144e+1 ⁸ (6.15e-1)	8.6947e+1 ⁷ (9.82e+0)	- 1.2327e+2 ² (4.65e+0)	- 1.4205e+2 ⁶ (2.74e+0)	- 1.3966e+2 ² (1.01e+1)	- 1.9903e+2 ² (2.09e+0)	- 1.8960e+2 ² (2.73e+0)	- 1.8938e+2 ² (2

Table 23: Mean and standard deviations (in parenthesis) of the HV indicator obtained by MOEAs using the MOEA/D framework on MOPs with irregular PF shapes. The two best mean values per MOP are highlighted in grayscale, where the darker one corresponds to the best one. The symbols “+”, “-”, and “=” are placed when the MOEA performs significantly better, significantly worse, or statistically equivalent to MOEA/D based on a one-tailed Wilcoxon test using a significance level of $\alpha = 0.05$. The % of satisfaction refers to the percentage of MOPs where the MOEA performs significantly better than MOEA/D. The superscripts are the obtained rank in the comparison.

MOP	Obj.	Gen.	MOEA/D	AdaW	MOEA/D-AdaRSE	MOEA/D-AdaGAE	MOEA/D-AdaMPT	MOEA/D-AdaCOU	MOEA/D-AdaPT	MOEA/D-AdaKRA
DTLZ5	3	400	5.4617e+0 ⁸ (5.13e-4)	5.5063e+0 ⁸ (6.92e-3)	5.5045e+0 ⁸ (1.74e-3)	5.4978e+0 ⁸ (1.43e-3)	5.5004e+0 ⁸ (2.09e-3)	5.5046e+0 ⁸ (1.82e-3)	5.5047e+0 ⁸ (2.14e-3)	5.5053e+0 ⁸ (1.84e-3)
	5	600	3.1028e+0 ⁸ (9.07e-4)	3.1277e+0 ⁸ (1.18e-2)	3.1296e+0 ⁸ (1.08e-2)	3.1293e+0 ⁸ (1.16e-2)	3.1298e+0 ⁸ (8.48e-3)	3.1310e+0 ⁸ (6.87e-3)	3.1302e+0 ⁸ (5.59e-3)	3.1302e+0 ⁸ (7.73e-3)
	8	750	2.4715e+0 ⁸ (7.74e-4)	2.4921e+0 ⁸ (1.61e+0)	2.5016e+0 ⁸ (1.61e-1)	2.5006e+0 ⁸ (1.87e-1)	2.5009e+0 ⁸ (2.38e-1)	2.5038e+0 ⁸ (6.94e-2)	2.5017e+0 ⁸ (1.06e-1)	2.5018e+0 ⁸ (1.37e-1)
	10	1000	9.8787e+0 ⁸ (3.98e-3)	9.8522e+0 ⁸ (3.98e-1)	1.0014e+0 ⁹ (4.11e-1)	1.0013e+0 ⁹ (4.35e-1)	1.0012e+0 ⁹ (4.30e-1)	1.0024e+0 ⁹ (2.06e-1)	1.0014e+0 ⁹ (3.47e-1)	1.0016e+0 ⁹ (3.42e-1)
DTLZ6	3	400	4.4612e+0 ⁸ (4.50e-5)	5.5051e+0 ⁸ (4.08e-3)	5.5053e+0 ⁸ (1.65e-1)	5.4960e+0 ⁸ (9.18e-4)	5.4994e+0 ⁸ (4.65e-4)	5.5052e+0 ⁸ (2.68e-4)	5.5054e+0 ⁸ (1.68e-4)	5.5053e+0 ⁸ (2.94e-4)
	5	600	3.1897e+0 ⁸ (2.01e-4)	3.1915e+0 ⁸ (4.17e-2)	3.1922e+0 ⁸ (2.52e-3)	3.1921e+0 ⁸ (2.50e-3)	3.1922e+0 ⁸ (3.26e-3)	3.1925e+0 ⁸ (2.21e-3)	3.1923e+0 ⁸ (1.36e-3)	3.1923e+0 ⁸ (2.44e-3)
	8	750	2.5480e+0 ⁸ (8.29e-2)	2.5520e+0 ⁸ (2.65e-1)	2.5535e+0 ⁸ (1.92e-2)	2.5536e+0 ⁸ (1.91e-2)	2.5555e+0 ⁸ (2.48e-2)	2.5558e+0 ⁸ (1.29e-2)	2.5533e+0 ⁸ (1.82e-2)	2.5533e+0 ⁸ (2.19e-2)
	10	1000	1.0189e+0 ⁸ (3.96e-1)	1.0211e+0 ⁸ (6.81e-1)	1.0241e+0 ⁸ (5.33e-1)	1.0213e+0 ⁸ (2.96e-1)	1.0215e+0 ⁸ (3.26e-1)	1.0213e+0 ⁸ (7.70e-2)	1.0213e+0 ⁸ (8.64e-2)	1.0213e+0 ⁸ (4.18e-0)
DTLZ7	3	1000	6.5714e+0 ⁸ (2.71e-0)	6.5872e+0 ⁸ (5.84e-3)	6.6044e+0 ⁸ (3.14e-3)	6.5954e+0 ⁸ (5.36e-3)	6.5985e+0 ⁸ (3.12e-3)	6.6026e+0 ⁸ (3.64e-3)	6.6033e+0 ⁸ (4.09e-3)	6.6033e+0 ⁸ (3.60e-3)
	5	1000	2.4212e+0 ⁸ (3.09e-0)	2.5295e+0 ⁸ (1.37e-1)	2.5235e+0 ⁸ (3.72e-1)	2.5046e+0 ⁸ (3.67e-1)	2.4085e+0 ⁸ (3.92e-1)	2.4085e+0 ⁸ (3.13e-1)	2.5236e+0 ⁸ (3.79e-1)	2.52408e+0 ⁸ (3.24e-1)
	8	1000	1.6326e+0 ⁸ (3.01e-0)	1.8750e+0 ⁸ (2.23e+0)	1.8424e+0 ⁸ (9.57e-1)	1.8106e+0 ⁸ (1.01e+0)	1.8261e+0 ⁸ (1.00e+0)	1.8173e+0 ⁸ (2.75e+0)	1.8242e+0 ⁸ (1.03e+0)	1.8281e+0 ⁸ (6.05e-1)
	10	1500	6.2176e+0 ⁸ (2.35e+0)	7.2826e+0 ⁸ (4.30e+0)	6.9682e+0 ⁸ (9.52e-1)	6.9851e+0 ⁸ (1.82e+0)	6.9774e+0 ⁸ (1.74e+0)	7.1055e+0 ⁸ (1.36e+0)	6.8022e+0 ⁸ (6.32e+0)	6.7905e+0 ⁸ (4.18e+0)
WFG2	3	400	7.8827e+0 ⁸ (1.17e-0)	7.8686e+0 ⁸ (1.62e-2)	7.8810e+0 ⁸ (1.87e-2)	7.8509e+0 ⁸ (1.39e-3)	7.8577e+0 ⁸ (1.35e-3)	7.8576e+0 ⁸ (1.80e-2)	7.8556e+0 ⁸ (1.63e-3)	7.8776e+0 ⁸ (1.77e-2)
	5	750	3.1938e+0 ⁸ (1.80e-2)	3.1900e+0 ⁸ (2.06e-2)	3.1944e+0 ⁸ (1.68e-2)	3.1946e+0 ⁸ (1.55e-2)	3.1940e+0 ⁸ (1.62e-2)	3.1934e+0 ⁸ (1.78e-2)	3.1941e+0 ⁸ (1.10e-2)	3.1945e+0 ⁸ (1.31e-2)
	8	1500	2.5563e+0 ⁸ (1.35e-0)	2.5536e+0 ⁸ (9.18e-1)	2.5526e+0 ⁸ (1.01e-1)	2.5556e+0 ⁸ (1.16e-1)	2.5554e+0 ⁸ (1.31e-1)	2.5562e+0 ⁸ (1.20e-1)	2.5556e+0 ⁸ (1.19e-1)	2.5562e+0 ⁸ (1.53e-1)
	10	2000	1.0230e+0 ⁸ (3.81e-1)	1.0232e+0 ⁸ (3.94e-1)	1.0232e+0 ⁸ (3.09e-1)	1.0232e+0 ⁸ (3.19e-1)	1.0232e+0 ⁸ (2.99e-1)	1.0231e+0 ⁸ (3.01e-1)	1.0231e+0 ⁸ (3.92e-1)	1.0231e+0 ⁸ (4.01e-0)
WFG3	3	400	7.0879e+0 ⁸ (1.25e-0)	6.9990e+0 ⁸ (4.99e-2)	7.0631e+0 ⁸ (2.37e-0)	7.0480e+0 ⁸ (2.11e-2)	7.0536e+0 ⁸ (1.81e-2)	7.0616e+0 ⁸ (1.95e-2)	7.0606e+0 ⁸ (1.96e-2)	7.0625e+0 ⁸ (1.87e-2)
	5	750	2.8695e+0 ⁸ (3.09e-2)	2.8266e+0 ⁸ (3.44e-1)	2.9028e+0 ⁸ (1.71e-1)	2.8917e+0 ⁸ (1.26e-1)	2.8942e+0 ⁸ (1.19e-1)	2.9268e+0 ⁸ (1.10e-1)	2.9126e+0 ⁸ (1.15e-1)	2.9182e+0 ⁸ (9.61e-2)
	8	1500	2.2840e+0 ⁸ (1.79e-0)	2.2093e+0 ⁸ (3.41e+0)	2.2299e+0 ⁸ (2.42e+0)	2.2132e+0 ⁸ (3.16e+0)	2.2305e+0 ⁸ (2.17e-0)	2.2349e+0 ⁸ (1.12e+0)	2.2287e+0 ⁸ (2.61e+0)	2.2387e+0 ⁸ (2.45e+0)
	10	2000	1.9129e+0 ⁸ (5.57e+0)	9.0405e+0 ⁷ (1.25e+1)	8.9662e+0 ⁷ (1.32e+1)	8.9756e+0 ⁷ (1.28e+1)	8.9824e+0 ⁷ (9.53e-0)	9.3078e+0 ⁷ (8.84e-0)	9.3945e+0 ⁷ (8.01e+0)	9.3945e+0 ⁷ (8.01e+0)
DTLZ1 ⁻¹	3	400	5.4412e+0 ⁸ (6.86e-0)	5.4012e+0 ⁸ (1.88e-2)	5.4980e+0 ⁸ (4.80e-3)	5.4927e+0 ⁸ (4.01e-3)	5.4955e+0 ⁸ (2.00e-3)	5.4977e+0 ⁸ (2.64e-3)	5.5004e+0 ⁸ (2.76e-3)	5.5010e+0 ⁸ (3.48e-3)
	5	600	8.8038e+0 ⁸ (8.61e-0)	1.0886e+0 ⁹ (4.91e-1)	1.1088e+0 ⁹ (4.70e-2)	1.0701e+0 ⁹ (4.59e-2)	1.0820e+0 ⁹ (5.59e-2)	1.1285e+0 ⁹ (1.76e-3)	1.1292e+0 ⁹ (1.72e-3)	1.1120e+0 ⁹ (1.74e-2)
	8	750	6.9671e+0 ⁸ (5.21e-1)	1.9710e+0 ⁸ (2.05e-1)	2.0413e+0 ⁸ (1.43e-1)	1.9386e+0 ⁸ (2.50e-1)	2.0411e+0 ⁸ (1.70e-1)	2.0731e+0 ⁸ (2.67e-1)	2.0712e+0 ⁸ (1.75e-2)	2.0711e+0 ⁸ (5.99e-2)
	10	1000	6.8175e+0 ⁸ (4.76e-1)	2.8561e+0 ⁸ (6.92e-1)	2.9397e+0 ⁸ (1.45e-1)	2.8311e+0 ⁸ (2.26e-1)	2.9519e+0 ⁸ (1.37e-1)	2.9366e+0 ⁸ (7.31e-2)	2.9358e+0 ⁸ (5.28e-2)	2.9393e+0 ⁸ (5.45e-2)
DTLZ2 ⁻¹	3	250	6.6097e+0 ⁸ (3.15e-0)	6.7062e+0 ⁸ (4.58e-3)	6.6984e+0 ⁸ (3.37e-3)	6.6904e+0 ⁸ (3.67e-3)	6.6952e+0 ⁸ (3.82e-3)	6.6988e+0 ⁸ (5.33e-3)	6.6988e+0 ⁸ (2.27e-3)	6.6986e+0 ⁸ (3.20e-3)
	5	350	1.3713e+0 ⁸ (1.25e-0)	1.7739e+0 ⁸ (2.47e-2)	1.7614e+0 ⁸ (3.42e-2)	1.7554e+0 ⁸ (3.23e-2)	1.7500e+0 ⁸ (3.43e-2)	1.7552e+0 ⁸ (2.60e-2)	1.7552e+0 ⁸ (1.53e-2)	1.7548e+0 ⁸ (2.43e-2)
	8	500	2.1948e+0 ⁸ (6.53e-1)	4.6462e+0 ⁸ (2.96e-1)	4.4648e+0 ⁸ (2.96e-1)	4.5330e+0 ⁸ (4.24e-1)	4.5285e+0 ⁸ (3.60e-1)	4.4231e+0 ⁸ (2.98e-1)	4.1537e+0 ⁸ (2.05e-1)	4.1568e+0 ⁸ (3.49e-1)
	10	750	3.1434e+0 ⁸ (1.29e-1)	8.5839e+0 ⁸ (9.27e-1)	8.2273e+0 ⁸ (8.85e-1)	8.5157e+0 ⁸ (9.73e-1)	8.5001e+0 ⁸ (1.05e-0)	7.3269e+0 ⁸ (5.95e-1)	7.0474e+0 ⁸ (5.12e-1)	7.0474e+0 ⁸ (4.95e-1)
DTLZ3 ⁻¹	3	1000	6.6067e+0 ⁸ (7.57e-0)	6.7087e+0 ⁸ (3.54e-3)	6.6900e+0 ⁸ (2.46e-3)	6.6904e+0 ⁸ (2.04e-3)	6.6984e+0 ⁸ (2.55e-3)	6.6957e+0 ⁸ (3.08e-3)	6.6993e+0 ⁸ (2.48e-3)	6.6984e+0 ⁸ (4.77e-3)
	5	1000	1.3710e+0 ⁸ (1.18e-0)	1.7777e+0 ⁸ (6.02e-2)	1.7654e+0 ⁸ (2.30e-2)	1.7536e+0 ⁸ (5.20e-2)	1.7538e+0 ⁸ (4.21e-2)	1.7560e+0 ⁸ (4.04e-2)	1.7554e+0 ⁸ (2.11e-2)	1.7554e+0 ⁸ (2.64e-2)
	8	1000	2.1466e+0 ⁸ (5.15e-1)	4.5850e+0 ⁸ (6.50e-1)	4.4439e+0 ⁸ (6.47e-1)	4.5044e+0 ⁸ (5.75e-1)	4.5319e+0 ⁸ (5.50e-1)	4.3247e+0 ⁸ (2.93e-1)	4.1569e+0 ⁸ (3.60e-1)	4.1538e+0 ⁸ (2.88e-1)
	10	1500	3.1820e+0 ⁸ (1.08e-0)	8.5390e+0 ⁸ (9.27e-1)	8.2273e+0 ⁸ (8.85e-1)	8.5157e+0 ⁸ (9.73e-1)	8.5001e+0 ⁸ (1.05e-0)	7.0476e+0 ⁸ (4.03e-1)	7.0469e+0 ⁸ (4.95e-1)	7.0469e+0 ⁸ (4.95e-1)
DTLZ5 ⁻¹	3	600	6.6069e+0 ⁸ (5.98e-3)	6.7059e+0 ⁸ (3.44e-3)	6.6966e+0 ⁸ (2.04e-3)	6.6964e+0 ⁸ (2.36e-3)	6.6903e+0 ⁸ (2.05e-3)	6.6951e+0 ⁸ (3.74e-3)	6.6990e+0 ⁸ (2.55e-3)	6.6983e+0 ⁸ (6.21e-3)
	5	1000	1.3709e+0 ⁸ (2.91e-0)	1.7779e+0 ⁸ (2.02e-0)	1.7626e+0 ⁸ (2.44e-2)	1.7602e+0 ⁸ (3.86e-2)	1.7609e+0 ⁸ (2.42e-2)	1.7540e+0 ⁸ (1.92e-2)	1.7529e+0 ⁸ (2.14e-2)	1.7523e+0 ⁸ (2.62e-2)
	8	1000	2.1151e+0 ⁸ (9.03e-1)	4.5472e+0 ⁸ (2.56e-1)	4.2692e+0 ⁸ (1.81e-0)	4.2038e+0 ⁸ (5.25e-0)	4.2028e+0 ⁸ (3.49e-0)	3.9904e+0 ⁸ (4.05e-0)	4.0448e+0 ⁸ (1.67e-0)	4.0132e+0 ⁸ (2.31e-0)
	10	1500	3.2433e+0 ⁸ (1.41e-0)	9.1331e+0 ⁸ (1.50e-1)	7.6419e+0 ⁸ (4.03e+0)	7.6074e+0 ⁸ (5.01e+0)	8.1591e+0 ⁸ (4.17e+0)	8.6948e+0 ⁸ (2.37e+0)	8.6593e+0 ⁸ (4.87e-1)	8.6454e+0 ⁸ (2.54e-0)
DTLZ6 ⁻¹	3	400	6.6195e+0 ⁸ (6.92e-0)	6.7708e+0 ⁸ (3.44e-3)	6.7084e+0 ⁸ (2.17e-3)	6.7076e+0 ⁸ (2.13e-3)	6.7071e+0 ⁸ (2.13e-3)	6.7021e+0 ⁸ (2.45e-3)	6.7112e+0 ⁸ (2.22e-3)	6.7109e+0 ⁸ (1.97e-3)
	5	600	1.4127e+0 ⁸ (5.61e-1)	1.7947e+0 ⁸ (2.10e-2)	1.7832e+0 ⁸ (1.87e-2)	1.7763e+0 ⁸ (2.79e-2)	1.7744e+0 ⁸ (1.92e-2)	1.7744e+0 ⁸ (2.14e-2)	1.7752e+0 ⁸ (1.26e-2)	1.7752e+0 ⁸ (1.98e-2)
	8	750	2.3013e+0 ⁸ (6.20e-1)	4.8427e+0 ⁸ (2.03e-1)	4.6544e+0 ⁸ (2.02e-1)	4.6917e+0 ⁸ (3.38e-1)	4.6971e+0 ⁸ (2.10e-1)	4.5272e+0 ⁸ (1.72e-1)	4.4494e+0 ⁸ (2.31e-1)	4.4573e+0 ⁸ (2.58e-1)
	10	1000	3.1107e+0 ⁸ (1.54e-1)	9.1316e+0 ⁸ (1.50e-1)	8.7927e+0 ⁸ (4.18e-1)	8.7610e+0 ⁸ (5.49e-1)	8.7143e+0 ⁸ (5.32e-1)	7.8288e+0 ⁸ (6.29e-1)	7.8432e+0 ⁸ (5.77e-1)	7.8432e+0 ⁸ (5.77e-1)
WFG2 ⁻¹	3	400	6.1177e+0 ⁸ (2.97e-3)	6.7077e+0 ⁸ (4.54e-3)	6.6973e+0 ⁸ (2.08e-3)	6.6948e+0 ⁸ (3.97e-3)	6.6958e+0 ⁸ (4.29e-3)	6.6974e+0 ⁸ (9.43		

Table 24: Mean and standard deviations (in parenthesis) of the SPD indicator obtained by MOEAs using the MOEA/D framework on MOPs with irregular PF shapes. The two best mean values per MOP are highlighted in grayscale, where the darker tone corresponds to the best one. The symbols “+”, “-”, and “=” are placed when the MOEA performs significantly better, significantly worse, or statistically equivalent to MOEA/D based on a one-tailed Wilcoxon test using a significance level of $\alpha = 0.05$. The % of satisfaction refers to the percentage of MOPs where the MOEA performs significantly better than MOEA/D. The superscripts are the obtained rank in the comparison.

MOP	Obj.	Gen.	MOEA/D	AdaW	MOEA/D-AdaRSE	MOEA/D-AdaGAE	MOEA/D-AdaMPT	MOEA/D-AdaCOU	MOEA/D-AdaPT	MOEA/D-AdaKRA
DTLZ5	3	400	9.5807e+0 ⁸ (2.44e-3)	1.0475e+1 ¹ (1.78e-2)	1.0441e+1 ⁴ (8.88e-3) +	1.0363e+1 ⁷ (2.12e-2) +	1.0301e+1 ⁶ (1.89e-2) +	1.0443e+1 ² (6.95e-3) +	1.0404e+1 ³ (8.30e-3) +	1.0443e+1 ³ (8.42e-3) +
	5	600	8.2579e+0 ⁸ (9.33e-3)	2.1431e+1 ² (1.63e+0)	1.7421e+1 ⁴ (2.46e+0) +	1.5919e+1 ⁷ (2.04e+0) +	1.7384e+1 ⁵ (1.96e+0) +	1.6918e+1 ¹⁰ (2.53e+0) +	1.9041e+1 ³ (3.25e+0) +	1.9787e+1 ² (3.27e+0) +
	8	750	1.0713e+1 ² (1.13e+0)	4.4308e+1 ³ (3.67e+0) +	1.9340e+1 ⁵ (3.18e+0) +	1.7078e+1 ⁷ (2.91e+0) +	1.7232e+1 ⁶ (2.87e+0) +	2.3886e+1 ¹¹ (3.11e+0) +	2.5869e+1 ² (5.38e+0) +	2.6729e+1 ² (6.09e+0) +
	10	1000	1.1711e+1 ² (1.75e+0)	6.8069e+1 ³ (9.41e+0) +	2.4657e+1 ⁵ (3.57e+0) +	2.2109e+1 ⁷ (3.71e+0) +	2.3311e+1 ⁶ (2.84e+0) +	3.2873e+1 ¹² (3.29e+0) +	4.0410e+1 ² (3.29e+0) +	3.9336e+1 ² (4.97e+0) +
DTLZ6	3	400	9.5793e+0 ⁸ (4.56e-6)	1.0473e+1 ² (1.07e-3)	1.0466e+1 ³ (1.78e-3) +	1.0370e+1 ⁷ (9.99e-3) +	1.0409e+1 ⁶ (6.80e-3) +	1.0466e+1 ² (2.26e-3) +	1.0467e+1 ² (1.54e-3) +	1.0466e+1 ² (3.07e-3) +
	5	600	6.5083e+0 ⁸ (9.17e-6)	1.6178e+1 ² (7.19e-1)	1.6193e+1 ⁴ (1.25e+0) +	1.0080e+1 ⁷ (1.17e+0) +	1.0271e+1 ⁶ (1.24e+0) +	1.1208e+1 ¹¹ (1.08e+0) +	1.3733e+1 ² (1.68e+0) +	1.3841e+1 ² (1.48e+0) +
	8	750	7.1162e+0 ⁸ (3.62e-6)	3.2469e+1 ² (5.03e+0) +	1.4508e+1 ⁵ (1.51e+0) +	1.3983e+1 ⁷ (1.37e+0) +	1.4234e+1 ⁶ (1.99e+0) +	1.6121e+1 ¹¹ (1.47e+0) +	1.7707e+1 ² (1.63e+0) +	1.8140e+1 ² (1.48e+0) +
	10	1000	7.6380e+0 ⁸ (2.46e-6)	3.9083e+1 ² (5.15e+0) +	1.5855e+1 ⁵ (1.55e+0) +	1.5698e+1 ⁷ (1.63e+0) +	1.5812e+1 ⁶ (1.96e+0) +	2.1001e+1 ¹² (1.33e+0) +	2.0968e+1 ² (1.80e+0) +	2.0508e+1 ² (1.72e+0) +
DTLZ7	3	1000	2.1486e+1 ⁸ (4.51e-1)	2.4268e+1 ² (1.74e-1) +	2.3538e+1 ³ (1.24e-1) +	2.3290e+1 ⁷ (0.99e-1) +	2.3663e+1 ⁶ (4.02e-1) +	2.3421e+1 ² (5.02e-1) +	2.3594e+1 ² (6.66e-1) +	2.3510e+1 ² (4.28e-1) +
	5	1000	7.4502e+0 ⁸ (4.56e-0)	1.4146e+2 ² (8.57e+0) +	1.2045e+2 ⁴ (1.19e+1) +	1.2224e+2 ² (1.24e+1) +	1.2197e+2 ² (1.37e+1) +	1.1139e+2 ⁹ (0.88e+0) +	1.2048e+2 ² (0.56e+0) +	1.1813e+2 ² (1.55e+1) +
	8	1000	7.3342e+0 ⁸ (2.93e+0)	1.5401e+2 ² (7.15e-1) +	1.2041e+2 ⁴ (1.17e+0) +	1.2002e+2 ² (1.82e+0) +	1.2076e+2 ² (8.41e-1) +	1.1522e+2 ² (5.07e+0) +	1.1944e+2 ² (2.45e+0) +	1.2057e+2 ² (1.40e+0) +
	10	1500	1.1017e+2 ² (3.43e+0)	2.7490e+2 ² (1.09e-1) +	1.9084e+2 ³ (1.71e+0) +	1.9095e+2 ² (2.29e+0) +	1.8818e+2 ¹⁰ (1.39e+0) +	1.8762e+2 ² (3.26e+0) +	1.8866e+2 ² (2.84e+0) +	
WFG2	3	400	1.8528e+1 ⁸ (5.66e-1)	2.0577e+1 ² (2.51e-1) +	1.8938e+1 ³ (3.79e-1) +	1.8586e+1 ⁷ (1.17e+0) +	1.8855e+1 ⁶ (1.17e+0) +	1.8909e+1 ¹¹ (4.08e-1) +	1.8890e+1 ² (3.98e-1) +	
	5	750	3.6648e+1 ⁸ (1.42e-1)	4.0413e+1 ² (7.11e-1) +	3.6620e+1 ⁹ (3.93e-1) +	3.6860e+1 ² (5.63e-1) +	3.6447e+1 ⁷ (1.17e+0) +	3.6401e+1 ¹¹ (1.54e-1) +	3.6650e+1 ² (4.19e-1) +	
	8	1500	4.4107e+1 ⁸ (1.28e-0)	5.3898e+1 ² (6.15e+0) +	4.4674e+1 ⁹ (9.42e-1) +	4.4657e+1 ¹⁰ (1.12e-0) +	4.4657e+1 ² (5.56e-1) +	4.4384e+1 ¹¹ (1.18e-0) +	4.4666e+1 ² (8.92e-1) +	
	10	2000	5.2334e+1 ⁸ (1.51e+0)	6.4138e+1 ² (1.54e+0) +	5.2559e+1 ⁹ (1.67e+0) +	5.3047e+1 ¹² (9.91e-1) +	5.3236e+1 ² (1.31e+0) +	5.2704e+1 ¹¹ (1.35e-0) +	5.2535e+1 ² (9.84e-1) +	5.2683e+1 ² (1.20e-0) +
WFG3	3	400	1.1865e+1 ⁸ (4.21e-1)	1.2456e+1 ² (3.77e-1) +	1.2155e+1 ³ (3.56e-1) +	1.2286e+1 ⁶ (3.87e-1) +	1.2414e+1 ² (3.72e-1) +	1.2232e+1 ² (3.28e-1) +	1.2671e+1 ² (3.29e-1) +	1.2507e+1 ² (2.88e-1) +
	5	750	2.1421e+1 ⁸ (5.49e-1)	3.7416e+1 ² (1.49e-0) +	3.8083e+1 ³ (1.66e-0) +	3.3418e+1 ⁷ (1.22e+0) +	3.4912e+1 ⁶ (1.56e-0) +	3.8644e+1 ² (1.52e-0) +	4.2810e+1 ² (1.45e-0) +	4.3013e+1 ² (7.65e-1) +
	8	1500	2.2470e+1 ⁸ (1.43e-0)	7.6903e+1 ² (4.18e-0) +	6.9430e+1 ⁹ (2.97e-0) +	6.0497e+1 ¹² (3.20e+0) +	6.4438e+1 ² (2.83e-0) +	7.0528e+1 ² (1.88e-0) +	6.9787e+1 ² (1.99e-0) +	
	10	2000	2.5701e+1 ⁸ (2.68e-0)	1.2711e+2 ² (3.87e-0) +	1.1130e+2 ² (4.28e-0) +	1.9550e+1 ¹² (4.76e-0) +	1.0735e+2 ² (3.79e-0) +	1.0944e+2 ² (3.86e-0) +	1.1045e+2 ² (2.57e-0) +	
DTLZ1 ⁻¹	3	400	2.0007e+1 ⁸ (4.06e-3)	2.2560e+1 ² (1.55e-1) +	2.3103e+1 ⁵ (6.64e-2) +	2.3154e+1 ² (3.04e-2) +	2.3134e+1 ² (3.24e-2) +	2.3134e+1 ² (3.28e-1) +	2.3134e+1 ² (4.43e-2) +	2.3124e+1 ² (4.64e-2) +
	5	600	2.5066e+1 ⁸ (5.97e-3)	6.6327e+1 ² (6.16e-1) +	6.9180e+1 ⁴ (4.18e-1) +	6.2651e+1 ⁷ (1.15e-0) +	6.5006e+1 ² (8.41e-0) +	7.2901e+1 ¹¹ (1.59e-0) +	7.1487e+1 ² (1.42e-1) +	7.5150e+1 ² (1.55e-1) +
	8	750	2.5842e+1 ⁸ (8.50e-1)	1.0498e+2 ² (1.79e-0) +	1.0518e+2 ² (7.55e-1) +	1.0226e+2 ² (0.14e-0) +	1.0943e+2 ² (7.24e-1) +	9.0079e+1 ¹⁵ (6.55e-1) +	9.9250e+1 ² (8.87e-1) +	
	10	1000	2.5626e+1 ⁸ (1.16e-0)	1.6242e+2 ² (3.32e-0) +	1.5338e+2 ² (2.06e-0) +	1.6403e+2 ² (1.18e-0) +	1.5303e+2 ² (8.87e-1) +	1.5248e+2 ² (6.36e-1) +	1.5227e+2 ² (6.09e-1) +	
DTLZ2 ⁻¹	3	250	2.7603e+1 ⁸ (5.77e-2)	3.0716e+1 ² (3.80e-1) +	3.0463e+1 ⁴ (3.87e-1) +	2.9313e+1 ⁷ (6.03e-1) +	2.9780e+1 ⁵ (4.58e-1) +	2.9625e+1 ² (4.19e-1) +	3.0512e+1 ² (3.31e-1) +	3.0603e+1 ² (3.56e-1) +
	5	350	3.5972e+1 ⁸ (1.01e-1)	1.2416e+2 ² (1.51e+0) +	1.1975e+2 ² (1.30e+0) +	1.0701e+2 ⁷ (2.14e+0) +	1.0976e+2 ² (1.27e+0) +	1.2323e+1 ² (2.78e-1) +	1.2323e+1 ² (5.88e-1) +	1.2187e+1 ² (5.28e-1) +
	8	500	7.1649e+1 ⁸ (6.52e+0)	1.4632e+2 ² (4.86e-1) +	1.4158e+2 ² (2.18e+0) +	1.2799e+2 ² (3.45e-0) +	1.3482e+2 ² (2.10e-0) +	1.4517e+2 ² (1.54e-0) +	1.4367e+2 ² (2.23e-0) +	1.4243e+2 ² (2.77e-0) +
	10	750	8.2515e+1 ⁸ (7.90e-1)	2.5865e+2 ² (2.30e-0) +	2.3742e+2 ² (3.40e-0) +	2.1275e+2 ² (2.95e-0) +	2.3237e+2 ² (3.05e-0) +	2.4433e+2 ² (3.99e-0) +	2.4086e+2 ² (3.64e-0) +	2.4118e+2 ² (3.95e-0) +
DTLZ3 ⁻¹	3	1000	2.7632e+1 ⁸ (1.14e-2)	3.1006e+1 ² (3.80e-1) +	3.1256e+1 ² (1.84e-1) +	3.0693e+1 ⁷ (3.73e-1) +	3.0792e+1 ⁵ (3.10e-1) +	3.0765e+1 ² (4.53e-1) +	3.1276e+1 ² (1.78e-1) +	3.1224e+1 ² (2.83e-1) +
	5	1000	3.5957e+1 ⁸ (4.27e-2)	2.4131e+2 ² (1.99e-0) +	1.2140e+2 ⁴ (1.11e-0) +	1.0628e+2 ⁷ (1.93e-0) +	1.0201e+2 ² (1.07e-0) +	1.2510e+1 ² (6.55e-1) +	1.2320e+1 ² (5.88e-1) +	1.2187e+1 ² (5.28e-1) +
	8	1000	7.8256e+1 ⁸ (3.89e-0)	1.4565e+2 ² (7.46e-1) +	1.2424e+2 ² (1.66e-0) +	1.2491e+2 ² (3.13e-0) +	1.3321e+2 ² (2.25e-0) +	1.4246e+2 ² (1.13e-0) +	1.4474e+2 ² (1.90e-0) +	1.4489e+2 ² (1.47e-0) +
	10	1500	8.7145e+1 ⁸ (1.10e-1)	2.5788e+2 ² (9.97e-1) +	2.4039e+2 ² (3.78e-0) +	2.2109e+2 ² (3.04e-0) +	2.2409e+2 ² (3.26e-0) +	2.4397e+2 ² (3.86e-0) +	2.4397e+2 ² (4.10e-0) +	
DTLZ4 ⁻¹	3	600	2.7639e+1 ⁸ (1.54e-1)	3.1361e+1 ² (1.54e-1) +	3.1263e+1 ² (1.84e-1) +	3.1361e+1 ⁷ (1.87e-1) +	3.0857e+1 ⁶ (2.76e-1) +	3.0857e+1 ² (2.36e-1) +	3.1321e+1 ² (1.27e-1) +	3.1321e+1 ² (1.27e-1) +
	5	1000	3.5945e+1 ⁸ (9.83e-3)	1.3173e+2 ² (6.77e-1) +	1.2595e+2 ² (6.41e-1) +	1.1777e+2 ² (8.82e-1) +	1.1950e+2 ² (1.01e-0) +	1.2688e+2 ² (3.28e-1) +	1.2356e+2 ² (5.66e-1) +	1.2356e+2 ² (4.81e-1) +
	8	1250	8.3004e+1 ⁸ (5.30e-0)	1.4016e+2 ² (2.03e-0) +	1.4196e+2 ² (2.54e-0) +	1.3706e+2 ² (2.90e-0) +	1.4036e+2 ² (2.50e-0) +	1.4708e+2 ² (1.59e-0) +	1.4549e+2 ² (2.07e-0) +	1.4546e+2 ² (2.07e-0) +
	10	1500	6.5395e+1 ⁸ (1.272e-0)	2.5153e+2 ² (5.08e-0) +	1.5977e+2 ² (2.09e-0) +	1.5622e+2 ² (1.94e-0) +	1.5856e+2 ² (4.24e-0) +	1.5489e+2 ² (2.79e-0) +	1.5493e+2 ² (1.27e-0) +	1.5493e+2 ² (1.27e-0) +
DTLZ5 ⁻¹	3	400	1.7804e+1 ⁸ (3.17e-2)	1.8223e+1 ² (6.23e-1) +	1.7474e+1 ⁴ (2.86e-1) +	1.7733e+1 ⁷ (6.63e-1) +	1.7937e+1 ² (7.32e-1) +	1.7780e+1 ² (7.85e-1) +	1.7773e+1 ² (8.55e-1) +	1.7580e+1 ² (1.10e-0) +
	5	750	5.1541e+1 ⁸ (8.03e-1)	4.0415e+1 ² (9.72e-1) +	4.0206e+1 ⁴ (2.54e-0) +	3.8399e+1 ⁷ (8.56e-1) +	3.9412e+1 ² (0.04e-0) +	1.1798e+2 ² (4.20e-1) +	1.1511e+2 ² (5.56e-1) +	1.1506e+2 ² (4.78e-1) +
	8	1500	1.3283e+1 ⁸ (8.04e-1)	6.4802e+1 ² (1.08e+0) +	5.5978e+1 ² (3.85e-0) +	5.3260e+1 ² (2.68e-0) +	5.1654e+1 ⁷ (6.66e-0) +	6.1069e+2 ² (1.43e-0) +	1.4069e+2 ² (2.05e-0) +	1.4174e+2 ² (1.50e-0) +
	10	2000	1.3202e+1 ⁸ (8.30e-1)	8.7819e+1 ² (1.18e-0) +	7.1449e+1 ² (1.06e-0) +	6.9204e+1 ⁷ (9.86e-0) +	7.7859e+1<			

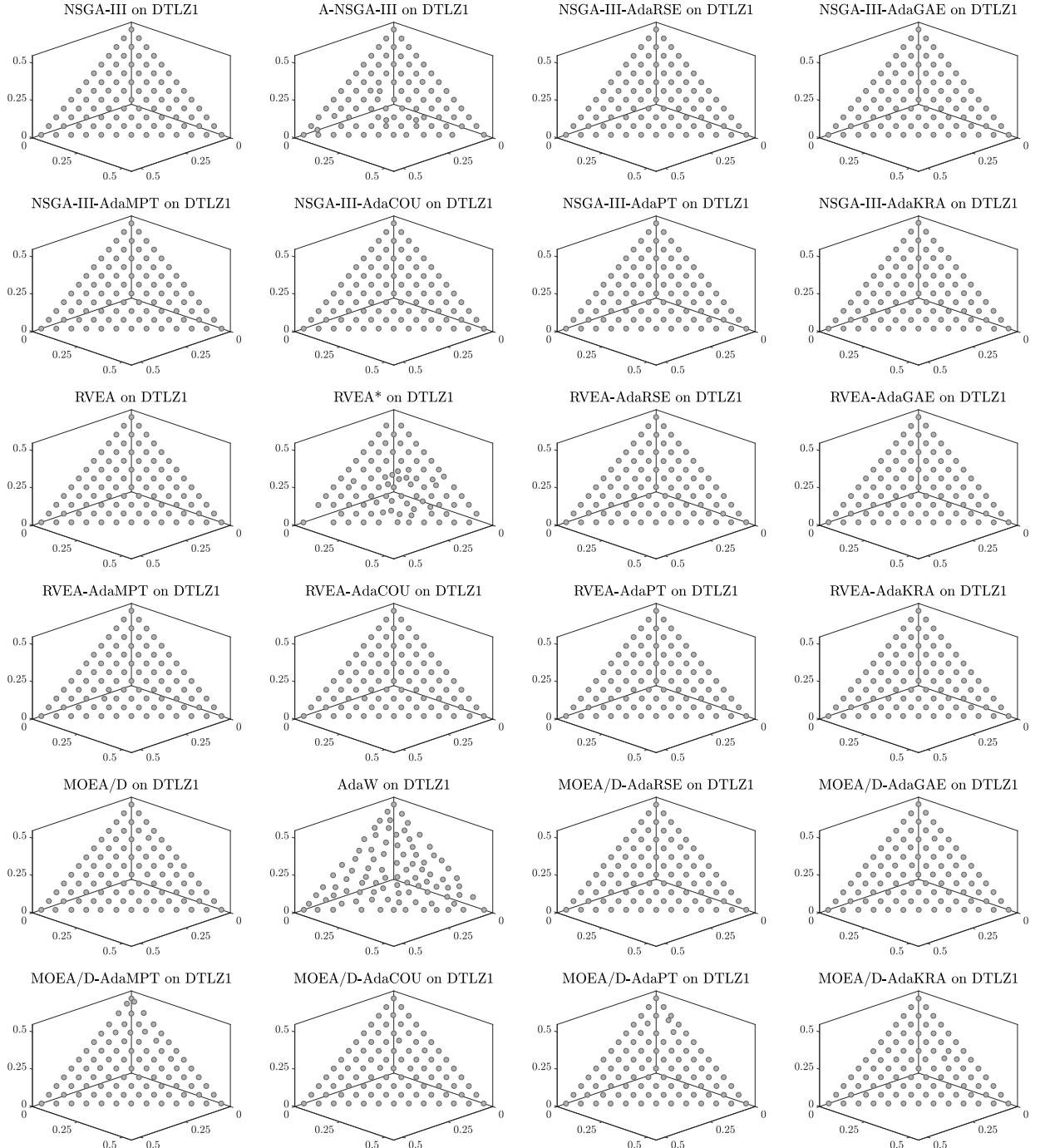


Figure 10: Final populations with the median HV value among 30 independent runs of MOEAs using the NSGA-III, RVEA, and MOEA/D frameworks on DTLZ1 with 3 objective functions.

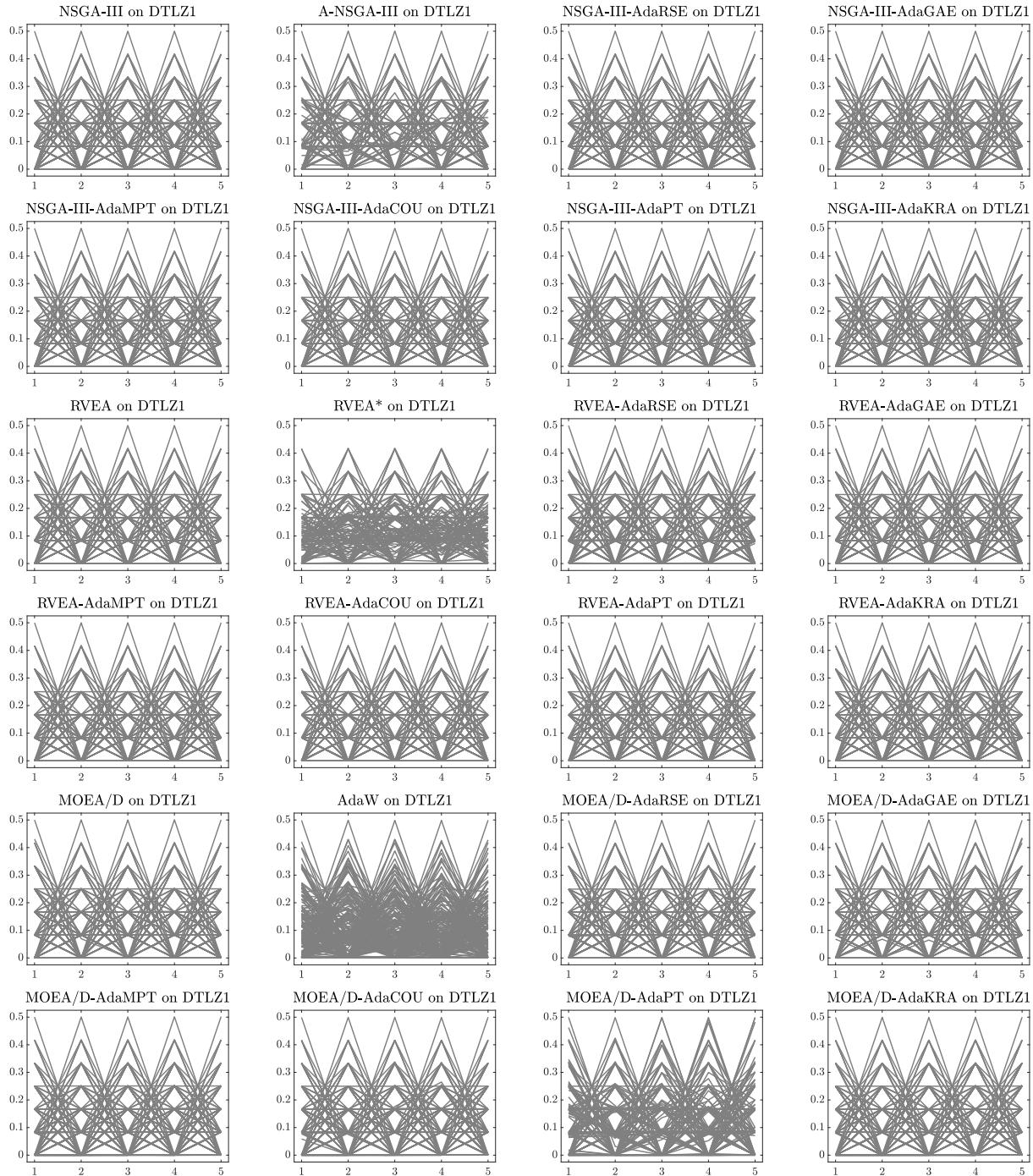


Figure 11: Final populations with the median HV value among 30 independent runs of MOEAs using the NSGA-III, RVEA, and MOEA/D frameworks on DTLZ1 with 5 objective functions.

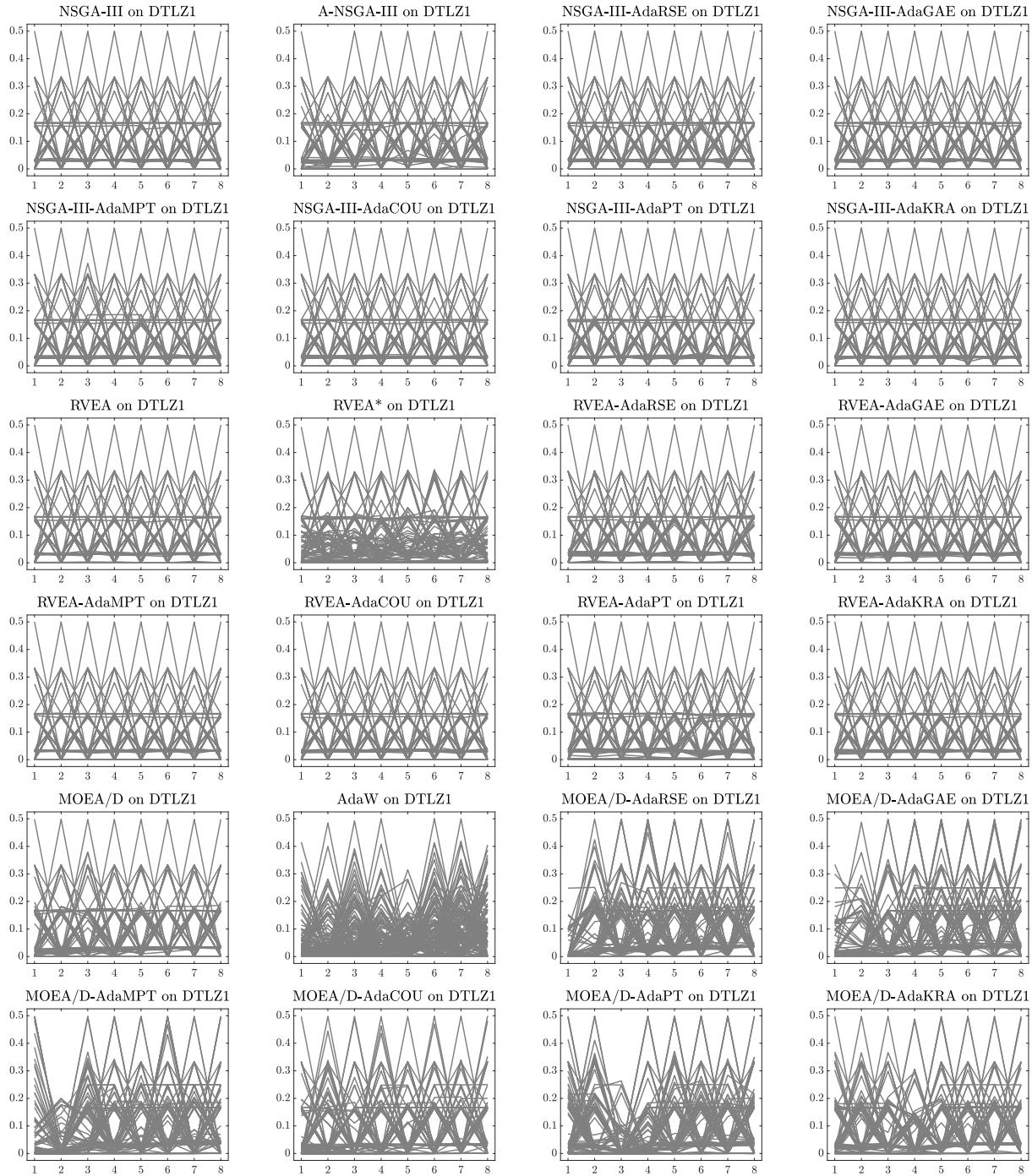


Figure 12: Final populations with the median HV value among 30 independent runs of MOEAs using the NSGA-III, RVEA, and MOEA/D frameworks on DTLZ1 with 8 objective functions.

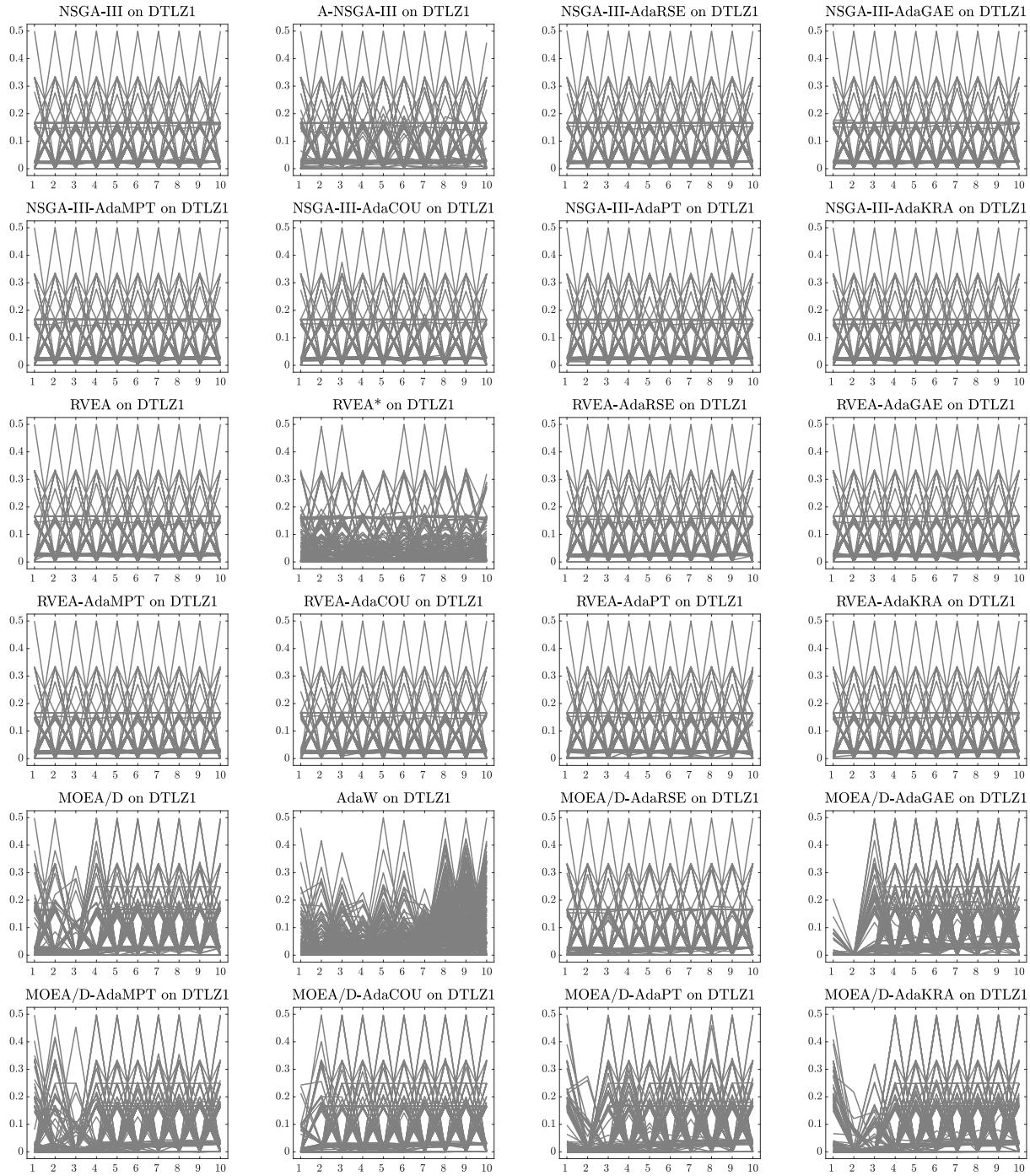


Figure 13: Final populations with the median HV value among 30 independent runs of MOEAs using the NSGA-III, RVEA, and MOEA/D frameworks on DTLZ1 with 10 objective functions.

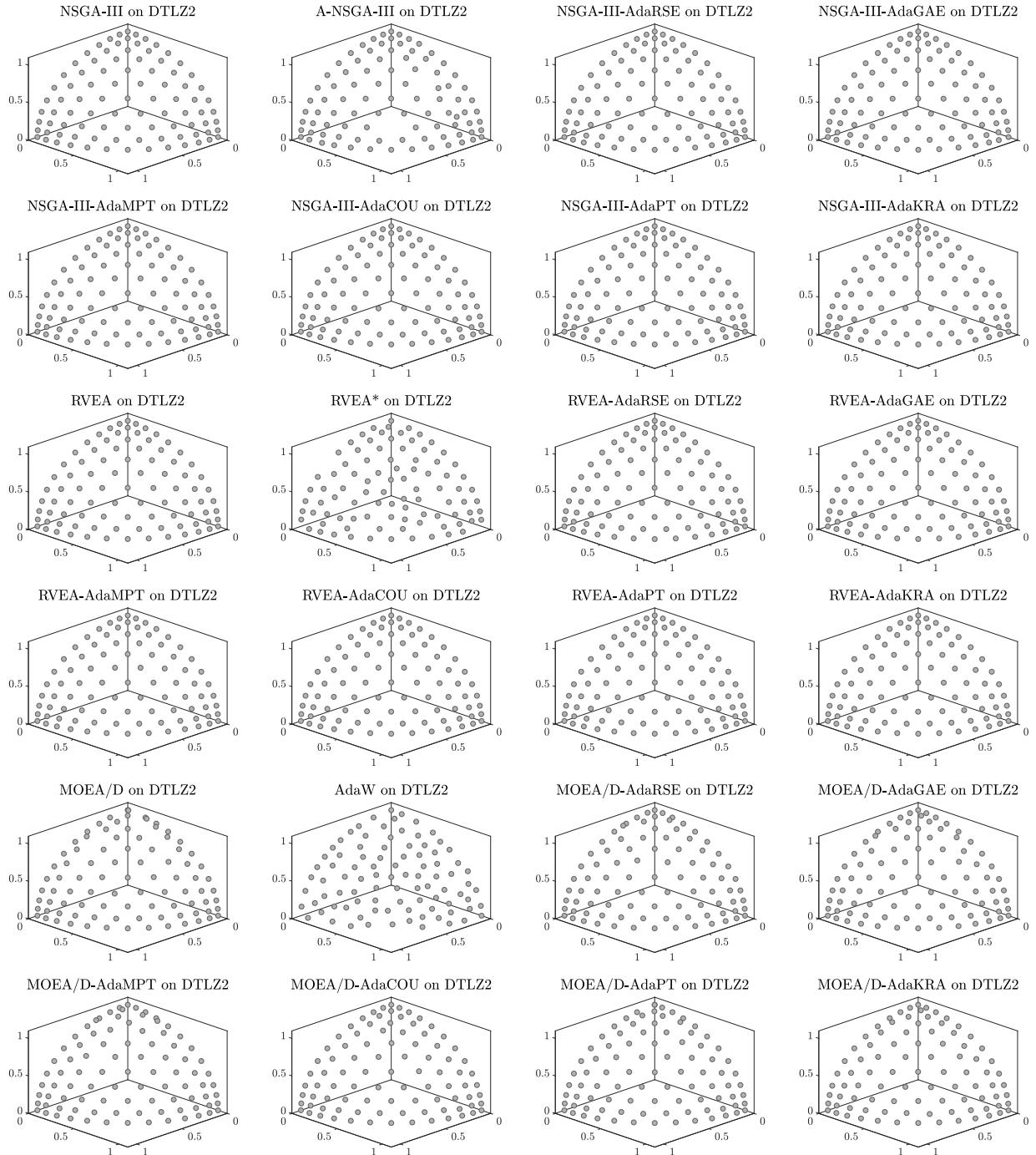


Figure 14: Final populations with the median HV value among 30 independent runs of MOEAs using the NSGA-III, RVEA, and MOEA/D frameworks on DTLZ2 with 3 objective functions.

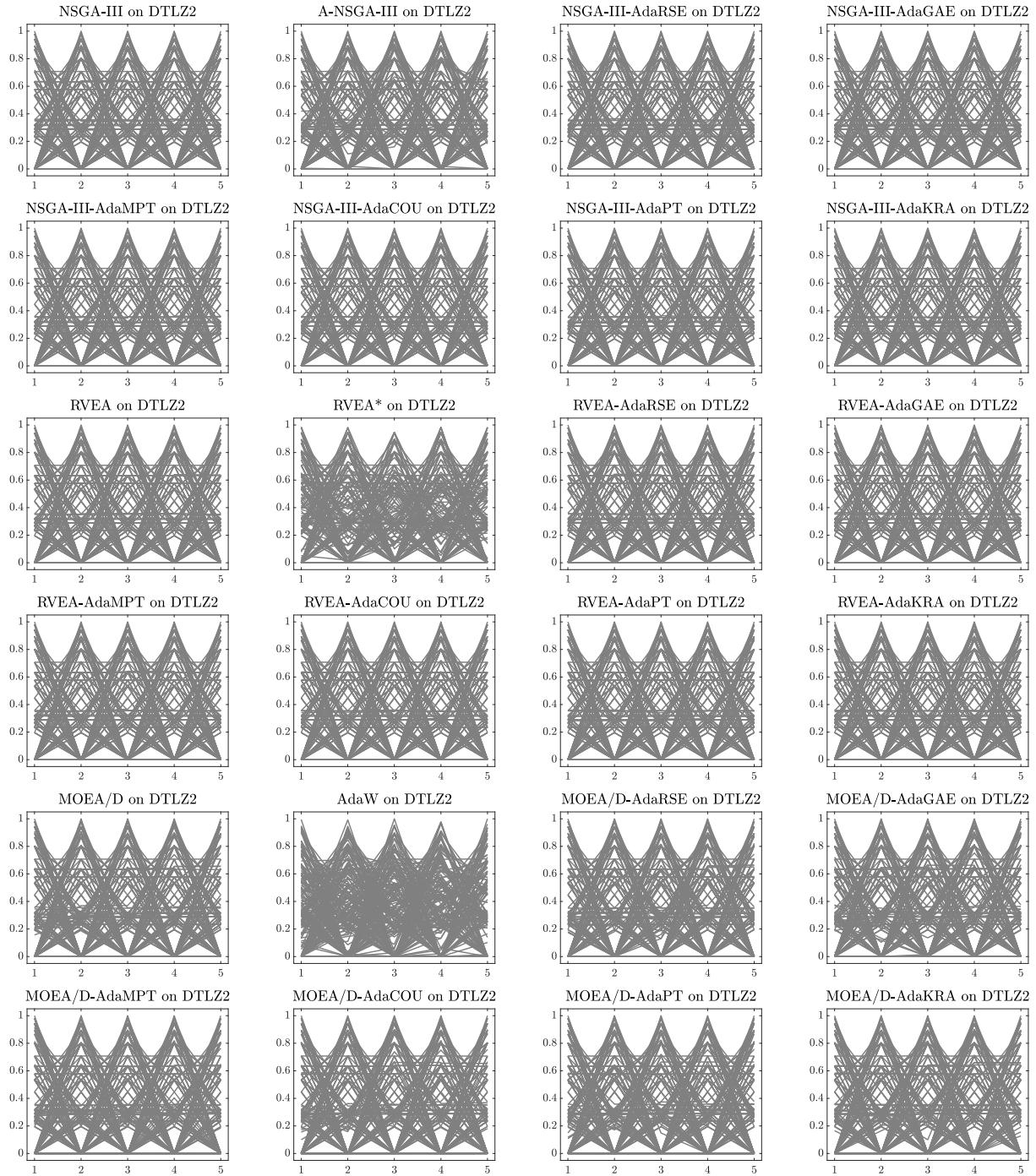


Figure 15: Final populations with the median HV value among 30 independent runs of MOEAs using the NSGA-III, RVEA, and MOEA/D frameworks on DTLZ2 with 5 objective functions.

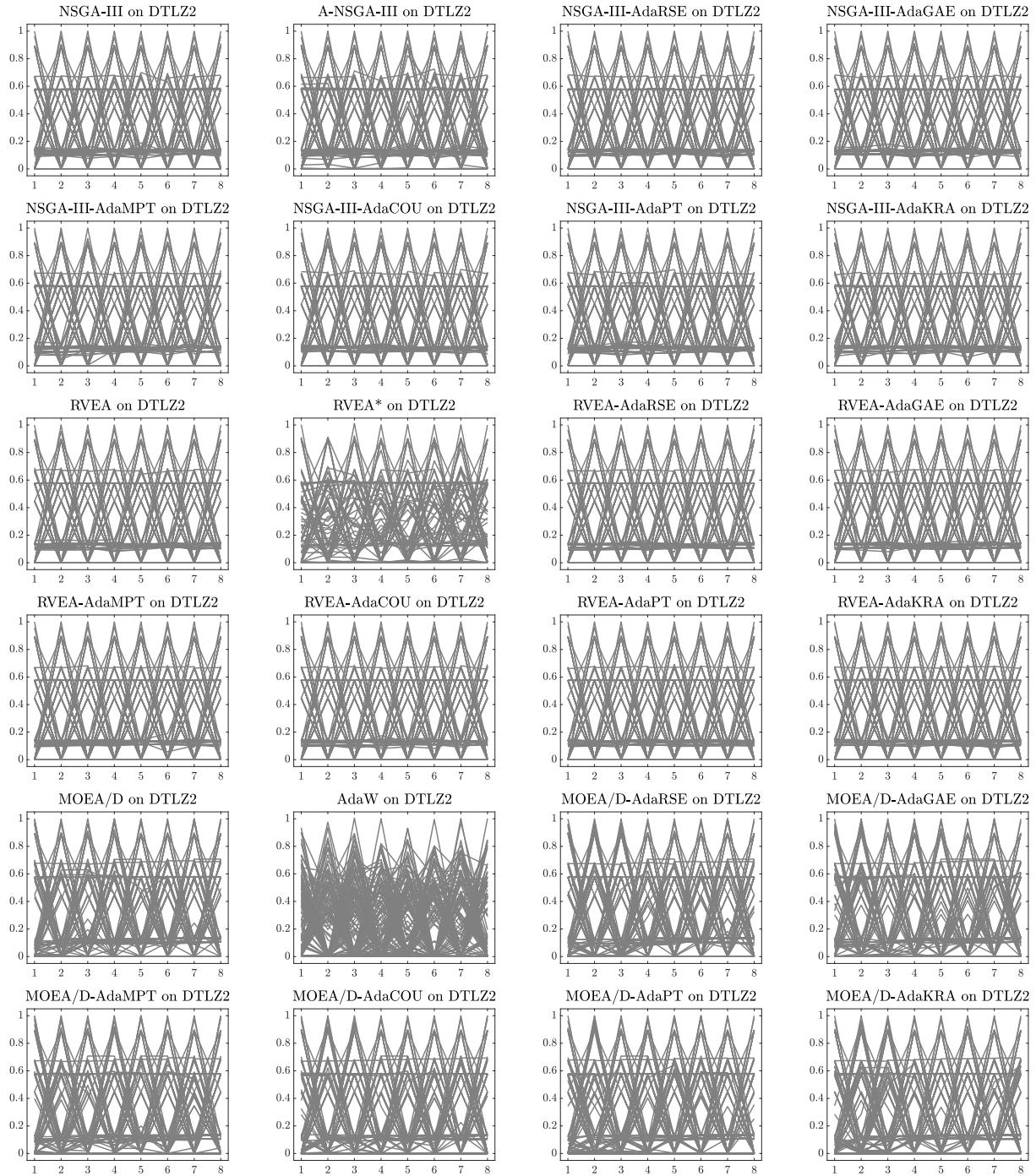


Figure 16: Final populations with the median HV value among 30 independent runs of MOEAs using the NSGA-III, RVEA, and MOEA/D frameworks on DTLZ2 with 8 objective functions.

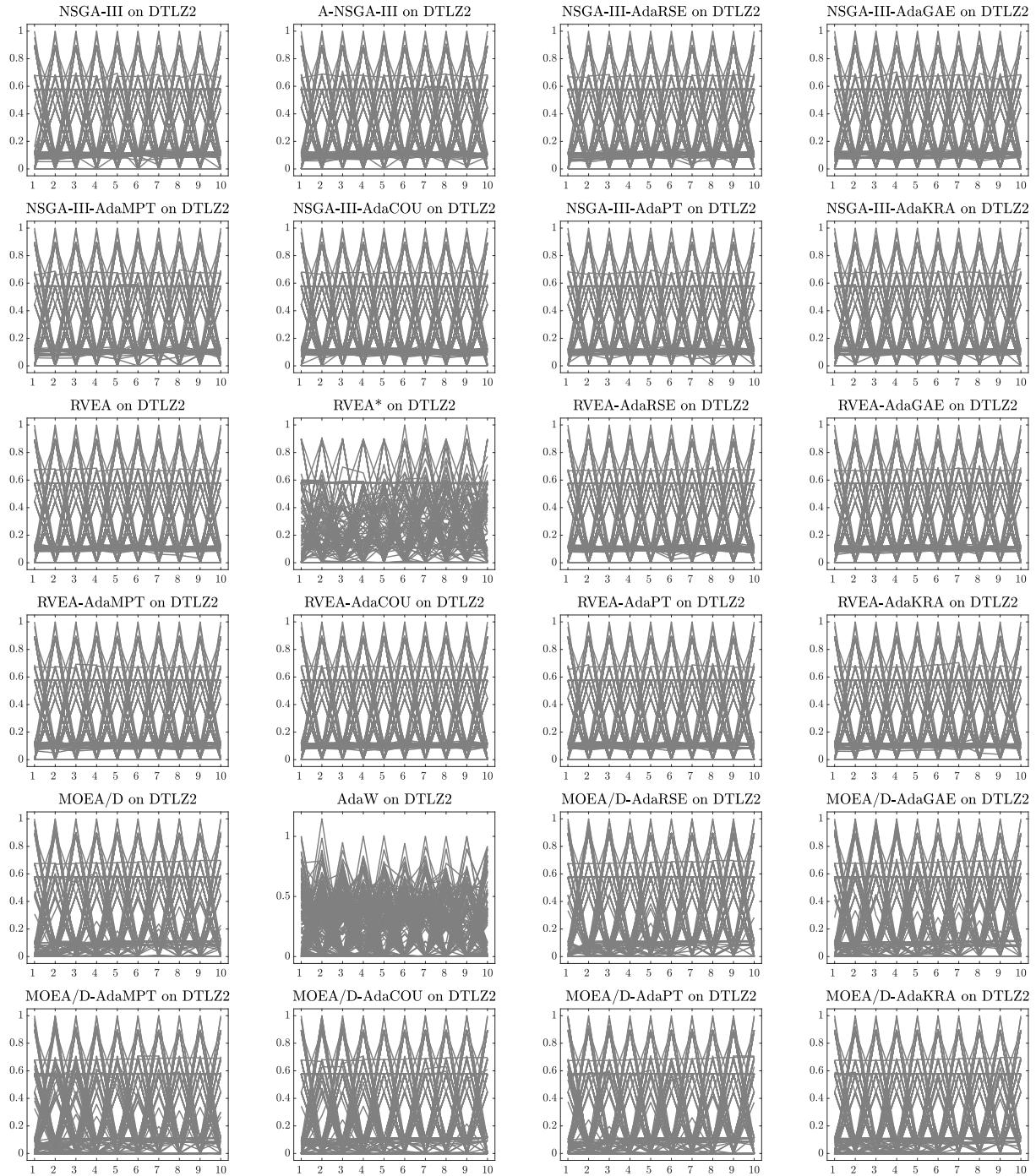


Figure 17: Final populations with the median HV value among 30 independent runs of MOEAs using the NSGA-III, RVEA, and MOEA/D frameworks on DTLZ2 with 10 objective functions.

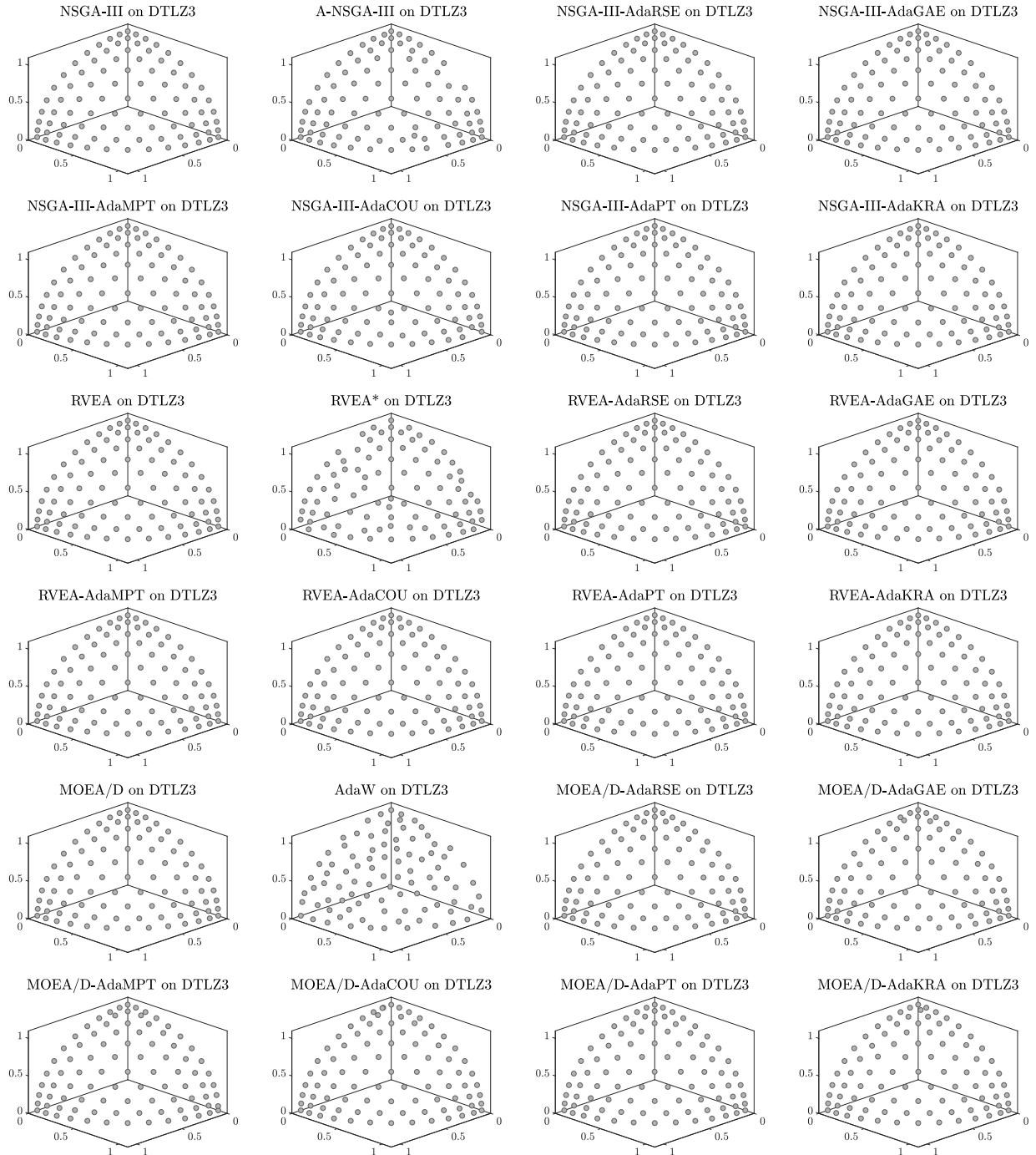


Figure 18: Final populations with the median HV value among 30 independent runs of MOEAs using the NSGA-III, RVEA, and MOEA/D frameworks on DTLZ3 with 3 objective functions.

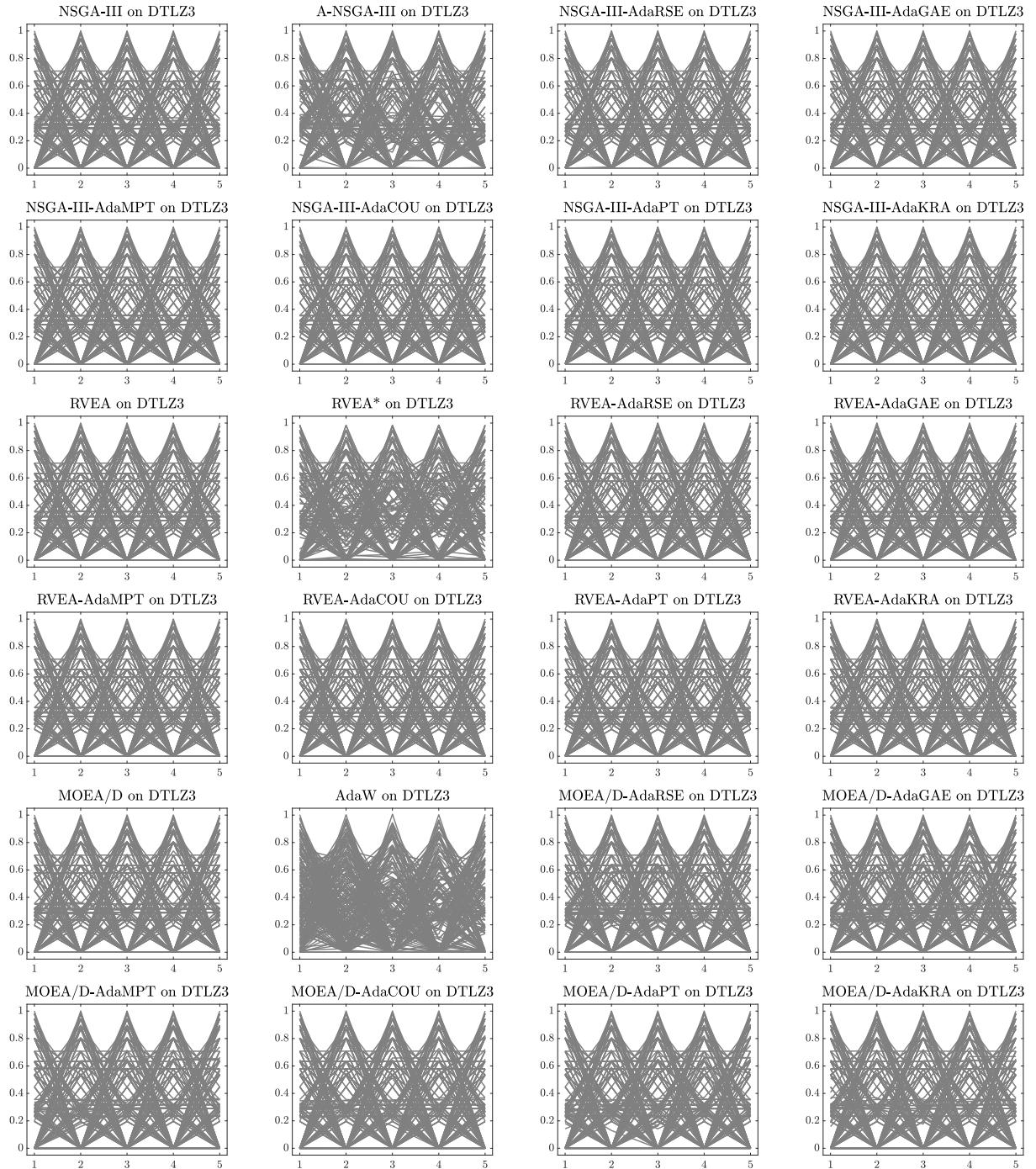


Figure 19: Final populations with the median HV value among 30 independent runs of MOEAs using the NSGA-III, RVEA, and MOEA/D frameworks on DTLZ3 with 5 objective functions.

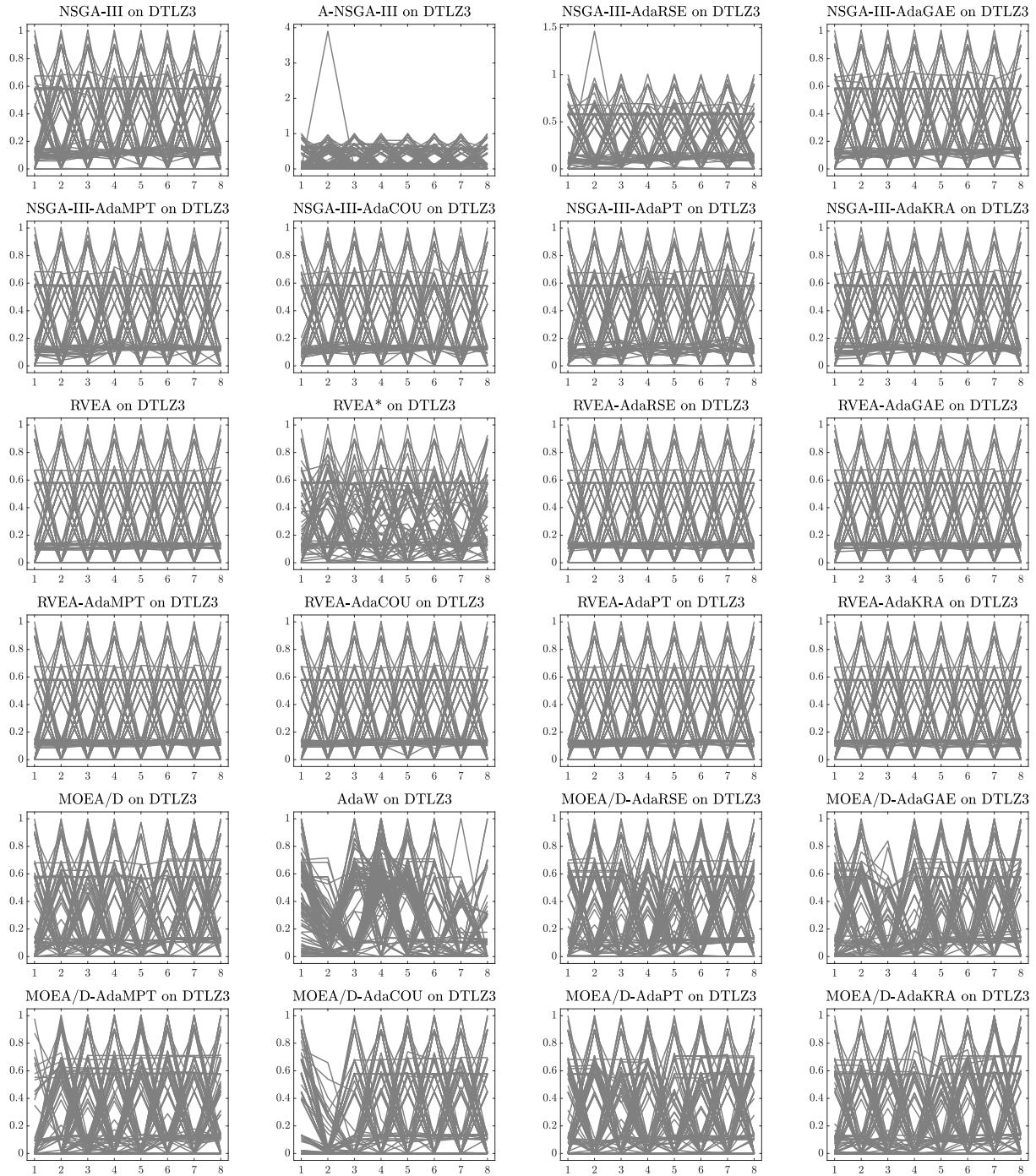


Figure 20: Final populations with the median HV value among 30 independent runs of MOEAs using the NSGA-III, RVEA, and MOEA/D frameworks on DTLZ3 with 8 objective functions.

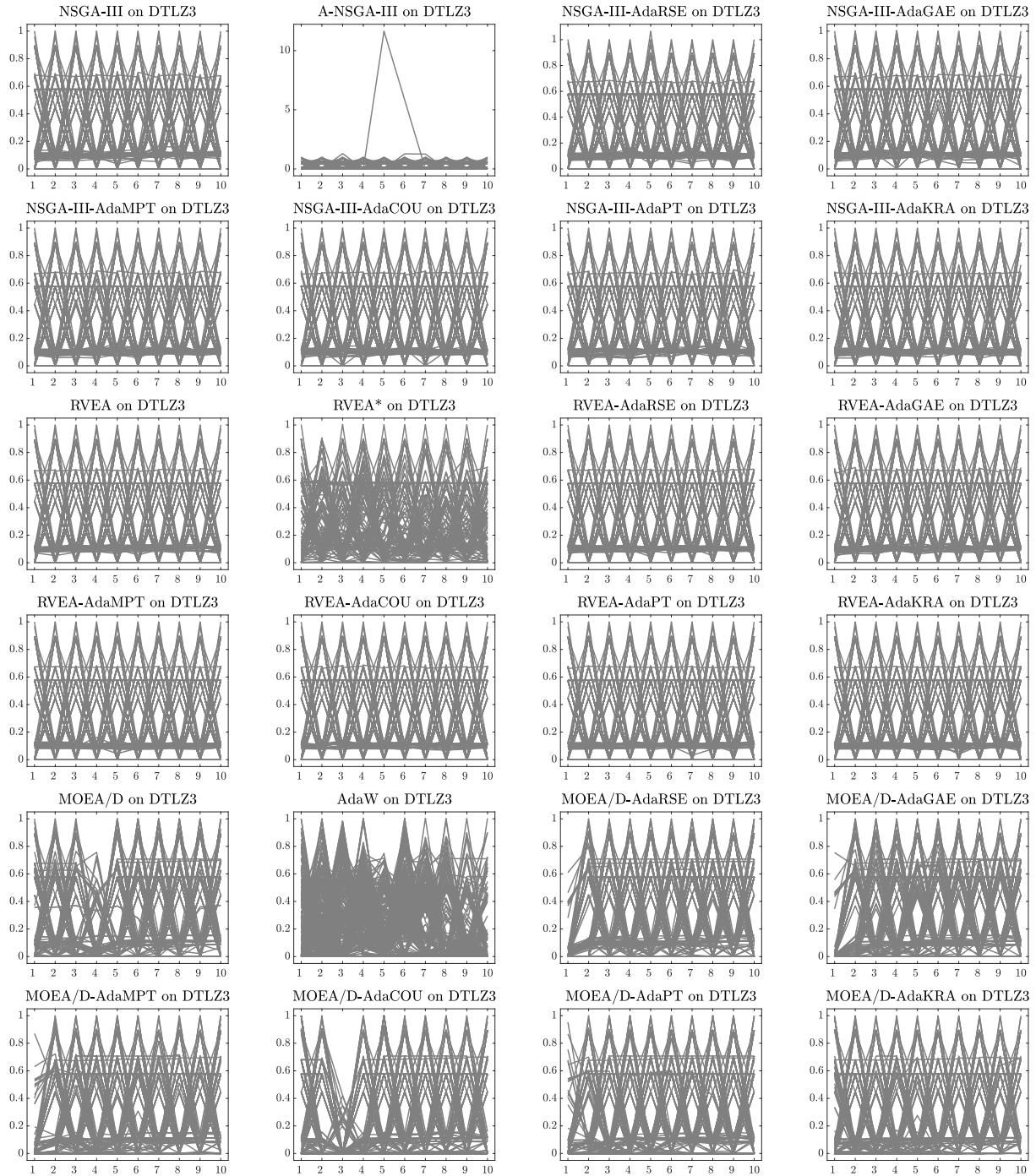


Figure 21: Final populations with the median HV value among 30 independent runs of MOEAs using the NSGA-III, RVEA, and MOEA/D frameworks on DTLZ3 with 10 objective functions.

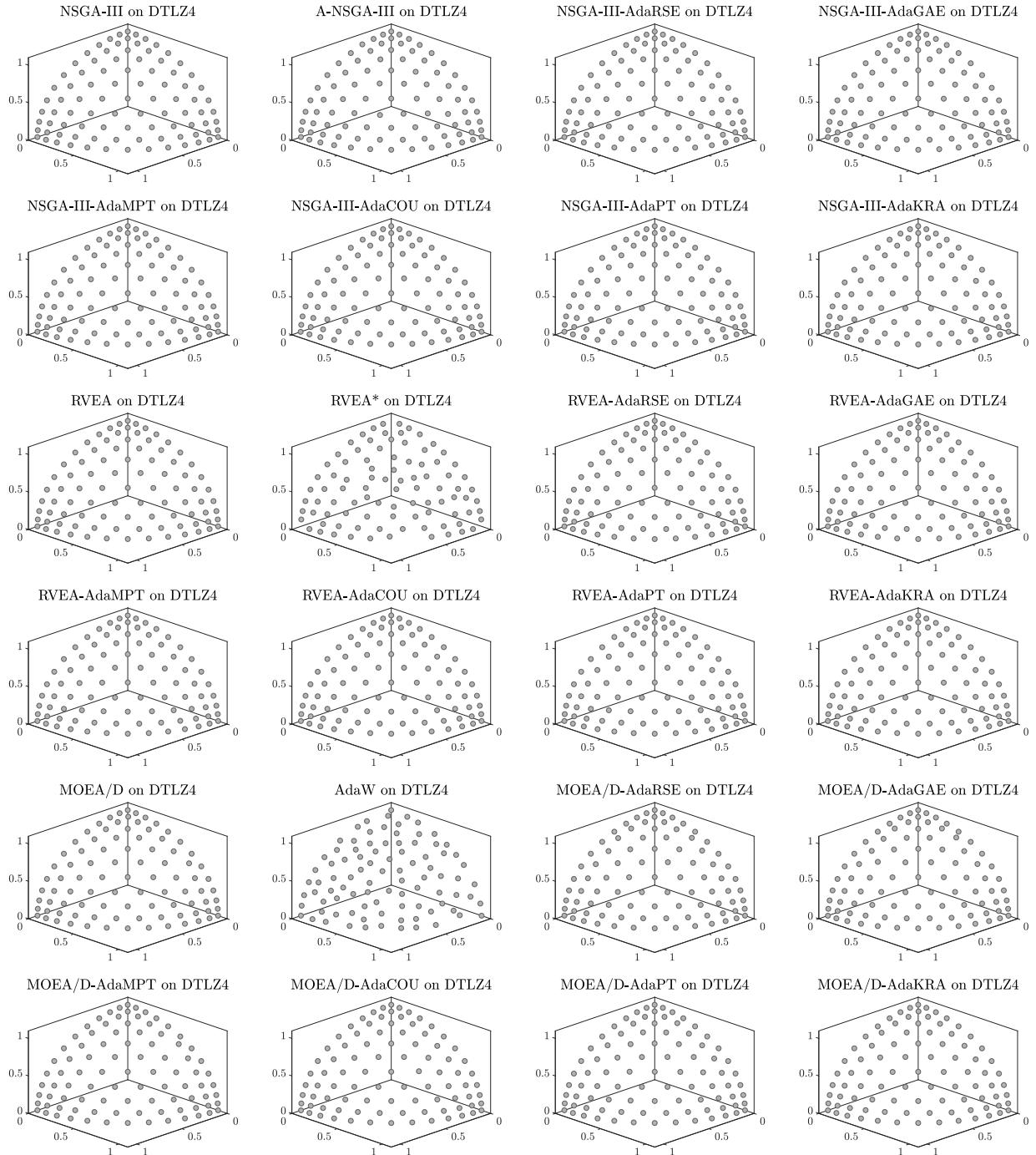


Figure 22: Final populations with the median HV value among 30 independent runs of MOEAs using the NSGA-III, RVEA, and MOEA/D frameworks on DTLZ4 with 3 objective functions.

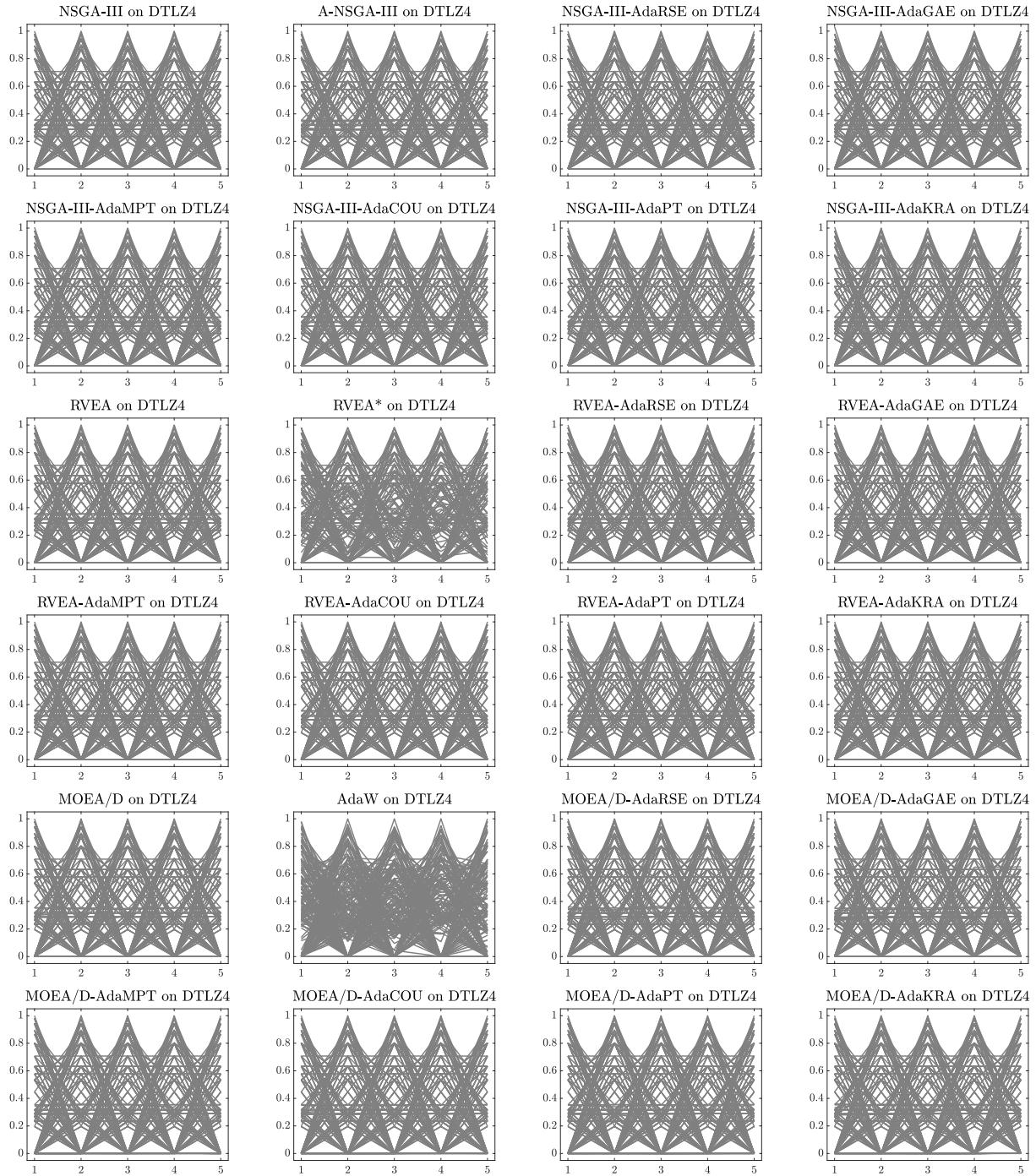


Figure 23: Final populations with the median HV value among 30 independent runs of MOEAs using the NSGA-III, RVEA, and MOEA/D frameworks on DTLZ4 with 5 objective functions.

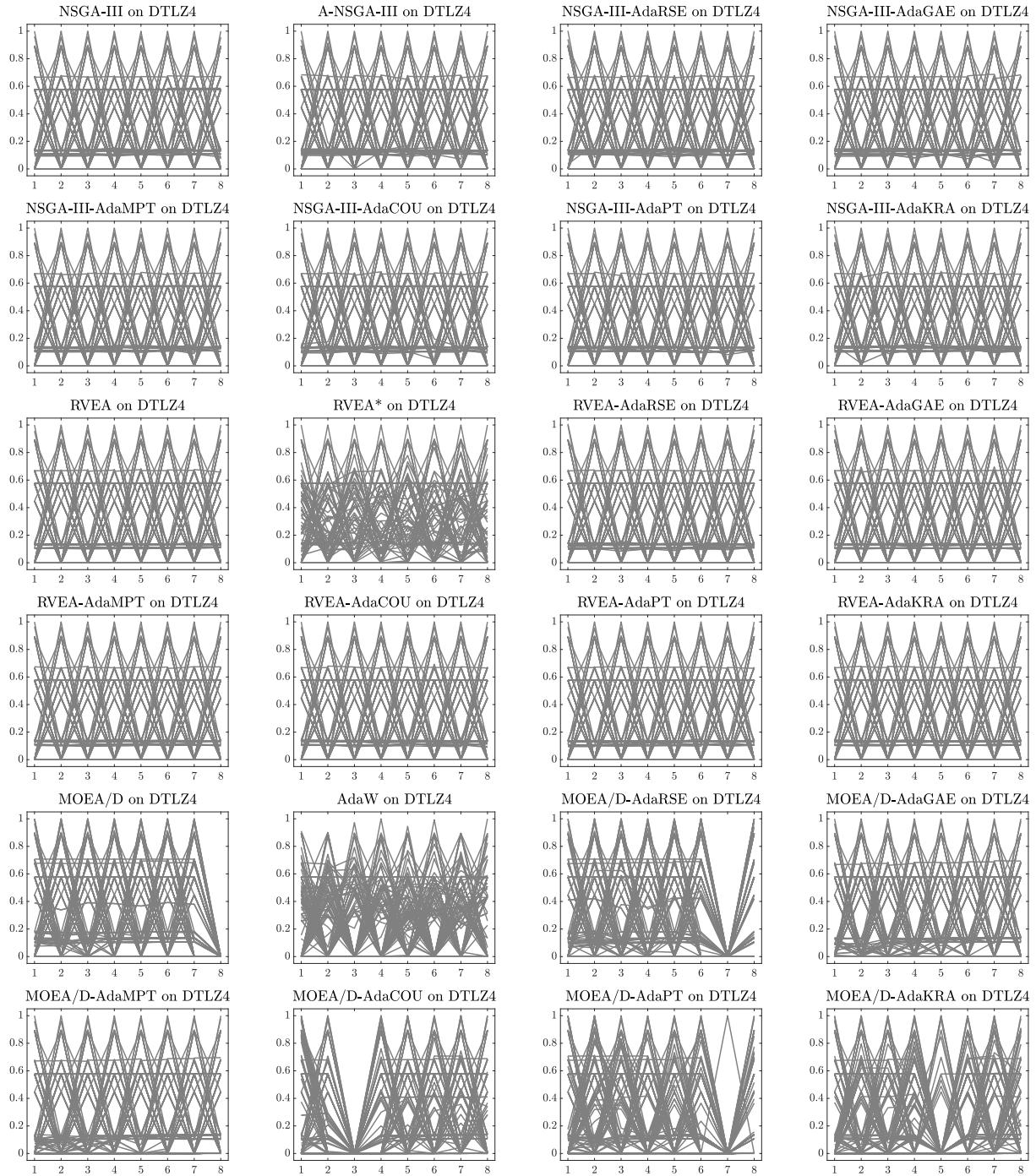


Figure 24: Final populations with the median HV value among 30 independent runs of MOEAs using the NSGA-III, RVEA, and MOEA/D frameworks on DTLZ4 with 8 objective functions.

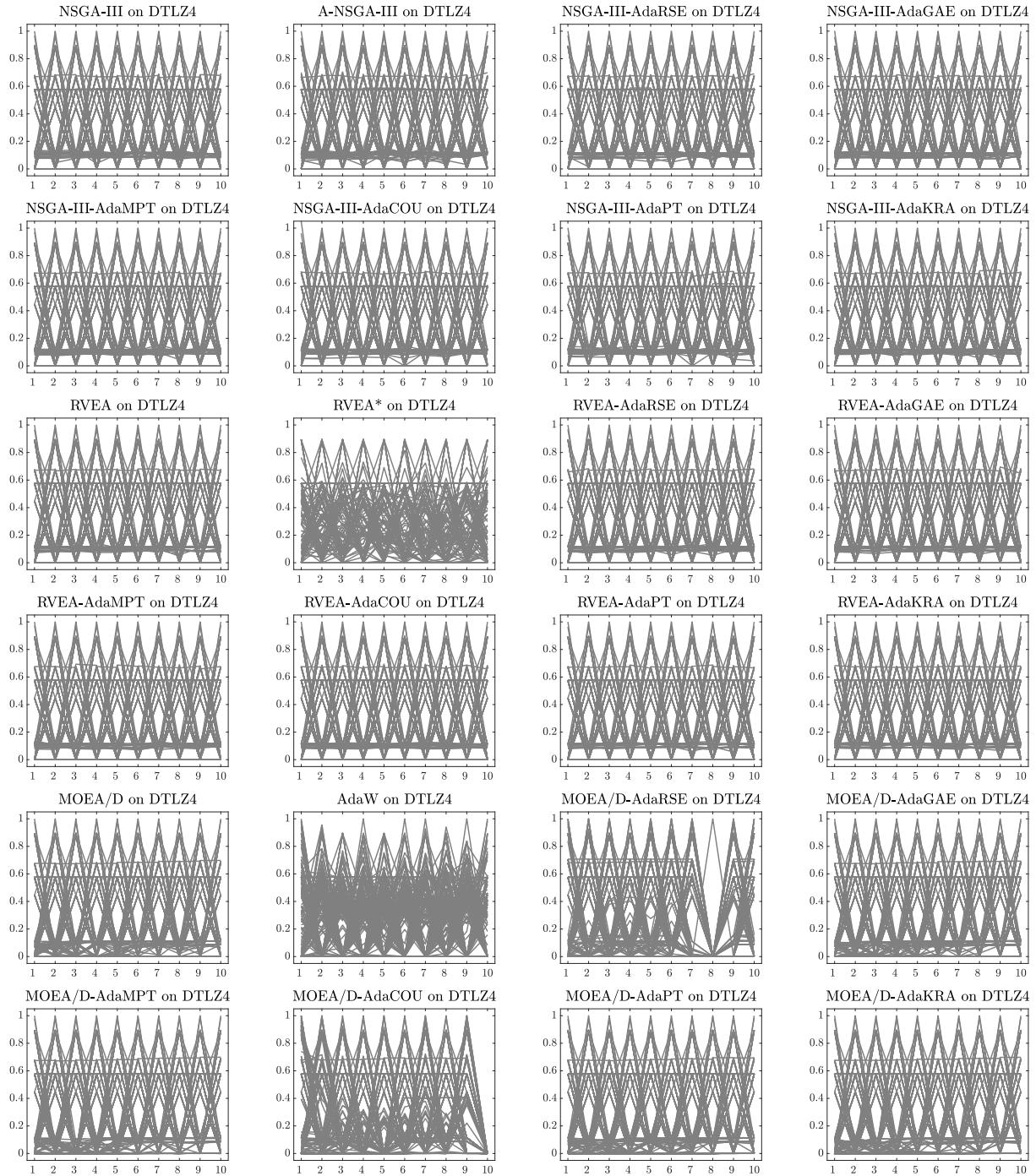


Figure 25: Final populations with the median HV value among 30 independent runs of MOEAs using the NSGA-III, RVEA, and MOEA/D frameworks on DTLZ4 with 10 objective functions.

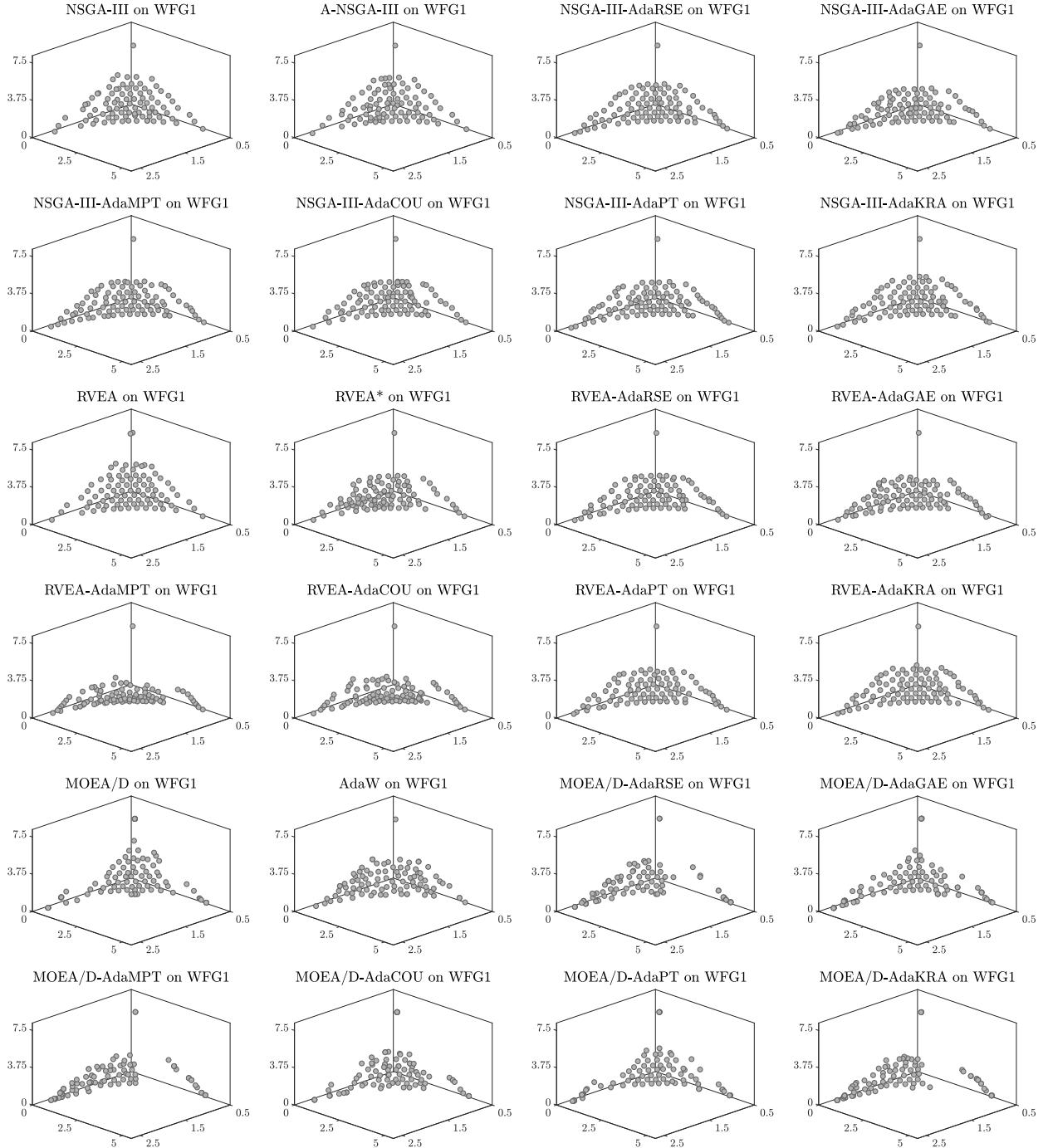


Figure 26: Final populations with the median HV value among 30 independent runs of MOEAs using the NSGA-III, RVEA, and MOEA/D frameworks on WFG1 with 3 objective functions.

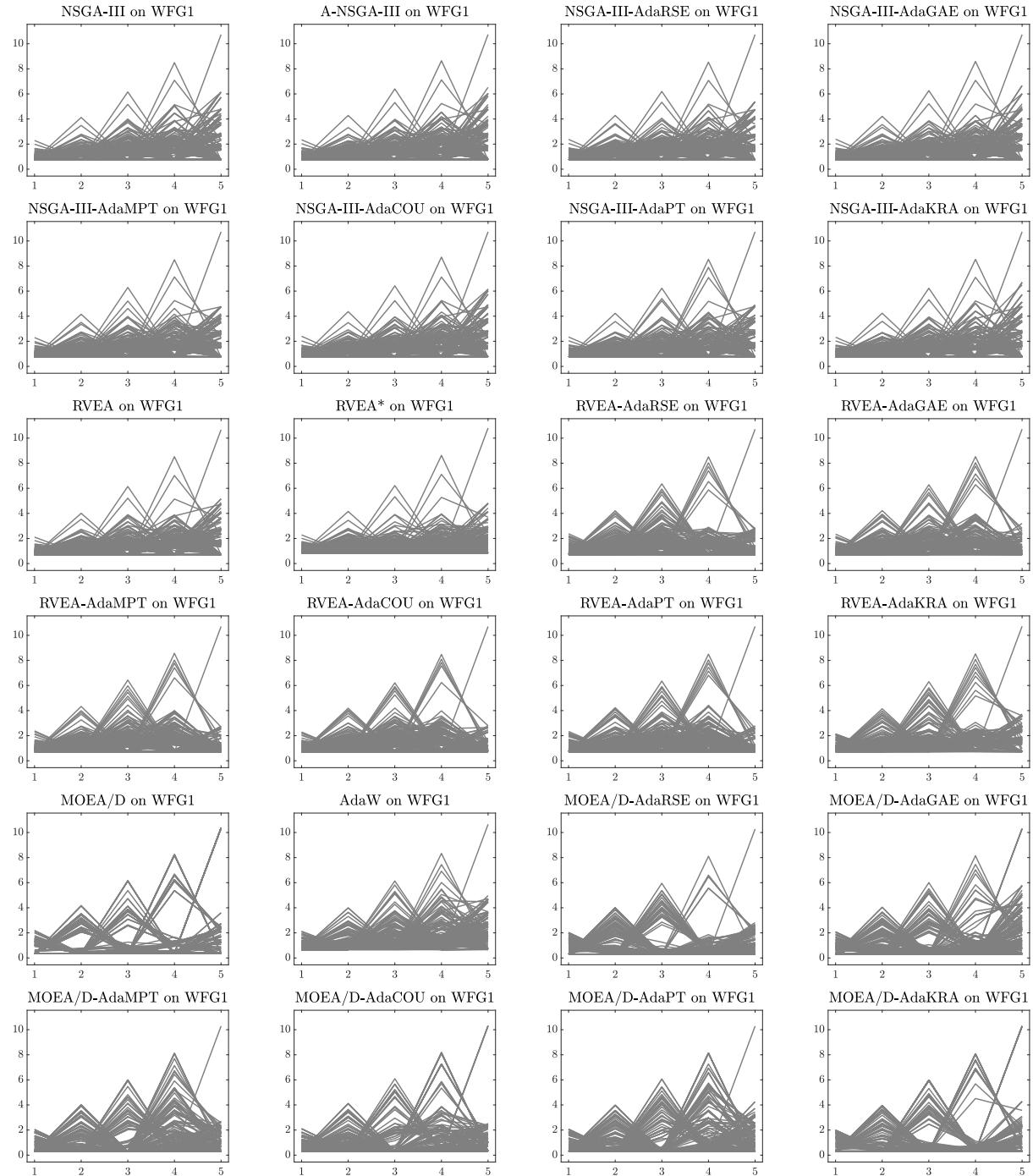


Figure 27: Final populations with the median HV value among 30 independent runs of MOEAs using the NSGA-III, RVEA, and MOEA/D frameworks on WFG1 with 5 objective functions.

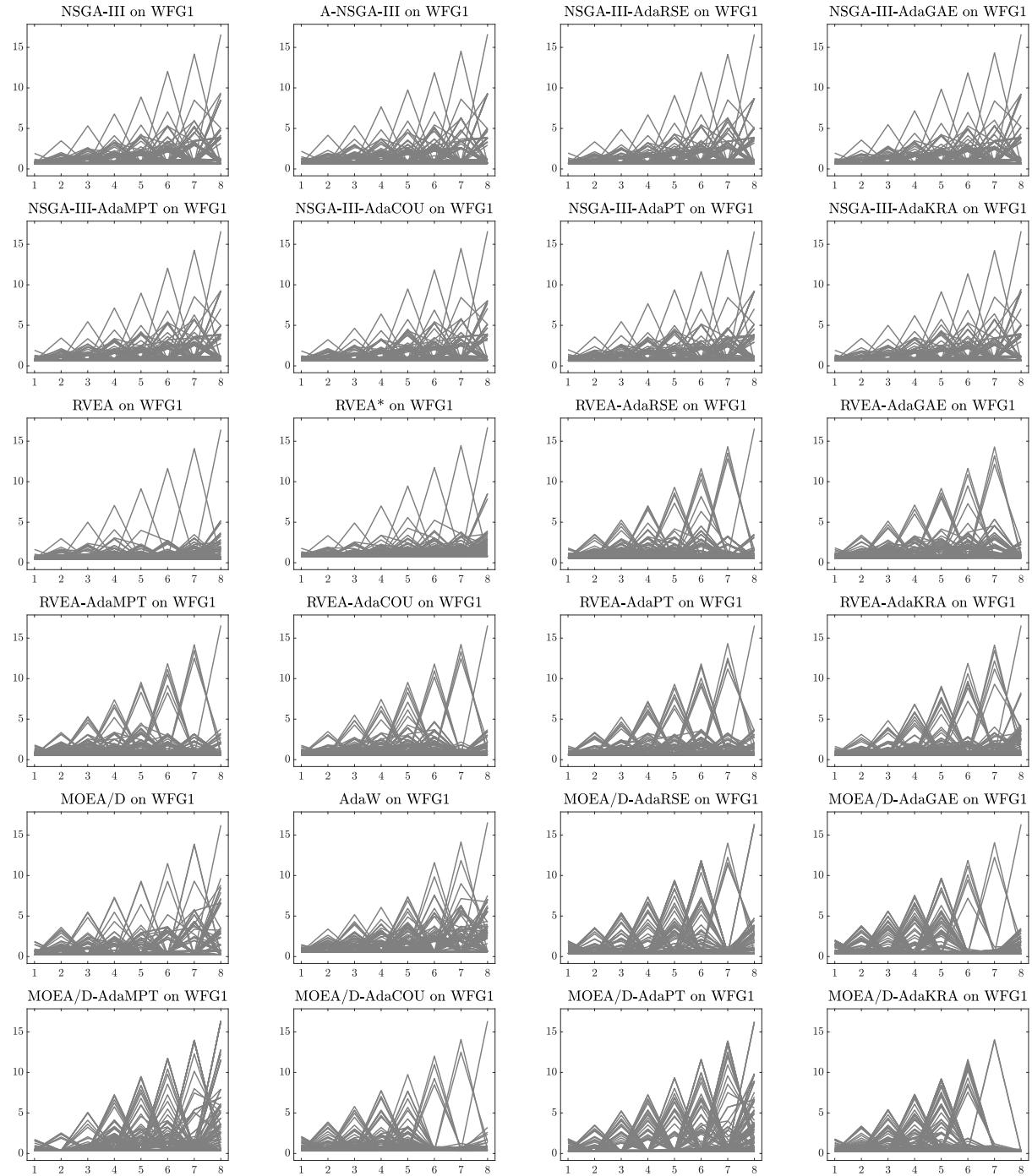


Figure 28: Final populations with the median HV value among 30 independent runs of MOEAs using the NSGA-III, RVEA, and MOEA/D frameworks on WFG1 with 8 objective functions.

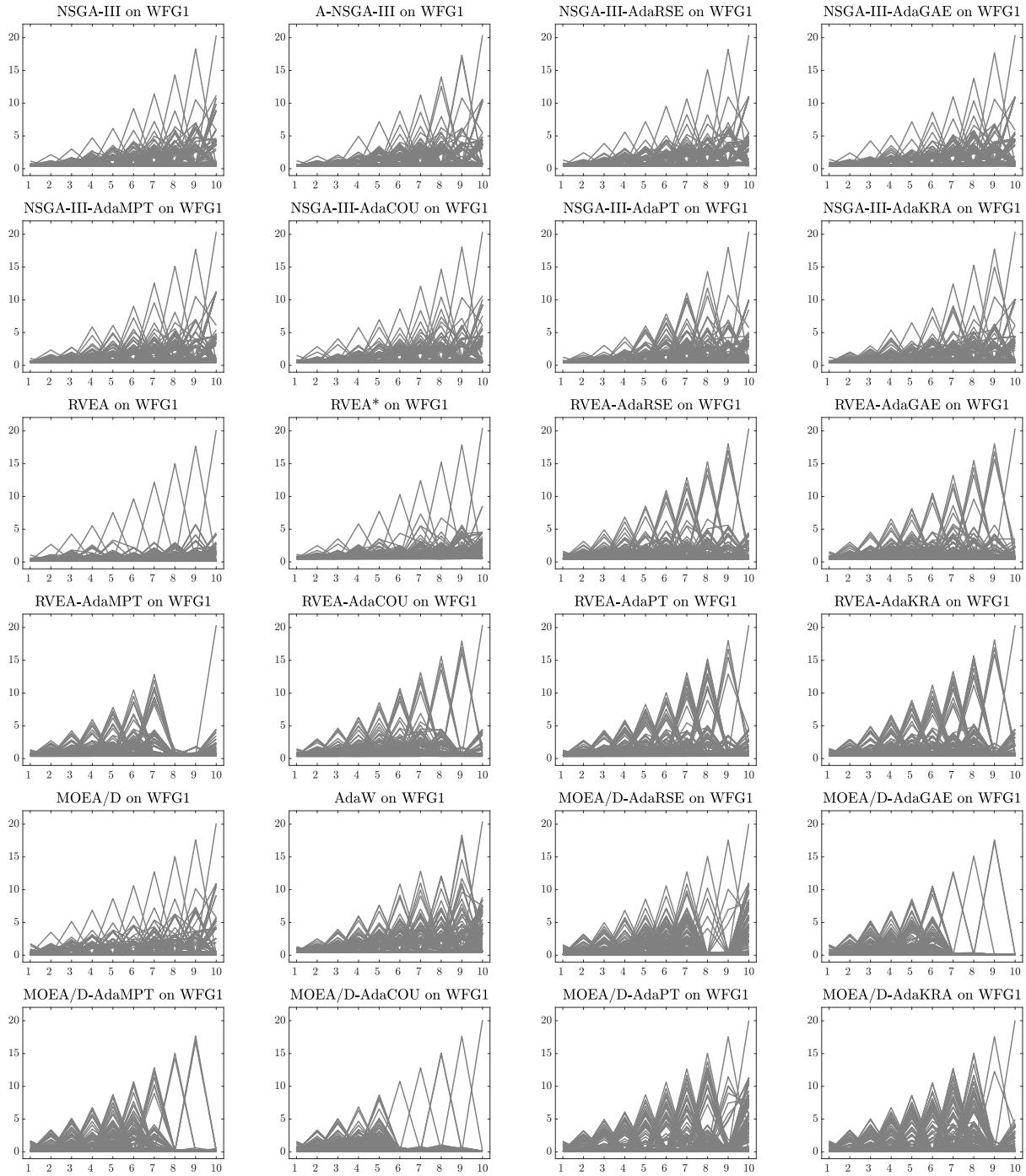


Figure 29: Final populations with the median HV value among 30 independent runs of MOEAs using the NSGA-III, RVEA, and MOEA/D frameworks on WFG1 with 10 objective functions.

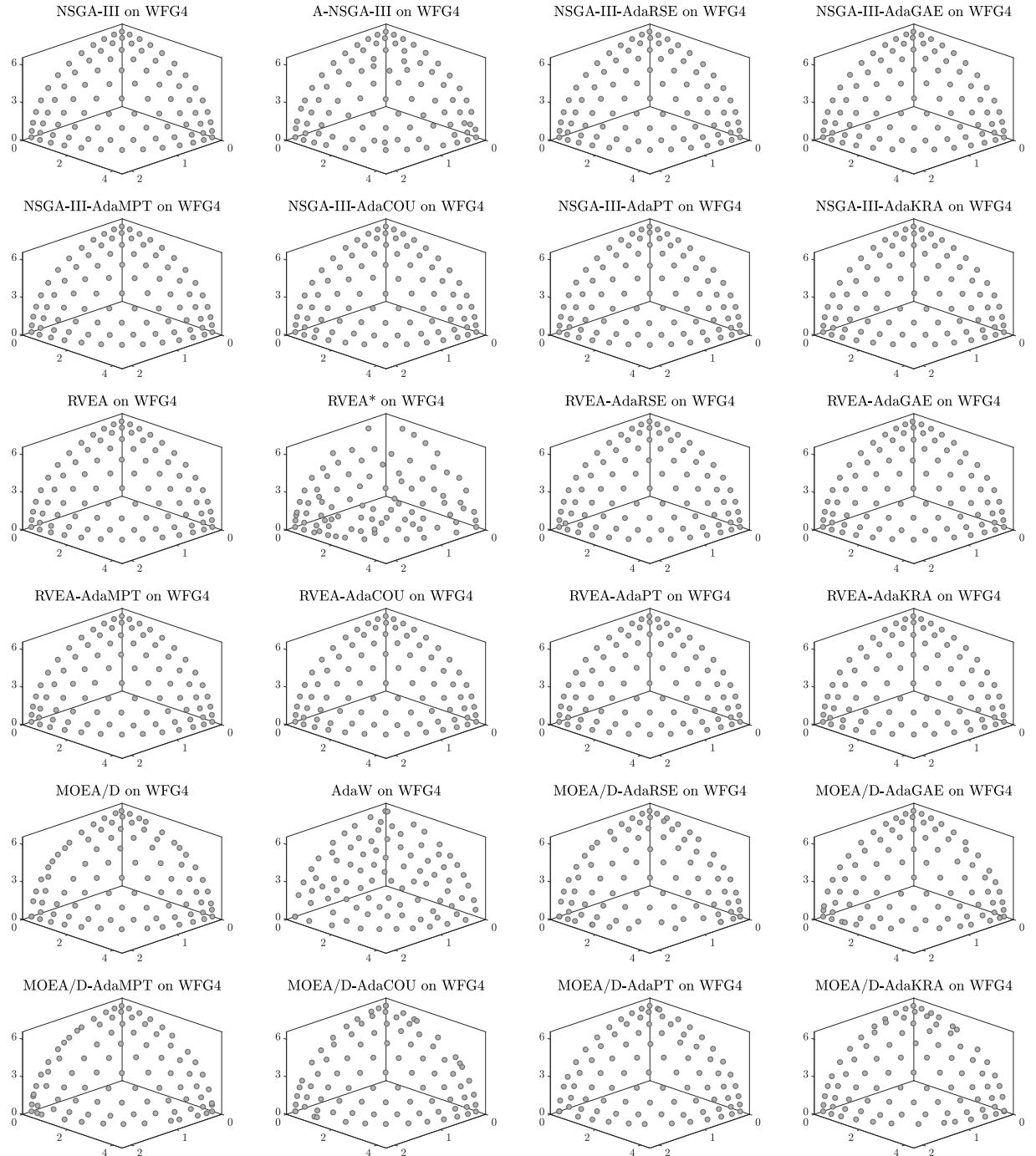


Figure 30: Final populations with the median HV value among 30 independent runs of MOEAs using the NSGA-III, RVEA, and MOEA/D frameworks on WFG4 with 3 objective functions.

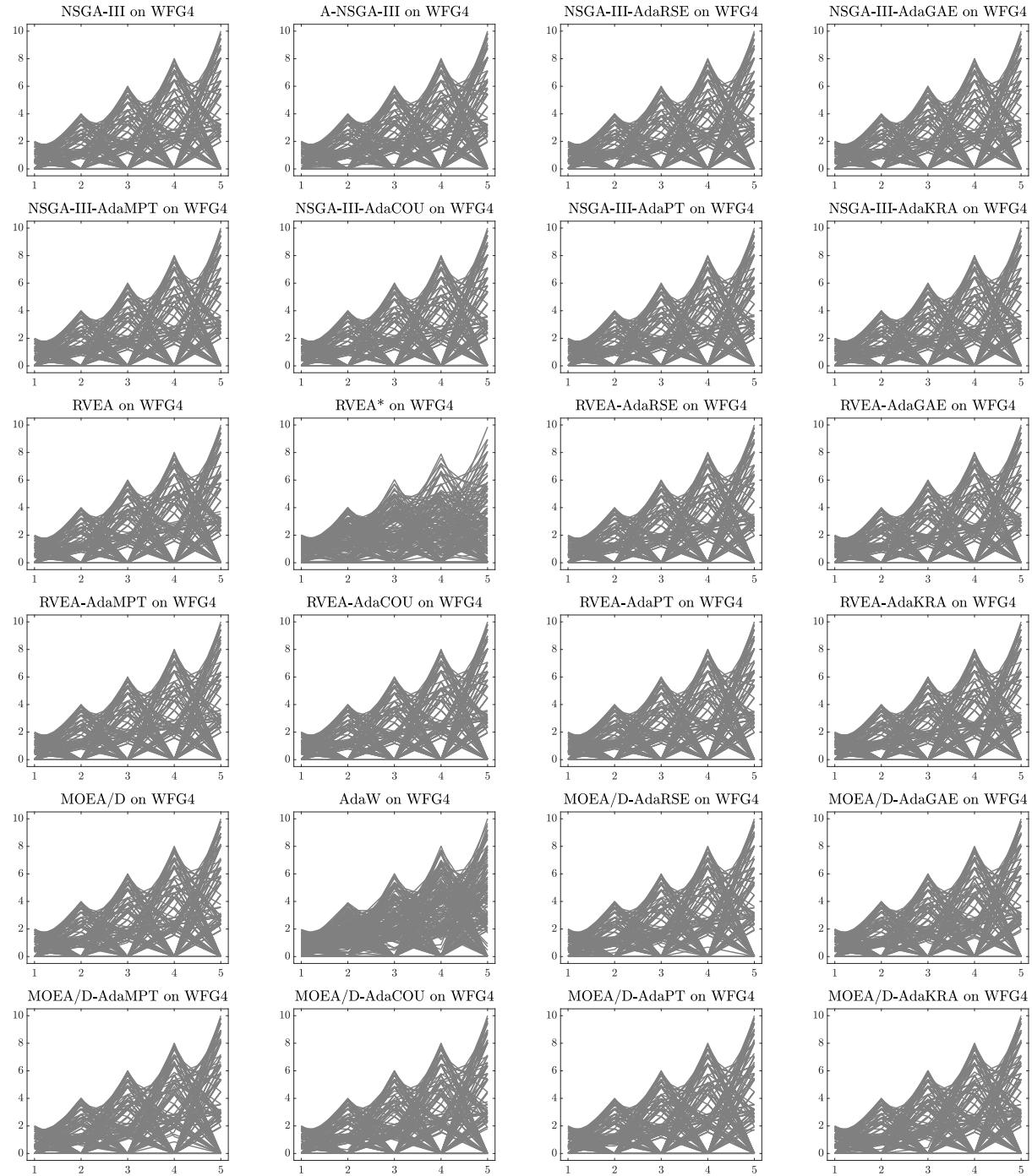


Figure 31: Final populations with the median HV value among 30 independent runs of MOEAs using the NSGA-III, RVEA, and MOEA/D frameworks on WFG4 with 5 objective functions.

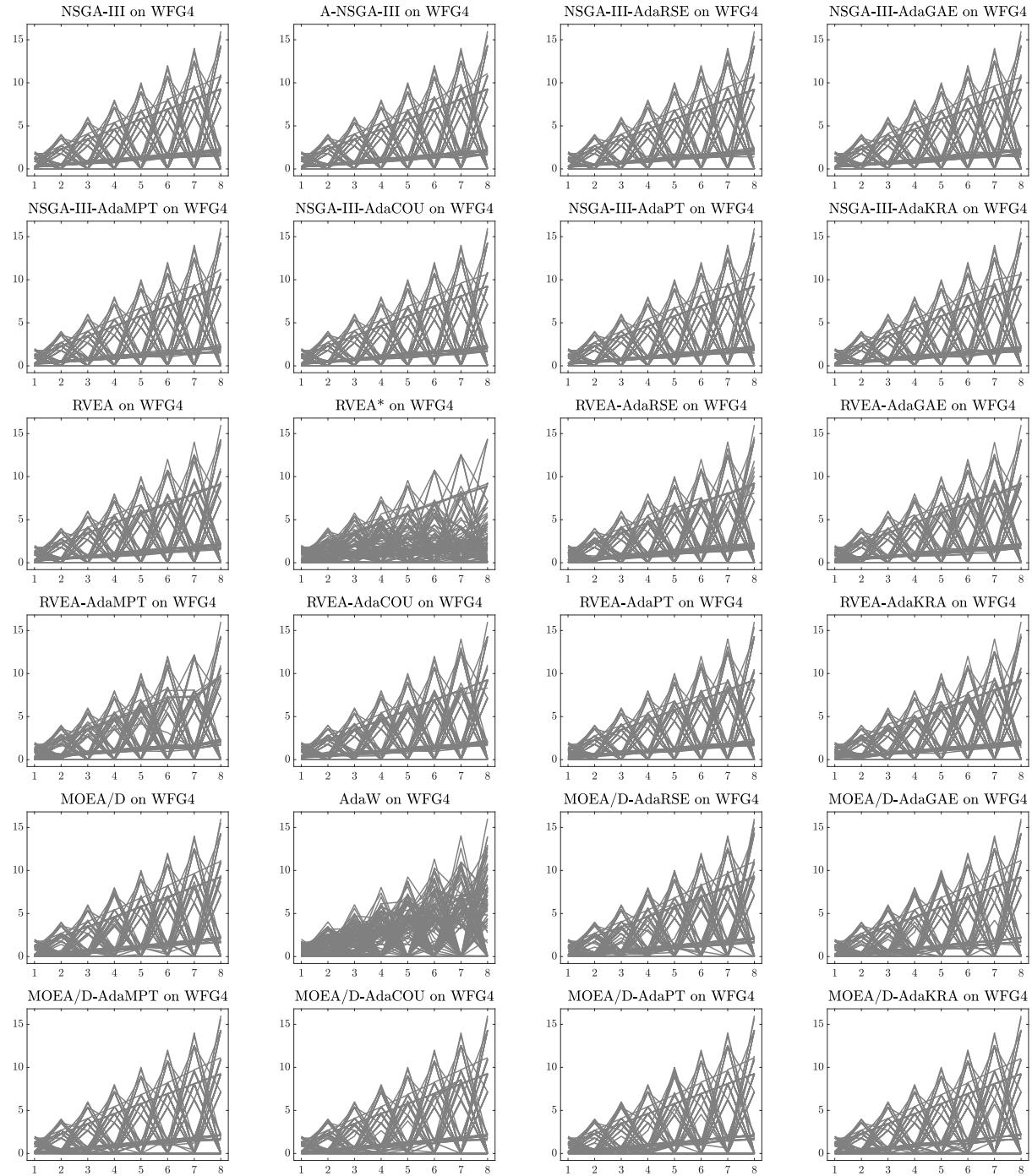


Figure 32: Final populations with the median HV value among 30 independent runs of MOEAs using the NSGA-III, RVEA, and MOEA/D frameworks on WFG4 with 8 objective functions.

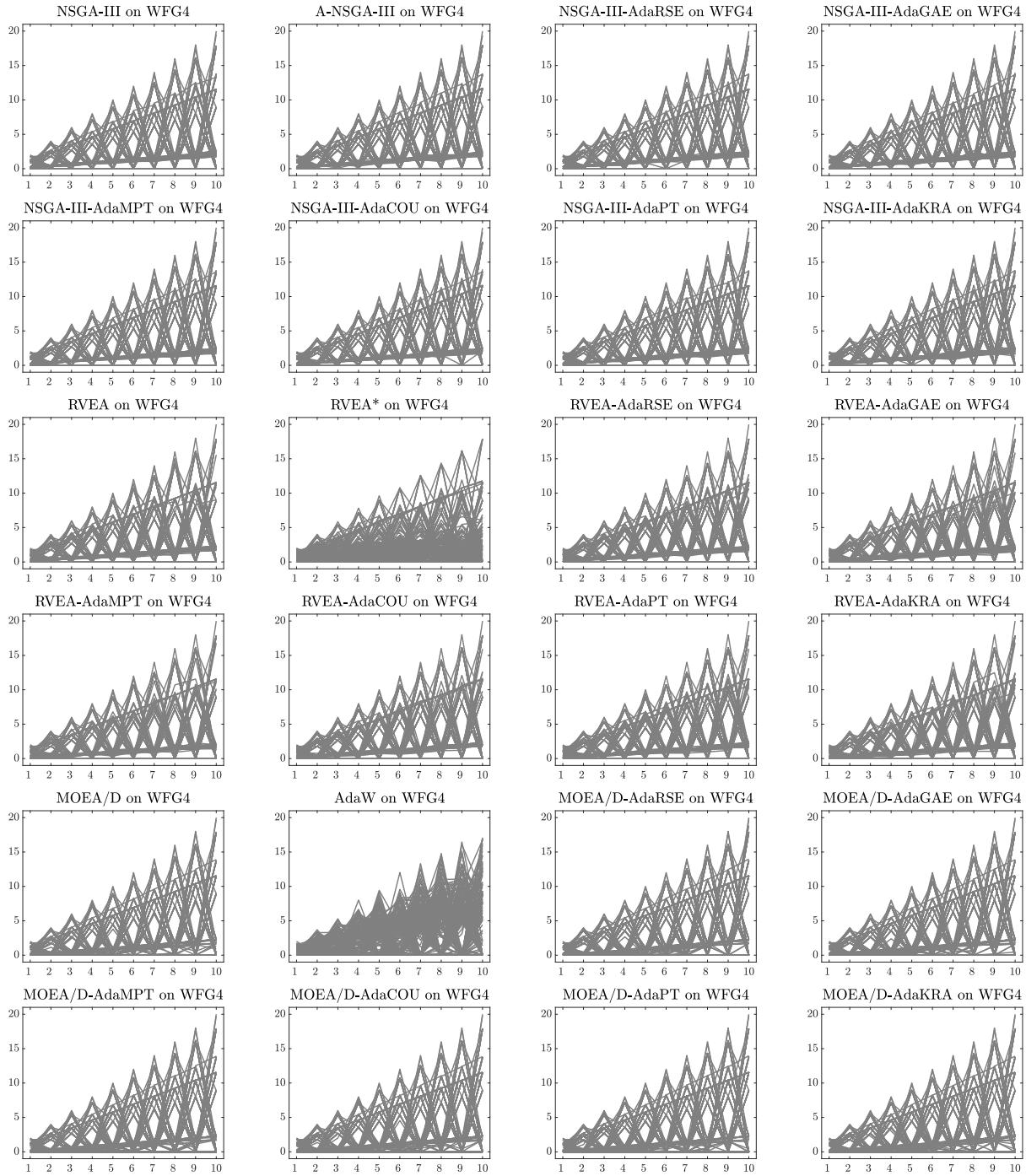


Figure 33: Final populations with the median HV value among 30 independent runs of MOEAs using the NSGA-III, RVEA, and MOEA/D frameworks on WFG4 with 10 objective functions.

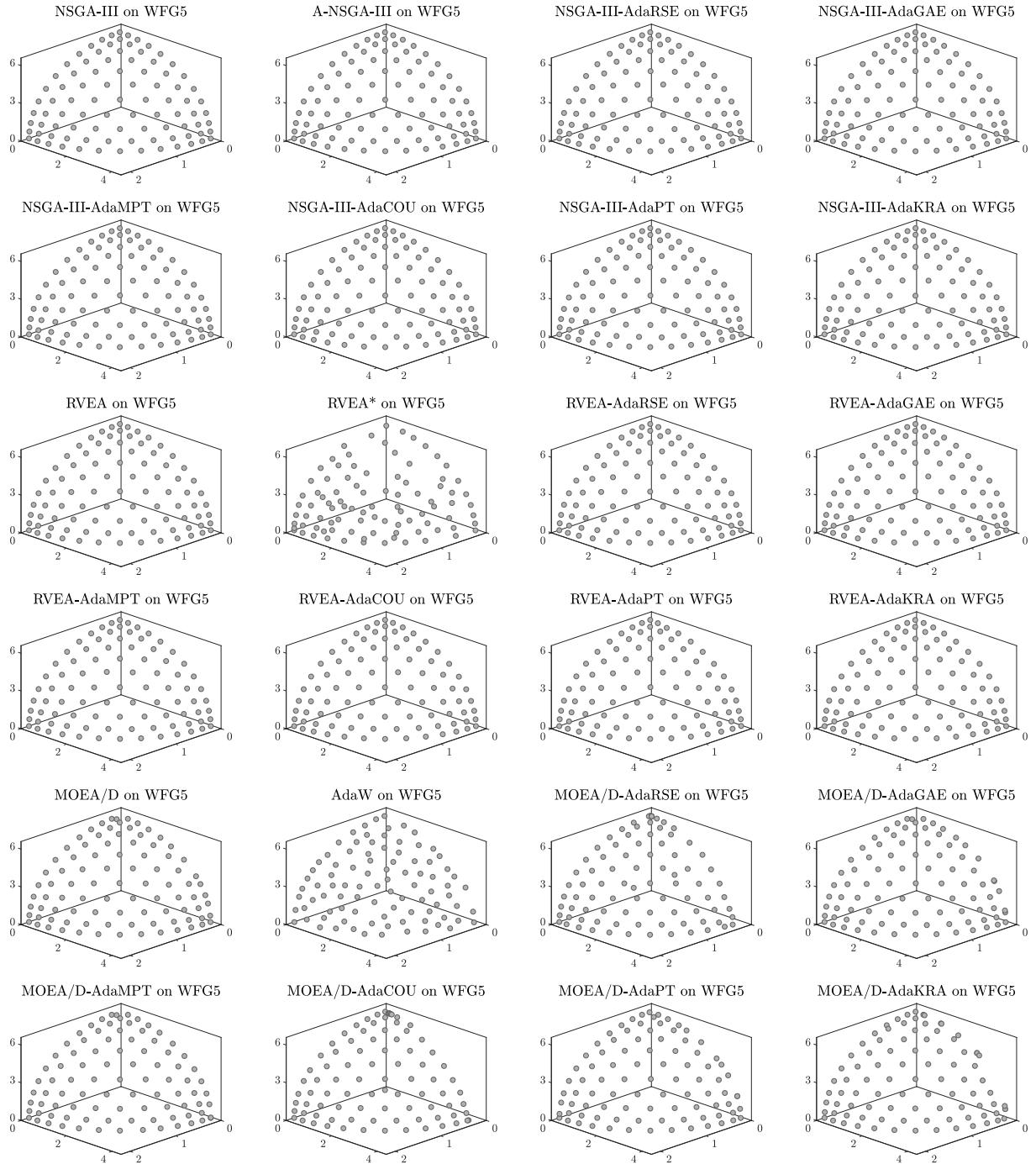


Figure 34: Final populations with the median HV value among 30 independent runs of MOEAs using the NSGA-III, RVEA, and MOEA/D frameworks on WFG5 with 3 objective functions.

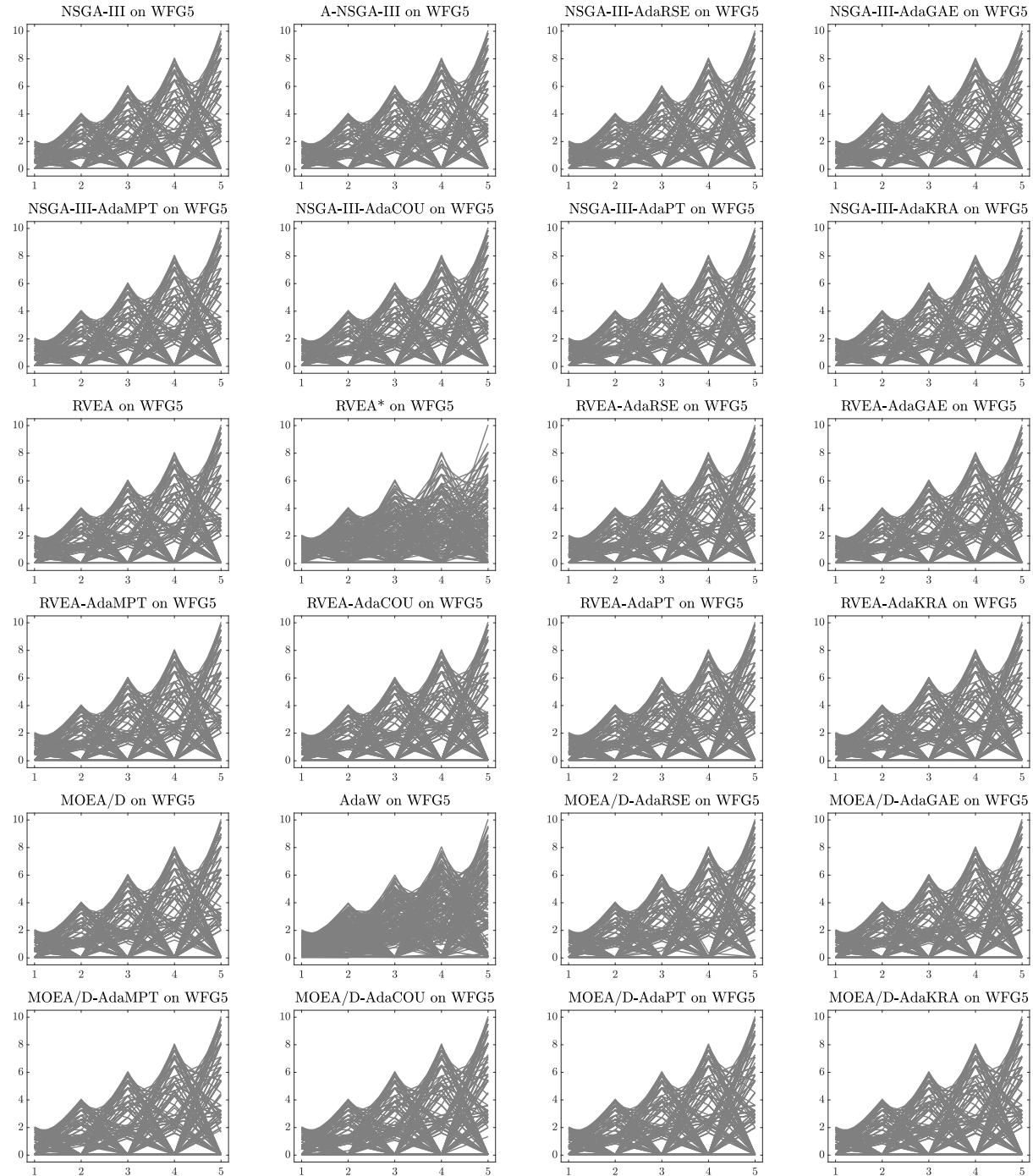


Figure 35: Final populations with the median HV value among 30 independent runs of MOEAs using the NSGA-III, RVEA, and MOEA/D frameworks on WFG5 with 5 objective functions.

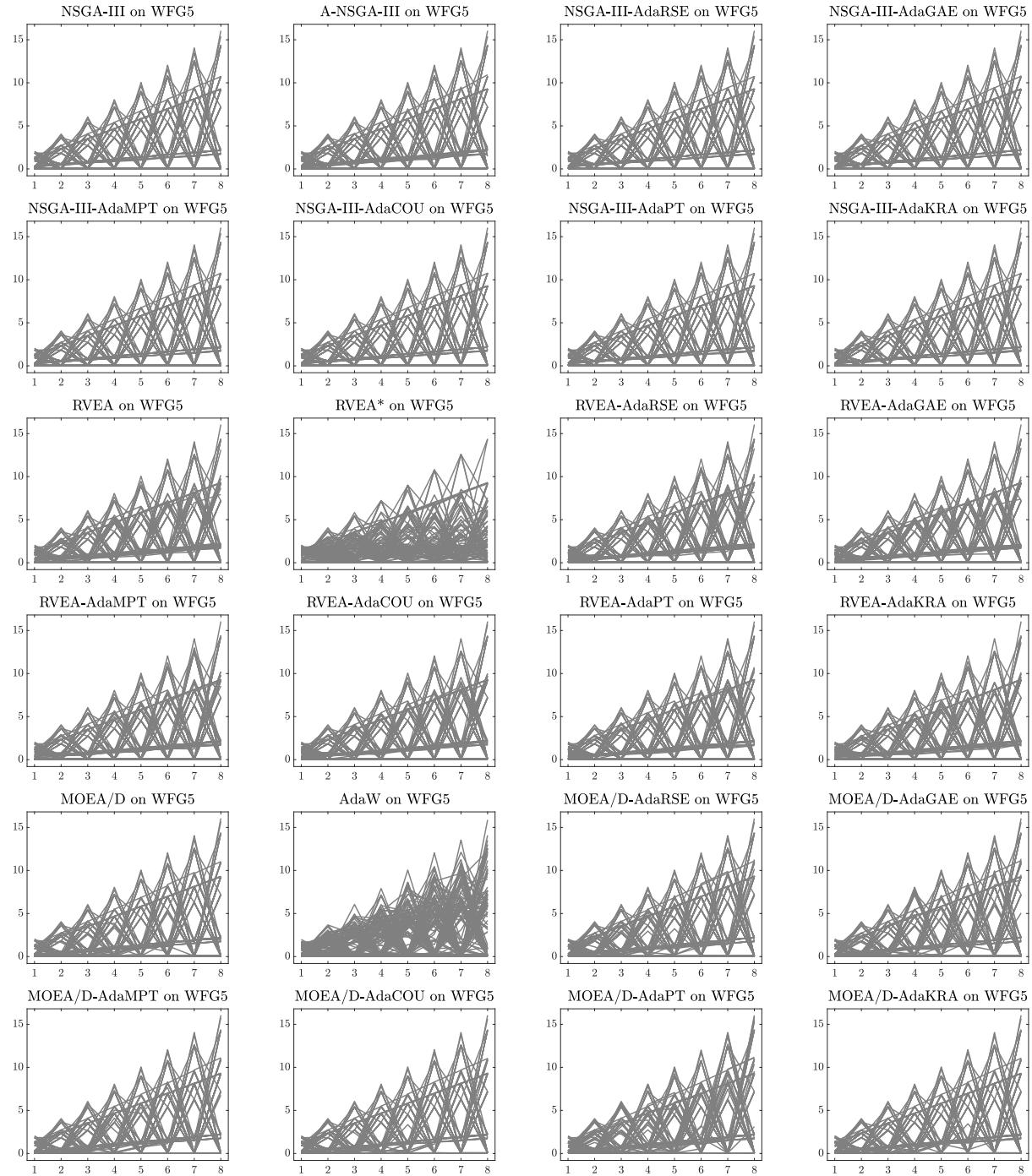


Figure 36: Final populations with the median HV value among 30 independent runs of MOEAs using the NSGA-III, RVEA, and MOEA/D frameworks on WFG5 with 8 objective functions.

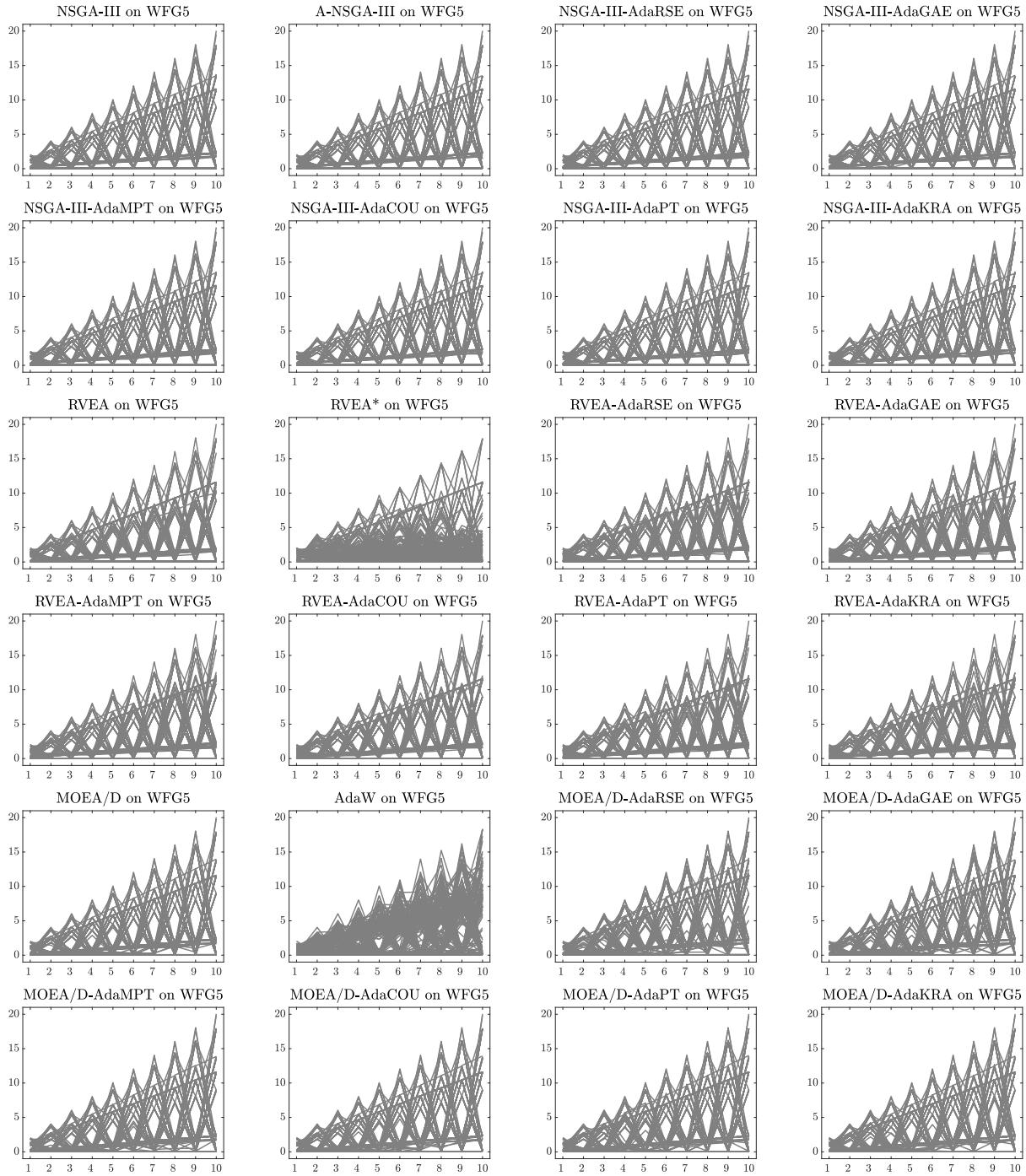


Figure 37: Final populations with the median HV value among 30 independent runs of MOEAs using the NSGA-III, RVEA, and MOEA/D frameworks on WFG5 with 10 objective functions.

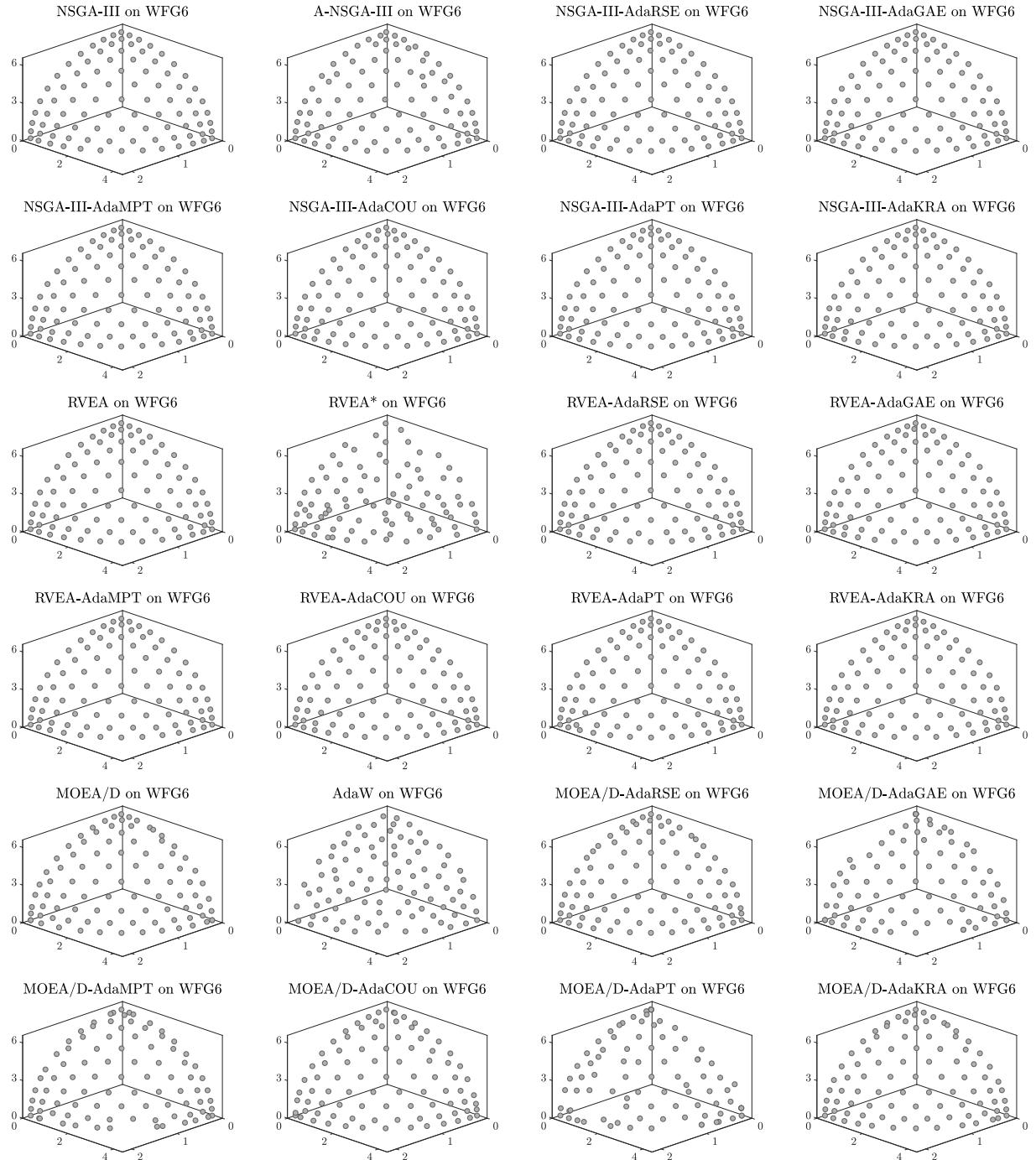


Figure 38: Final populations with the median HV value among 30 independent runs of MOEAs using the NSGA-III, RVEA, and MOEA/D frameworks on WFG6 with 3 objective functions.

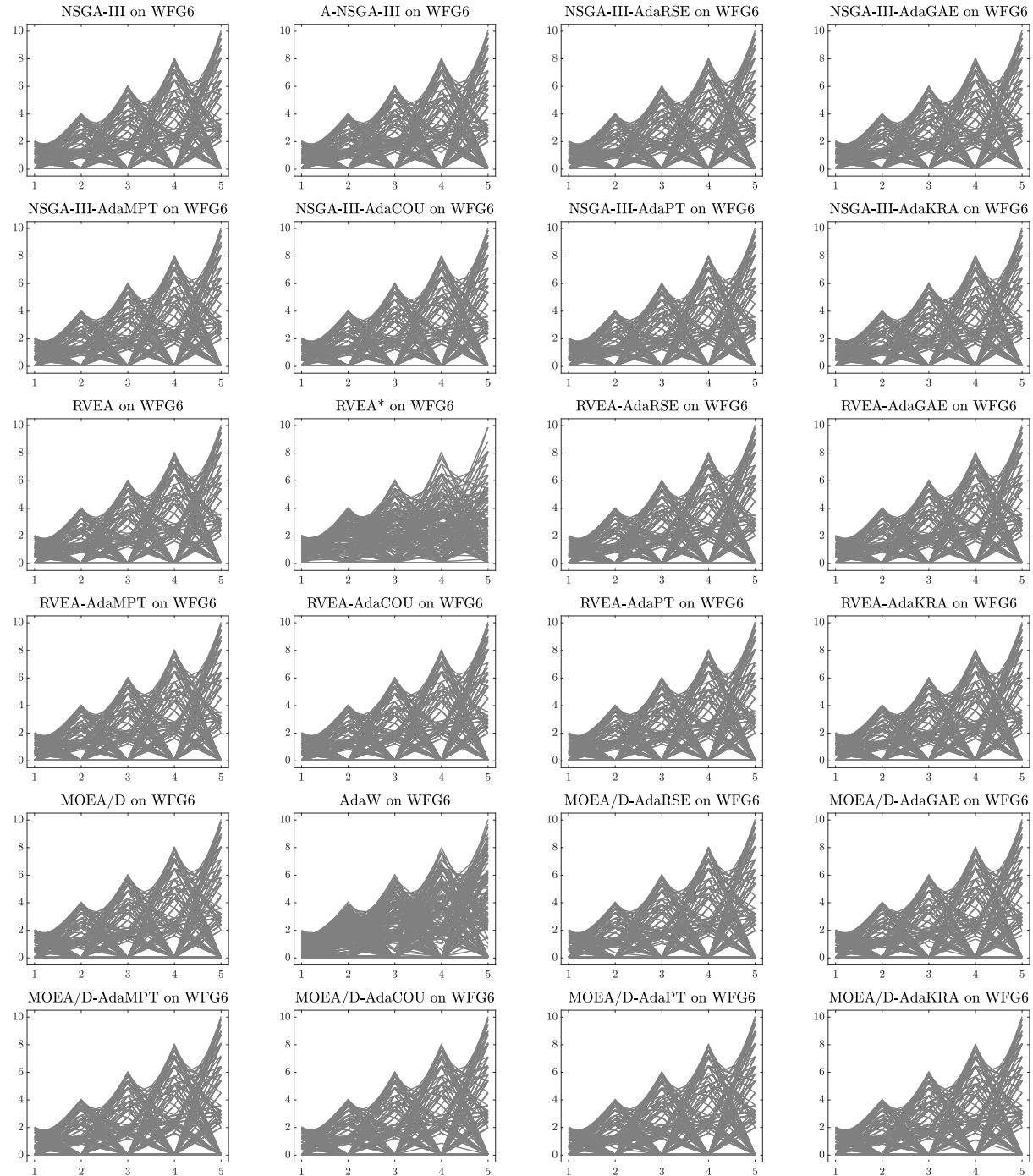


Figure 39: Final populations with the median HV value among 30 independent runs of MOEAs using the NSGA-III, RVEA, and MOEA/D frameworks on WFG6 with 5 objective functions.

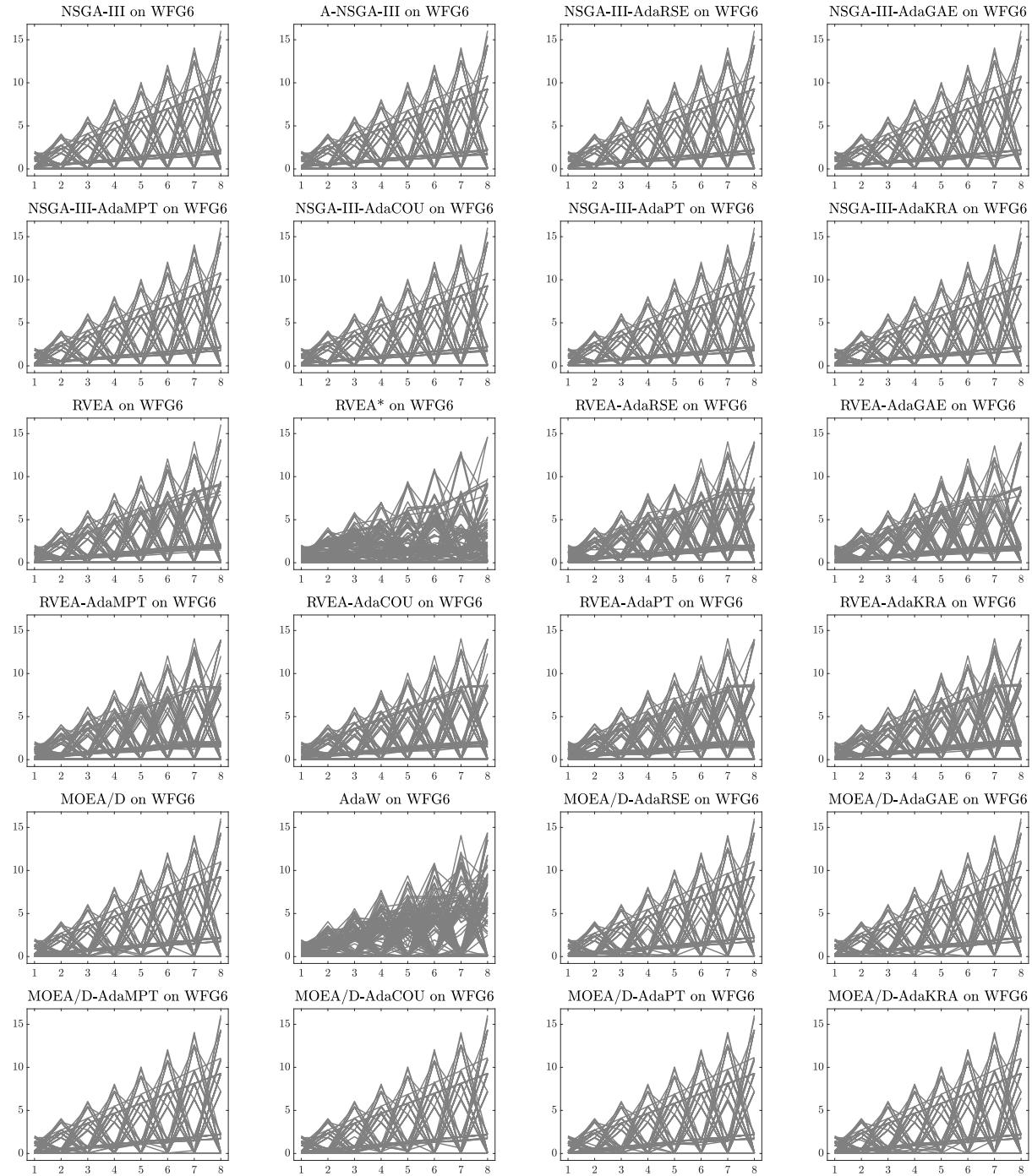


Figure 40: Final populations with the median HV value among 30 independent runs of MOEAs using the NSGA-III, RVEA, and MOEA/D frameworks on WFG6 with 8 objective functions.

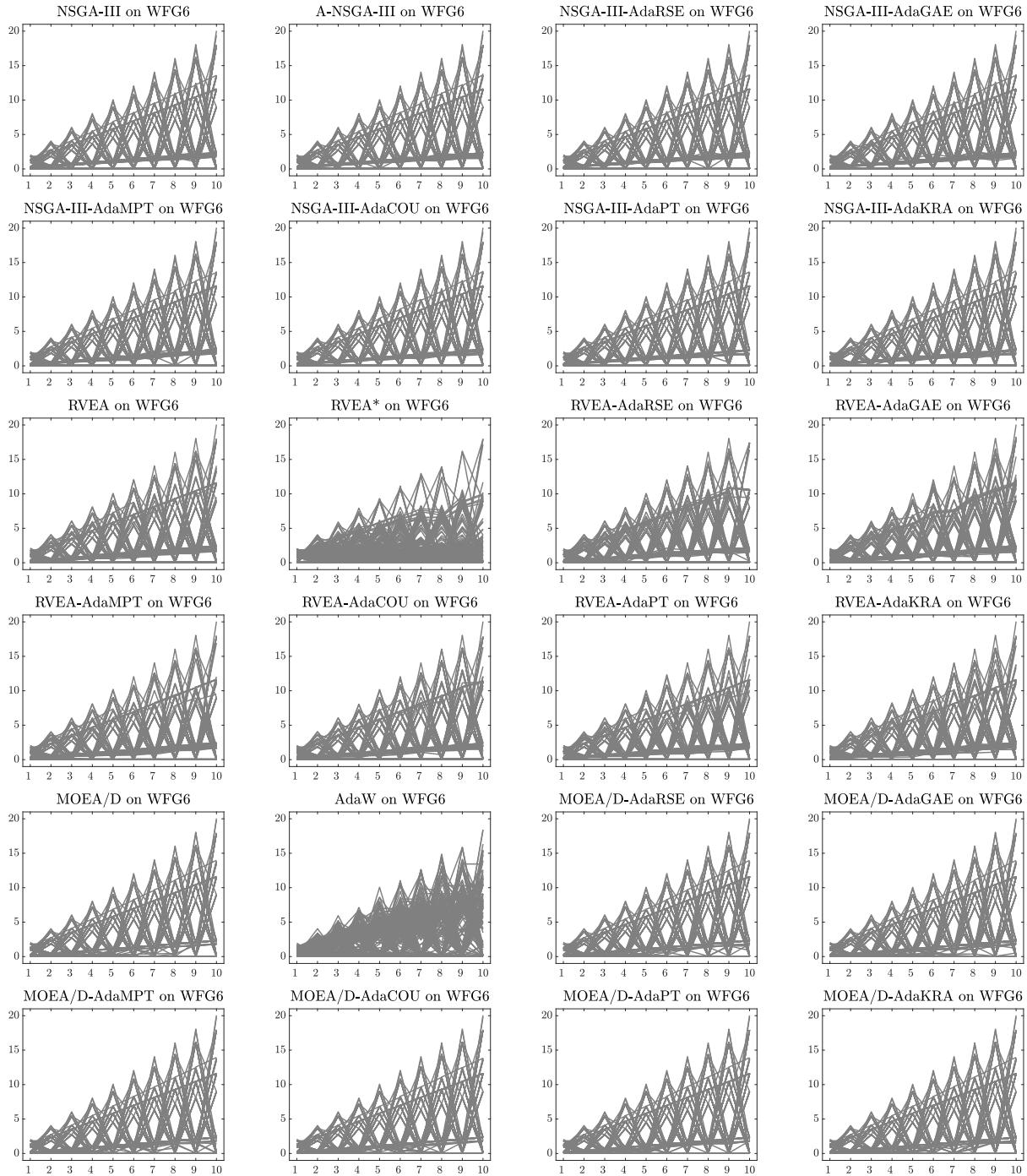


Figure 41: Final populations with the median HV value among 30 independent runs of MOEAs using the NSGA-III, RVEA, and MOEA/D frameworks on WFG6 with 10 objective functions.

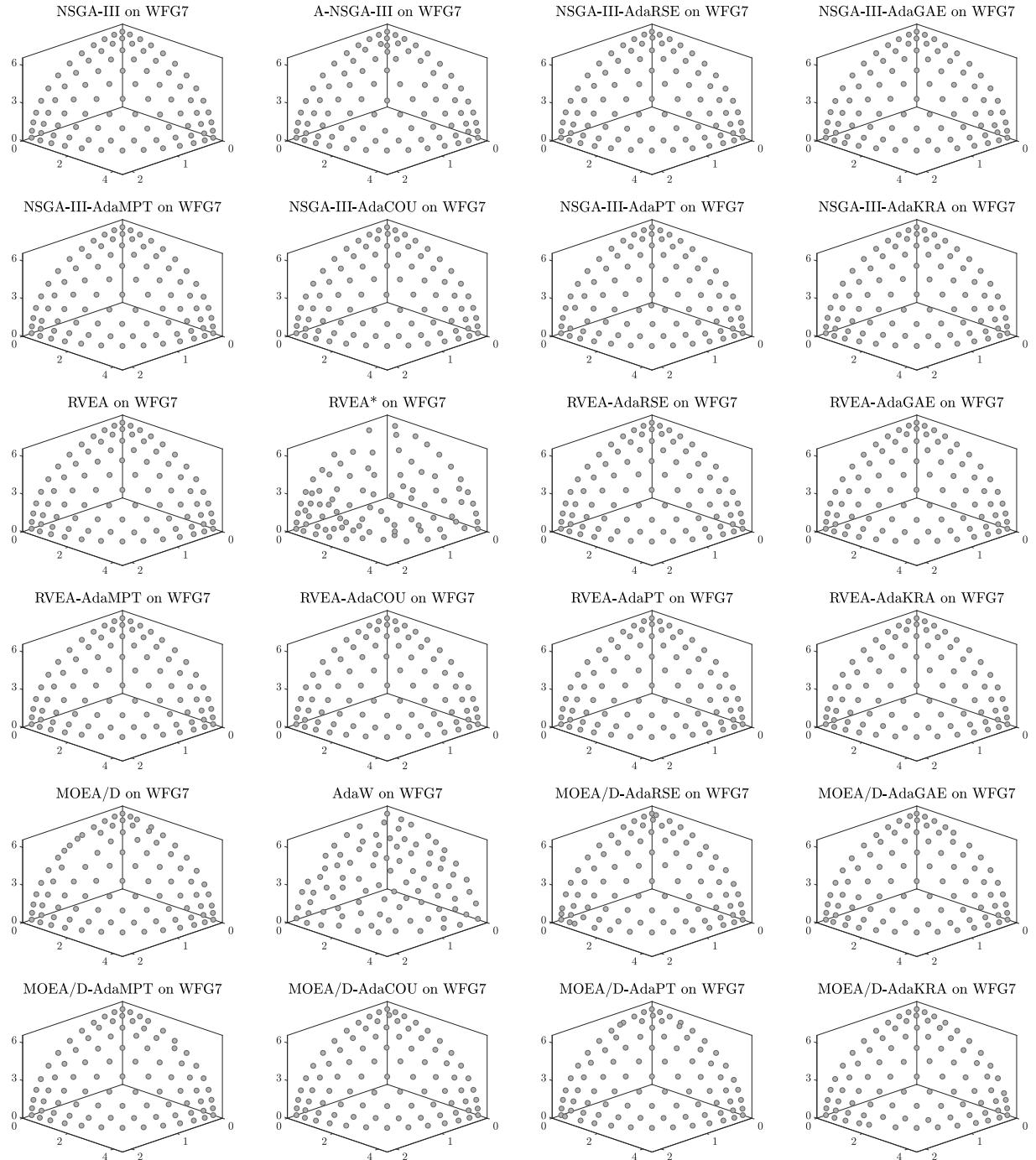


Figure 42: Final populations with the median HV value among 30 independent runs of MOEAs using the NSGA-III, RVEA, and MOEA/D frameworks on WFG7 with 3 objective functions.

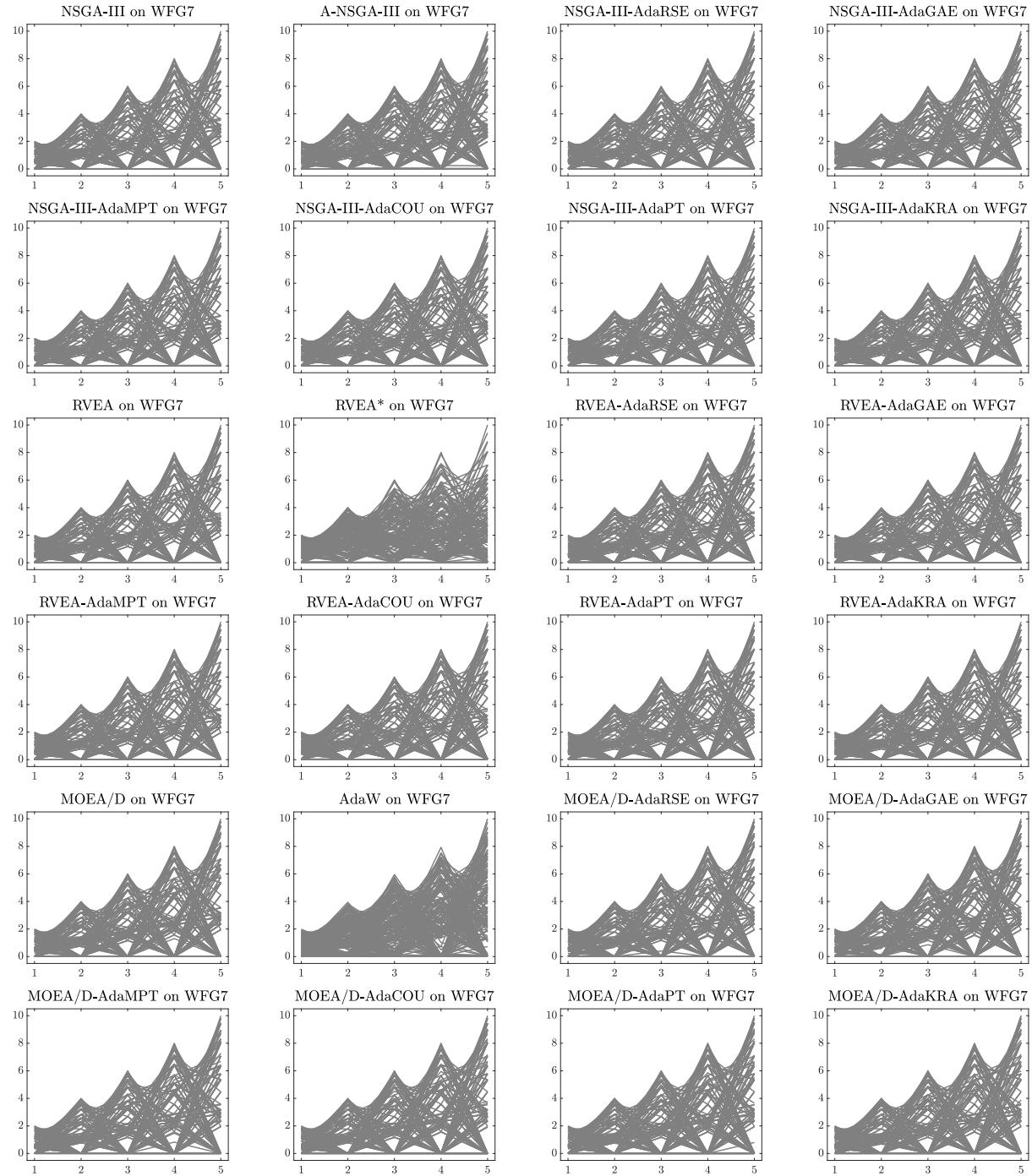


Figure 43: Final populations with the median HV value among 30 independent runs of MOEAs using the NSGA-III, RVEA, and MOEA/D frameworks on WFG7 with 5 objective functions.

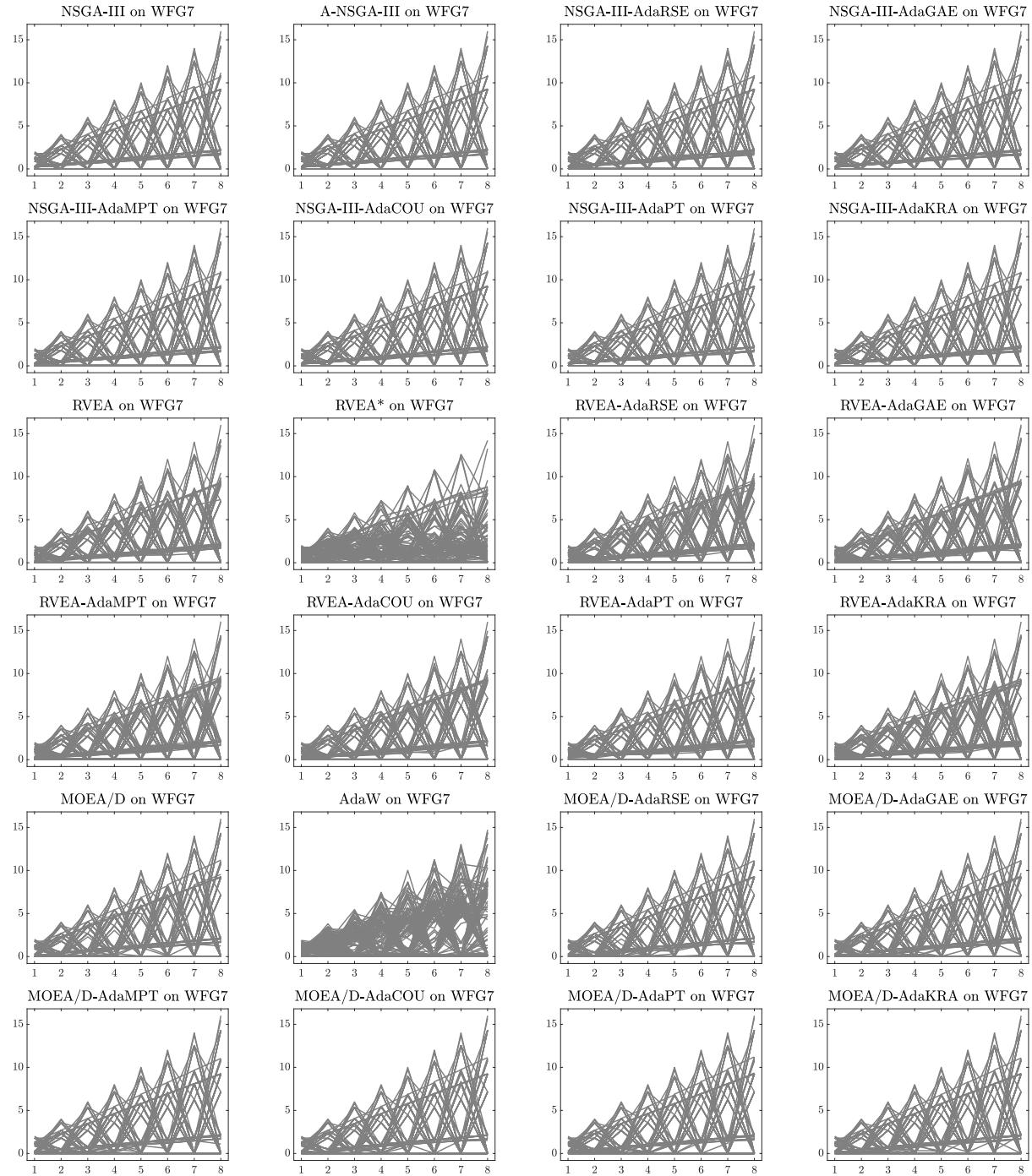


Figure 44: Final populations with the median HV value among 30 independent runs of MOEAs using the NSGA-III, RVEA, and MOEA/D frameworks on WFG7 with 8 objective functions.

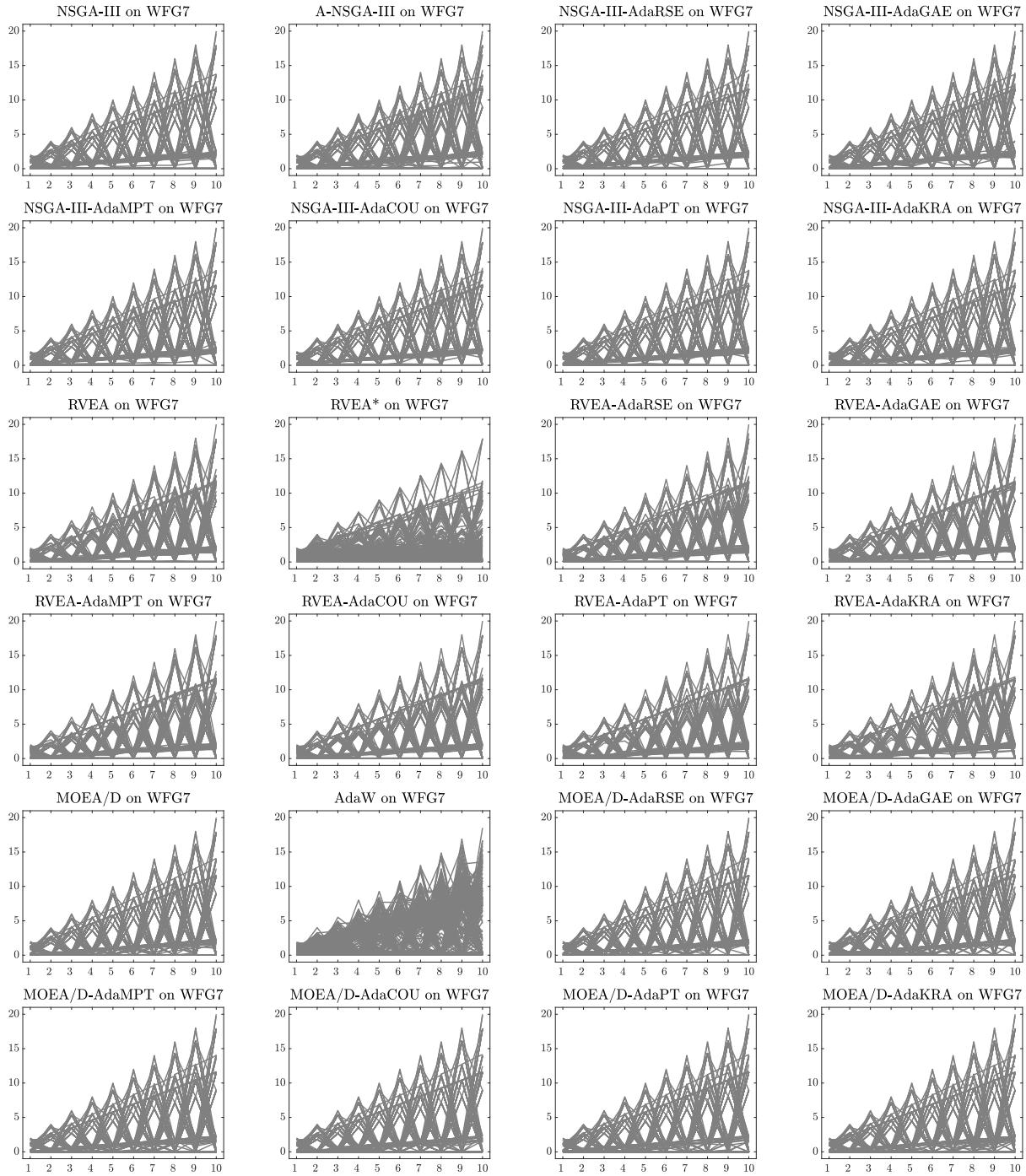


Figure 45: Final populations with the median HV value among 30 independent runs of MOEAs using the NSGA-III, RVEA, and MOEA/D frameworks on WFG7 with 10 objective functions.

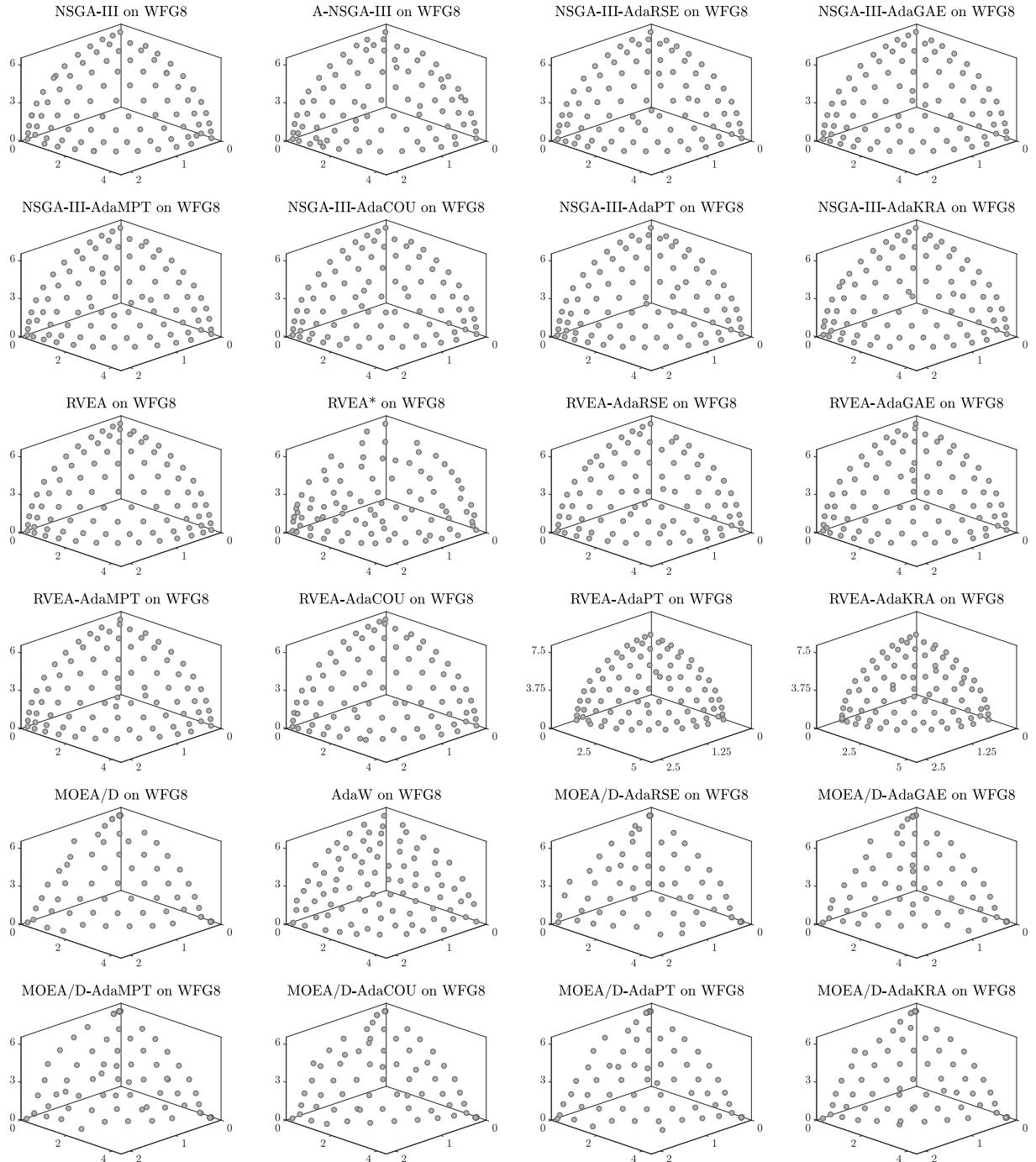


Figure 46: Final populations with the median HV value among 30 independent runs of MOEAs using the NSGA-III, RVEA, and MOEA/D frameworks on WFG8 with 3 objective functions.

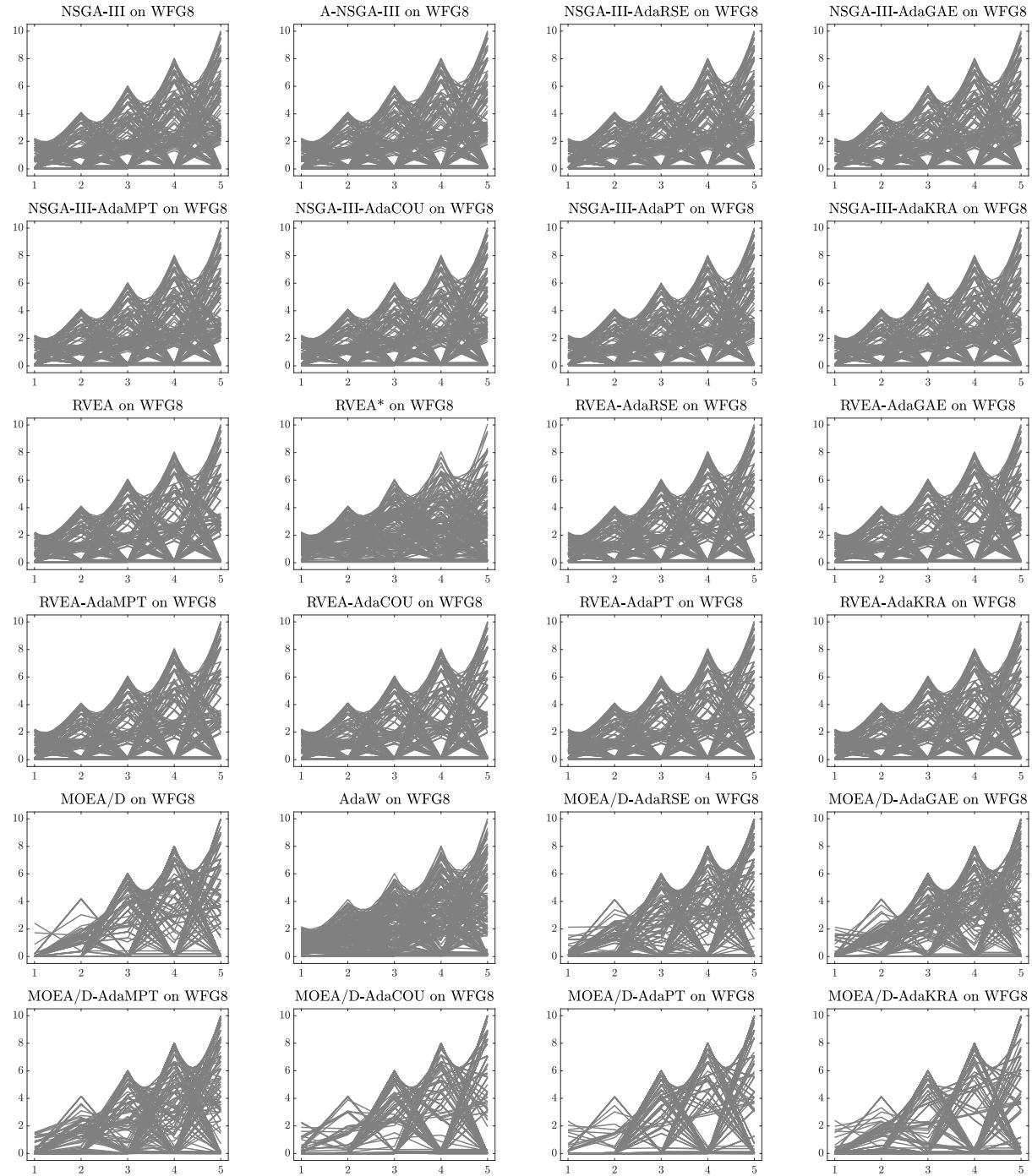


Figure 47: Final populations with the median HV value among 30 independent runs of MOEAs using the NSGA-III, RVEA, and MOEA/D frameworks on WFG8 with 5 objective functions.

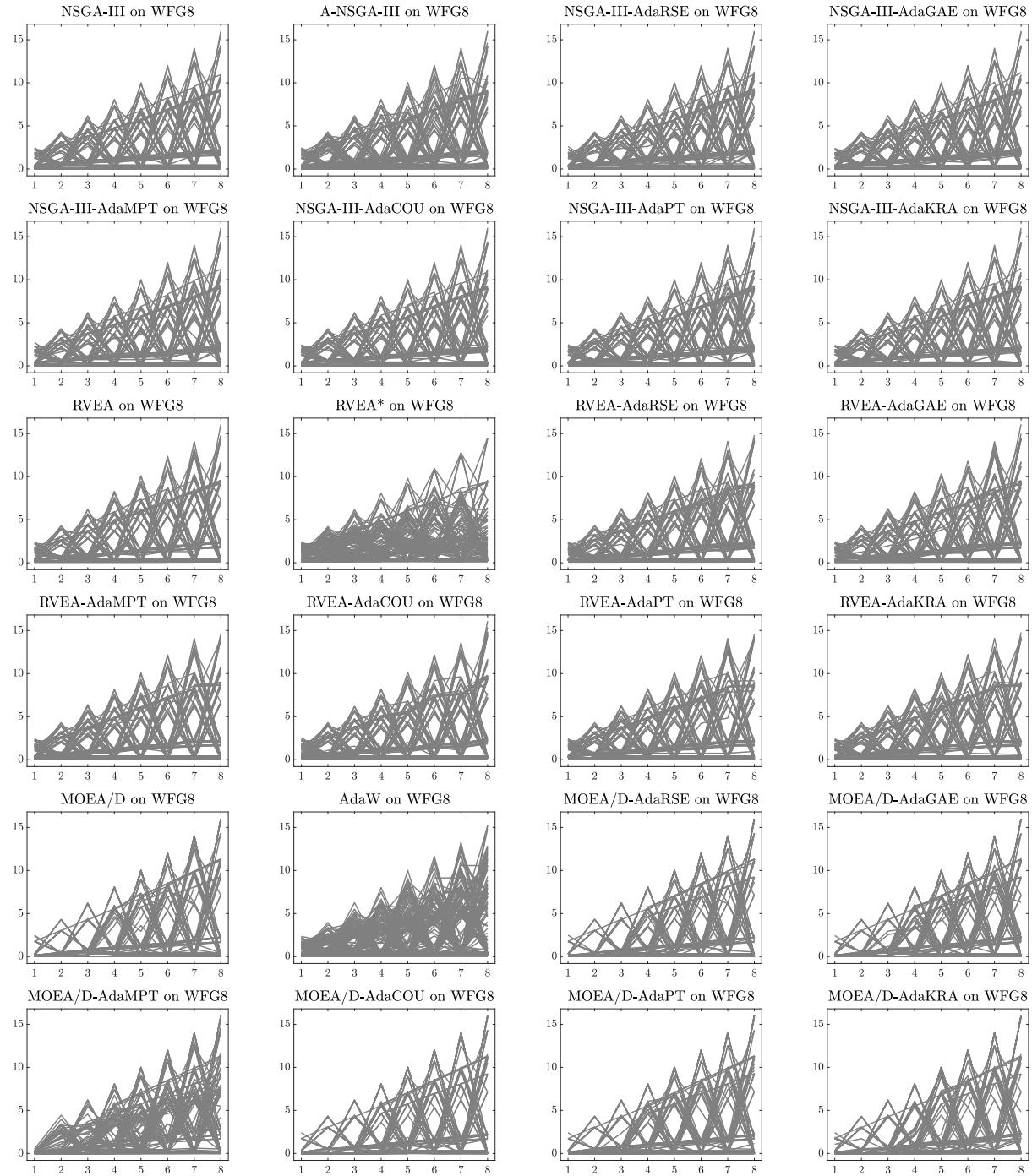


Figure 48: Final populations with the median HV value among 30 independent runs of MOEAs using the NSGA-III, RVEA, and MOEA/D frameworks on WFG8 with 8 objective functions.

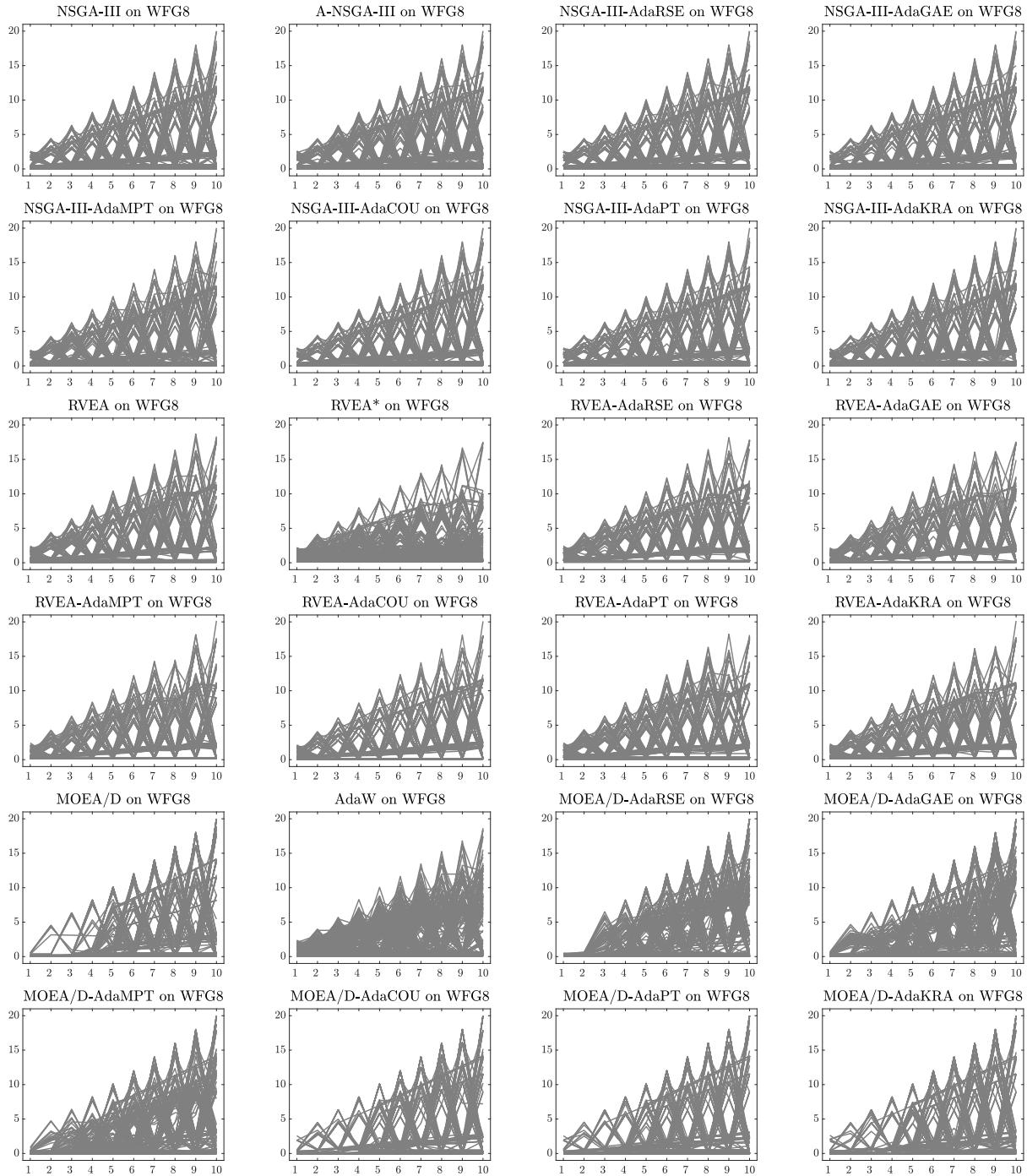


Figure 49: Final populations with the median HV value among 30 independent runs of MOEAs using the NSGA-III, RVEA, and MOEA/D frameworks on WFG8 with 10 objective functions.

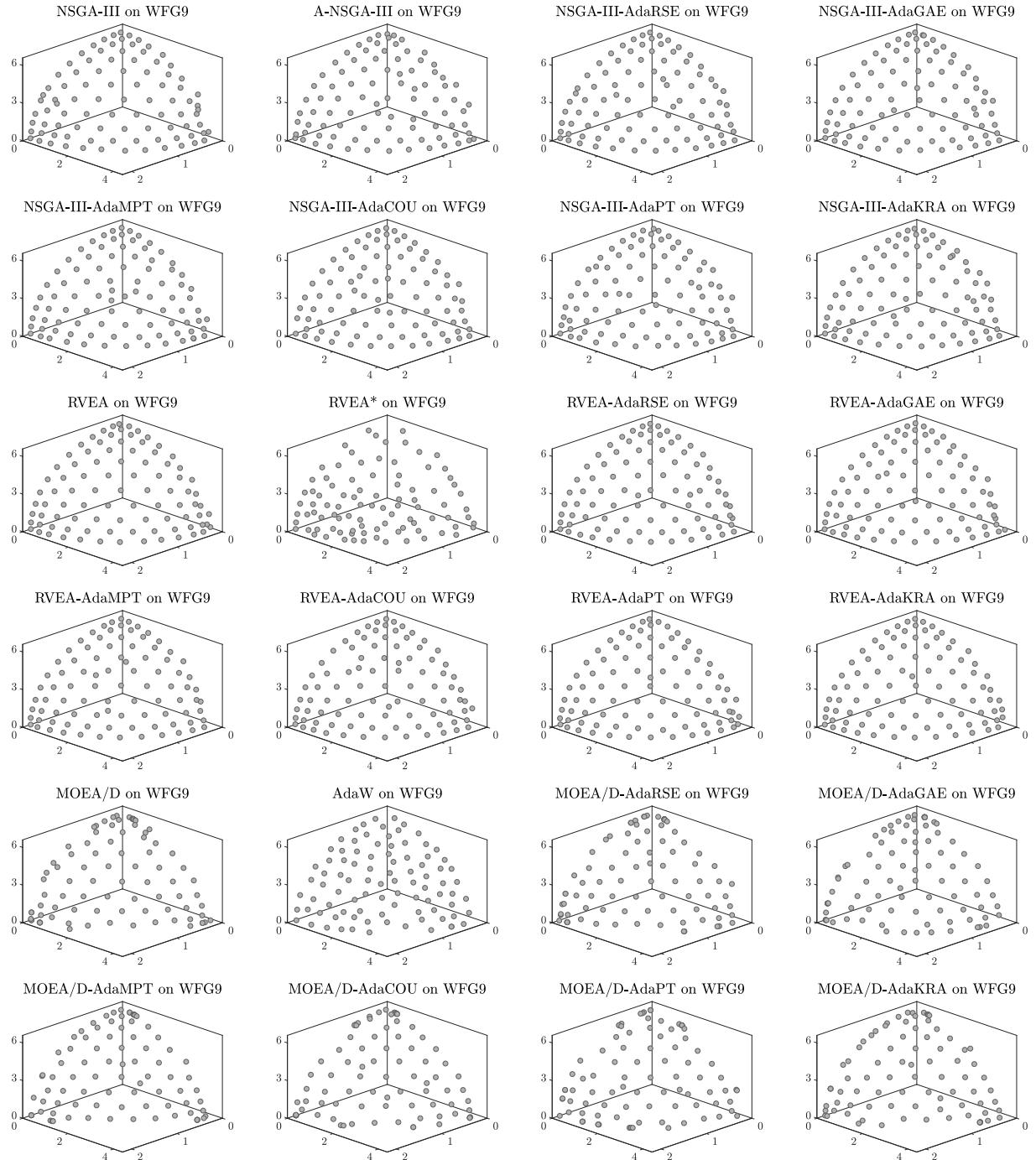


Figure 50: Final populations with the median HV value among 30 independent runs of MOEAs using the NSGA-III, RVEA, and MOEA/D frameworks on WFG9 with 3 objective functions.

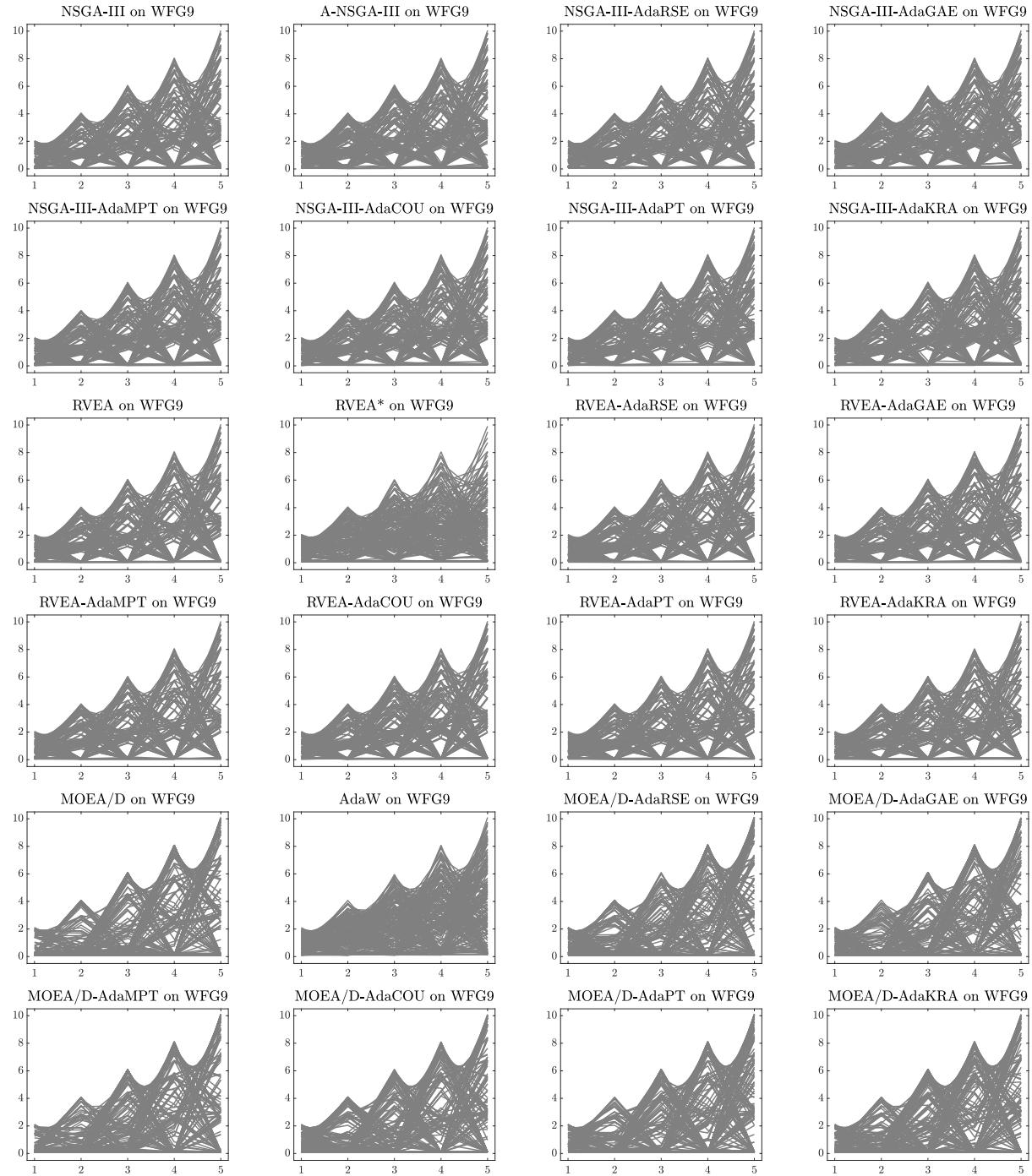


Figure 51: Final populations with the median HV value among 30 independent runs of MOEAs using the NSGA-III, RVEA, and MOEA/D frameworks on WFG9 with 5 objective functions.

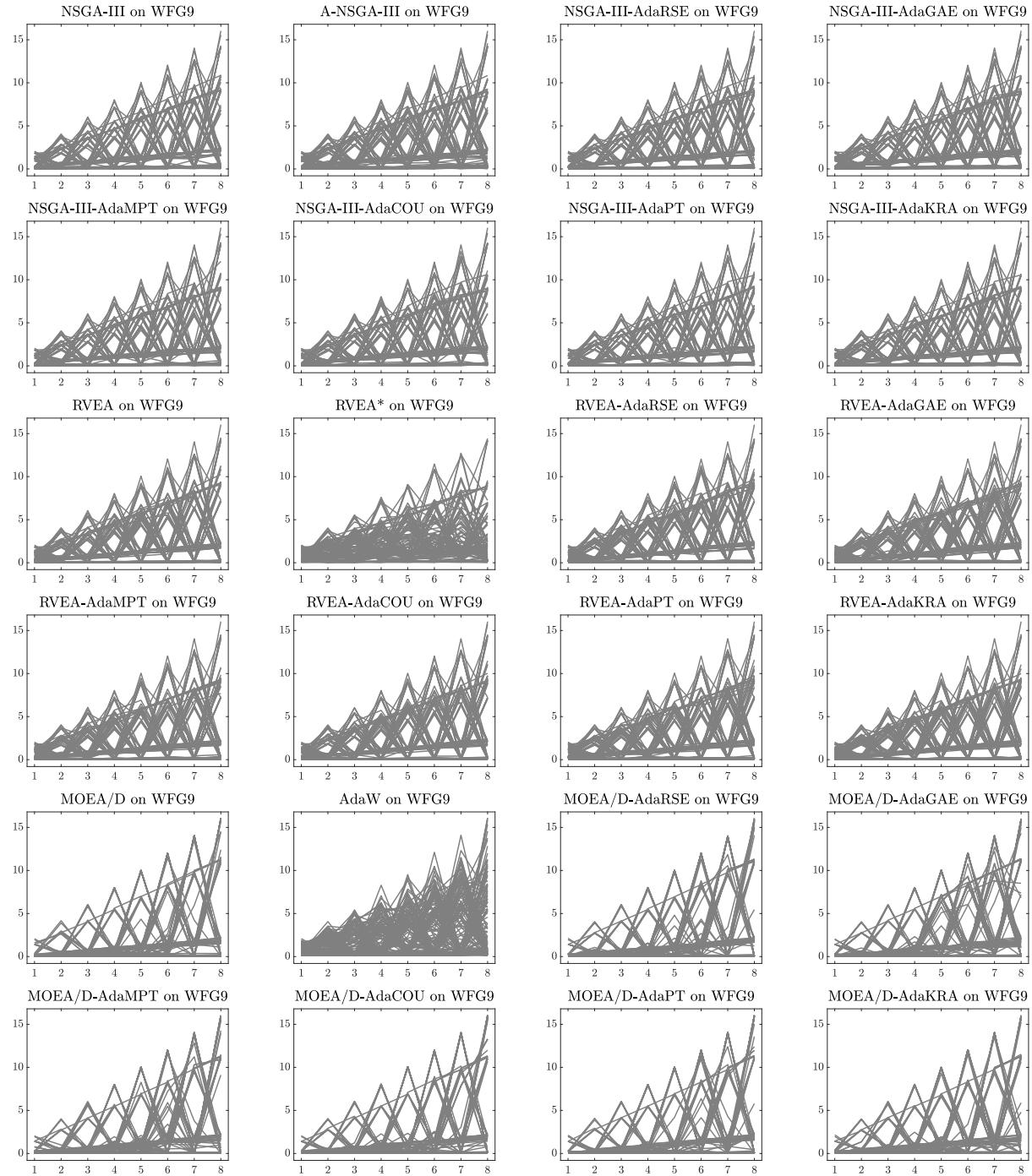


Figure 52: Final populations with the median HV value among 30 independent runs of MOEAs using the NSGA-III, RVEA, and MOEA/D frameworks on WFG9 with 8 objective functions.

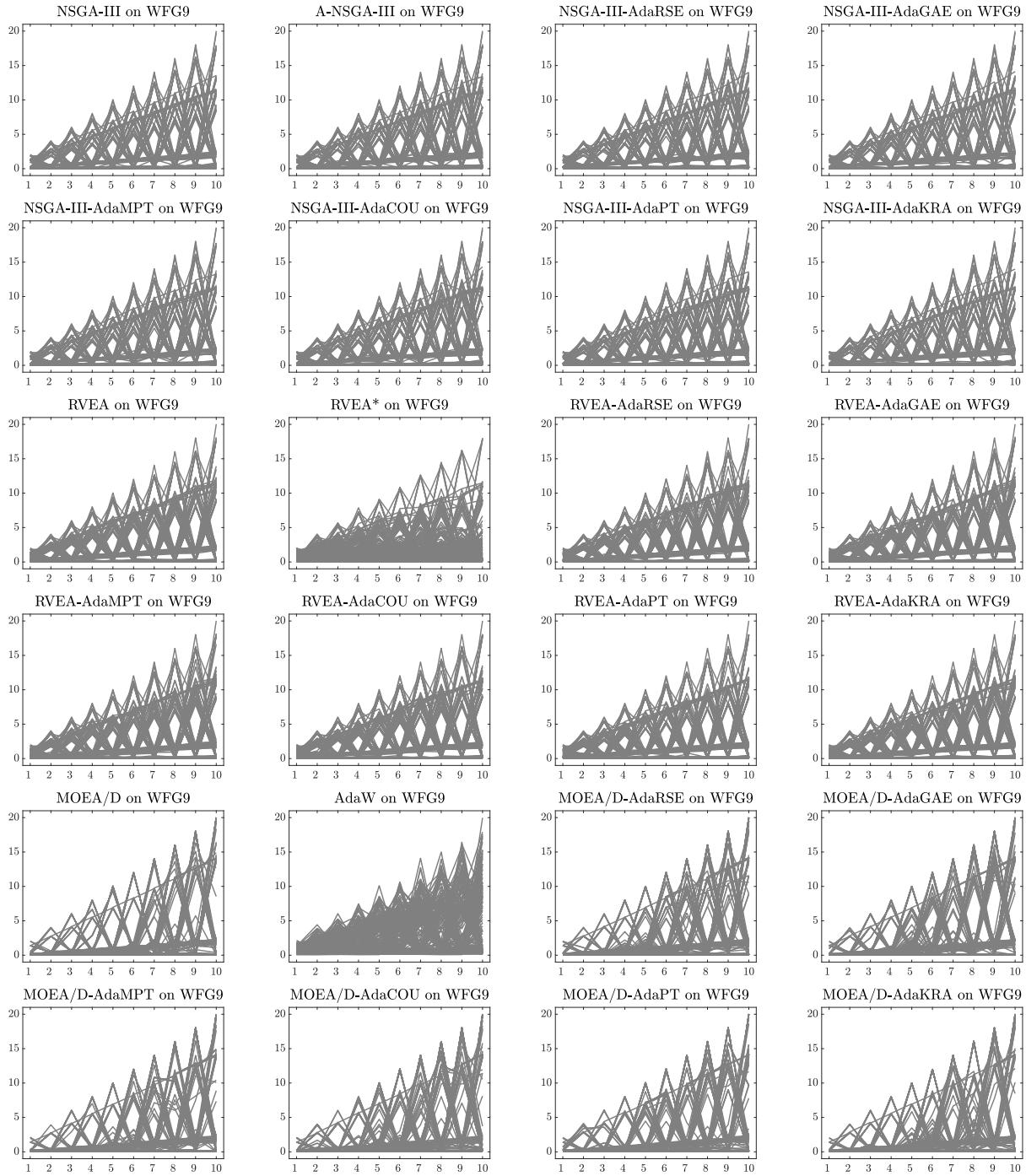


Figure 53: Final populations with the median HV value among 30 independent runs of MOEAs using the NSGA-III, RVEA, and MOEA/D frameworks on WFG9 with 10 objective functions.

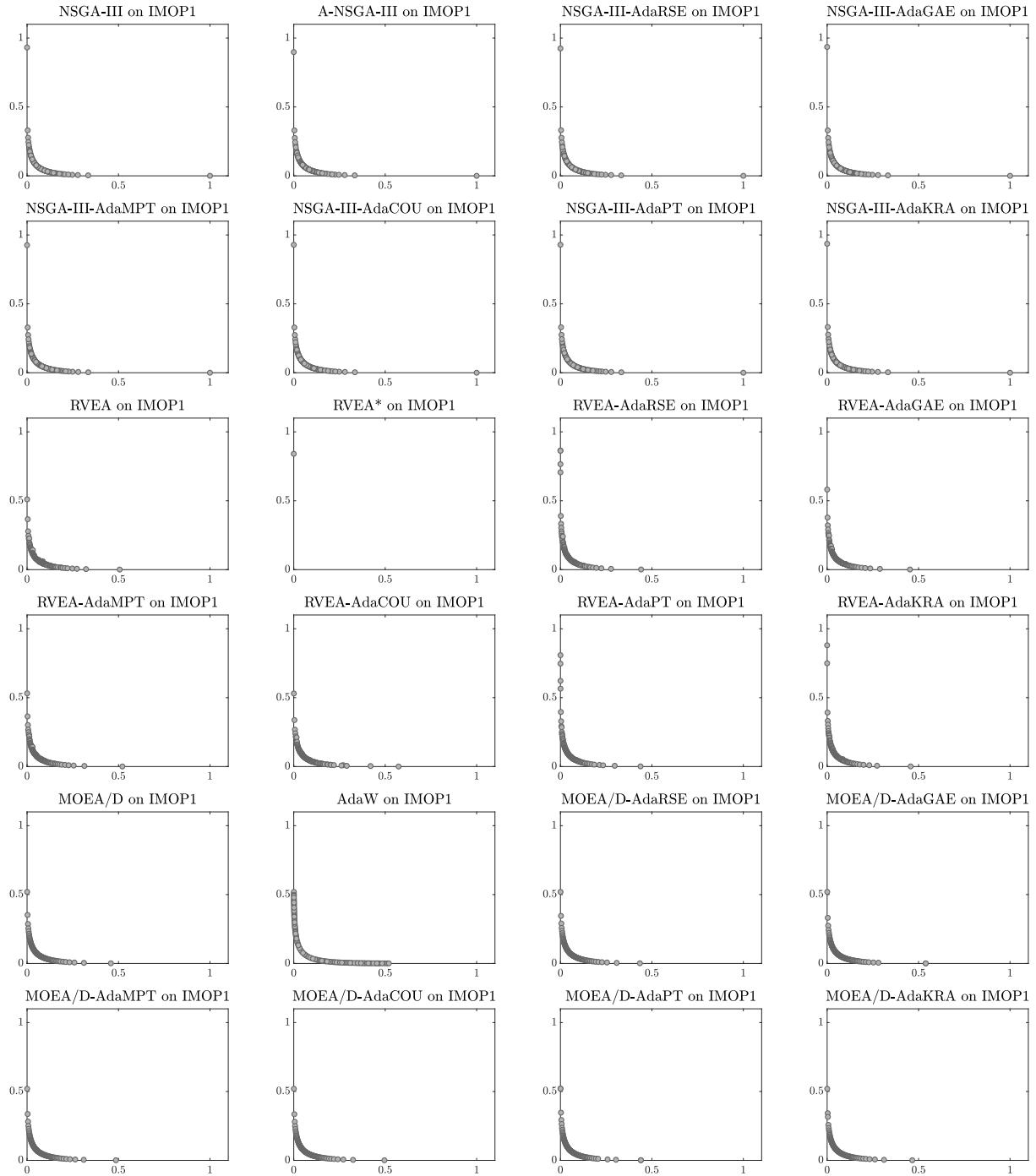


Figure 54: Final populations with the median HV value among 30 independent runs of MOEAs using the NSGA-III, RVEA, and MOEA/D frameworks on IMOP1.

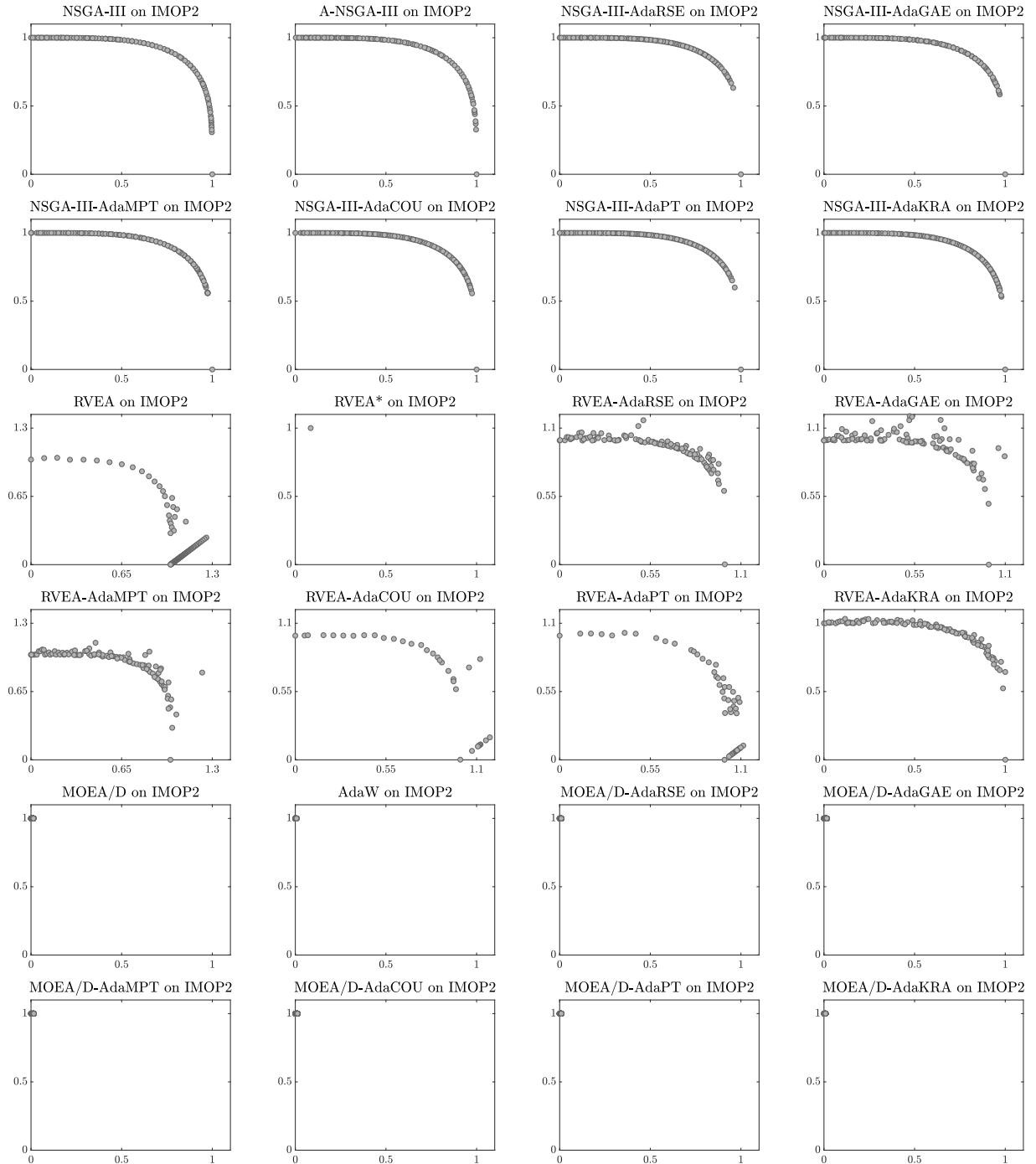


Figure 55: Final populations with the median HV value among 30 independent runs of MOEAs using the NSGA-III, RVEA, and MOEA/D frameworks on IMOP2.

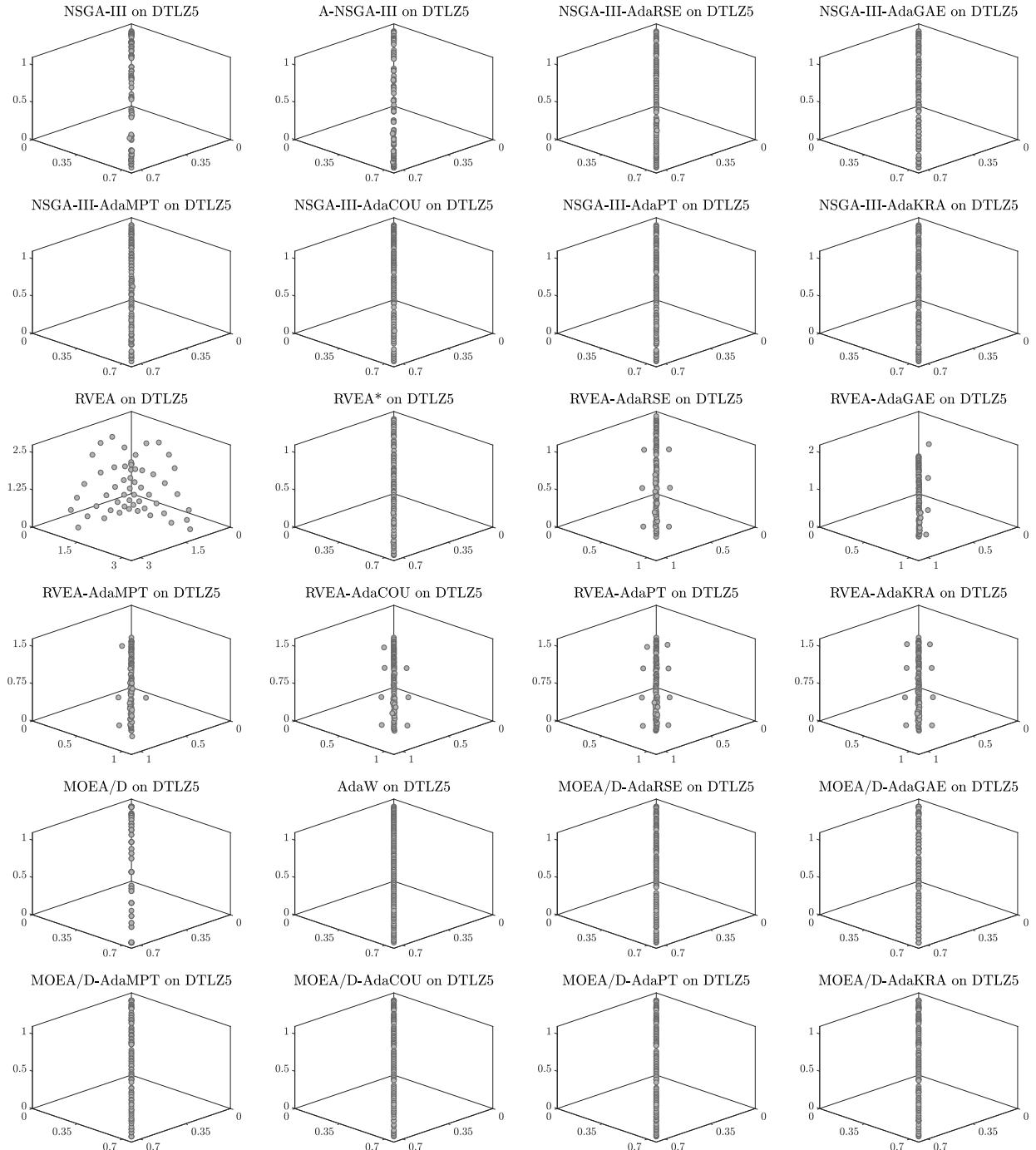


Figure 56: Final populations with the median HV value among 30 independent runs of MOEAs using the NSGA-III, RVEA, and MOEA/D frameworks on DTLZ5 with 3 objective functions.

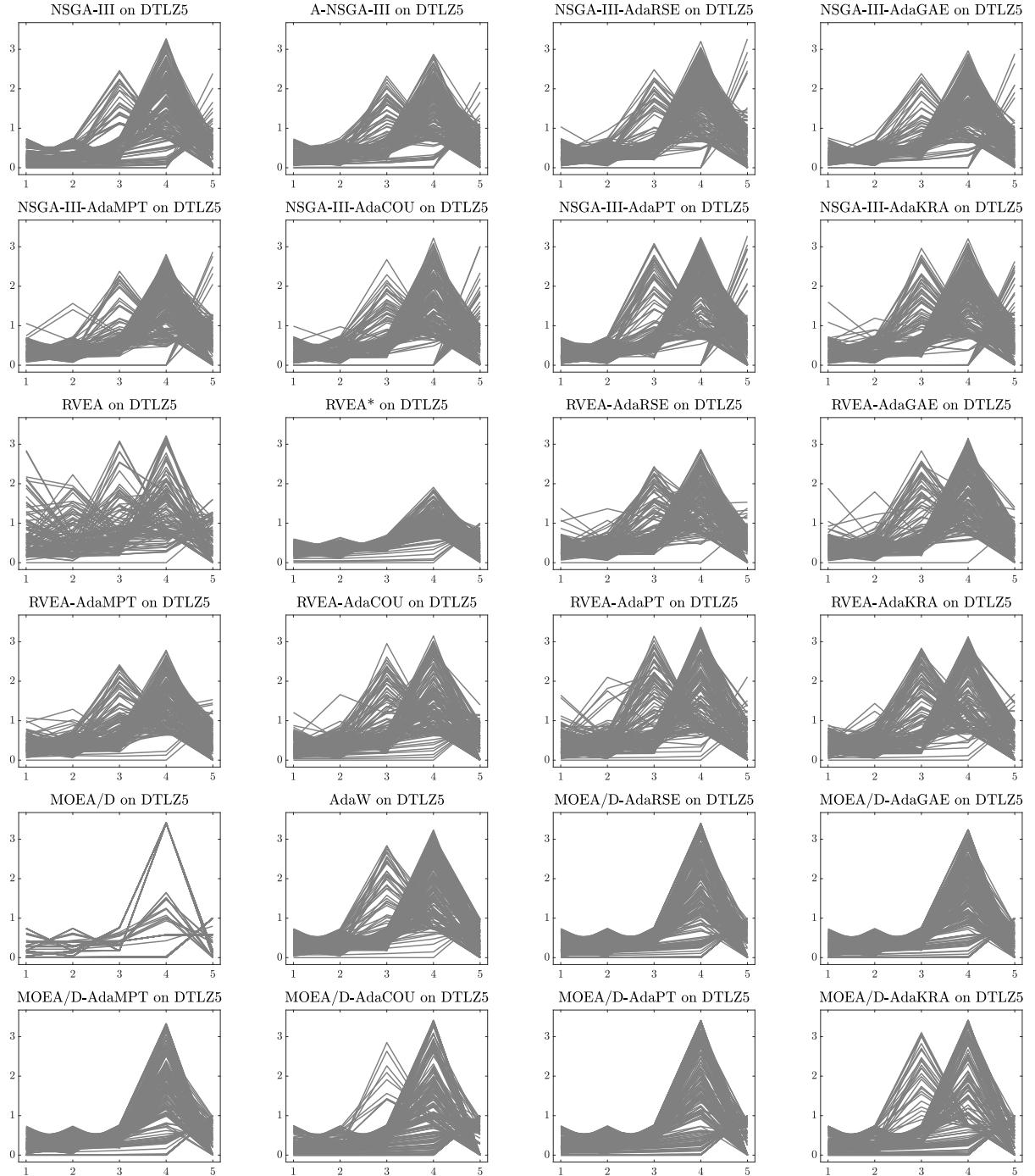


Figure 57: Final populations with the median HV value among 30 independent runs of MOEAs using the NSGA-III, RVEA, and MOEA/D frameworks on DTLZ5 with 5 objective functions.

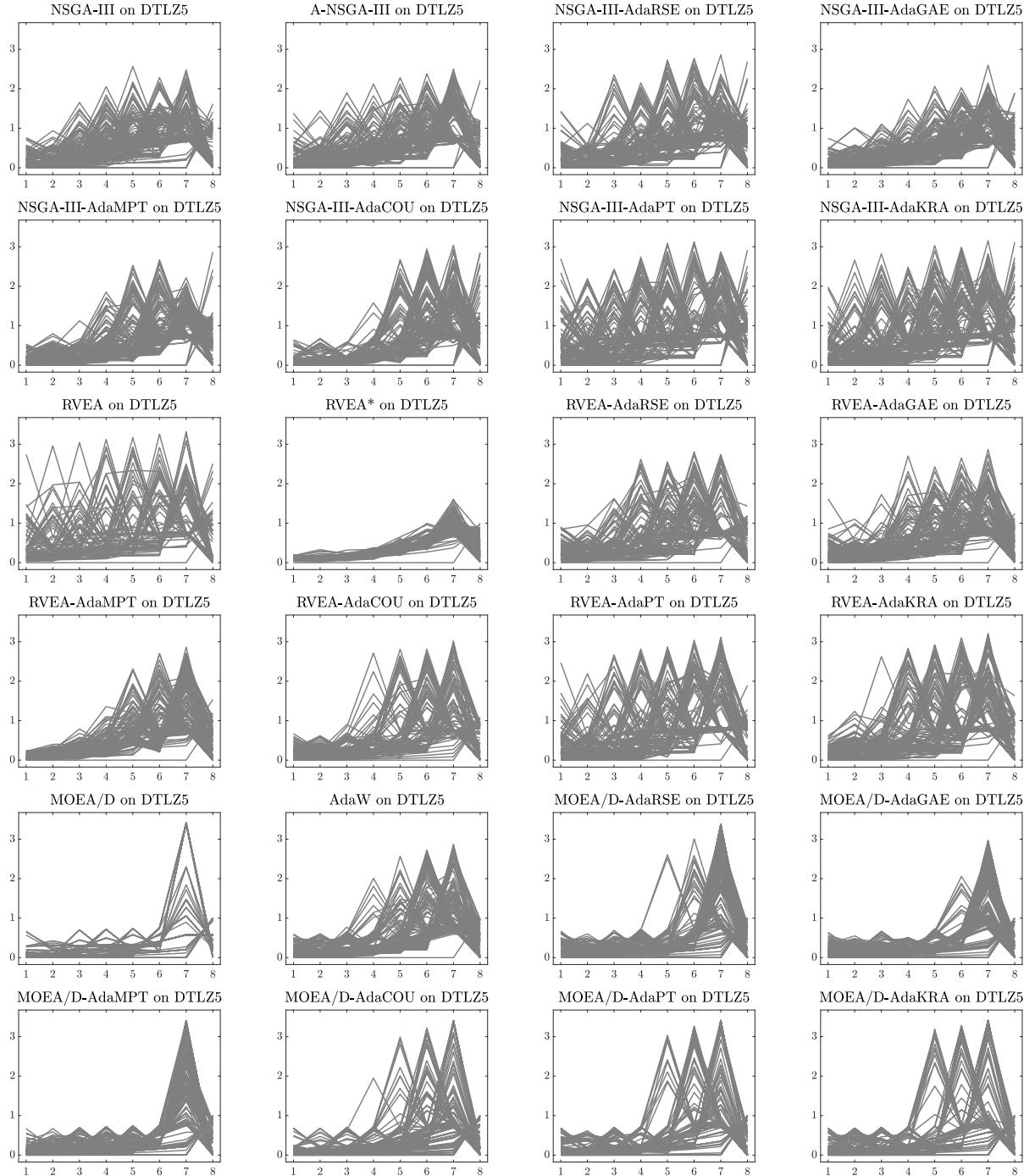


Figure 58: Final populations with the median HV value among 30 independent runs of MOEAs using the NSGA-III, RVEA, and MOEA/D frameworks on DTLZ5 with 8 objective functions.

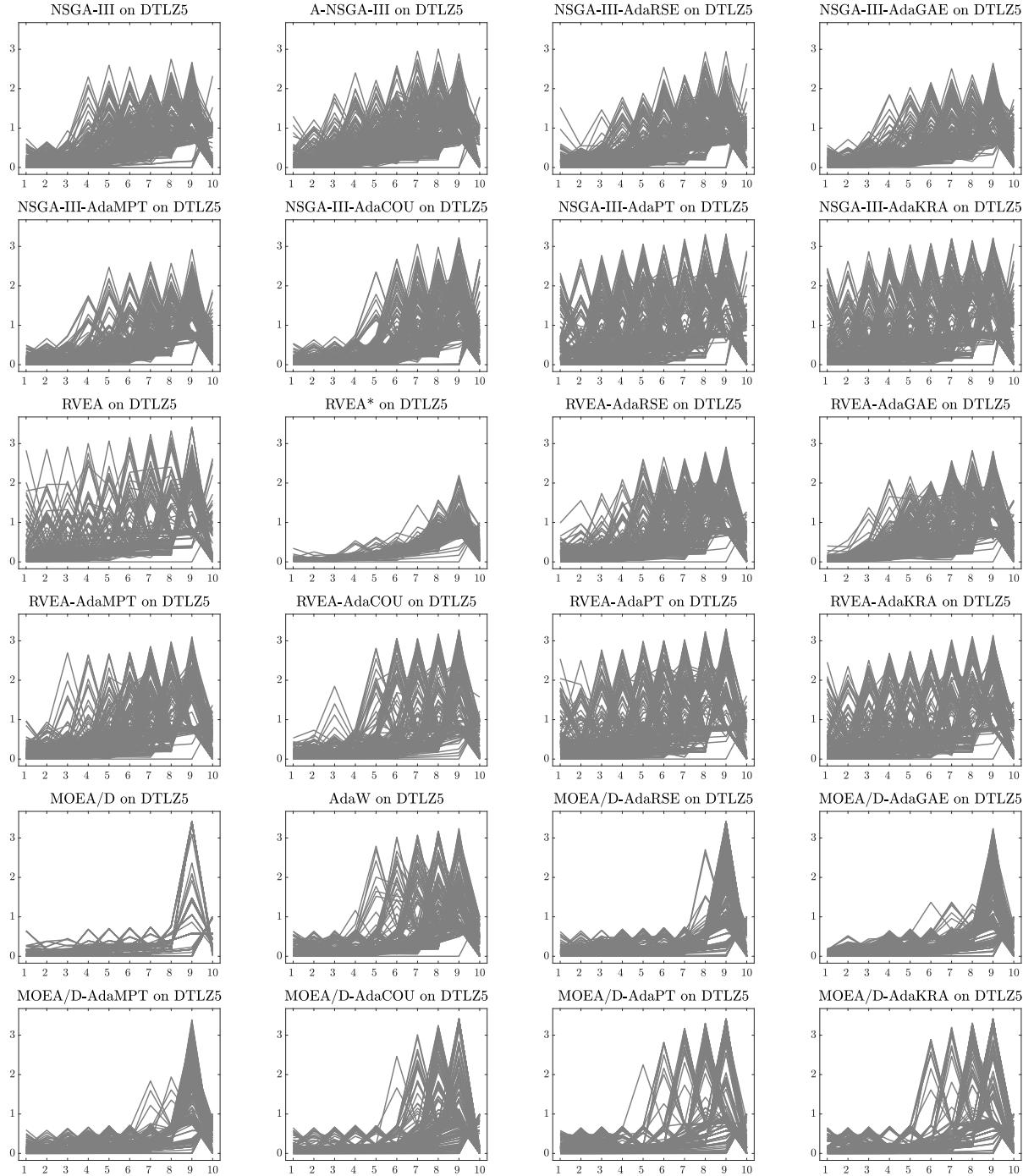


Figure 59: Final populations with the median HV value among 30 independent runs of MOEAs using the NSGA-III, RVEA, and MOEA/D frameworks on DTLZ5 with 10 objective functions.

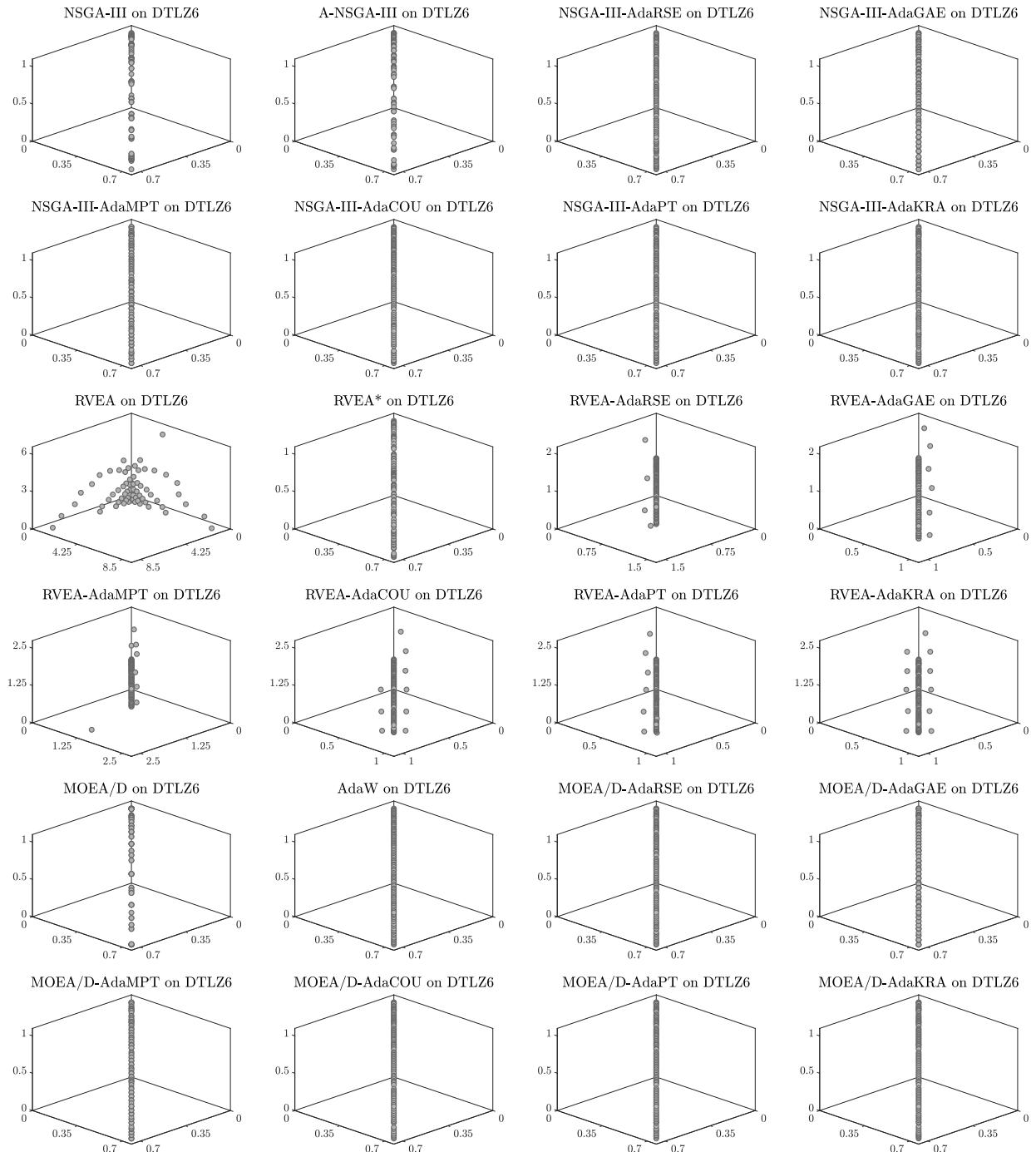


Figure 60: Final populations with the median HV value among 30 independent runs of MOEAs using the NSGA-III, RVEA, and MOEA/D frameworks on DTLZ6 with 3 objective functions.

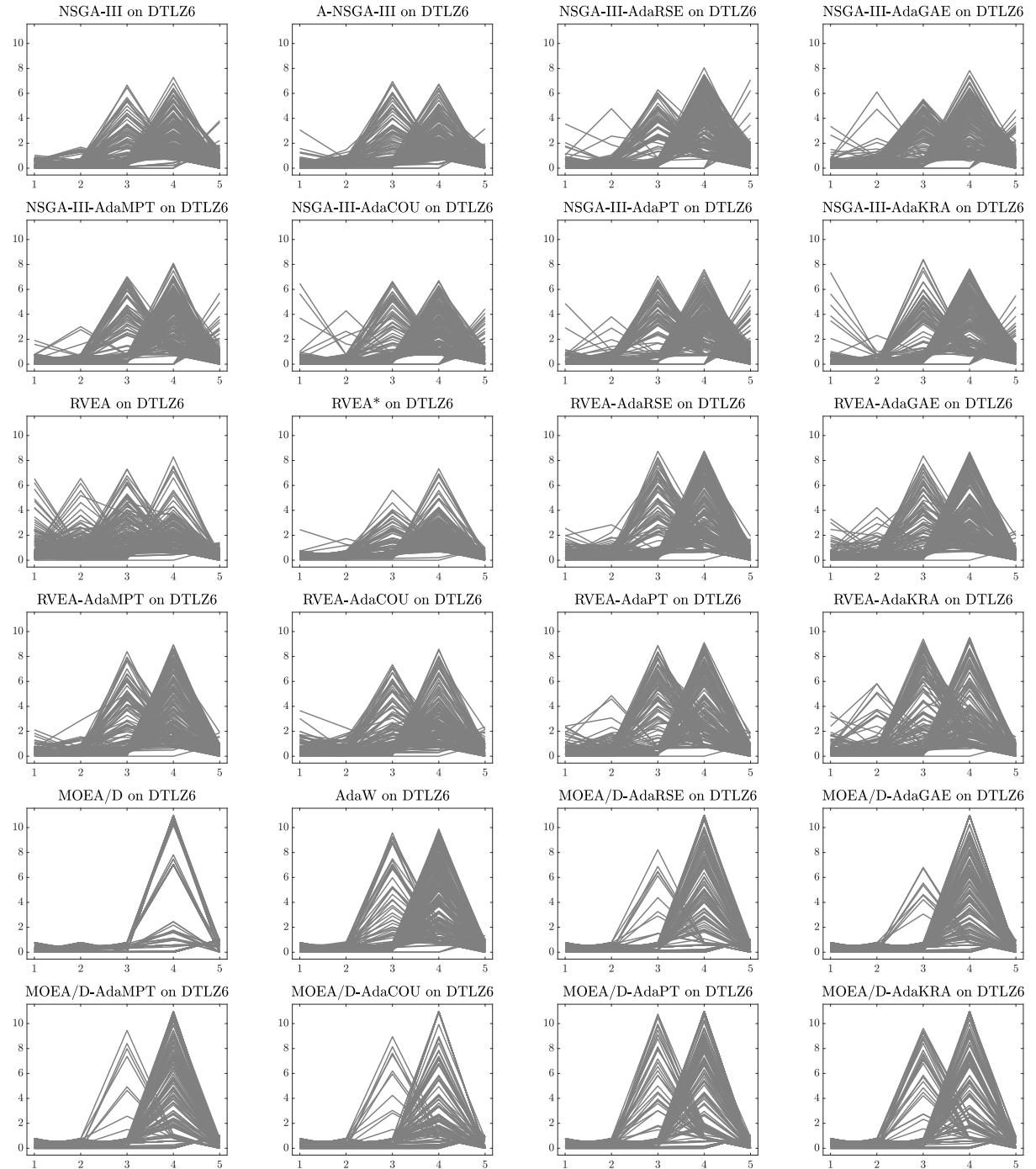


Figure 61: Final populations with the median HV value among 30 independent runs of MOEAs using the NSGA-III, RVEA, and MOEA/D frameworks on DTLZ6 with 5 objective functions.

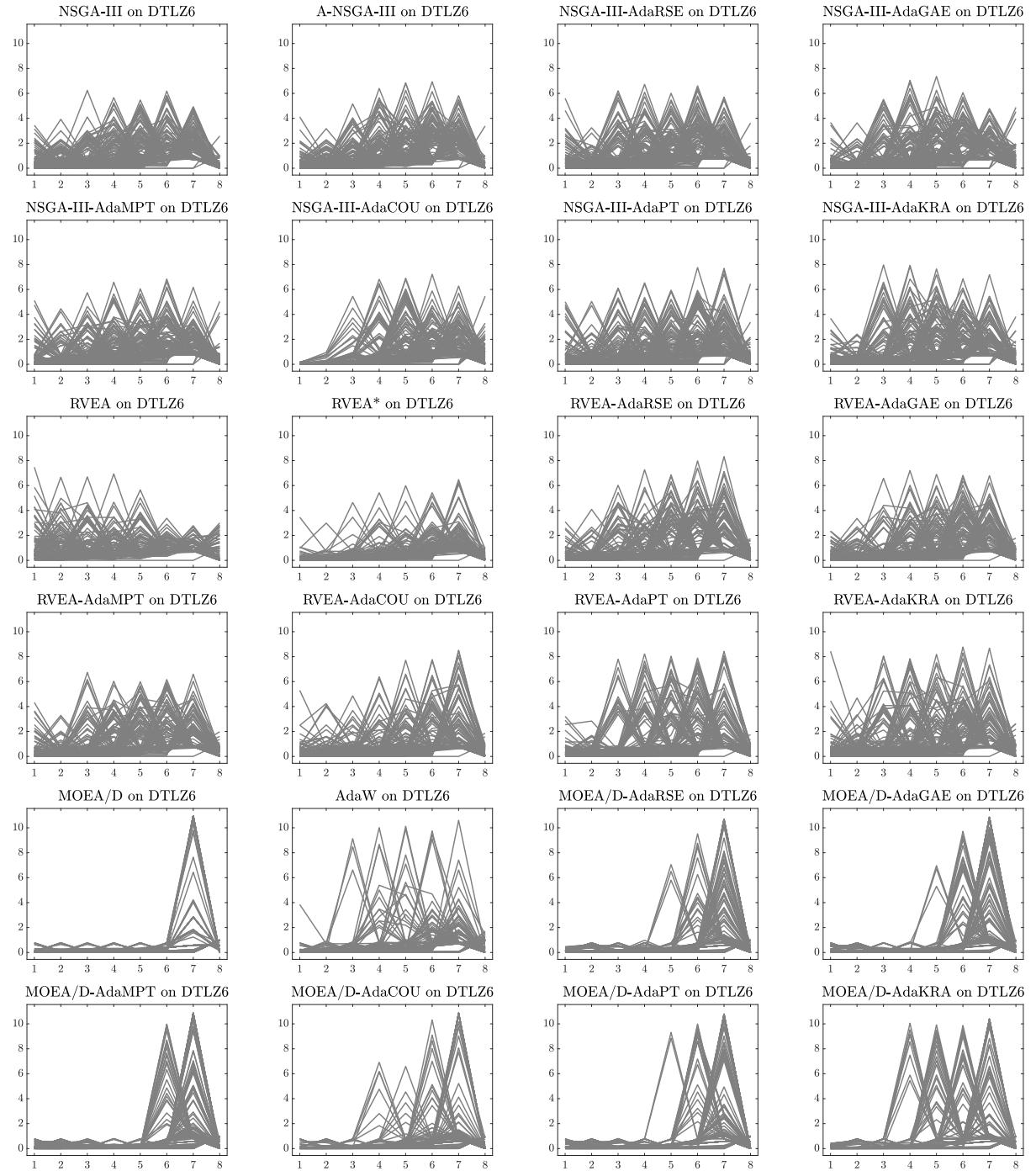


Figure 62: Final populations with the median HV value among 30 independent runs of MOEAs using the NSGA-III, RVEA, and MOEA/D frameworks on DTLZ6 with 8 objective functions.

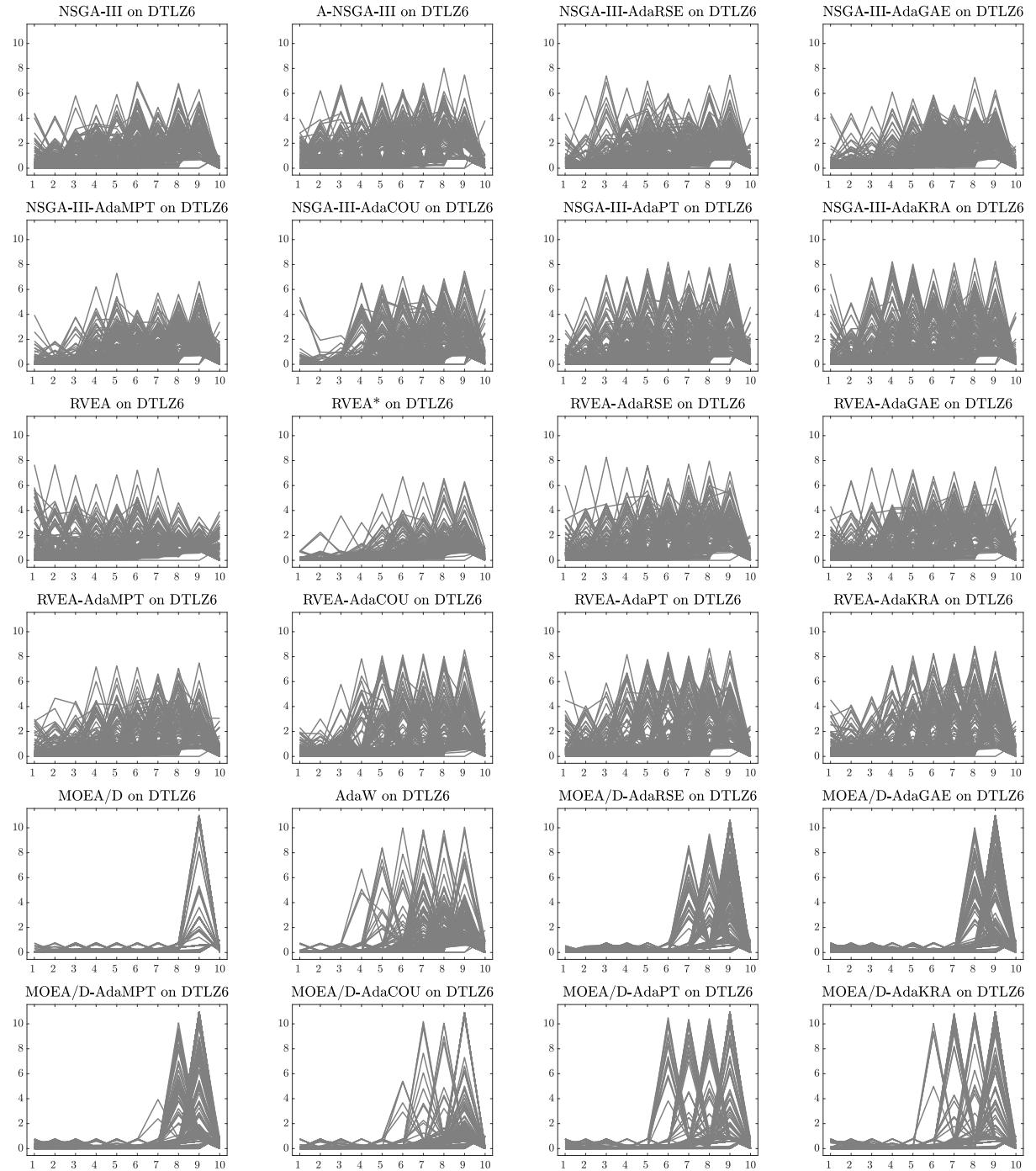


Figure 63: Final populations with the median HV value among 30 independent runs of MOEAs using the NSGA-III, RVEA, and MOEA/D frameworks on DTLZ6 with 10 objective functions.

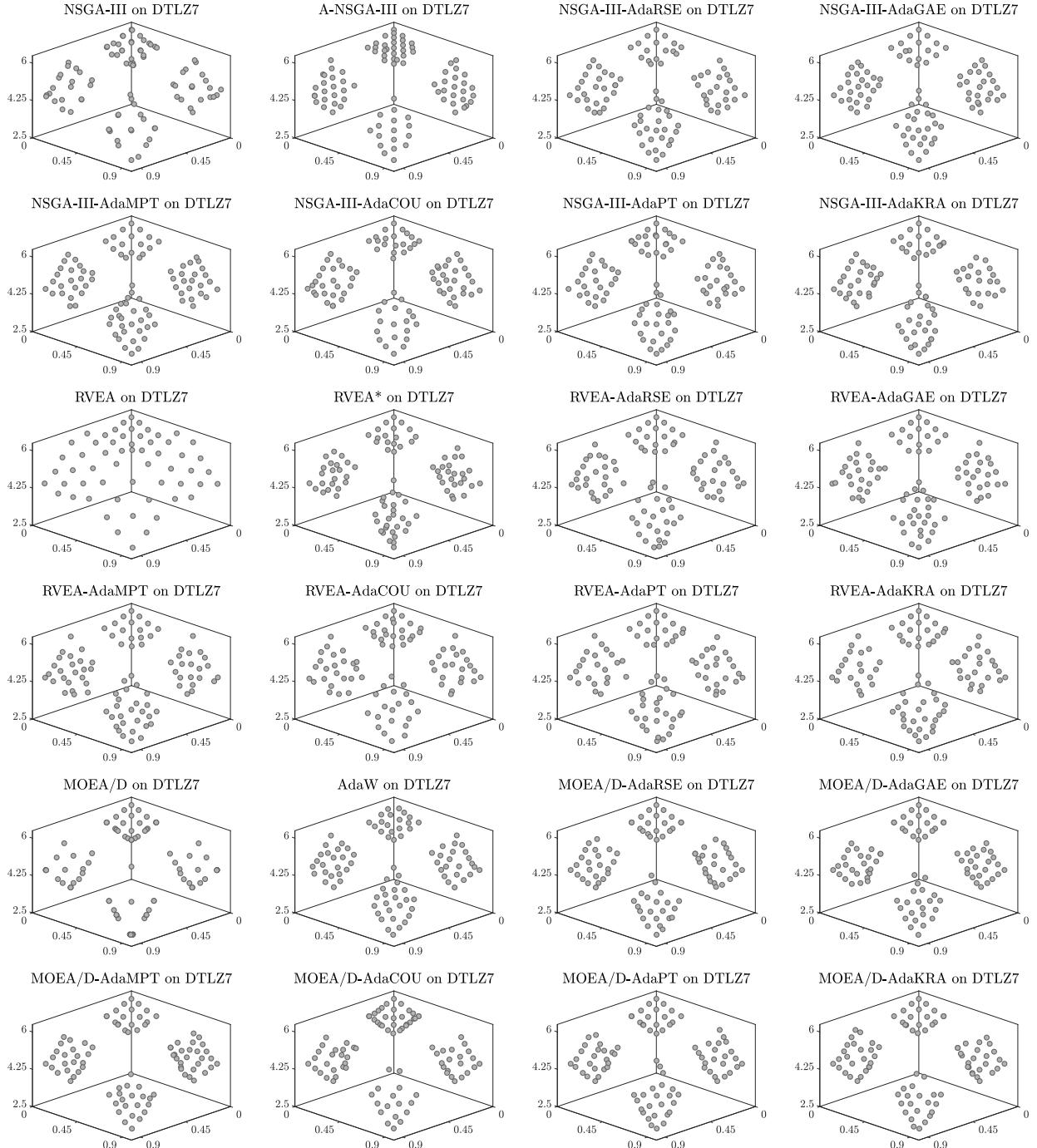


Figure 64: Final populations with the median HV value among 30 independent runs of MOEAs using the NSGA-III, RVEA, and MOEA/D frameworks on DTLZ7 with 3 objective functions.

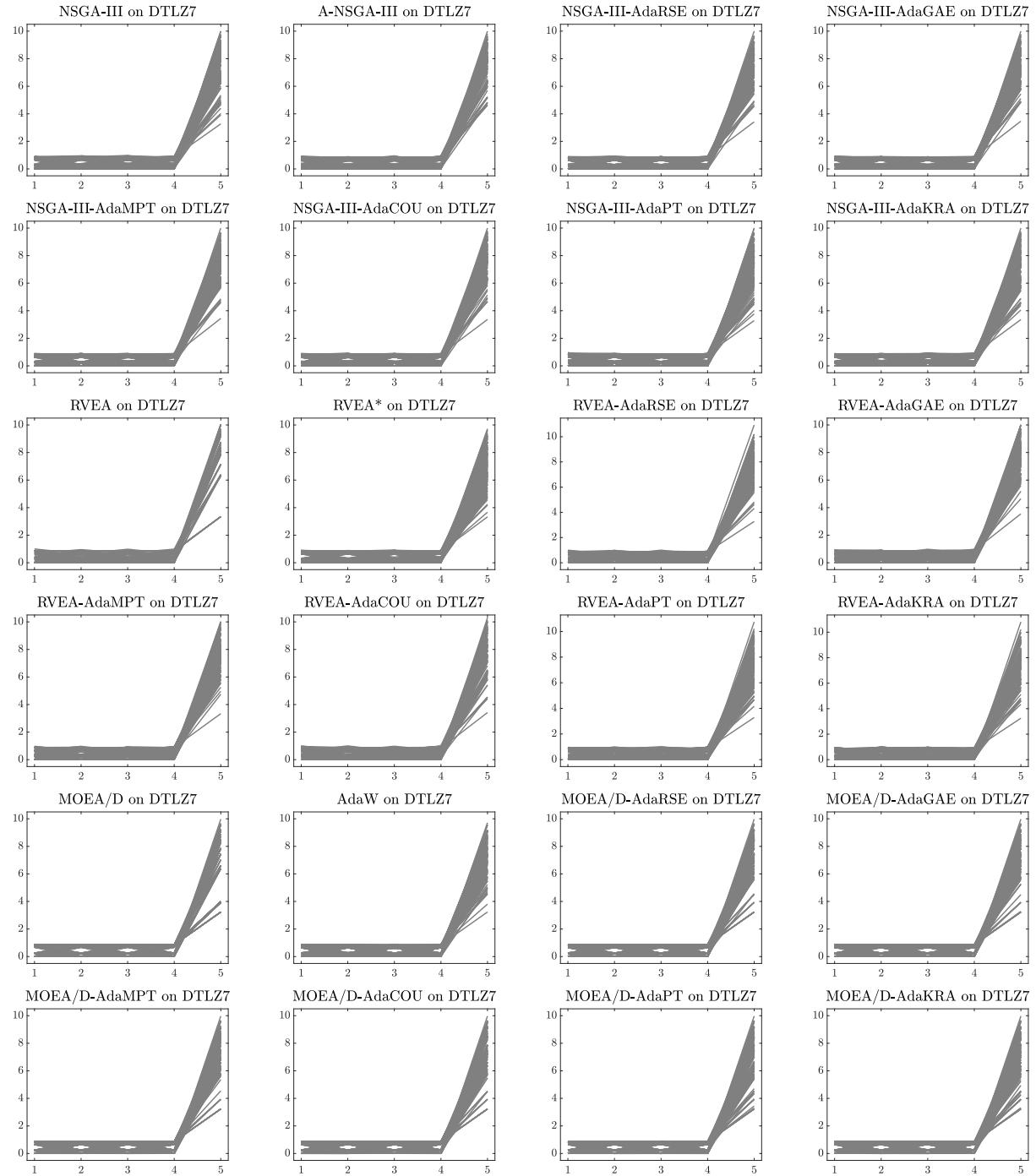


Figure 65: Final populations with the median HV value among 30 independent runs of MOEAs using the NSGA-III, RVEA, and MOEA/D frameworks on DTLZ7 with 5 objective functions.

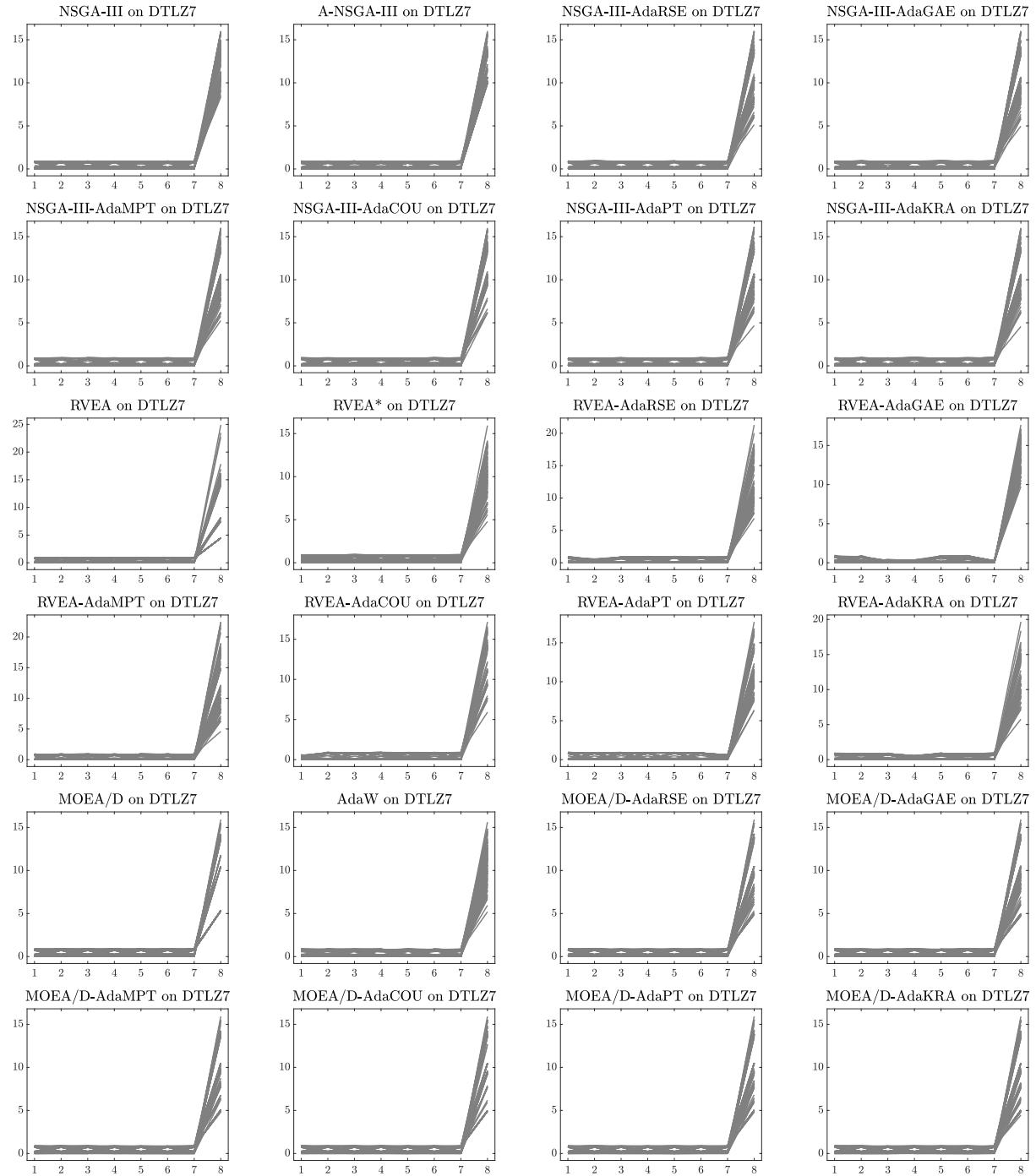


Figure 66: Final populations with the median HV value among 30 independent runs of MOEAs using the NSGA-III, RVEA, and MOEA/D frameworks on DTLZ7 with 8 objective functions.

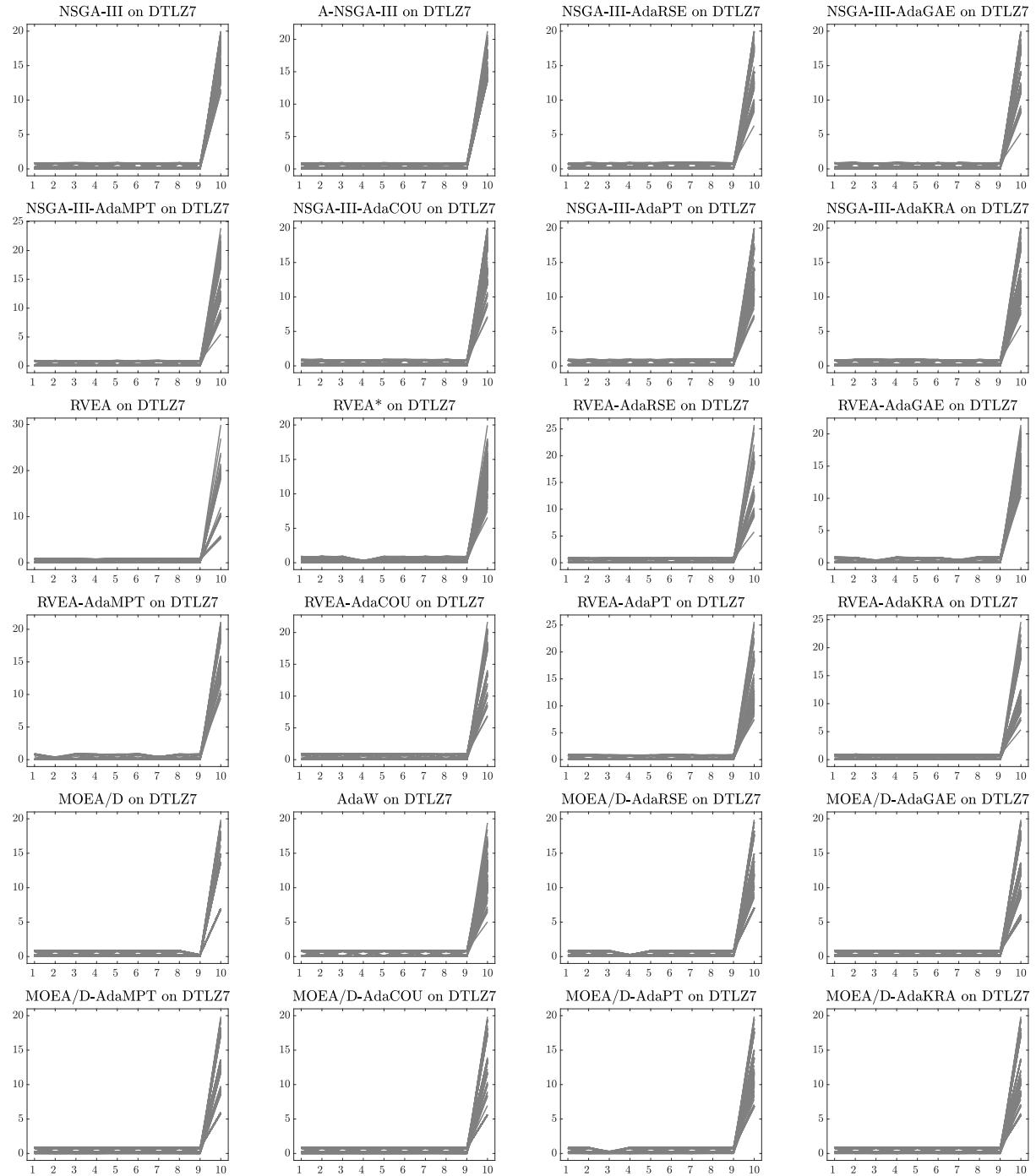


Figure 67: Final populations with the median HV value among 30 independent runs of MOEAs using the NSGA-III, RVEA, and MOEA/D frameworks on DTLZ7 with 10 objective functions.

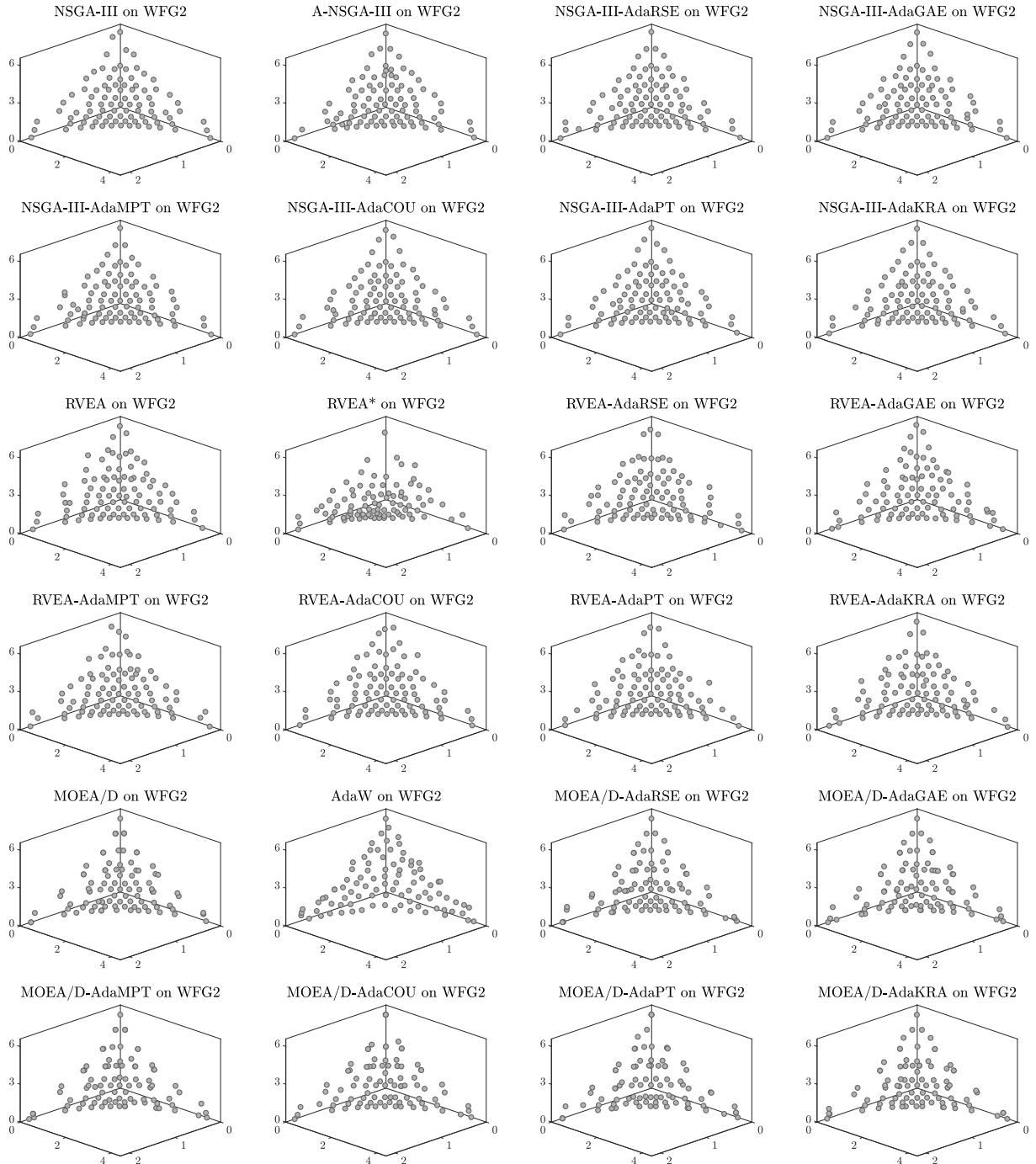


Figure 68: Final populations with the median HV value among 30 independent runs of MOEAs using the NSGA-III, RVEA, and MOEA/D frameworks on WFG2 with 3 objective functions.

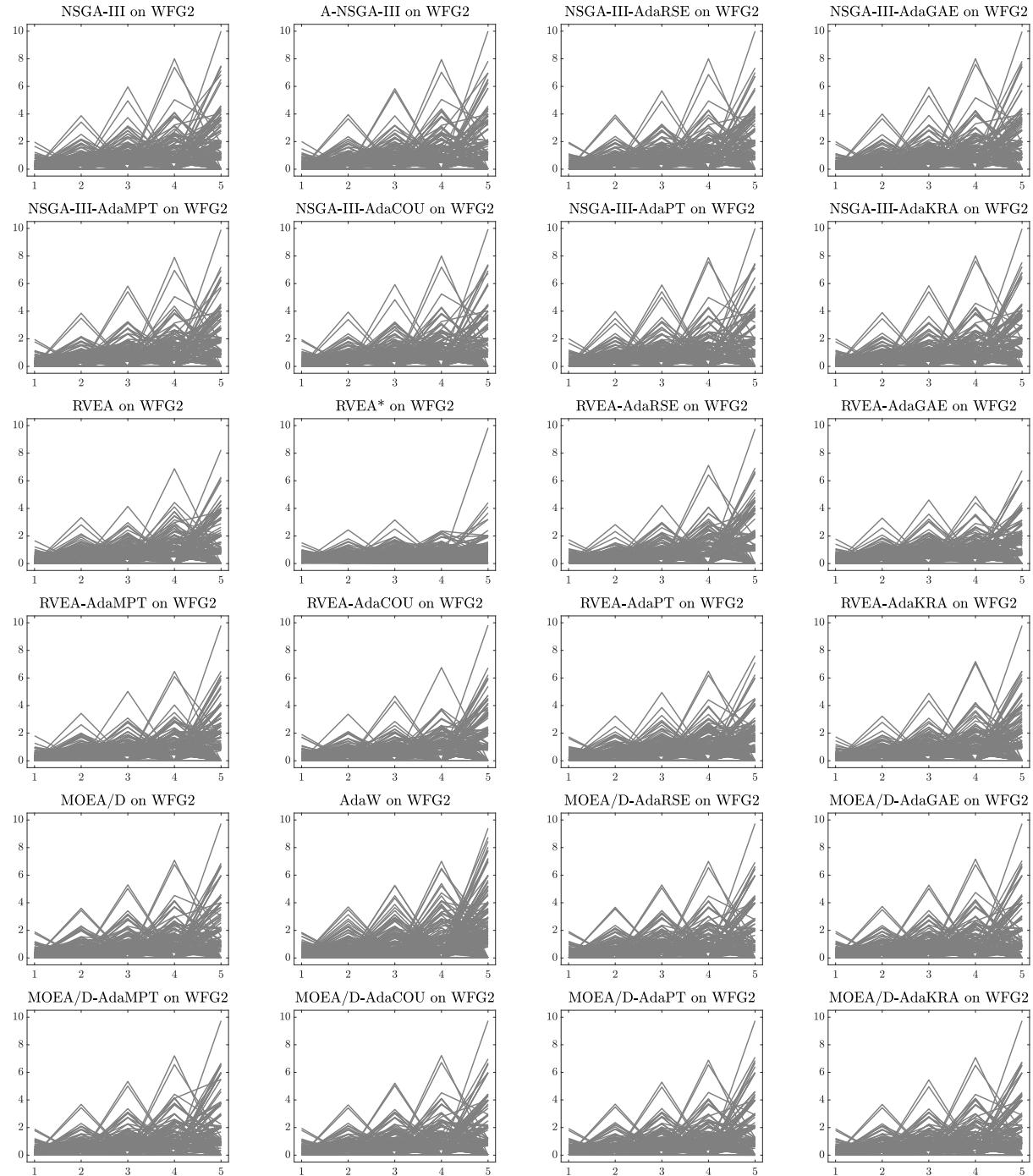


Figure 69: Final populations with the median HV value among 30 independent runs of MOEAs using the NSGA-III, RVEA, and MOEA/D frameworks on WFG2 with 5 objective functions.

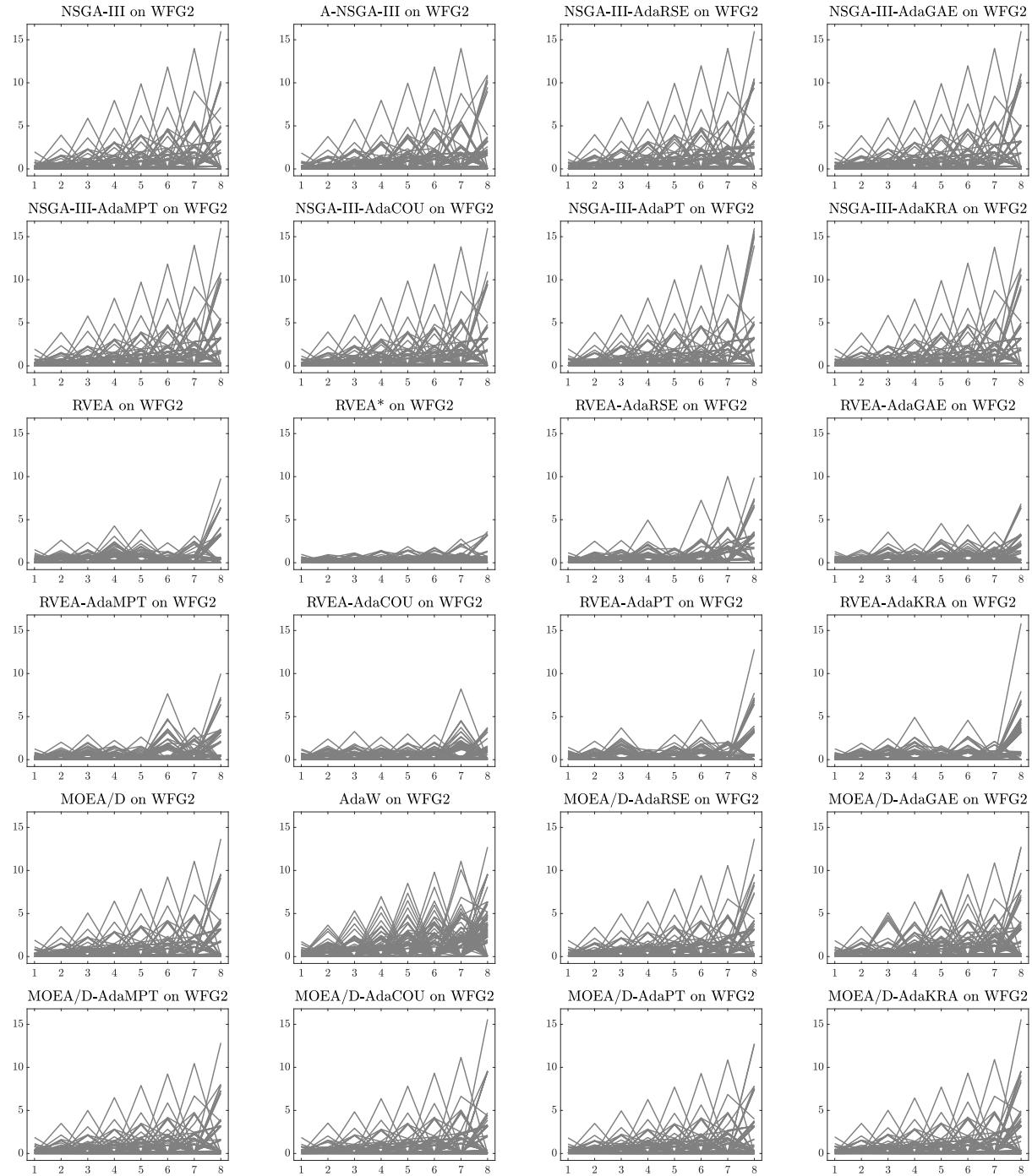


Figure 70: Final populations with the median HV value among 30 independent runs of MOEAs using the NSGA-III, RVEA, and MOEA/D frameworks on WFG2 with 8 objective functions.

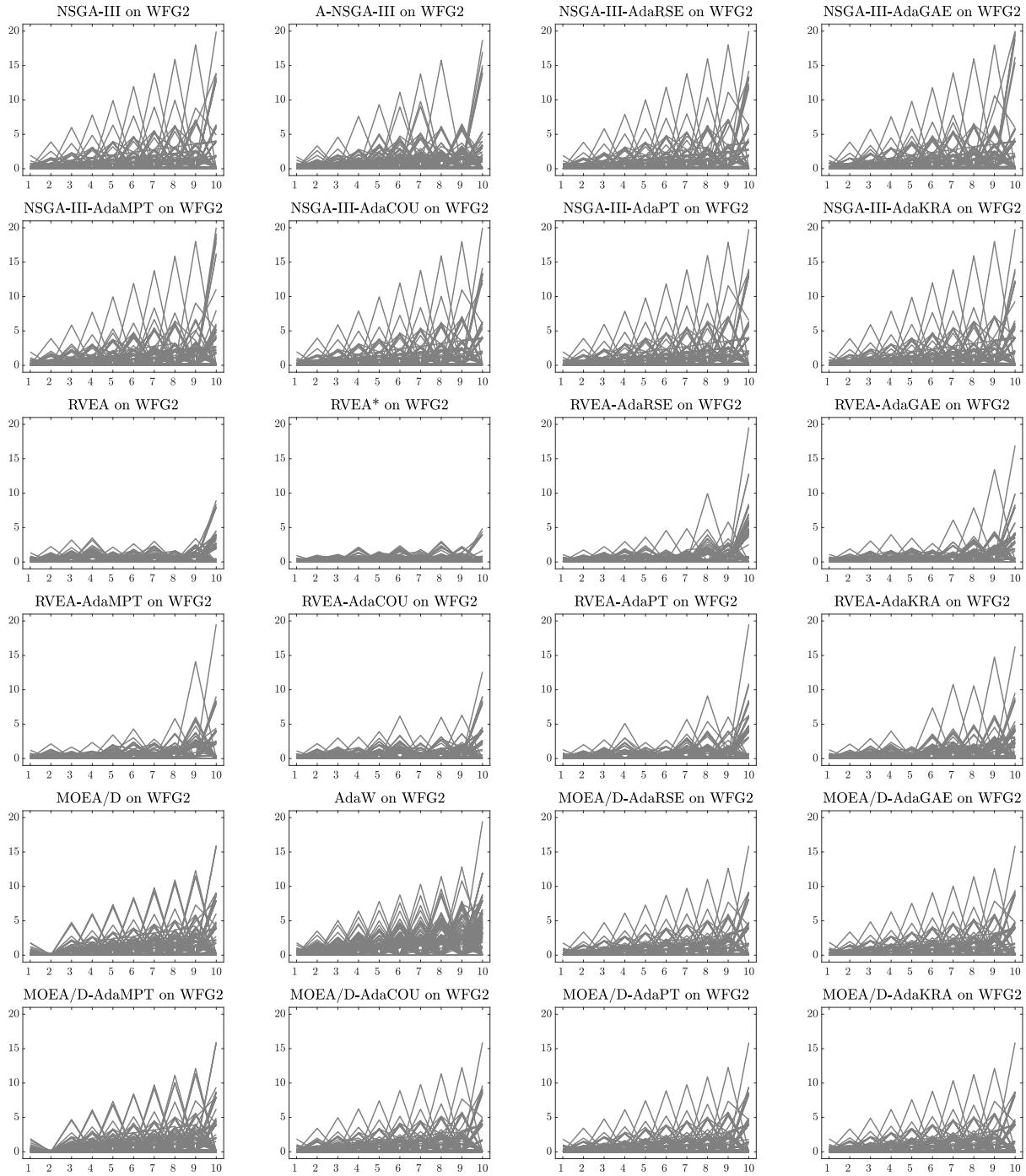


Figure 71: Final populations with the median HV value among 30 independent runs of MOEAs using the NSGA-III, RVEA, and MOEA/D frameworks on WFG2 with 10 objective functions.

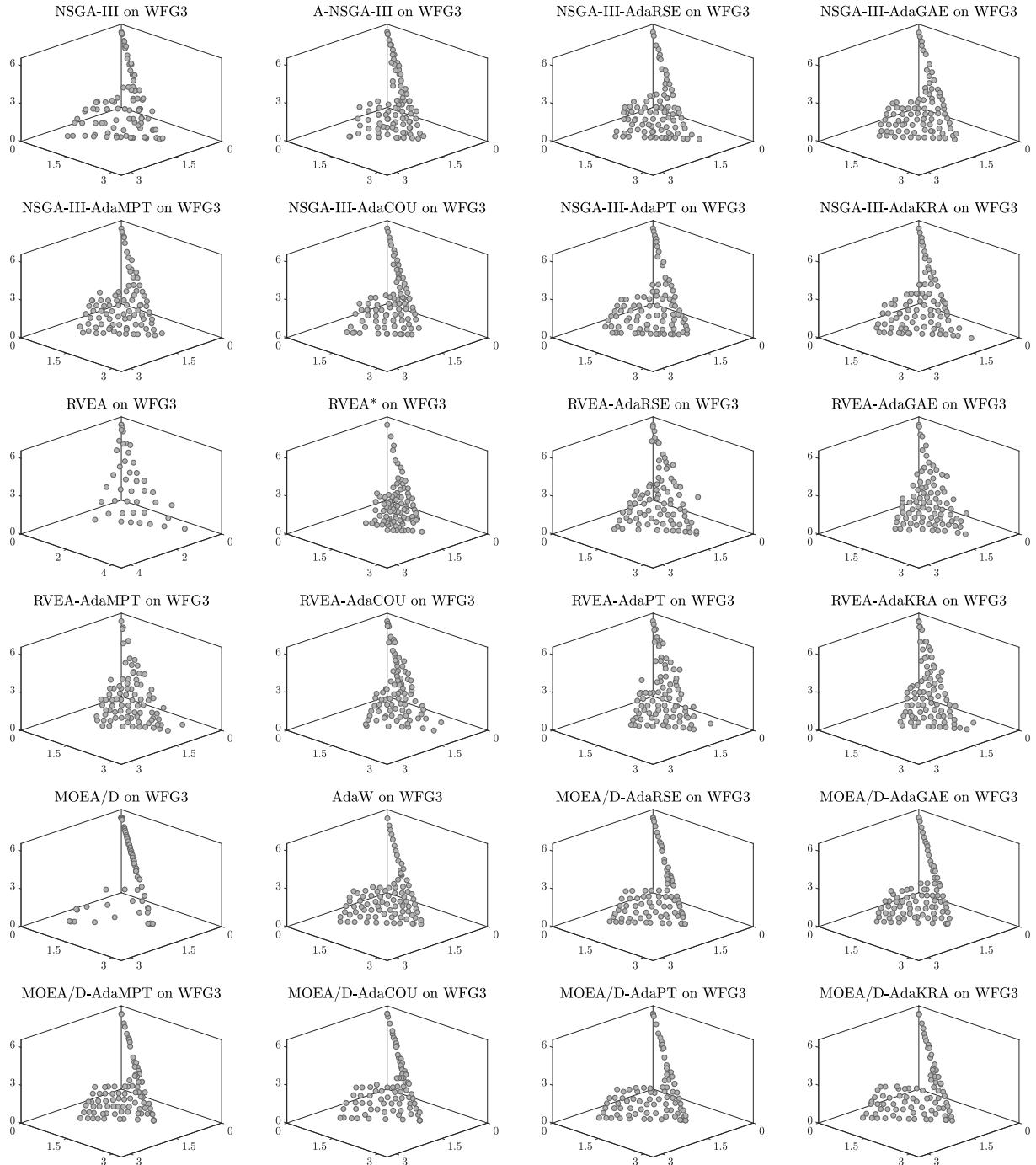


Figure 72: Final populations with the median HV value among 30 independent runs of MOEAs using the NSGA-III, RVEA, and MOEA/D frameworks on WFG3 with 3 objective functions.

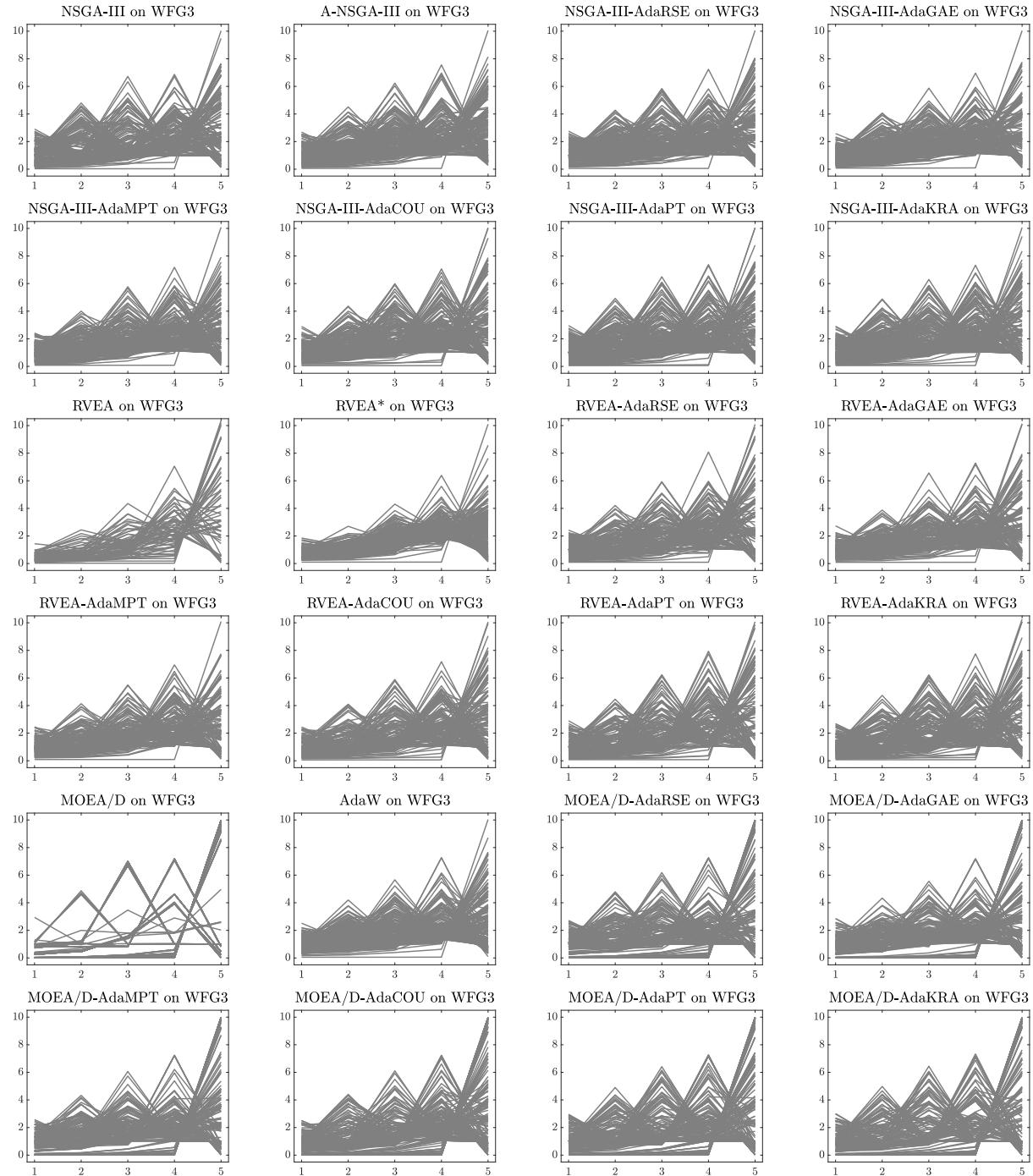


Figure 73: Final populations with the median HV value among 30 independent runs of MOEAs using the NSGA-III, RVEA, and MOEA/D frameworks on WFG3 with 5 objective functions.

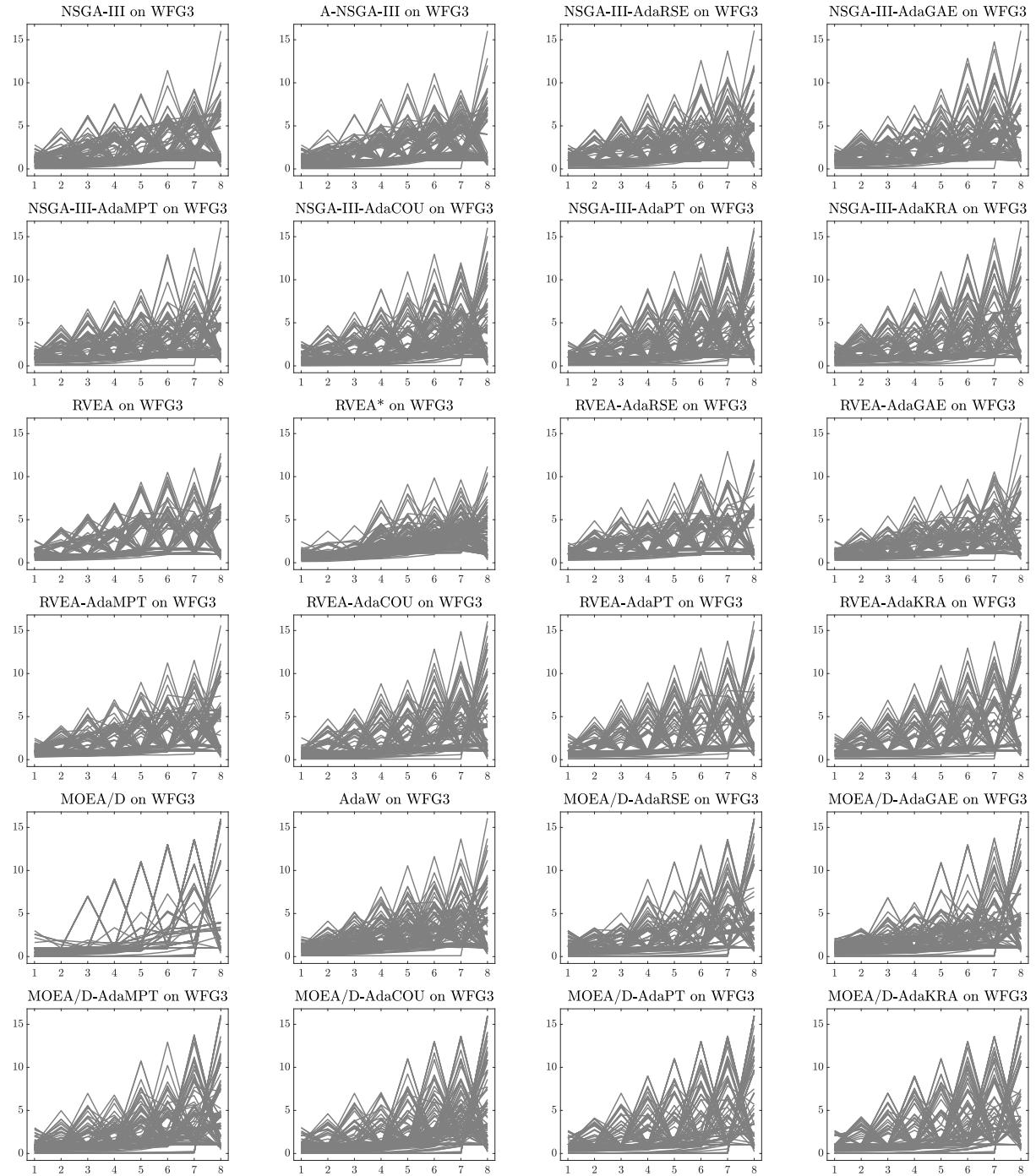


Figure 74: Final populations with the median HV value among 30 independent runs of MOEAs using the NSGA-III, RVEA, and MOEA/D frameworks on WFG3 with 8 objective functions.

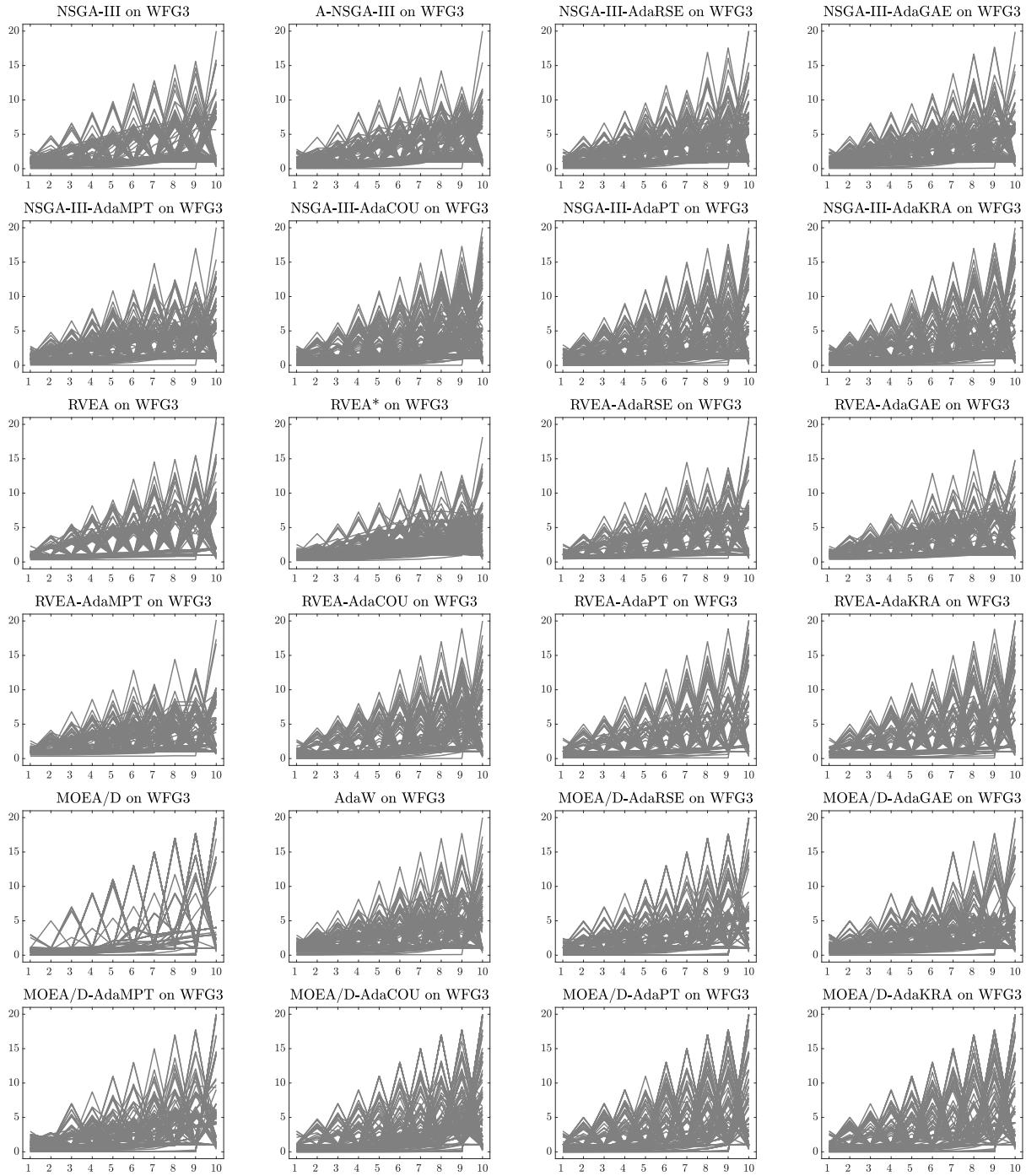


Figure 75: Final populations with the median HV value among 30 independent runs of MOEAs using the NSGA-III, RVEA, and MOEA/D frameworks on WFG3 with 10 objective functions.

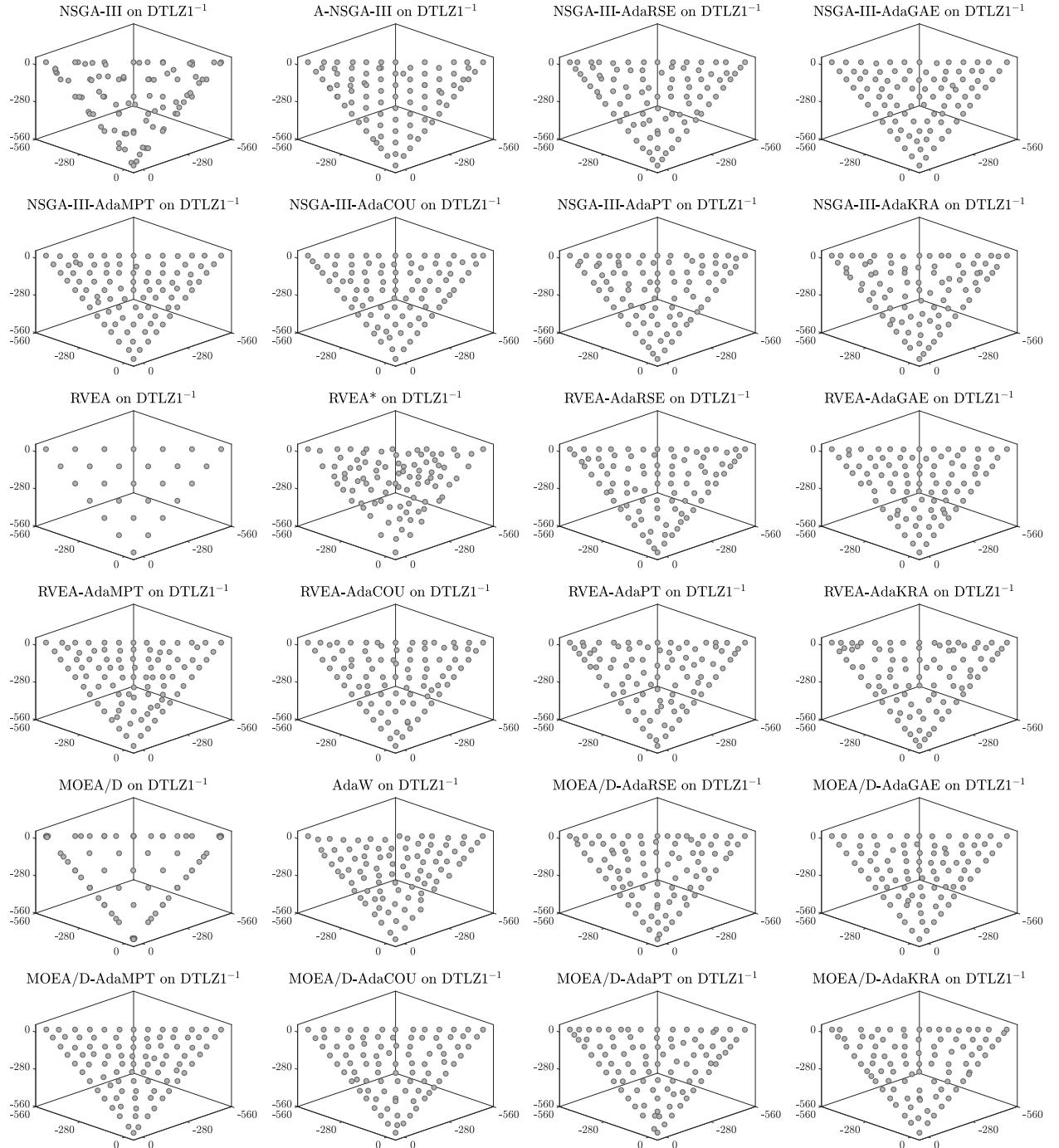


Figure 76: Final populations with the median HV value among 30 independent runs of MOEAs using the NSGA-III, RVEA, and MOEA/D frameworks on $DTLZ1^{-1}$ with 3 objective functions.

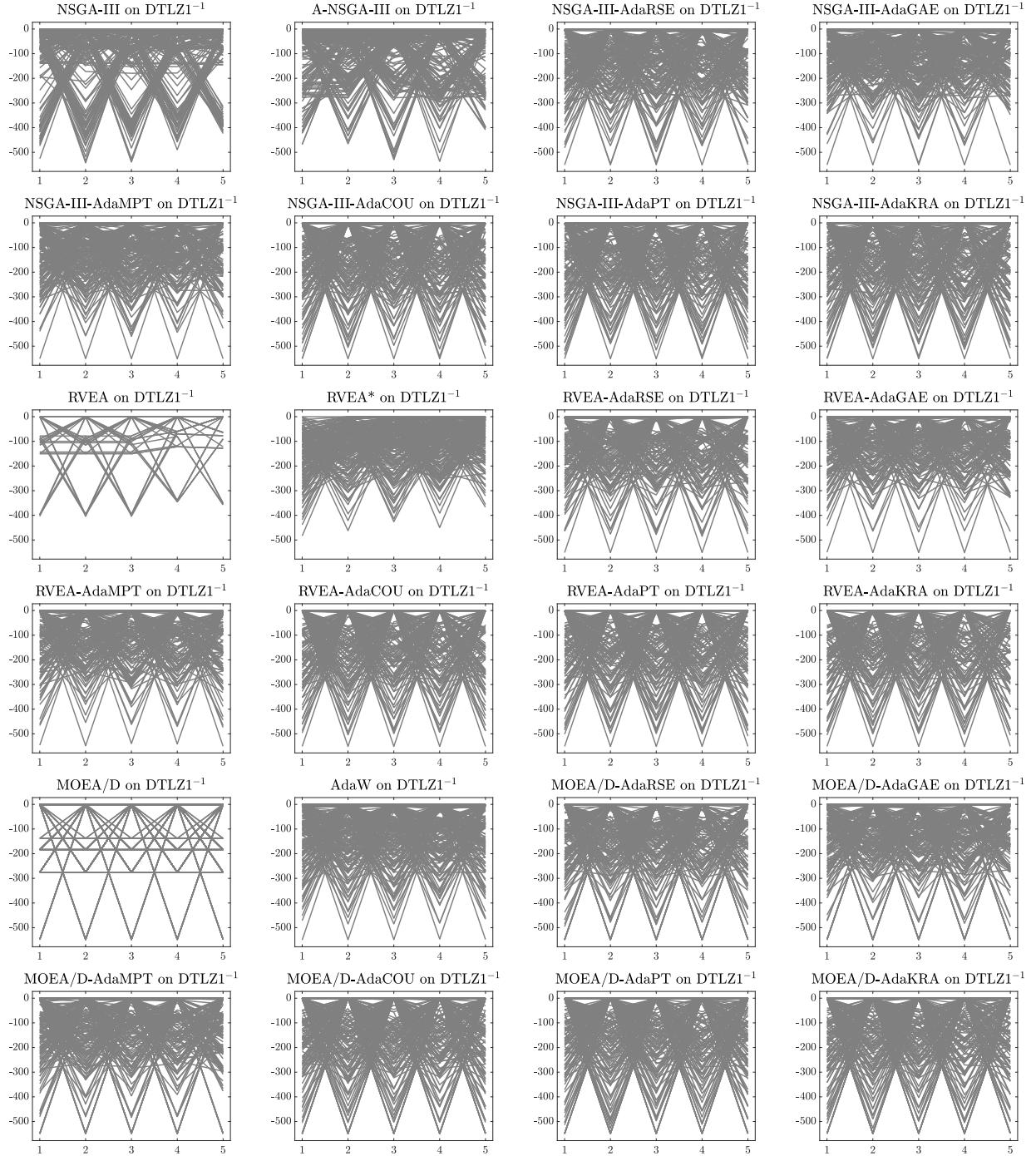


Figure 77: Final populations with the median HV value among 30 independent runs of MOEAs using the NSGA-III, RVEA, and MOEA/D frameworks on DTLZ1⁻¹ with 5 objective functions.

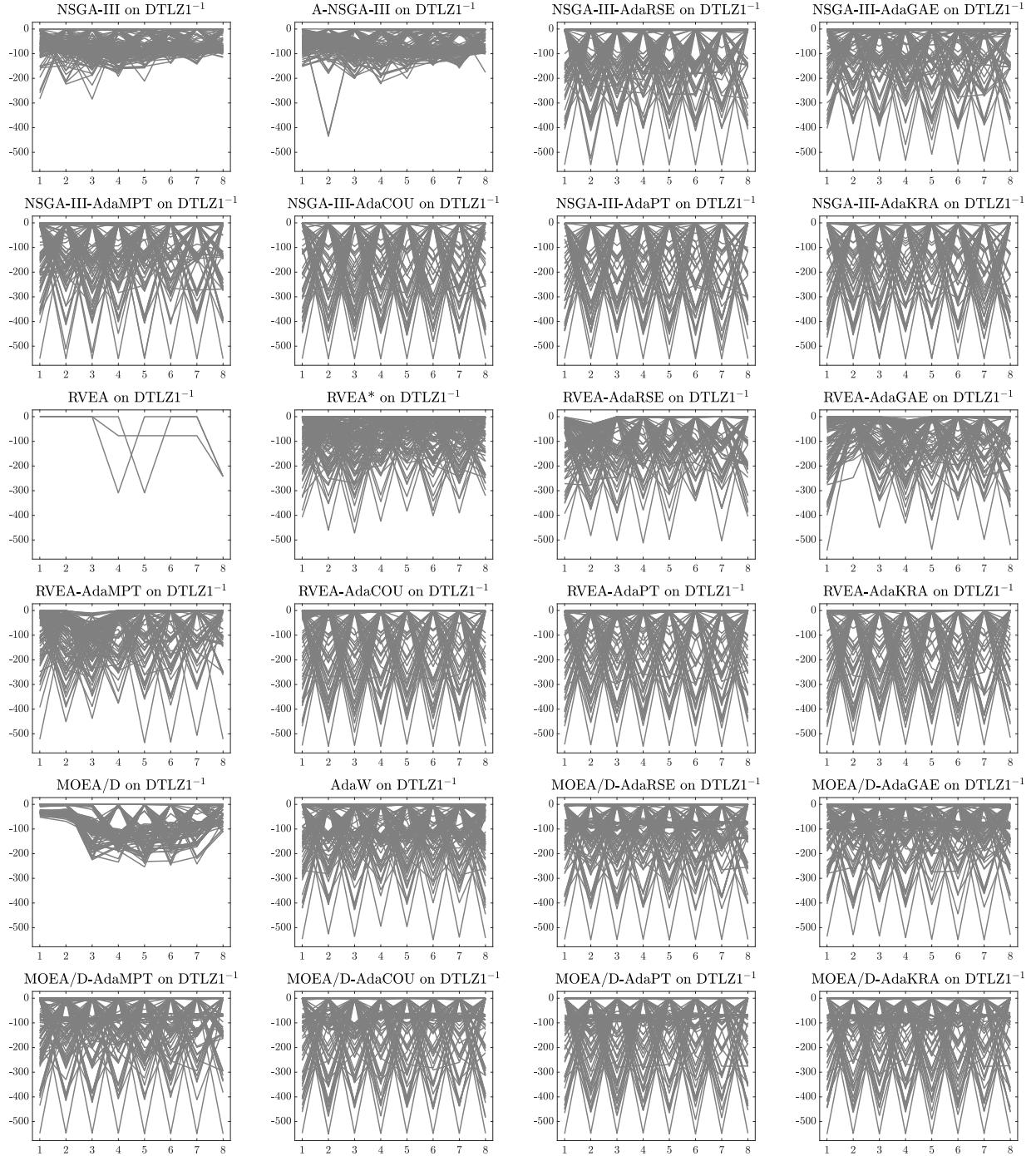


Figure 78: Final populations with the median HV value among 30 independent runs of MOEAs using the NSGA-III, RVEA, and MOEA/D frameworks on $DTLZ1^{-1}$ with 8 objective functions.

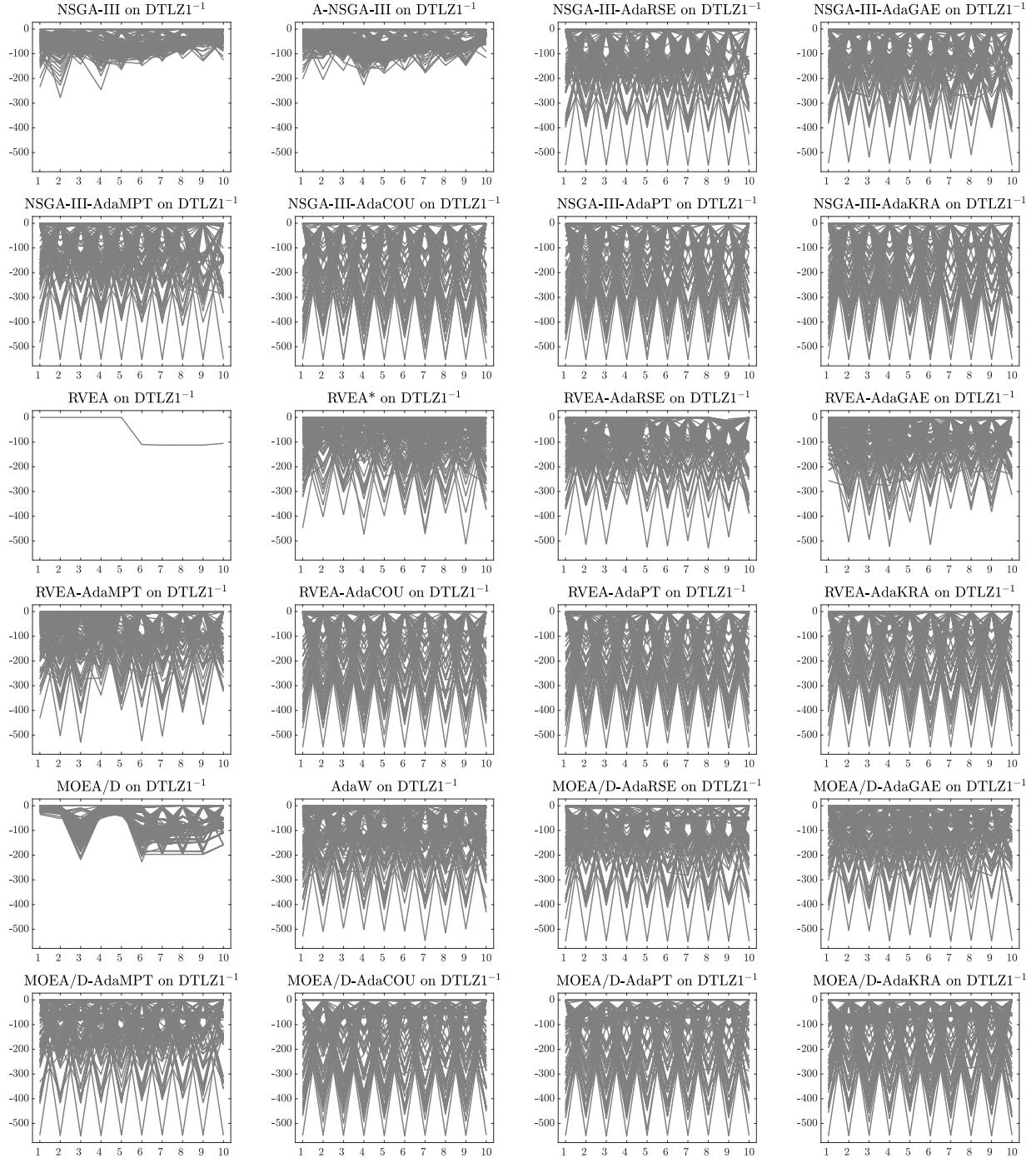


Figure 79: Final populations with the median HV value among 30 independent runs of MOEAs using the NSGA-III, RVEA, and MOEA/D frameworks on $DTLZ1^{-1}$ with 10 objective functions.

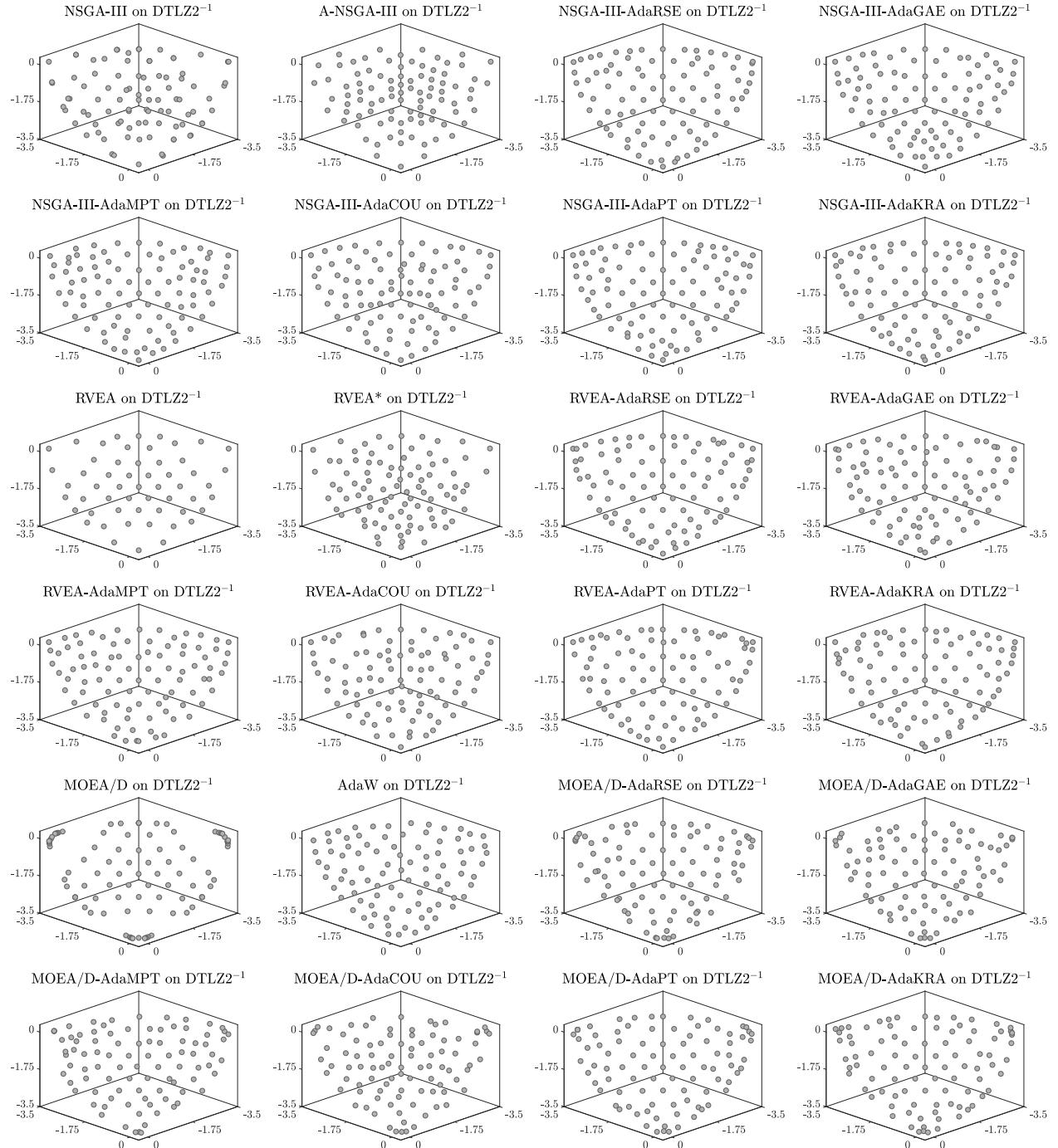


Figure 80: Final populations with the median HV value among 30 independent runs of MOEAs using the NSGA-III, RVEA, and MOEA/D frameworks on $DTLZ2^{-1}$ with 3 objective functions.

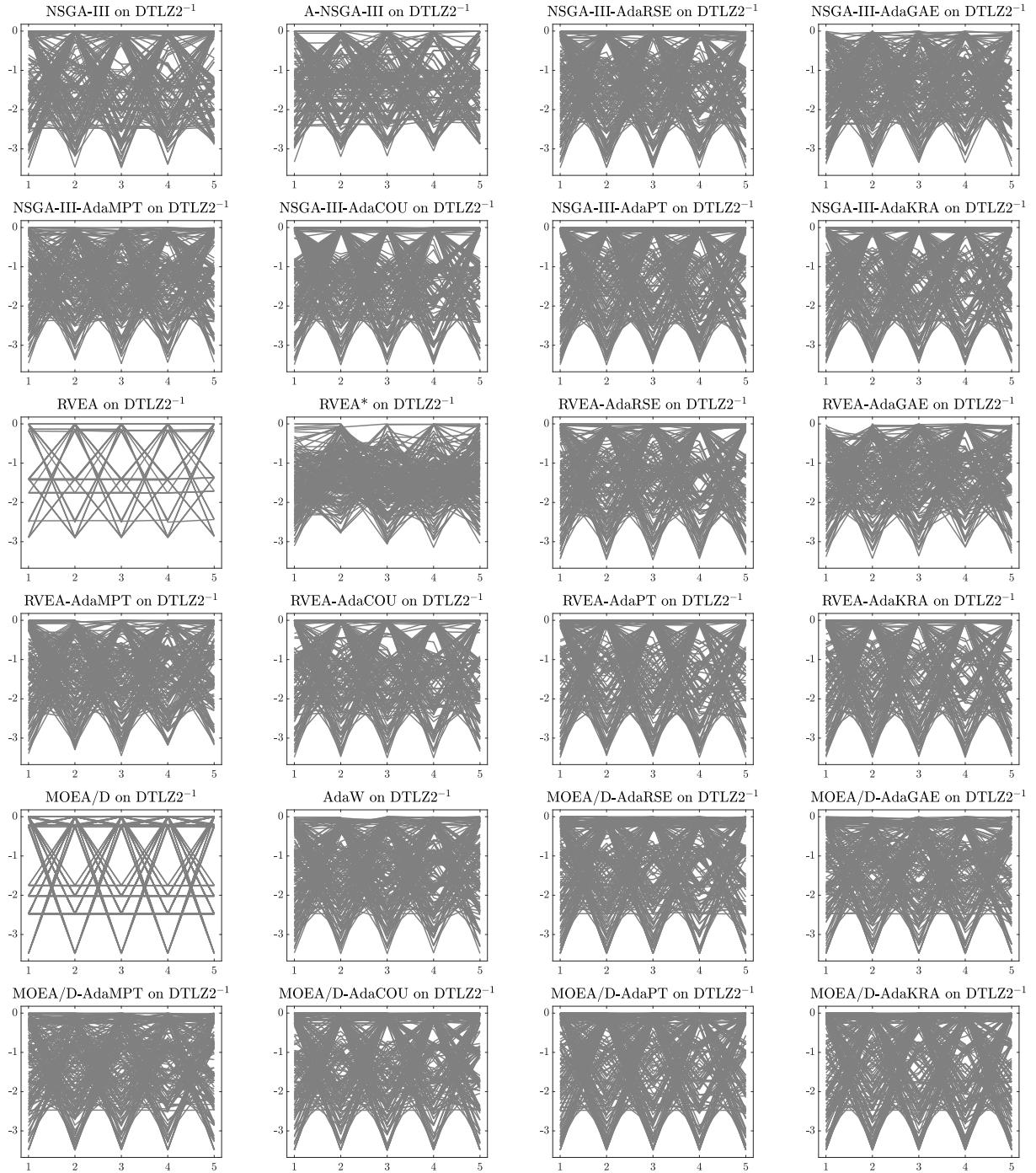


Figure 81: Final populations with the median HV value among 30 independent runs of MOEAs using the NSGA-III, RVEA, and MOEA/D frameworks on DTLZ2⁻¹ with 5 objective functions.

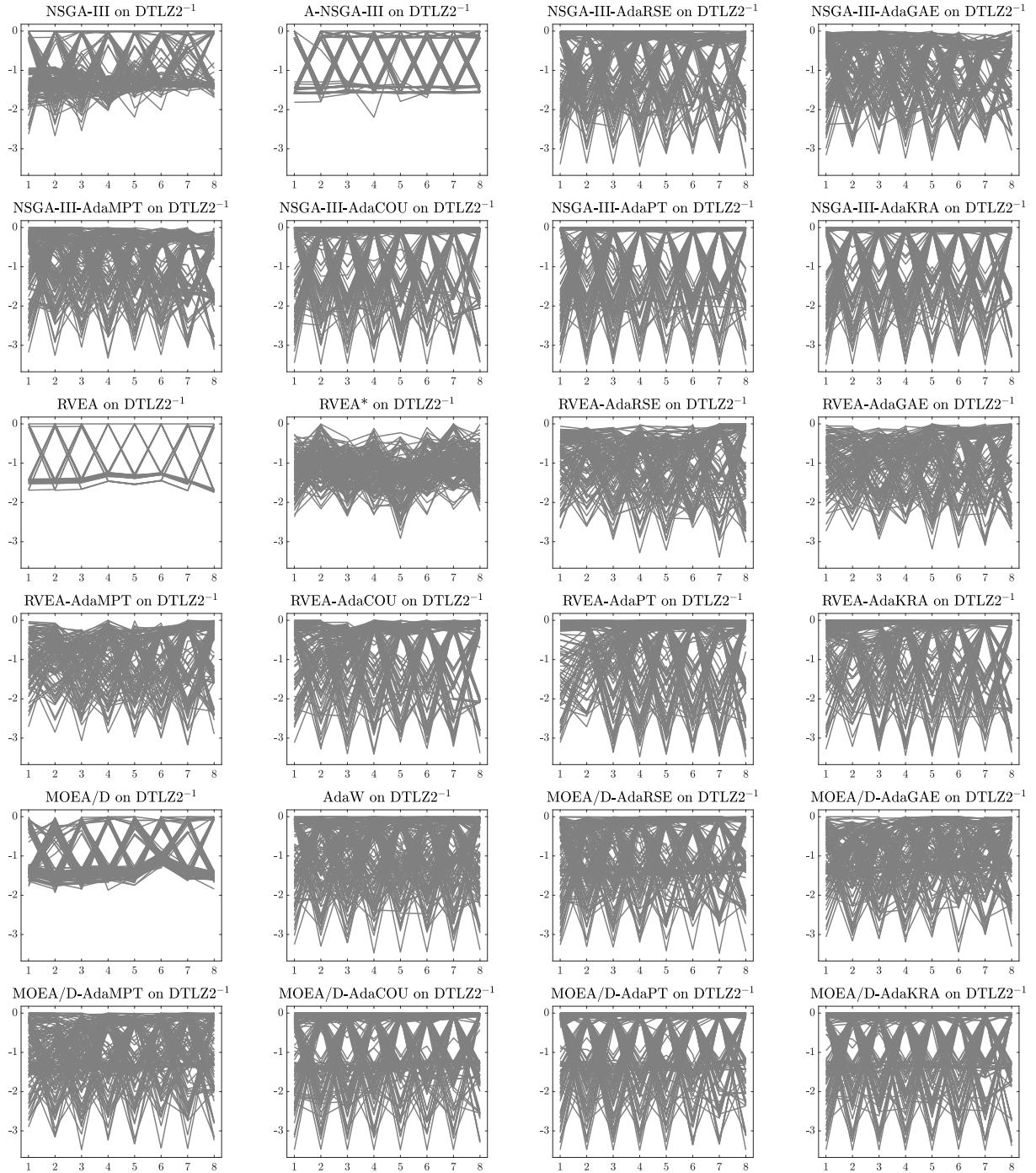


Figure 82: Final populations with the median HV value among 30 independent runs of MOEAs using the NSGA-III, RVEA, and MOEA/D frameworks on DTLZ2⁻¹ with 8 objective functions.

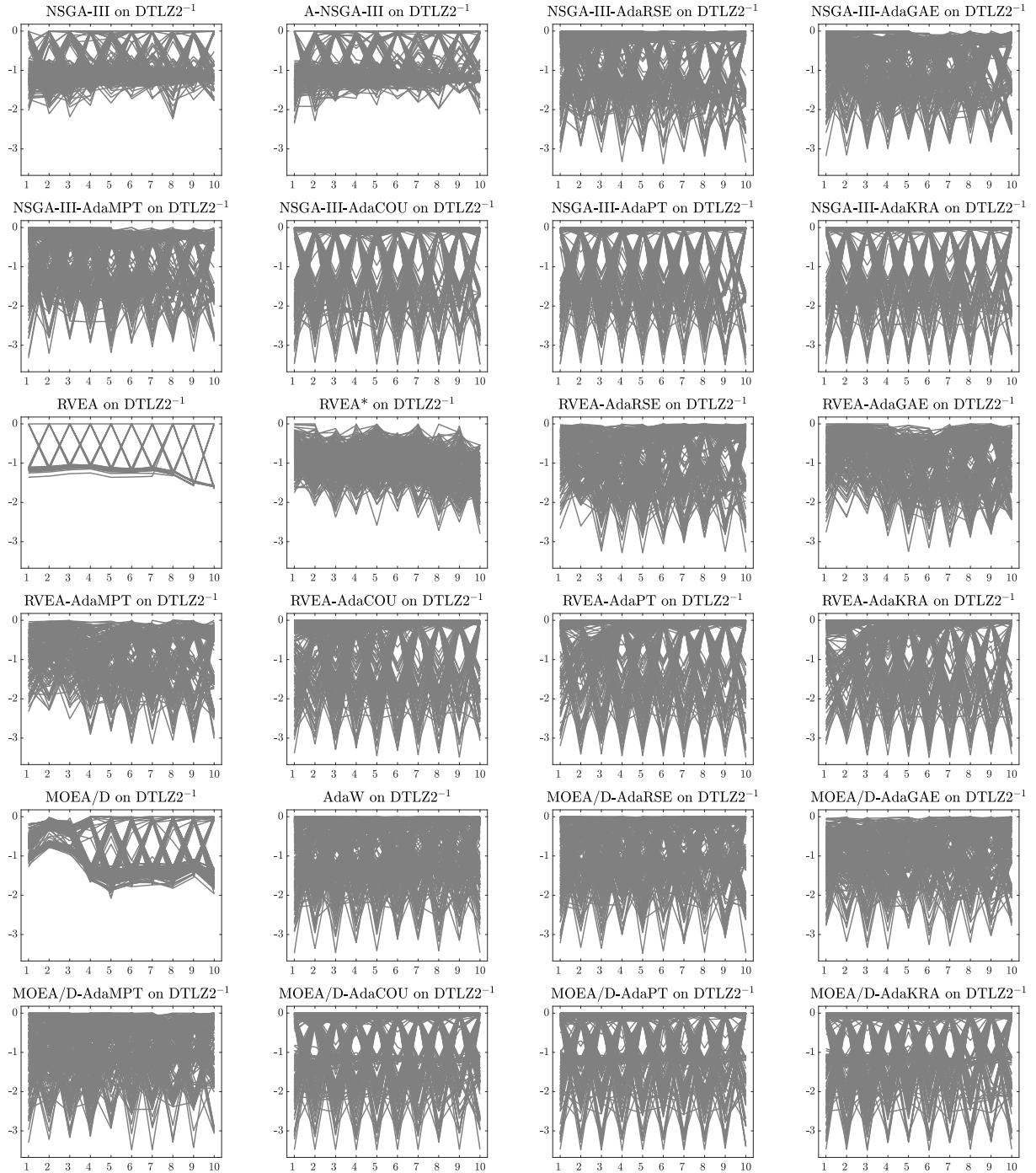


Figure 83: Final populations with the median HV value among 30 independent runs of MOEAs using the NSGA-III, RVEA, and MOEA/D frameworks on $DTLZ2^{-1}$ with 10 objective functions.

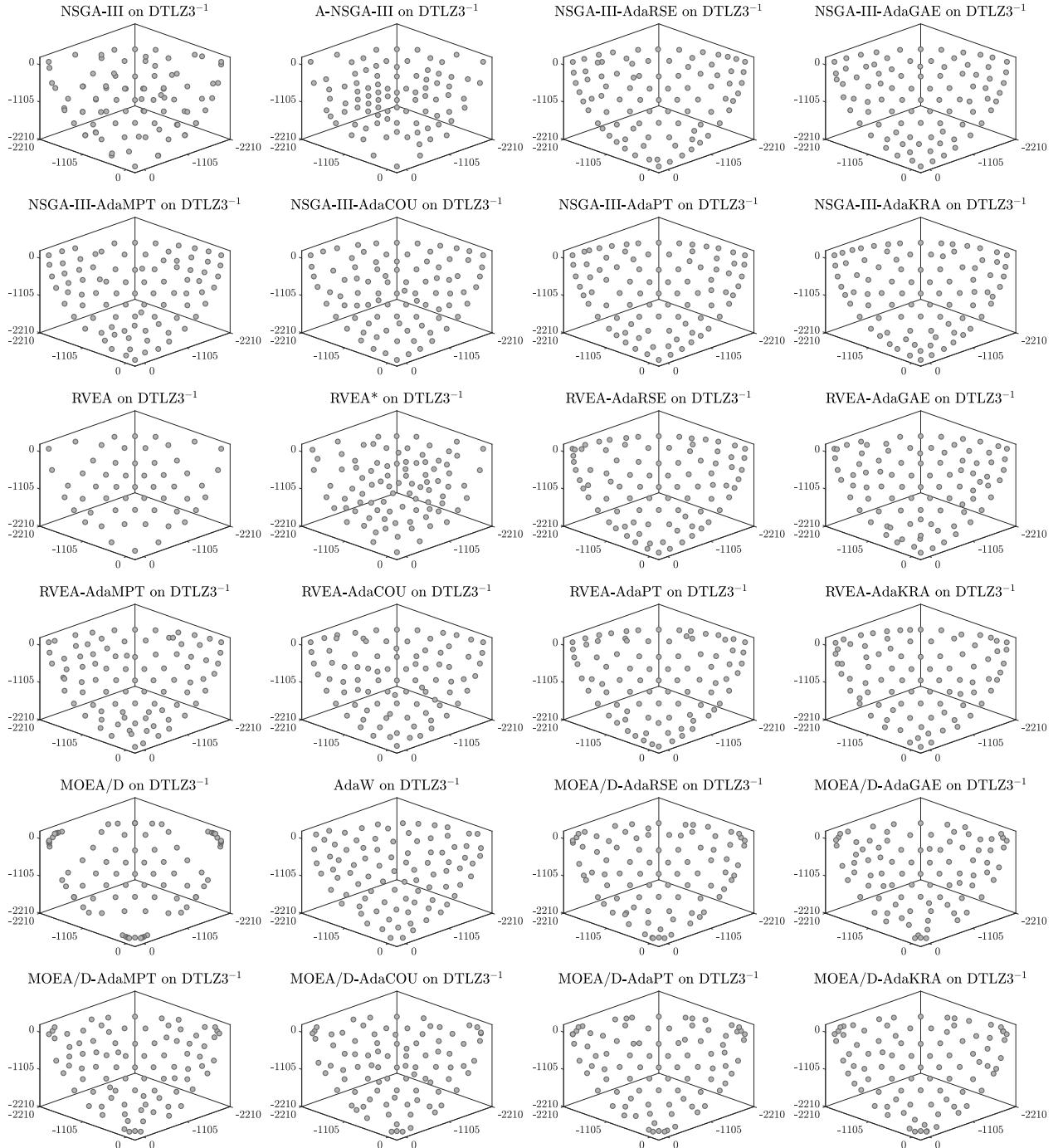


Figure 84: Final populations with the median HV value among 30 independent runs of MOEAs using the NSGA-III, RVEA, and MOEA/D frameworks on $DTLZ3^{-1}$ with 3 objective functions.

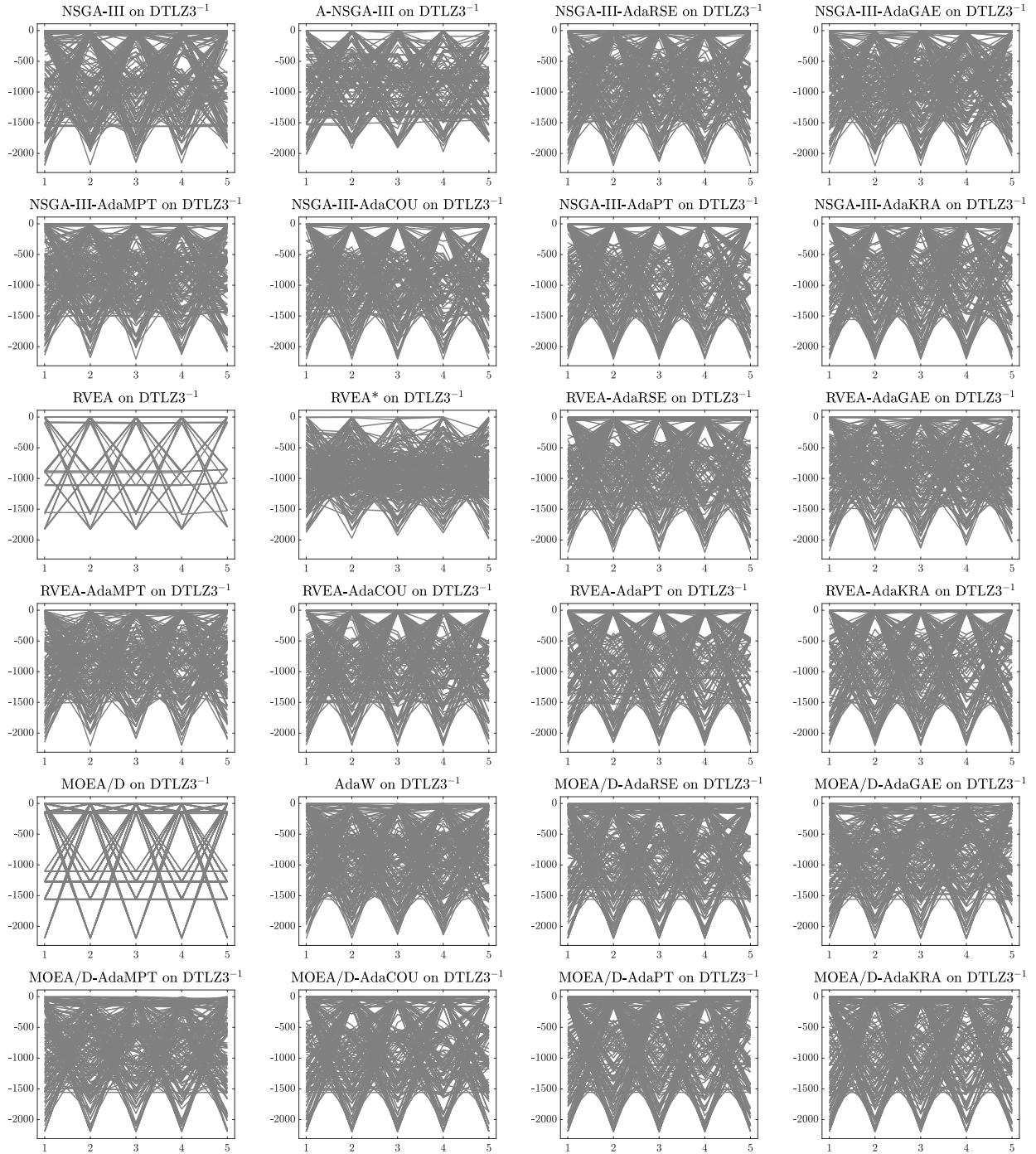


Figure 85: Final populations with the median HV value among 30 independent runs of MOEAs using the NSGA-III, RVEA, and MOEA/D frameworks on DTLZ3⁻¹ with 5 objective functions.

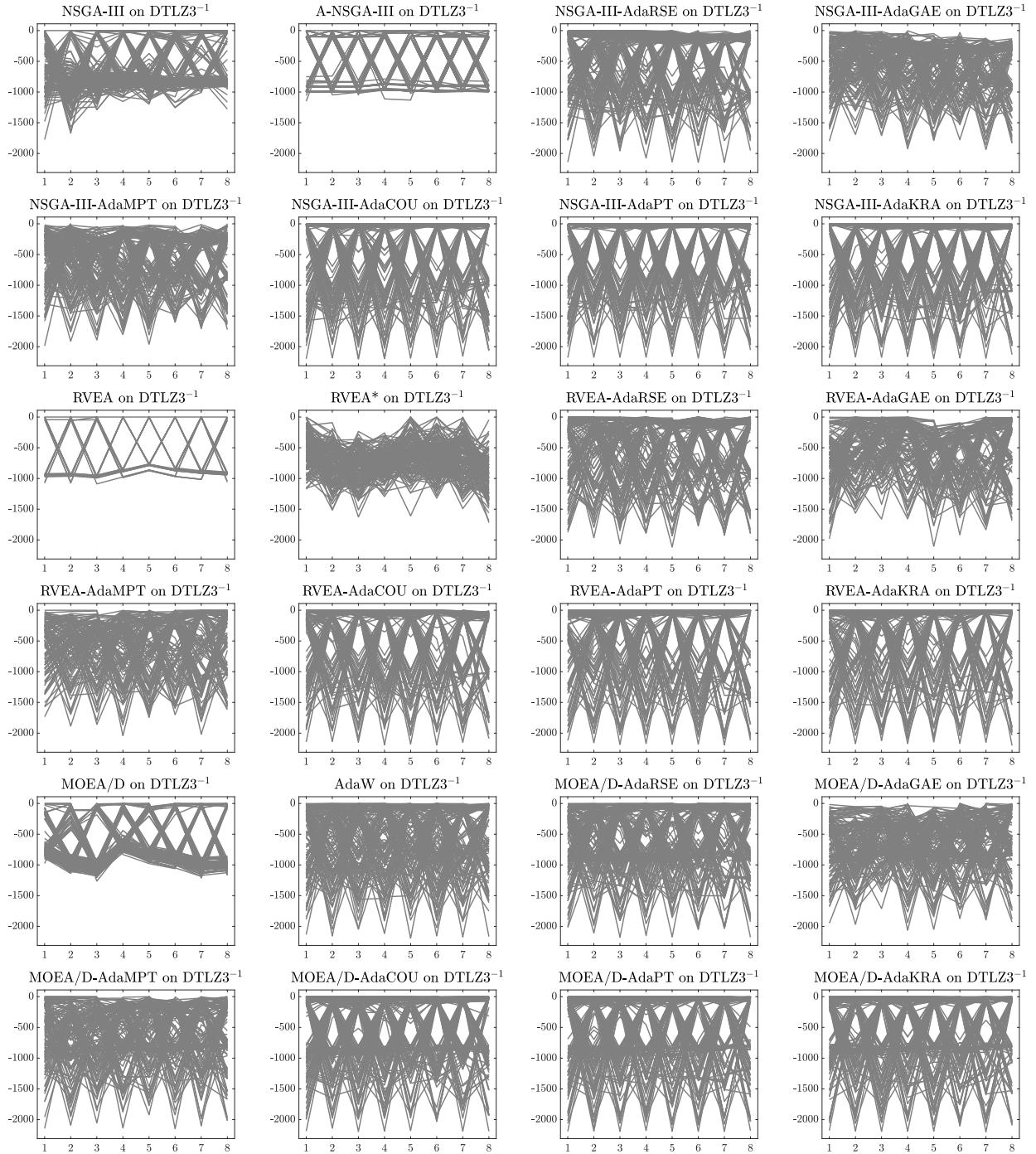


Figure 86: Final populations with the median HV value among 30 independent runs of MOEAs using the NSGA-III, RVEA, and MOEA/D frameworks on DTLZ3^{-1} with 8 objective functions.

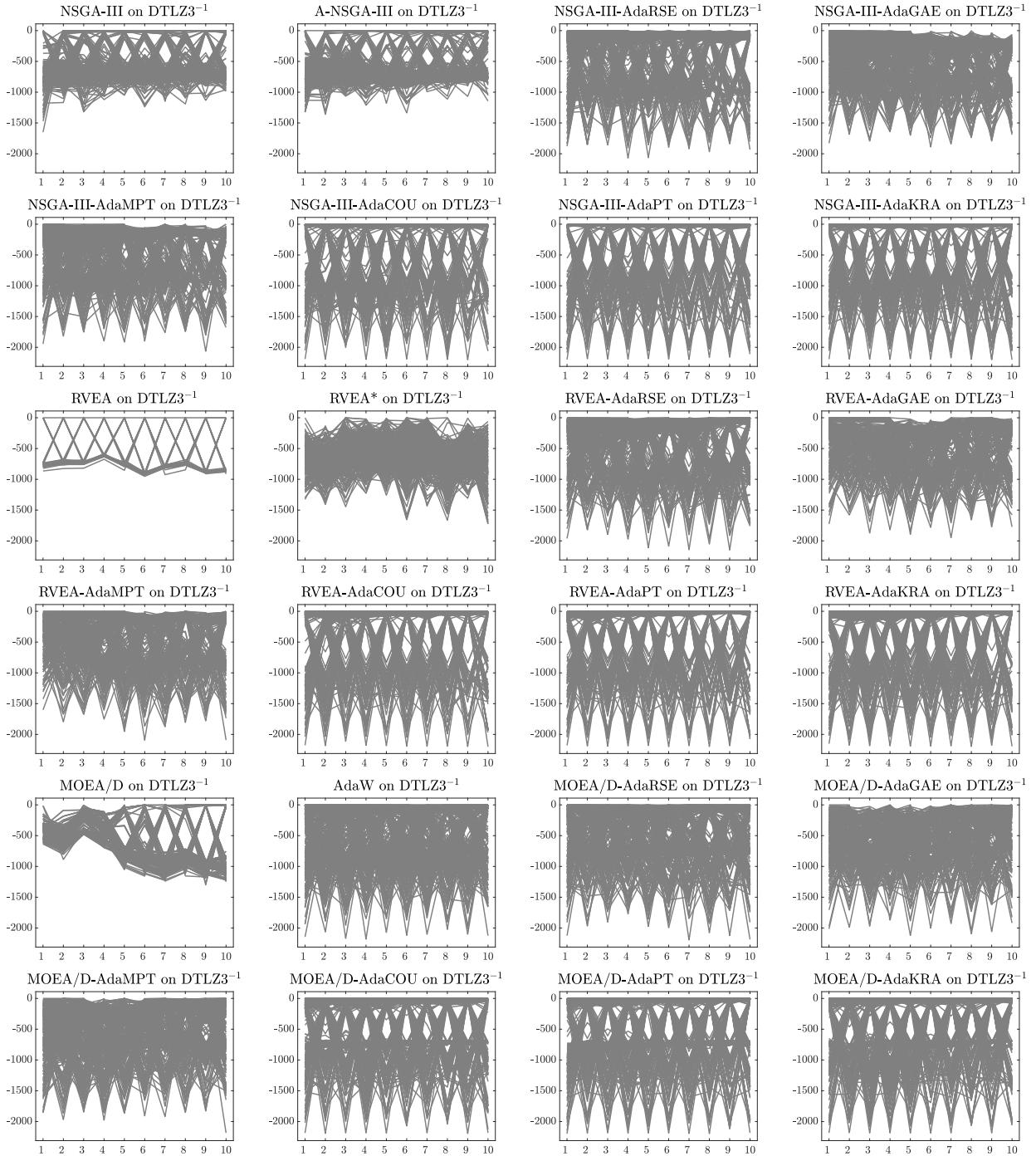


Figure 87: Final populations with the median HV value among 30 independent runs of MOEAs using the NSGA-III, RVEA, and MOEA/D frameworks on DTLZ3^{-1} with 10 objective functions.

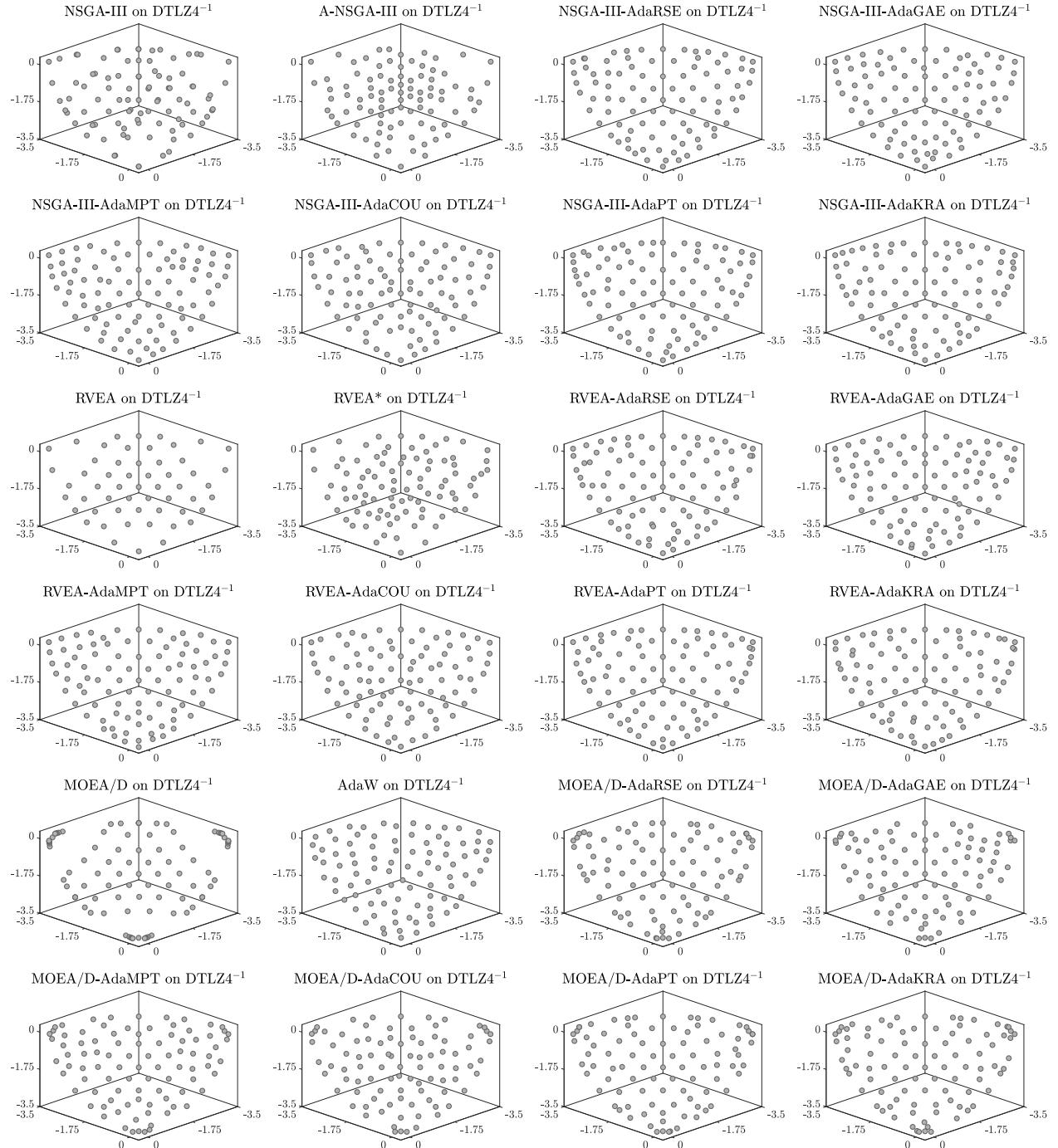


Figure 88: Final populations with the median HV value among 30 independent runs of MOEAs using the NSGA-III, RVEA, and MOEA/D frameworks on $DTLZ4^{-1}$ with 3 objective functions.

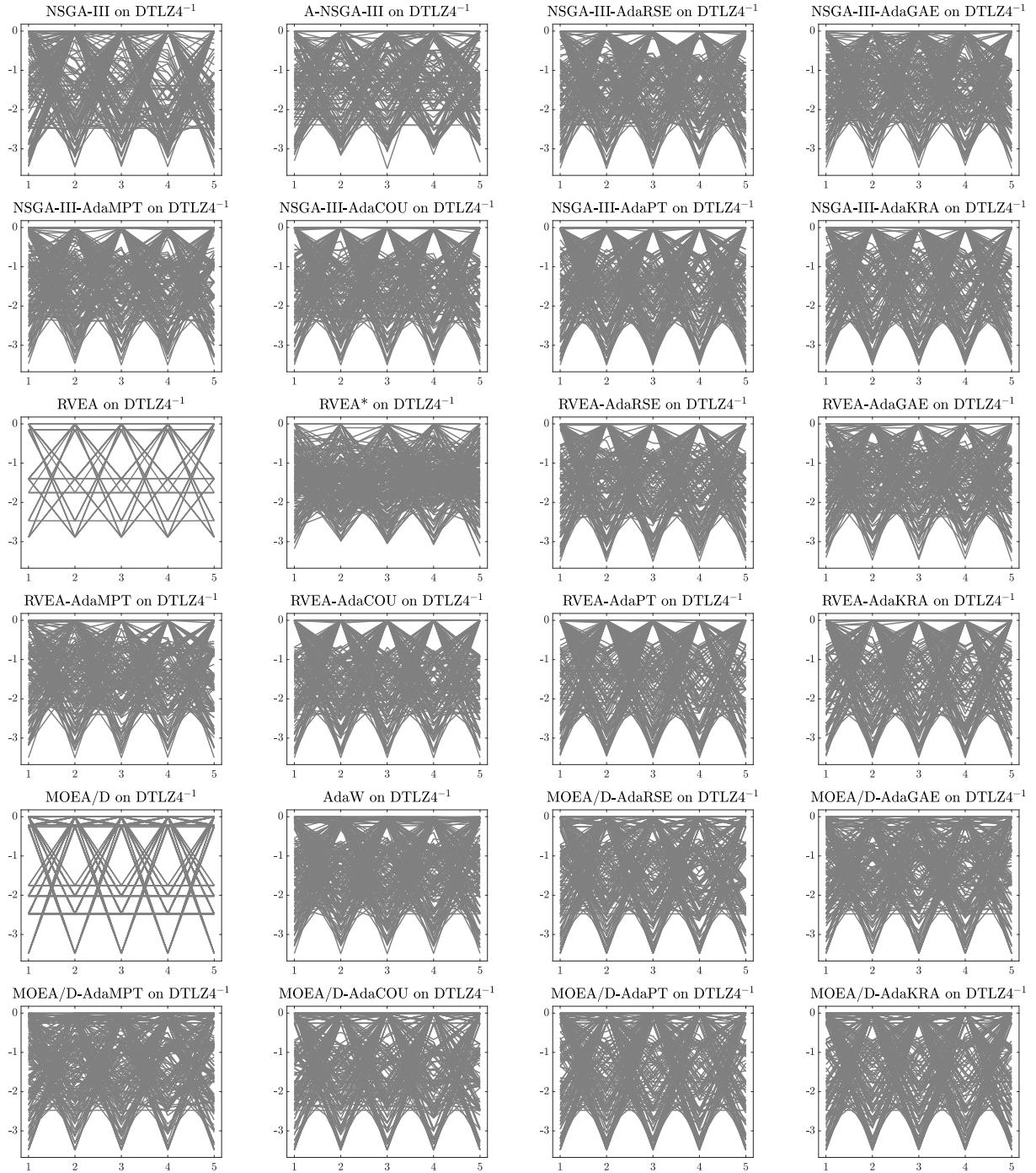


Figure 89: Final populations with the median HV value among 30 independent runs of MOEAs using the NSGA-III, RVEA, and MOEA/D frameworks on DTLZ4⁻¹ with 5 objective functions.

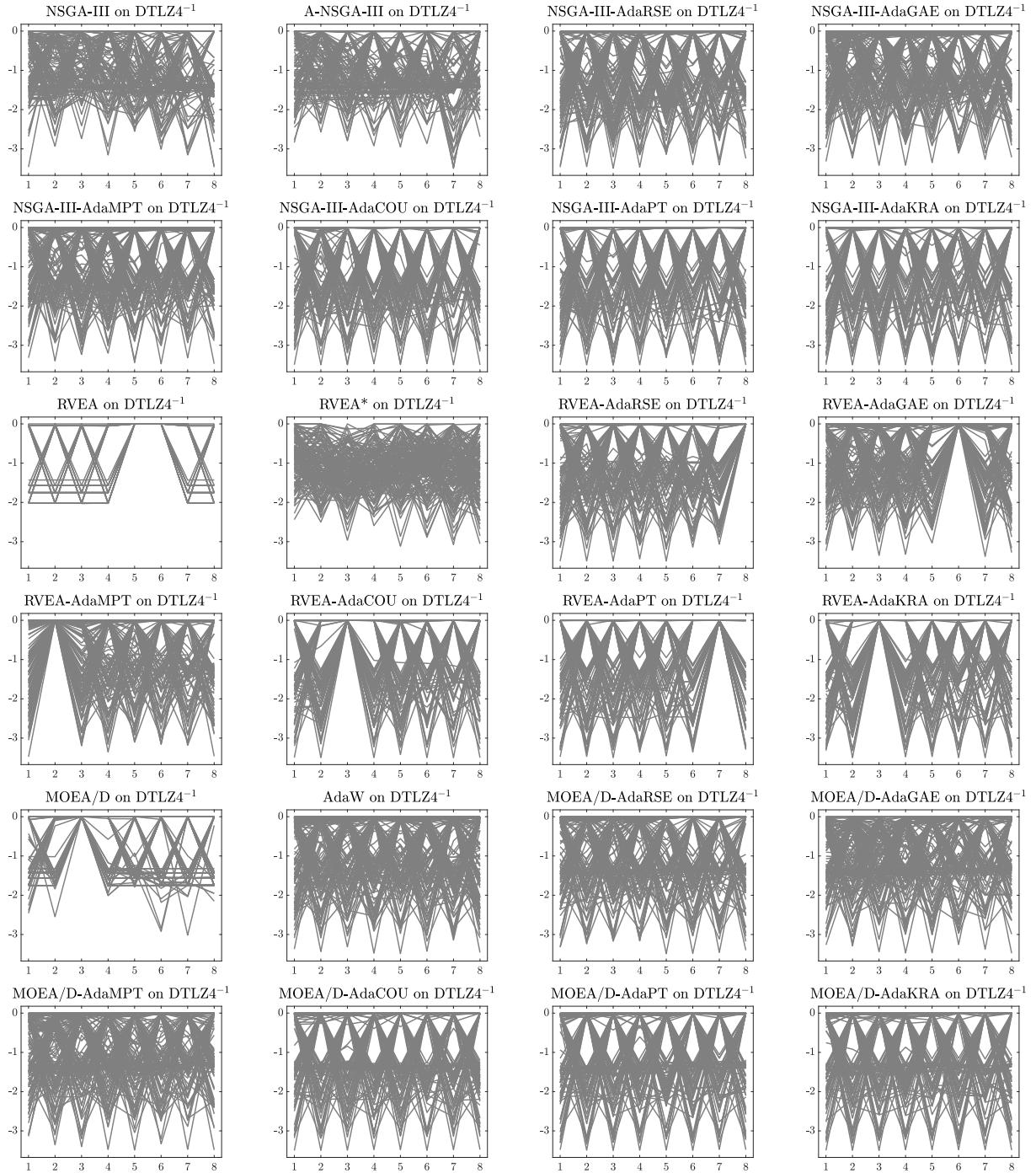


Figure 90: Final populations with the median HV value among 30 independent runs of MOEAs using the NSGA-III, RVEA, and MOEA/D frameworks on DTLZ4⁻¹ with 8 objective functions.

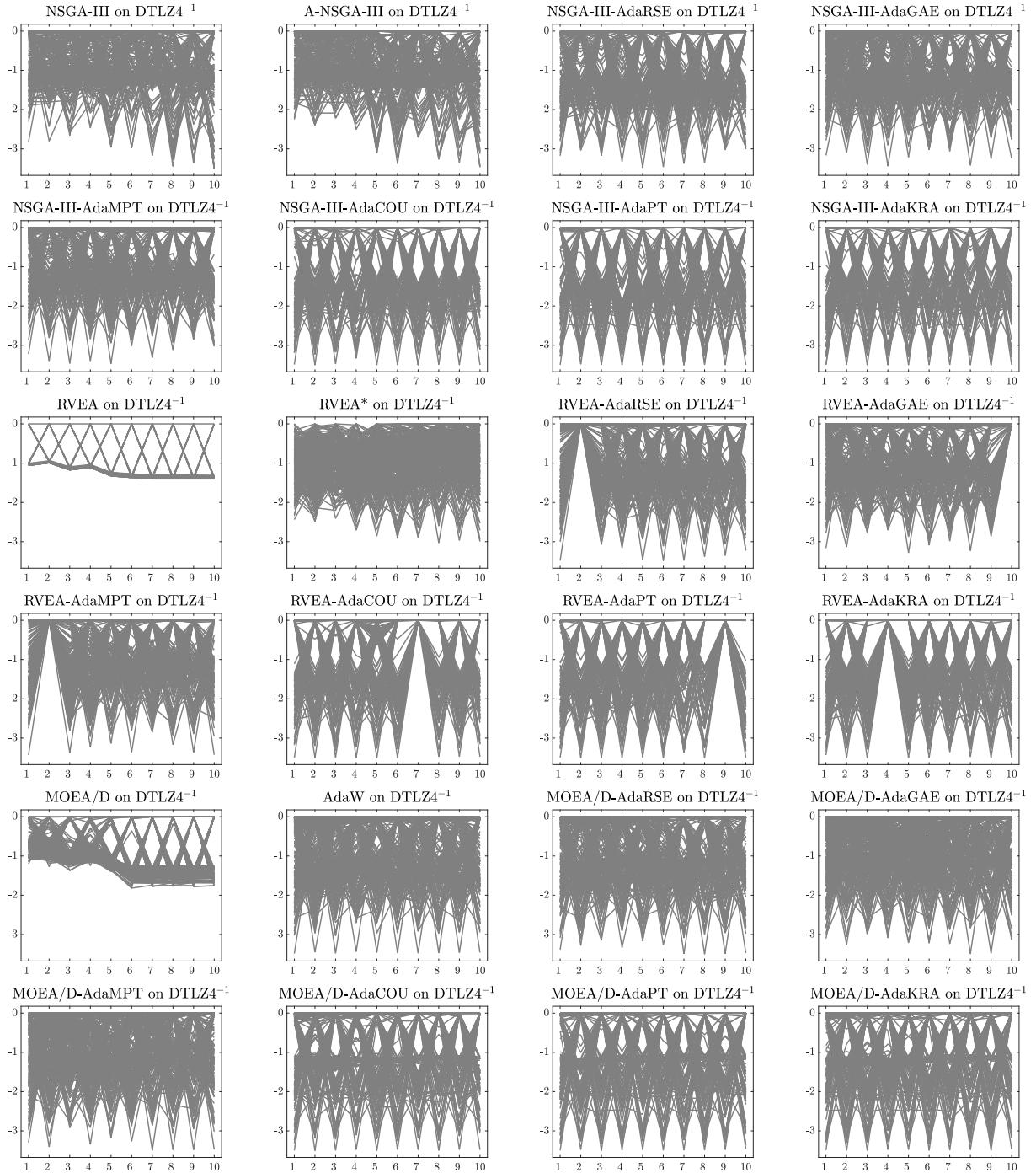


Figure 91: Final populations with the median HV value among 30 independent runs of MOEAs using the NSGA-III, RVEA, and MOEA/D frameworks on $DTLZ4^{-1}$ with 10 objective functions.

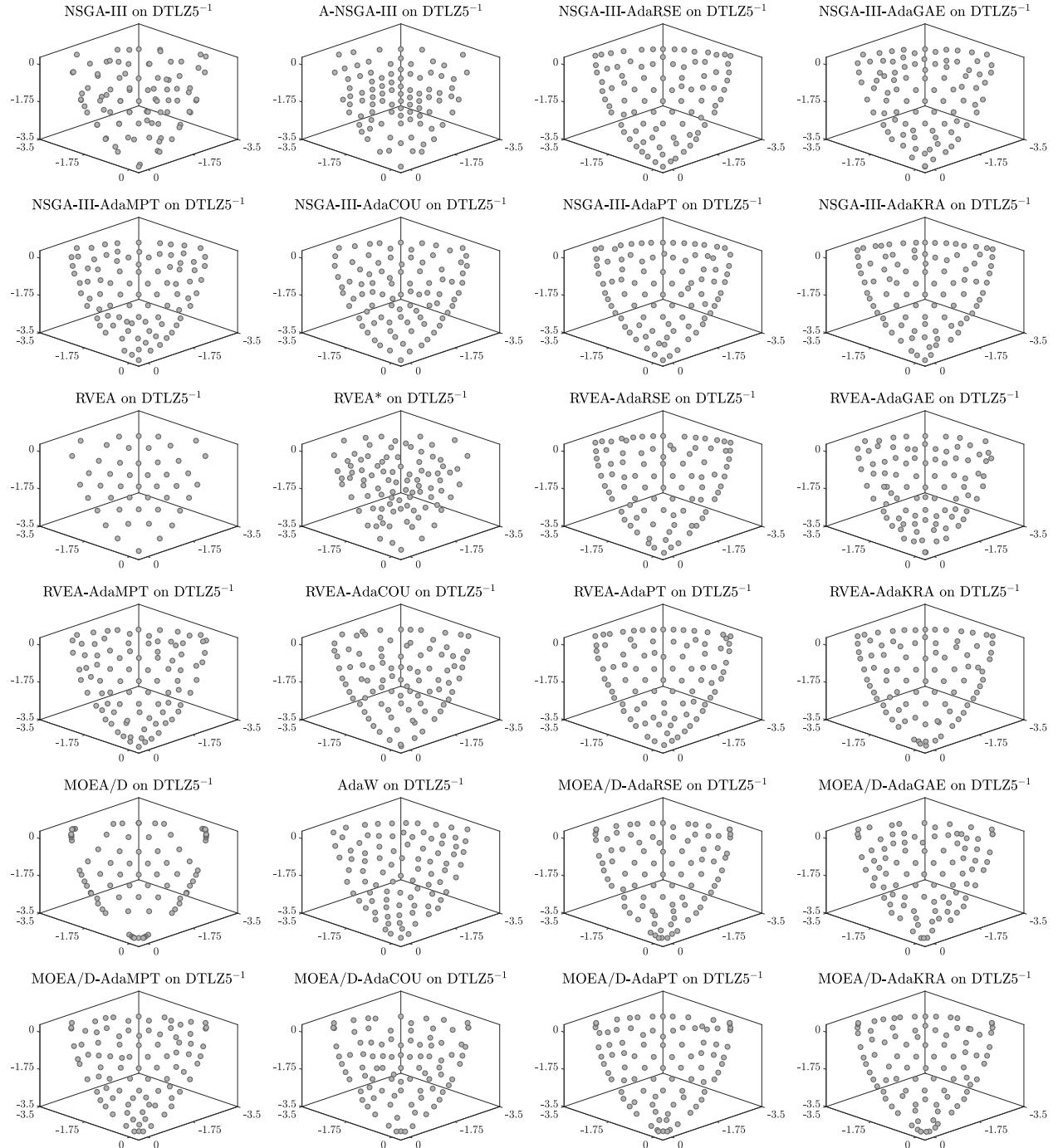


Figure 92: Final populations with the median HV value among 30 independent runs of MOEAs using the NSGA-III, RVEA, and MOEA/D frameworks on $DTLZ5^{-1}$ with 3 objective functions.

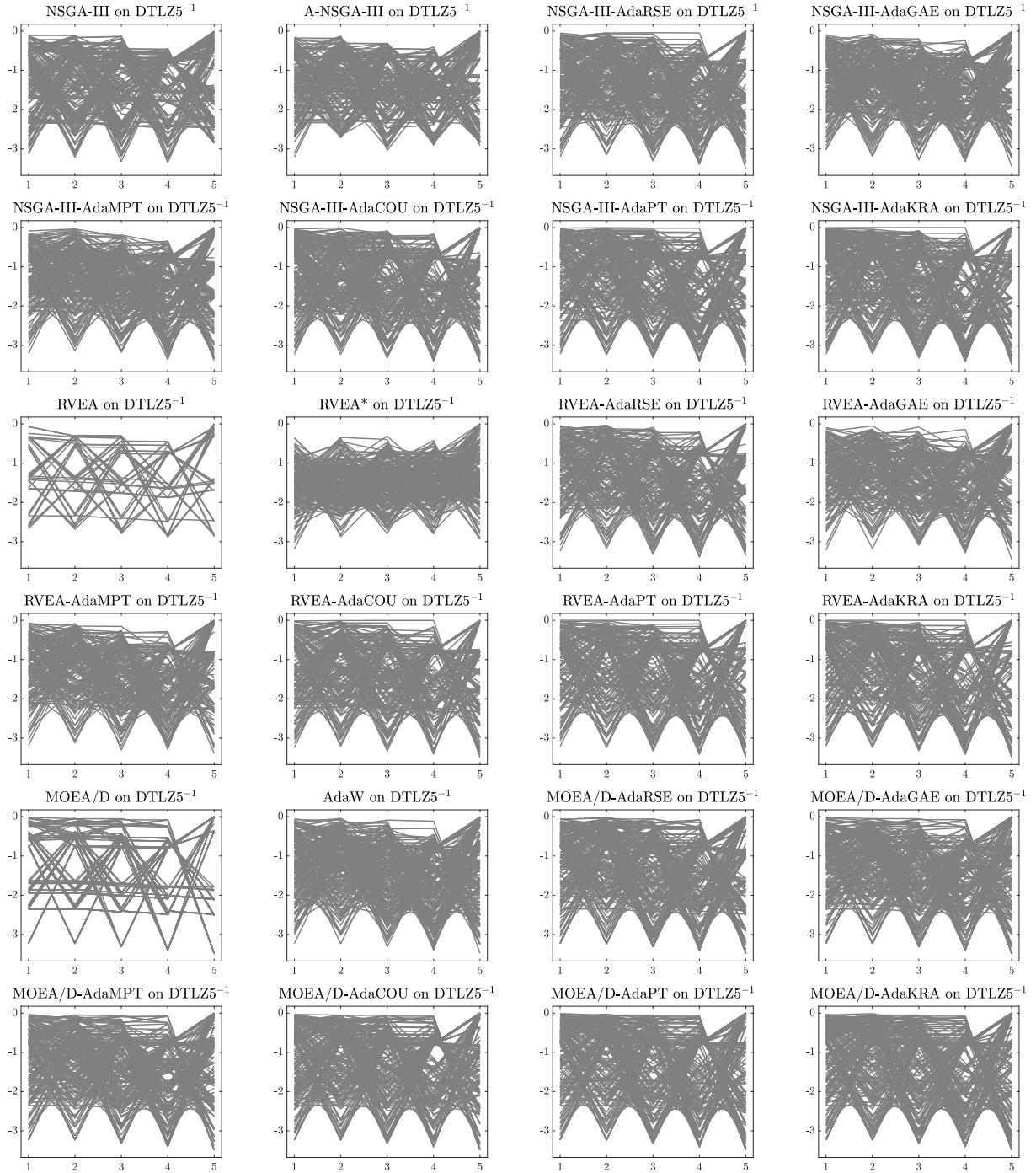


Figure 93: Final populations with the median HV value among 30 independent runs of MOEAs using the NSGA-III, RVEA, and MOEA/D frameworks on $DTLZ5^{-1}$ with 5 objective functions.

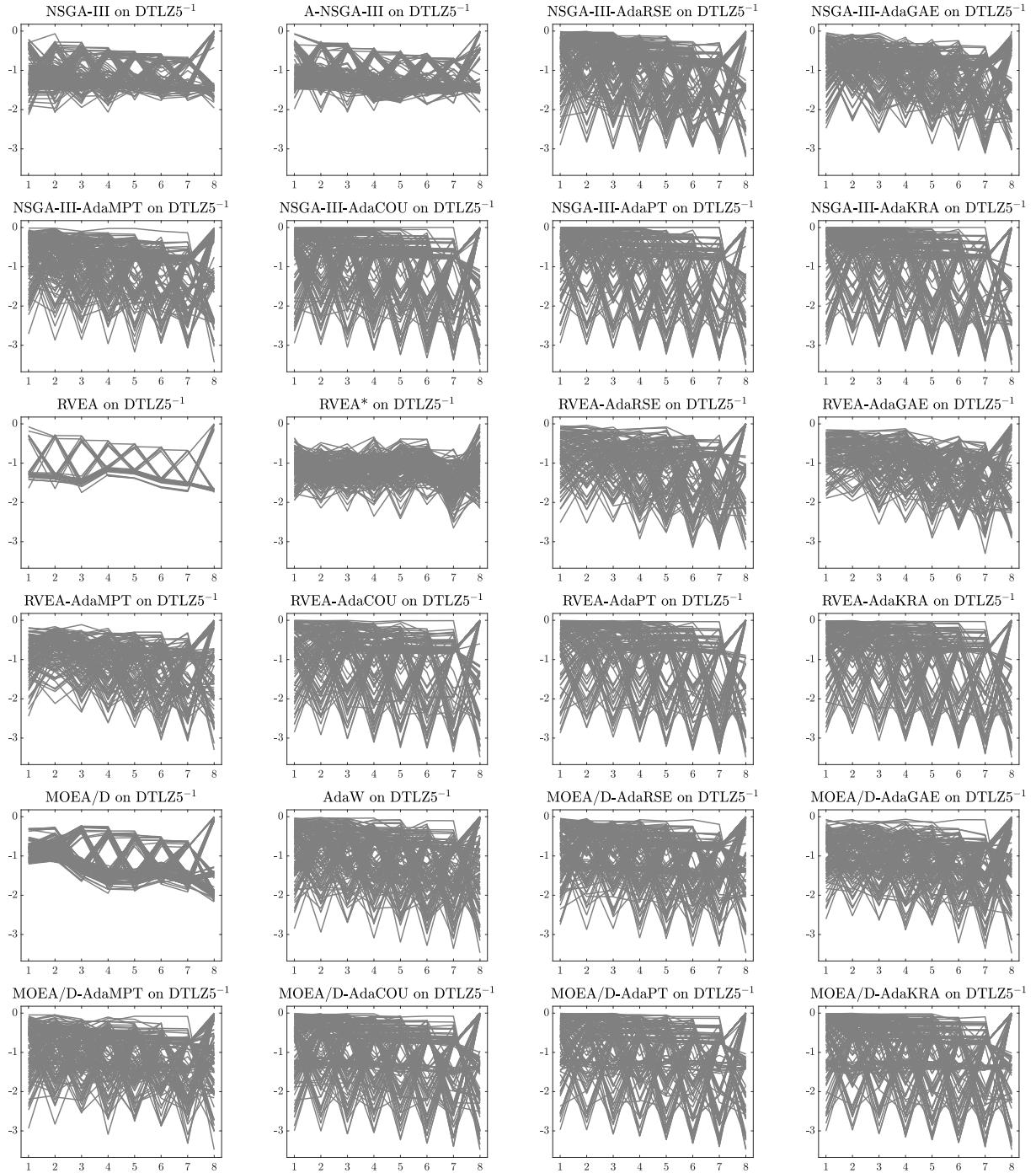


Figure 94: Final populations with the median HV value among 30 independent runs of MOEAs using the NSGA-III, RVEA, and MOEA/D frameworks on DTLZ5⁻¹ with 8 objective functions.

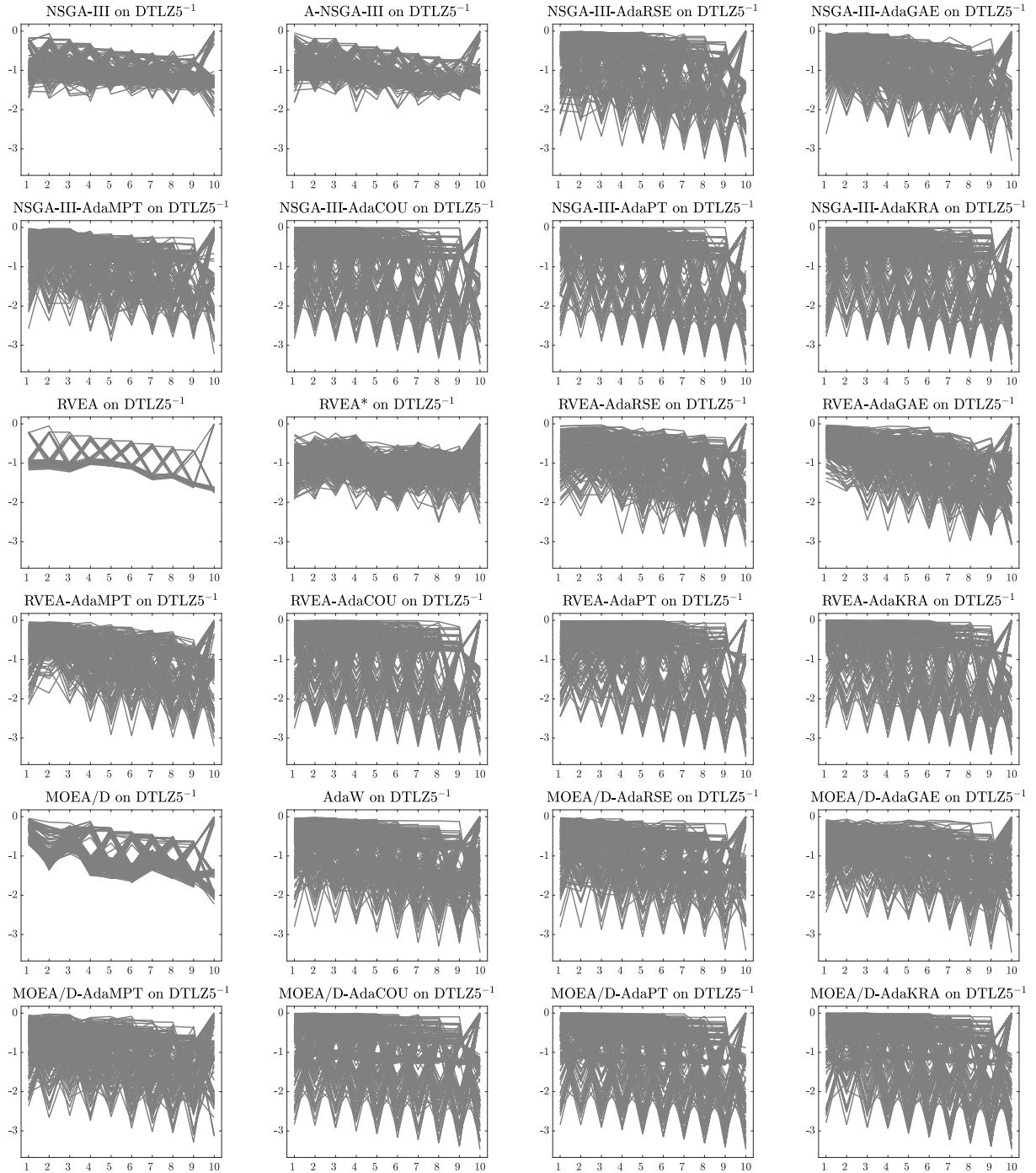


Figure 95: Final populations with the median HV value among 30 independent runs of MOEAs using the NSGA-III, RVEA, and MOEA/D frameworks on DTLZ5⁻¹ with 10 objective functions.

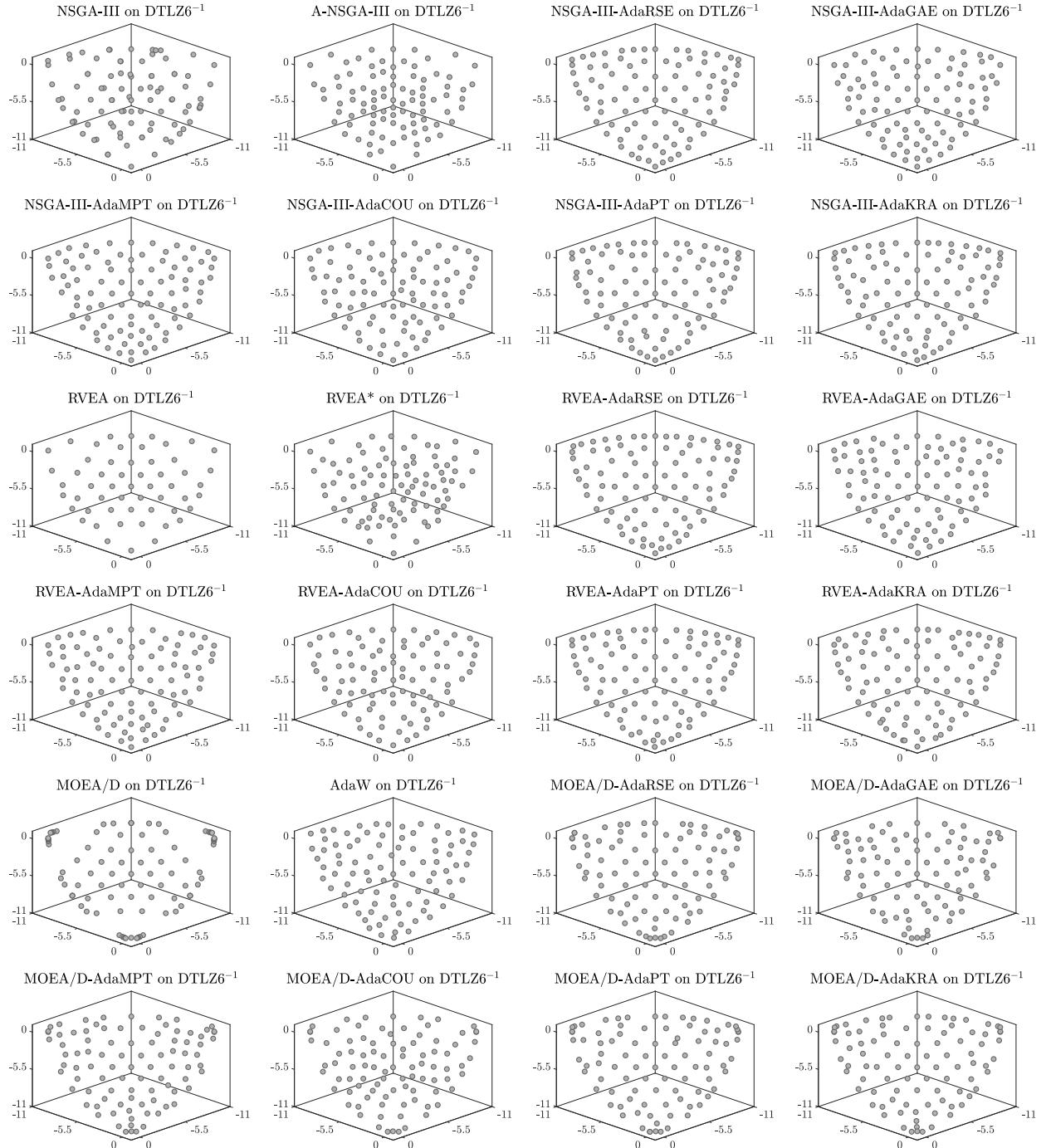


Figure 96: Final populations with the median HV value among 30 independent runs of MOEAs using the NSGA-III, RVEA, and MOEA/D frameworks on $DTLZ6^{-1}$ with 3 objective functions.

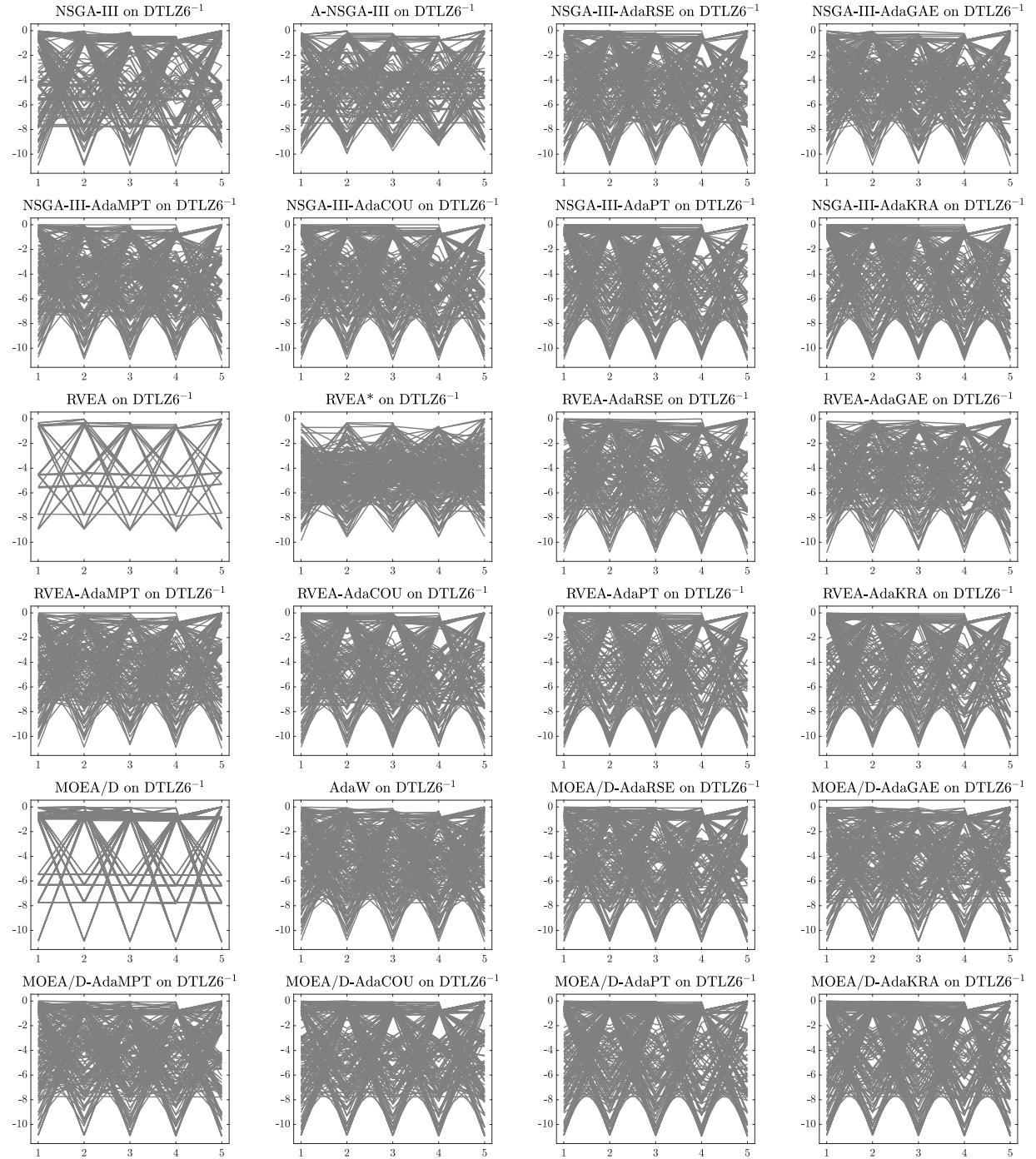


Figure 97: Final populations with the median HV value among 30 independent runs of MOEAs using the NSGA-III, RVEA, and MOEA/D frameworks on DTLZ6⁻¹ with 5 objective functions.

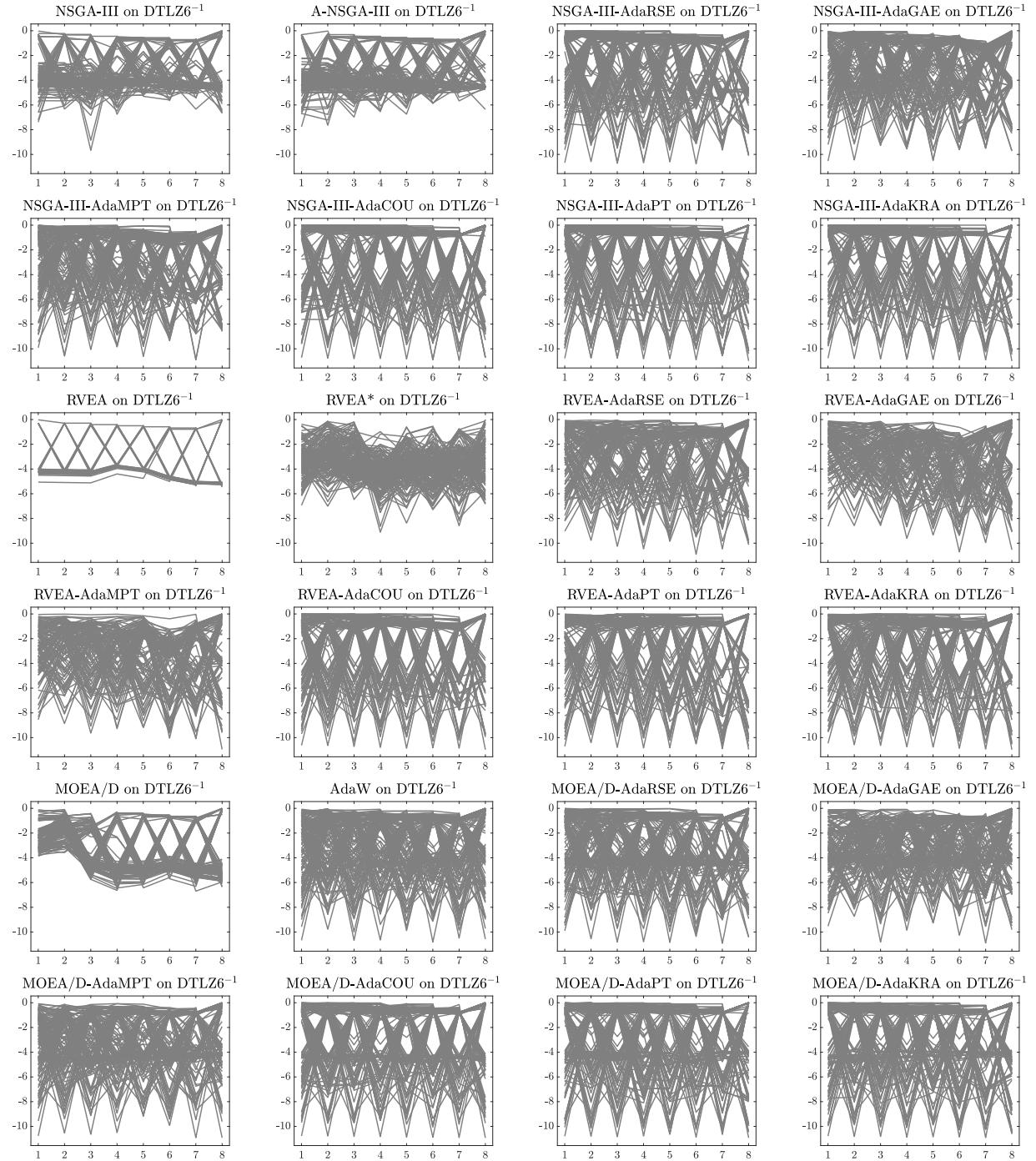


Figure 98: Final populations with the median HV value among 30 independent runs of MOEAs using the NSGA-III, RVEA, and MOEA/D frameworks on $DTLZ6^{-1}$ with 8 objective functions.

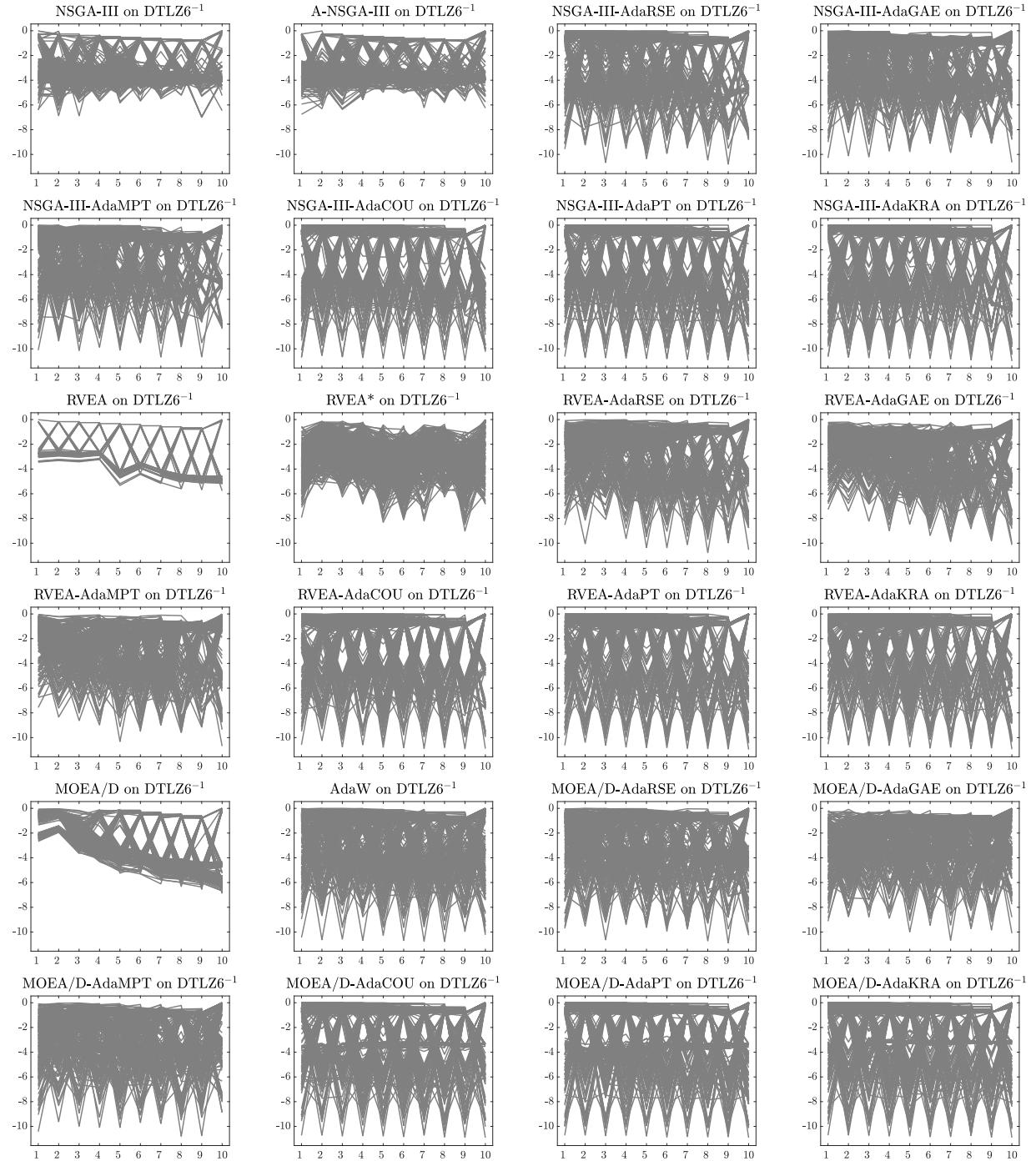


Figure 99: Final populations with the median HV value among 30 independent runs of MOEAs using the NSGA-III, RVEA, and MOEA/D frameworks on DTLZ6⁻¹ with 10 objective functions.

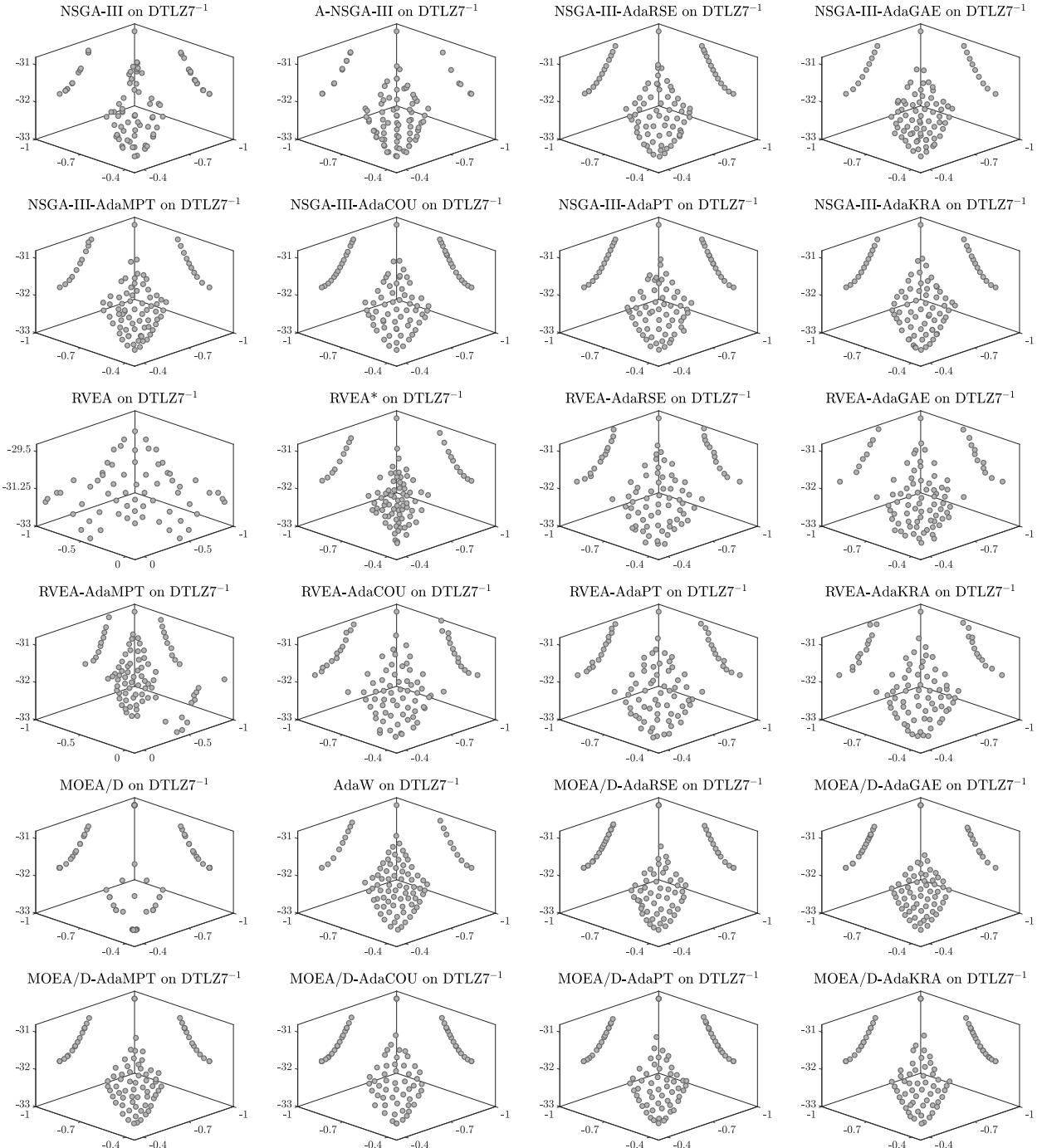


Figure 100: Final populations with the median HV value among 30 independent runs of MOEAs using the NSGA-III, RVEA, and MOEA/D frameworks on $DTLZ7^{-1}$ with 3 objective functions.

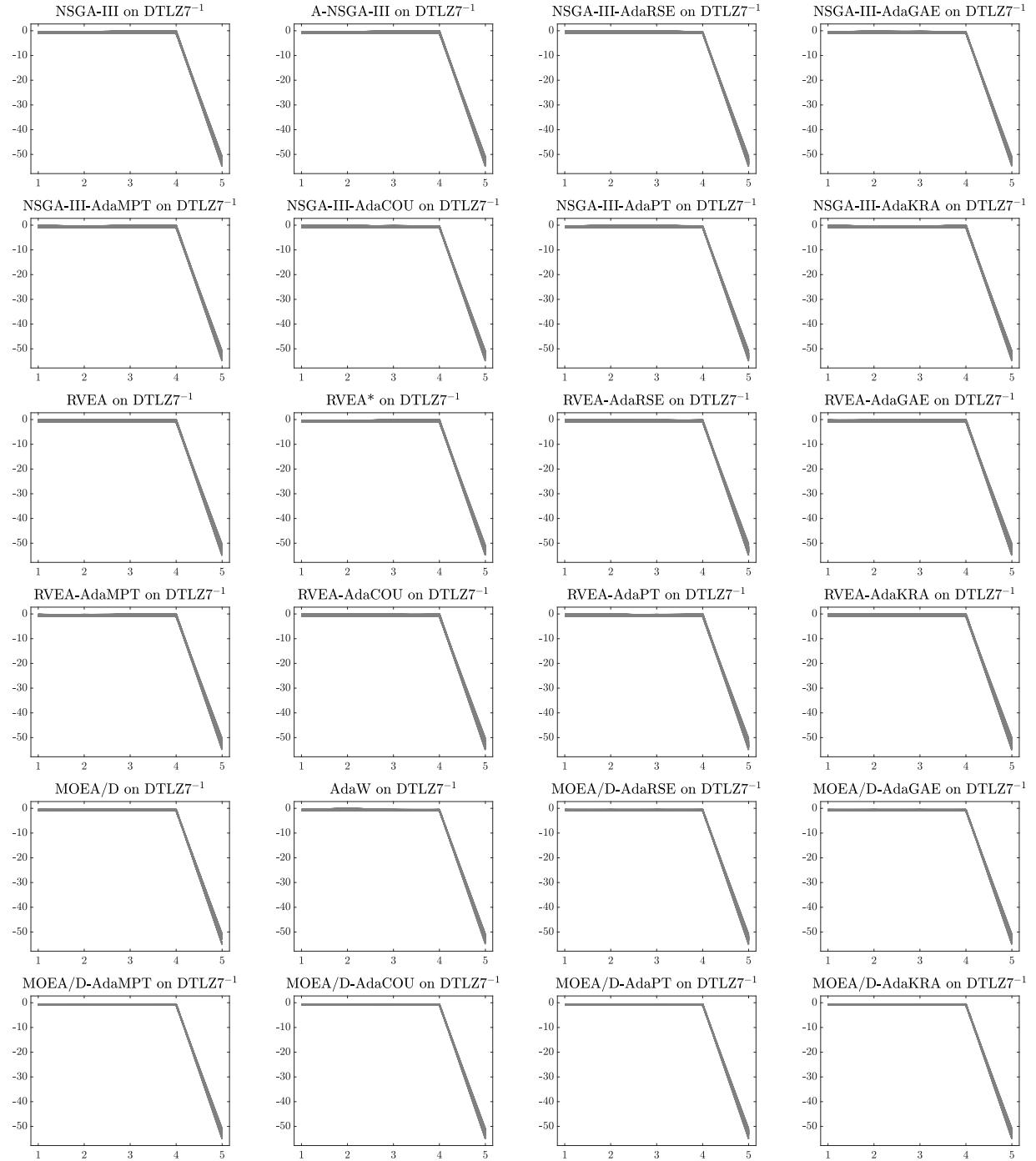


Figure 101: Final populations with the median HV value among 30 independent runs of MOEAs using the NSGA-III, RVEA, and MOEA/D frameworks on $DTLZ7^{-1}$ with 5 objective functions.

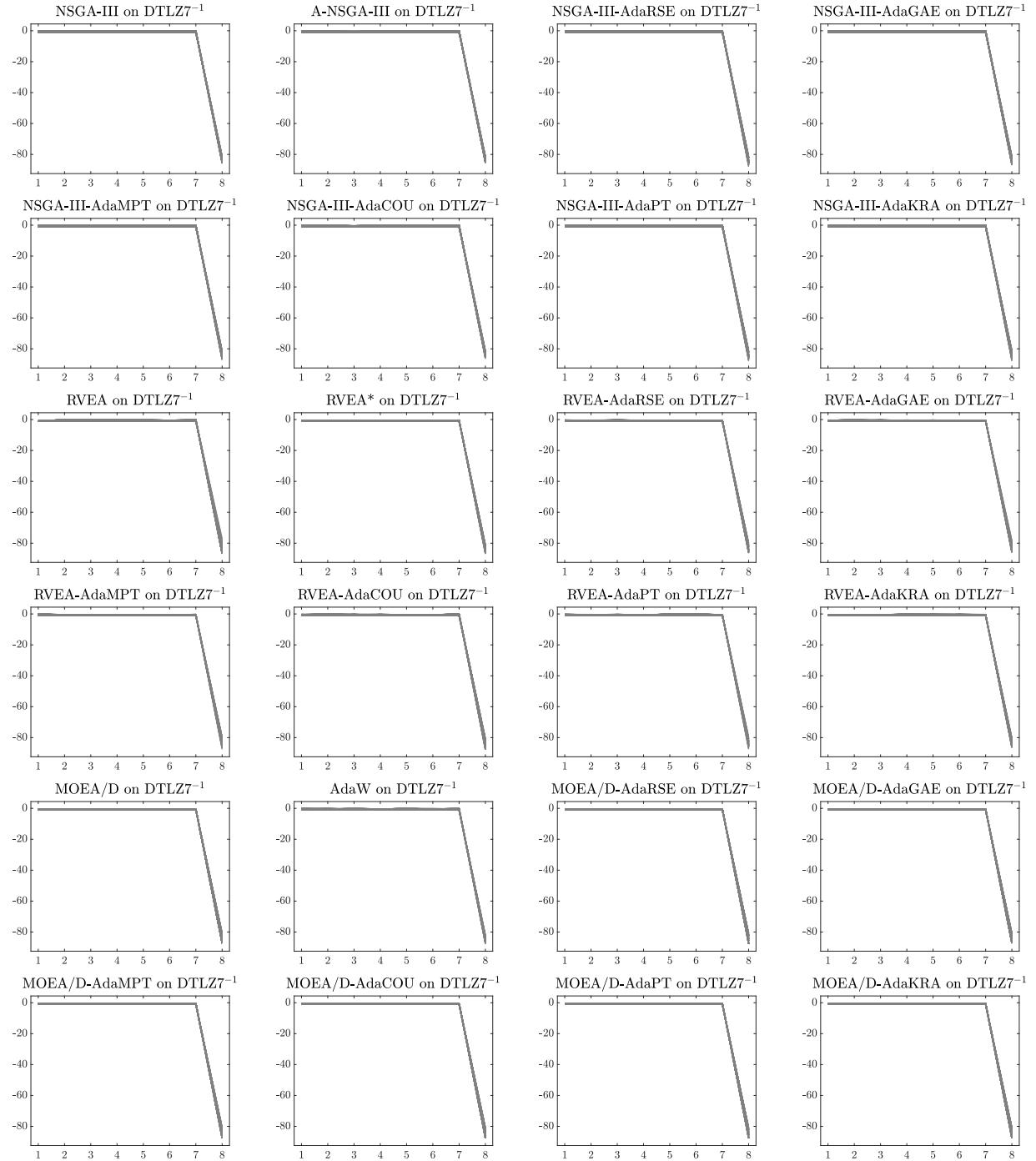


Figure 102: Final populations with the median HV value among 30 independent runs of MOEAs using the NSGA-III, RVEA, and MOEA/D frameworks on $DTLZ7^{-1}$ with 8 objective functions.

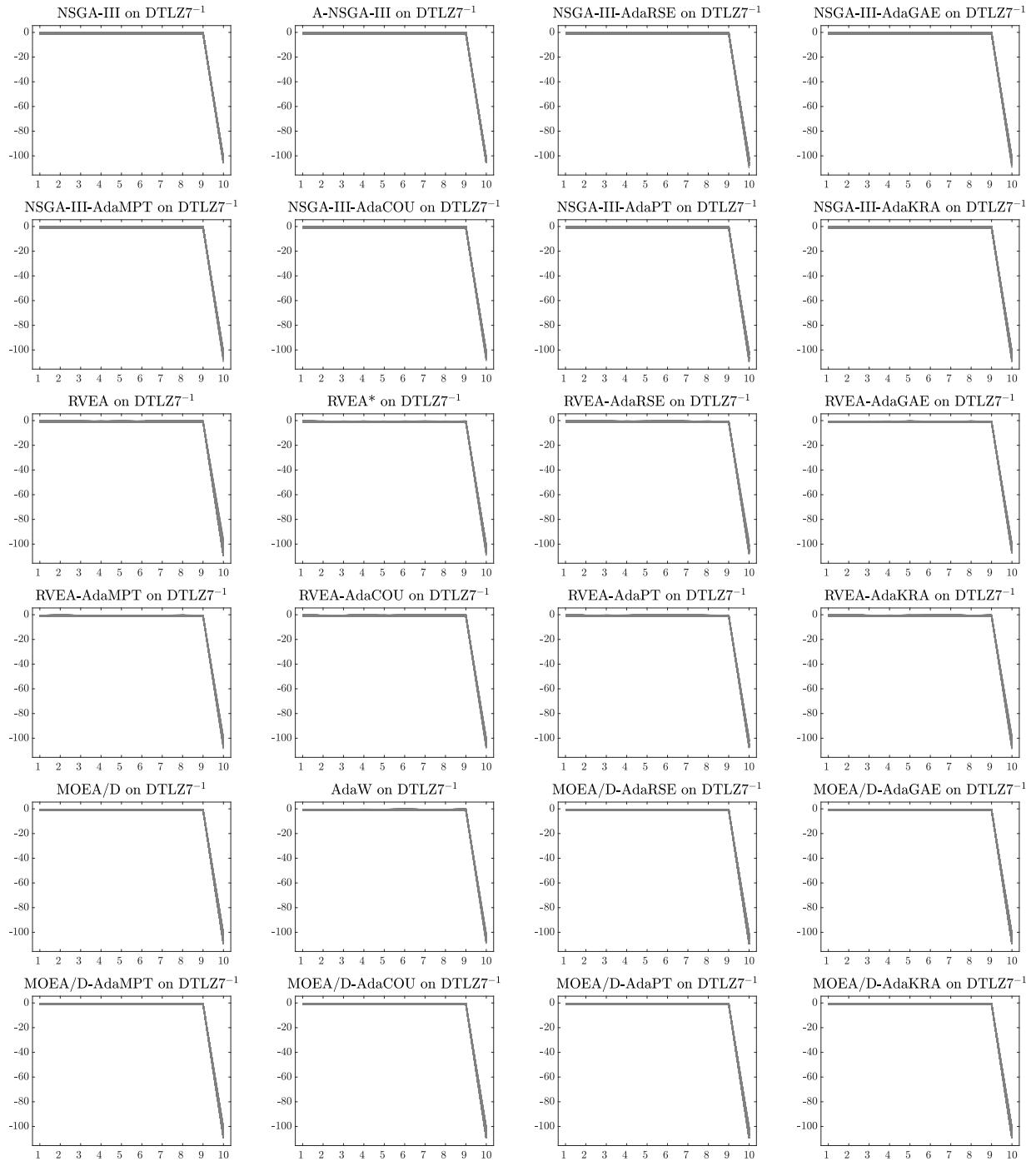


Figure 103: Final populations with the median HV value among 30 independent runs of MOEAs using the NSGA-III, RVEA, and MOEA/D frameworks on DTLZ7⁻¹ with 10 objective functions.

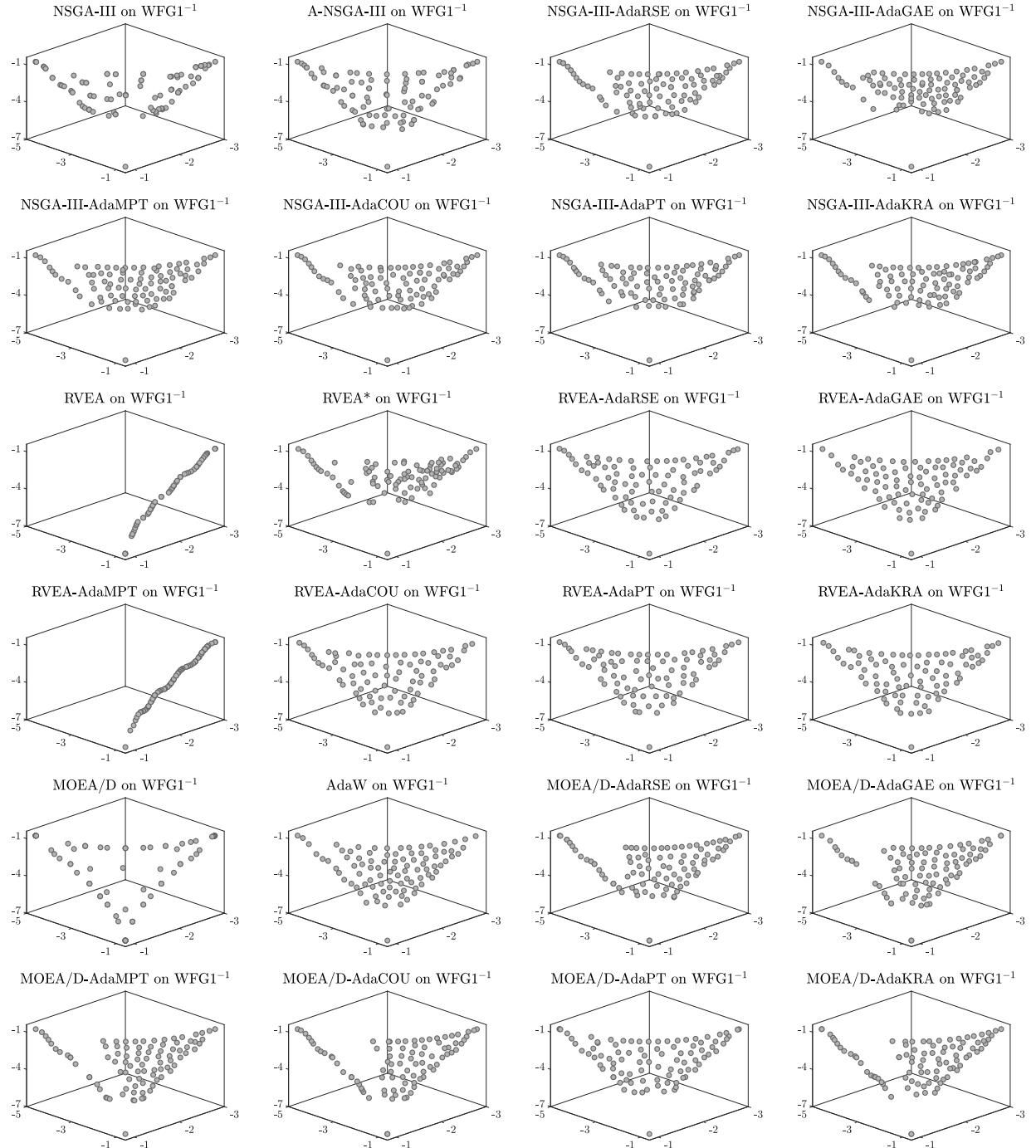


Figure 104: Final populations with the median HV value among 30 independent runs of MOEAs using the NSGA-III, RVEA, and MOEA/D frameworks on WFG1^{-1} with 3 objective functions.

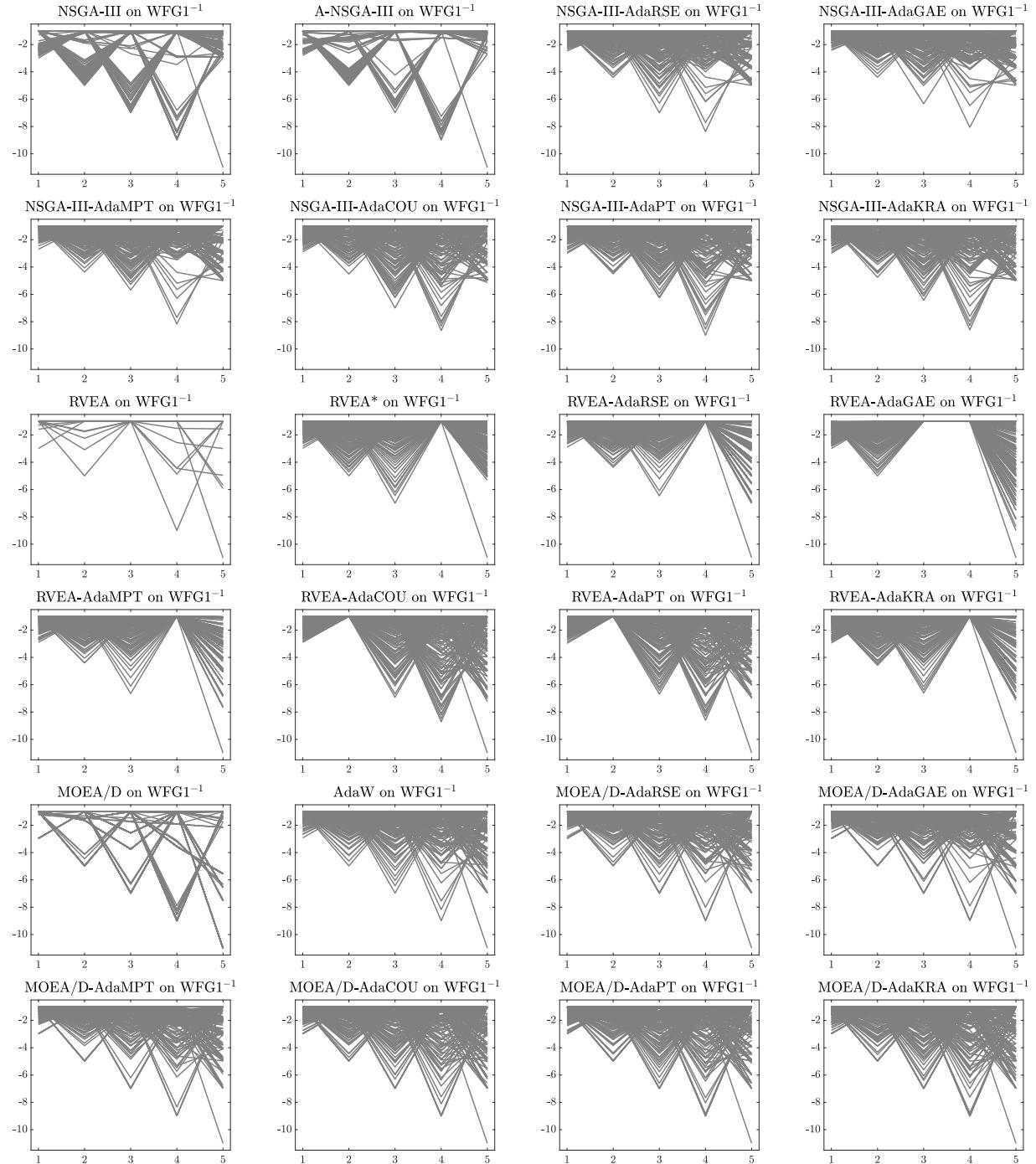


Figure 105: Final populations with the median HV value among 30 independent runs of MOEAs using the NSGA-III, RVEA, and MOEA/D frameworks on WFG1^{-1} with 5 objective functions.

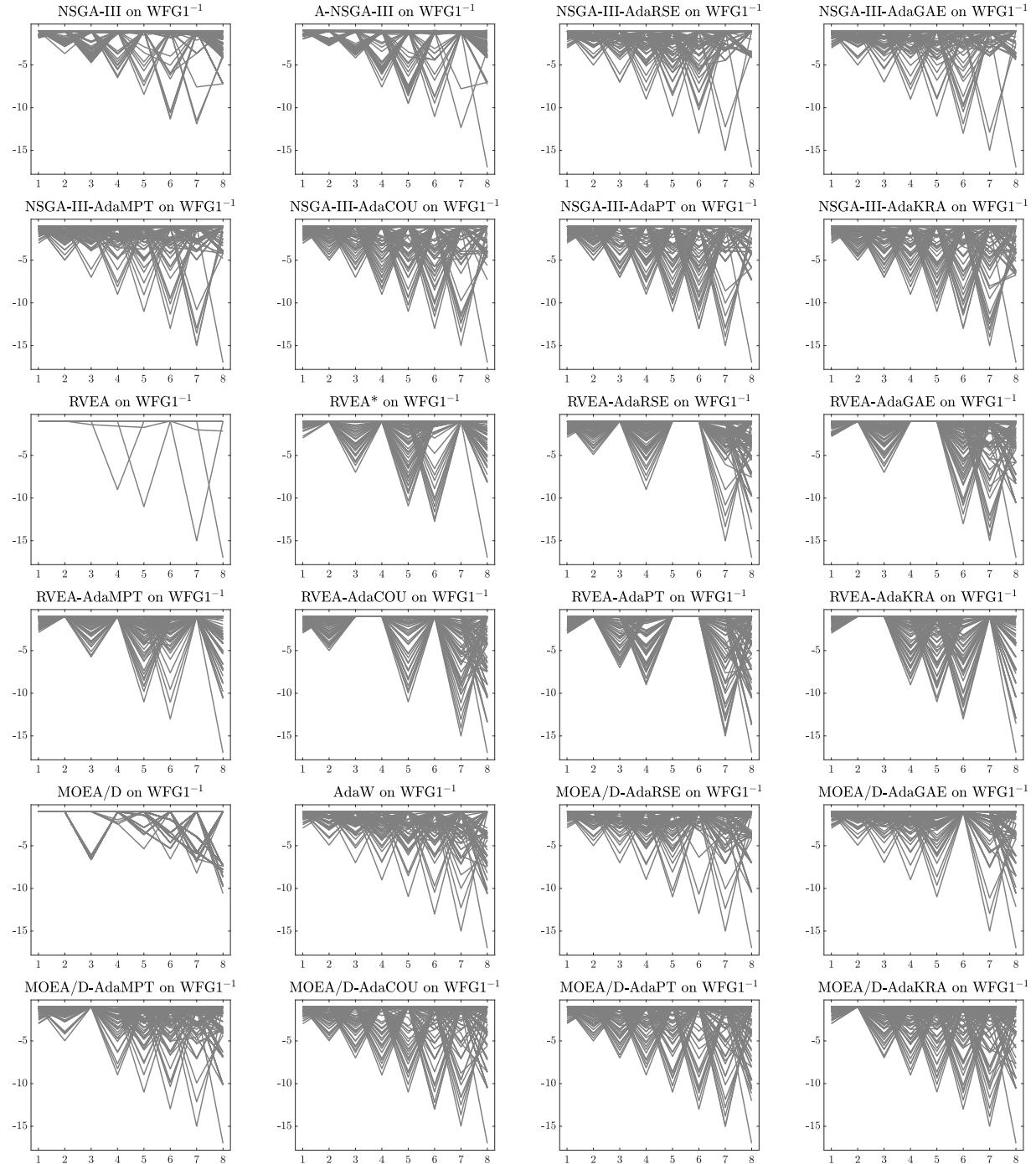


Figure 106: Final populations with the median HV value among 30 independent runs of MOEAs using the NSGA-III, RVEA, and MOEA/D frameworks on WFG1^{-1} with 8 objective functions.

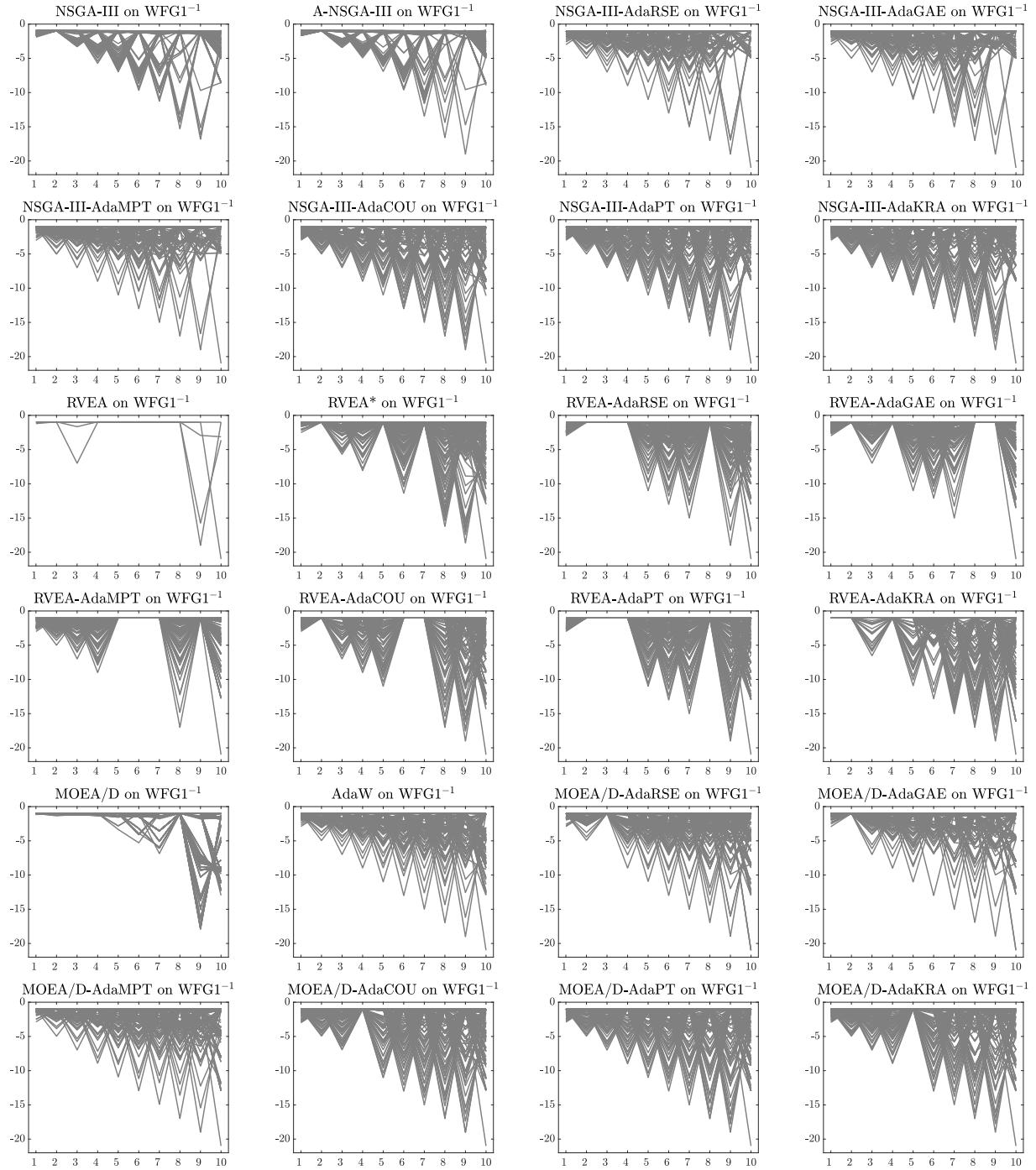


Figure 107: Final populations with the median HV value among 30 independent runs of MOEAs using the NSGA-III, RVEA, and MOEA/D frameworks on WFG1⁻¹ with 10 objective functions.

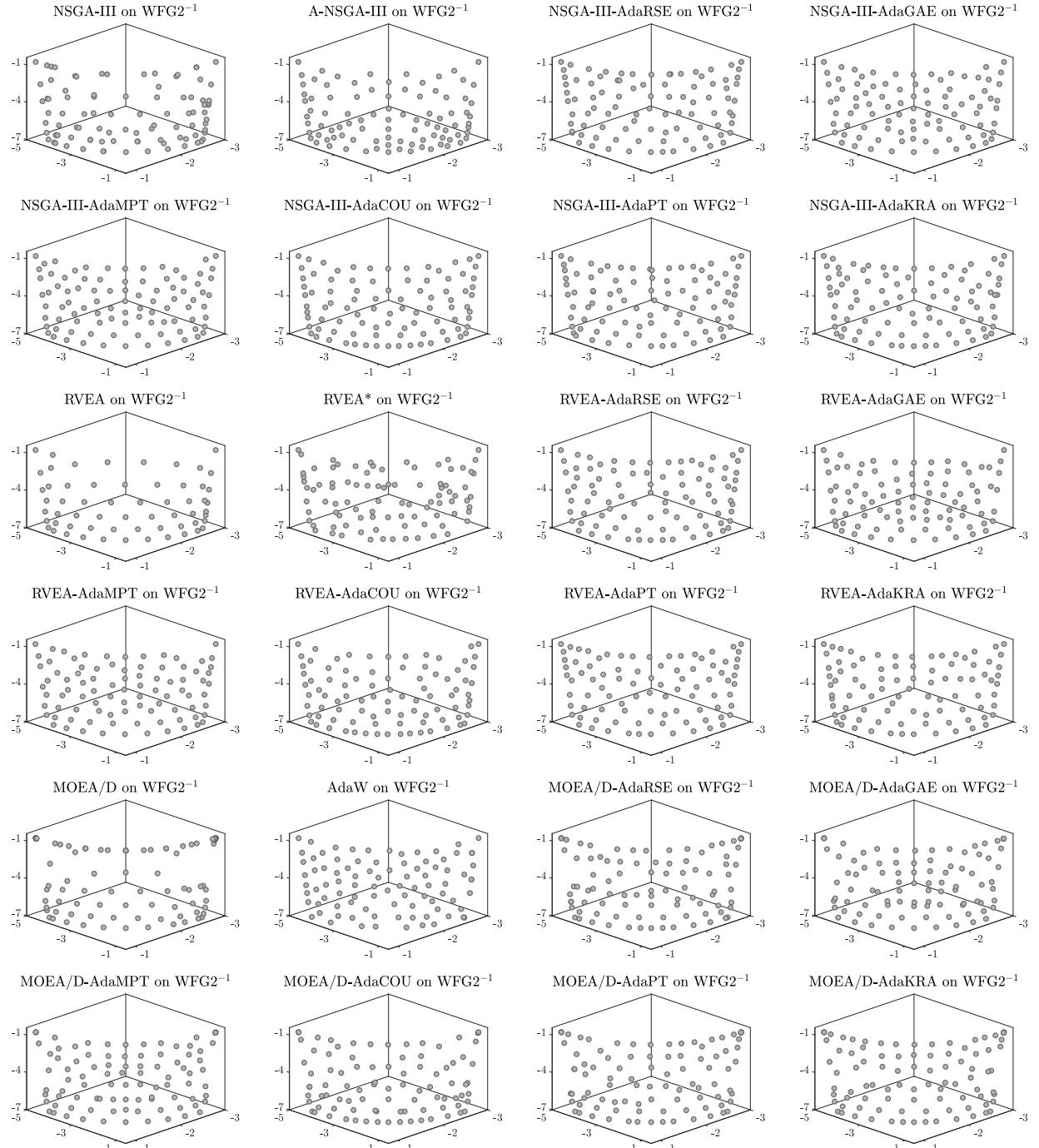


Figure 108: Final populations with the median HV value among 30 independent runs of MOEAs using the NSGA-III, RVEA, and MOEA/D frameworks on WFG2^{-1} with 3 objective functions.

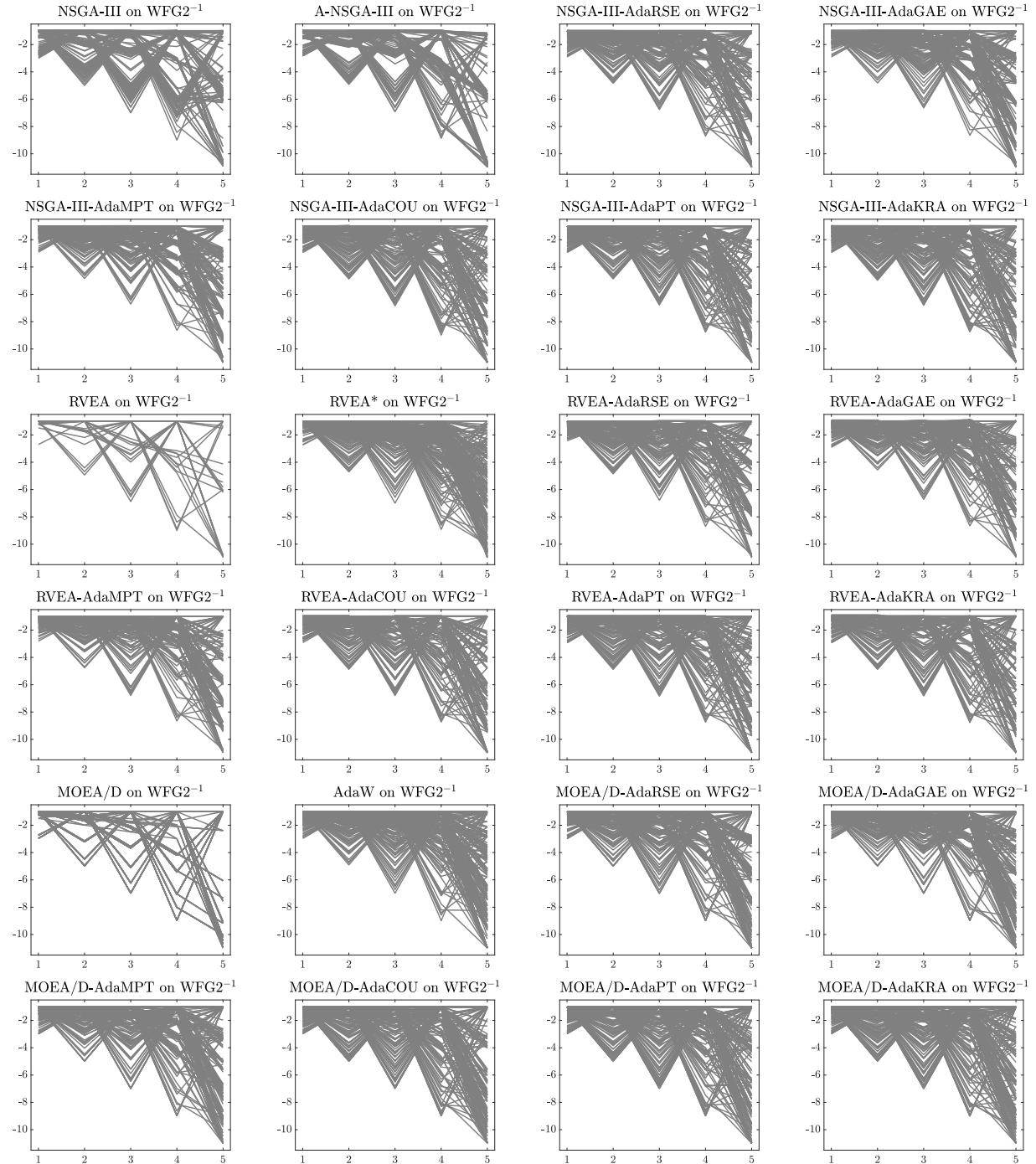


Figure 109: Final populations with the median HV value among 30 independent runs of MOEAs using the NSGA-III, RVEA, and MOEA/D frameworks on WFG2^{-1} with 5 objective functions.

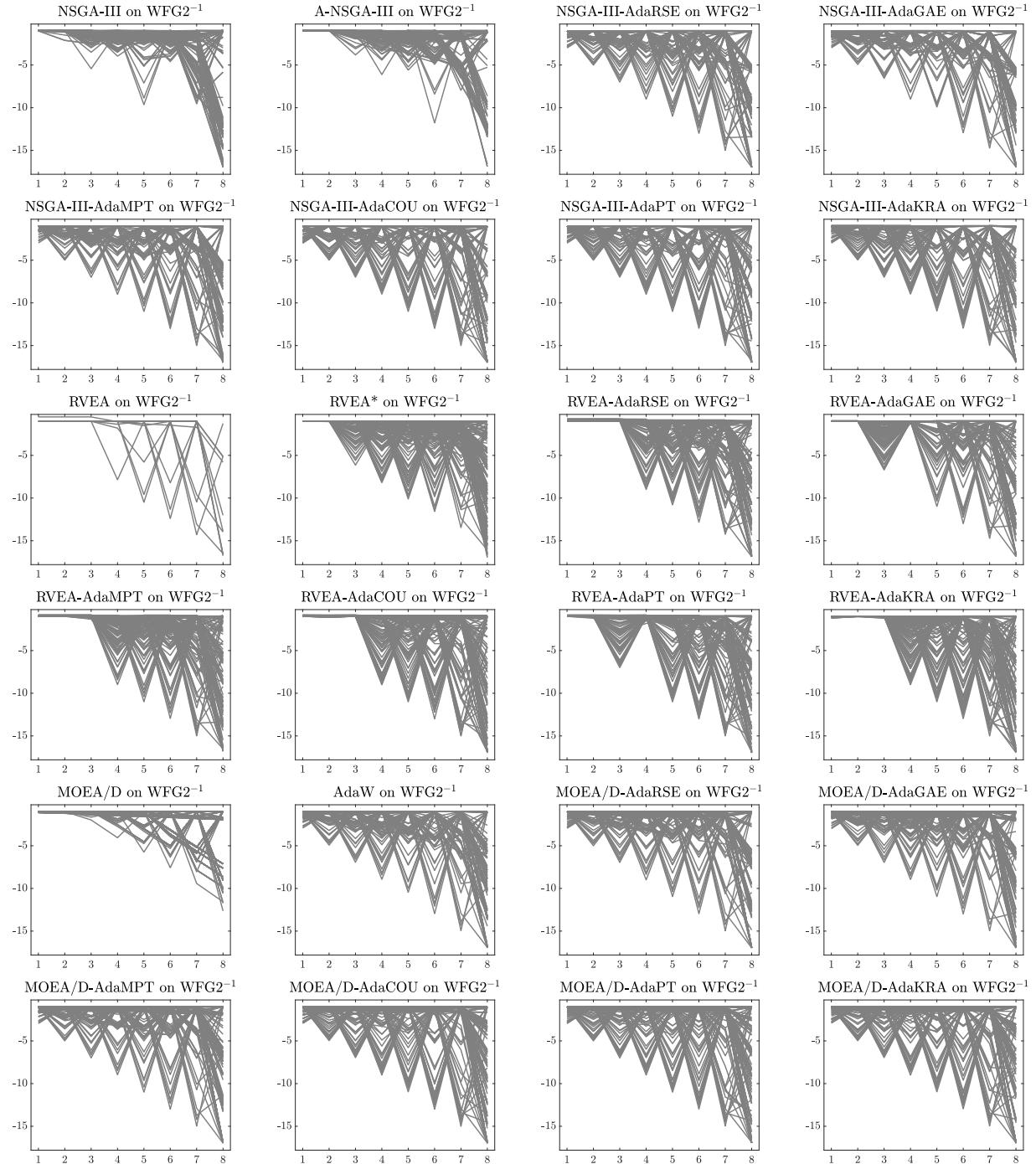


Figure 110: Final populations with the median HV value among 30 independent runs of MOEAs using the NSGA-III, RVEA, and MOEA/D frameworks on WFG2^{-1} with 8 objective functions.

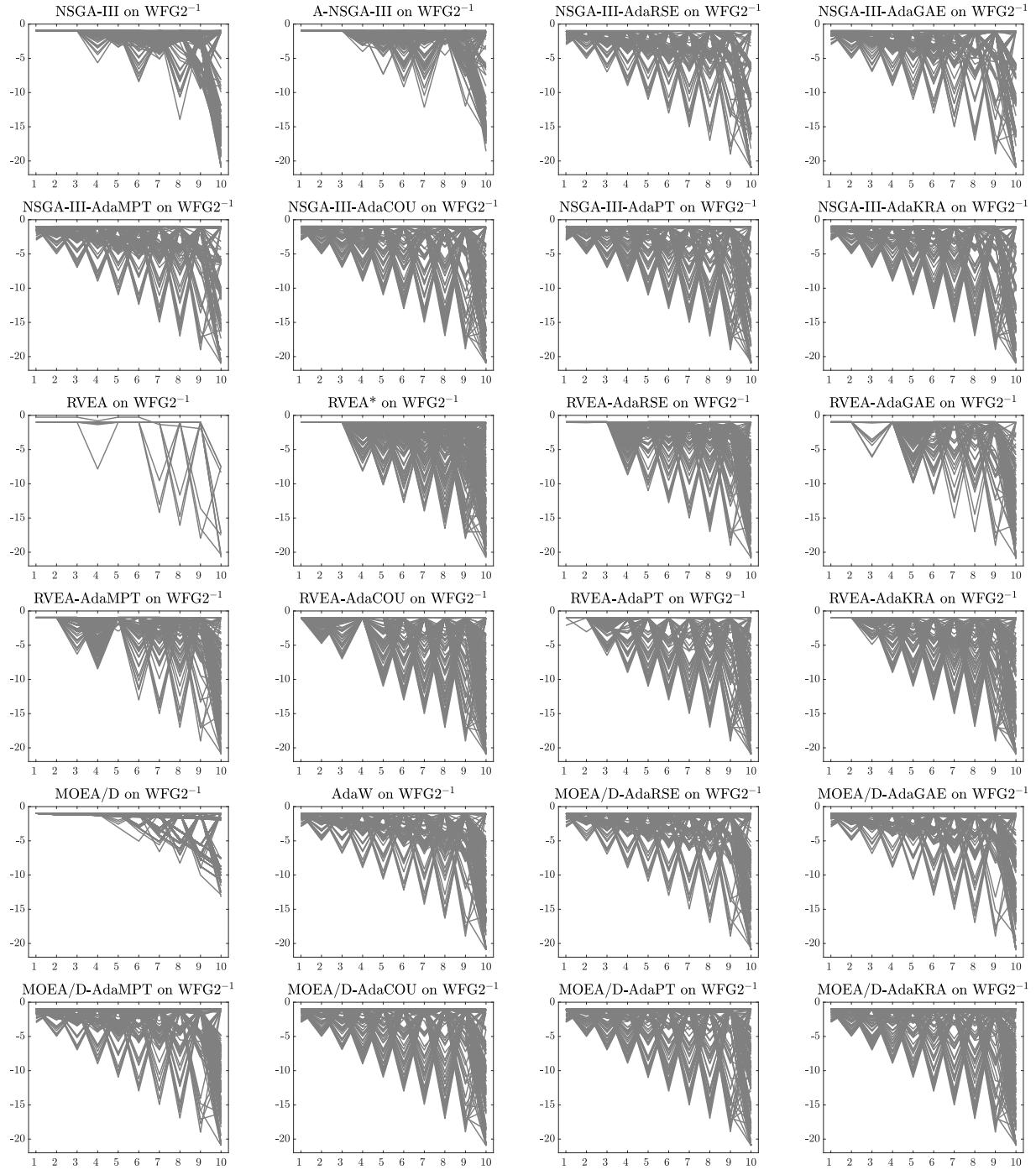


Figure 111: Final populations with the median HV value among 30 independent runs of MOEAs using the NSGA-III, RVEA, and MOEA/D frameworks on WFG2^{-1} with 10 objective functions.

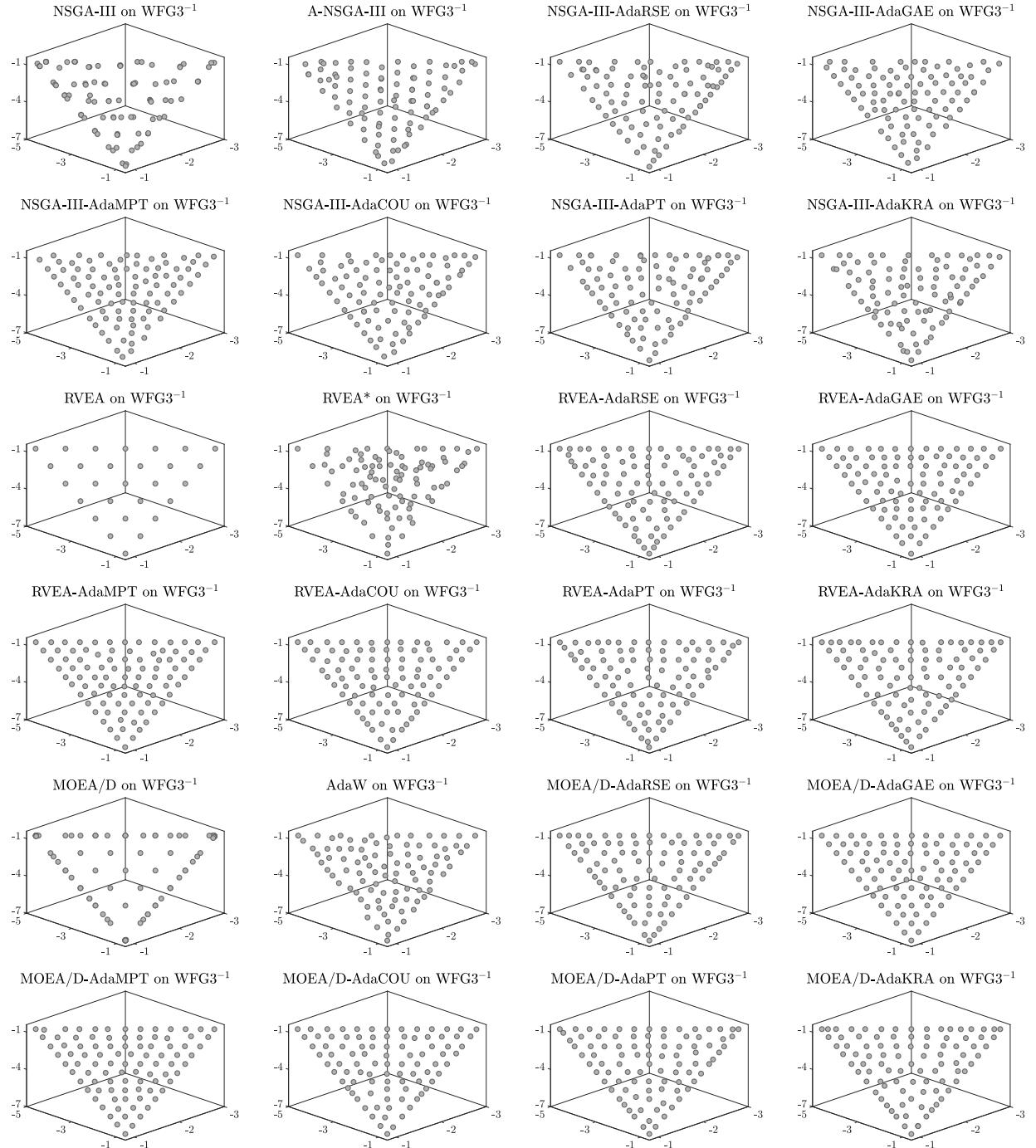


Figure 112: Final populations with the median HV value among 30 independent runs of MOEAs using the NSGA-III, RVEA, and MOEA/D frameworks on WFG3^{-1} with 3 objective functions.

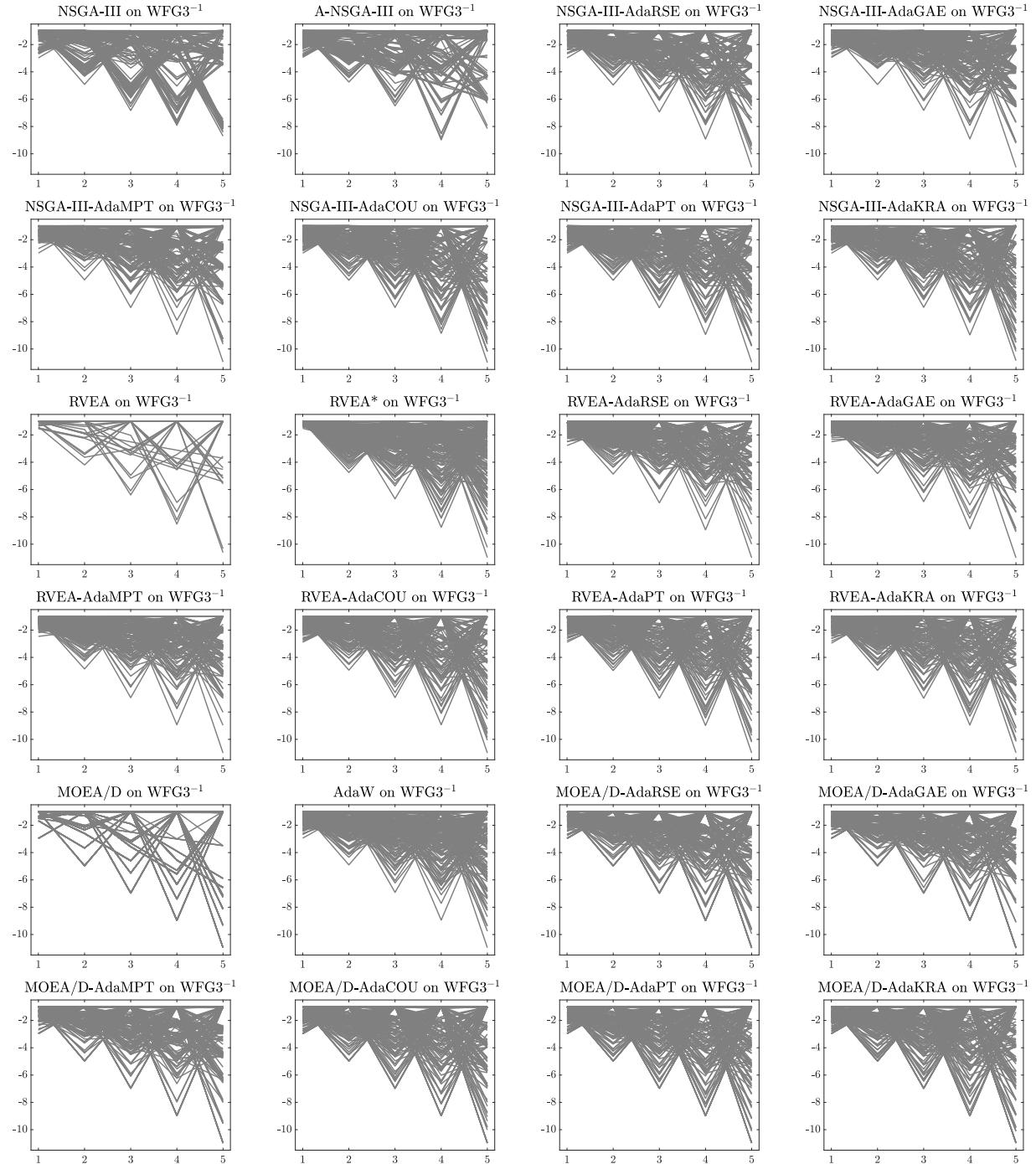


Figure 113: Final populations with the median HV value among 30 independent runs of MOEAs using the NSGA-III, RVEA, and MOEA/D frameworks on WFG3^{-1} with 5 objective functions.

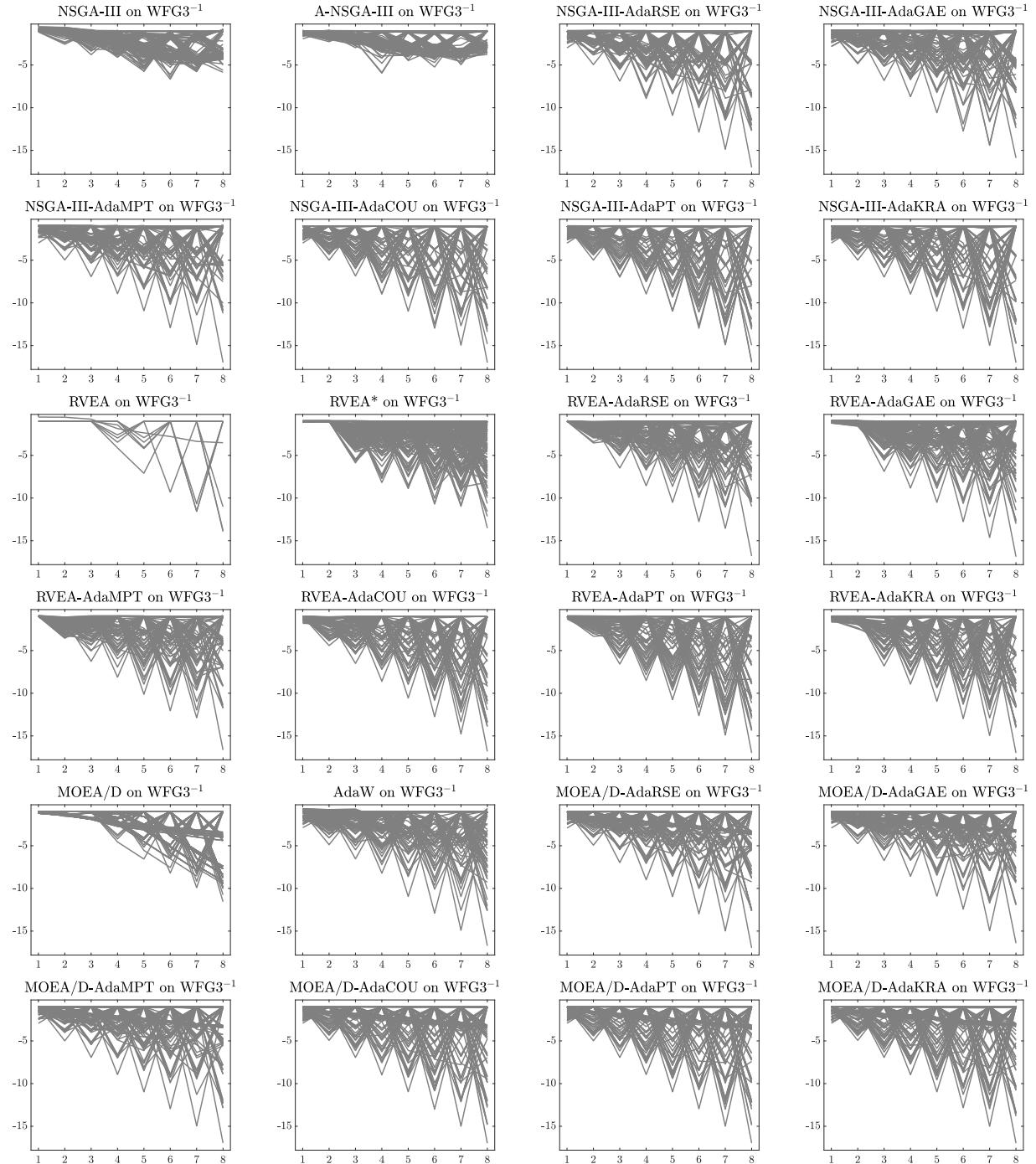


Figure 114: Final populations with the median HV value among 30 independent runs of MOEAs using the NSGA-III, RVEA, and MOEA/D frameworks on WFG3⁻¹ with 8 objective functions.

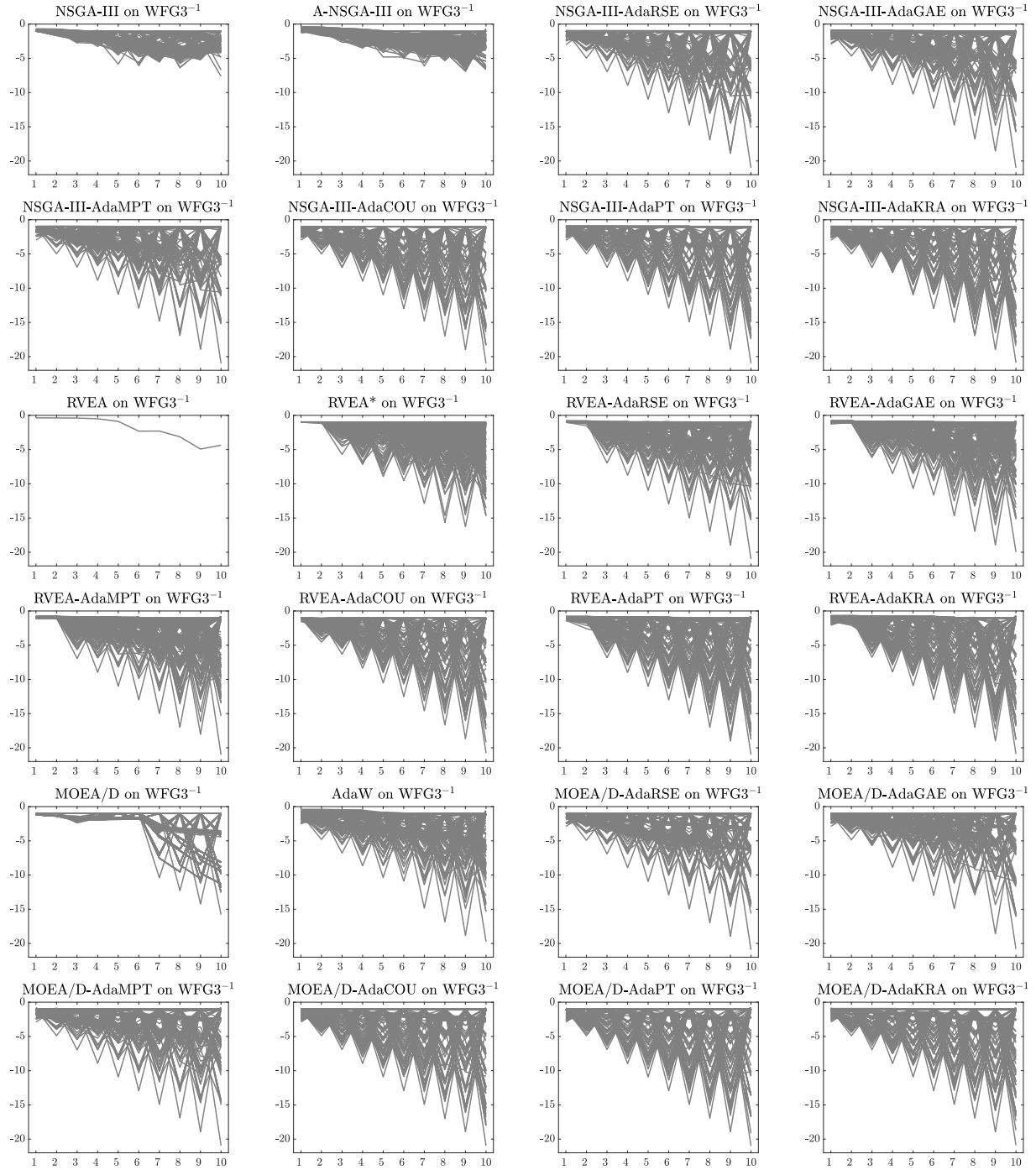


Figure 115: Final populations with the median HV value among 30 independent runs of MOEAs using the NSGA-III, RVEA, and MOEA/D frameworks on WFG3^{-1} with 10 objective functions.

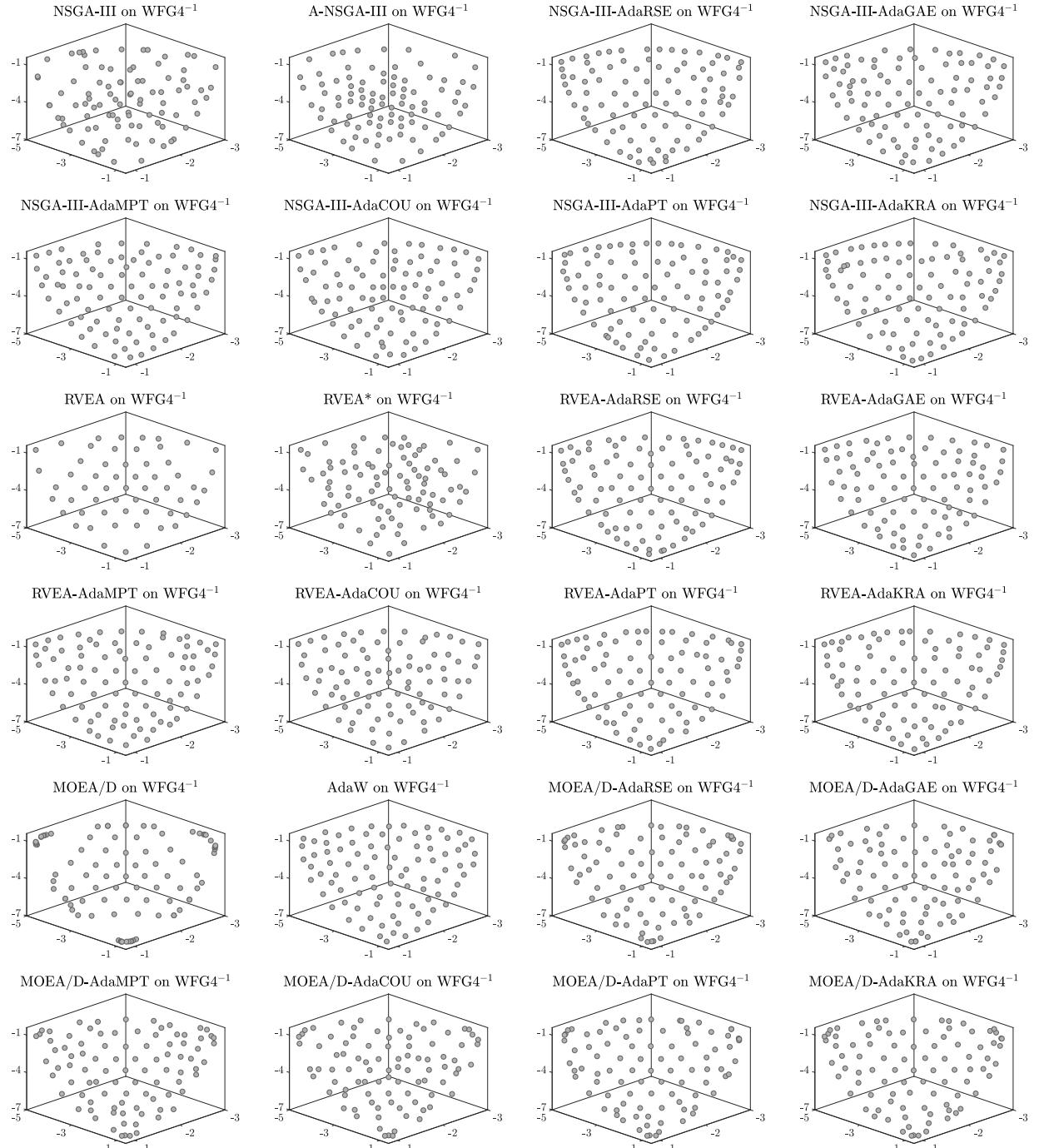


Figure 116: Final populations with the median HV value among 30 independent runs of MOEAs using the NSGA-III, RVEA, and MOEA/D frameworks on WFG4^{-1} with 3 objective functions.

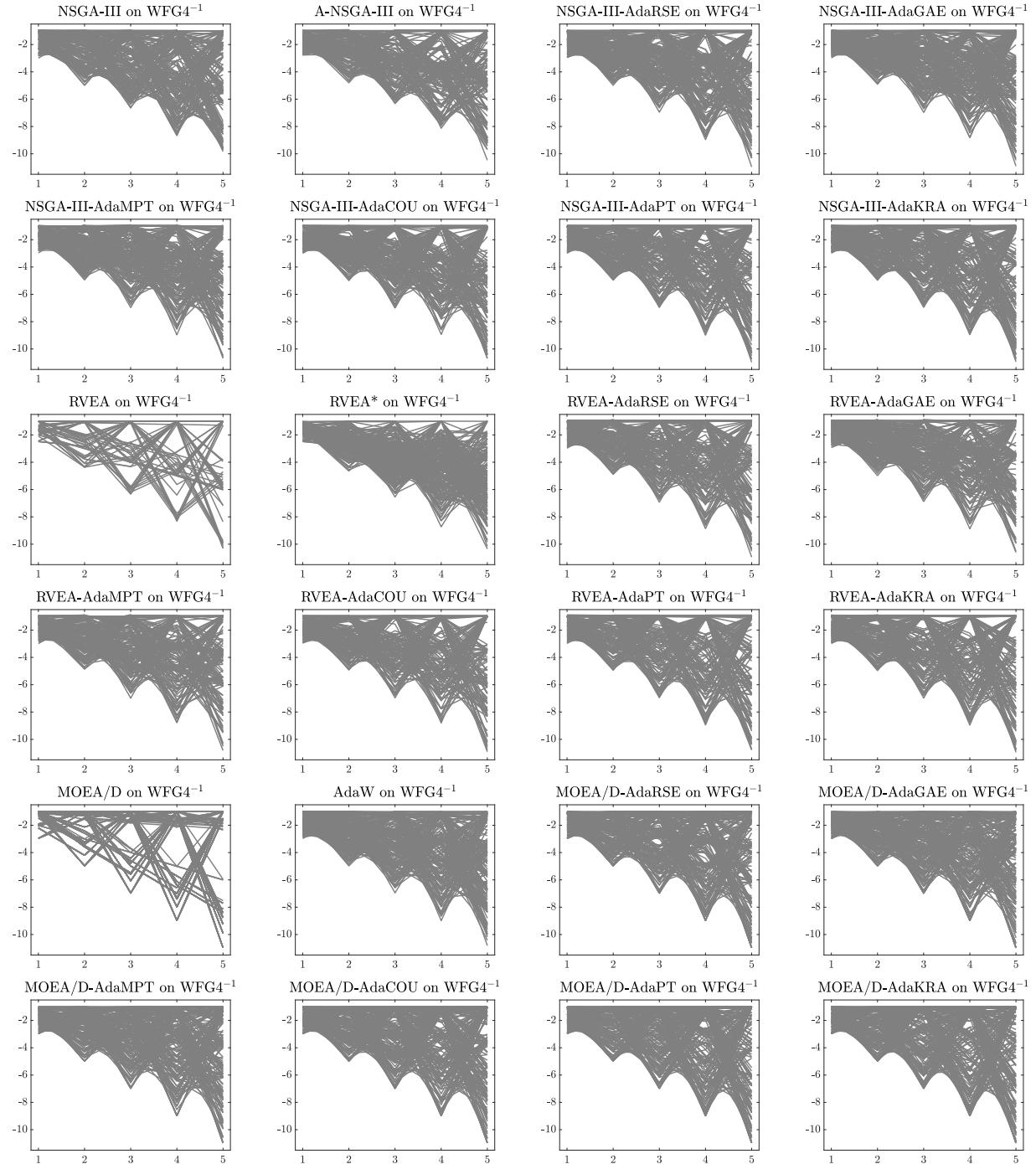


Figure 117: Final populations with the median HV value among 30 independent runs of MOEAs using the NSGA-III, RVEA, and MOEA/D frameworks on WFG4^{-1} with 5 objective functions.

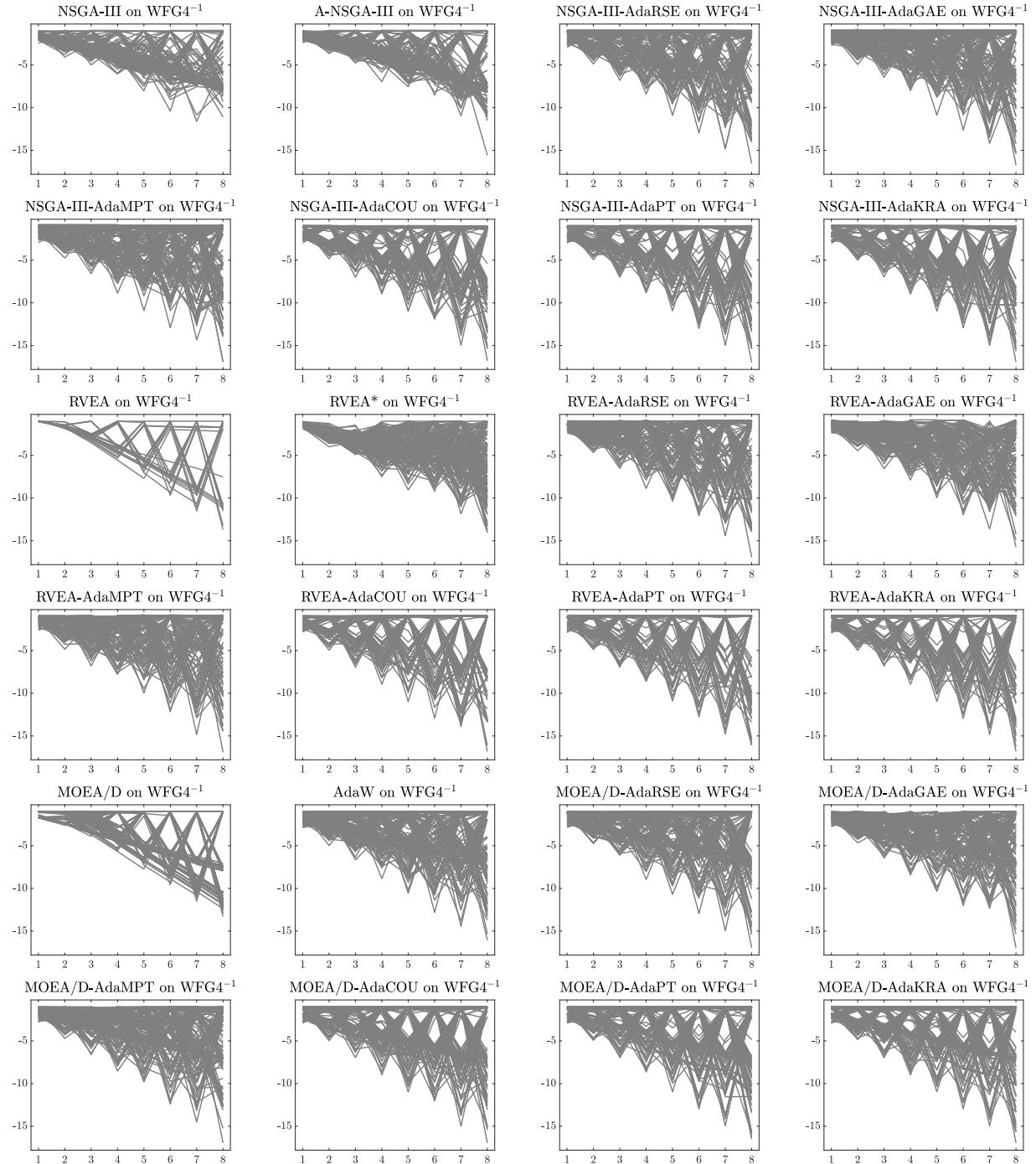


Figure 118: Final populations with the median HV value among 30 independent runs of MOEAs using the NSGA-III, RVEA, and MOEA/D frameworks on WFG4^{-1} with 8 objective functions.

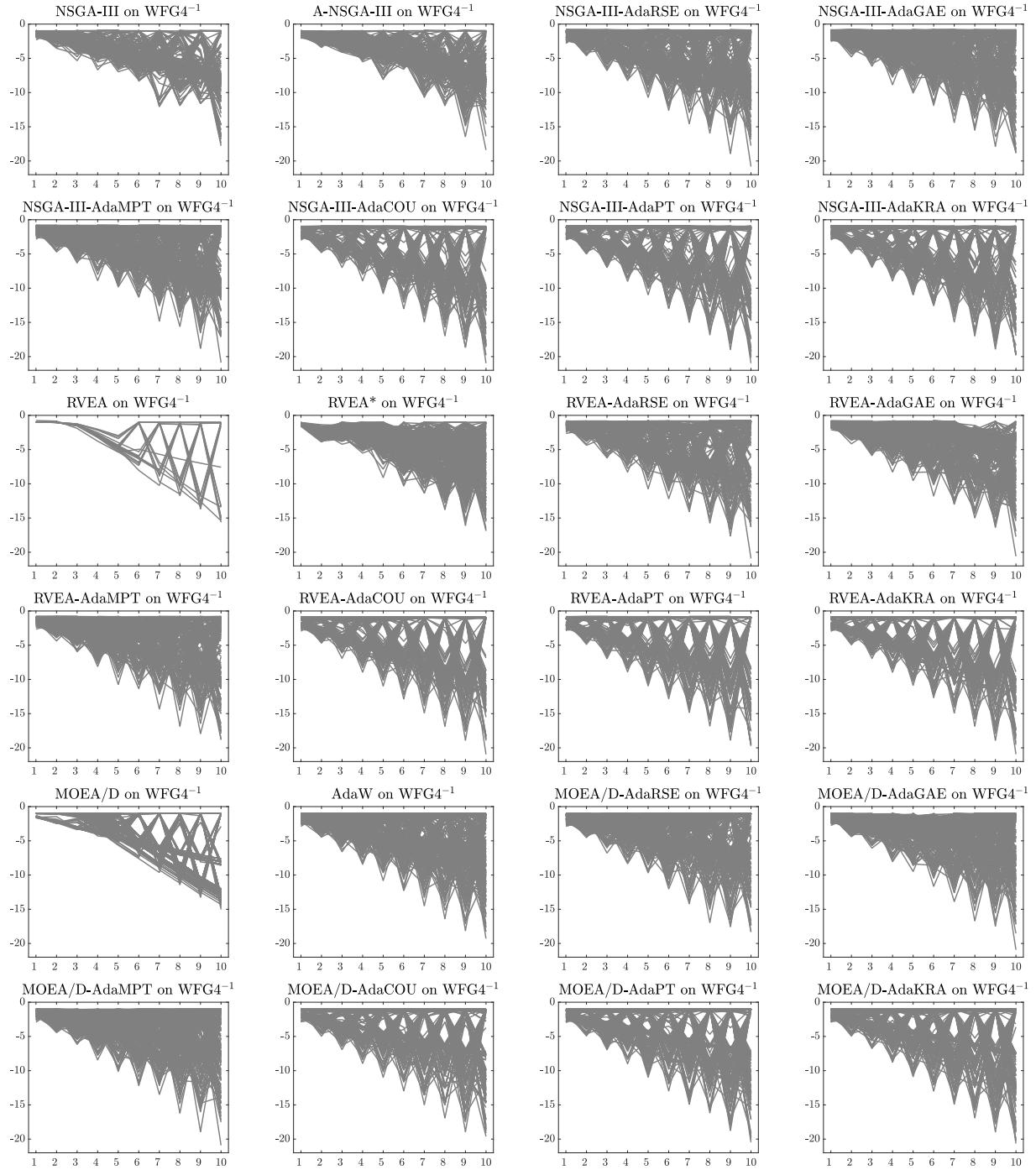


Figure 119: Final populations with the median HV value among 30 independent runs of MOEAs using the NSGA-III, RVEA, and MOEA/D frameworks on WFG4⁻¹ with 10 objective functions.

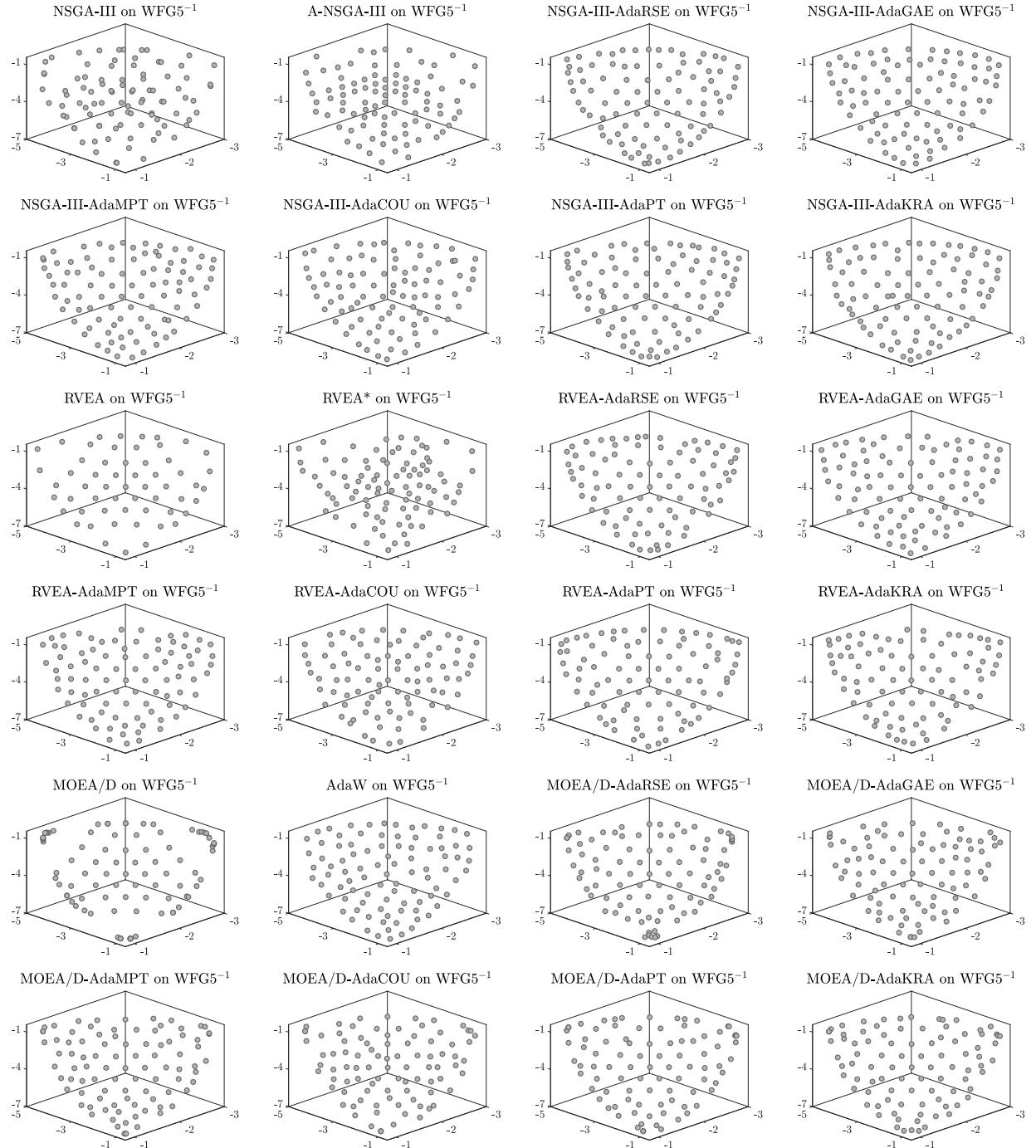


Figure 120: Final populations with the median HV value among 30 independent runs of MOEAs using the NSGA-III, RVEA, and MOEA/D frameworks on WFG5⁻¹ with 3 objective functions.

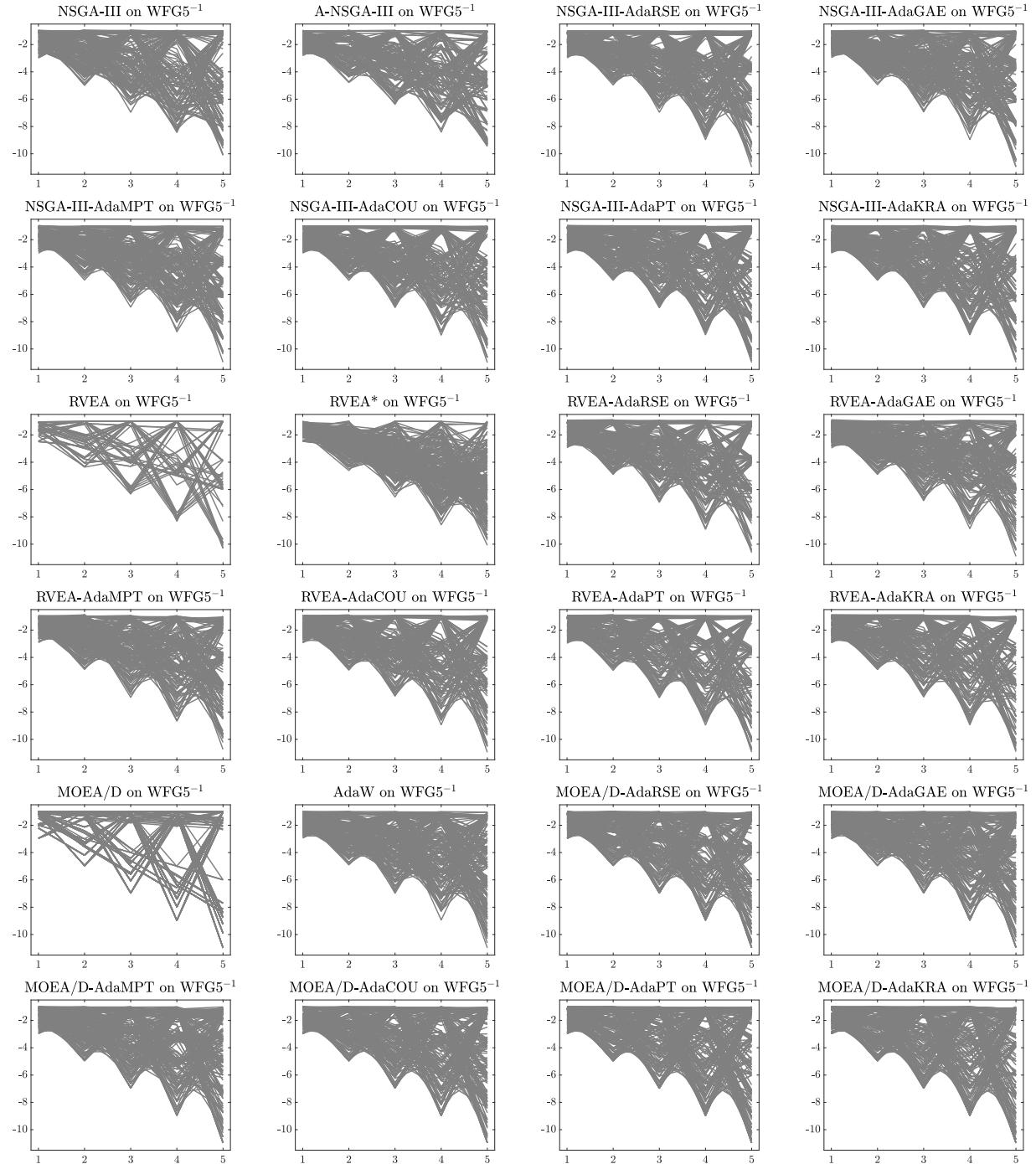


Figure 121: Final populations with the median HV value among 30 independent runs of MOEAs using the NSGA-III, RVEA, and MOEA/D frameworks on WFG5^{-1} with 5 objective functions.

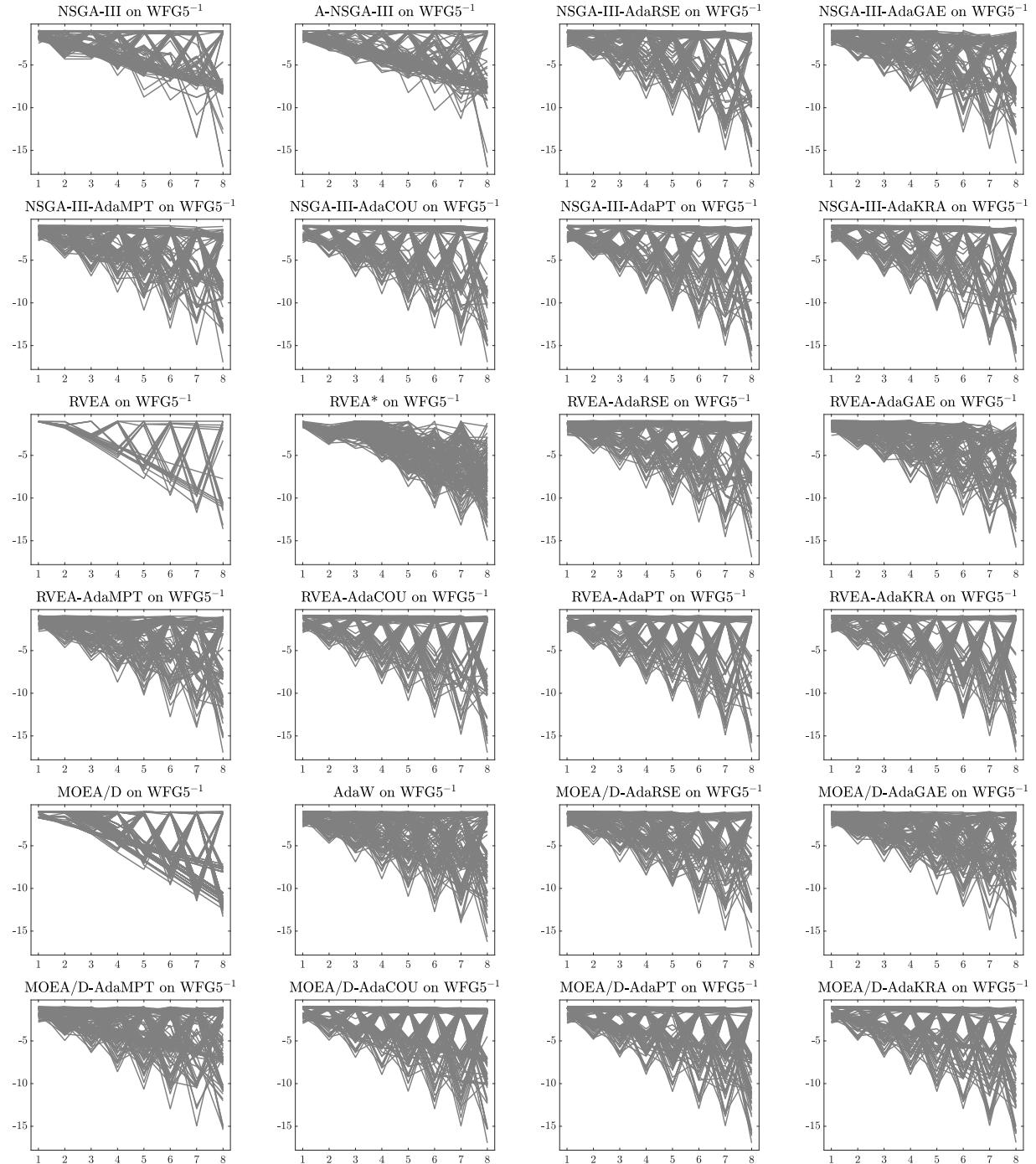


Figure 122: Final populations with the median HV value among 30 independent runs of MOEAs using the NSGA-III, RVEA, and MOEA/D frameworks on WFG5^{-1} with 8 objective functions.

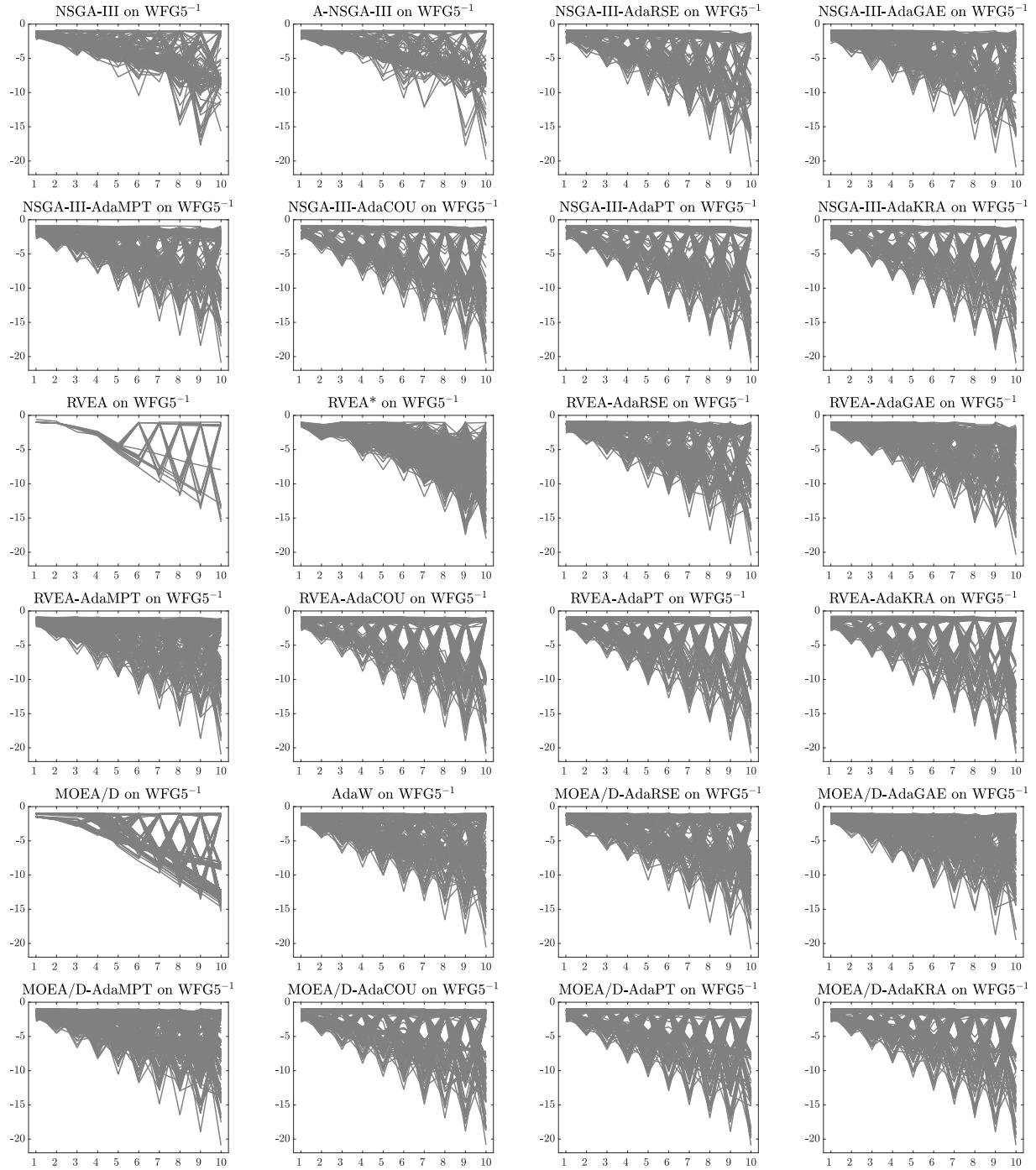


Figure 123: Final populations with the median HV value among 30 independent runs of MOEAs using the NSGA-III, RVEA, and MOEA/D frameworks on WFG5⁻¹ with 10 objective functions.

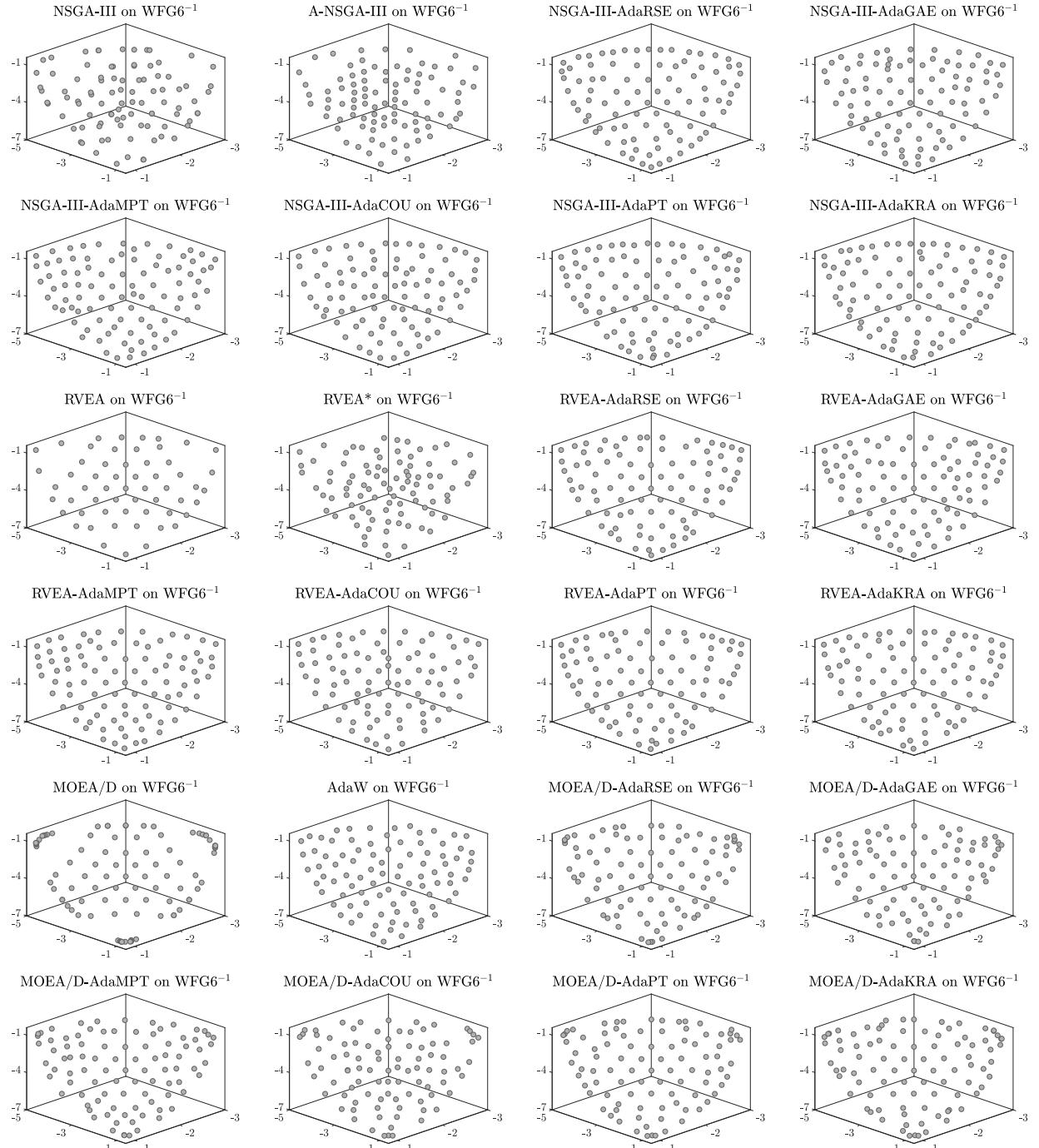


Figure 124: Final populations with the median HV value among 30 independent runs of MOEAs using the NSGA-III, RVEA, and MOEA/D frameworks on WFG6^{-1} with 3 objective functions.

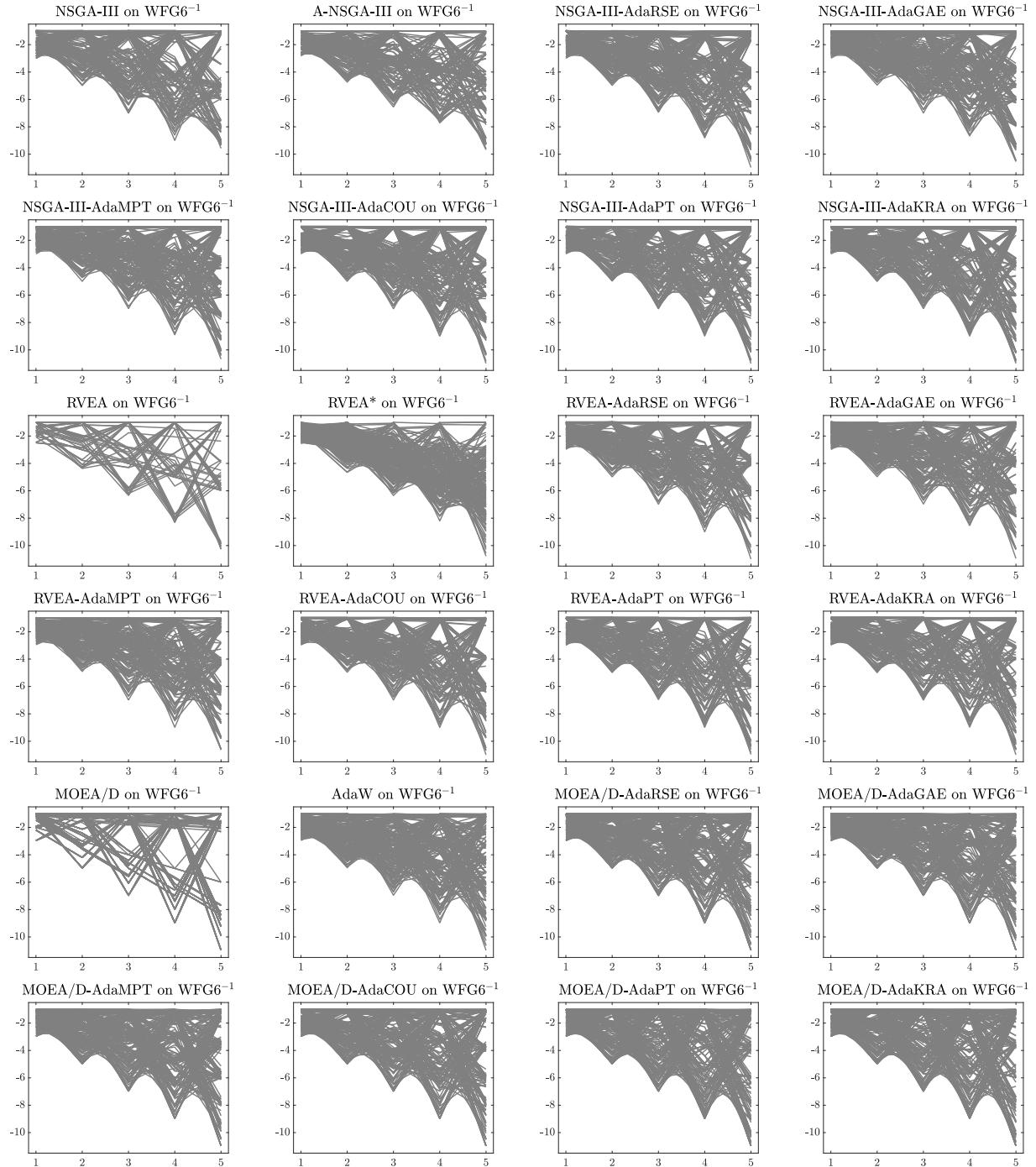


Figure 125: Final populations with the median HV value among 30 independent runs of MOEAs using the NSGA-III, RVEA, and MOEA/D frameworks on WFG6^{-1} with 5 objective functions.

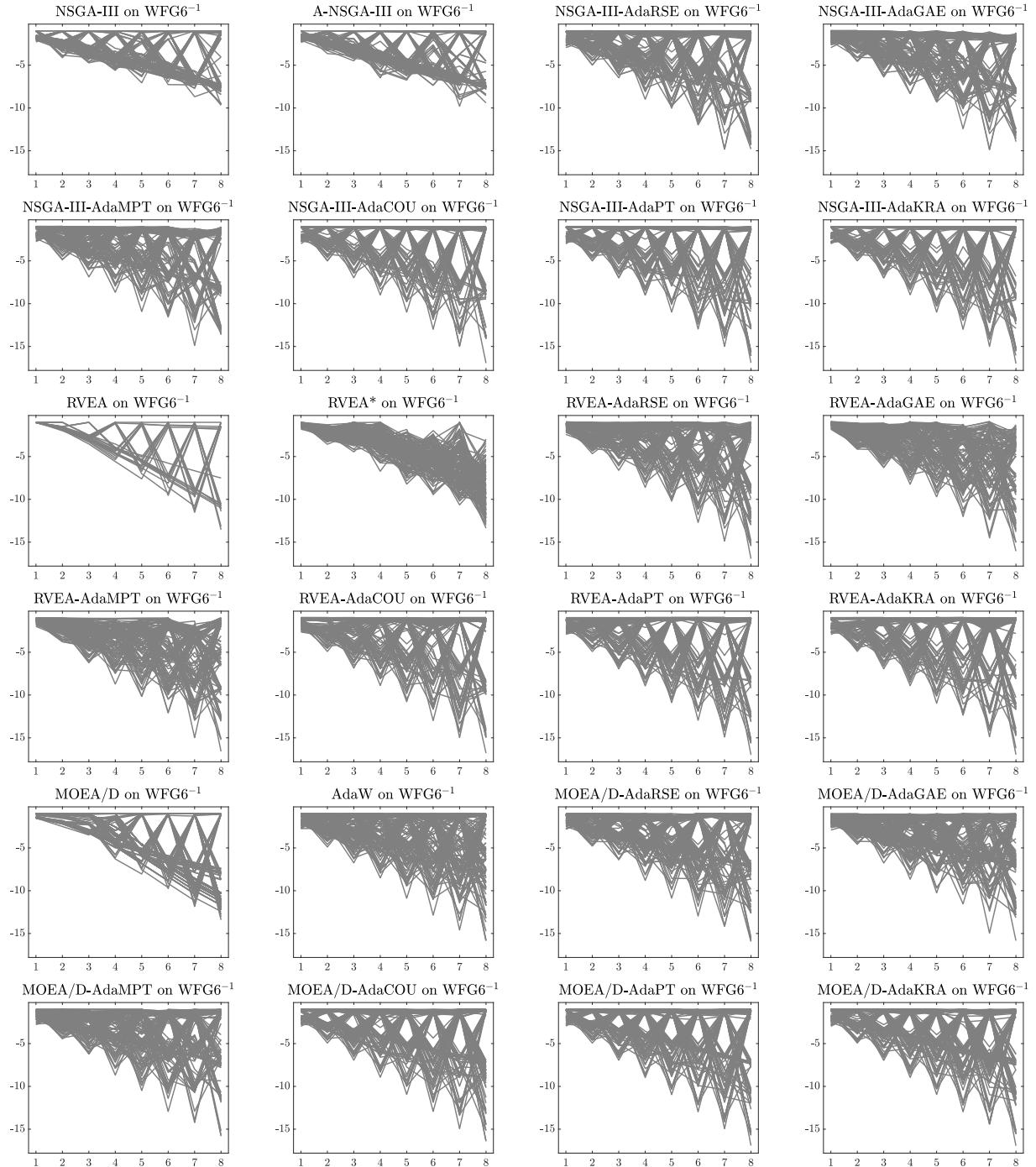


Figure 126: Final populations with the median HV value among 30 independent runs of MOEAs using the NSGA-III, RVEA, and MOEA/D frameworks on WFG6^{-1} with 8 objective functions.

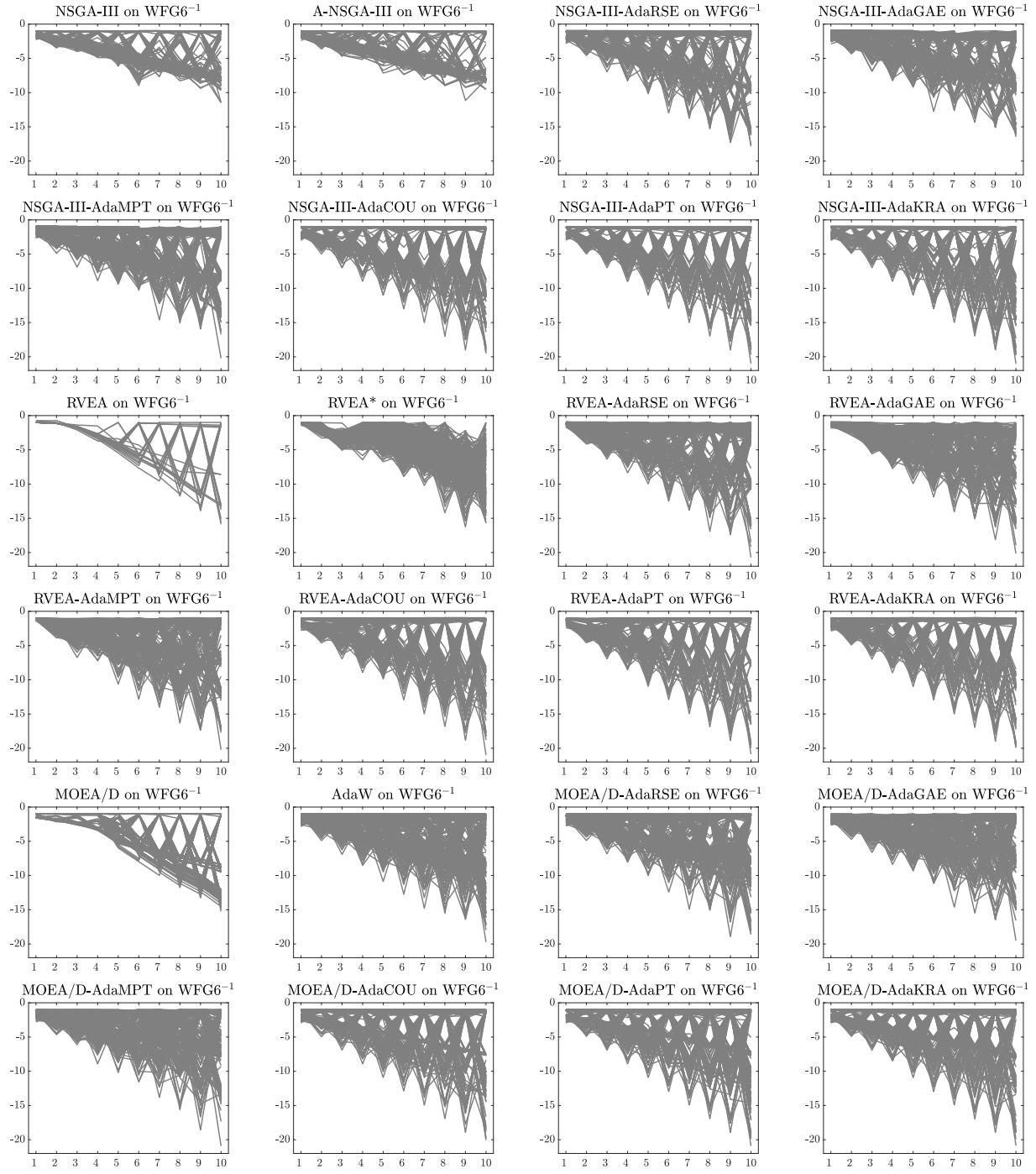


Figure 127: Final populations with the median HV value among 30 independent runs of MOEAs using the NSGA-III, RVEA, and MOEA/D frameworks on WFG6⁻¹ with 10 objective functions.

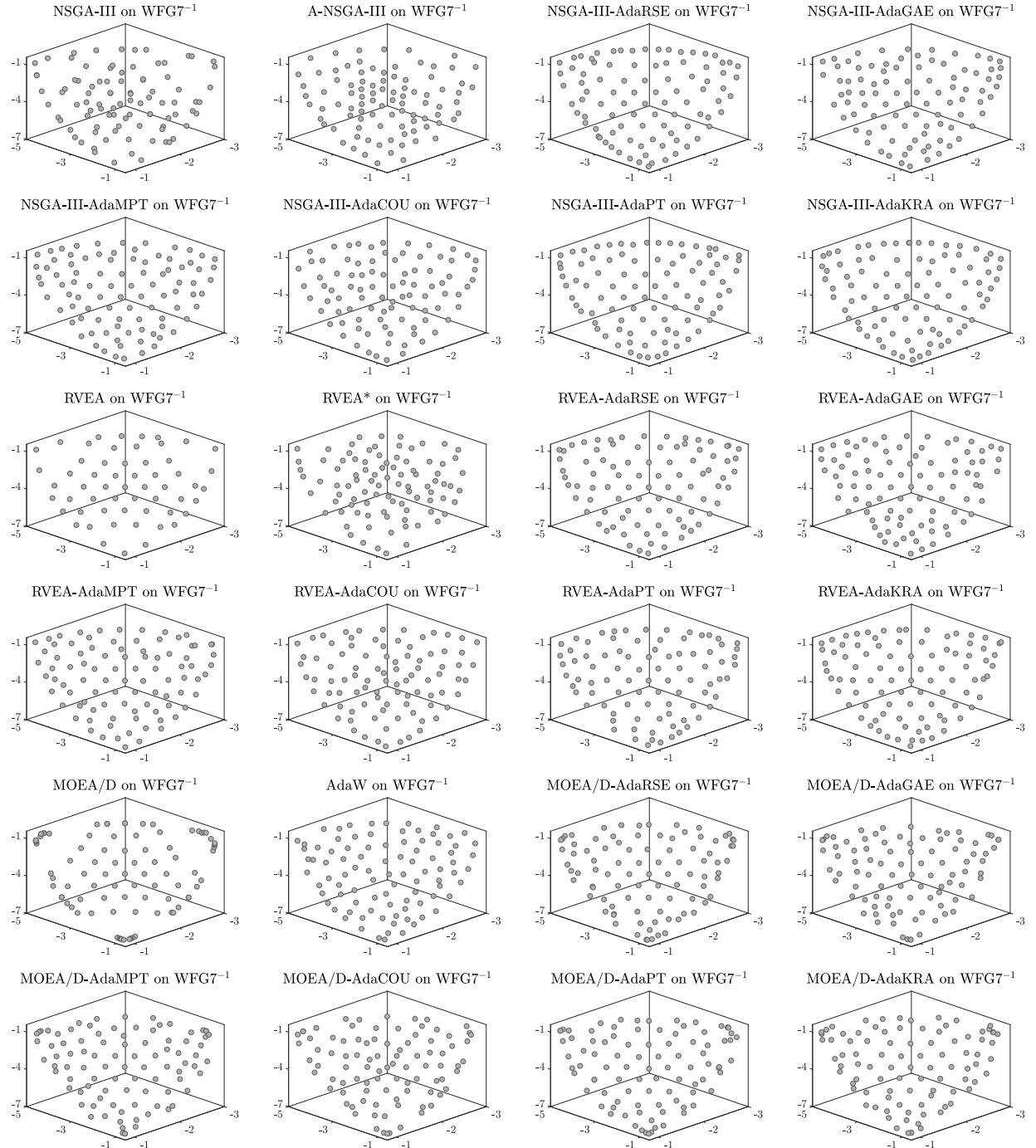


Figure 128: Final populations with the median HV value among 30 independent runs of MOEAs using the NSGA-III, RVEA, and MOEA/D frameworks on WFG7^{-1} with 3 objective functions.

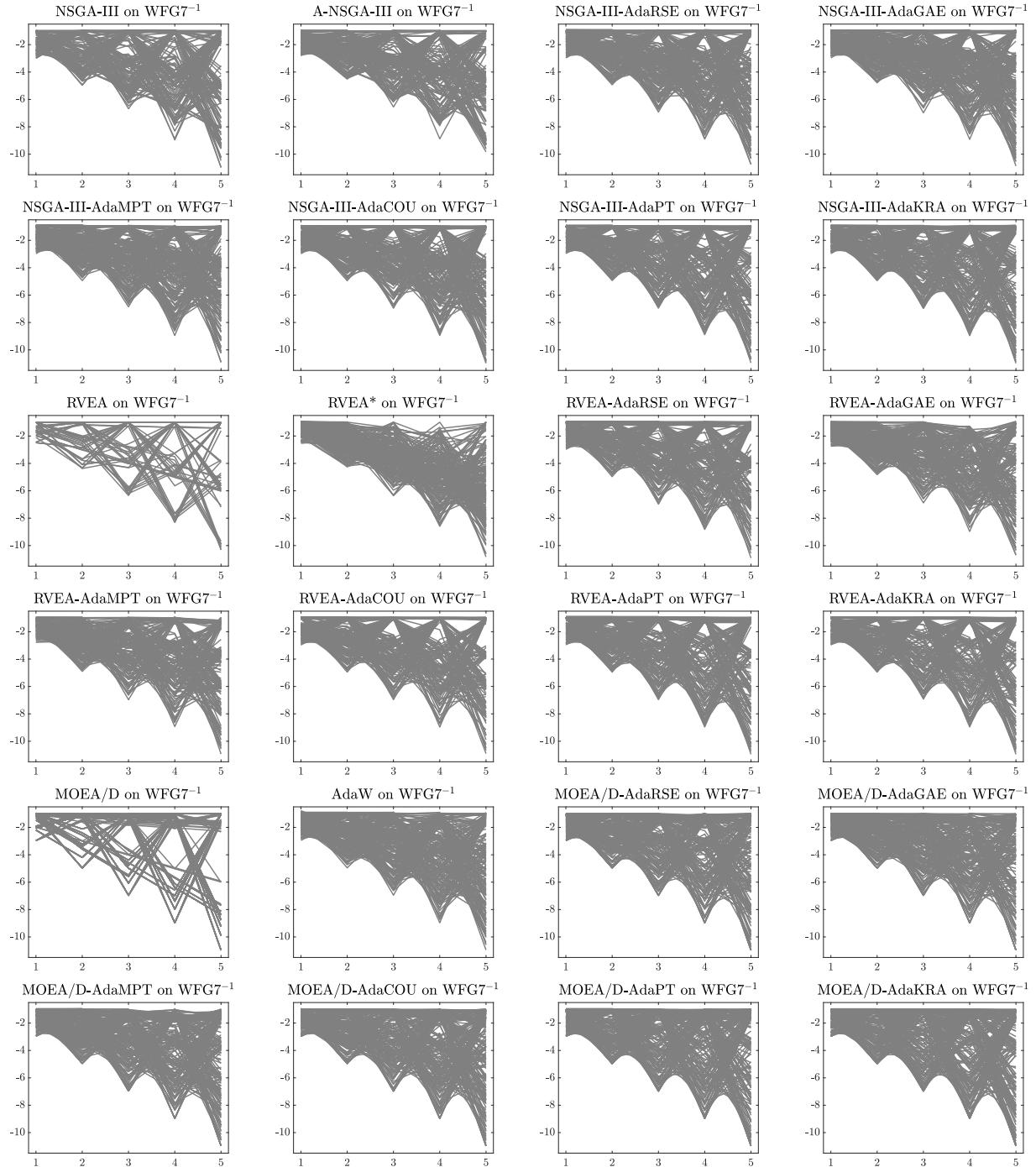


Figure 129: Final populations with the median HV value among 30 independent runs of MOEAs using the NSGA-III, RVEA, and MOEA/D frameworks on WFG7^{-1} with 5 objective functions.

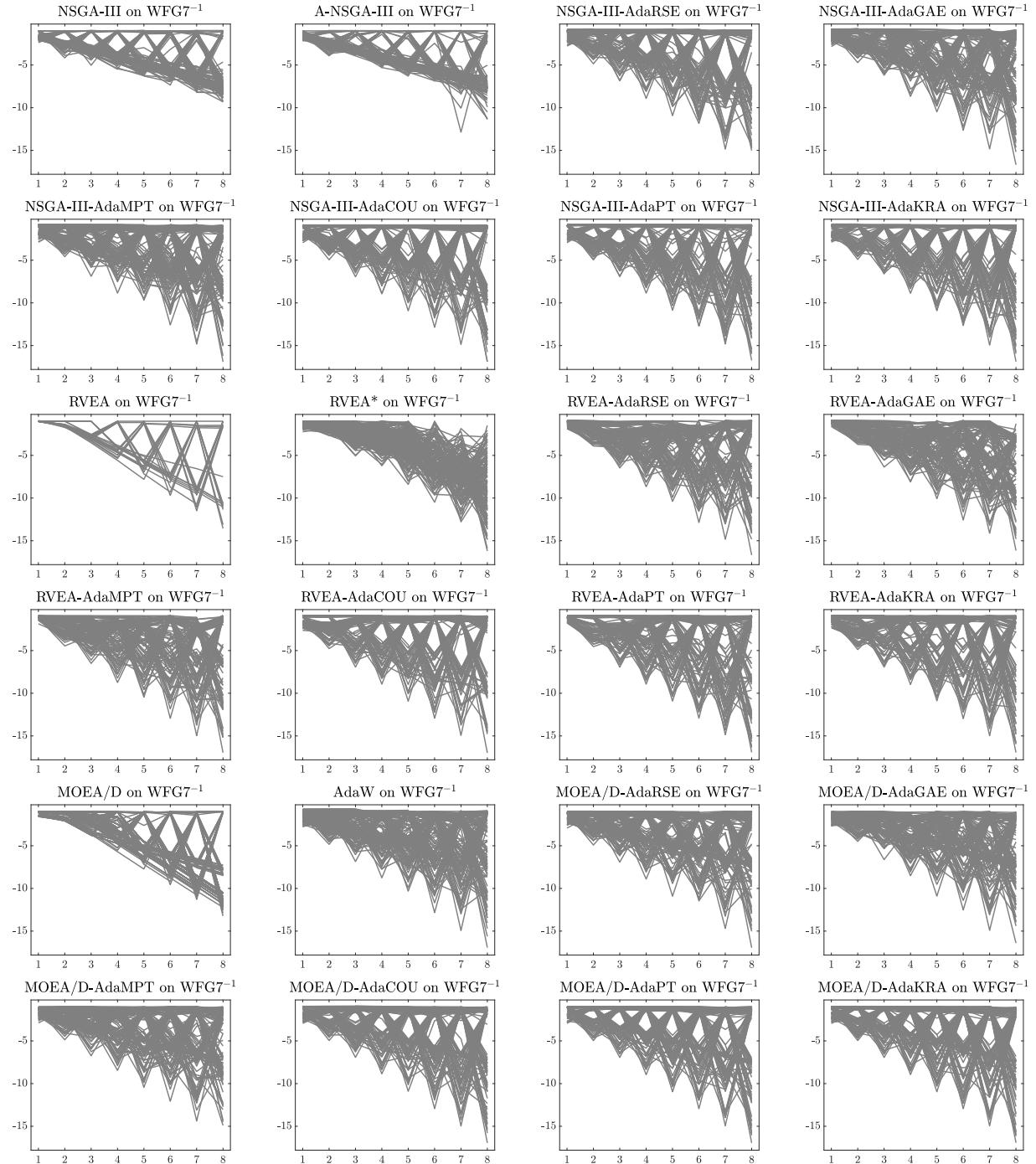


Figure 130: Final populations with the median HV value among 30 independent runs of MOEAs using the NSGA-III, RVEA, and MOEA/D frameworks on WFG7^{-1} with 8 objective functions.

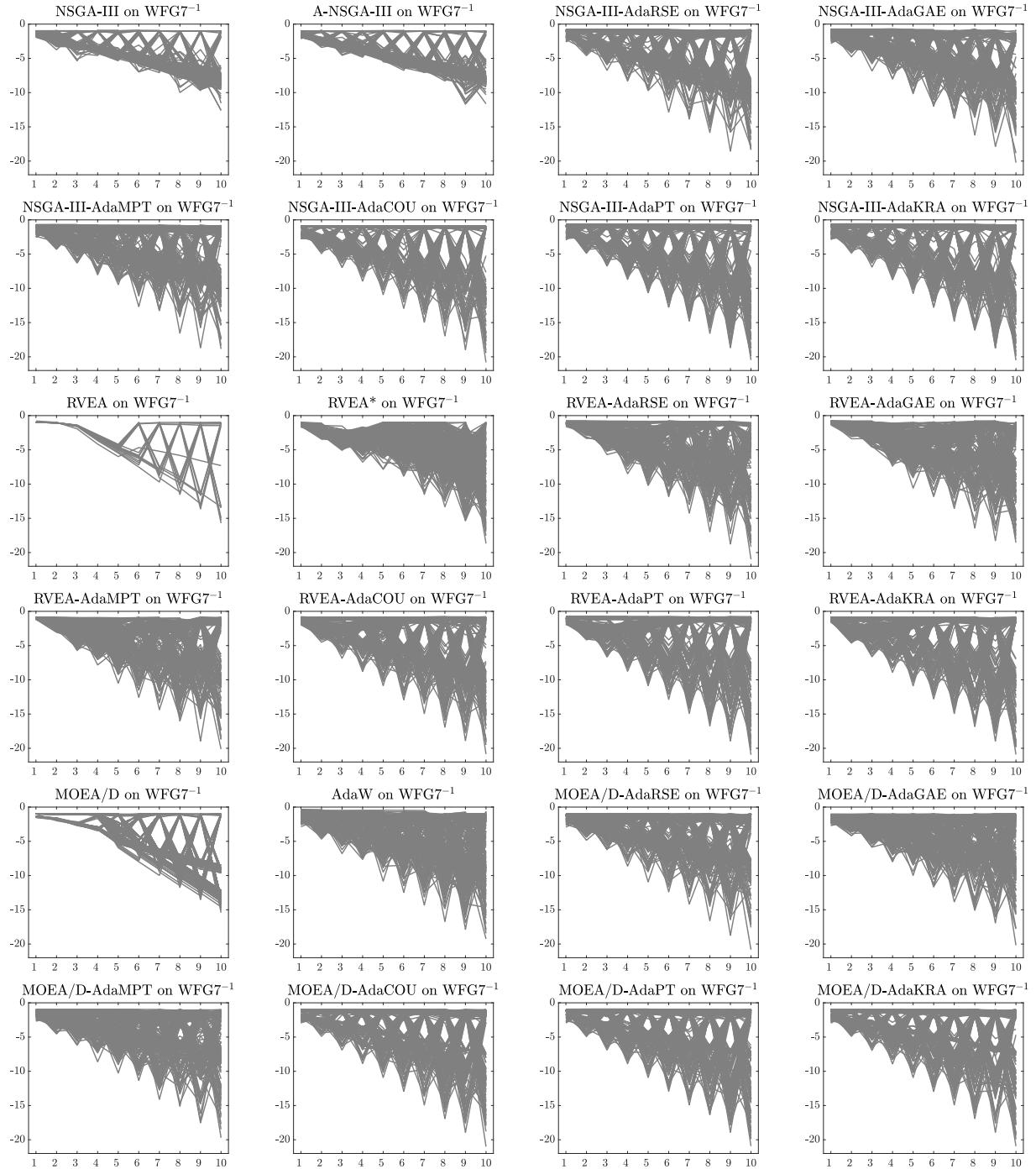


Figure 131: Final populations with the median HV value among 30 independent runs of MOEAs using the NSGA-III, RVEA, and MOEA/D frameworks on WFG7⁻¹ with 10 objective functions.

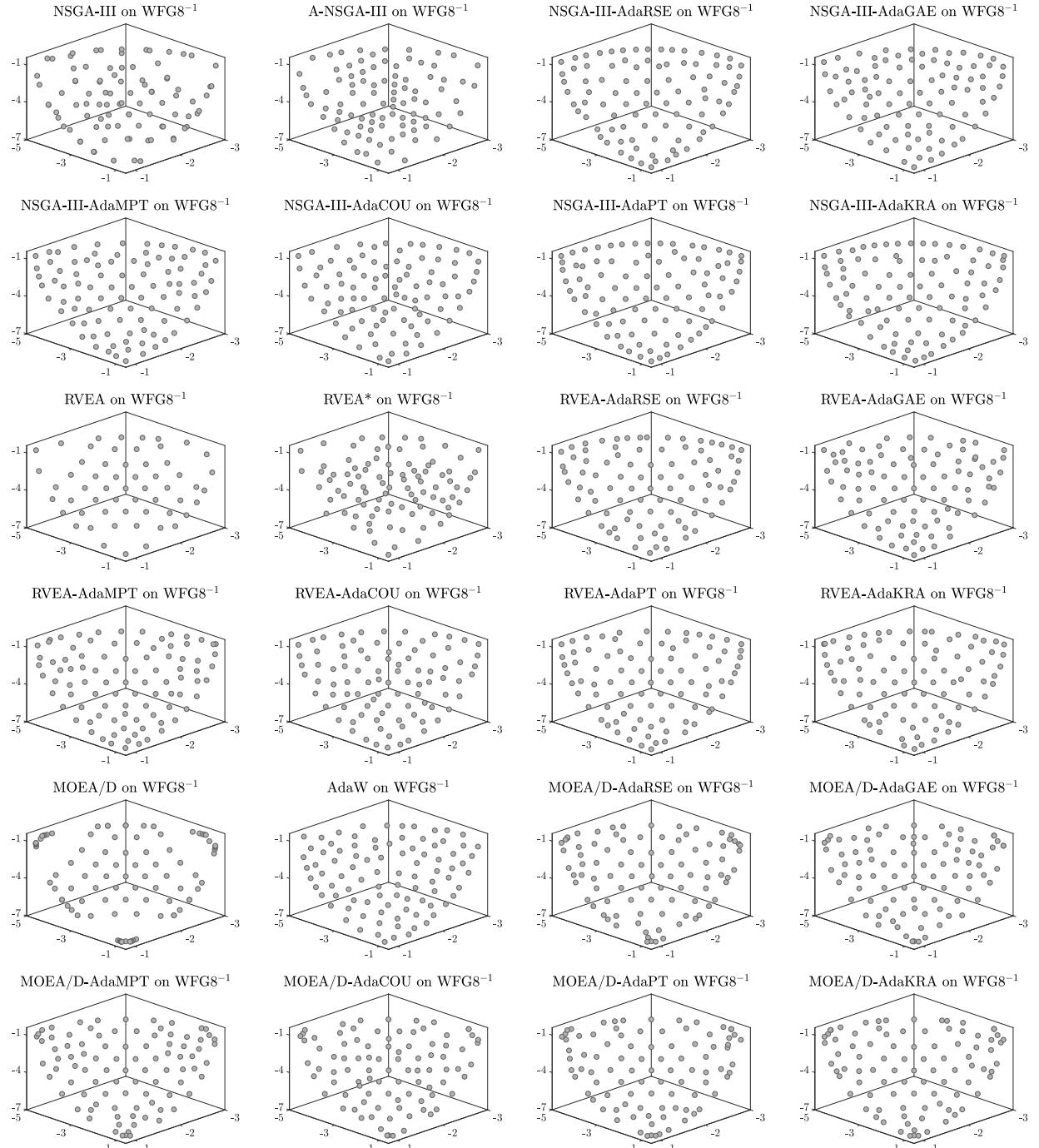


Figure 132: Final populations with the median HV value among 30 independent runs of MOEAs using the NSGA-III, RVEA, and MOEA/D frameworks on WFG8^{-1} with 3 objective functions.

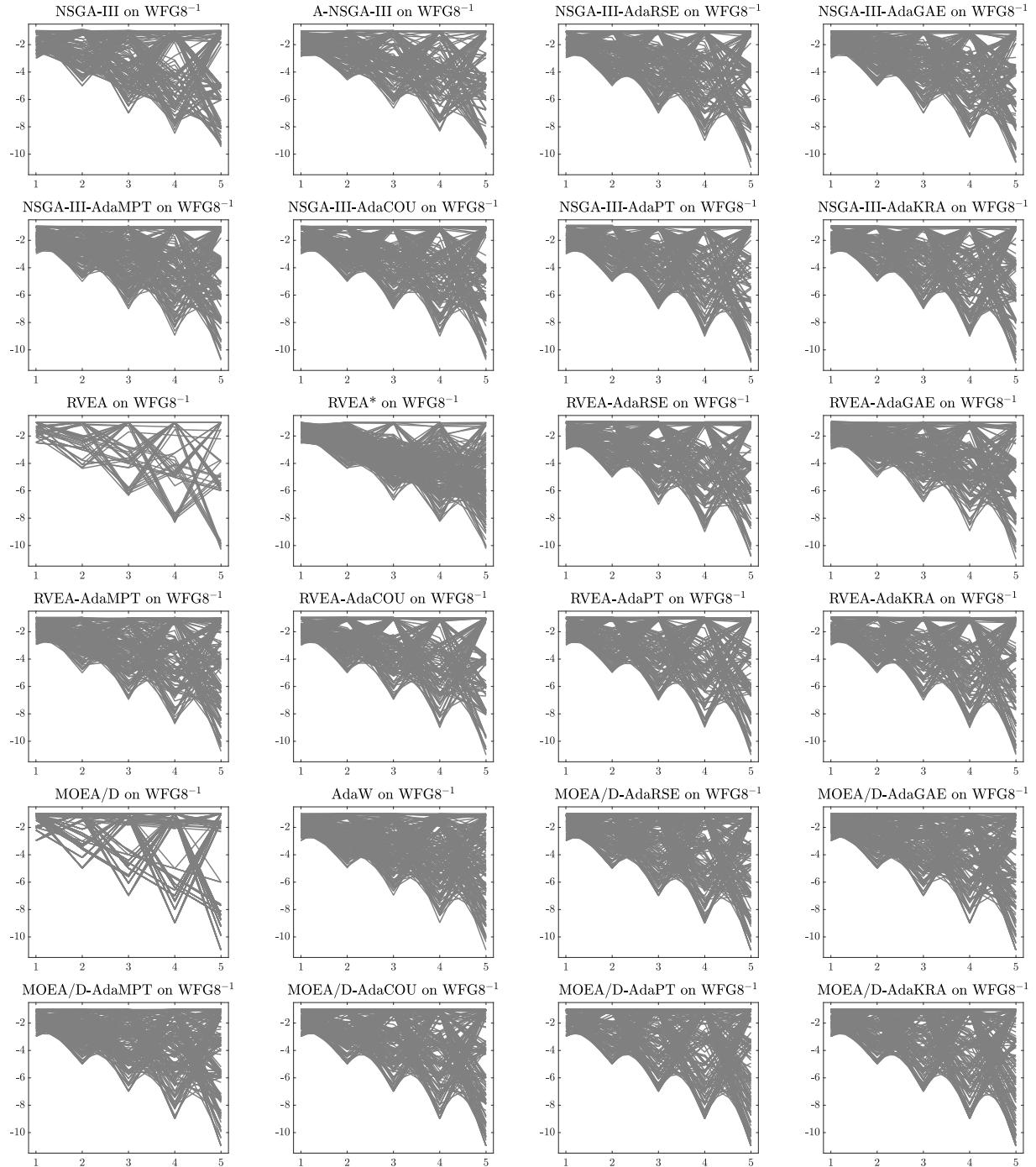


Figure 133: Final populations with the median HV value among 30 independent runs of MOEAs using the NSGA-III, RVEA, and MOEA/D frameworks on WFG8^{-1} with 5 objective functions.

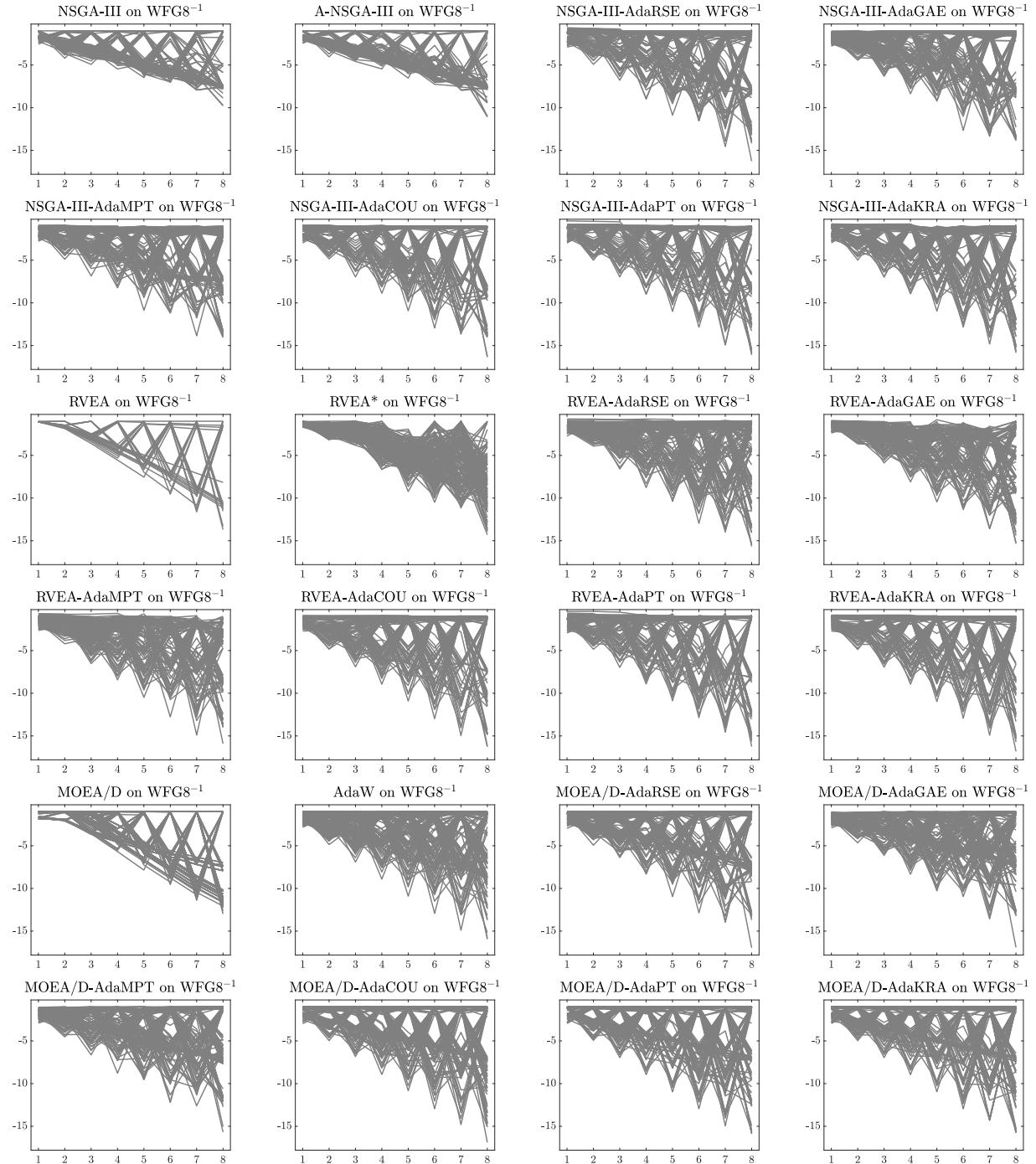


Figure 134: Final populations with the median HV value among 30 independent runs of MOEAs using the NSGA-III, RVEA, and MOEA/D frameworks on WFG8^{-1} with 8 objective functions.

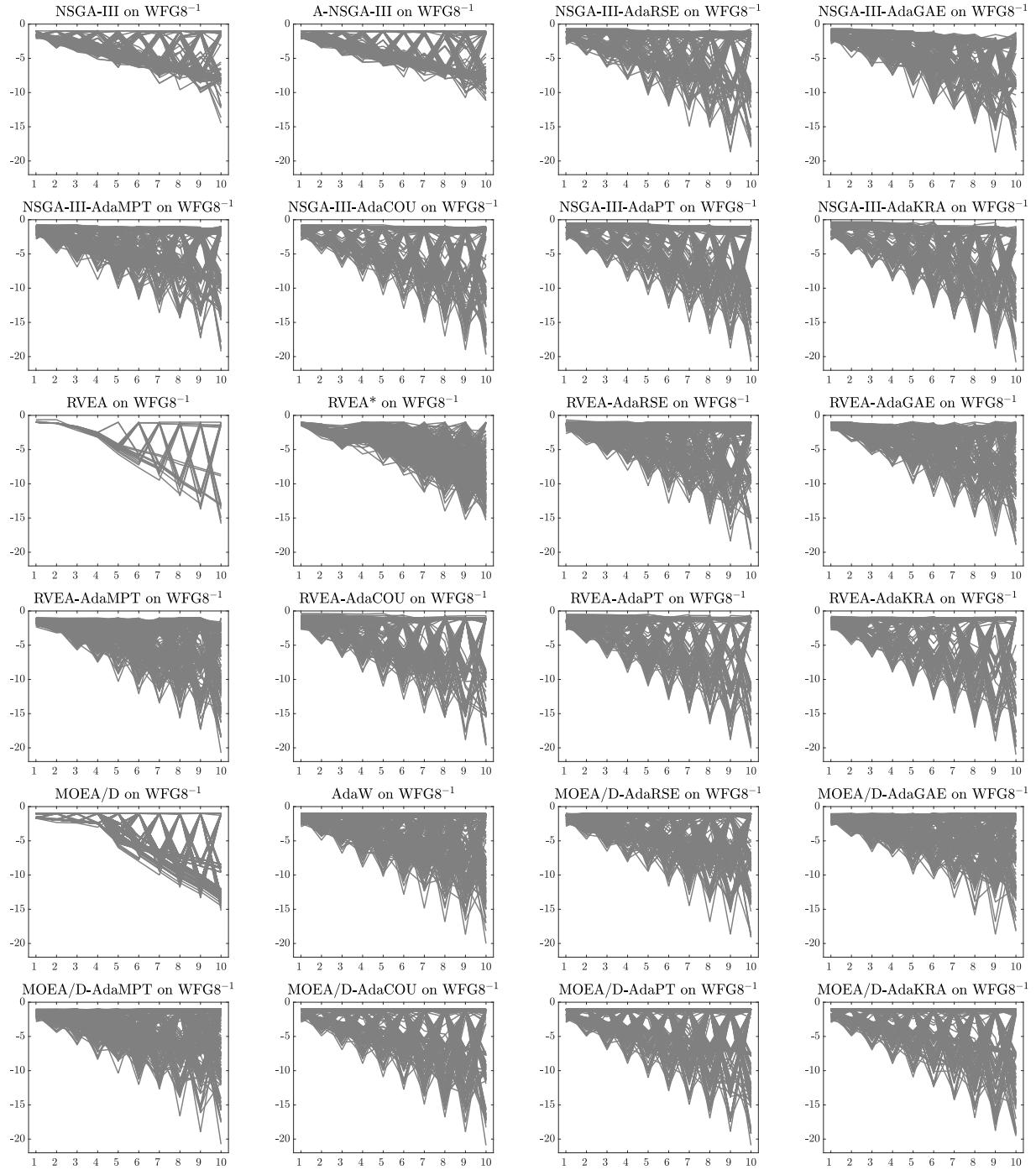


Figure 135: Final populations with the median HV value among 30 independent runs of MOEAs using the NSGA-III, RVEA, and MOEA/D frameworks on WFG8^{-1} with 10 objective functions.

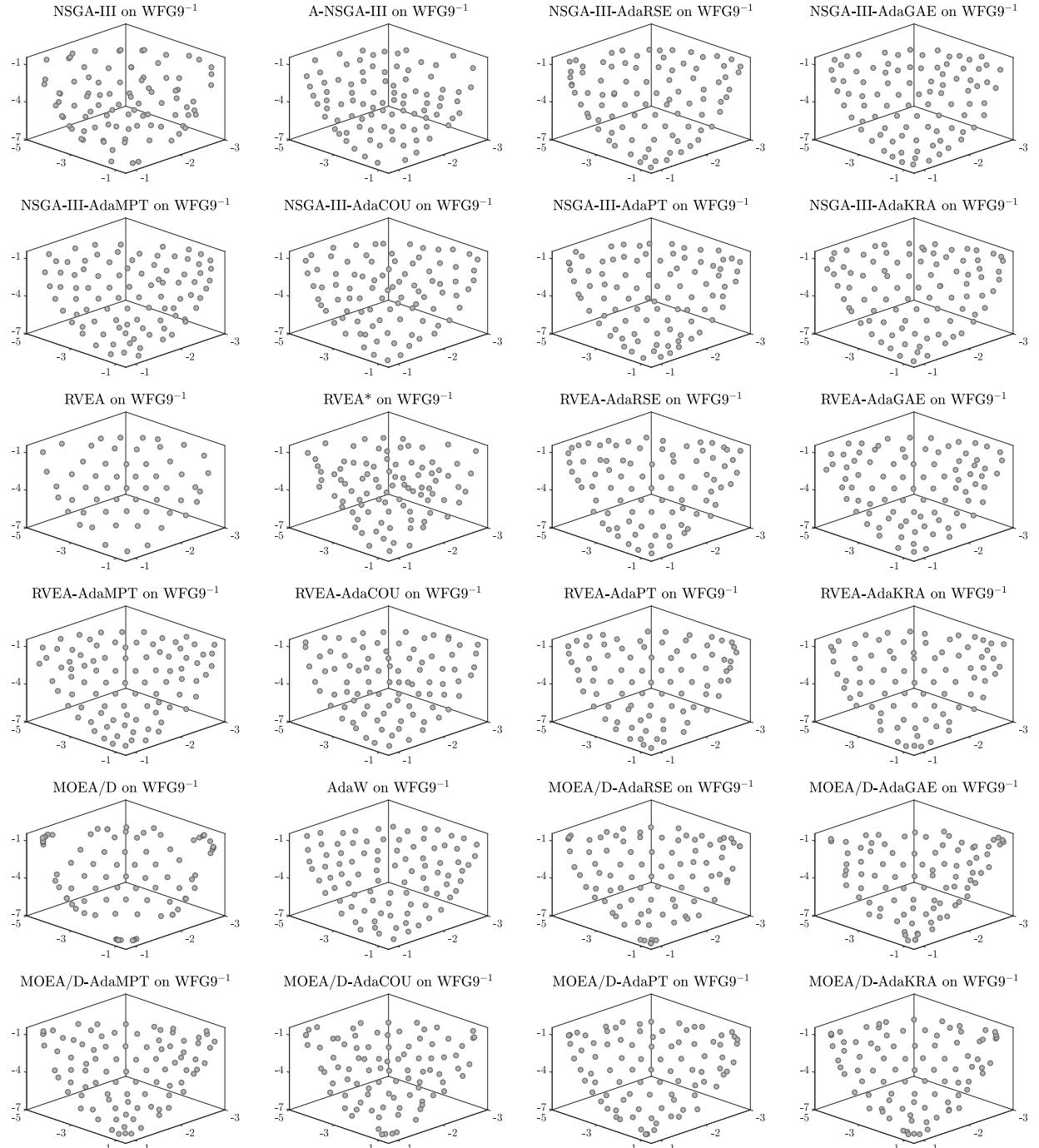


Figure 136: Final populations with the median HV value among 30 independent runs of MOEAs using the NSGA-III, RVEA, and MOEA/D frameworks on WFG9^{-1} with 3 objective functions.

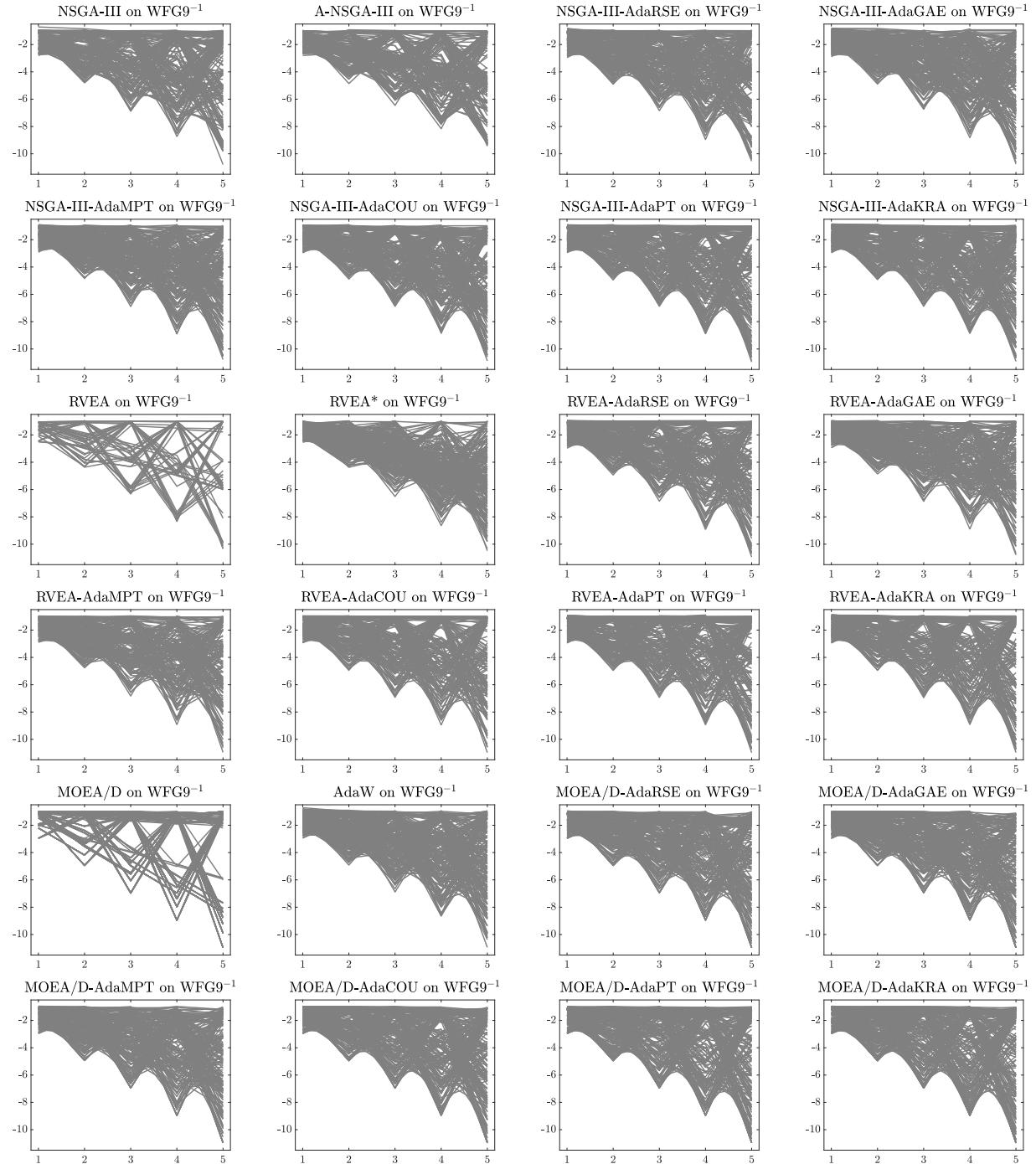


Figure 137: Final populations with the median HV value among 30 independent runs of MOEAs using the NSGA-III, RVEA, and MOEA/D frameworks on WFG9^{-1} with 5 objective functions.

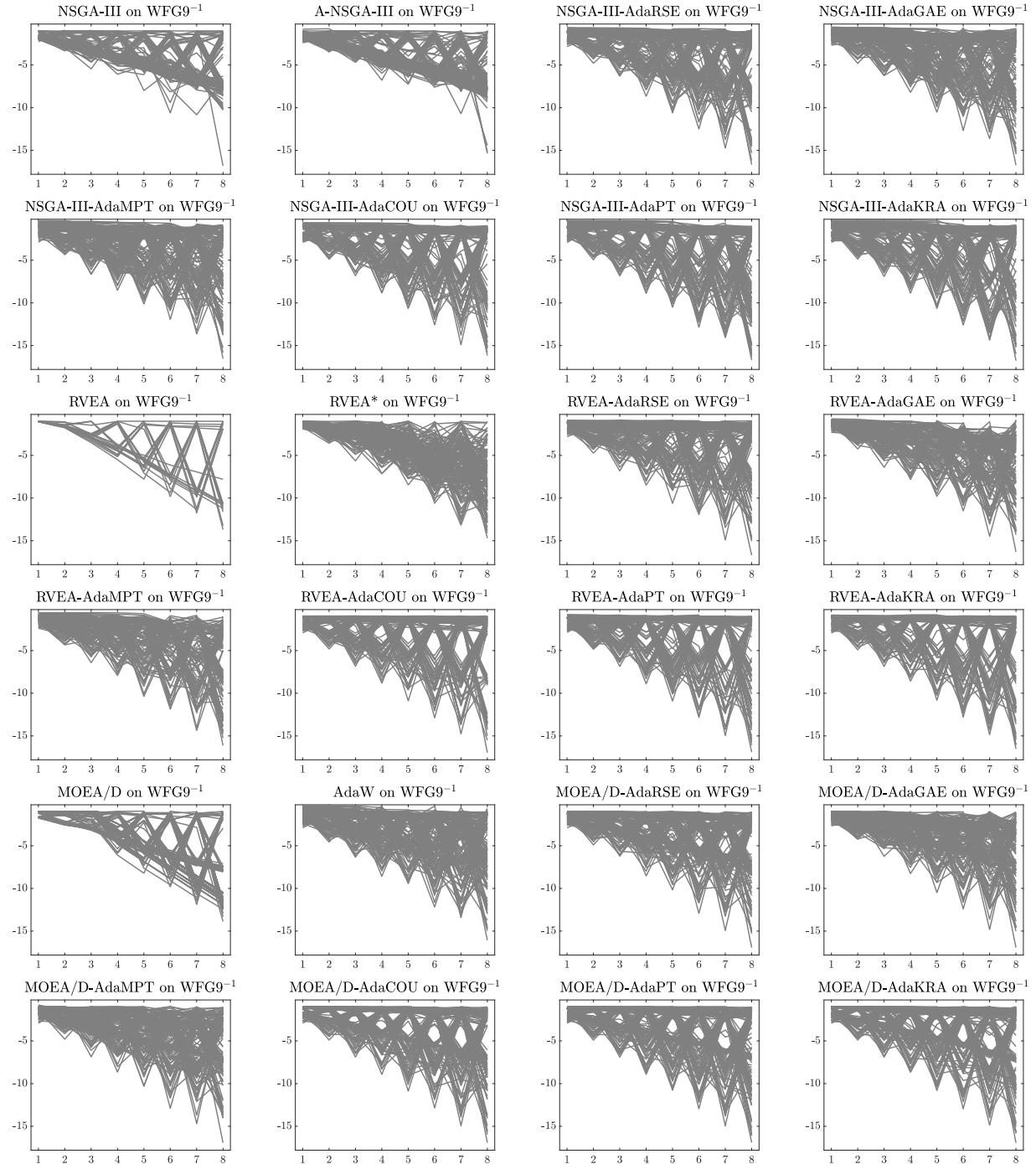


Figure 138: Final populations with the median HV value among 30 independent runs of MOEAs using the NSGA-III, RVEA, and MOEA/D frameworks on WFG9⁻¹ with 8 objective functions.

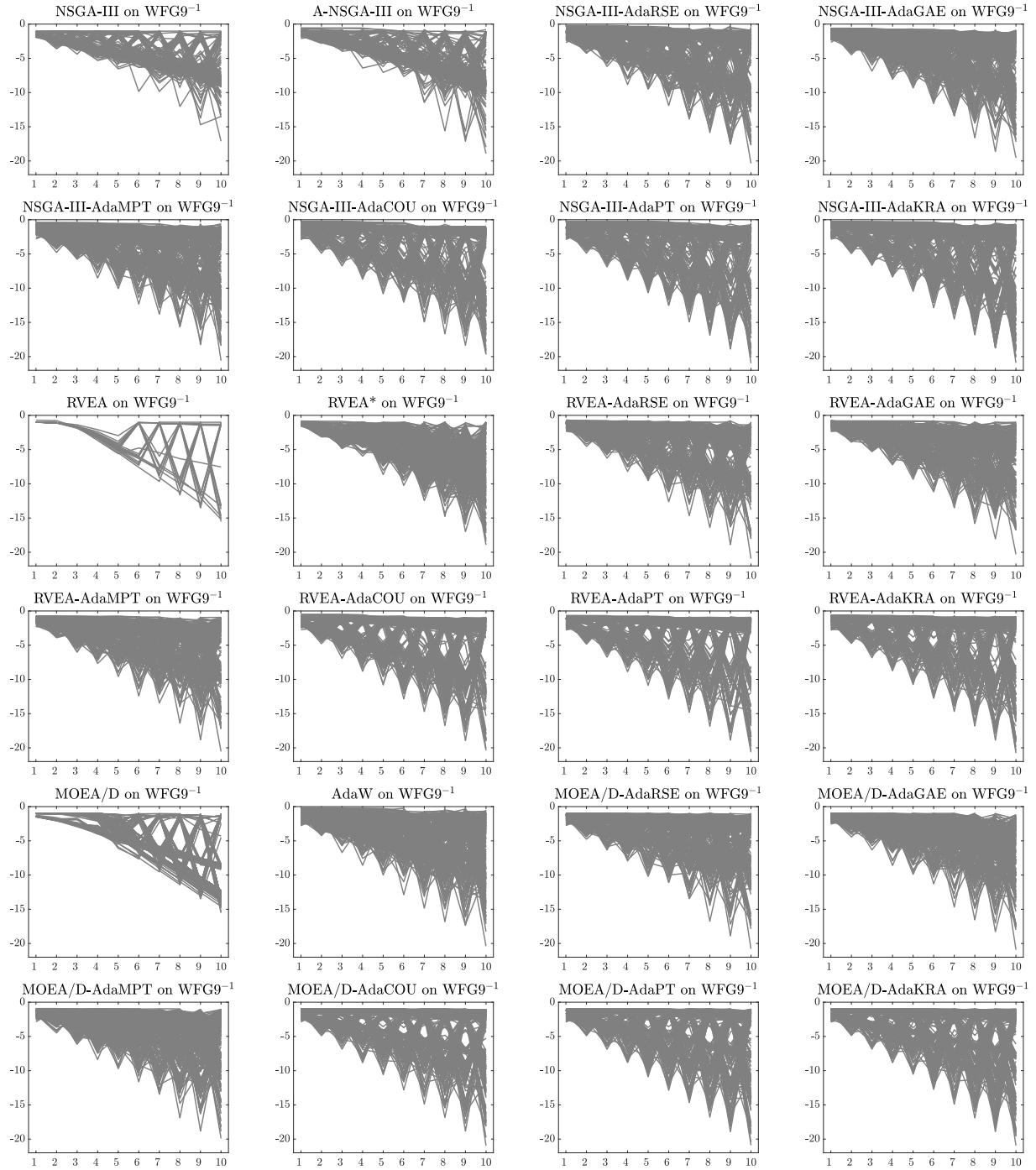


Figure 139: Final populations with the median HV value among 30 independent runs of MOEAs using the NSGA-III, RVEA, and MOEA/D frameworks on WFG9⁻¹ with 10 objective functions.

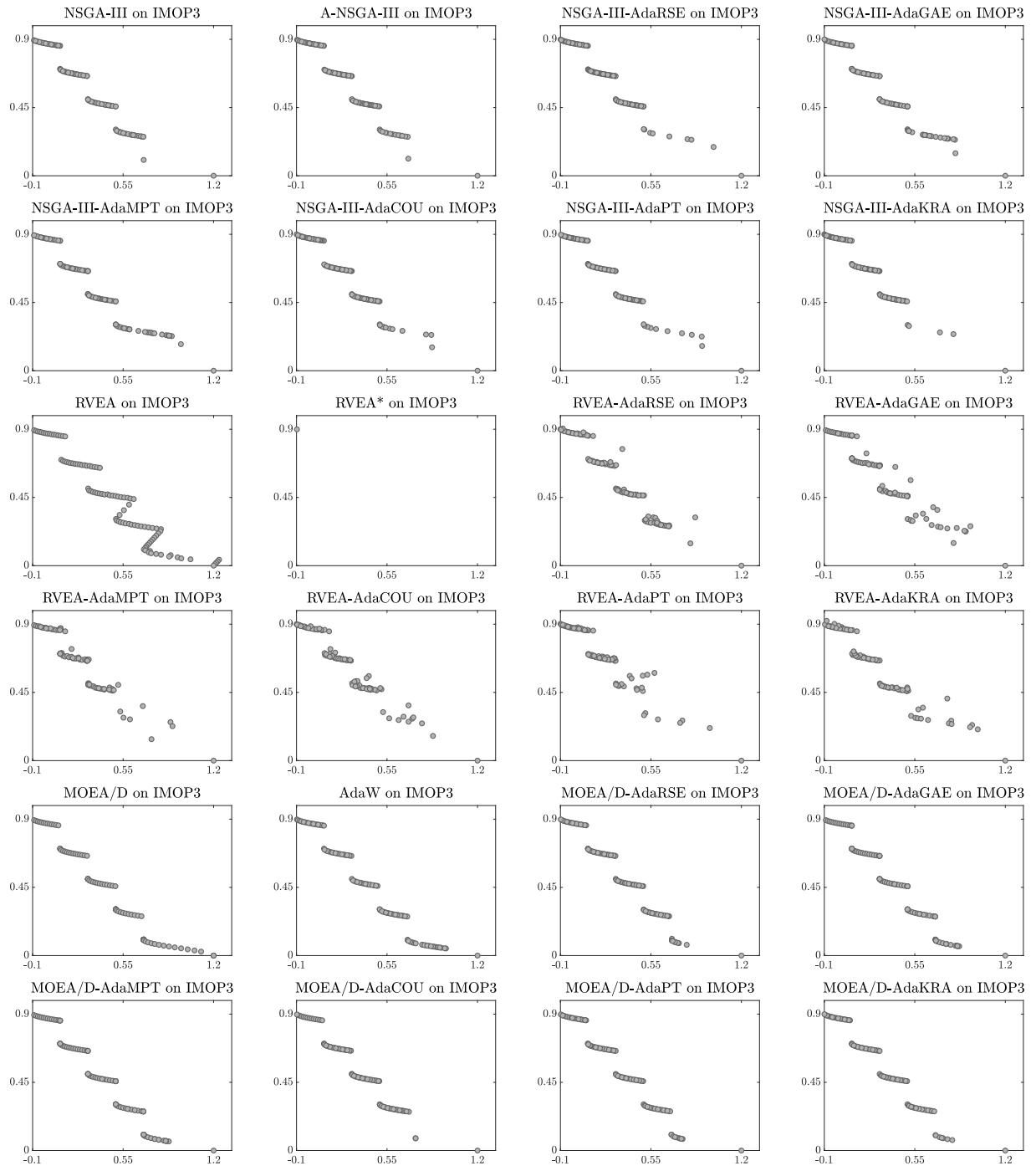


Figure 140: Final populations with the median HV value among 30 independent runs of MOEAs using the NSGA-III, RVEA, and MOEA/D frameworks on IMOP3.

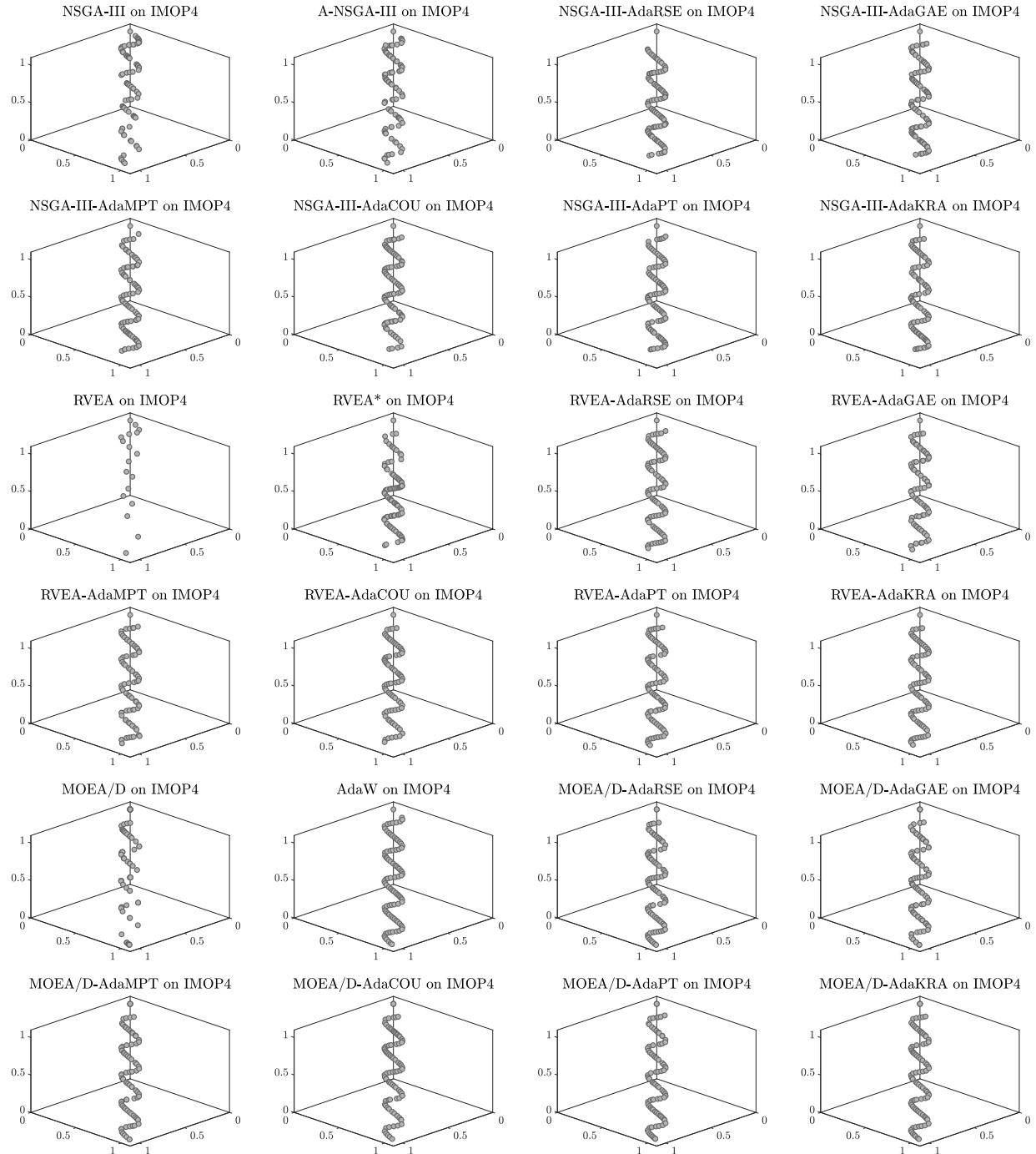


Figure 141: Final populations with the median HV value among 30 independent runs of MOEAs using the NSGA-III, RVEA, and MOEA/D frameworks on IMOP4.

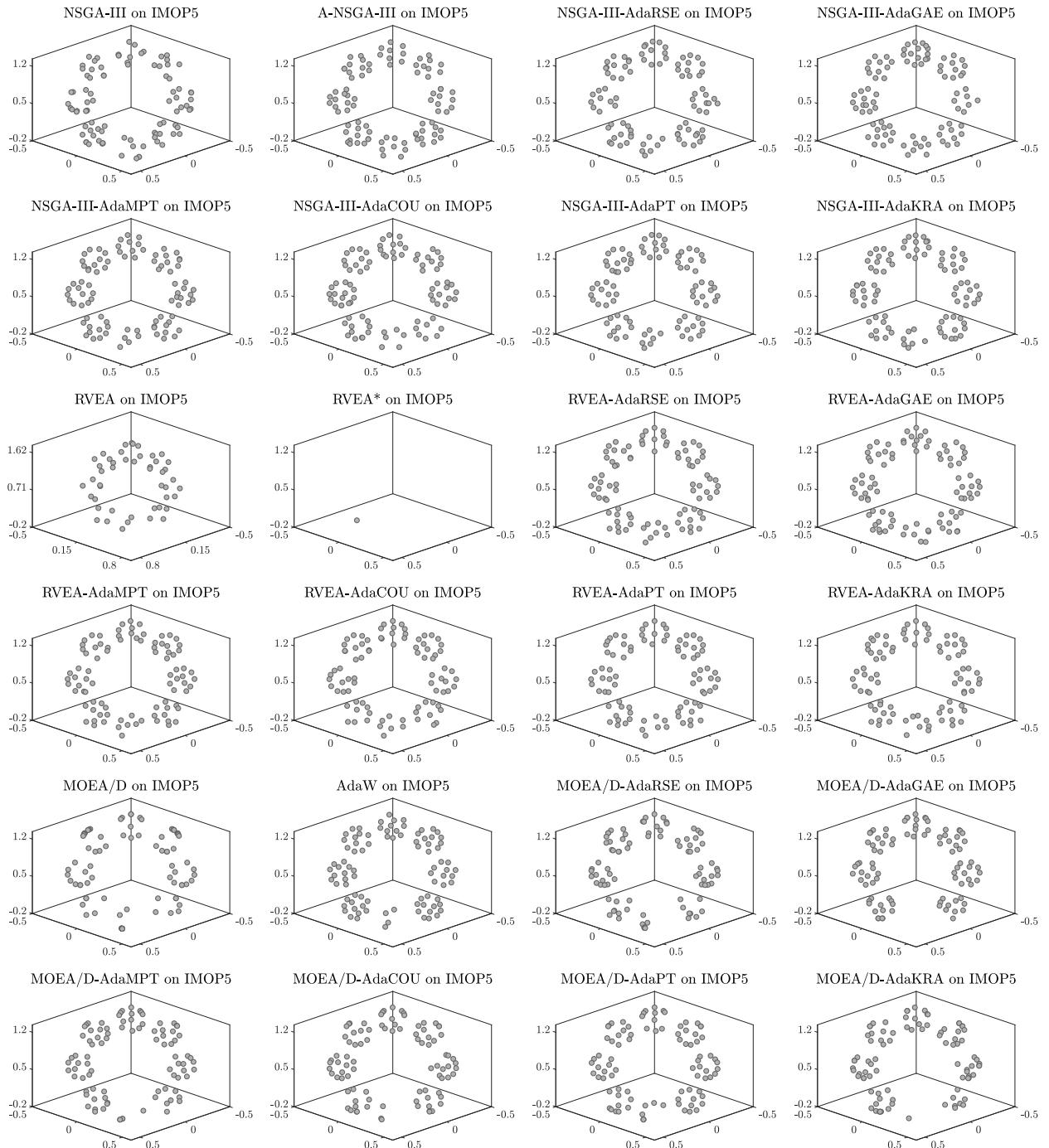


Figure 142: Final populations with the median HV value among 30 independent runs of MOEAs using the NSGA-III, RVEA, and MOEA/D frameworks on IMOP5.

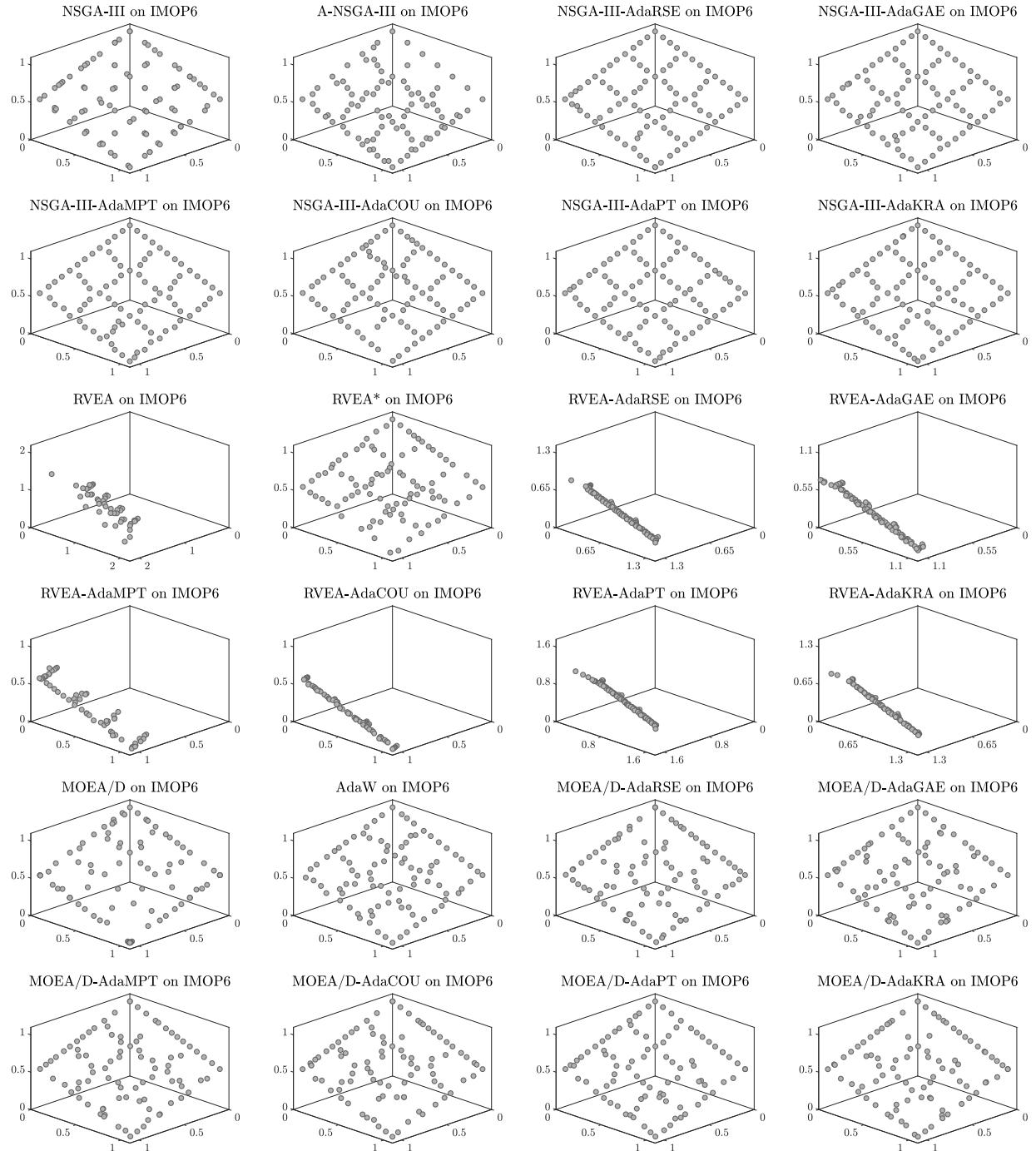


Figure 143: Final populations with the median HV value among 30 independent runs of MOEAs using the NSGA-III, RVEA, and MOEA/D frameworks on IMOP6.

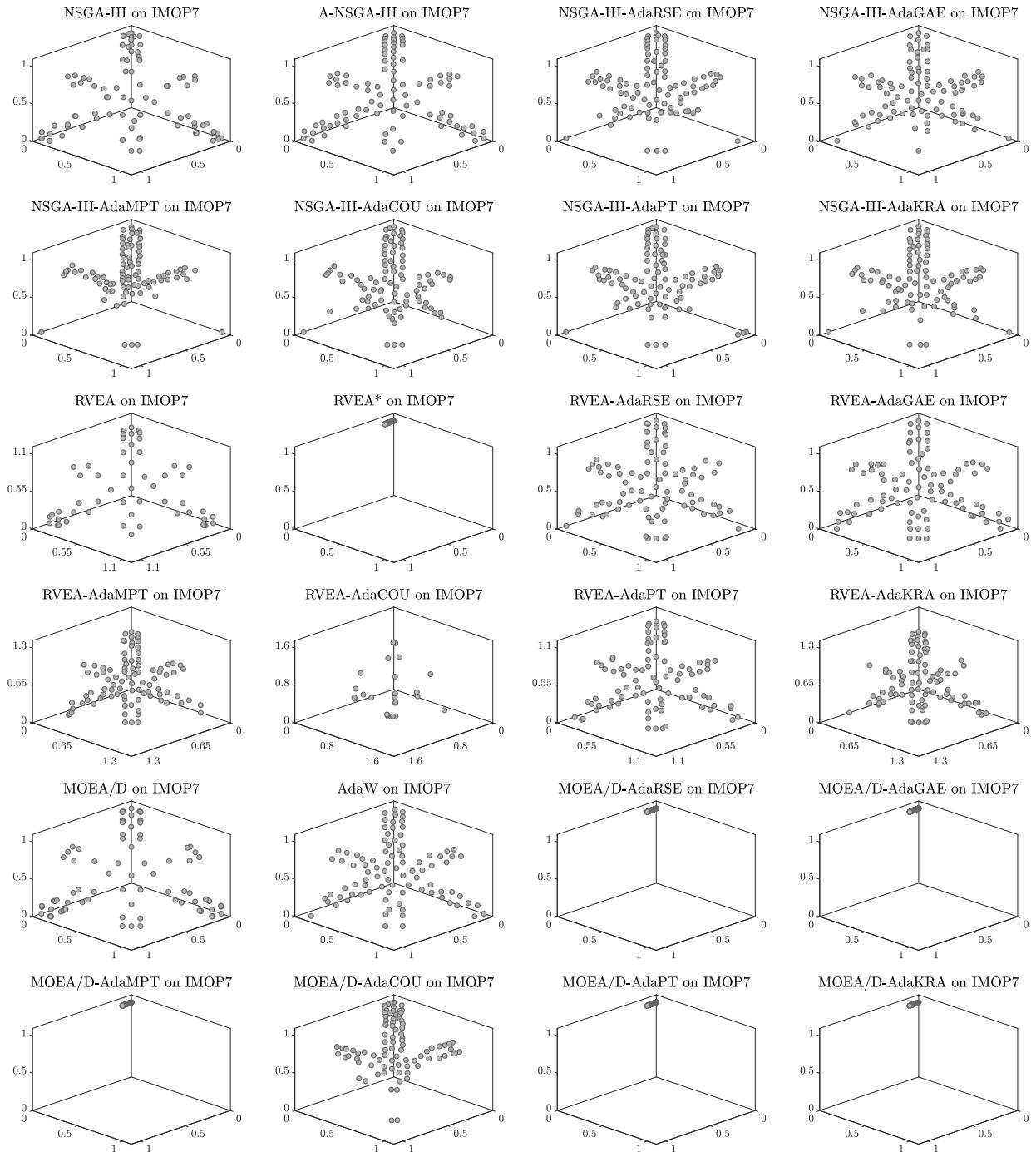


Figure 144: Final populations with the median HV value among 30 independent runs of MOEAs using the NSGA-III, RVEA, and MOEA/D frameworks on IMOP7.

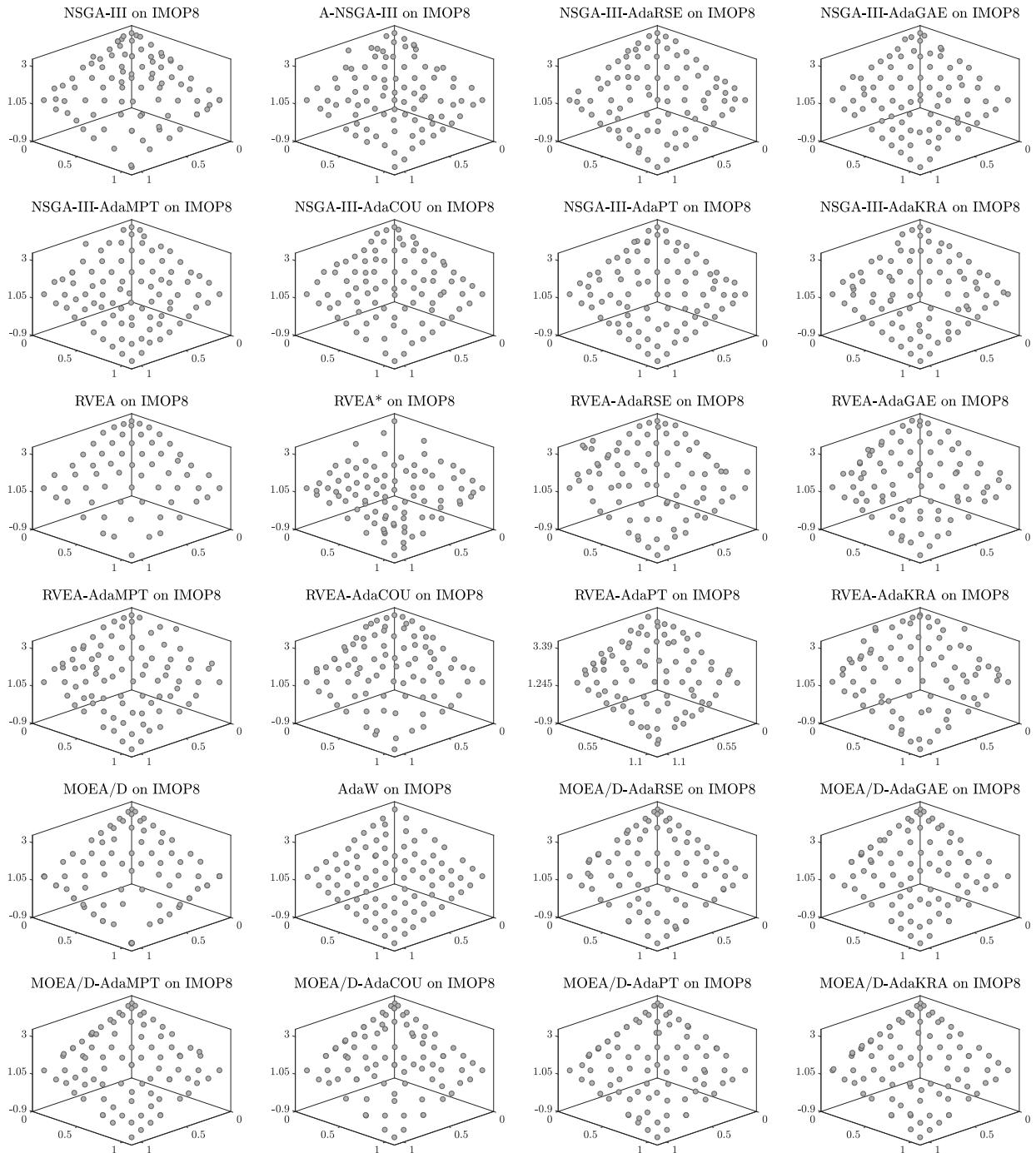


Figure 145: Final populations with the median HV value among 30 independent runs of MOEAs using the NSGA-III, RVEA, and MOEA/D frameworks on IMOP8.

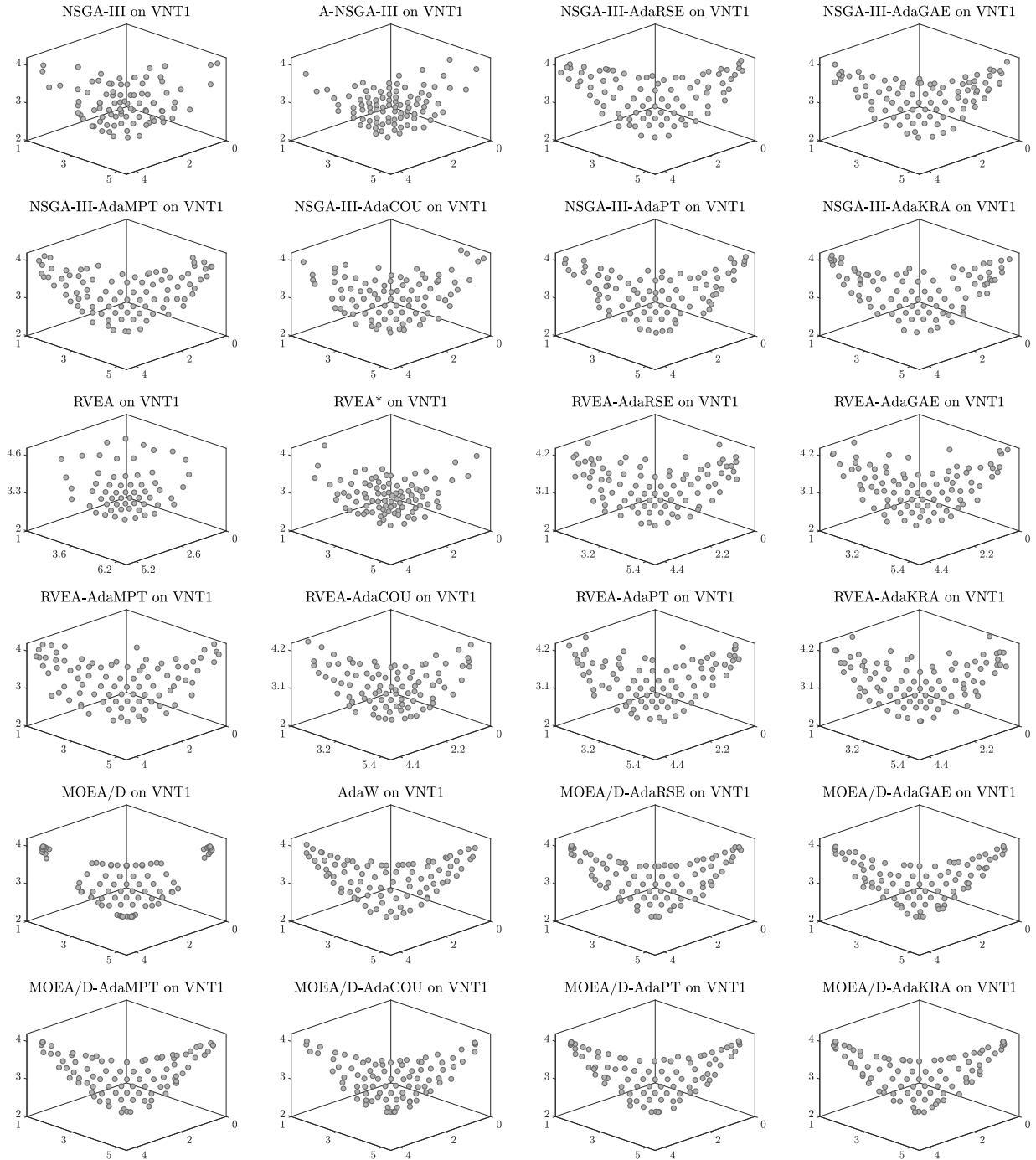


Figure 146: Final populations with the median HV value among 30 independent runs of MOEAs using the NSGA-III, RVEA, and MOEA/D frameworks on VNT1.

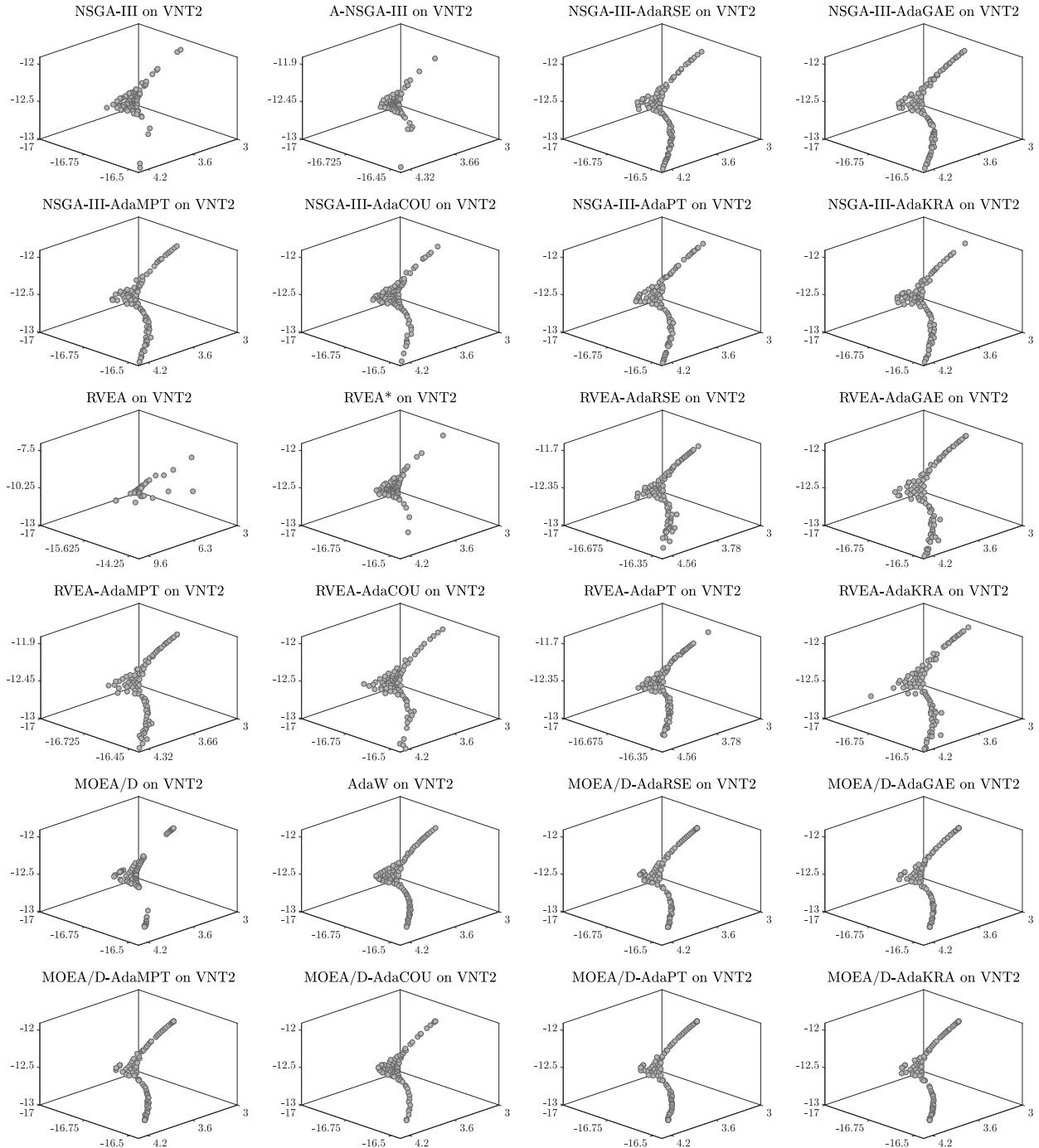


Figure 147: Final populations with the median HV value among 30 independent runs of MOEAs using the NSGA-III, RVEA, and MOEA/D frameworks on VNT2.

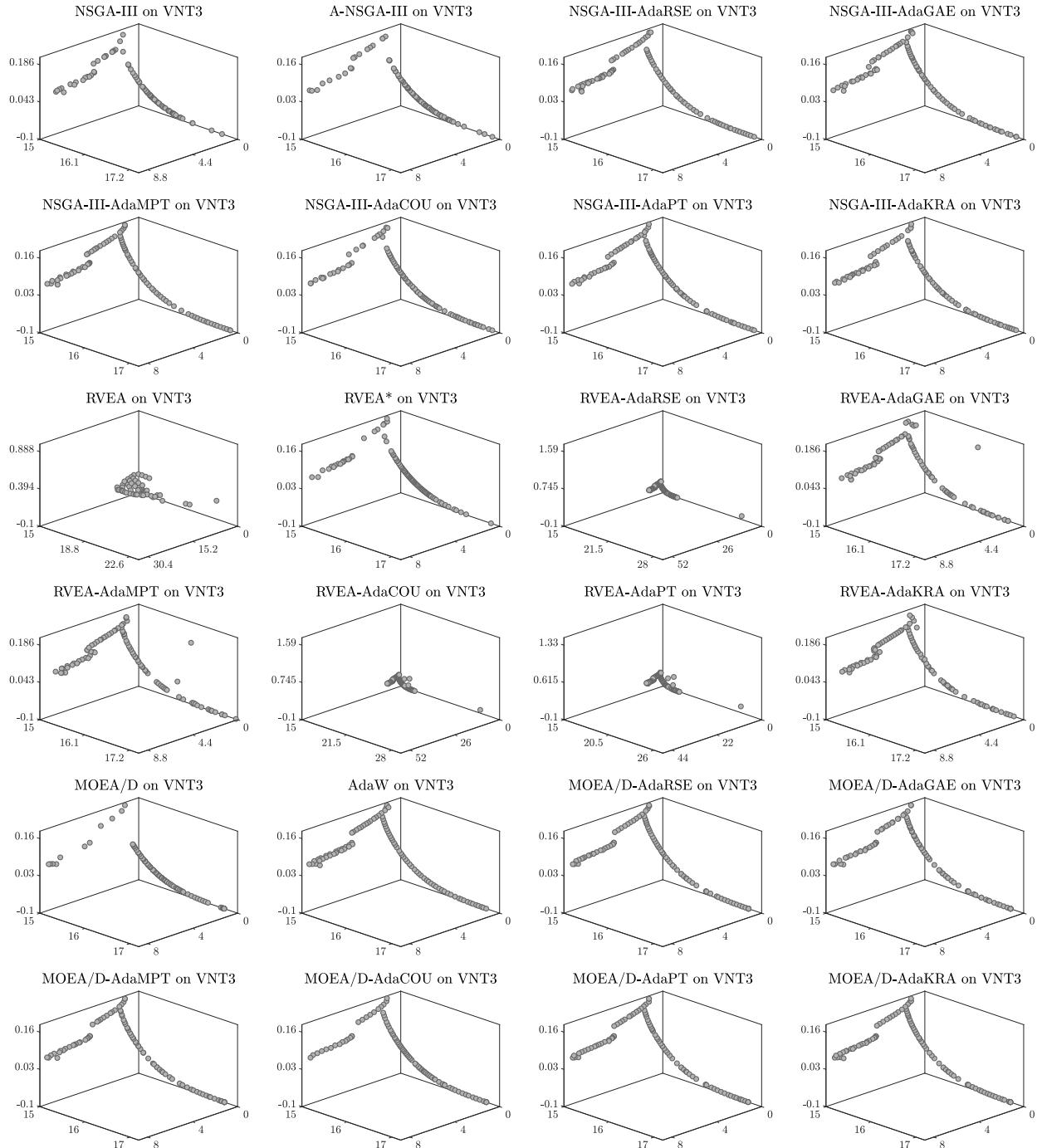


Figure 148: Final populations with the median HV value among 30 independent runs of MOEAs using the NSGA-III, RVEA, and MOEA/D frameworks on VNT3.

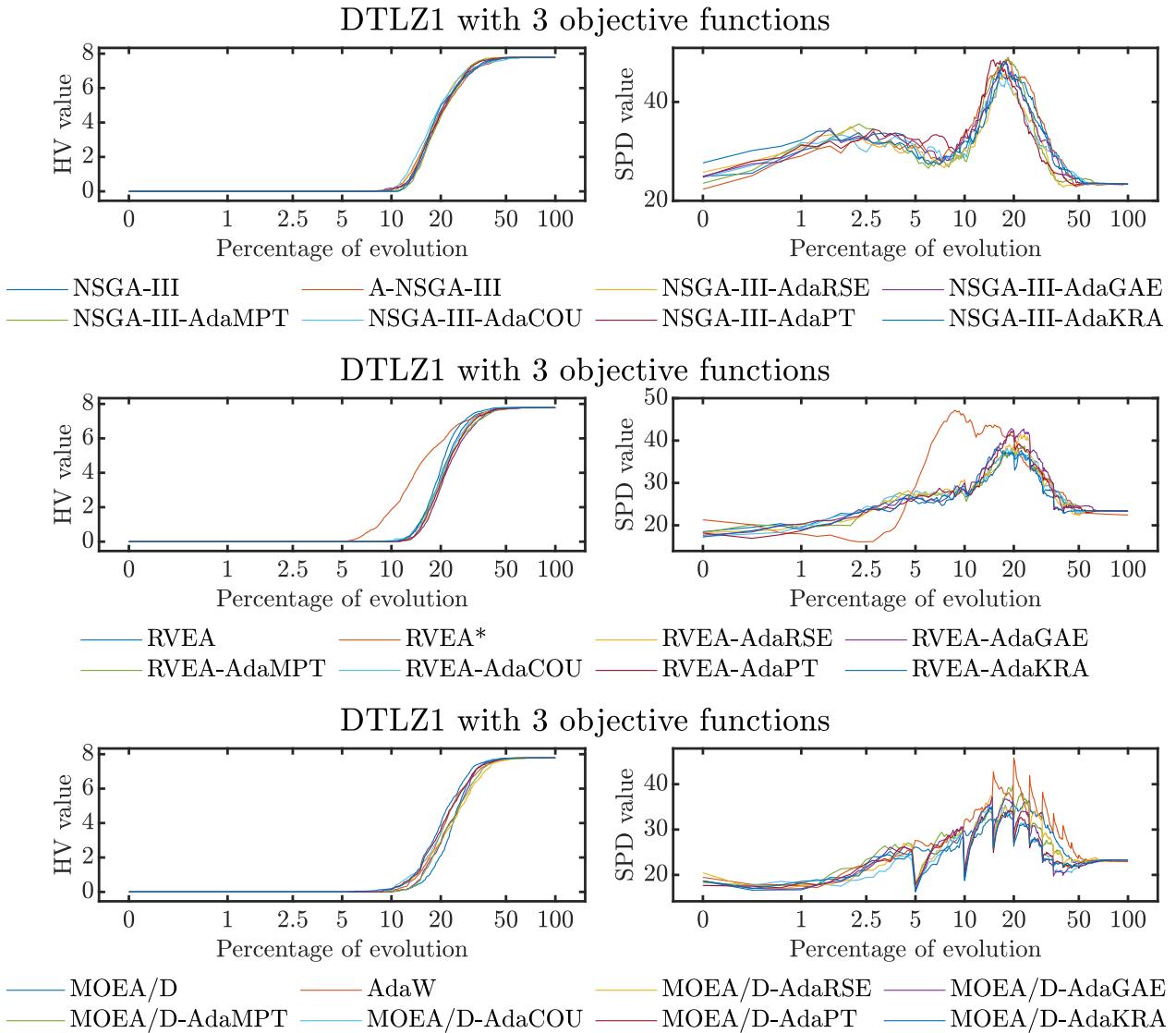


Figure 149: Convergence and diversity graphs with the mean HV value and SPD value of 30 independent runs of MOEAs using the NSGA-III, RVEA, and MOEA/D frameworks on DTLZ1 with 3 objective functions.

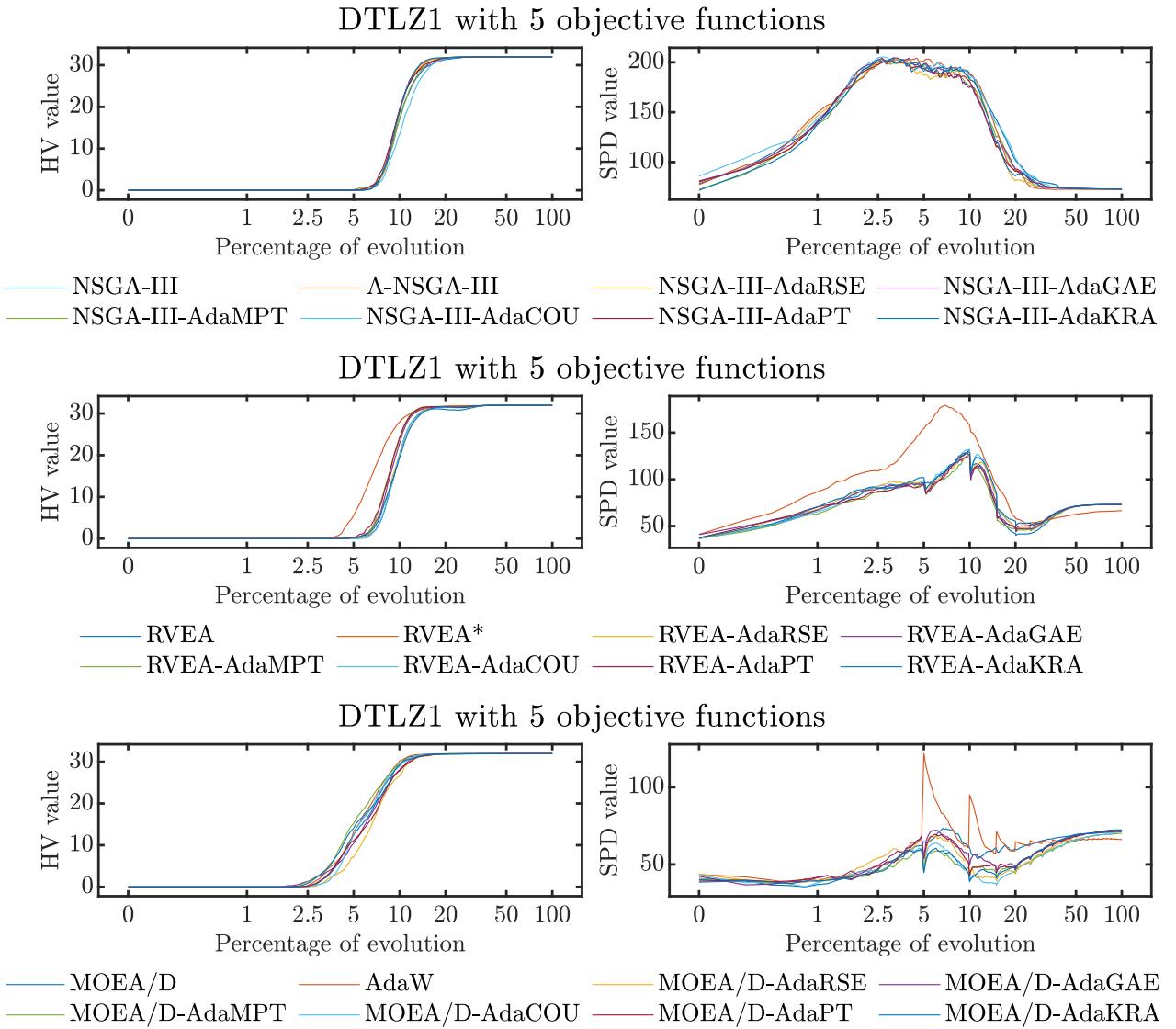


Figure 150: Convergence and diversity graphs with the mean HV value and SPD value of 30 independent runs of MOEAs using the NSGA-III, RVEA, and MOEA/D frameworks on DTLZ1 with 5 objective functions.

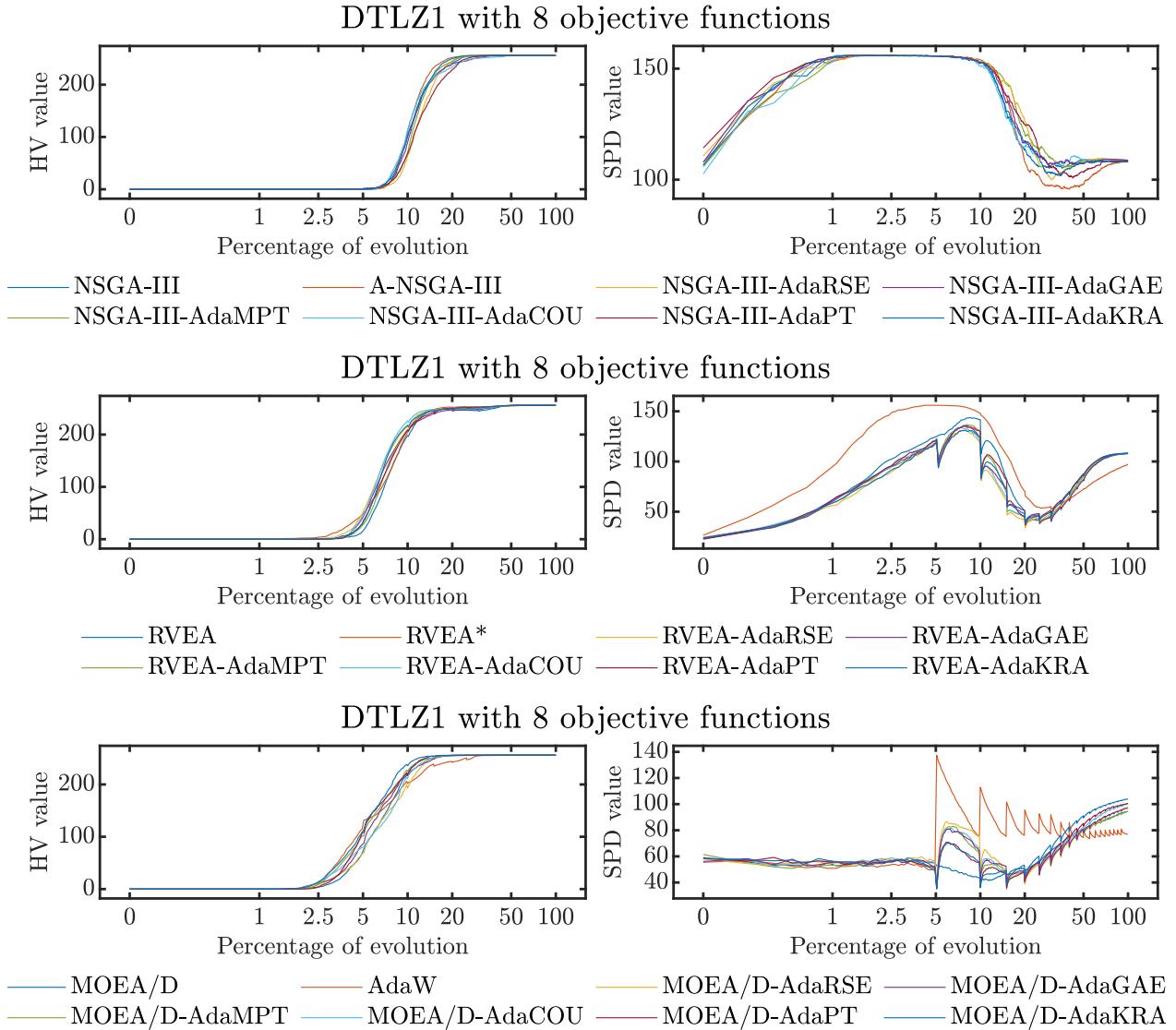


Figure 151: Convergence and diversity graphs with the mean HV value and SPD value of 30 independent runs of MOEAs using the NSGA-III, RVEA, and MOEA/D frameworks on DTLZ1 with 8 objective functions.

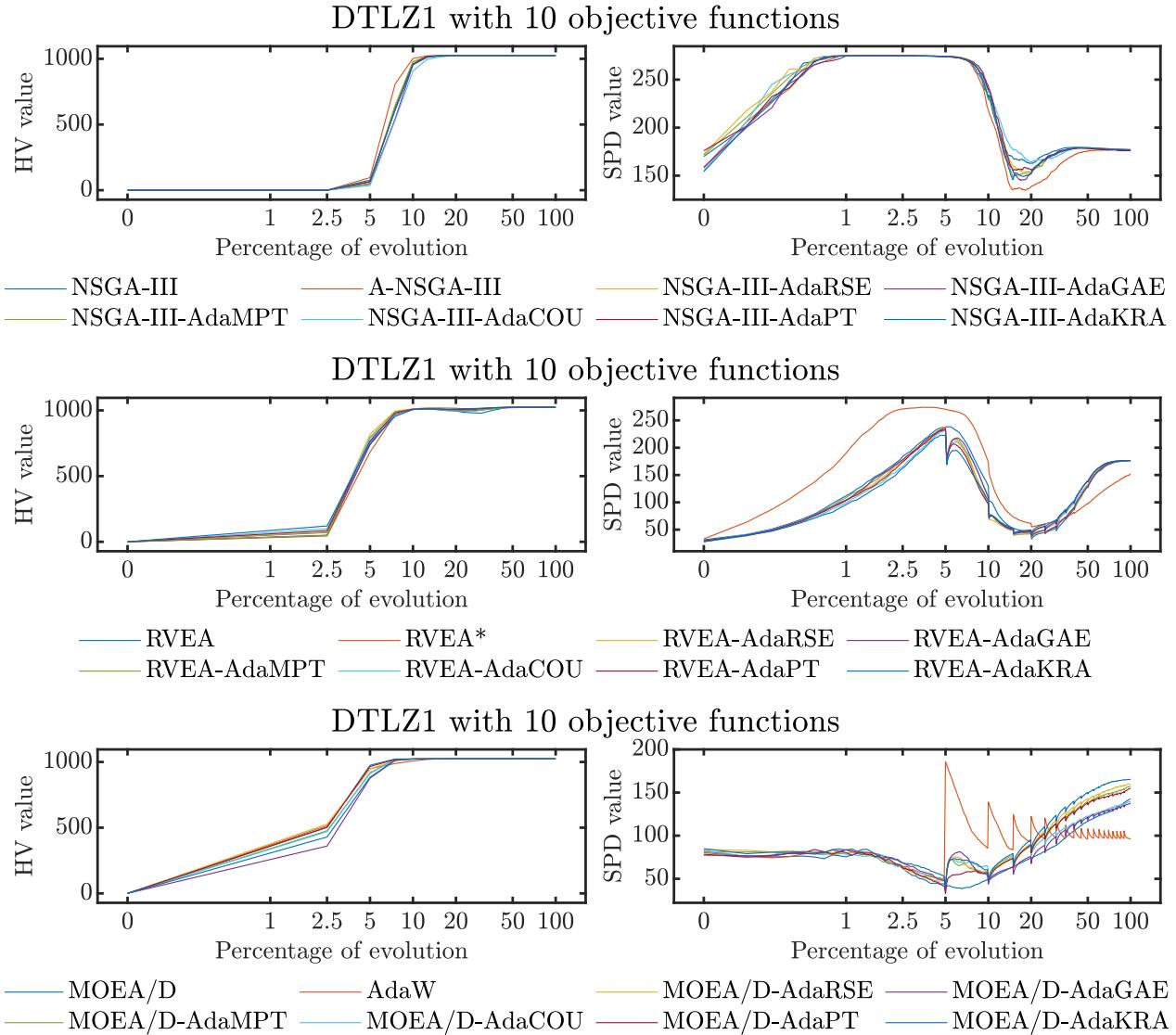


Figure 152: Convergence and diversity graphs with the mean HV value and SPD value of 30 independent runs of MOEAs using the NSGA-III, RVEA, and MOEA/D frameworks on DTLZ1 with 10 objective functions.

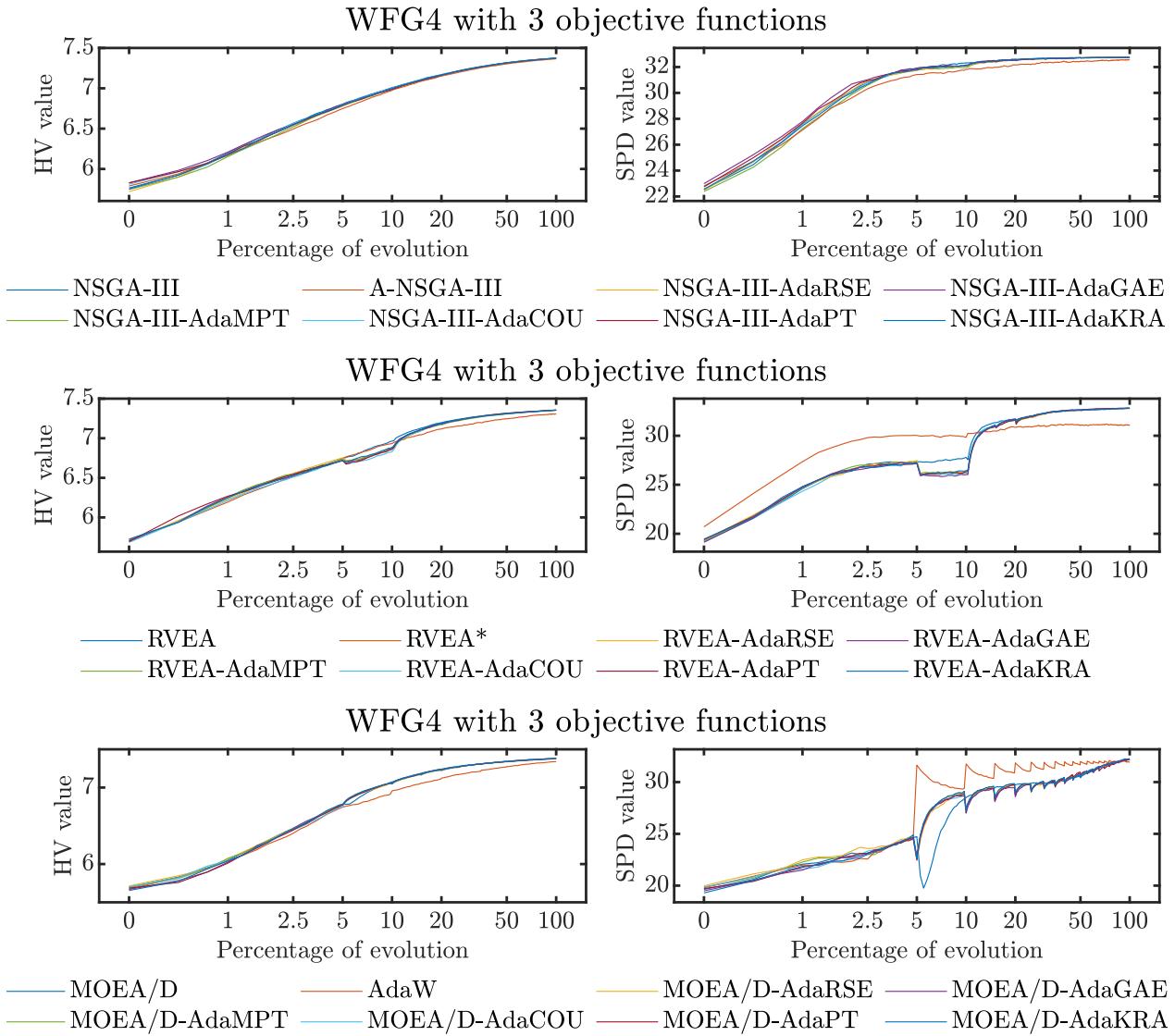


Figure 153: Convergence and diversity graphs with the mean HV value and SPD value of 30 independent runs of MOEAs using the NSGA-III, RVEA, and MOEA/D frameworks on WFG4 with 3 objective functions.

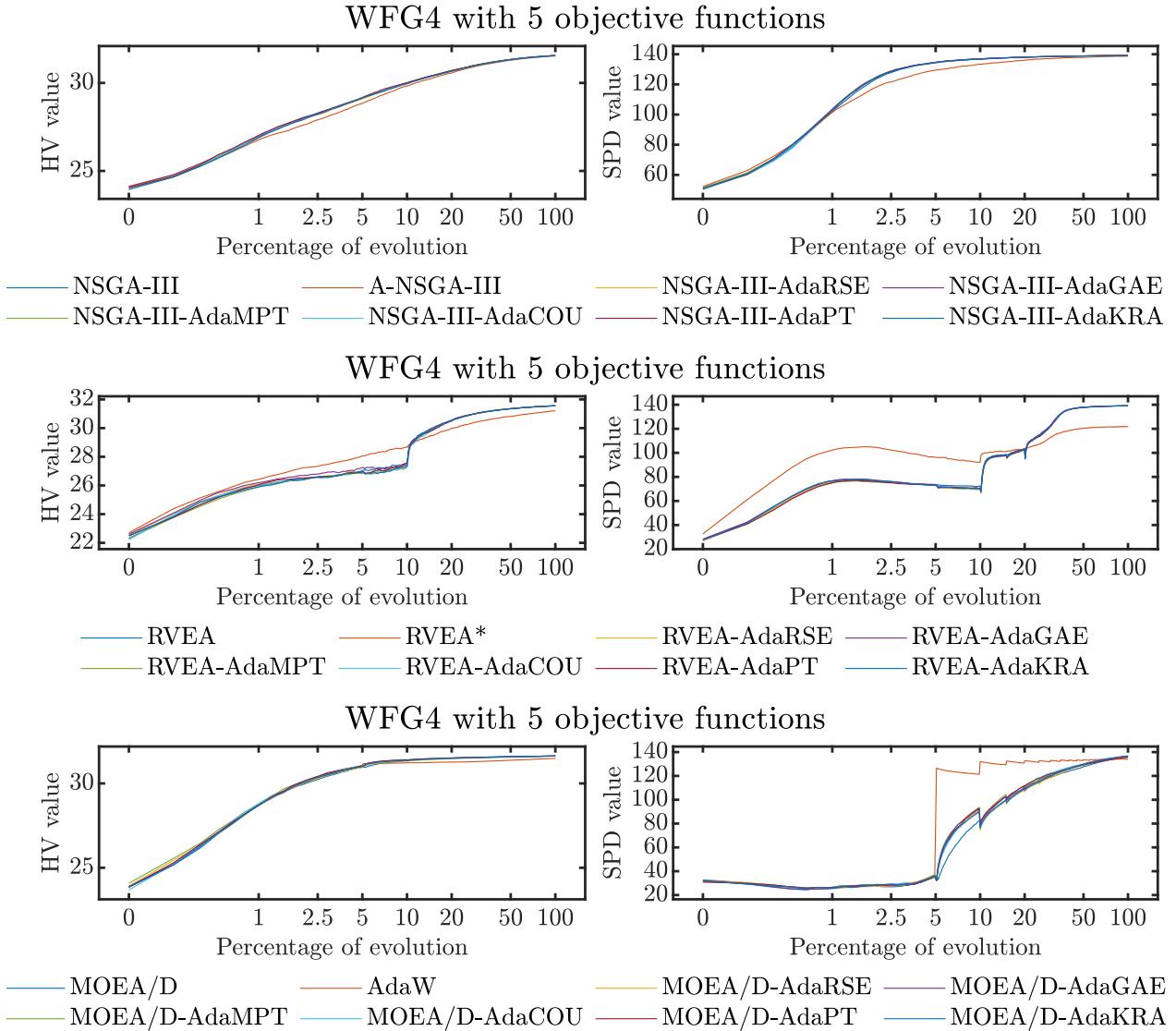


Figure 154: Convergence and diversity graphs with the mean HV value and SPD value of 30 independent runs of MOEAs using the NSGA-III, RVEA, and MOEA/D frameworks on WFG4 with 5 objective functions.

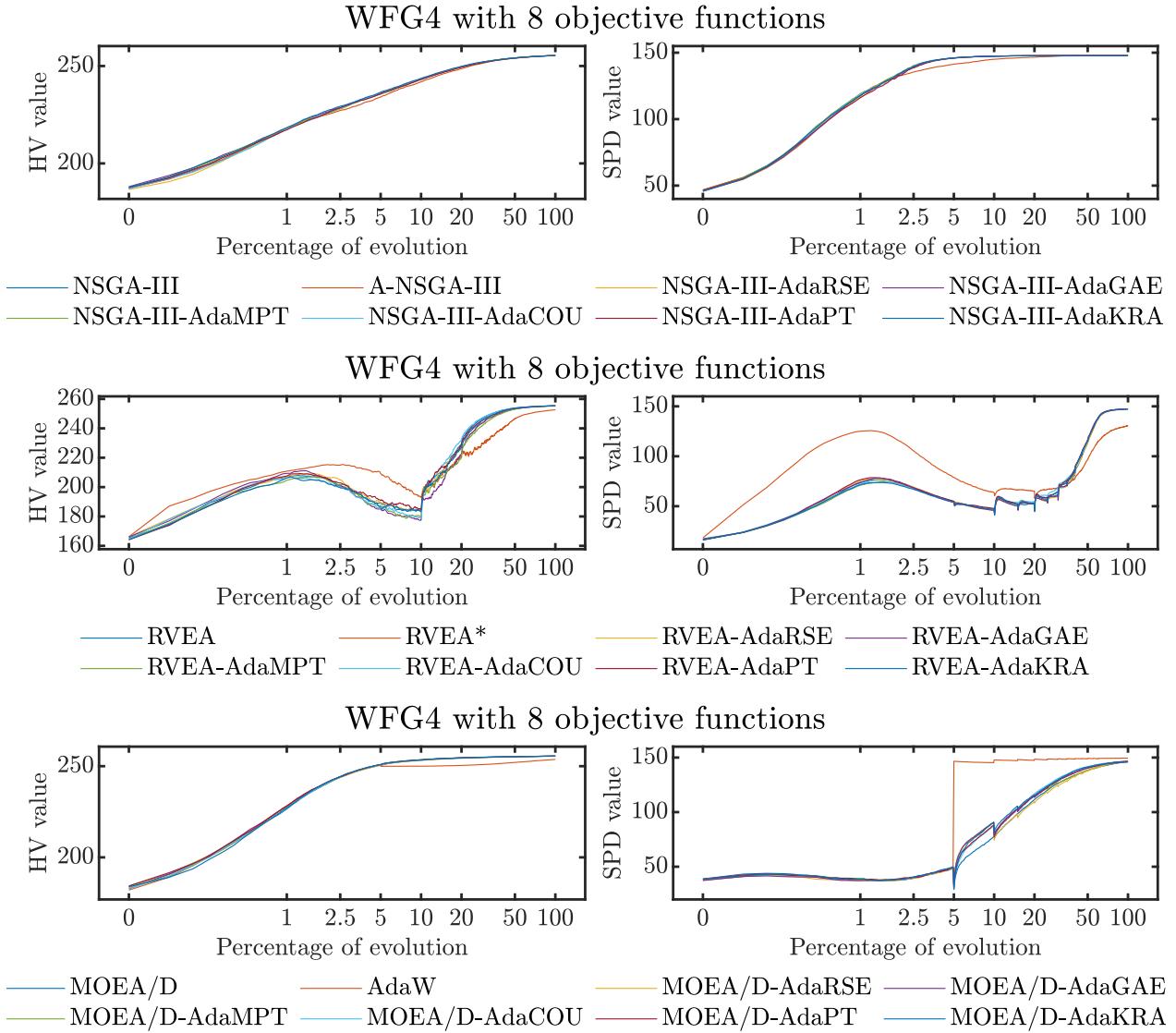


Figure 155: Convergence and diversity graphs with the mean HV value and SPD value of 30 independent runs of MOEAs using the NSGA-III, RVEA, and MOEA/D frameworks on WFG4 with 8 objective functions.

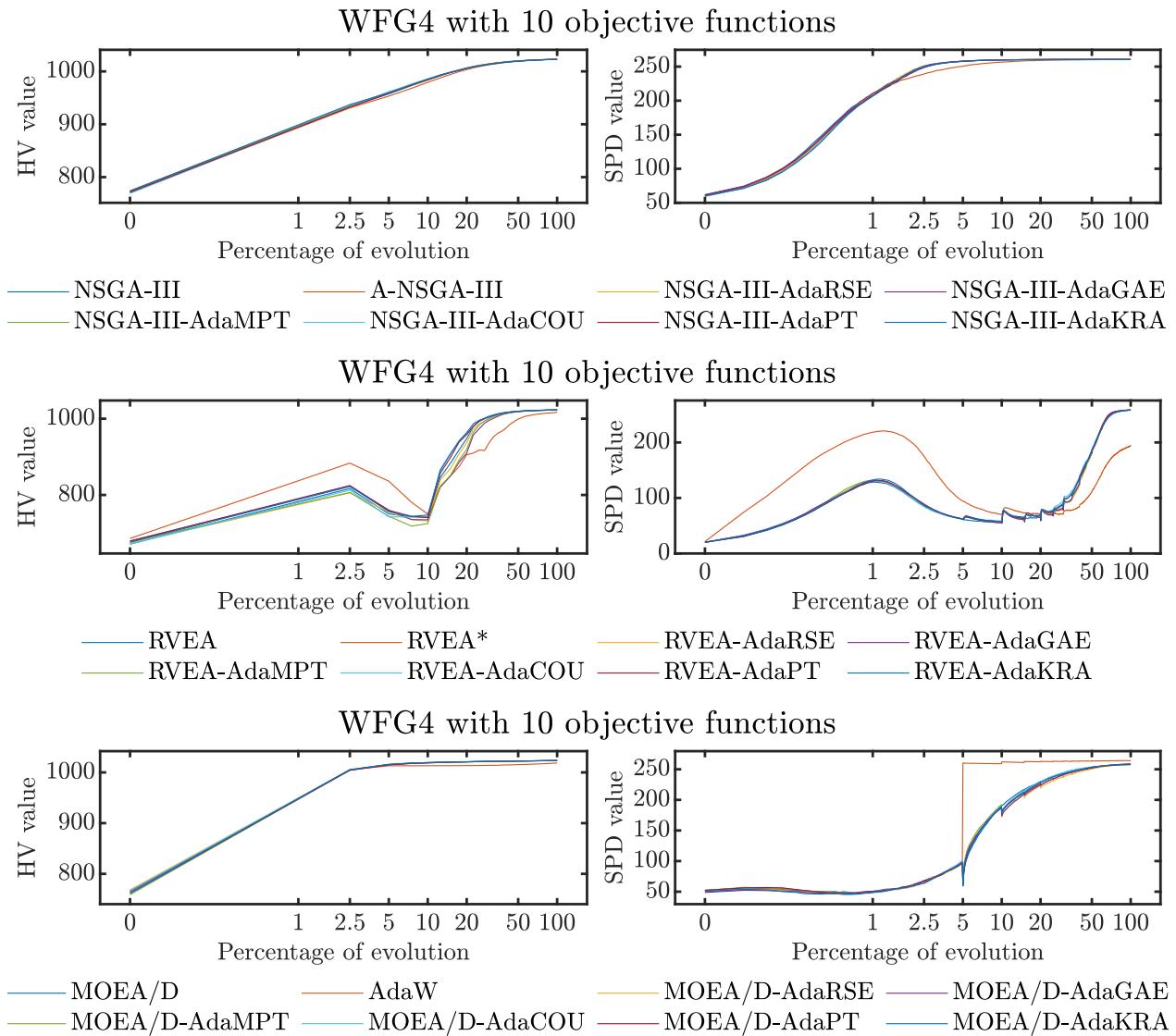


Figure 156: Convergence and diversity graphs with the mean HV value and SPD value of 30 independent runs of MOEAs using the NSGA-III, RVEA, and MOEA/D frameworks on WFG4 with 10 objective functions.

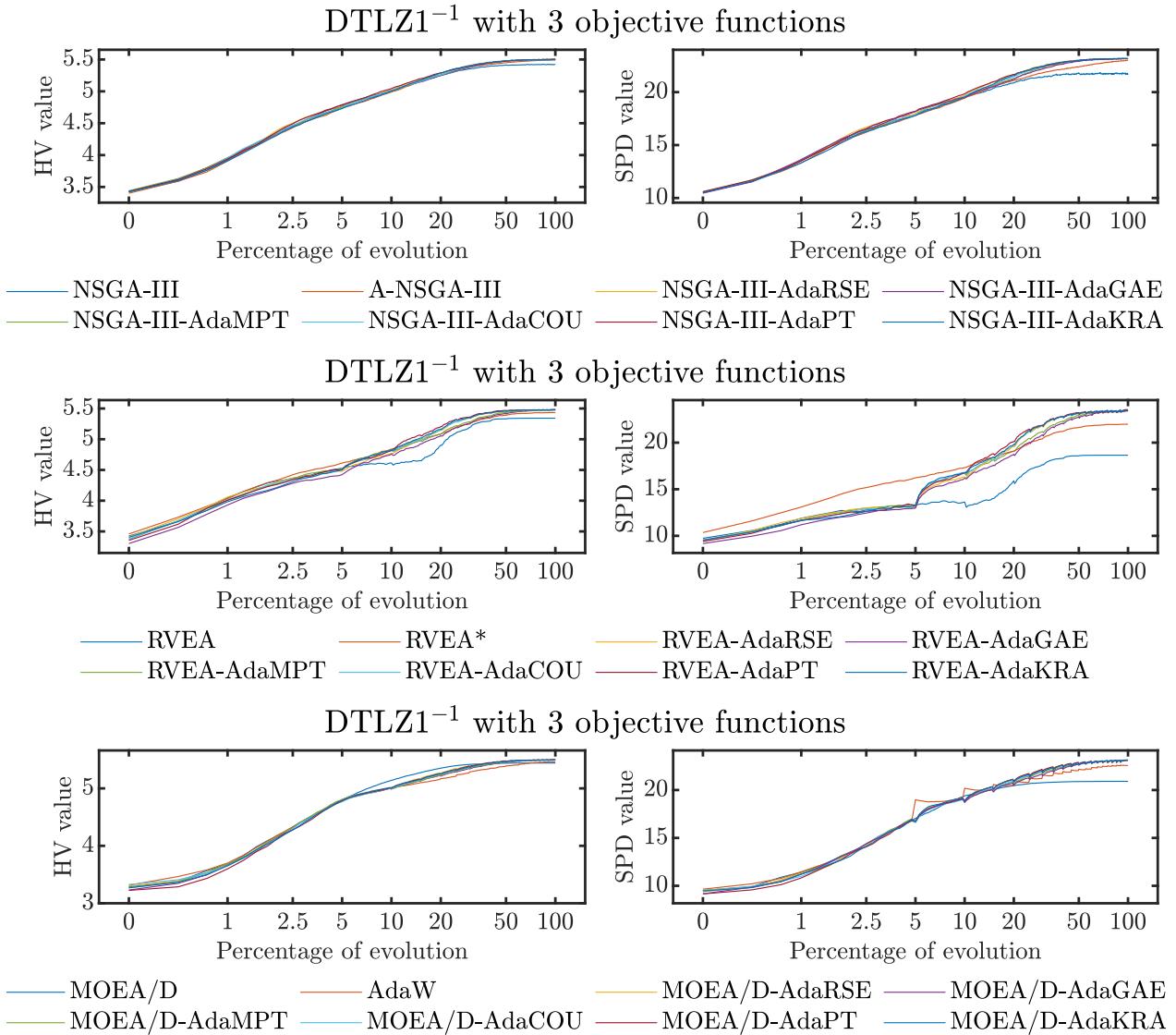


Figure 157: Convergence and diversity graphs with the mean HV value and SPD value of 30 independent runs of MOEAs using the NSGA-III, RVEA, and MOEA/D frameworks on DTLZ1⁻¹ with 3 objective functions.

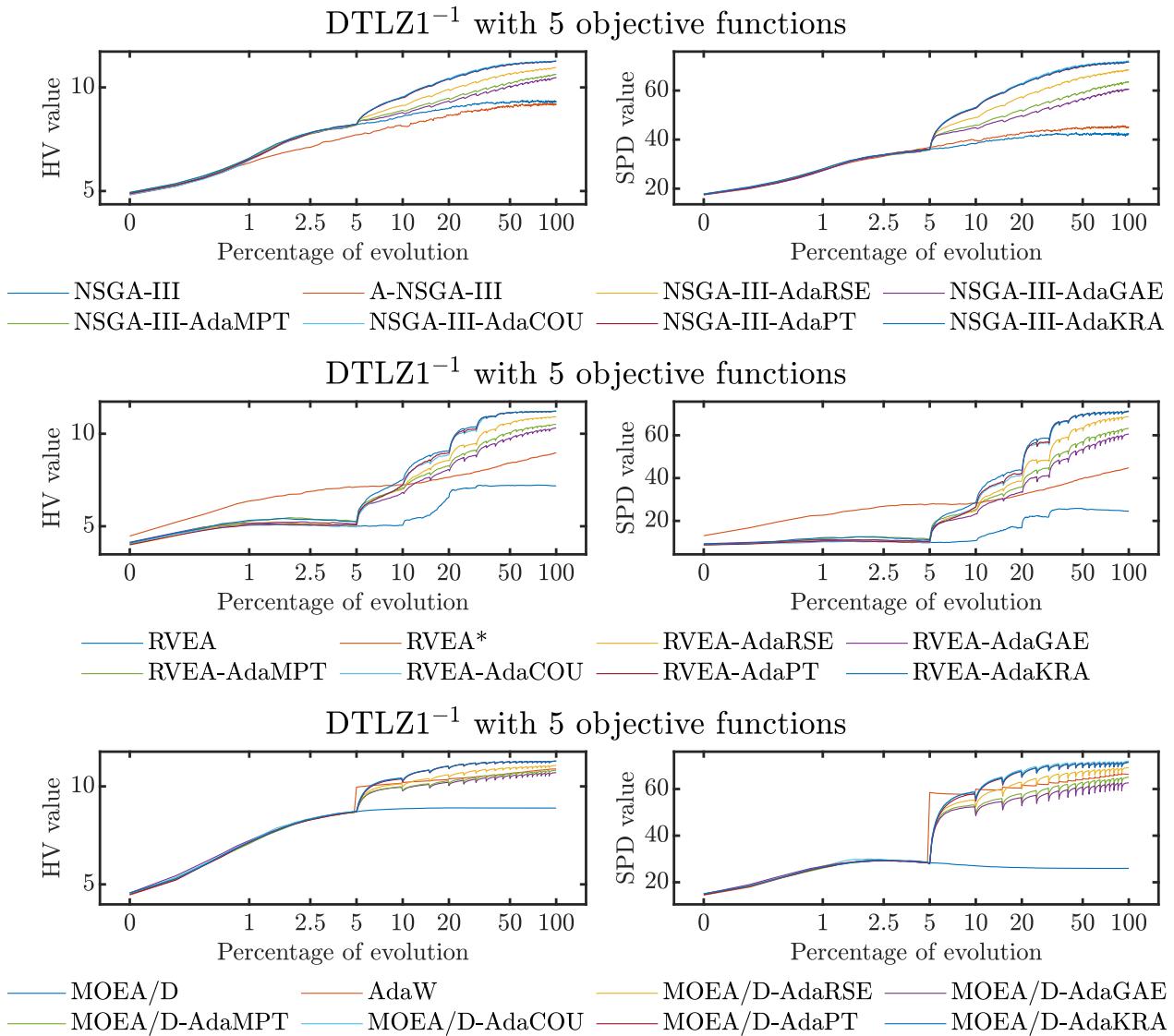


Figure 158: Convergence and diversity graphs with the mean HV value and SPD value of 30 independent runs of MOEAs using the NSGA-III, RVEA, and MOEA/D frameworks on DTLZ1⁻¹ with 5 objective functions.

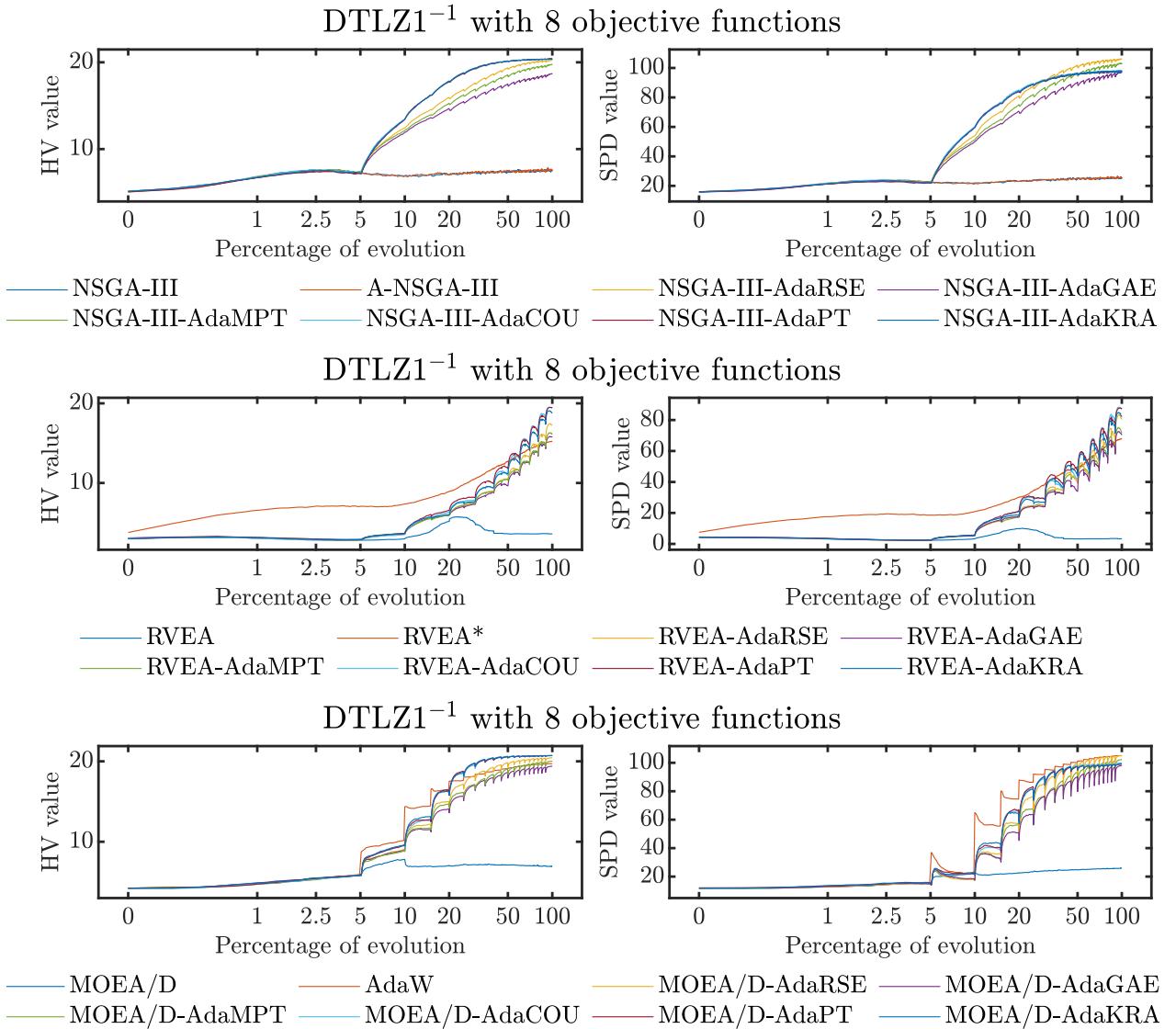


Figure 159: Convergence and diversity graphs with the mean HV value and SPD value of 30 independent runs of MOEAs using the NSGA-III, RVEA, and MOEA/D frameworks on DTLZ1⁻¹ with 8 objective functions.

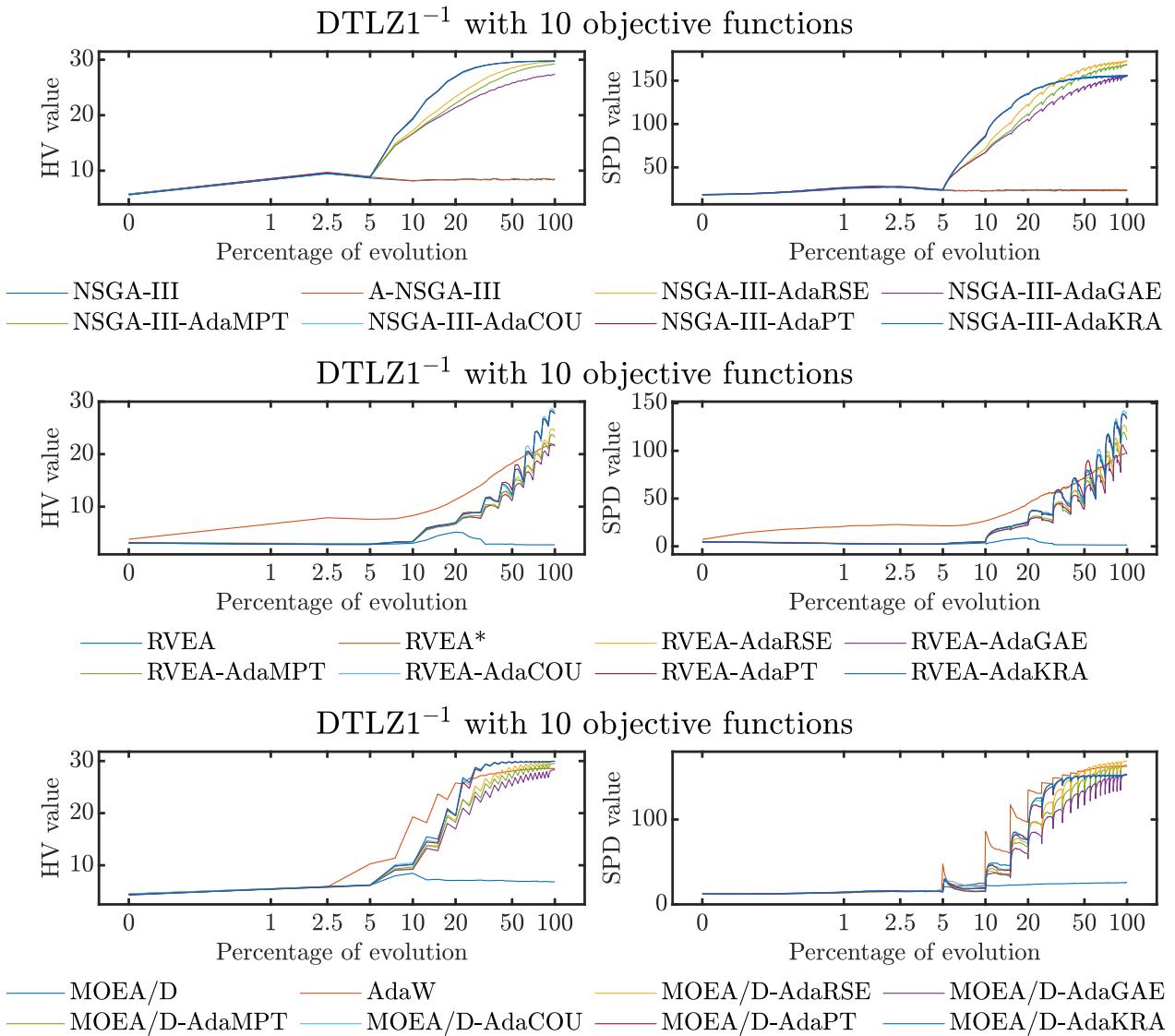


Figure 160: Convergence and diversity graphs with the mean HV value and SPD value of 30 independent runs of MOEAs using the NSGA-III, RVEA, and MOEA/D frameworks on DTLZ1⁻¹ with 10 objective functions.

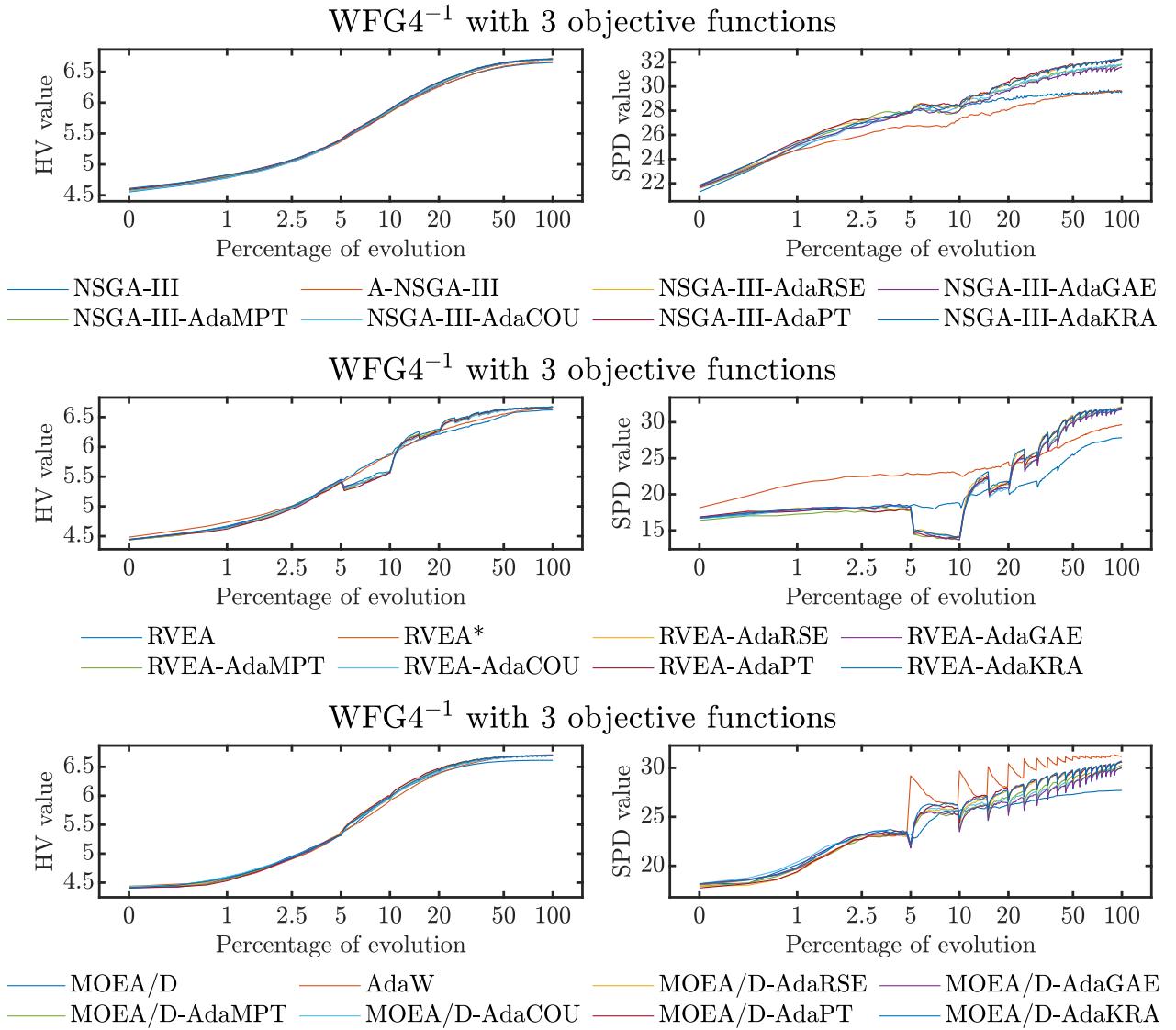


Figure 161: Convergence and diversity graphs with the mean HV value and SPD value of 30 independent runs of MOEAs using the NSGA-III, RVEA, and MOEA/D frameworks on WFG4⁻¹ with 3 objective functions.

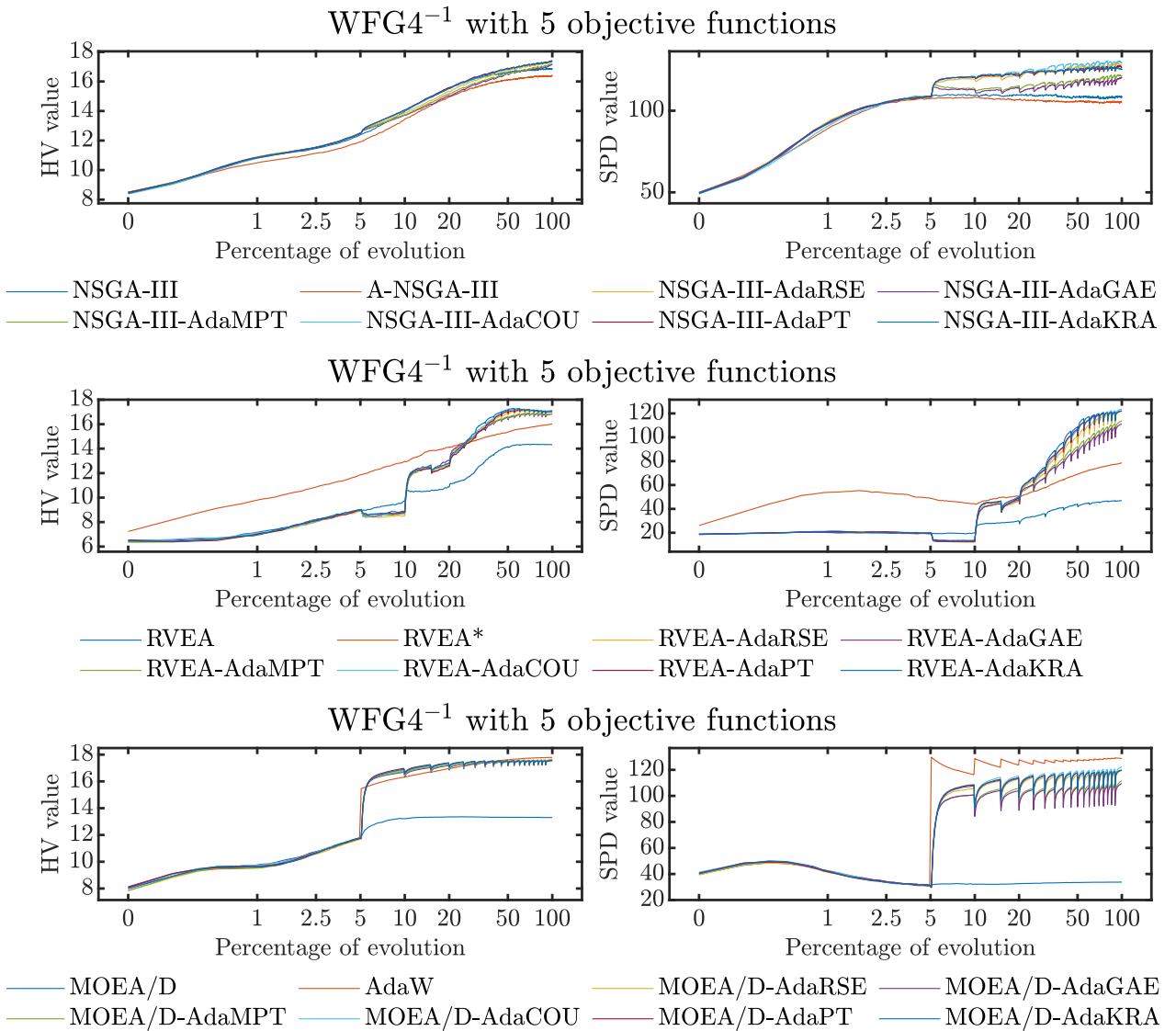


Figure 162: Convergence and diversity graphs with the mean HV value and SPD value of 30 independent runs of MOEAs using the NSGA-III, RVEA, and MOEA/D frameworks on WFG4⁻¹ with 5 objective functions.

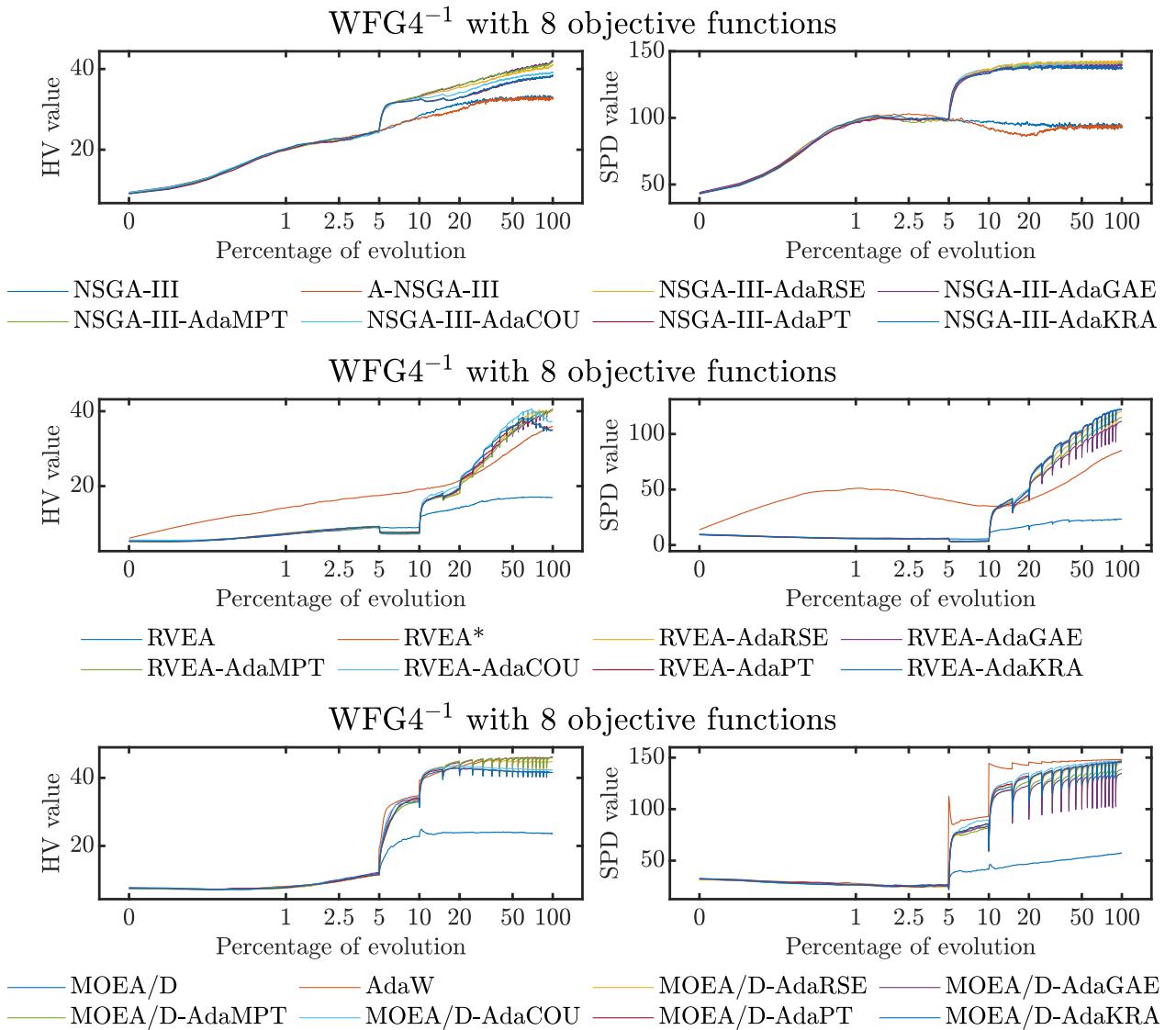


Figure 163: Convergence and diversity graphs with the mean HV value and SPD value of 30 independent runs of MOEAs using the NSGA-III, RVEA, and MOEA/D frameworks on WFG4⁻¹ with 8 objective functions.

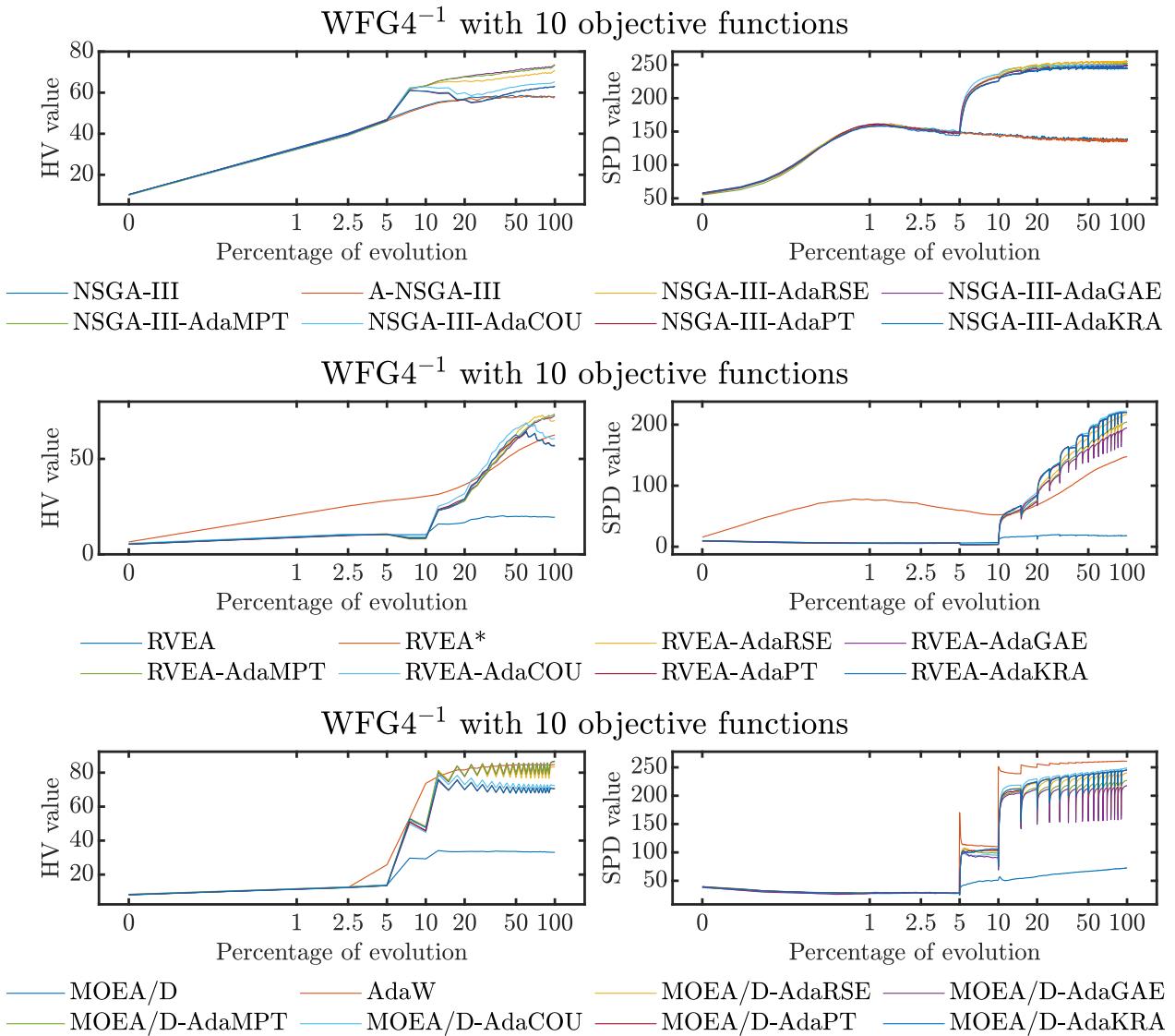


Figure 164: Convergence and diversity graphs with the mean HV value and SPD value of 30 independent runs of MOEAs using the NSGA-III, RVEA, and MOEA/D frameworks on WFG4⁻¹ with 10 objective functions.